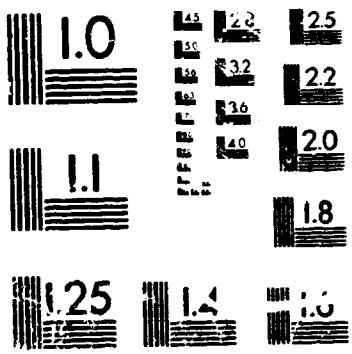

FINAL REPORT

REGENERABLE BIOCIDE DELIVERY UNIT

VOLUME 1

SEPTEMBER 1992

Prepared by

James E. Atwater
Richard R. Wheeler, Jr.

Contract No. NAS9-18361

Lyndon B. Johnson Space Center
National Aeronautics and Space Administration
Houston, TX 77058

UMPQUA RESEARCH COMPANY
AEROSPACE DIVISION
P.O. BOX 791 - 125 VOLUNTEER WAY
MYRTLE CREEK, OR 97457
TELE: (503) 863-7770
FAX: (503) 863-7775

URC 80356

FINAL REPORT

REGENERABLE BIOCIDE DELIVERY UNIT

VOLUME 1

SEPTEMBER 1992

Prepared by

James E. Atwater
Richard R. Wheeler, Jr.

Contract No. NAS9-18361

Lyndon B. Johnson Space Center
National Aeronautics and Space Administration
Houston, TX 77058

UMPQUA RESEARCH COMPANY
AEROSPACE DIVISION
P.O. BOX 791 - 125 VOLUNTEER WAY
MYRTLE CREEK, OR 97457
TELE: (503) 863-7770
FAX: (503) 863-7775

URC 80356

Table of Contents

Section	Volume 1.	Page
	PROJECT SUMMARY	i
1	INTRODUCTION	1-1
2	REGENERATIVE MICROBIAL CHECK VALVE (RMCV) AUTONOMOUS TEST STANDS	2-1
	2.0 Overview	2-2
	2.1 RMCV Test Stand Design and Construction	2-3
	2.1.1 The Regenerative Microbial Check Valve Circuit	2-3
	2.1.2 The Multiplexed RMCV Test Stand	2-6
	2.1.3 System On-line Iodine Monitor	2-6
	2.1.4 RMCV Test Stand Control	2-8
	2.1.5 RMCV Influent Temperature Control Circuits	2-10
	2.2 RMCV Test Stand Operation	2-14
3	CHEMISTRY OF THE RMCV CHALLENGE SOLUTIONS	3-1
	3.0 Overview	3-2
	3.1 Ersatz Reclaimed Potable Water	3-2
	3.2 Ersatz Reclaimed Hygiene Water	3-2
	3.3 Ersatz Humidity Condensate	3-3
	3.4 Ersatz Urine Distillate	3-6
4	THE DIODE ARRAY SPECTROPHOTOMETER AS RMCV TEST STAND ON-LINE IODINE MONITOR	4-1
	4.0 Overview	4-1
	4.1 Diode Array Spectrophotometer Quantitative Methodology	4-3
	4.2 Calibration	4-9
	4.2.1 Ersatz Reclaimed Potable Water	4-10
	4.2.2 Ersatz Reclaimed Hygiene Water	4-13
	4.2.3 Ersatz Humidity Condensate	4-13
	4.2.4 Ersatz Urine Distillate	4-13
	4.3 Long Term RMCV Life Cycle Tests	4-24
	4.4 Parametric RMCV Tests	4-26
	4.5 Kinetic Studies	4-27
	4.6 Prototype RMCV	4-27
5	RMCV SMALL COLUMN LIFE CYCLE TESTS	5-1
	5.0 Overview	5-2
	5.1 RMCV-1: Ersatz Reclaimed Potable Water	5-4
	5.2 RMCV-2: Ersatz Reclaimed Hygiene Water	5-11

TABLE OF CONTENTS (Continued)

	5.3	RMCV-3: Ersatz Humidity Condensate	5-23
	5.4	RMCV-4: Ersatz Urine Distillate	5-31
	5.5	Conclusions	5-41
6		RMCV PARAMETRIC TESTING	6-1
	6.0	Overview	6-2
	6.1	Residence Time Experiments	6-3
	6.2	Iodine Crystal Size Experiments	6-12
	6.3	RMCV Operation at High and Low pH	6-25
	6.4	Amberlite 401S Resin Tests	6-28
7		RMCV CHEMISTRY	7-1
	7.0	Overview	7-2
	7.1	The Chemistry of Aqueous I_2 Speciation	7-3
		7.1.1 Aqueous I_2 Equilibria at 25 °C	7-3
		7.1.2 Numerical Solution of Multiple Equilibria	7-6
		7.1.3 True Equilibrium I_2 Speciation at 25 °C	7-8
		7.1.4 Pseudo-equilibrium (fast) Speciation at 25 °C	7-11
		7.1.5 Kinetics of Equilibrium Speciation at 25 °C	7-27
	7.2	Chemistry and Kinetics of I_2 Loss in Ersatz Humidity Condensate and Ersatz Urine Distillate	7-40
		7.2.1 I_2 Decay in Ersatz Humidity Condensate	7-41
		7.2.2 I_2 Decay in Ersatz Urine Distillate	7-52
		7.2.3 I_2 Decay Conclusions	7-54
	7.3	The Search for Iodinated Organics	7-57
8		RMCV SUPER-IODINATION FOR MICROBIAL DECONTAMINATION	8-1
	8.0	Overview	8-2
	8.1	Production of Super-iodinated Water	8-2
	8.2	Disinfection of Surfaces using Super-iodinated Water	8-4
	8.3	Control of Biofilm using Super-iodinated Water	8-4
	8.4	Conclusions	8-9
9		MATERIALS COMPATIBILITY WITH ELEMENTAL IODINE	9-1
	9.0	Overview	9-2
	9.1	Corrosion of Stainless Steels by I_2	9-3
		9.1.1 Exposure to Saturated Iodine Solution	9-3
		9.1.2 Exposure to Moist Crystalline I_2	9-12
		9.1.3 Exposure to Dry Crystalline I_2	9-12
	9.2	Corrosion of Titanium by I_2	9-12
	9.3	Corrosion of Hasteloy C and Hasteloy G by I_2	9-19

TABLE OF CONTENTS (Continued)

	9.3.1	Corrosion of Hasteloy C	9-19
	9.3.2	Corrosion of Hasteloy G	9-19
9.4	Compatibility of Organic Materials with I_2		0-23
9.5	Analysis of Saturated I_2 Solutions for Dissolved Metals		9-24
9.6	Conclusions		9-24
10	PROTOTYPE REGENERATIVE MICROBIAL CHECK VALVE DEVELOPMENT		10-1
10.0	Overview		10-2
10.1	Prototype RMCV Design		10-2
10.1.1		MCV and Solid I_2 Bed Sizing	10-2
10.1.2		RMCV Flow Path Hardware	10-8
10.1.3		The Prototype RMCV Control System	10-11
10.1.4		The On-Line Iodine Monitor	10-12
10.2	The Integrated Prototype RMCV		10-16
10.3	The Prototype RMCV Operational Test		10-16
10.4	Conclusions		10-21
11	CONCLUSIONS		11-1
12	REFERENCES AND BIBLIOGRAPHY		12-1

Volume 2

APPENDIX I - PROJECT SOFTWARE

APPENDIX II - PROTOTYPE RMCV OPERATIONS MANUAL

LIST OF FIGURES

Figure No.		Page
1.1	Block Diagram of the Regenerative Microvial Check Valve (RMCV)	1-3
2.1	Schematic Illustration of Individual Small Column Scale RMCV	2-4
2.2	Integrated RMCV Test Stand Schematic	2-7
2.3	Schematic Illustration of RMCV Test Stand Control Architecture	2-8
2.4	1.7 °C Temperature Control Sub-system	2-11
2.5	26.7 °C Temperature Control Sub-system	2-13
2.6	Black and White Facsimile of RMCV Test Stand Color VGA Screen - Washout Mode	2-17
2.7	Black and White Facsimile of RMCV Test Stand Color VGA Screen - with Regeneration	2-18
4.1	UV-VIS Spectrum of 0.4 mg/L I^- in DI Water	4-3
4.2	UV-VIS Spectrum of 2.0 mg/L I_2 in DI Water	4-4
4.3	UV-VIS Spectrum of 2.0 mg/L I^-, 4.0 mg/L I_2 in DI Water	4-5
4.4	UV-VIS Spectra of RMCV Challenge Solution Matrices	4-8
4.5	Calibration of 1 cm Path-length Cell in DI Wateer	4-11
4.6	Calibration of 10 cm Path-length Cell in DI Water	4-12
4.7	10 cm Cell-Ersatz Reclaimed Hygiene Water - DI Blank	4-14
4.8	10 cm Cell-Ersatz Reclaimed Hygiene Water (RHW) - RHW Blank	4-15
4.9	1 cm Cell-Ersatz Humidity Condensate - DI Water Blank	4-16
4.10	1 cm Cell-Ersatz Humidity Condensate (HC) - HC Matrix Blank	4-17
4.11	5 cm Cell-Ersatz Humidity Condensate (HC) - HC Matrix Blank	4-18
4.12	10 cm Cell-Ersatz Humidity Condensate - DI Water Blank	4-19
4.13	10 cm Cell-Ersatz Humidity Condensate (HC) - HC Matrix Blank	4-20
4.14	5 cm Cell-Ersatz Urine Distillate (UD) - UD Matrix Blank	4-21
4.15	10 cm Cell-Ersatz Urine Distillate - DI Water Blank	4-22
4.16	10 cm Cell-Ersatz Urine Distillate (UD) - UD Matrix Blank	4-23
4.17	Iodide and Iodine at λ = 228 nm - DI Water Matrix	4-25
4.18	Constant Temperature Spectrometer Cell for Kinetics Experiments	4-28
5.1	RMCV Life Cycle Test - Ersatz Reclaimed Potable water - 0-500 L/cm^3	5-5
5.2	RMCV Life Cycle Test - Ersatz Reclaimed Potable water - 500-1000 L/cm^3	5-6
5.3	RMCV Life Cycle Test - Ersatz Reclaimed Potable water - 1000-1500 L/cm^3	5-7
5.4	RMCV Life Cycle Test - Ersatz Reclaimed Potable water - 1500-2000 L/cm^3	5-8

LIST OF FIGURES (Continued)

5.5	RMCV Life Cycle Test - Ersatz Reclaimed Potable water - 2000-2500 L/cm^3	5-9
5.6	RMCV Life Cycle Test - Ersatz Reclaimed Potable water - 2500-2556 L/cm^3	5-10
5.7	Cyclic Throughput - Ersatz Reclaimed Potable Water	5-12
5.8	Cyclic I_2 Depletion - Ersatz Reclaimed Potable Water	5-12
5.9	Cyclic I_2 Depletion - Ersatz Reclaimed Potable Water	5-13
5.10	I_2 Depletion During Regeneration - Ersatz Reclaimed Potable Water	5-13
5.11	Cyclic Throughput During Regeneration - Ersatz Reclaimed Potable Water	5-14
5.12	RMCV Life Cycle Test - Ersatz Reclaimed Hygiene Water: 0-500 L/cm^3	5-15
5.13	RMCV Life Cycle Test - Ersatz Reclaimed Hygiene Water: 500-1000 L/cm^3	5-16
5.14	RMCV Life Cycle Test - Ersatz Reclaimed Hygiene Water: 1000-1500 L/cm^3	5-17
5.15	RMCV Life Cycle Test - Ersatz Reclaimed Hygiene Water: 1500-2000 L/cm^3	5-18
5.16	RMCV Life Cycle Test - Ersatz Reclaimed Hygiene Water: 2000-2394 L/cm^3	5-19
5.17	Cyclic I_2 Depletion - Ersatz Reclaimed Hygiene Water	5-21
5.18	I_2 Depletion During Regeneration - Ersatz Reclaimed Hygiene Water	5-21
5.19	Cyclic Throughput - Ersatz Reclaimed Hygiene Water	5-22
5.20	Cyclic I_2 Depletion During Regeneration - Ersatz Reclaimed Hygiene Water	5-22
5.21	Cyclic Throughput During Regeneration - Ersatz Reclaimed Hygiene Water	5-23
5.22	RMCV Life Cycle Test - Ersatz Humidity Condensate: 0-500 L/cm^3	5-25
5.23	RMCV Life Cycle Test - Ersatz Humidity Condensate: 500-1000 L/cm^3	5-26
5.24	RMCV Life Cycle Test - Ersatz Humidity Condensate: 1000-1500 L/cm^3	5-27
5.25	RMCV Life Cycle Test - Ersatz Humidity Condensate: 1500-2000 L/cm^3	5-28
5.26	RMCV Life Cycle Test - Ersatz Humidity Condensate: 2000-2500 L/cm^3	5-29
5.27	RMCV Life Cycle Test - Ersatz Humidity Condensate: 2500-2533 L/cm^3	5-30
5.28	Cyclic I_2 Depletion - Ersatz Humidity Condensate	5-32
5.29	Cyclic I$^-$ Depletion - Ersatz Humidity Condensate	5-32
5.30	Cyclic Throughput - Ersatz Humidity Condensate	5-33
5.31	Cyclic I_2 Depletion During Regeneration - Ersatz Humidity Condensate	5-33
5.32	Cyclic Throughput During Regeneration - Ersatz Humidity Condensate	5-34
5.33	RMCV Life Cycle Test - Ersatz Urine Distillate: 0-500 L/cm^3	5-35
5.34	RMCV Life Cycle Test - Ersatz Urine Distillate: 500-1000 L/cm^3	5-36
5.35	RMCV Life Cycle Test - Ersatz Urine Distillate: 1000-1500 L/cm^3	5-37
5.36	RMCV Life Cycle Test - Ersatz Urine Distillate: 1500-2000 L/cm^3	5-38

LIST OF FIGURES (Continued)

5.37	RMCV Life Cycle Test - Ersatz Urine Distillate: 2000-2500 L/cm^3	5-39
5.38	RMCV Life Cycle Test - Ersatz Urine Distillate: 2500-2533 L/cm^3	5-40
5.39	Cyclic I_2 Depletion - Ersatz Urine Distillate	5-42
5.40	Cyclic I$^-$ Depletion - Ersatz Urine Distillate	5-42
5.41	Cyclic Throughput - Ersatz Urine Distillate	5-43
5.42	Cyclic I_2 Depletion During Regeneration - Ersatz Urine Distillsate	5-43
5.43	Cyclic Throughput during Regeneration - Ersatz Urine Distillate	5-44
6.1	Residence Time Experiments: Ersatz Reclaimed Potable Water MCV = 0.203 min., I_2 Bed = 0.553 min.	6-4
6.2	Residence Time Experiments: Ersatz Reclaimed Potable Water MCV = 0.212 min., Crystal Bed = 0.577 min.	6-5
6.3	Residence Time Experiments: Ersatz Reclaimed Potable Water MCV = 0.294 min., Crystal Bed = 0.801 min.	6-6
6.4	Residence Time Experiments: Ersatz Reclaimed Potable Water MCV = 0.464 min., Crystal Bed = 1.216 min.	6-7
6.5	Residence Time Experiments: Ersatz Humidity Condensate MCV = 0.198 min., I_2 Bed = 0.640 min.	6-9
6.6	Residence Time Experiments: Ersatz Humidity Condensate MCV = 0.202 min., I_2 Bed = 0.649 min.	6-10
6.7	Residence Time Experiments: Ersatz Humidity Condensate MCV = 0.379 min., I_2 Bed = 1.032 min.	6-11
6.8	Effluent I_2 versus Residence Time	6-13
6.9	I_2 Loading Rate during Regeneration versus MCV Residence Time	6-14
6.10	Size Distribution of I_2 Crystals	6-14
6.11	850 - 1180 µ Crystal Bed Washout	6-15
6.12	600 - 850 µ Crystal Bed Washout	6-16
6.13	425 - 600 µ Crystal Bed Washout	6-17
6.14	300 - 425 µ Crystal Bed Washout	6-18
6.15	<300 µ Crystal Bed Washout	6-19
6.16	Aqueous I_2 versus Crystal Size - 1.0 Min. Residence Time	6-21
6.17	Aqueous I_2 versus Crystal Size - 0.4 Min. Residence Time	6-21
6.18	Aqueous I_2 versus Crystal Size - 0.2 Min. Residence Time	6-22
6.19	Aqueous I_2 versus Crystal Size - 0.1 Min. Residence Time	6-22
6.20	300 - 425 µ Crystal Bed Effluent versus Residence Time	6-23
6.21	425 - 600 µ Crystal Bed Effluent versus Residence Time	6-23
6.22	600 - 850 µ Crystal Bed Effluent versus Residence Time	6-24
6.23	850 - 1180 µ Crystal Bed Effluent versus Residence Time	6-24
6.24	RMCV Challenged with HCl Solution at pH = 2	6-26
6.25	RMCV Challenged with HCl Solution at pH = 4	6-26
6.26	RMCV Challenged with NaOH at pH = 8	6-27
6.27	RMCV Challenged with NaOH at pH = 10	6-27

LIST OF FIGURES (Continued)

6.28	Amberlite 401S - Ersatz Reclaimed Potable Water	6-29
6.29	Amberlite 401S - Ersatz Reclaimed Hygiene Water	6-29
6.30	Amberlite 401S - Ersatz Humidity Condensate	6-30
6.31	Amberlite 401S - Ersatz Urine Distillate	6-30
7.1	Equilibrium of I_2 Vapor as a Function of Aqueous I_2	7-3
7.2	Equilibrium Iodine Speciation - 300 mg/L I	7-9
7.3	Equilibrium Iodine Speciation - 10 mg/L I	7-10
7.4	Equilibrium Iodine Speciation - 4 mg/L I	7-12
7.5	Equilibrium Iodine Speciation - 2 mg/L I	7-13
7.6	Equilibrium Fractional Occurence of I_2 versus Total I	7-14
7.7	Equilibrium Fractional Occurence of I^- versus Total I	7-15
7.8	Equilibrium Fractional Occurence of I_3^- versus Total I	7-16
7.9	Equilibrium Fractional Occurence of IO_3^- versus Total I	7-17
7.10	Pseudo-equilibrium Iodine Speciation versus pH - 300 mg/l Total I	7-19
7.11	Pseudo-equilibrium Iodine Speciation versus pH - 10 mg/l Total I	7-20
7.12	Pseudo-equilibrium Iodine Speciation versus pH - 4 mg/l Total I	7-21
7.13	Pseudo-equilibrium Iodine Speciation versus pH - 2 mg/l Total I	7-22
7.14	Pseudo-equilibrium Speciation - (2 mg/l I_2 + 0.2 mg/L I^-)	7-24
7.15	Pseudo-equilibrium Speciation - (2 mg/l I_2 + 0.6 mg/L I^-)	7-25
7.16	Pseudo-equilibrium Speciation - (2 mg/l I_2 + 1.0 mg/L I^-)	7-22
7.17	I_2 Speciation Kinetics - 300 mg/L I at pH = 7	7-29
7.18	I_2 Speciation Kinetics - 4.0 mg/L I at pH = 7	7-31
7.19	I_2 Speciation Kinetics - 2.0 mg/L I at pH = 7	7-32
7.20	I_2 Speciation Kinetics - 300 mg/L I at pH = 6	7-33
7.21	I_2 Speciation Kinetics - 4.0 mg/L I at pH = 6	7-34
7.22	I_2 Speciation Kinetics - 2.0 mg/L I at pH = 7	7-35
7.23	I_2 Speciation Kinetics - 4.0 mg/L I at pH = 5	7-36
7.24	I_2 Speciation Kinetics - 2.0 mg/L I at pH = 5	7-37
7.25	I_2 Speciation Kinetics at pH = 4	7-38
7.26	I_2 Speciation Kinetics at pH = 3	7-39
7.27	I_2 Decay in Ersatz Humidity Condensate Matrix	7-43
7.28	Ersatz Humidity Condensate - I_2	7-45
7.29	Time Series of UV-vis Spectra - I_2 in Ersatz Humidity Condensate	7-46
7.30	Elemental Iodine Decay in 2.5 mM Formic Acid	7-48
7.31	Iodine Reaction with Formic Acid	7-49
7.32	Formic Acid - I_2 Second Order Rate Model	7-50
7.33	Arrhenius Plot - I_2 in Formic Acid - 2nd Order Rate Constant	7-52
7.34	I_2 Decay in Ersatz Urine Distillate	7-53
7.35	I_2 in Ersatz Urine Distillate	7-53
7.36	Iodine Decay in Urine Distillate - 2nd Order Model	7-54

LIST OF FIGURES (Continued)

7.37	Project Decay of 4.0 mg/L I_2 in STS-45 Humidity Condensate	7-56
8.1	Solid State Crystal Bed Effluent I_2 concentration versus Throughput, 10 cm^3 bed volume - 10 cm^3/min flow rate	8-3
9.1	Iodine Corrosion Tests - 304 Stainless Steel	9-4
9.2	Iodine Corrosion Tests - 316 Stainless Steel	9-5
9.3	Iodine Corrosion Tests - 316L Stainless Steel	9-7
9.4	Iodine Corrosion Tests - 347 Stainless Steel	9-8
9.5	Iodine Corrosion Tests - 410 Stainless Steel	9-10
9.6	Iodine Corrosion Tests - Titanium - 2	9-13
9.7	Iodine Corrosion Tests - Titanium - 7	9-14
9.8	Iodine Corrosion Tests - Titanium - 9	9-15
9.9	Iodine Corrosion Tests - Titanium - 4901	9-17
9.10	Iodine Corrosion Tests - Hastelcy C	9-20
9.11	Iodine Corrosion Tests - Hasteloy G	9-21
9.12	Iodine Corrosion Tests - Teflon	9-25
9.13	Iodine Corrosion Tests - Polypropylene	9-26
9.14	Iodine Corrosion Tests - Viton A	9-27
9.15	Iodine Corrosion Tests - Teflon coated 302 SS Spring	9-29
10.1	Effluent I_2 versus MCV Residence Time During Regeneration	10-4
10.2	Regeneration Liquor I_2 versus Crystal Bed Residence Time	10-4
10.3	Bed Volume versus Flow Rate for Minimal Residence Times	10-5
10.4	Prototype RMCV Plumbing Schematic	10-7
10.5	100 cm^3 Stainless Steel Microbial Check Valve	10-9
10.6	Titanium Housing for 15.24 cm I_2 Crystal Bed	10-10
10.7	Prototype RMCV Control Schematic	10-12
10.8	Intercomparison of Prototype Effluent I_2 by Various Methods	10-14
10.9	Astro Iodine Bench Control Schematic	10-15
10.10	Integrated Prototype RMCV	10-17
10.11	6 Month Prototype RMCV Flow History	10-19
10.12	Prototype RMCV in Super-Iodination Mode	10-21

LIST OF TABLES

Table No.		Page
5.1	RMCV Life Cycle Test Results Summary	5-3
7.1	Summary of Iodine Decay Kinetics in 2.5 mM Formic Acid	7-51
8.1	Surface Contamination Super-iodination Test Results	8-5
8.2	Test Results for Super-iodination of the 24 Hour Biofilm	8-6
8.3	Test Results for Super-iodination of the 40 Hour Biofilm	8-6
8.4	Super-iodination of the 72 Hour Biofilm-Single Exposure	8-7
8.5	Super-iodination of the 72 Hour Biofilm-Multiple Exposure	8-7
8.6	Test Results for Super-iodination of the 88 Hour Biofilm	8-8
9.1	Corrosion Tests - 304 Stainless Steel	9-6
9.2	Corrosion Tests - 316 Stainless Steel	9-6
9.3	Corrosion Tests - 316L Stainless Steel	9-9
9.4	Corrosion Tests - 347 Stainless Steel	9-9
9.5	Corrosion Tests - 410 Stainless Steel	9-11
9.6	Corrosion Tests - Titanium - 2	9-11
9.7	Corrosion Tests - Titanium - 7	9-16
9.8	Corrosion Tests - Titanium - 9	9-16
9.9	Corrosion Tests - Titanium - 4901	9-18
9.10	Corrosion Tests - Hasteloy C	9-18
9.11	Corrosion Tests - Hasteloy G	9-22
9.12	Corrosion Tests - Teflon	9-22
9.13	Corrosion Tests - Polypropylene	9-28
9.14	Corrosion Tests - Viton A	9-28
9.15	Corrosion Tests - Teflon Coated Stainless Steel Springs	9-30

PROJECT SUMMARY

The Microbial Check Valve (MCV), which is currently used aboard the Shuttle Orbiter for disinfection of the potable water supply, is an expendable flow-through canister containing iodinated ion exchange resin. Means for extension of MCV life are desirable to avoid resupply penalties. The Phase I Regenerable Biocide Delivery Unit program demonstrated the feasibility of regenerating an MCV *in situ*, using a strong aqueous elemental iodine solution resulting from diversion of the MCV influent to a packed bed containing iodine crystals. In small column tests, eight manual regenerations of an MCV resin were accomplished. The term Regenerative Microbial Check Valve (RMCV) was adopted describing this new technology.

The Phase II program has resulted in the development of a full scale and fully autonomous prototype RMCV, capable of maintaining residual I_2 levels between 2.0 - 4.0 mg/L for prolonged periods. During six months of testing at the Space Station baseline flow rate of 120 cm^3/min, the prototype RMCV underwent nine regenerations. RMCV life cycle tests, using a variety of influent streams, were conducted over an eighteen month period to determine the useful lives of MCVs incorporating this new technology and to determine ultimate failure mechanisms. MCV life extensions of 130 fold were demonstrated, limited only by the Phase II performance period. Based upon this work, it is certain that RMCV units can be developed to provide unattended biocide addition for the thirty year life of Space Station *Freedom*, or for other longer duration applications such as a Lunar Base or Mars mission.

RMCV technology has also been demonstrated capable of delivering, on demand, a concentrated aqueous I_2 solution for potential use as a disinfectant during transient episodes of microbial surface contamination, for the control of biofilm formation, or as a preventative measure in systems which are particularly susceptible to the growth of microorganisms.

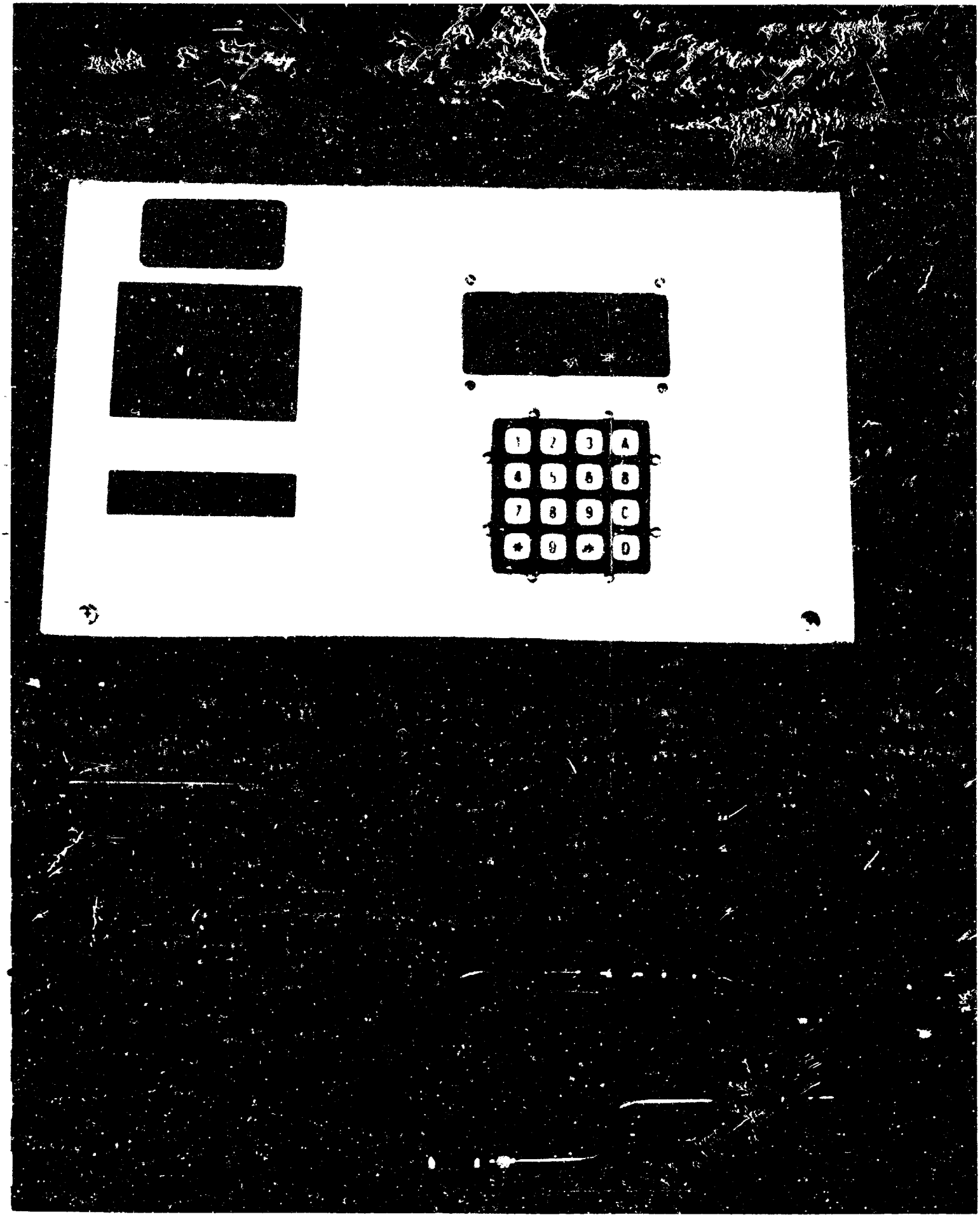

URC 80356

Prototype RMCV - Frontal View

ORIGINAL PAGE
COLOR PHOTOGRAPH

URC 80356

Prototype RMCV - Side View

ORIGINAL PAGE
COLOR PHOTOGRAPH

1

INTRODUCTION

Disinfection of the potable water supply aboard the Shuttle Orbiter is currently provided by the Microbial Check Valve (MCV)[87,88,89]. The MCV produces a significant microbial contact kill, and imparts a biocidal iodine residual to the water[62,82,127,290.291,292,368,421]. The MCV is an in-line, flow-through cartridge containing iodinated strong base anion exchange resin. Elemental iodine (I_2), in the form of complex polyiodide anions[52,136,168,189,190,191,194,195,237,250,369,414,435,453], is bound to the quaternary amine functional groups within the resin framework. As water flows through the MCV some of the polyiodide anions dissociate, resulting in the liberation of aqueous I_2.

The dissociation of elemental I_2 from the bound state as a complex anion, to the free aqueous state is an equilibrium process, and hence is reversible. In a flow-through situation, true equilibrium is not achieved. The amount of residual I_2 imparted to the process water stream at any given time is determined by the method of MCV resin preparation, the design of the MCV cannister, and the stage of the MCV in its useful life. The Orbiter MCV has a design life of 30 days. An MCV with a 90 day life is baselined for Space Station *Freedom*[53]. For longer duration applications, such as a Lunar Base or Mars mission, an extended life is desirable to avoid resupply penalties.

A method of *in situ* MCV regeneration using elemental iodine has been developed. The process is illustrated in Figure 1.1. During regeneration, water *en route* to the MCV first passes through a crystalline iodine bed where a concentration between 200 - 300 mg/L I_2 is attained. When introduced into the MCV, a reverse concentration gradient is established which favors loading of I_2 onto the resin, effecting regeneration of the MCV.

The initial demonstration of the concept was accomplished under the Phase I SBIR Contract No. NAS9 - 18113, entitled Regenerable Biocide Delivery Unit[90,222] which concluded August, 1989. In this work, eight successful regenerations were demonstrated using small column scale MCVs, and the term Regenerative Microbial Check Valve (RMCV)

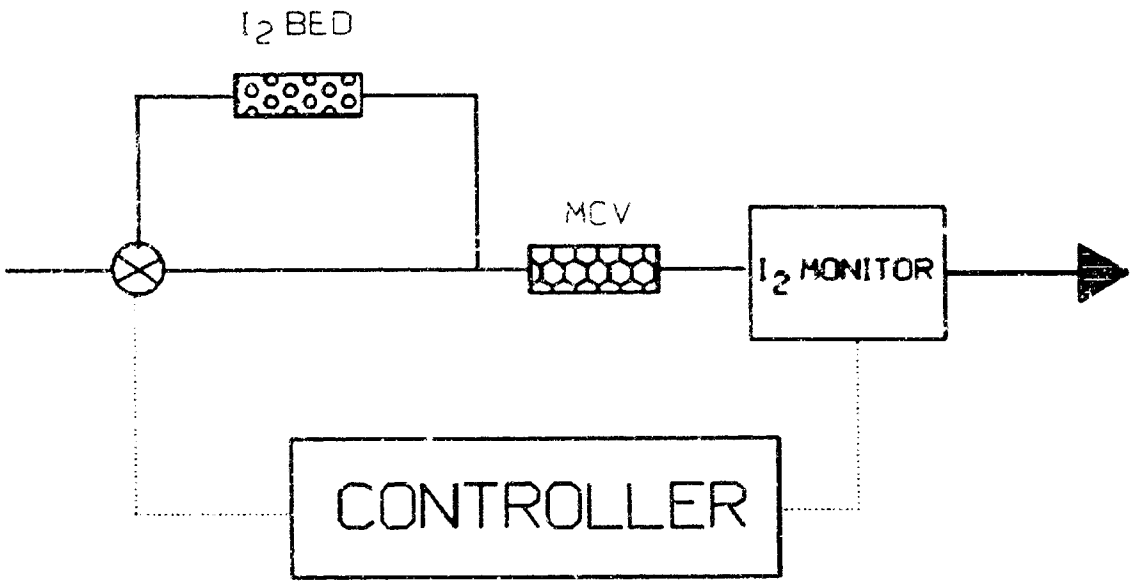

Figure 1.1 Block Diagram of the Regenerative Microbial Check Valve (RMCV).

was adopted to describe this technology

The generalized RMCV illustrated schematically in Figure 1.1 is typical of the fully autonomous units assembled and tested under the current development program, ranging from small column scale RMCVs to a full scale prototype system capable of accepting Space Station *Freedom* design flow rates. The autonomous RMCV consists of an MCV, I_2 Crystal Bed, diverter valve, iodine monitor, and controller. In the normal washout mode of operation, the process water stream is routed directly through the MCV cannister and the MCV effluent I_2 concentration is continuously tracked by the iodine monitor which transmits this information to the controller. When residual I_2 levels fall below 2.0 mg/L, the controller triggers the diverter valve to re-route flow first through the I_2 Crystal Bed and then through the MCV. When the MCV resin has been fully replenished, the controller switches the diverter valve back to its original position and flow is re-established directly to the MCV cannister. An operational I_2 concentration range between 4.0 - 2.0 mg/L was established for

the RMCV. The duration of the regeneration process is designed to replenish the MCV resin sufficiently for residual I_2 concentrations of 4.0 mg/L to be re-established.

This report details the advanced RMCV developments accomplished under the Phase II SBIR contract No. NAS9-18361 for the performance period September 16, 1990 - September 16, 1992. The report is organized into sections detailing: RMCV test stand design and operation, chemistry of the RMCV challenge streams, the diode array spectrophotometer as RMCV test stand on-line iodine monitor, small column long term RMCV life cycle tests, parametric testing, RMCV chemistry, RMCV super-iodination for microbial decontamination, compatibility of materials with elemental iodine, and prototype RMCV development and testing. The final section contains both the references cited in the text and a comprehensive bibliography of relevant literature. For convenience, the references are not organized in numerical order of citation. Instead they have been included in the bibliography as a whole, which is arranged alphabetically by author and numbered consecutively.

2

REGENERATIVE MICROBIAL CHECK VALVE (RMCV) AUTONOMOUS TEST STANDS

2.0 Overview.

Two fully autonomous Regenerative Microbial Check Valve (RMCV) Test Stands were designed, constructed, and programmed for the purposes of conducting small column long term regenerative life cycle tests and a variety of discrete parametric tests. Two vitually identical systems resulted from this effort, differing only slightly in the software used for control purposes.

The overall system design was driven by several key requirements. Foremost among these was the operational objective of continuously maintaining aqueous elemental iodine (I_2) concentrations in all RMCV effluent streams between a minimum value of 2.0 mg/L and a maximum value of 4.0 mg/L. The system was therefore required to sense RMCV effluent I_2 concentrations in real time in order to invoke regeneration at residual biocide levels < 2.0 mg/L. To function autonomously, with a minimum of operator intervention, it was required that the regeneration event be both initiated and terminated by the system. The size and level of complexity of the RMCV test stand was further established by the need for continuous unattended operation during extended periods of time, of up to four independent RMCV circuits. System complexity was further driven by the required capability of supplying selected RMCV influent challenge streams at both elevated and sub-ambient temperatures. From a logistics perspective, the scope of the Phase II work plan required development of a system capable of obtaining maximum data using a minimum of project personnel.

Control of each test stand was established using an IBM PC compatible 386SX personal computer. The Hewlett-Packard (HP) model 8452A diode array spectrophotometer was selected as the iodine monitor. Communication between the iodine monitor and host computer was obtained using a parallel interface. Steady flow of the RMCV challenge influents was maintained using a four channel peristaltic pump. One of four possible flowing streams was routed to the system iodine monitor using solenoid actuated valves controlled by direct digital output to a bank of solid state relays. Similarly intiation and termination of the

regeneration event was controlled by solenoid actuated valves. Temperatures were monitored using thermocouples and a digital thermometer with an RS-232C serial data link to the host computer. The system design and operation is described in detail below.

2.1 RMCV Test Stand Design and Construction.

Two computer controlled test stands were constructed for the continuous operation of a maximum of four small column scale RMCVs each. The four influent RMCV challenge streams included: ersatz reclaimed potable water, ersatz reclaimed hygiene water, ersatz urine distillate and ersatz humidity condensate. The chemical compositions of these challenge solutions are given in Section 3. Materials of construction were selected for their compatibility with the constituents of the RMCV aqu ous challenge streams.

Each RMCV Test Stand consists of four identical RMCV circuits plumbed in parallel. Downstream of the MCVs, the four flowing streams are multiplexed to a photodiode array UV - visible spectrophotometer, which serves as the on-line iodine monitor. Regeneration and stream selection for iodine monitoring are achieved under computer control. Unique to the third and fourth RMCV circuits, are temperature control units which produce ersatz urine distillate at 26.7 ^{o}C and humidity condensate at 1.7 ^{o}C.

2.1.1 The Regenerative Microbial Check Valve Circuit.

The essential details of an individual RMCV circuit are illustrated schematically in Figure 2.1. The RMCV challenge solution feedstock is contained within a 190 liter glass lined tank. The RMCV feed solution flows under the action of a Masterflex model 7520-35 (Cole-Parmer) peristaltic cartridge pump fitted with an attached Model 7519-00 four channel cartridge. The pump is rated at 3 A, 115 VAC and 50/60 Hz. The challenge solution flow rate is continuously adjustable via a rear mounted ten turn potentiometer or alternatively using a 4 - 20 mA external signal. The pump is capable of driving four streams within the 10 mL/min - 50 mL/min flow rate range required for either long term regnerative life cycle (real time) tests

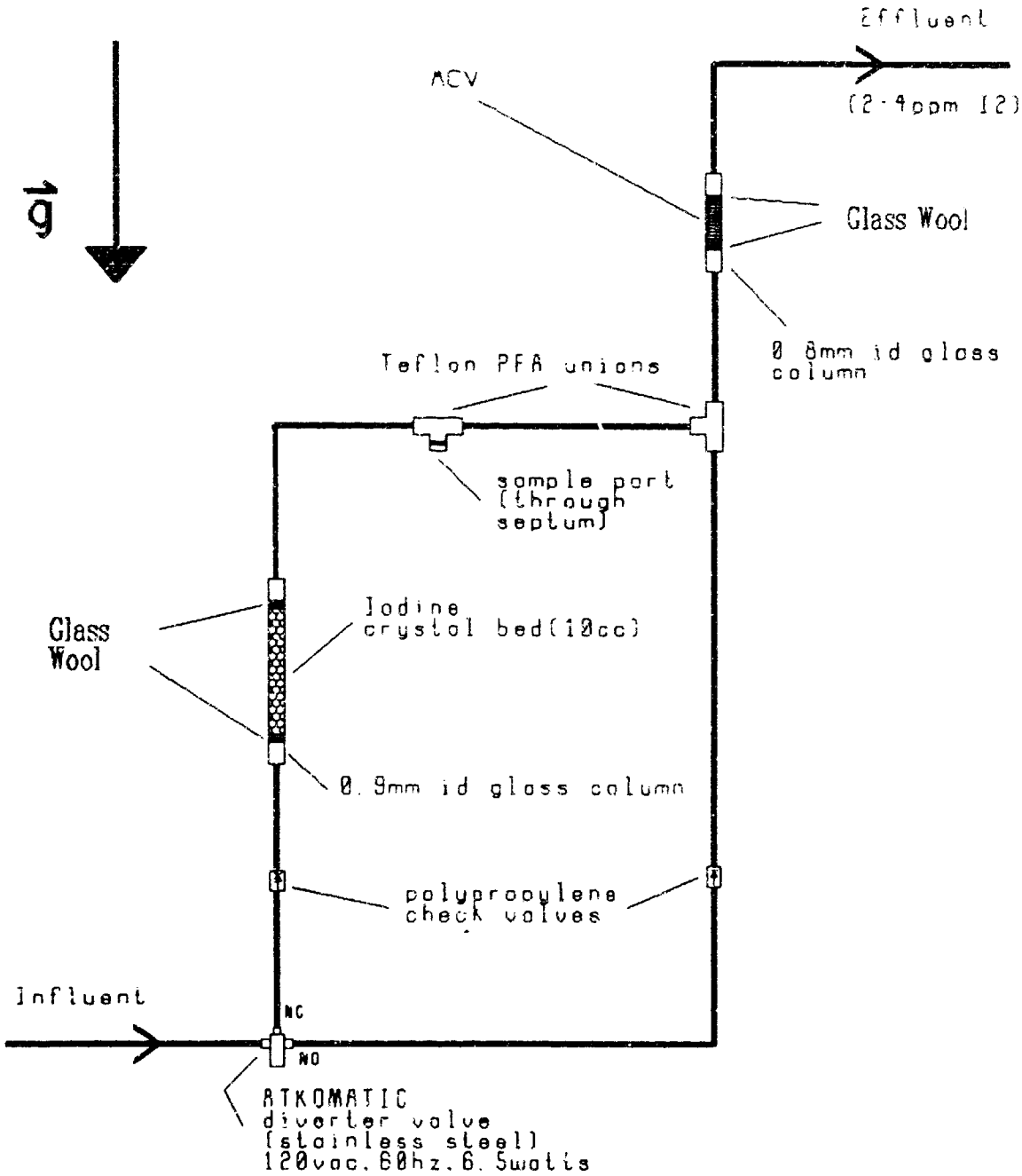

Figure 2.1 Schematic illustration of individual small column scale RMCV.

or the variety of parametric (accelerated) tests.

The conduit carrying RMCV challenge solution from the feed tank, through the peristaltic pump head, to the RMCV control solenoid valve is composed of Tygon tubing. The RMCV control valve is a two-way ATKOMATIC stainless steel solenoid actuated diverter valve (Cole Parmer 135-02). This regeration control valve is powered by 120 VAC and 60 Hz, consumes 6.5 watts, and is actuated either manually or under computer control via digital ouput to a solid state relay.

In the normal (elemental iodine washout) operational mode, flow is routed first through a polypropylene check valve and then directly to the inflow face of the MCV. The regeneration mode is invoked when power is applied to the solenoid. The RMCV control valve then directs the flow first past a second polypropylene check valve, then through the solid state iodine crystal regeneration bed. Downstream of the iodine crystal bed, the regeneration loop feeds back into the main stream using a Teflon - PFA union, and finally the regeneration stream flows into the MCV.

The solid state iodine crystal regeneration bed consists of a 0.9 mm ID borosilicate glass column packed with 10 cm^3 of iodine and held in place at each end with a glass wool plug. This configuration provides a residence time of approximately 0.8 minutes while flow is diverted in this direction. Downstream of the iodine crystal bed, glass or Teflon has been used where possible, to minimize the potential for interaction of iodine with the materials of construction. Located immediately downstream of the crystal bed is a sample port, made using a Teflon -PFA tee fitted with a septum such as that used for gas chromatography. This sample port serves to permit the collection of representative aliquots of the concentrated aqueous elemental iodine regeneration liquor.

Irrespective of the position of the RMCV control valve, the flowing stream of challenge solution is directed to the inflow face of the MCV. The small column scale MCV consists of a 0.8 mm ID borosilicate glass tube containing 2.5 cm^3 of iodinated resin. The

MCV resins were iodinated using Umpqua Research Company standard procedures for the preparation of resins, such as for those to be used in the Shuttle Orbiter or in UNIBEDs for Space Station *Freedom* multifiltration applications. The four MCVs used for the long term life cycle tests as well as those used for the bulk of the parametric testing were prepared using the standard iodinated resin used in the preparation of MCVs for Shuttle Orbiter missions. These resins typically have an anion exchange capacity for iodide of approximately 1.15 meq/cm^3 and initial total elemental iodine loadings of 2.30 mMole/cm^3. RMCVs prepared from Rohm and Haas Amberlite 401 S resin have undergone limited testing. MCV resins will be treated in greater detail in Sections 5 and 6 to follow.

2.1.2 The Multiplexed RMCV Test Stand.

Each RMCV Test Stand multiplexes four individual RMCV circuits as shown in Figure 2.2. The residual iodine containing effluent from each of the individual MCVs passes through a second solenoid actuated two-way Teflon valve, which routes each of the four challenge streams sequentially into the photodiode array spectrophotometer flow-through cell, where the concentration of aqueous iodine species is determined. The four Teflon solenoid actuated valves (Cole Parmer N-01367-72) are driven by a 12 VDC power supply. In the energized state, each valve consumes 3 W and is rated for pressures up to 30 psig. The Teflon valves can be operated either manually or via a solid state relay under computer control. In the normal operation mode, the solenoid is not energized and the RMCV challenge stream is routed to waste. When power is applied, the valve diverts its respective challenge solution flow to the diode array spectrophotometer's 10 cm path length quartz flow-through cell. The cell's effluent is carried to waste via Teflon tubing. This conduit provides a convenient means of sample collection for pH, conductivity and independent iodine determinations.

2.1.3 System On-line Iodine Monitor.

An HP model 8452A photodiode array spectrophotometer is used as the system on

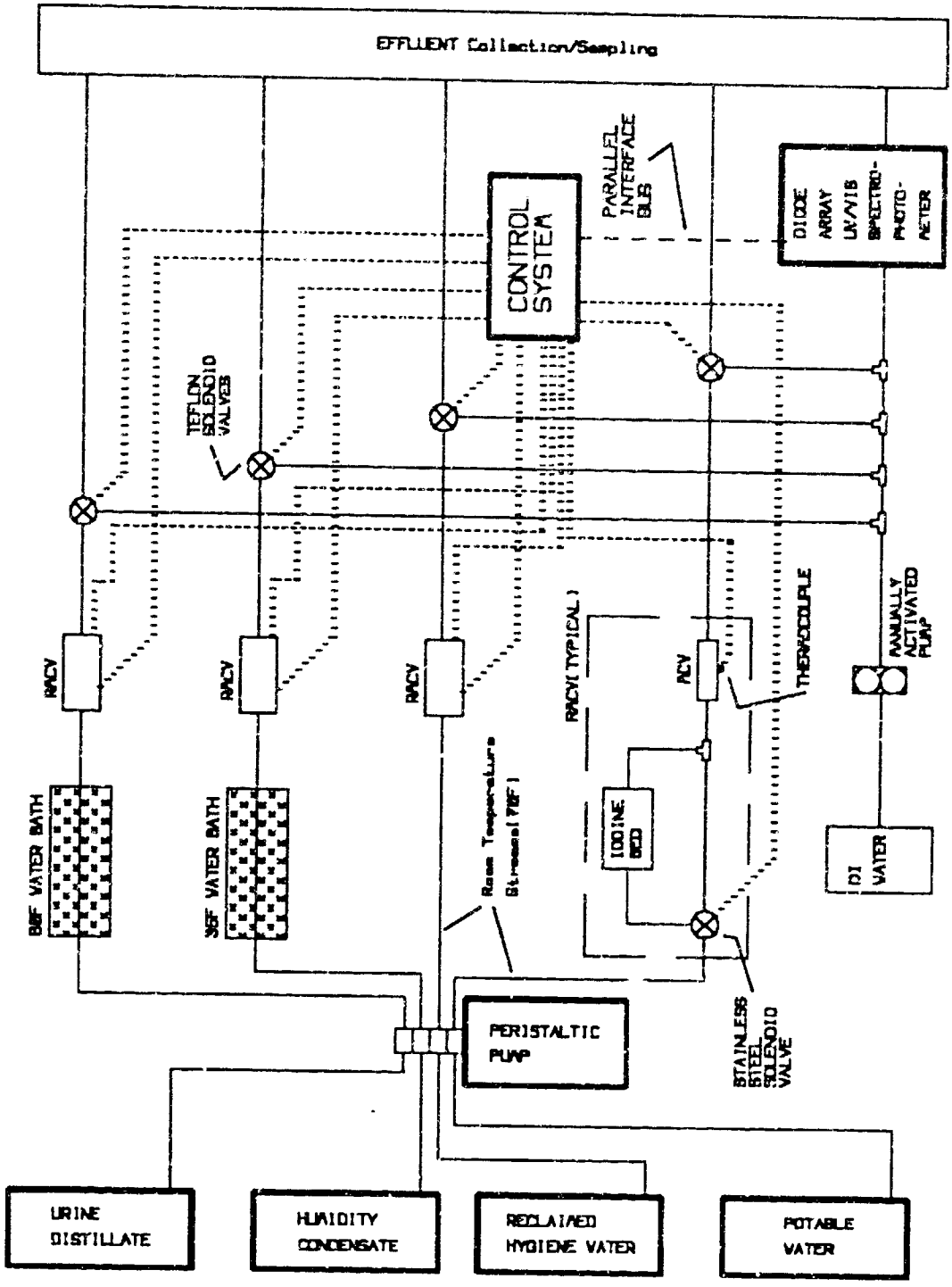

Figure 2.2 Integrated RMCV Test Stand Schematic.

line iodine monitor. It is a single beam instrument with 316 photodiodes yielding a spectral resolution of 2 nm in the wavelength (λ) range between 190 - 820 nm, covering both the ultraviolet (UV) and visible (VIS) regions of the absorption spectrum. The instrument dedicated to the long term RMCV life cycle test stand used a 10 cm path length UV quartz flow-through spectrophotometer cell throughout the course of this experiment. The second test stand has been variously configured with 1 cm, 5 cm and 10 cm path length flow-through quartz spectrophotometer cells, dependent upon the needs of individual experiments.

2.1.4 RMCV Test Stand Control.

The overall RMCV contol scheme is illustrated in Figure 2.3. A 16 MHz, 386 SX IBM compatible microcomputer provides overall system control of each of the RMCV test stands. Basic features of these identical computer systems include 1 Mb RAM, Color VGA monitor, 40 Mb RLL fixed disk, 5 1/4" 1.2 Mb and 3 1/2" 1.44 Mb floppy disk drives.

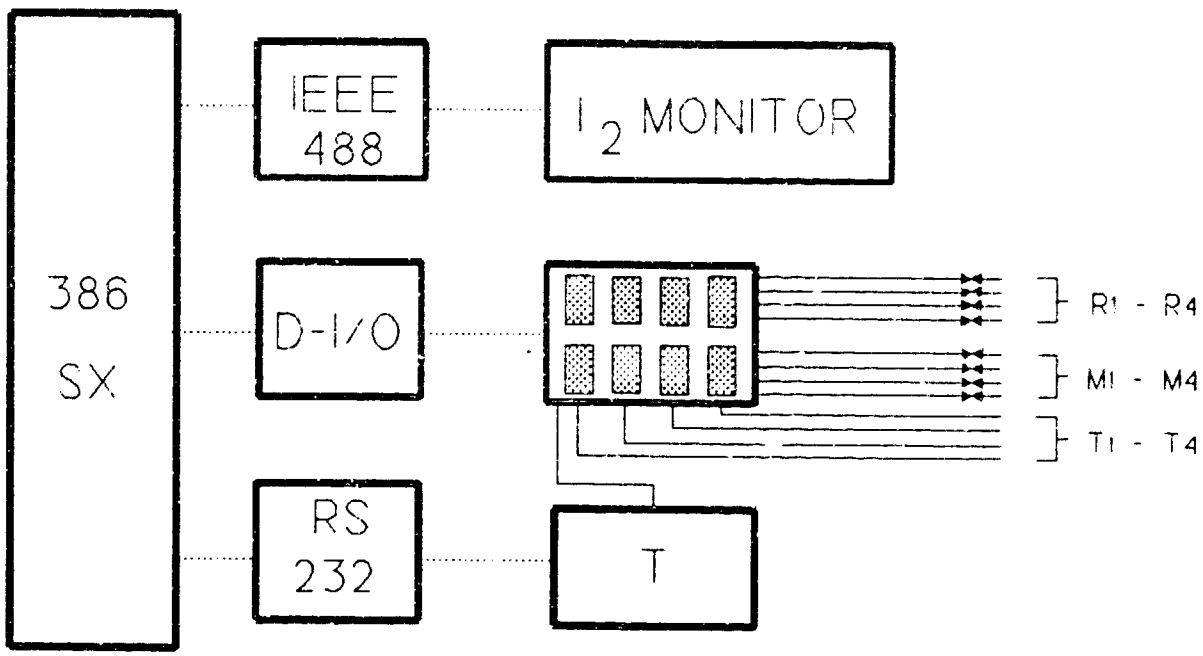

Figure 2.3 Schematic Illustration of RMCV Test Stand Control Architecture.

The HP 8452A diode array spectrophotometer is not a stand alone instrument. It was designed to operate only under computer control. In the analytical laboratory, the spectrophotometer is typically interfaced (parallel or serial) to an IBM compatible 80286 PC or better with a minimum of EGA graphics capability. Using HP proprietary software, the computer - spectrophotometer combination functions as a dedicated instrument.

For the purposes of using the diode array spectrophotometer as the RMCV test stand system iodine monitor, a different approach was required. As the HP control software does not have multi-tasking capability, and as our computer system was required to provide other monitoring and control functions beyond those necessary to serve the diode array spectrophotometer, fundamental spectrometric control subroutines were embedded in the system master control program RMCV.EXE. This master program was written using Microsoft QuickBasic Version 4.5, an enhanced and compiled version of the BASIC language. The use of this primitive programming language was necessitated by the availability of diode array spectrophotometer control function subroutines in this language only. A listing of the RMCV.BAS source code is included in Appendix I. System control of the iodine monitor is implemented via an IEEE-488 (HPIB, GPIB) parallel interface bus linking the 386 SX computer with the diode array spectrophotmeter. Use of the diode array spectrometer as the system iodine monitor is treated in extensive detail in Section 4.

Each of a maximum of four flowing RMCV effluent streams are sequentially routed to the system iodine monitor. Computer control of the four Teflon two-way valves responsible for flow switching through the iodine monitor is effected using an ACCESS model IOD-24 buffered 24-bit digital Input/Output (I/O) board. The I/O board occupies a single 16 bit site on the 386 SX motherboard. The digital I/O lines are routed to an externally mounted ACCESS model ROB-8 solid state relay board housing eight solid state relays, one for each test stand solenoid valve. Relays 1 - 4 (M1 - M4 in Figure 2.3) are responsible for multiplexing the four RMCV effluents to the system iodine monitor and correspond to ersatz

reclaimed potable water, ersatz reclaimed hygiene water, ersatz humidity condensate, and ersatz urine distillate RMCV effluents respectively. The chemistry of these four challenge streams is presented in Section 3. The architecture of the control program allows any combination of these four streams to be operated at a given time.

The temperatures measured by four type K thermocouples mounted to each MCV resin bed are also multiplexed using relays 1 - 4. The thermocouples are designated T1 - T4 and correspond to the temperatures of the RMCVs challenged with ersatz reclaimed potable water, ersatz reclaimed hygiene water, ersatz humidity condensate, and ersatz urine distillate challenge streams respectively. At the same time that a given relay switches RMCV effluent flow into the system iodine monitor, it also switches the appropriate thermocouple signal to the Newport model 269 - D1 digital thermocouple thermometer. The temperature is then transmitted via a serial RS-232C data transfer to the computer's COM 1 port.

Based upon the quantitative information obtained by the system iodine monitor, the computer also controls the MCV regeneration process. Regeneration events are invoked using the digital I/O board to control the solid state relays 5 - 8 (R1 - R4 in Figure 2.3) corresponding to ersatz reclaimed potable water, ersatz reclaimed hygiene water, ersatz humidity condensate, and ersatz urine distillate regeneration control valves respectively. Regeneration is invoked by applying power to the appropriate solenoid valve.

2.1.5 RMCV Influent Temperature Control Circuits.

The features of the RMCV test apparatus outlined above are common to each of the four circuits corresponding to the four designated MCV challenge streams. The ersatz urine distillate and ersatz humidity condensate streams present the additional requirement for temperature adjustment to approximately 26.7 ^{o}C and 1.7 ^{o}C respectively.

The cooling system used to produce 1.7 ^{o}C ersatz humidity condensate is shown schematically in Figure 2.4. Upstream of the RMCV control solenoid, ersatz humidity condensate is pumped through a series of stainless steel coils maintained at 1.7 ^{o}C in a 6 liter

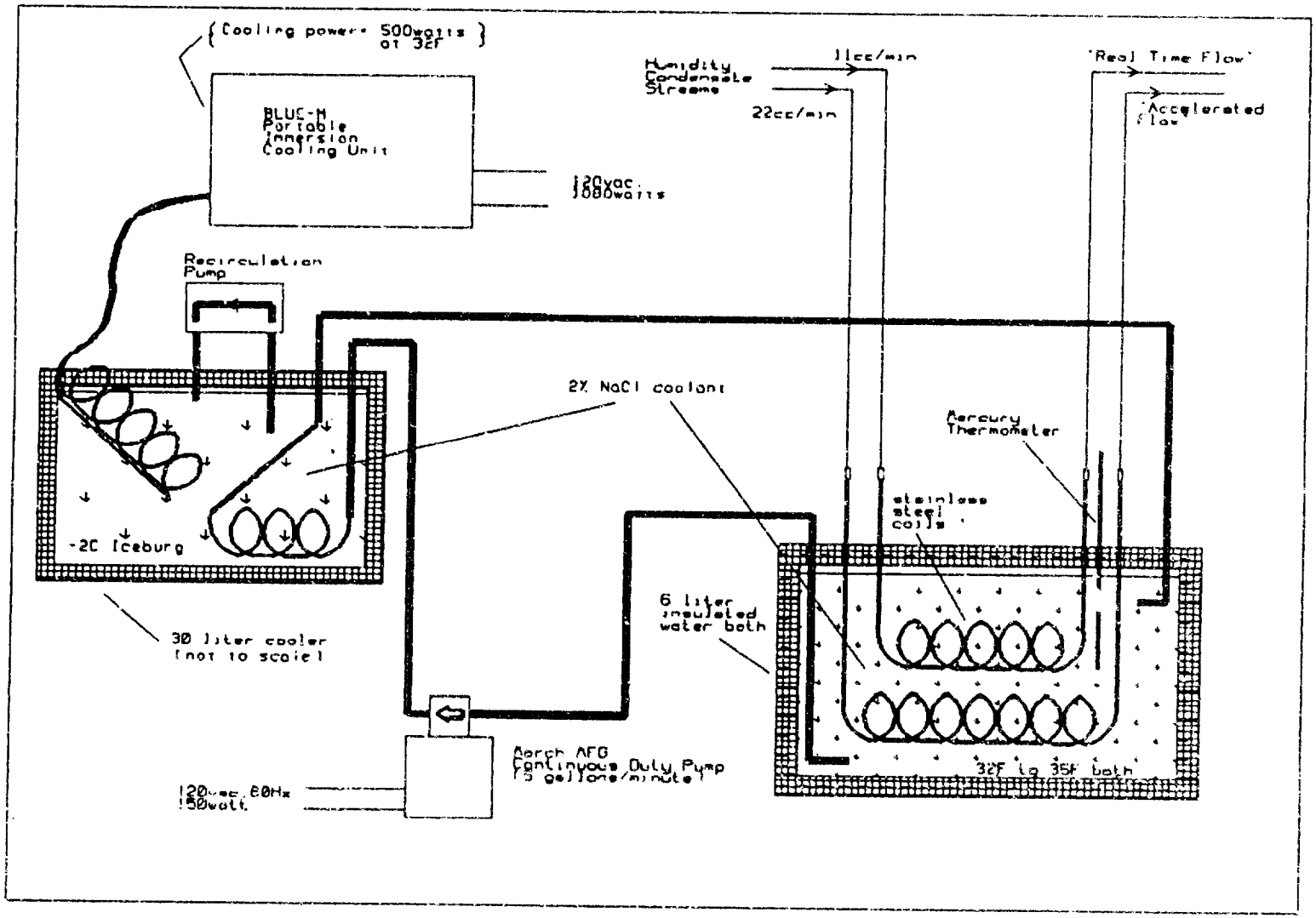

Figure 2.4 1.7 °C Temperature Control Sub-system

insulated water bath. A MARCH Mfg. model 1A-MD-1 continuous duty pump is used to recirculate water between the insulated water bath and a 30 liter coolant reservoir at a flow rate of approximately 3.8 L/min. The pump draws 0.45 A at 115 VAC and 50/60 Hz. The reservoir is maintained at -2 °C by a Blue-M model D-3115-O-C portable immersion cooling unit. The cooling unit consumes 1080 watts at 120 VAC and 50/60 Hz, and provides 500 watts of cooling power. Salt (NaCl) is added to the coolant water to depress the freezing point to the desired temperature. A MARCH Mfg. model AC-2CP-MD recirculating pump provides continuous flow of water in the liquid state across the cooling coils and the formed ice at approximately 20 L/min. This pump operates at 3000 rpm and is rated at 1.5 A for 115V AC and 50/60 Hz.. Temperature control is achieved through a feedback circuit to the immersion cooler from a K type thermocouple mounted within the cooling coils. Temperature of the primary cooling bath is further stabilized by an ice - water equilibrium at the freezing point, which directs minor thermal transients into phase changes, rather than temperature changes. The sub-system provides temperature stability of ± 1 °C .

The 26.7 °C ersatz urine distillate heating system is illustrated schematically in Figure 2.5. Upstream of the RMCV control solenoid, ersatz urine distillate is routed through a series of stainless steel coils maintained at 26.7 °C in a 6 liter capacity insulated water bath. Stainless steel coils are used to maximize heat transfer. A MARCH Mfg. model AC-2CP-MD continuous duty pump is used to recirculate water at approximately 20 L/min between the insulated bath and a 1.4 liter stainless steel cylinder wrapped with 209 watt heat tape. The temperature of the bath is monitored using a J - type immersion thermocouple, whose signal is fed to an OMEGA model CN-1200 Process Variable Controller which applies power to the heat tape, as required. The controller is set to maintain 26.7 °C in the bath. All electrical components of this sub-system operate using 120 VAC and 50/60 Hz line current. The sub-system provides temperature stability of ± 1 °C.

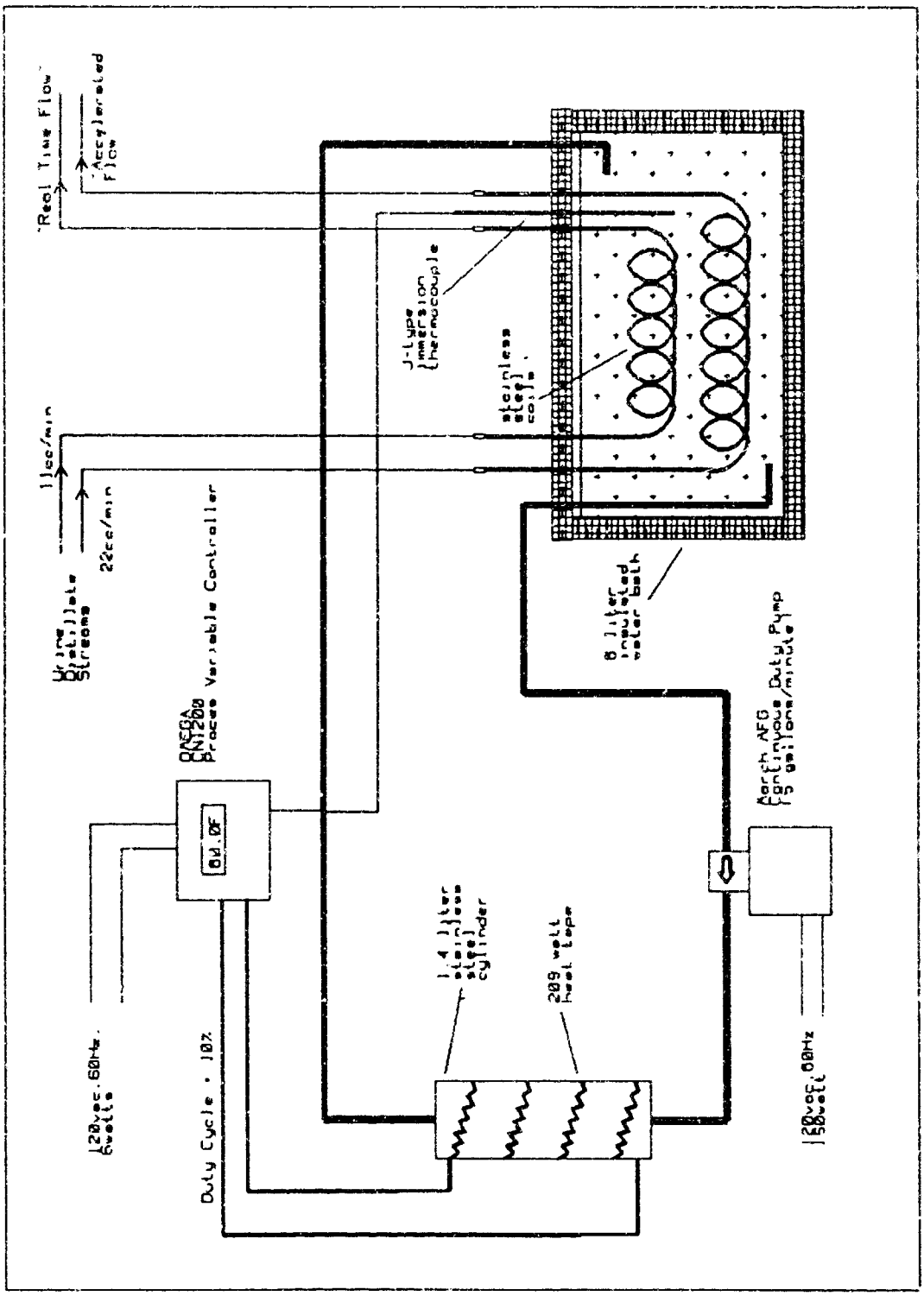

Figure 2.5 26.7 °C Temperature Control Sub-system

2.2 RMCV Test Stand Operation.

Challenge solutions are prepared within the 190 liter glass lined feed tanks from pre-made refrigerated concentrates. Newly made up RMCV feed tanks are mixed sequentially using a recirculating pump which draws from the bottoms and delivers to the tops of the storage tanks until uniform compositions are obtained.

Once the feed solutions are well mixed, flow through the RMCV circuits is established using the four channel peristaltic cartridge pump. For routine operation, flow rates in the range of 10 - 12 mL/min are set using a ten turn potentiometer. Flow rates are determined manually using a graduated cyclinder and a stopwatch. Prior to the initiation of computer control, with all solid state relays in the de-energized state, flow is routed directly to each MCV and the effluents are routed directly to waste. In this condition, both the solid state elemental iodine crystal regeneration beds and the system iodine monitor are bypassed.

Autonomous operation of the RMCV Test Stand is initiated by entering the IO directory on the C: partition of the fixed disk drive and invoking the RMCV program. The control program immediately sets all solid state relays to the power off condition and then prompts the user to fill the system iodine monitor flow-through cell with a deionized (DI) water blank. The blank spectrum thus obtained is subtracted by the diode array spectrophotometer from all subsequent spectra collected until the RMCV control program is terminated. The user is then prompted to enter whether or not (Y/N) each of the four RMCV challenge streams is flowing.

The control program routes the first RMCV effluent to the system iodine monitor by energizing the solid state relay controlling the appropriate Teflon® two-way valve. Normally the iodinated RMCV effluent flows through the quartz spectrophotomer cell for a twenty minute period prior to acquisition of the spectrum. This time span is necessary for the previous cell contents to be completely replaced. After twenty minutes, a spectrum is acquired, net absorbances at selected wavelengths are passed along the parallel interface to

the computer, and iodine values are calculated and stored on both the fixed disk, and for backup purposes on a 1.44 Mb floppy disk in the B: drive. If the elemental iodine values are 2.0 mg/L or greater the computer de-energizes the current relay and energizes the next relay in sequence, thus routing a new RMCV effluent to the system iodine monitor.

If the residual I_2 level falls below 2.0 mg/L, the flow of that particular RMCV effluent stream is maintained to the system iodine monitor and regeneration is invoked by energizing the appropriate stainless steel two-way valve via digital output to the corresponding solid state relay. During regeneration, spectra are acquired at five minute intervals. Flow through the iodine monitor does not index to the next sequential RMCV effluent until the regeneration event is terminated. Thus only one RMCV can undergo regeneration at a time. Criteria for termination of regeneration, used in the small column scale RMCV test stands involve both preset times and effluent iodine concentration levels and will be discussed in more detail in Sections 5 and 6 of this report covering long term life cycle testing and parametric testing respectively.

The sequence of events is portrayed on the system VGA color monitor where a graph representing each of the four RMCV circuits is displayed. On each graph a time series of iodine monitor test results is presented as a histogram. In this representation, the height of each bar indicates the total concentration of iodine species in mg/L. The lower most purple region of the bar indicates the concentration of elemental iodine. Located above this region is a blue colored area whose height indicates approximate iodide concentration. The status of each of the eight solid state relays is also indicated on the VGA screen by color. Red indicates that the relay and the corresponding solenoid valve are energized. A green color indicates that the relay is not energized. These colors correspond to the colors emmitted by status indicating LEDs mounted beside the solid state relays on the ROB-8 circuit board. The computer screen also indicates both the current time and the time of last spectral acquisition.

A black and white facsimile of a typical RMCV long term life cycle test stand color

VGA monitor display is shown in Figure 2.6. Clockwise, begining with the upper left hand corner, the graphs represent RMCV 1 - ersatz reclaimed potable water, RMCV 2 - ersatz reclaimed hygiene water, RMCV 3 - ersatz humidity condensate, and RMCV 4 - ersatz urine distillate. In this example the potable water stream is washing out from approximately 4 mg/L I_2 to 3.4 mg/l; the reclaimed hygiene water stream is washing out from 4 mg/L - 3.2 mg/L; the humidity condensate stream is oscillating between 2.3 - 3.0 mg/l; and the urine distillate stream is dropping from 3.3 - 2.8 mg/L.

A regeneration event for the humidity condensate stream is shown in Figure 2.7. In this display the large gaps in the graphs for RMCVs 1, 2, and 4 are attributable to the regeneration of RMCV 3 challenged with ersatz humidity condensate. The system iodine monitor follows the entire course of the MCV regeneration, during which the sampling periodicity is increased to once every five minutes. The elemental iodine concentrations can be seen to rise from 7.2 mg/L to > 10 mg/L over the course of the regeneration. It is also evident that once regeneration terminates, normal washout begins with residual I_2 levels of approximately 4 mg/L.

The systems are normally operated continuously until the challenge stream feed tanks are depleted, at which time the systems are shut down for routine maintenance. Quadratic calibration coefficients for calculation of iodine and iodide values in any of the RMCV effluent matrices can be changed while autonomous operation continues via keyboard commands. The time interval between sampling events can also be changed via keyboard entry.

During the approximate eighteen month operational history of the Test Stand dedicated to the long term RMCV life cycle tests, the system has proven to be surprisingly robust. The most frequent cause of loss of autonomous control has been due to rare transient interuptions in laboratory power causing program execution to cease. In such cases, flows to the RMCVs are re-established as soon as power returns, but control functions remain suspended until the computers are manually re-booted and the control programs are restarted.

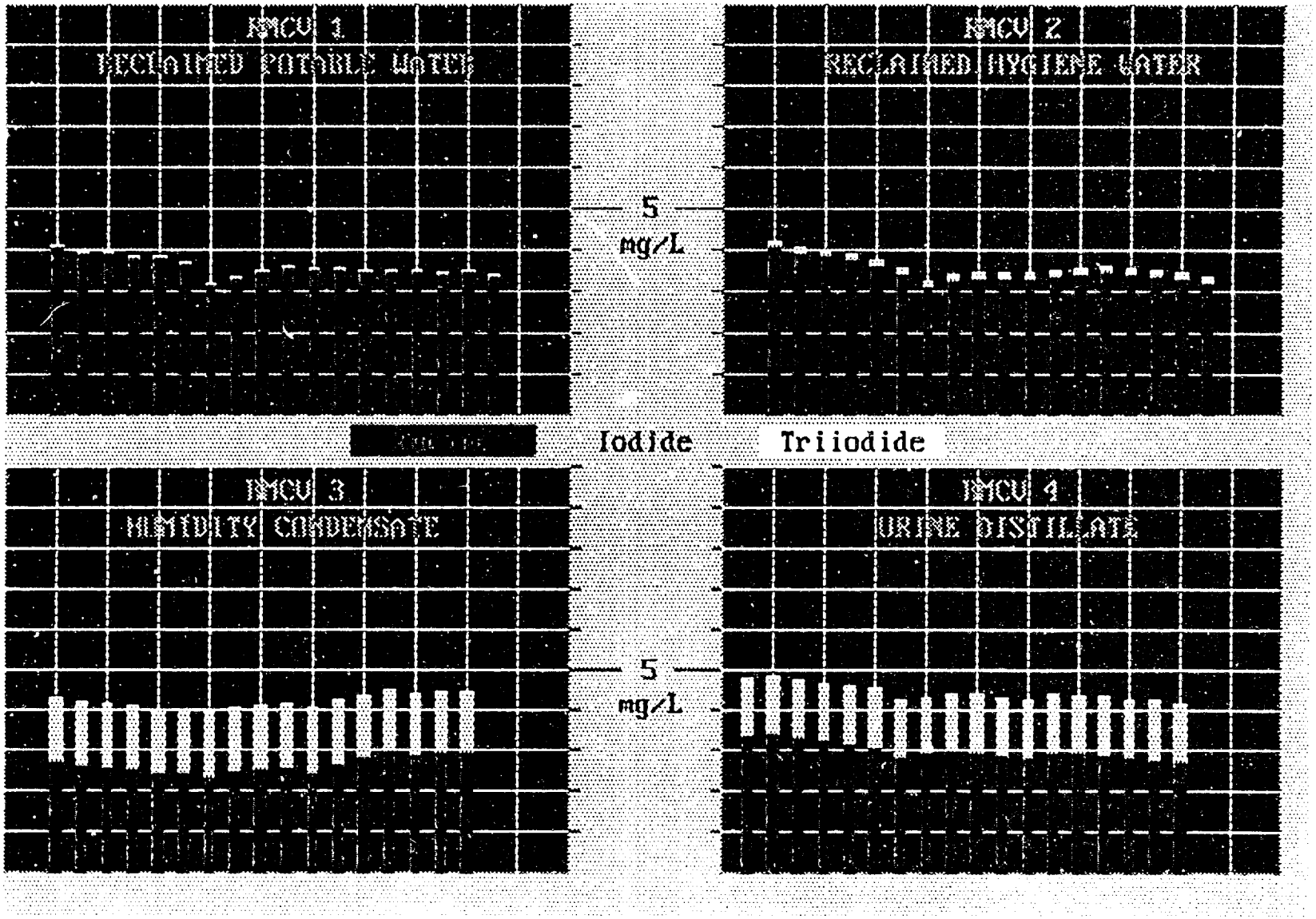

Figure 2.6 Black and White Facsimile of RMCV Test Stand Color VGA Screen - Washout Mode

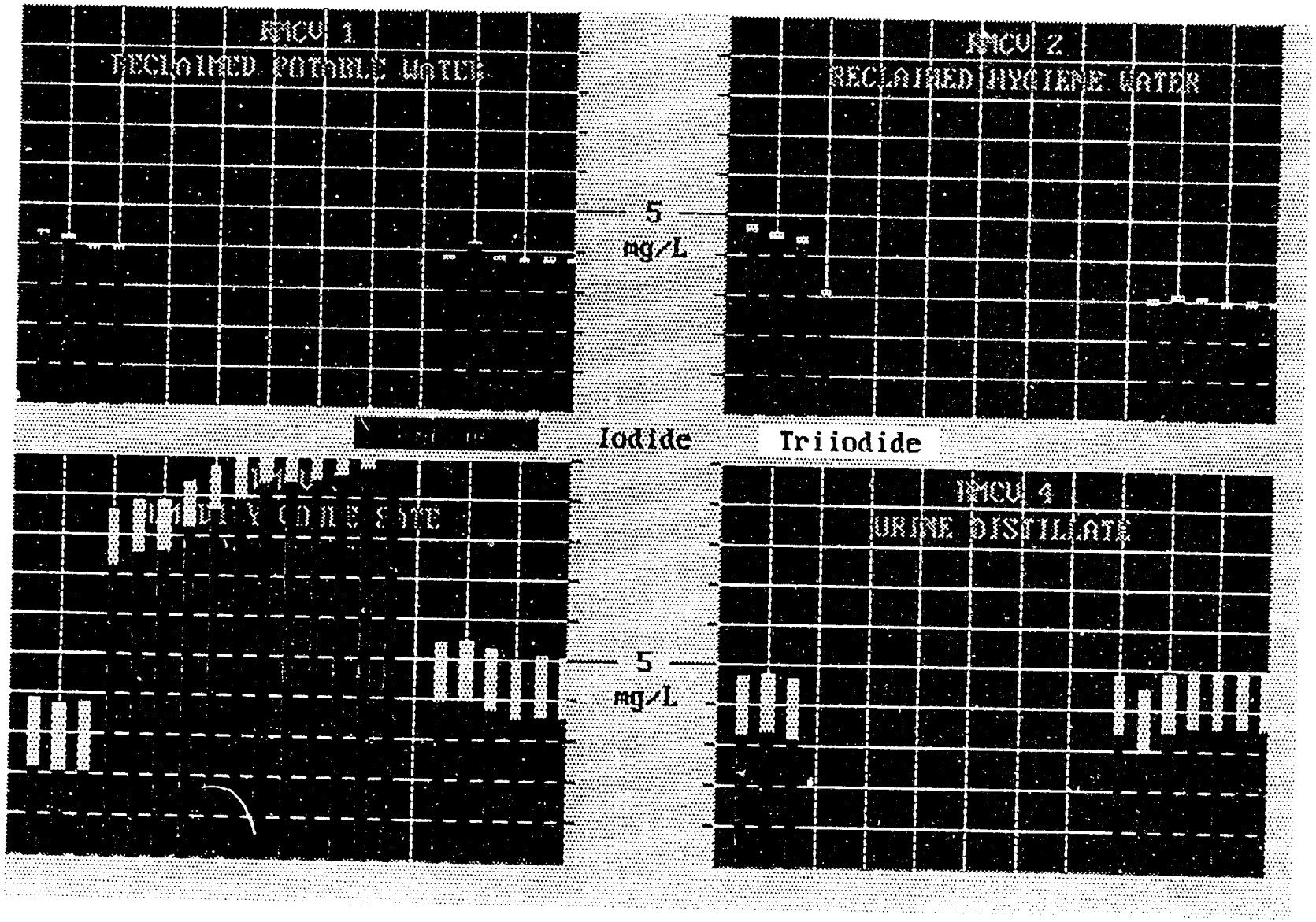

Figure 2.7 Black and White Facsimile of RMCV Test Stand Color VGA Screen - with Regeneration

One solid state relay, one stainless steel valve, and two Teflon valves have been replaced. Two of the recirculating pumps in the 1.7 °C temperature control sub-system have been replaced. Tubing through the Masterflex pump cartridges has required replacement at approximate six week intervals to maintain desired flowrates. Glass wool plugs at the inflow faces of both the MCVs and the iodine crystal regeneration beds have plugged with particulate matter requiring replacement to prevent the build up of unacceptably high pressures. Routine maintenance during shutdowns primarily involves tightening of the various fittings and tubing connections to prevent leaks.

3

CHEMISTRY of the RMCV CHALLENGE SOLUTIONS

3.0 Overview.

A prime objective of the RMCV development activity was to characterize the system response when challenged with a range of influent contaminant streams, varying in chemical composition between the pure water ideal case and significantly contaminated waters representative of streams from reclamation processes encountered in closed loop regenerative life support systems. The four challenge streams selected were: ersatz reclaimed potable water, ersatz reclaimed hygiene water, ersatz humidity condensate, and ersatz urine distillate. The chemical compositions are outlined below.

3.1 Ersatz Reclaimed Potable Water.

Laboratory grade deionized water was selected as reasonably representative of reclaimed waters suitable for human consumption. The deionized (DI) water used in this study was prepared from tap water by treatment with Culligan mixed bed ion exchangers and sorption/filtration media. The laboratory DI water ranges typically between pH 5.5 and pH 7.0, exhibits conductivities between 0.1 µS/cm and 5.0 µS/cm, and contains Total Organic Carbon (TOC) ≤ 1.0 mg/L and Total Inorganic Carbon (TIC) ≅ 0.5 mg/L. Chloroform, resulting from chlorination of the public drinking water supply, is the only trace organic substance which has been identified. Chloroform typically occurs at levels ≅ 0.5 µg/L. The water has been tested for all EPA regulated drinking water contaminants, including the fifty-nine Method 502.2 volatile organic chemicals[419], with chloroform being the only organic analyte detected. Microflora are typically present in the DI water at levels ranging between $5 \times 10^4 - 2 \times 10^5$ CFU/mL and consist predominately of *Pseudomonas pickettii*.

3.2 Ersatz Reclaimed Hygiene Water.

The composition of this challenge stream represents water which has been sufficiently

purified for use as shower or wash water but insufficiently purified for human consumption. Routine make-up was achieved using concentrates dissolved in DI water, diluted to volume inside the RMCV feed tank with DI water, and mixed with a recirculating pump. Bacterial counts for this challenge stream ranged between 1.5×10^3 - 1.9×10^4 CFU/cm^3.

Contaminant	Structure	mg/L	TOC mg/L
Urea	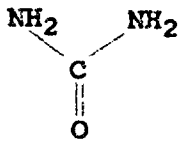	12.5	2.50
Ethanol		2.0	1.04
Acetone	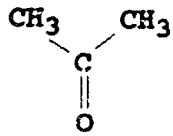	2.0	1.24
Sodium Chloride	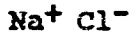	1.0	0
		$\Sigma = 17.5$	$\Sigma = 4.78$

3.3 Ersatz Humidity Condensate.

The chemical composition of the humidity condensate model used throughout this study represents a collection of known and suspected humidity condensate constituents in relatively high concentrations for the purpose of rigorously challenging ion exchange media. To this end, the chemical compositon of the subject model is heavily weighted toward ionic or ionizable substances in contrast to ersatz humidity condensate models designed to challenge other processes such as catalytic oxidation[1]. The model is a simplification of the humidity condensate model designed to challenge multifiltration UNIBEDs for Space Station *Freedom*, prior to unification of the water reclamation streams. The model was simplified by the

elimination of trace contaminants occuring at levels less than 1 mg/L and by the elimination of thiourea. Routine make-up was achieved using concentrates dissolved in DI water, diluted to volume inside the RMCV feed tank with DI water, and mixed with a recirculating pump. Microbial counts in this challenge stream ranged between < 10 - 3.4 x 10^4 CFU/cm^3. The chemical composition is given below.

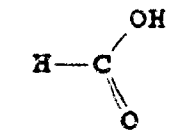

Formic Acid 115 mg/L (30.01 mg/L as TOC)

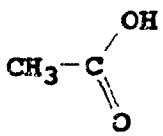

Acetic Acid 75 mg/L (30.00 mg/L as TOC)

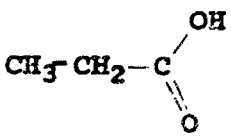

Propionic Acid 62 mg/L (30.16 mg/L as TOC)

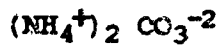

Ammonium Carbonate 35 mg/L (0.0 mg/L as TOC)

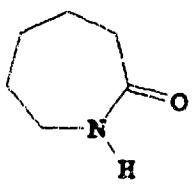

Caprolactam 24 mg/L (16.78 mg/L as TOC)

Ethanol 5 mg/L (2.61 mg/L as TOC)

Ersatz Humidity Condensate Continued

Methanol 5 mg/L (1.87 mg/L as TOC)

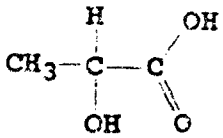

Lactic Acid 5 mg/L (2.00 mg/L as TOC)

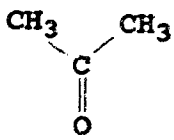

Acetone 3 mg/L (1.86 mg/L as TOC)

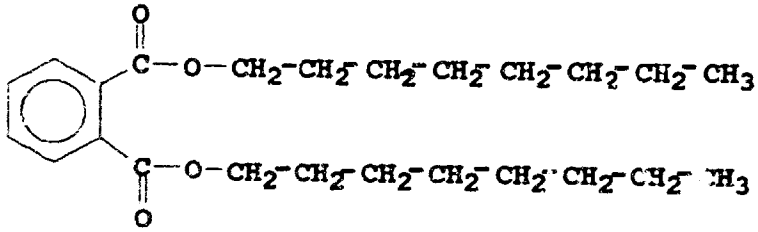

Dioctylphthalate 3 mg/L (2.21 mg/L as TOC)

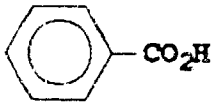

Benzoic Acid 3 mg/L (2.07 mg/L as TOC)

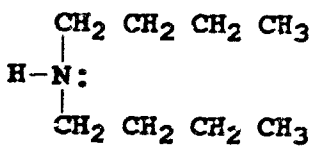

Di-n-butylamine 2 mg/L (1.49 mg/L as TOC)

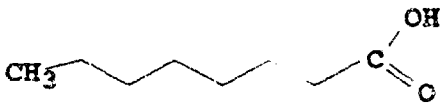

Caprylic Acid 2 mg/L (1.33 mg/L as TOC)
(Octanoic)

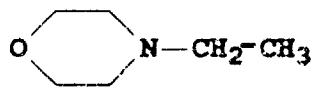

N-ethyl morpholine 2 mg/L (1.25 mg/L as TOC)

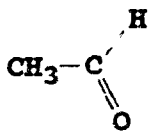

Acetaldehyde 2 mg/L (1.09 mg/L as TOC)

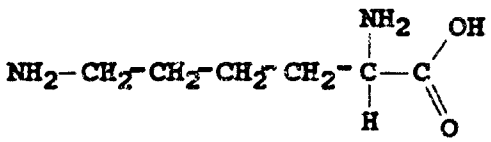

Lysine 2.0 mg/L (0.99 mg/L as TOC)

Σ = 345 mg/L Σ = 123.72 mg/L TOC

3.4 Ersatz Urine Distillate.

The ersatz urine distillate challenge stream represents an assemblage of possible contaminants in relatively high concentrations. Routine make-up was achieved using concentrates dissolved in DI water, diluted to volume inside the RMCV feed tank with DI water, and mixed with a recirculating pump. Microbial populations in this challenge stream

ranged between 5.0 x 10^2 - 6.0 x 10^4 CFU/cm^3. The chemical composition follows.

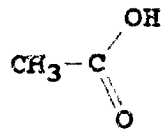

Acetic Acid	30 mg/L	(12.00 mg/L as TOC)

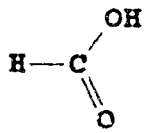

Formic Acid	10 mg/L	(2.60 mg/L as TOC)

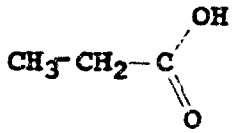

Propionic Acid	10 mg/L	(4.86 mg/L as TOC)

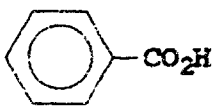

Benzoic Acid	2.0 mg/L	(1.38 mg/L as TOC)

Ethanol	2.0 mg/L	(1.04 mg/L as TOC)

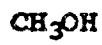

Methanol	1.0 mg/L	(0.37 mg/L as TOC)

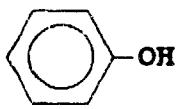

Phenol	0.6 mg/L	(0.46 mg/L as TOC)
	Σ = 55.6 mg/L	Σ = 22.71 mg/L TOC

4

THE DIODE ARRAY SPECTROPHOTOMETER as RMCV TEST STAND ON-LINE IODINE MONITOR

4.0 Overview.

Absorbance in the 460 nm region of the visible spectrum has been used extensively for the determination of aqueous elemental iodine[6,19,74,374-376], and was used successfully to monitor iodine levels near the solubility limit in the Phase I increment of the RMCV development effort[90,222]. An on-line I_2 monitor using absorbance at 466 nm was developed by Walsh et al[34,427]. The iodine bench, currently under development by Astro International Corporation as a component of the Space Station *Freedom* Process Control Water Quality Monitor (PCWQM), uses absorbance at 470 nm to quantify I_2 levels in an aqueous stream flowing at a nominal 120 cm^3/min[12,13,116,215,216]. Building upon this foundation, UV-visible absorbance spectrophotometry was selected as the analytical method of choice for incorporation into the autonomous RMCV test stands.

The HP model 8452A diode array spectrophotometer has several features which make it an attractive choice for applications such as the small column scale RMCV test stand on-line iodine monitors. Among these are: the wide dynamic wavelength (λ) range from 190 nm in the ultraviolet (UV) through the visible (VIS) region of the spectrum to 820 nm in near infrared (IR); the rapid rate of spectral acquisition; minimization of moving parts required for operation of the instrument (in contrast to scanning UV-VIS instruments); and the relative ease with which the instrument can be integrated as a component into a larger computer controlled system.

For this study three sample cells with optical path lengths of 1 cm, 5 cm and 10 cm were used. The 1 cm path length cell used is a conventional HP 89062A square 80µL flow-through cuvette. The 5 cm and 10 cm cells are both UV grade quartz cylinders with Teflon PTFE stoppers. These two cells differ only in their lengths along the horizontal axis. Holes have been drilled through the Teflon stoppers at each end, through which Teflon tubing has been inserted as the source of influent from the RMCVs and as the conduit for effluent to

waste, in the flow-through configuration.

4.1 Diode Array Spectrophotometer Quantitative Methodology.

An absorbance (A) spectrum of 0.4 mg/L aqueous iodide (I^-), acquired using a 10 cm path length cell, is shown in Figure 4.1. Sharp absorbance maxima are evident at λ = 196 nm and λ = 228 nm. Figure 4.2 presents the spectrum of 2.0 mg/L aqueous elemental iodine (I_2) also acquired using a 10 cm path length cell. In the full scale representation of 4.2a the absorbance maximum at λ = 204 nm is shown. Below, in the expanded scale depiction presented as Figure 4.2b, two additional maxima at λ = 270 nm and λ = 460 nm are evident.

The situation becomes more complex when a mixed iodine-iodide spectrum is examined. Figure 4.3 presents the spectrum of 4.0 mg/L I_2 in the presence of 2.0 mg/L I^-. In the full scale spectrum shown in 4.3a it can be seen that the absorption regions for I_2, with a maximum at λ = 204 nm, and the absorption regions for I^-, with a maximum at λ = 228 nm, overlap and fuse into a single asymmetric absorption region from which quantitative information about either species cannot be easily extracted.

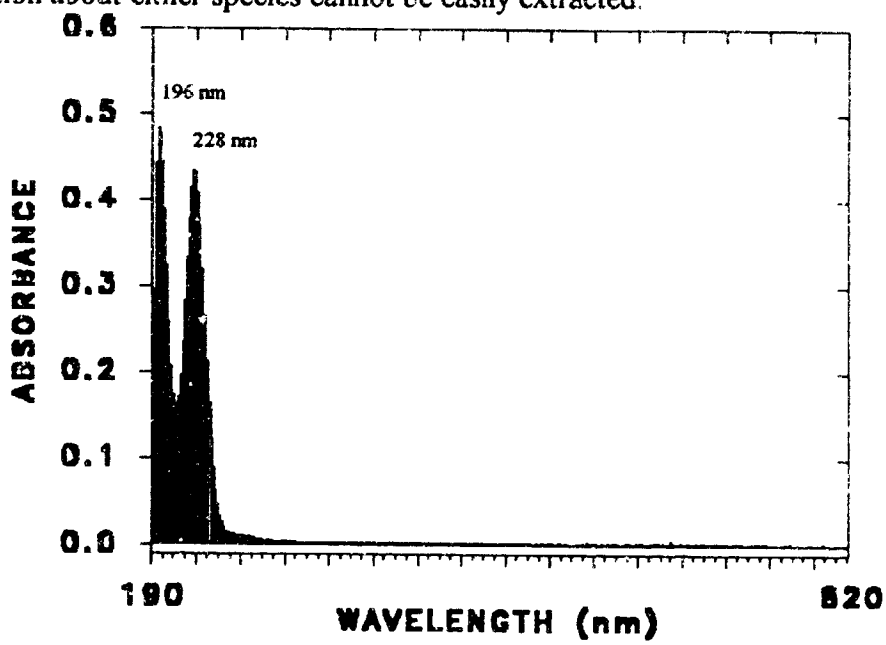

Figure 4.1 UV-VIS Spectrum of 0.4 mg/L I^- in DI Water.

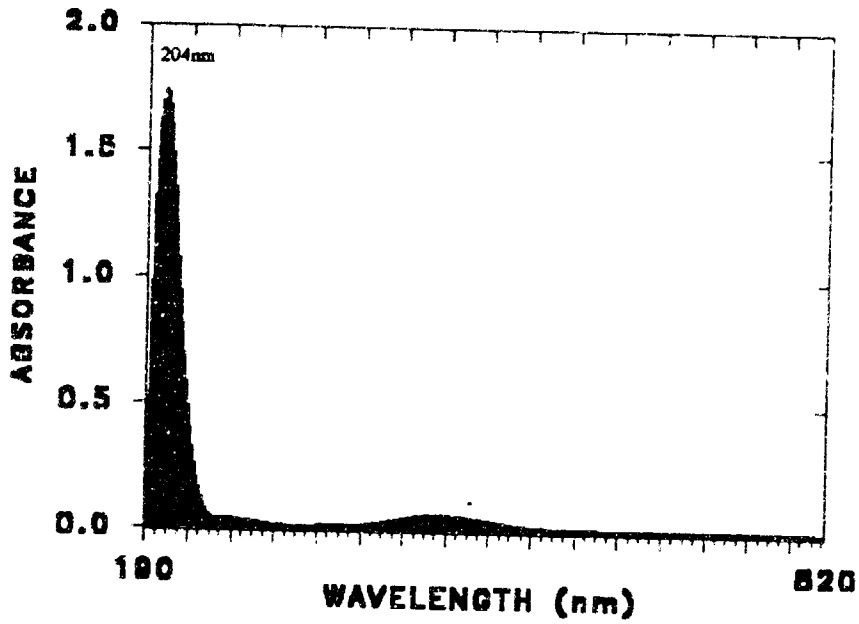

a) Full Scale Spectrum

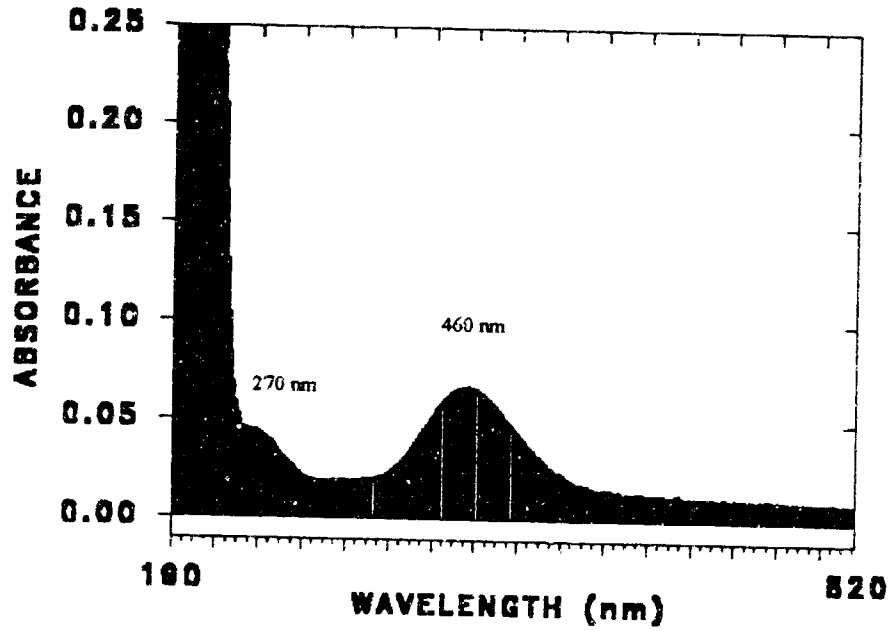

b) Expanded Scale Spectrum

Figure 4.2 UV-VIS Spectrum of 2.0 mg/L I_2 in DI Water

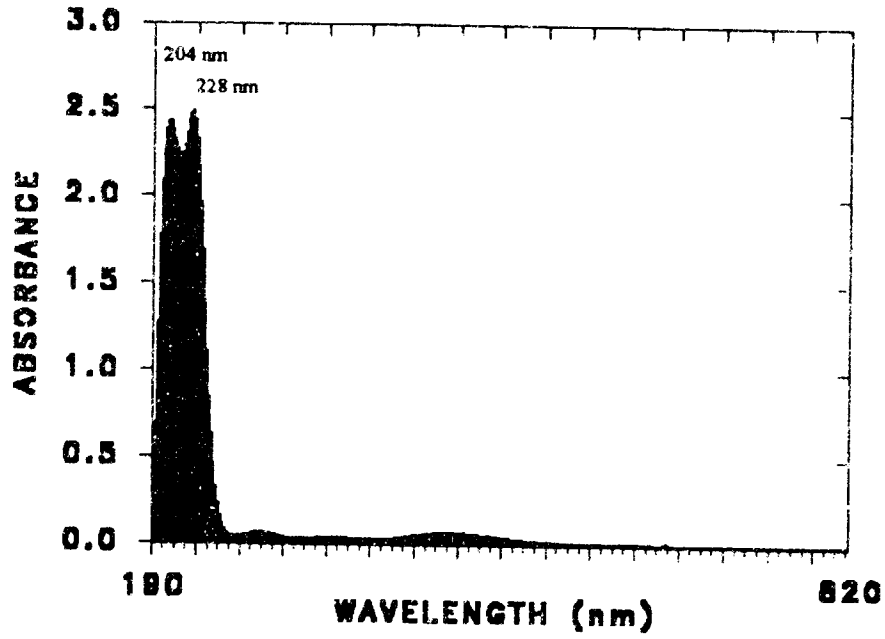

a) Full Scale Spectrum

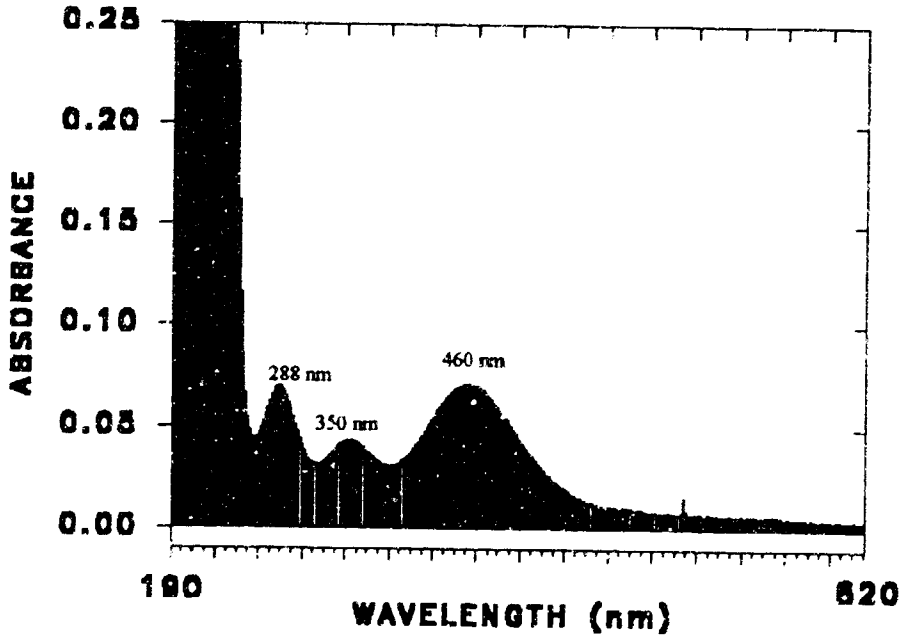

b) Expanded Scale Spectrum

Figure 4.3 UV - VIS spectrum of 2.0 mg/L I^-, 4.0 mg/L I_2 in DI Water.

The expanded scale spectrum for this mixture, shown in 4.3b, reveals poor resolution of the relative maximum at λ = 270 nm attrubutable to I_2. Examination of longer wavelengths reveals two new relative maxima in the high ultraviolet at λ = 288 and λ = 350 nmAbsorbance in these regions is due to the presence of the triiodide (I_3^-) anion formed by the equilibrium reaction between elemental iodine and the iodide anion,

$$I_2 + I^- \Leftrightarrow I_3^- \qquad K_{eq} = \frac{[I_3^-]}{[I_2][I^-]} = 710.$$

Further upscale in the visible spectral region is the λ = 460 nm relative I_2 absorbance maximum which remains well resolved but rests upon an elevated baseline resulting from the presence of I^- in the mixture.

Spectra of non-iodinated matrix blanks corresponding to the four RMCV challenge solutions are given in Figure 4.4. The DI water spectrum of Figure 4.4a, representing the ersatz reclaimed potable water matrix, is featureless. This is because the spectrophotometer is routinely zeroed using a DI water blank. Some slight spectral features can be seen in the ersatz reclaimed hygiene water matrix as shown in Figure 4.4b. Very strong spectral features, dominated by marked absorbance in the UV region between 200 nm - 230 nm, are characteristic of the ersatz humidity condensate matrix shown in Figure 4.4c. To a somewhat lesser extent, similar features are evident in the ersatz urine distillate matrix spectrum given in Figure 4.4d.

Through a series of hasty calibration experiments, it became clear that the disparate matrix absorbance characteristics of the four RMCV challenge streams under investigation required that four separate calibrations of the diode array spectrophotometer be undertaken, one for each subject matrix. It was also determined that the method of Burger and Liebhafsky[74] as applied by Schultz et al.[374-376] was not practical for the on-line monitoring requirments of the RMCV test program. In this method absorbances at wavelengths of 288

nm, 350 nm and 460 nm are measured, I_2 and I_3^- concentrations are calculated by simultaneous solution of a system of linear equations, and I^- concentration is determined indirectly from the equilibrium expression using the calculated I_2 and I_3^- levels. While an excellent method for aqueous streams such as DI water in which the iodinated species are the primary contaminants absorbing in the 200 nm - 600 nm λ region, the method presents too manydifficulties in terms of maintaining separate calibrations for each of the four subject matrices, particularly in light of the then unknown effects of long term instrument drift and other factors attributable to prolonged periods of unattended continuous operation.

Instead, it was decided to use an adaptation of the methods used by Walsh et al.[424] and by Dougherty et al.[116] for long term continuous iodine monitoring in a flow-through situation, namely monitoring the absorbance in the 460 nm region relative to the baseline at longer wavelengths, to correct for matrix effects and to correct for the effects of the presence of variable quantities of I^-. In addition to this, we found that an approximate iodide value can be obtained using the 228 nm λ region calibrated for both I_2 and I^-. By using the known I_2 concentration derived from the 460 nm wavelength, the absorbance attributable to I_2 at 228 nm can be subtracted. The resulting difference between the corrected absorbance at this wavelength and that of the pure non-iodinated matrix blank is then attributable to the presence of I^-. At the low mg/L iodine concentrations of interest to the RMCV development program, I_3^- values are extremely low and can be ignored.

For the purposes of practicality and also for the purposes of facilitating direct comparison of iodine data generated in the RMCV development work with the historical body of MCV related iodine data, it was decided to adopt the iodine speciation convention implicit to the leuco-crystal violet (LCV) colorimetric analytical methodology[85]. In this technique, I_2 concentration is determined directly, and total I concentration is determined after oxidation by oxone. I^- concentration is calculated as the difference between total I and I_2. The results obtained in this way are not strictly correct as both I_2 and I^- concentrations are equally

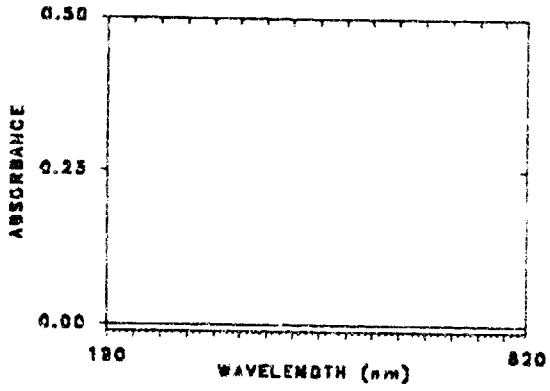

a) Ersatz Reclaimed Potable Water

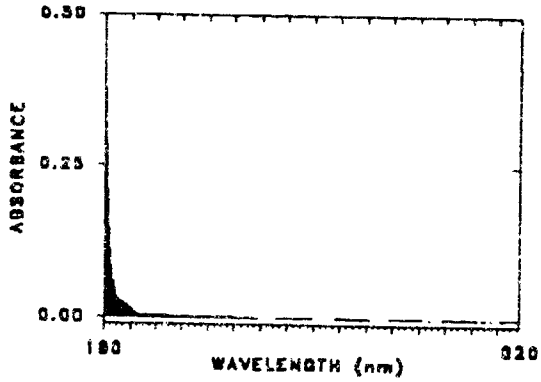

b) Ersatz Reclaimed Hygiene Water

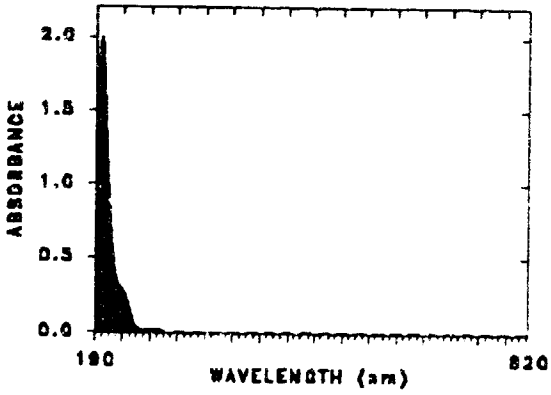

c) Ersatz Humidity Condensate

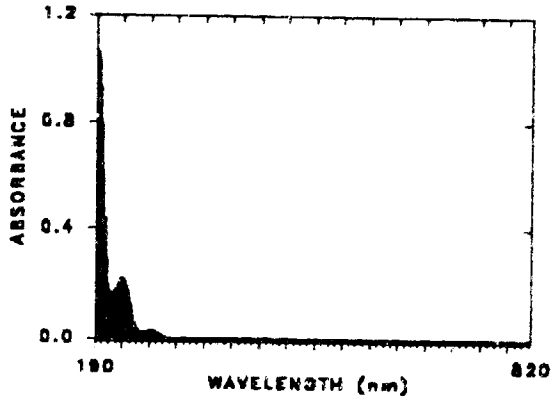

d) Ersatz Urine Distillate

Figure 4.4 UV-VIS Spectra of RMCV Challenge Solution Matrices.

diminished on a molar basis by the amount of I_3^- present. Also, this approach ignores the effects of hydrolytic disproportionation reactions resulting in the formation of other aqueous iodine species such as hypoiodous acid (HOI) and iodate (IO_3^-).

Both the kinetics and equilibrium of these hydrolysis reactions are examined in detail in Section 7 of this report. The results indicate that, at the pHs of the challenge solutions, and considering the elapsed times between addition of I_2 to the challenge streams at the MCVs and the analyses at the diode array spectrophotometer, the errors introduced by failure to consider other aqueous iodine species are not significant.

4.2 Calibration.

Each of the diode array spectrometers were calibrated prior to initiation of on-line monitoring. Once continuous operations had been initated, periodic calibration checks by the LCV colorimetric method were used to maintain calibrations during periods of uninterrupted operation. The frequency of calibration checks varied between daily and bi-weekly, with the frequency diminishing with time. The RMCV.EXE program was designed to accomodate on-line entry of quadratic recalibration factors for each of the four RMCV challenge streams without interruption of the autonomous test stand operation.

Initial calibrations of the diode array spectrometer were conducted using series of iodinated matrix solution standards spanning the absorbance range of the instrument for sample cells of 1 cm, 5 cm and 10 cm path-lengths. The aqueous standards were prepared from a refrigerated 1,000 mg/L I_2 stock solution in absolute ethanol. The stock solution was prepared using re-sublimed crystalline elemental iodine. The stability of this stock solution was confirmed by periodic LCV colorimetric analyses and further confirmed by thiosulfate titrations.

The resulting values for concentration versus absorbance ordered pairs were fitted to polynomials of appropriate degree by the method of least squares (L_2) and the goodness of fit

judged by the correlation coefficient (r^2)[384]. The calibration coefficients thus derived were then embedded in software controlling the appropriate RMCV test stand.

Experience in our laboratory has shown that at least some denatured ethanolic I_2 solutions are unstable. Such is the case when methyl-isobutyl-ketone (MIBK) is used as a denaturant. I_2 concentrations made up using this type of denatured ethanol rapidly decay by:

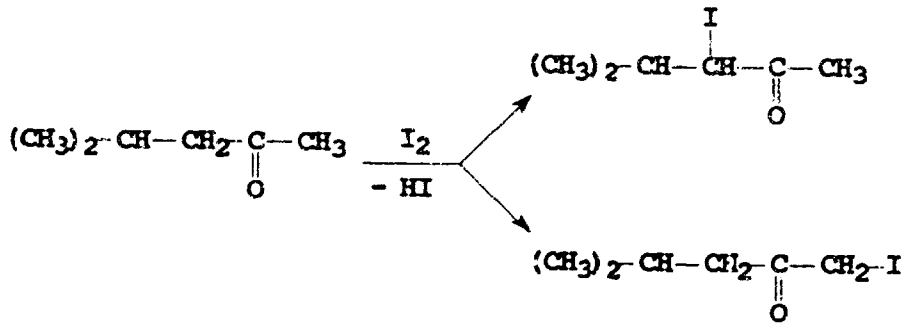

(Eqn. 4.1)

This problem is easily avoided by the use of absolute ethanol.

4.2.1 Ersatz Reclaimed Potable Water

The initial calibration experiments were carried out in DI water, representing the ersatz reclaimed potable water RMCV challenge stream. It was determined that for our system λ = 464 nm, 4 nm upscale from the absorbance maximum, was most suitable for monitoring aqueous I_2 concentrations. This finding is in close but not exact agreement with a previous study which concluded that the 466 nm wavelength was optimal[424].

The series of spectra acquired for calibration of the 1 cm path-length cell and the resulting calibration curve are shown in Figures 4.5a and 4.5b respectively. The calibration curve is linear for the concentration range between of 0 - 200 mg/L and yields an r^2 value of 0.9989 indicating good correlation. Similar spectra and calibration curves for the 10 cm path-length cell are given in Figure 4.6.

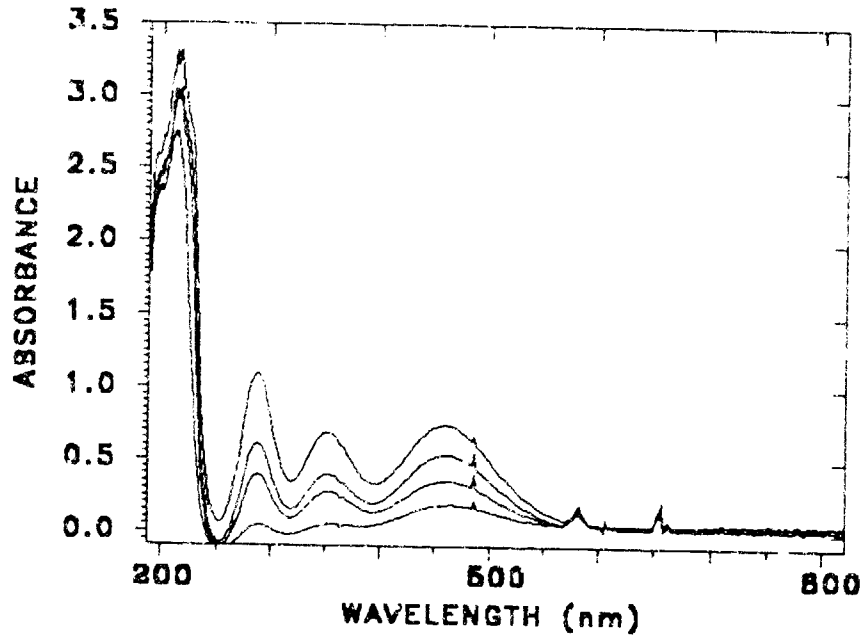

a) Calibration Spectra

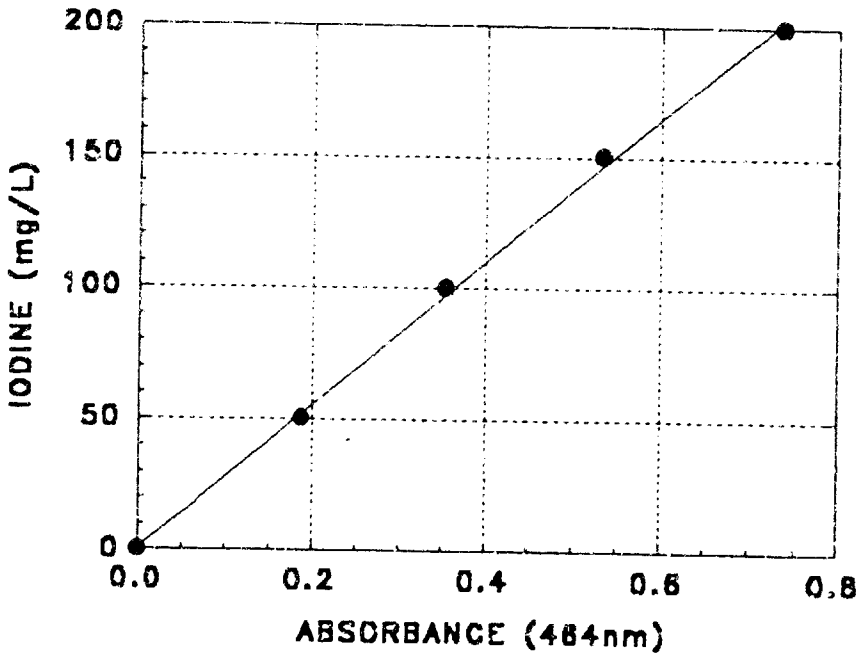

b) Calibration Curve - $[I_2]$ mg/L= 273.8 (A_{464} - A_{600}) + 0.44

r^2 = 0.9989

Figure 4.5 Calibration of 1 cm Path-length Cell in DI Water

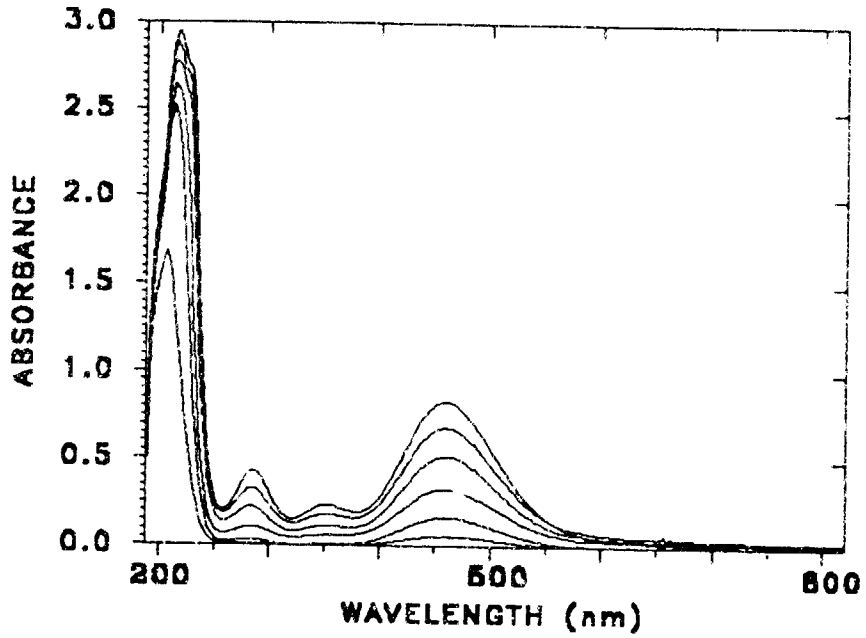

a) Calibration Spectra

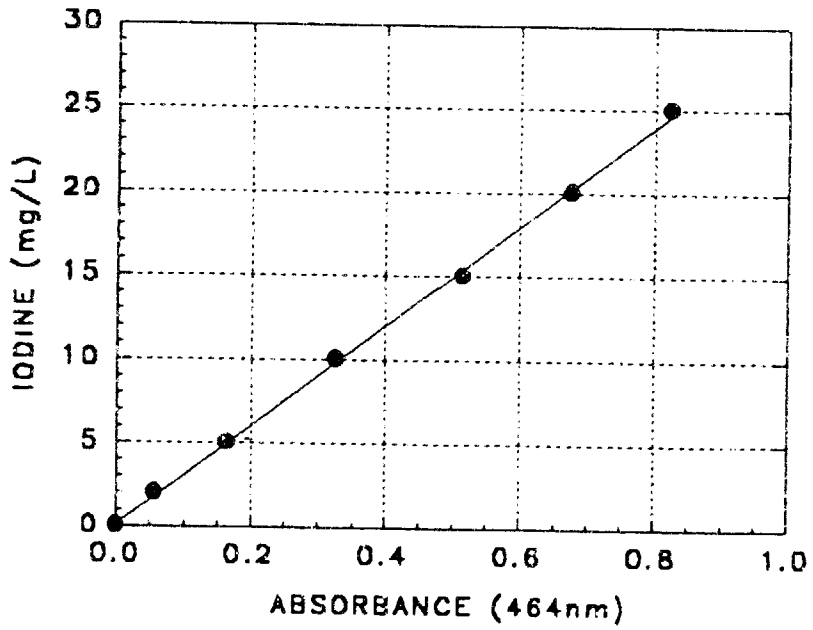

b) Calibration Curve - $[I_2]$ mg/L= 29.74 (A_{464} - A_{600}) + 0.09

$r^2 = 0.9991$

Figure 4.6 Calibration of 10 cm Path-length Cell in DI Water

4.2.2 Ersatz Reclaimed Hygiene Water.

The situation becomes somewhat more complex when matrices other than DI water are analyzed because the diode array spectrophotometer can only be zeroed with a single instrument blank. All subsequent measurements made by the instrument are relative to this initial instrument blank. In situations in which the spectrophotometer must quantify I_2 levels in multiple matrices, DI water is the obvious choice for the instrument blank. However, in cases such as with certain parametric tests or kinetics experiments in which only a single matrix is to be monitored, it is desirable to use the subject matrix to zero the instrument Spectra and resulting I_2 calibration curves for the 10 cm path-length cell are shown in Figures 4.7 and 4.8 for measurements made against a DI water and an ersatz reclaimed hygiene water instrument blank respectively.

4.2.3 Ersatz Humidity Condensate.

As the most chemically diverse of the RMCV challenge streams, this matrix exhibits the most intense and complex UV-VIS absorption spectrum. Correspondingly, the spectra collected using a DI water instrument blank are dramatically different from those collected against the matrix instrument blank in the $\lambda \leq 200$ nm region. Calibrations for the 1 cm pathlength cell are shown in Figures 4.9 and 4.10 against a DI water and the matrix blank respectively. Calibration of the 5 cm path-length cell against a matrix instrument blank is illustrated in Figure 4.11. Figures 4.12 and 4.13 represent the calibrations of the 10 cm path length cell using a DI water blank and a matrix blank respectively.

4.2.4 Ersatz Urine Distillate.

The contrasts between spectra collected with DI water and matrix instrument blanks for the ersatz urine distillate RMCV challenge stream are similar in scope to those of the ersatz humidity condensate matrix, and more pronounced than those of the two other

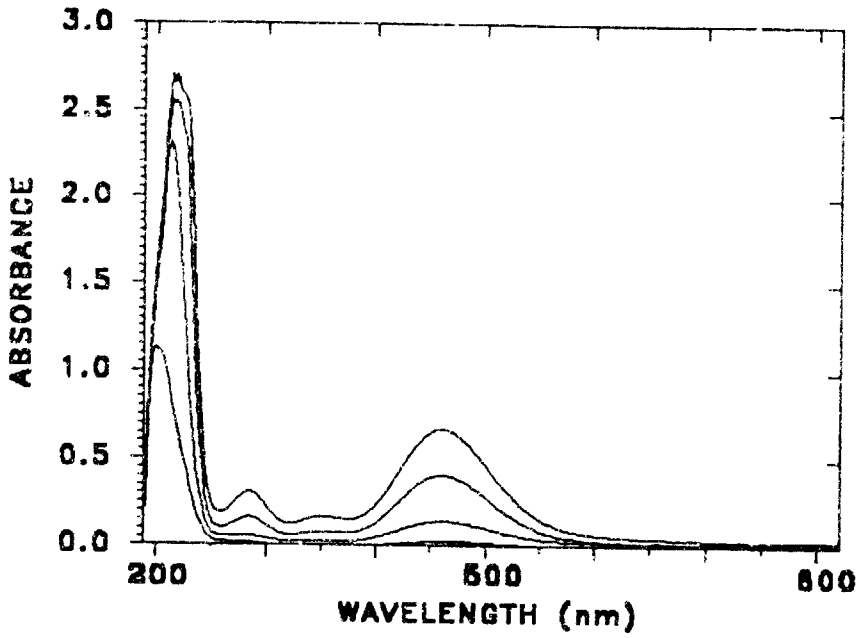

a) Calibration Spectra

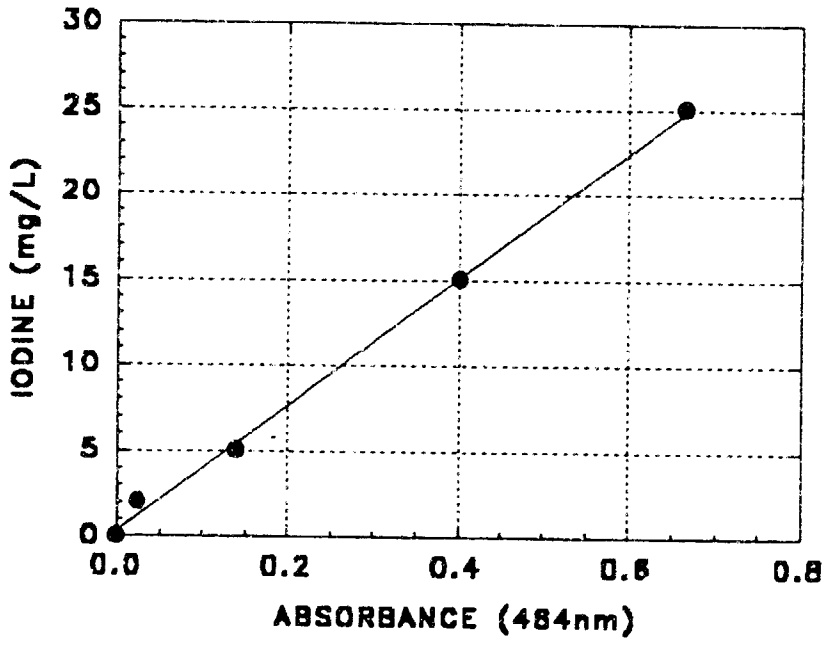

b) Calibration Curve - $[I_2]$ mg/L= 36.83 (A_{464} - A_{600}) + 0.30

r^2 = 0.9978

Figure 4.7 10 cm Cell -Ersatz Reclaimed Hygiene Water- DI Blank

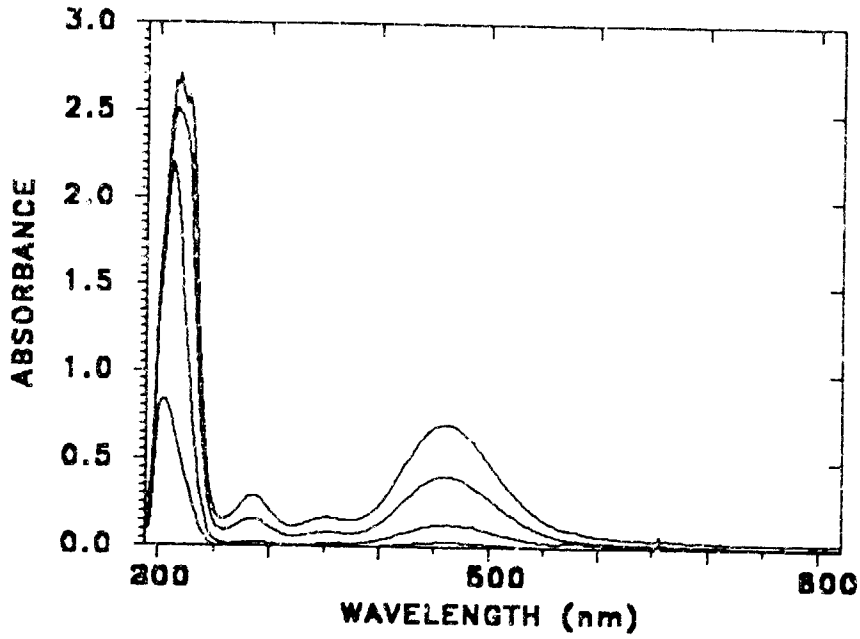

a) Calibration Spectra

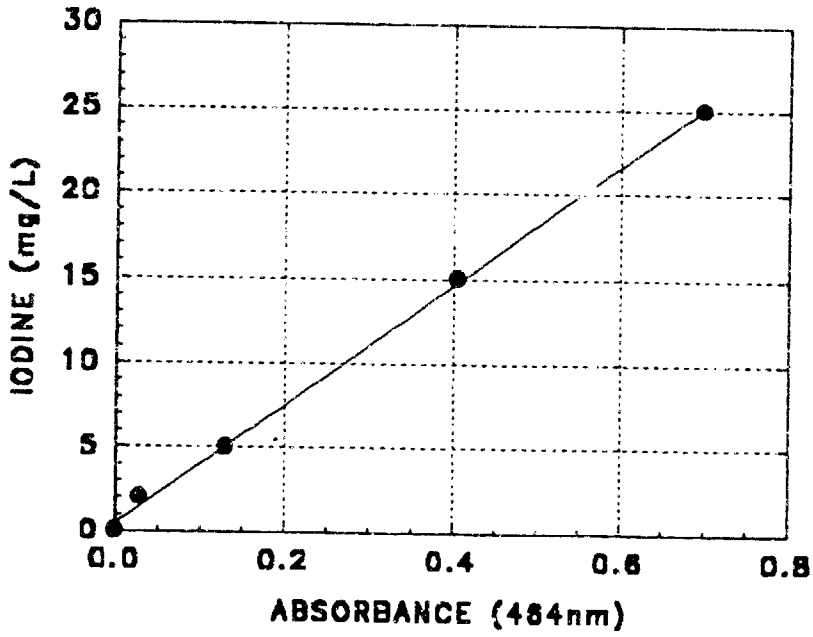

b) Calibration Curve - $[I_2]$ mg/L= 35.24 (A_{464} - A_{600}) + 0.49

$r^2 = 0.9988$

Figure 4.8 10 cm Cell - Ersatz Reclaimed Hygiene Water (RHW) - RHW Blank

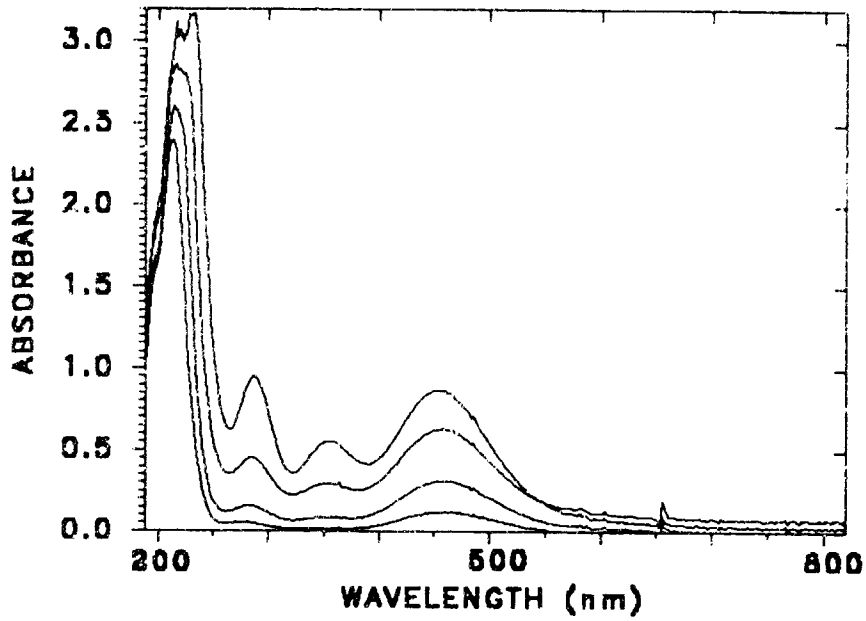

a) Calibration Spectra

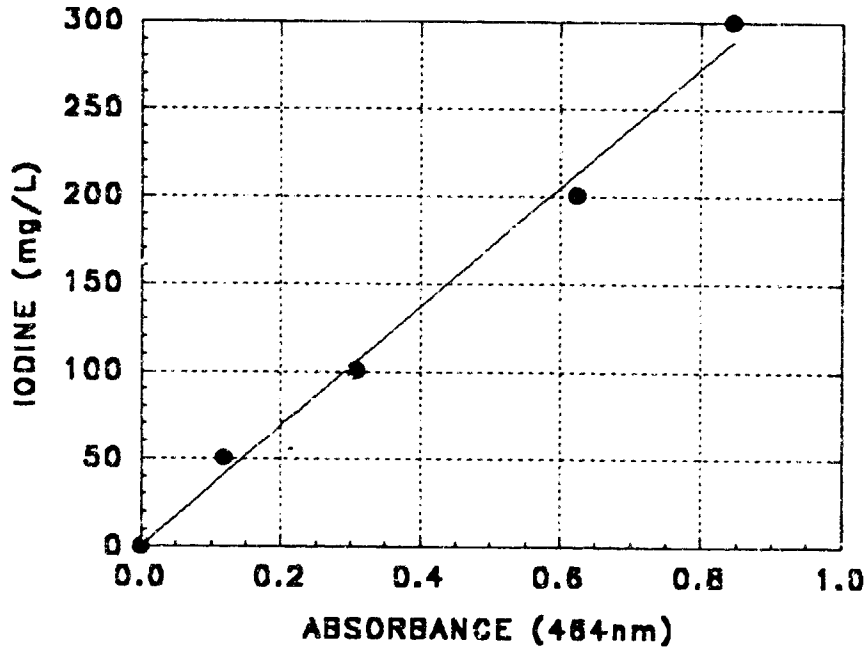

b) Calibration Curve - $[I_2]$ mg/L= 341.10 (A_{464} - A_{600}) + 0.46

$r^2 = 0.9930$

Figure 4.9 1 cm Cell - Ersatz Humidity Condensate - DI Water Blank

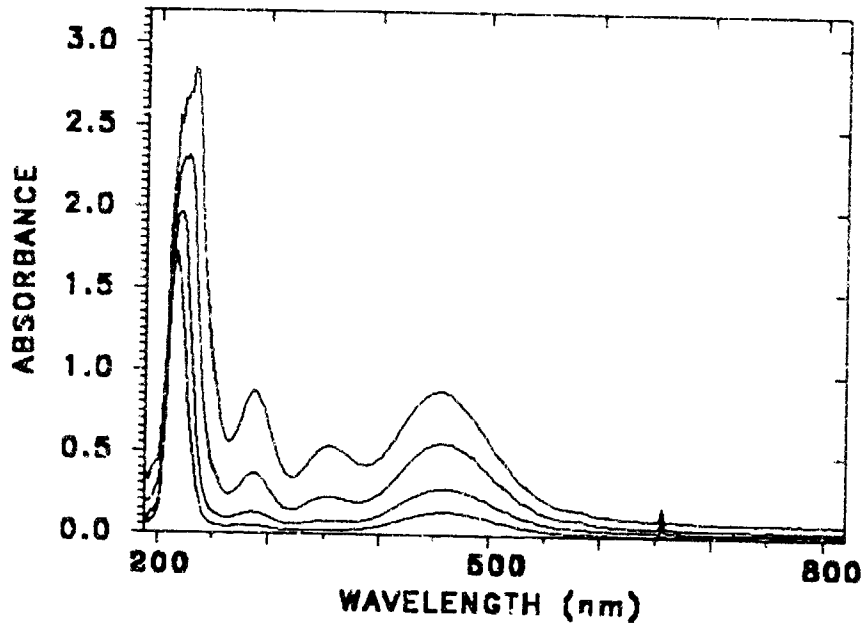

a) Calibration Spectra

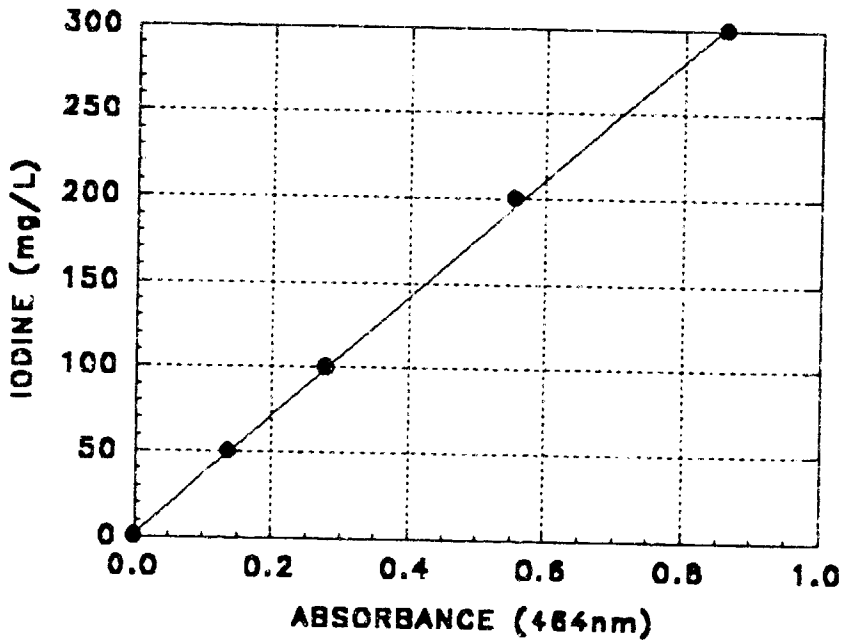

b) Calibration Curve - $[I_2]$ mg/L= 349.08 $(A_{464} - A_{600})$ + 2.03

$r^2 = 0.9995$

Figure 4.10 1 cm Cell - Ersatz Humidity Condensate (HC) - HC Matrix Blank

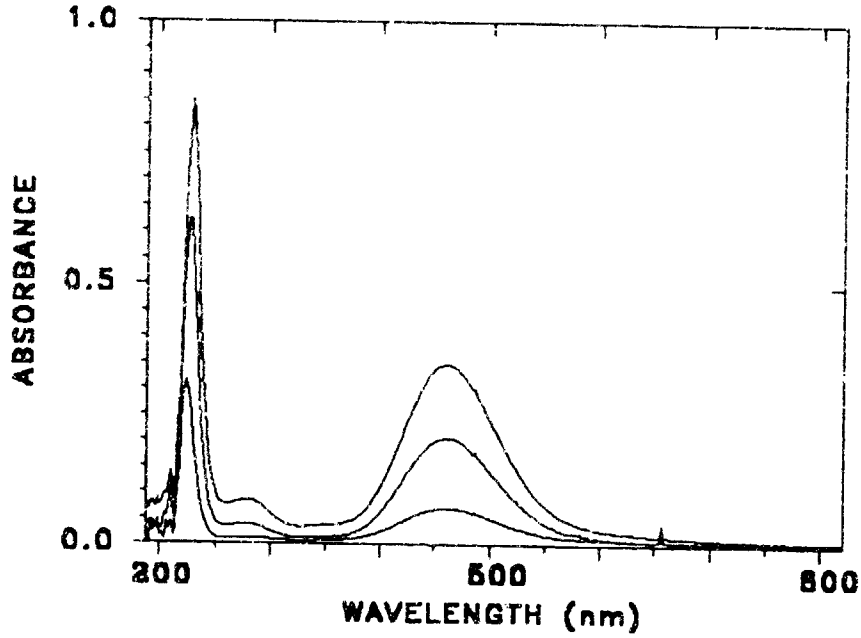

a) Calibration Spectra

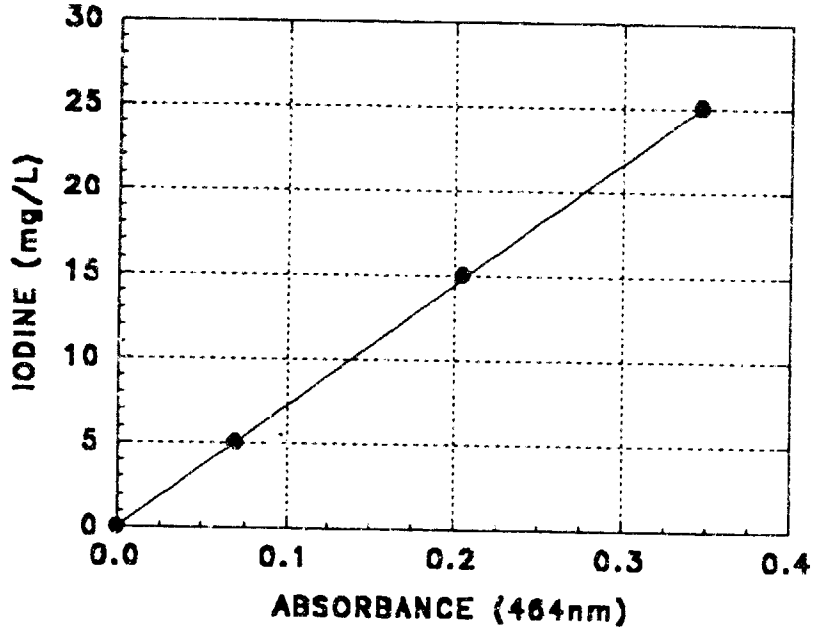

b) Calibration Curve - $[I_2]$ mg/L= 72.26 (A_{464} - A_{600}) + 0.01

$r^2 = 0.9999$

Figure 4.11 5 cm Cell - Ersatz Humidity Condensate (HC) - HC Matrix Blank

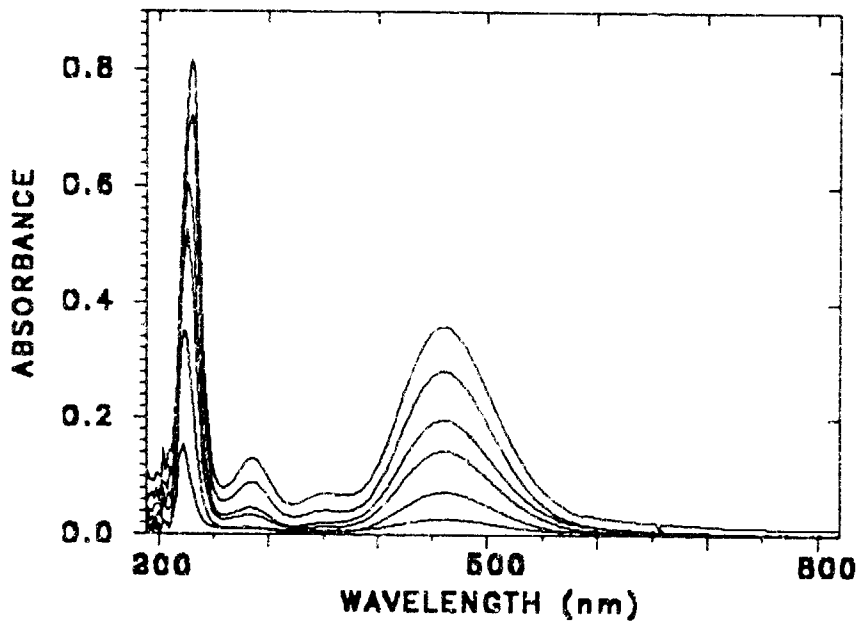

a) Calibration Spectra

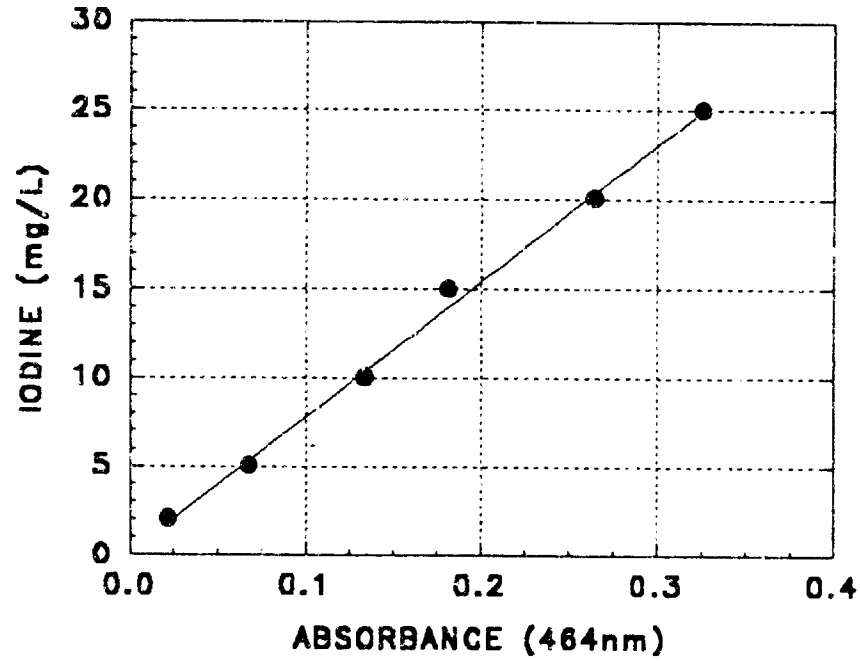

b) Calibration Curve - $[I_2]$ mg/L= 76.27 (A_{464} - A_{600}) + 0.14

$r^2 = 0.9966$

Figure 4.12 10 cm Cell - Ersatz Humidity Condensate - DI Water Blank

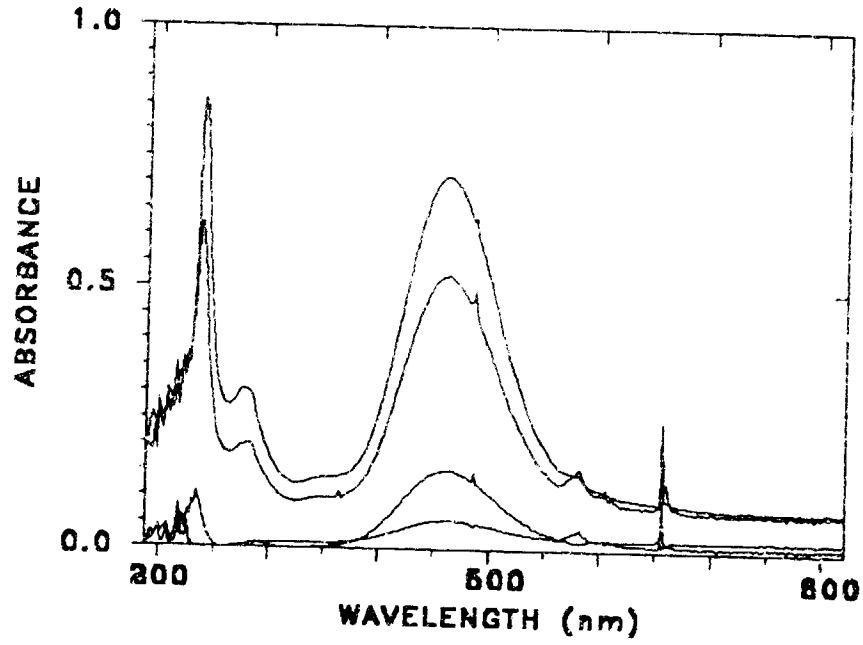

a) Calibration Spectra

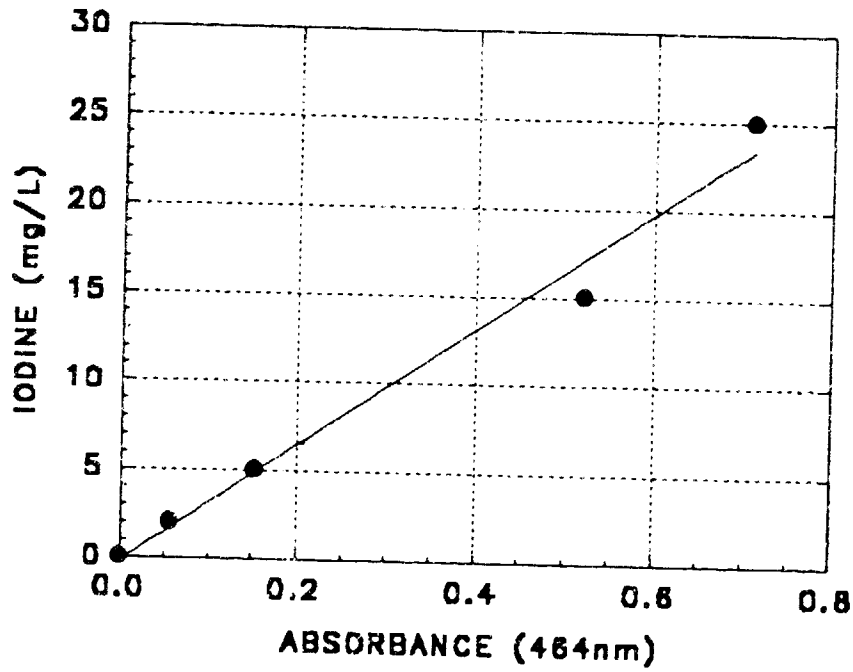

b) Calibration Curve - $[I_2]$ mg/L= 33.20 (A_{464} - A_{600}) - 0.19

$r^2 = 0.9833$

Figure 4.13 10 cm Cell - Ersatz Humidity Condensate (HC) - HC Matrix Blank

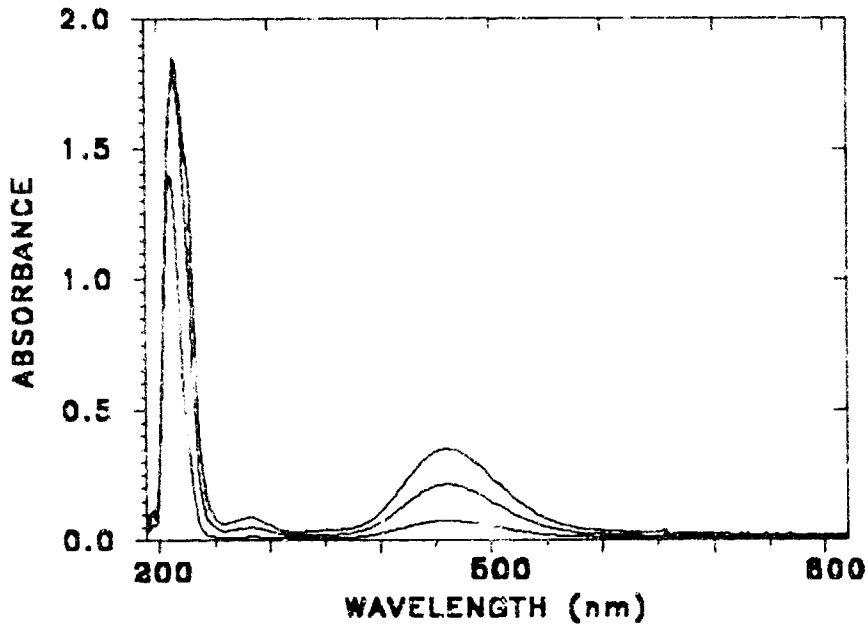

a) Calibration Spectra

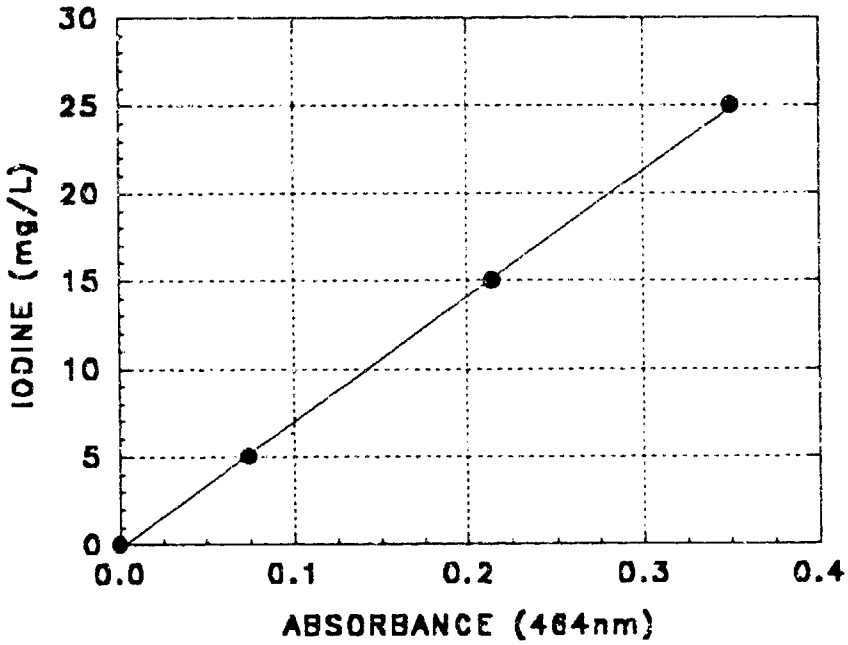

b) Calibration Curve - $[I_2]$ mg/L= 71.66 (A_{464} - A_{600}) + 0.20

$r^2 = 0.9997$

Figure 4.14 5 cm Cell - Ersatz Urine Distillate (UD) - UD Matrix Blank

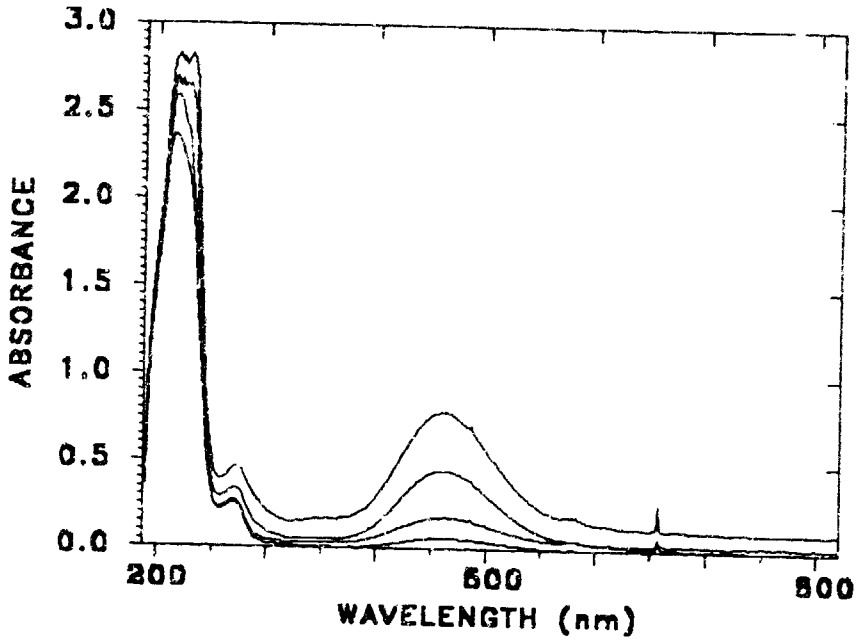

a) Calibration Spectra

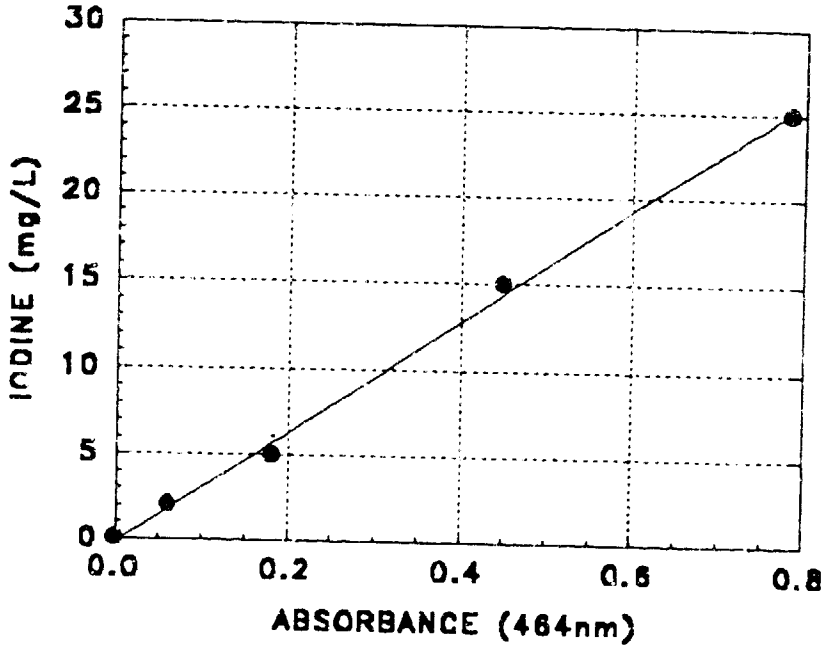

b) Calibration Curve - $[I_2]$ mg/L= 32.31 (A_{464} - A_{600}) - 0.15

$r^2 = 0.9978$

Figure 4.15 10 cm Cell - Ersatz Urine Distillate - DI Water Blank

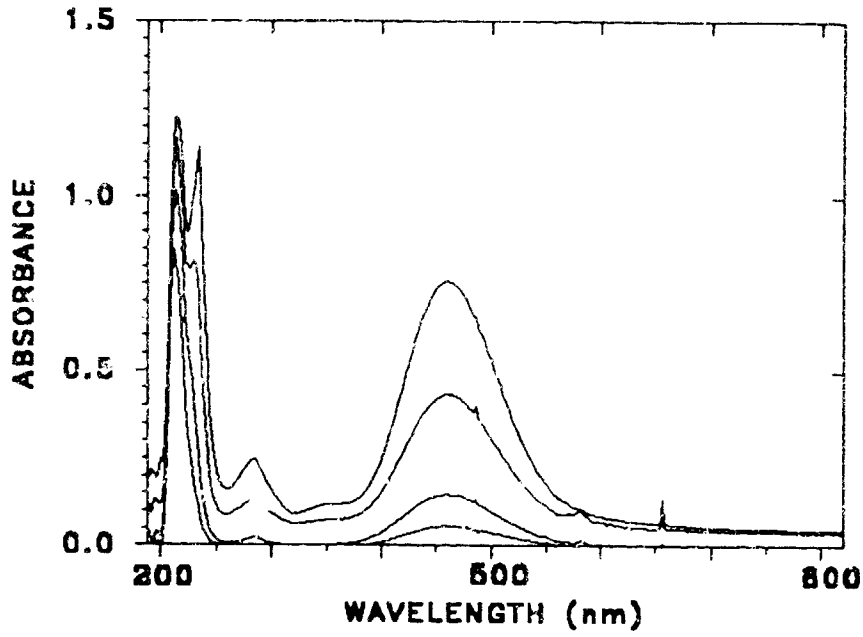

a) Calibration Spectra

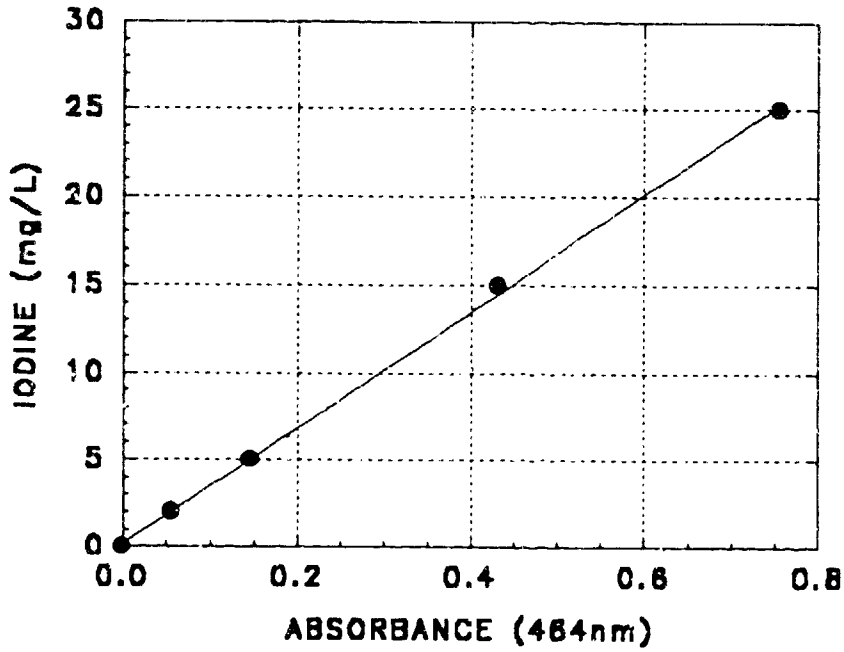

b) Calibration Curve - $[I_2]$ mg/L= 33.24 (A_{464} - A_{600}) + 0.17

$r^2 = 0.9993$

Figure 4.16 10 cm Cell - Ersatz Urine Distillate (UD) - UD Matrix Biank

matrices. Calibration for the 5 cm path length cell derived using a matrix instrument blank is presented in Figure 4.14. Figures 4.15 - 4.16 illustrate calibrations for this RMCV challenge stream arising from DI water and matrix instrument blanks respectively.

4.3 Long Term RMCV Life Cycle Tests.

For the diode array spectrophotometer serving the long term RMCV life cycle testing, the initial calibration factors derived by the methods outlined above were embedded in the RMCV.EXE master control program prior to commencement of system operation. Frequent calibration checks via the LCV method resulted in periodic recalibrations of the instrument by keyboard entry of quadratic calibration coefficients, without interruption of system operation, augmented by hard coding of new factors into software during periods of shutdown for challenge solution make up and routine maintenance.

The diode array spectrophotometer serving the long term life tests was the only instrument calibrated for the iodide anion. The initial I^- calibration was established by first determining the separate relationships between concentration and absorbance for I^- and I_2 at the 228 nm wavelength for the 10 cm pathlength cell. These relationships for the DI water matrix are illustrated in Figure 4.17a and 4.17b for I^- and I_2 respectively. After I_2 concentrations are calculated using absorbance at λ = 464 nm, the equivalent absorbance attributable to I_2 at λ = 228 nm is subtracted from the total absorbance at this wavelength. The net absorbance at λ = 228 nm is then used in the calculation of iodide. Matrix absorbance at the 228 nm wavelength is significant for both the ersatz humidity condensate and the ersatz urine distillate. The validity of the above procedure requires that matrix effects at this wavelength remain constant. Experience has shown this to be the case throughout the long term RMCV life cycle tests.

The accuracy of the calibrations of the instrument for iodide was checked by both the LCV colorimetric method and by use of a solid state iodide selective electrode. Due to the

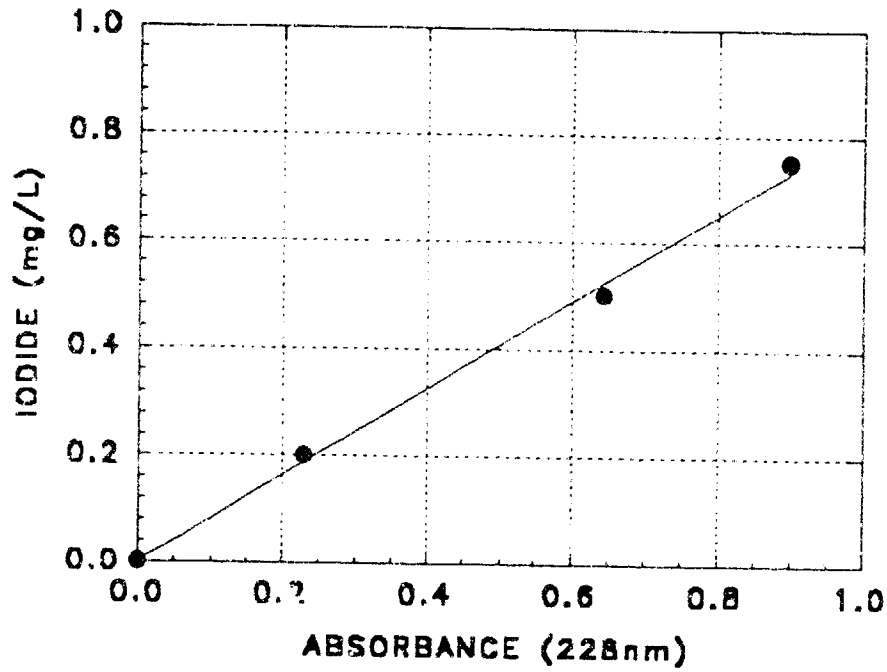

a) Iodide at 228 nm - $[I^-]$ mg/L = 0.8142 A_{228} - 0.0009

$r^2 = 0.9966$

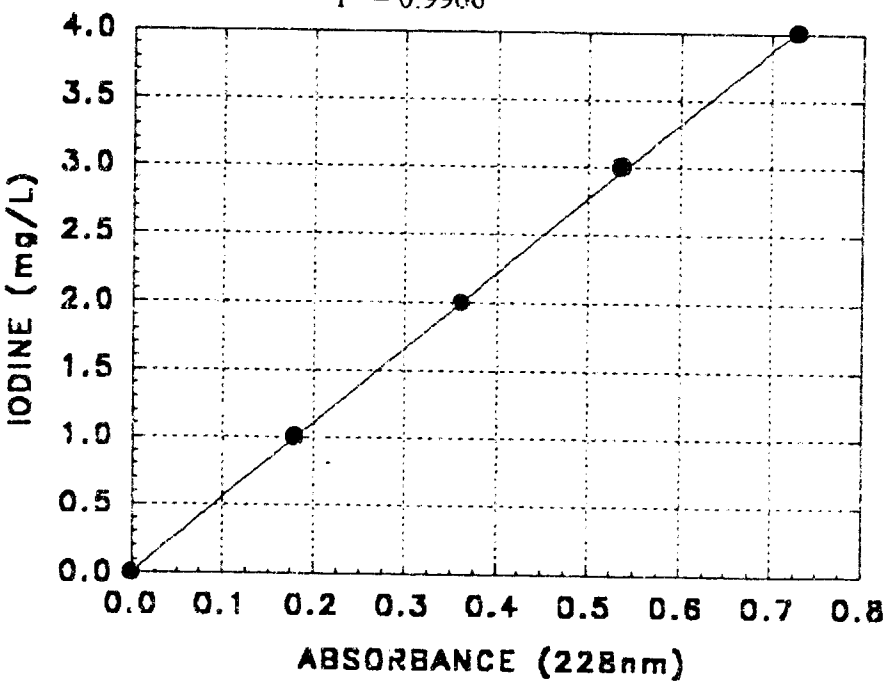

b) Iodine at 228 nm - $[I_2]$ mg/L = 5.51 A_{228} - 0.0079

$r^2 = 0.9998$

Figure 4.17 Iodide and Iodine at λ = 228 nm - DI Water Matrix.

complexity of the iodide calculational technique, adjustments to the calibrations for this parameter were made only by hard coding into software during times of system shut-down.

In the early stages of the long term RMCV life cycle test, frequent recalibrations were required. At the same time it was noted that a gradually increasing dull yellow-brown coloration was associated with the slow build up of adsorbed iodine on the inner surfaces of the spectrophotometer cell. In this context it seemed apparent that this sorption phenomenon was responsible for the frequent recalibrations due to the concomitant changes in the transmissive properties of the optical quartz. The adsorbed iodine was removed with difficulty by dissolution in polar organic solvents such as acetone, ethanol or methanol. Experienced proved that attempts to maintain cell cleanliness were counterproductive. The transition from no visable coloration on the cell surface to visable coloration required almost daily re-calibrations. However, after approximately two weeks of operation without cell cleaning, the level of adsorbed iodine equilibrated and stable calibrations could be maintained for several months. Afterward, less frequent recalibrations were dictated by the slow loss in intensity of the deuterium source lamp.

Over the course of the roughly eighteen month history of the long term life cycle tests, the diode array spectrophotometer proved itself to be remarkably robust. In this time of nearly continuous operation only two major instrument malfunctions occured. The first was the failure of the deuterium lamp power supply, the second was the failure of the deuterium lamp. Fortunately, parts from the second diode array spectrophotometer serving parametric and kinetics tests could be sacrificed to keep the long term tests operational while repairs were being made.

4.4 Parametric RMCV Tests.

The diode array spectrometer serving the second RMCV small column test stand devoted to parametric tests was calibrated variously for 1 cm, 5 cm, and 10 cm path-length

cells depending upon the concentration ranges encountered for the different experiments. The parametric studies were limited to the ersatz reclaimed potable water and the ersatz humidity condensate challenge streams, corresponding to the simplest and the most chemically complex of the contaminant matrices.

4.5 Kinetic Studies.

Kinetic studies were undertaken to characterize the rates and reactions of I_2 decay in ersatz humidity condensate and ersatz urine distillate. For the purposes of these tests calibrations of the 5 cm path-length cell were used for both matrices in the concentration range between 0 and 20 mg/L of I_2.

The spectrophotometer cell was thermally insulated and jacketed with a coil of tubing connected to a temperature control circuit as illustrated in Figure 4.18. The circuit consisted of a pump as a source of flow, a constant temperature bath containing water at the desired temperature and connected to tubing coils surrounding the spectrophotometer cell, an outer insulation layer for the cell, and a K-type thermocouple mounted at the cell and connected to a Newport model 269-D1 digital thermocouple thermometer, interfaced by RS-232C asynchronous serial data link to the controlling computer. Temperature regulation within the cell was $\pm$ 1 ^{o}C.

4.6 Prototype RMCV.

The second diode array spectrophotometer which was dedicated to parametric and kinetics experiments has also played an important role in the development of the prototype RMCV. At the beginning of prototype RMCV operation, the diode array spectrophotometer served as the system on-line iodine monitor, communicating with the RMVC system microcontroller by serial RS-232C data link. The spectrophotometer was kept on-line during the initial evaluation period for the PCWQM Iodine Bench as system monitor. After the

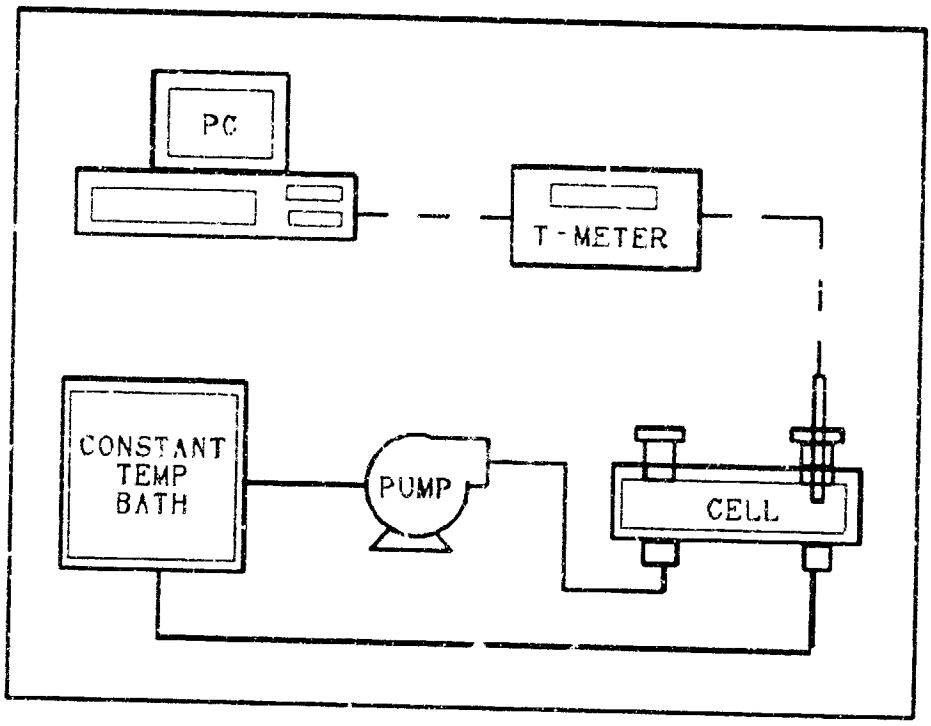

a) Temperature Control Circuit.

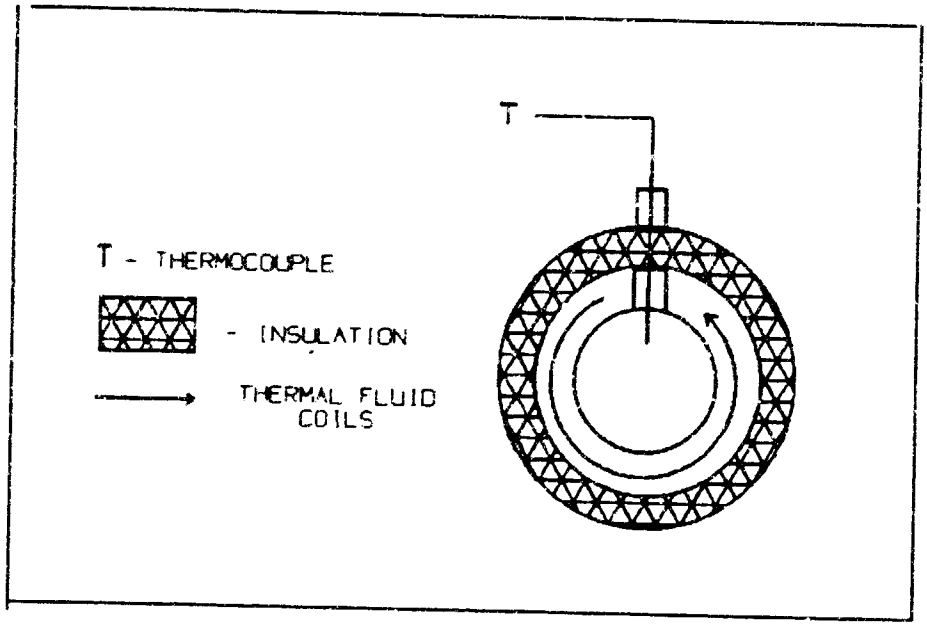

b) Jacketed Spectrophotometer Cell Cross Section

Figure 4.18 Constant Temperature Spectrometer Cell for Kinetics Experiments.

PCWQM Iodine Bench was judged satisfactory, the diode array spectrophotometer was taken off line. It served again as the on-line iodine monitor while the Iodine Bench was re-fitted with electronic control elements conformable with inclusion in the PRMCV.

5

RMCV SMALL COLUMN LIFE CYCLE TESTS

5.0 Overview.

For the purpose of determining the regenerable lives of RMCVs when challenged with a variety of contaminant streams, small column scale long term life cycle testing was conducted for a period of approximately eighteen months. Four RMCVs, each consisting of an MCV containing 2.5 cm^3 of iodinated anion exchange resin, and a 10 cm^3 bed of solid state elemental iodine, were incorporated into the RMCV Life Cycle Test Stand. The design and operation of the fully autonomous computer controlled test stand is presented in Section 2.

Four challenge streams were selected: ersatz reclaimed potable water, ersatz reclaimed hygiene water, ersatz humidity condensate, and ersatz urine distillate. These four challenge streams were used as influent for the units designated as RMCV-1, RMCV-2, RMCV-3 and RMCV-4 respectively. The chemistry of the challenge solutions is presented in Section 3. The respective feedstocks were prepared in bathces and stored in 190 L tanks. A flow rate of approximately 12.0 cm^3/min was established and maintained for each unit. This corresponded to a residence time within the MCV of approximately 0.21 minutes, and to a residence time within the I_2 crystal bed of approximately 0.82 minutes. (Residence times are discussed in greater detail in Section 6.) The small MCV volume and short MCV residence time were chosen to maximize the potential number of regenerations within the eighteen month performance period. Flow histories through the RMCVs were recorded as liters of flow per cm^3 of ion exchange resin, and abbreviated as L/cm^3 or as L/cc.

A desired operational I_2 concentration window of 4.00 mg/L - 2.00 mg/L was specified for each RMCV. Regenerations were invoked when the residual I_2 levels dropped below 2.00 mg/L. Regenerations were intended to raise the MCV resin I_2 loadings sufficiently to re-establish washout at 4.00 mg/L. During regeneration, I_2 concentrations in the regeneration liquor were initially at saturation levels of approximately 300 mg/L, but quickly stabilized at lower levels ranging between 200 - 225 mg/L, once flow through the

crystal bed was established. The I_2 levels in each RMCV effluent were determined in real-time by UV-VIS absorption spectrophotometric techniques using the photodiode array spectrophotometer. Analytical techniques and calibration procedures for this instrument are detailed in Section 4.

Following an intial shakedown period that spanned the first 200 L/cm^3 of throughput, continuous unattended operation was achieved and maintained. The system was shutdown aprroximately bi-weekly for routine maintenance and renewal of the RMCV challenge solutions. Otherwise, the system ran continuously for approximately eighteen months, with three of the four RMCVs totalling throughputs in excess of 2,500 L/cm^3. The system proved to be remarkably robust, undergoing a minimum of unscheduled down time. The life cycle test histories for each of the four RMCVs are summarized in Table 5.1. and presented in detail below.

Table 5.1 RMCV Life Cycle Test Results Summary.

Parameter	Units	Ersatz Reclaimed Potable Water	Ersatz Reclaimed Hygiene Water	Ersatz Humidity Condensate	Ersatz Urine Distillate
Σ Throughput	L/cm^3	2556	2393	2533	2611
Σ Cycles		167	312	218	176
Σ I_2 Washout	mg	20,021	37,208	19,365	18,217
Σ I^- Washout	mg	445	833	2,330	4,725
Average I_2 Concentration	mg/L	3.13	6.22	3.06	2.79
Average I^- Concentration	mg/L	0.07	0.14	0.37	0.70
Average pH		5.96	5.88	3.43	3.80
Ave. Cyclic Throughput	L/cm^3	16.49	7.67	11.62	14.84
Average Flow Rate	cm^3/min	11.80	11.35	11.81	11.86

5.1 RMCV-1: Ersatz Reclaimed Potable Water.

The RMCV serving the ersatz reclaimed potable water challenge stream was designated as RMCV-1. During the course of the long term life cycle testing this unit accumulated 2,555.6 L/cm^3 of total throughput. The average pH of the MCV effluent was 6.0. In excess of 20 grams of I_2 were imparted to the challenge stream at an average concentration of 3.13 mg/L. RMCV-1 experienced 167 cycles of washout and regeneration, with cyclic throughputs varying from 20 L/cm^3 per cycle to 10 L/cm^3 per cycle, for an overall average cyclic throughput of 16.5 L/cm^3. Using a typical expendable MCV design value of 20 L/cm^3, this constitutes a 128 fold extension of MCV life.

The life cycle test histories for RMCV-1 are shown in Figures 5.1, 5.2, 5.3, 5.4, 5 5, and 5.6, which present the first, second, third, fourth, fifth, and sixth 500 L/cm^3 increment of flow history respectively. These figures present RMCV effluent I_2 and I^- concentrations, pH, conductivity, and flow rate as functions of cumulative throughput. Regenerations are depicted as transient spikes of high elemental iodine concentration. These transient spikes are attributable to residence times optimized for a maximum number of regenerations during the life cycle test program and have been eliminated in the design of the prototype RMCV.

During the shakedown period, corresponding to the first 200 L/cm^3 of throughput, RMCV-1 exhibited erratic behavior. Once system hardware and software were debugged, stable operation, interrupted by only occasional system upsets, was achieved. Regenerations were given a minimum duration of 40 minutes, after which regeneration was terminated by an I_2 concentration greater than 10 mg/L. At approximately 455 L/cm^3, RMCV-1 over-regenerated due to a disruption of flow to the on-line I_2 monitor. To prevent recurrence, a maximum regeneration time of 120 minutes was coded into the RMCV.EXE master control program.

The predominant trend which became evident with the increase in cumulative flow through RMCV-1 was the gradual lessening of the cyclic throughput. By approximately 1200

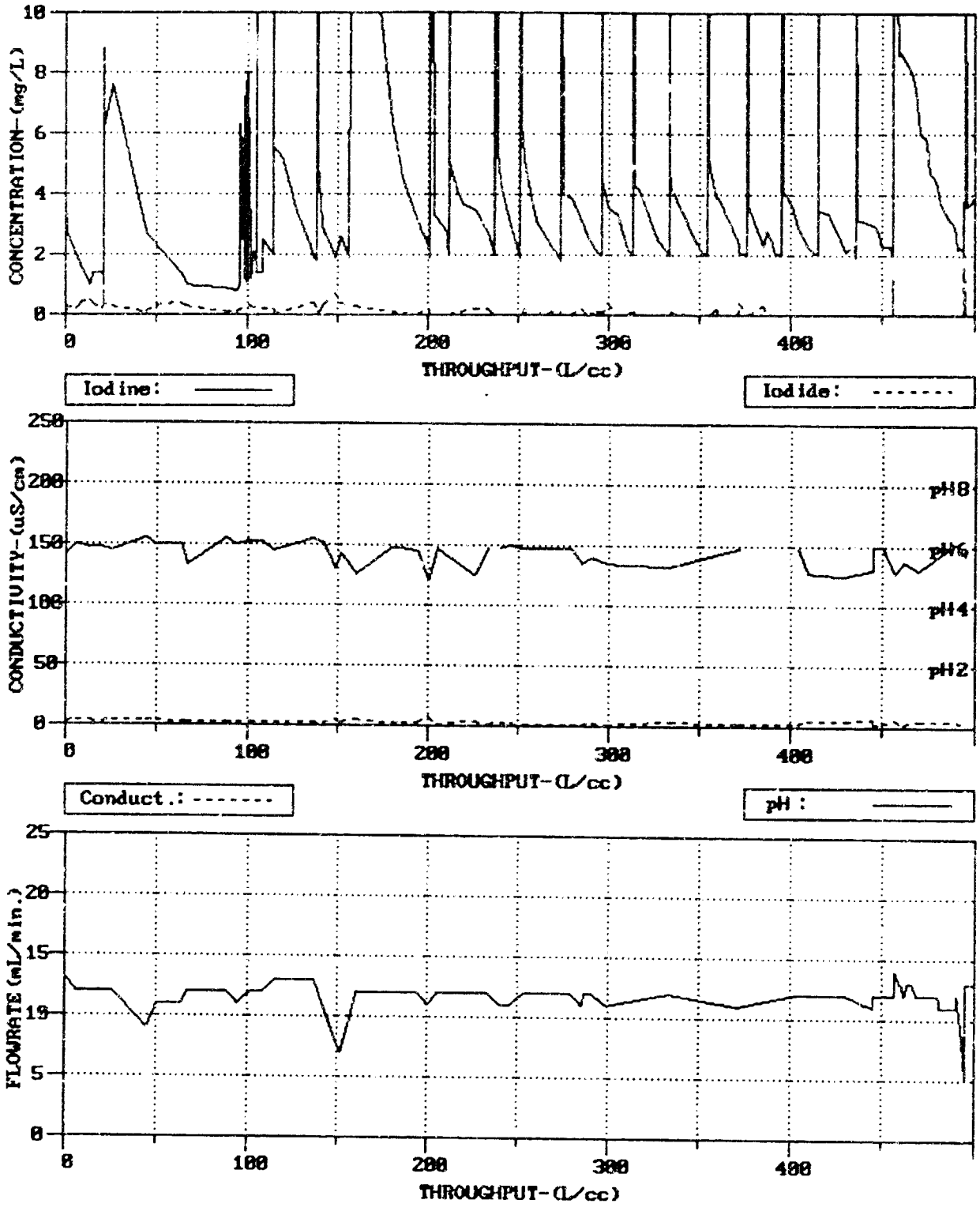

Figure 5.1 RMCV Life Cycle Test - Ersatz Reclaimed Potable Water - 0 - 500 L/cm^3

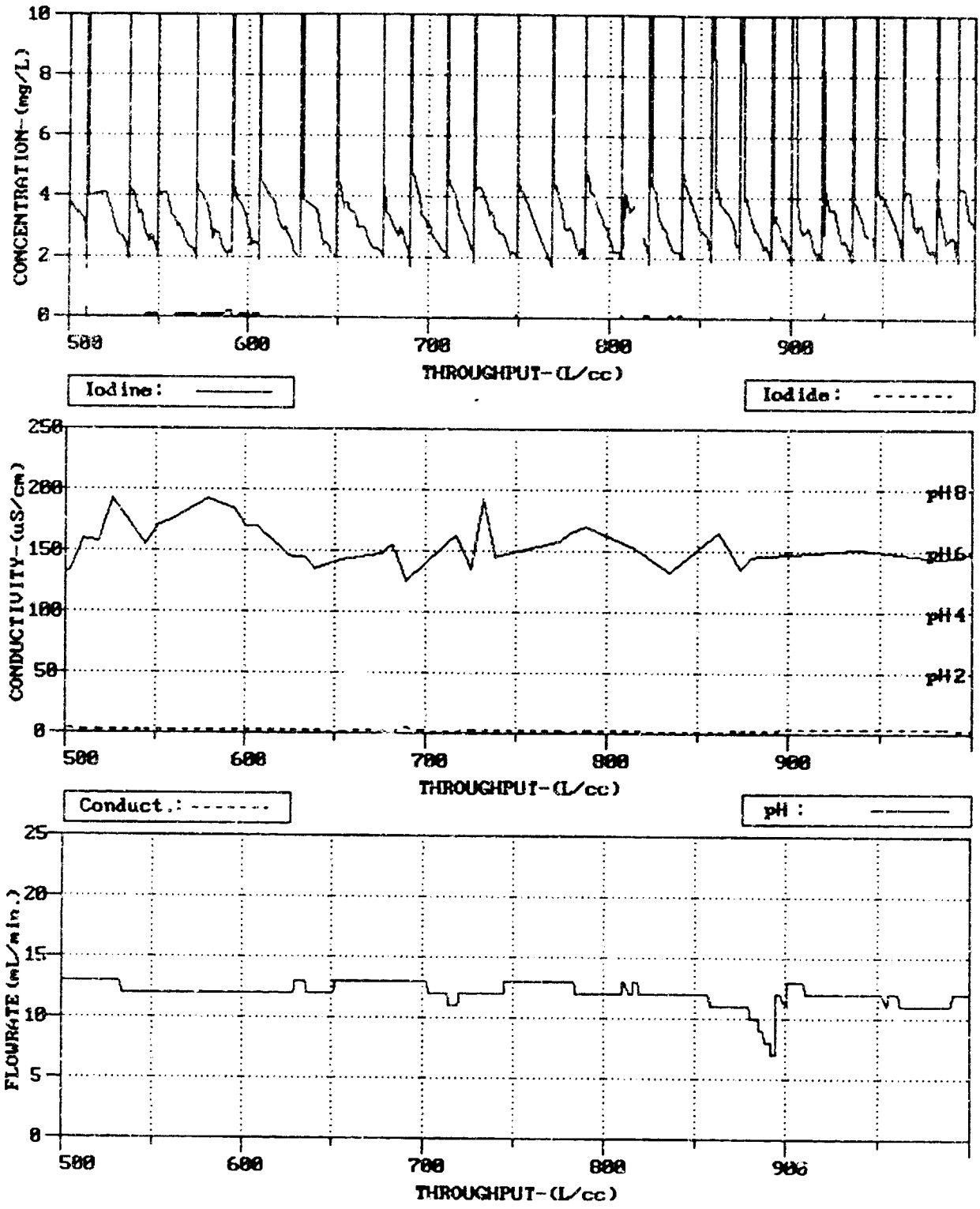

Figure 5.2 RMCV Life Cycle Test - Ersatz Reclaimed Potable Water: 500-1000 L/cm^3

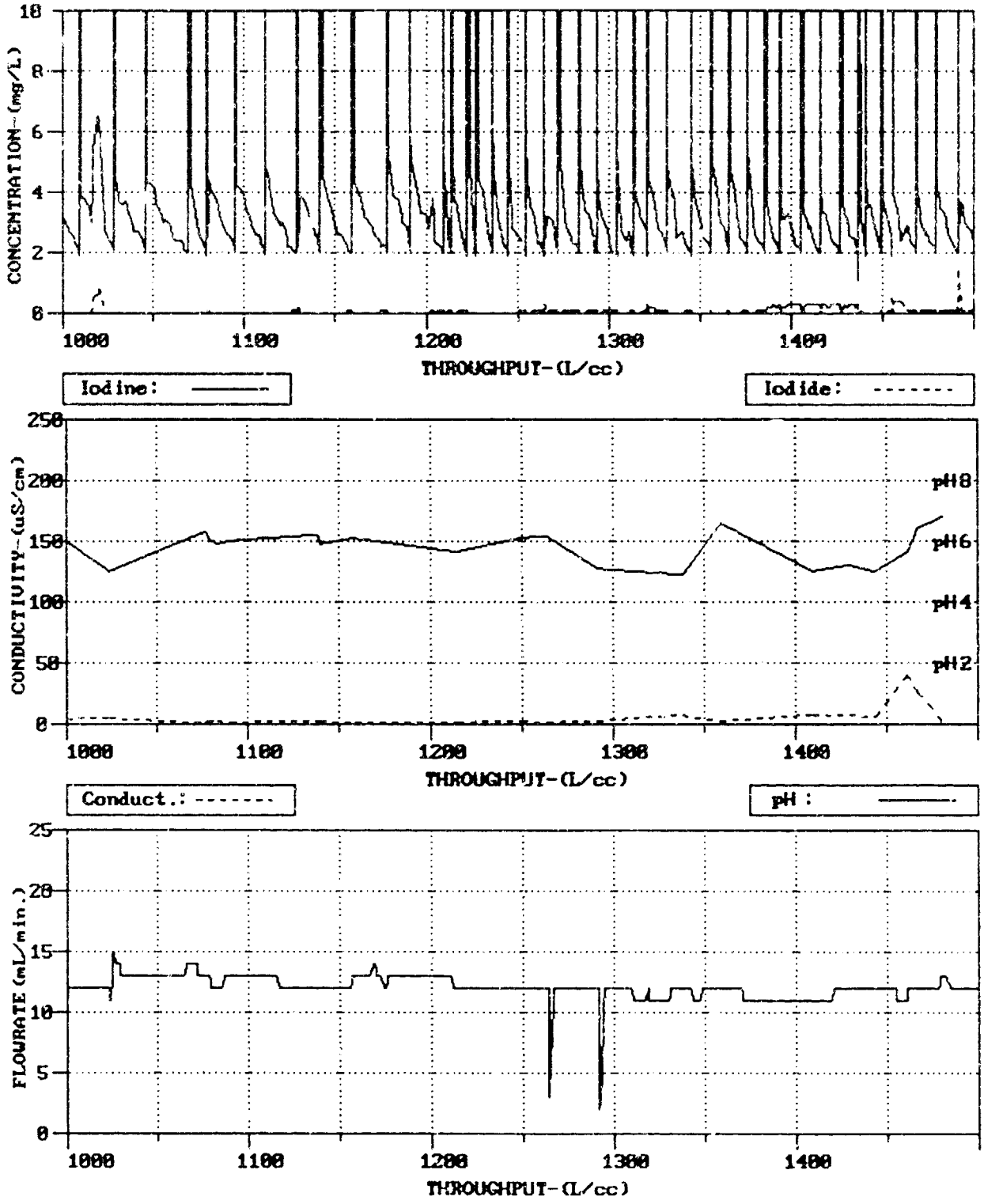

Figure 5.3 RMCV Life Cycle Test - Ersatz Reclaimed Potable Water: 1000-1500 L/cm^3

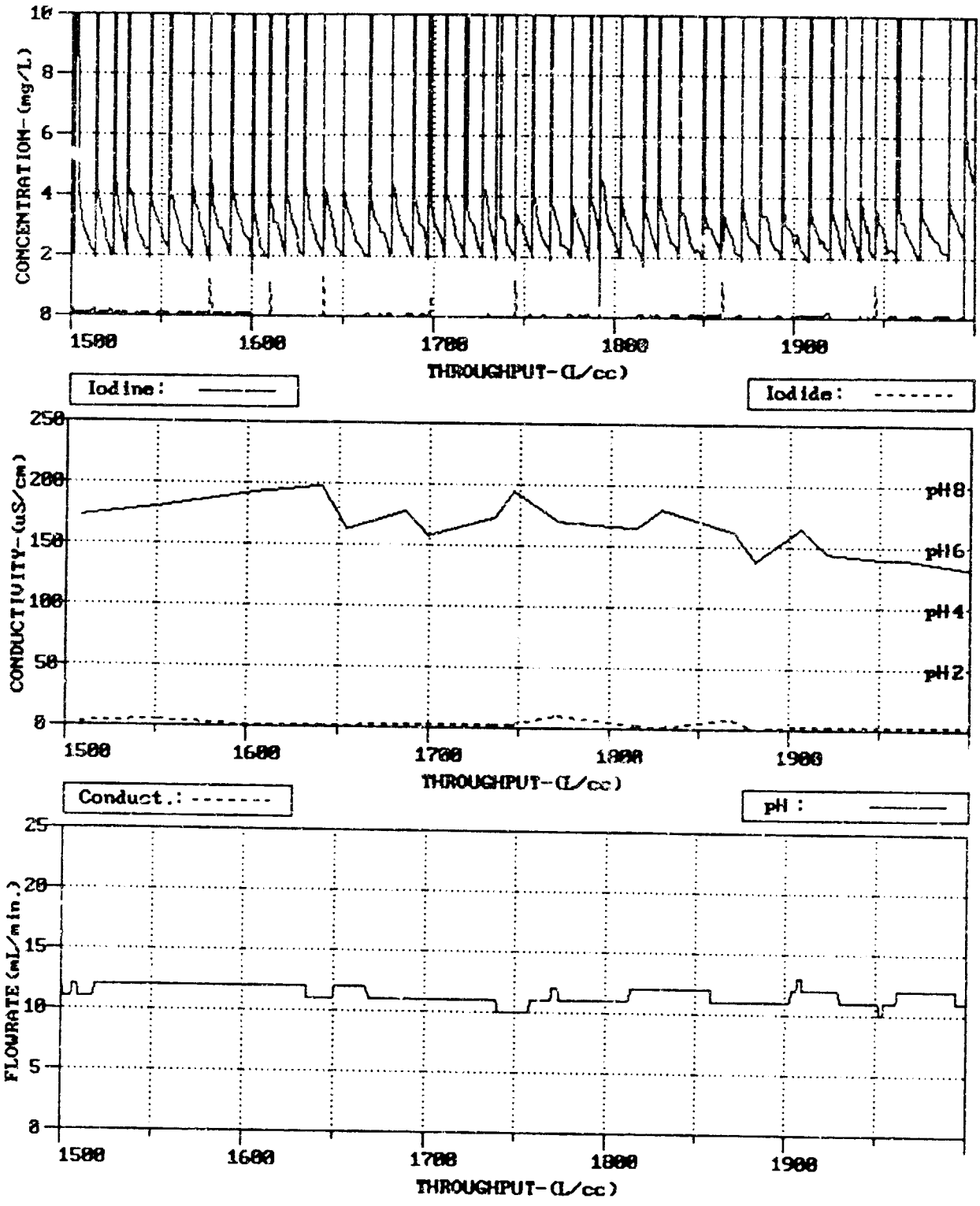

Figure 5.4 RMCV Life Cycle Test - Ersatz Reclaimed Potable Water 1500-2000 L/cm^3

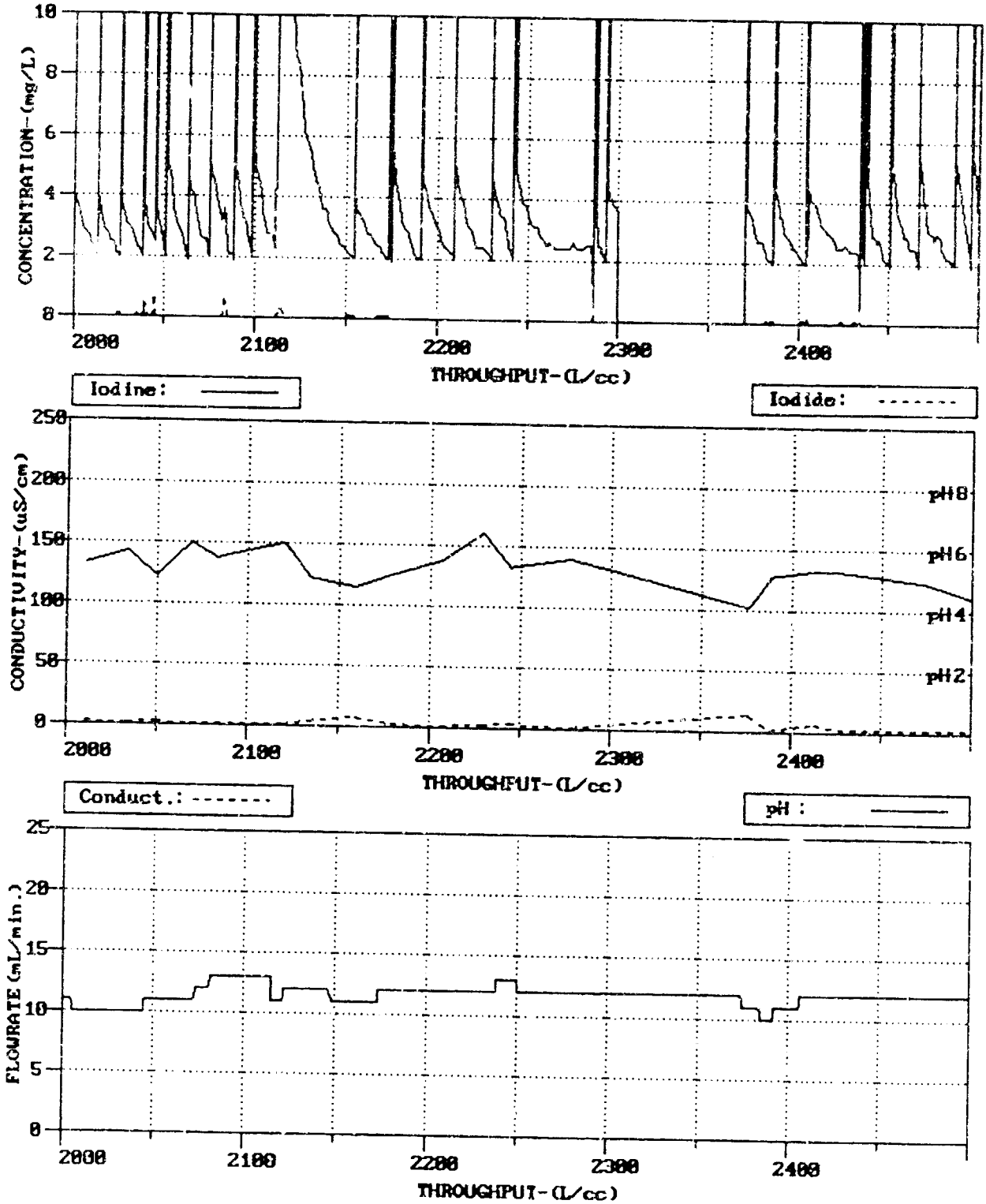

Figure 5.5 RMCV Life Cycle Test - Ersatz Reclaimed Potable Water. 2000-2500 L/cm^3.

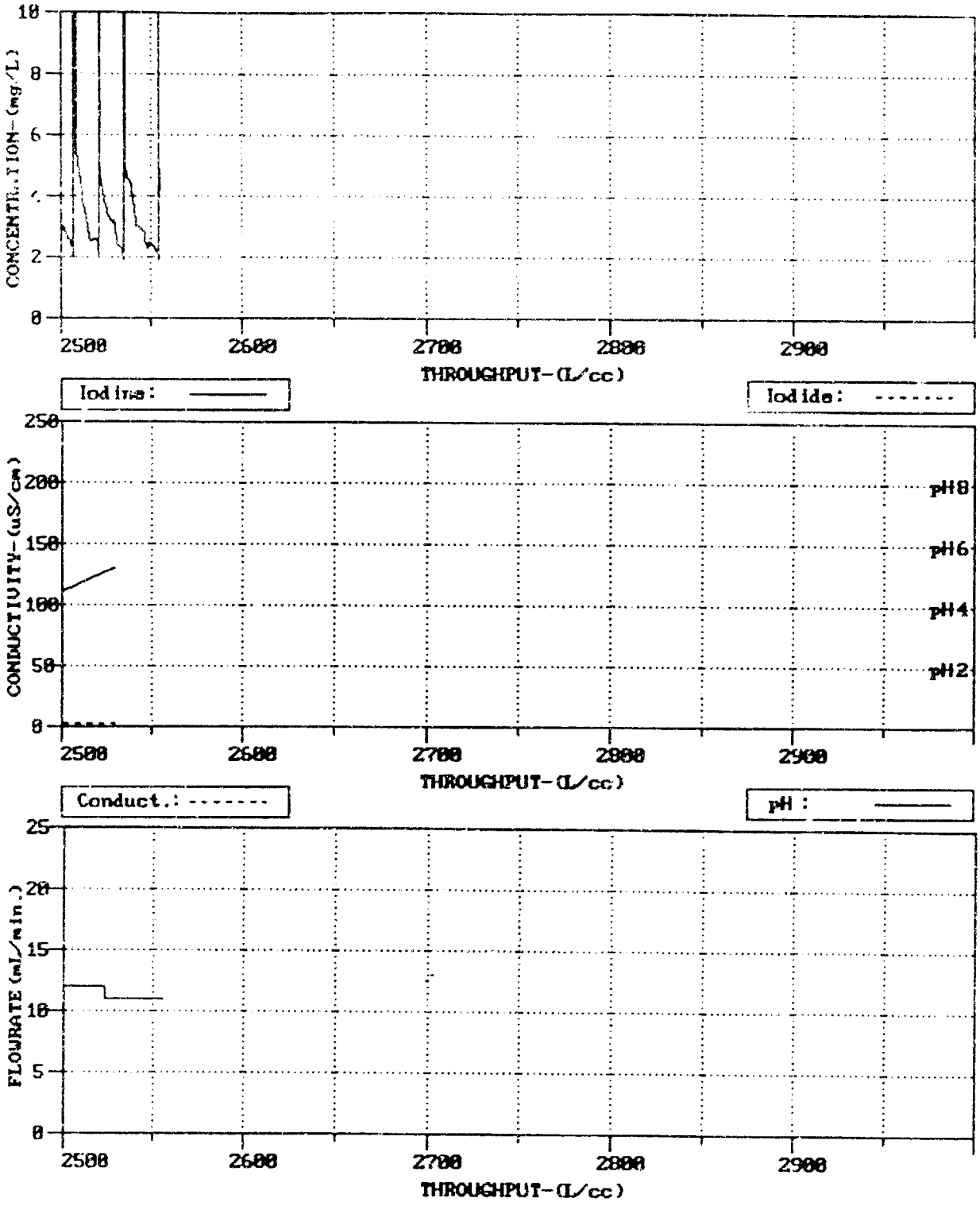

Figure 5.6 RMCV Life Cycle Test - Ersatz Reclaimed Potable Water : 2500 - 2556 L/cm^3.

L/cm^3 cyclic throughput had diminished to 12.5 L/cm^3, and afterward ranged between this value and a minimum of 10 L/cm^3. At approximately 1950 L/cm^3 of cumulative flow, the I_2 crystal bed, having been severely depleted, was replaced with 10 cm^3 of crystalline I_2. This resulted in a significant increase in the cyclic throughput. At approximately 2110 L/cm^3 another over-regeneration occured due to loss of flow to the on-line I_2 monitor. The regeration was terminated when the maximum time condition had been fulfilled. Iodine concentrations between 2300 - 2370 L/cm^3 were not recorded due to operator error. Flow to RMCV-1 was terminated at 2555.6 L/cm^3.

Cyclic throughput, cyclic I_2 depletion, and cyclic I^- depletion refer to the cumulative flow, cumulative elemental iodine loss from the MCV, and the cumulative iodide loss from the MCV for a given RMCV cycle of washout and regeneration. The values of these parameters for RMCV-1 versus cycle number are illustrated in Figures 5.7, 5.8, and 5.9 respectively. Considerable scatter of the data is evident, although trends are clearly discernable. Cyclic I_2 depletion correlates well with the observed trend in cyclic throughput. In the early stages of RMCV-1's flow history, corresponding to 18-20 L/cm^3 of throughput per cycle, approximately 180 mg I_2 were lost from the MCV resin during one complete cycle. I_2 depletion per cycle dropped to approximately 100 mg with the fall in cyclic throughput to the 10 L/cm^3 level, and then rose to the 140 mg level following replacement of the iodine crystal bed. No trends are evident in the depletion of I^-. MCV resin I_2 depletion and throughput during the regeneration phase of RMCV operation versus cycle number are illustrated in Figures 5.10 and 5.11 respectively.

5.2 RMCV-2: Ersatz Reclaimed Hygiene Water.

The RMCV serving the ersatz reclaimed hygiene water challenge stream was designated as RMCV-2. This unit accumulated 2,393.6 L/cm^3 of total throughput. The average pH of the MCV effluent was 5.9. More than 37 grams of I_2 were imparted to the

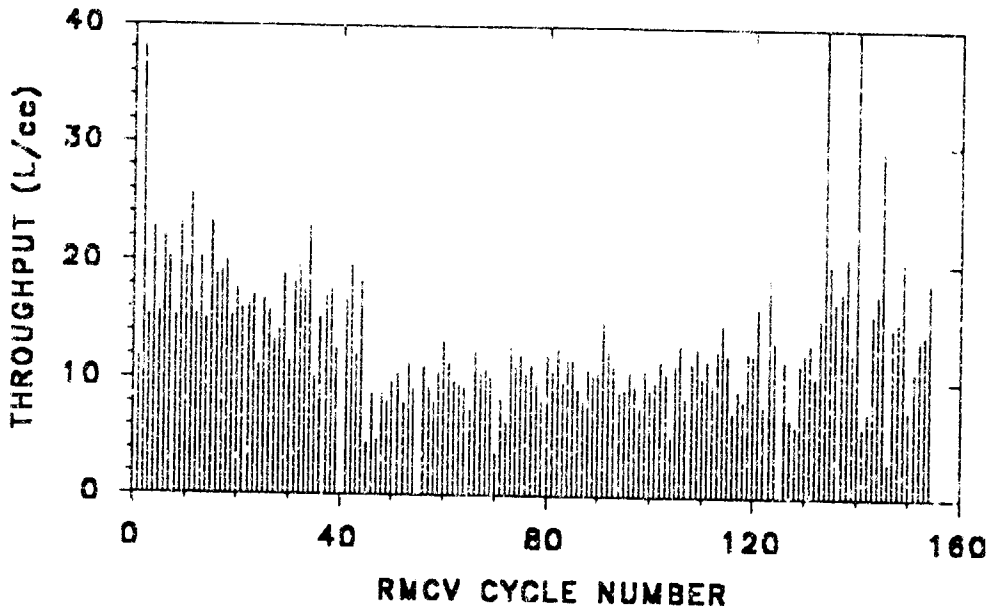

Figure 5.7 Cyclic Throughput - Ersatz Reclaimed Potable Water.

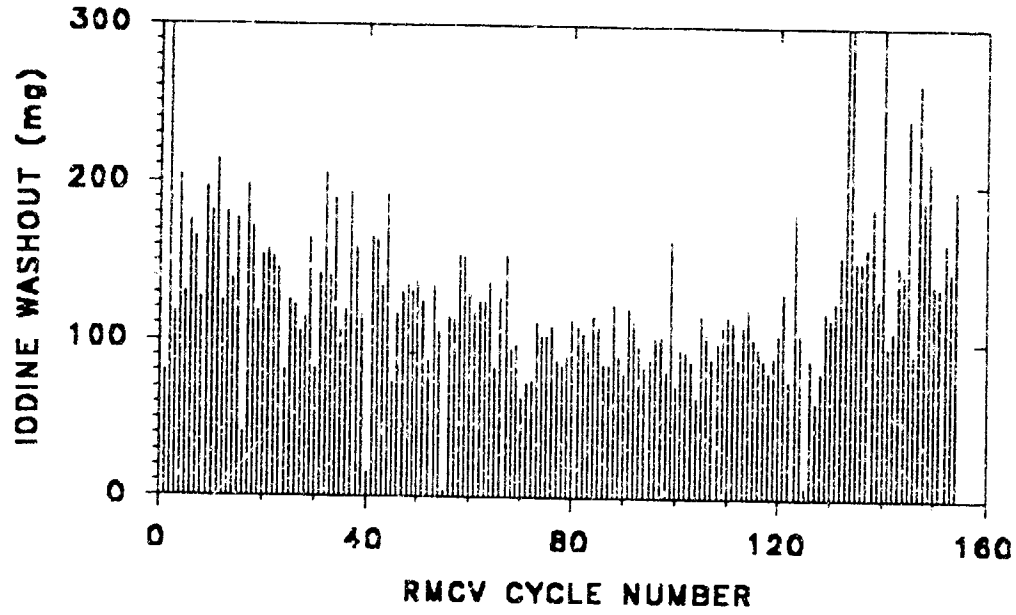

Figure 5.8 Cyclic I_2 Depletion - Ersatz Reclaimed Potable Water.

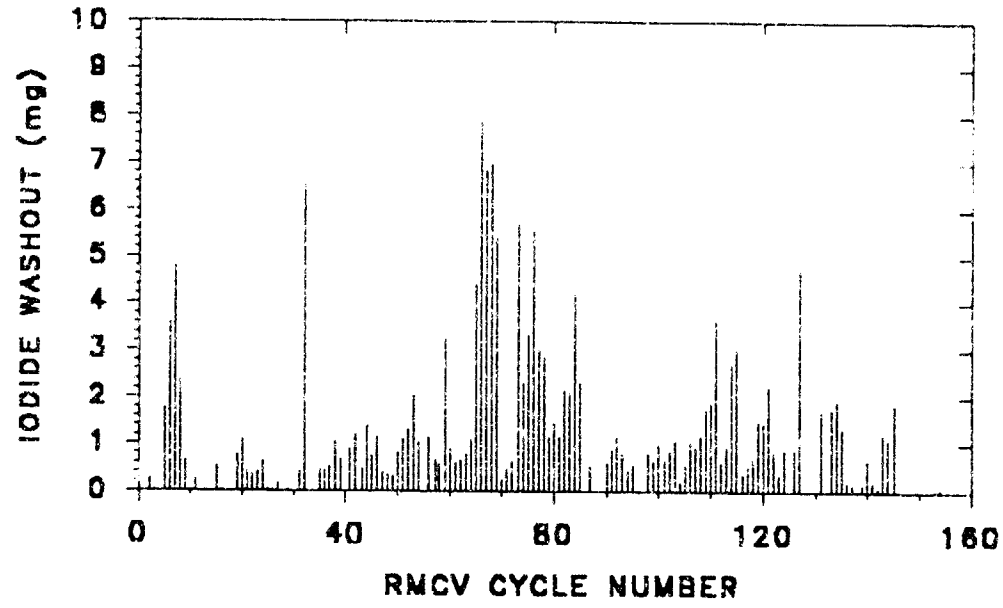

Figure 5.9 Cyclic I^- Depletion - Ersatz Reclaimed Potable Water.

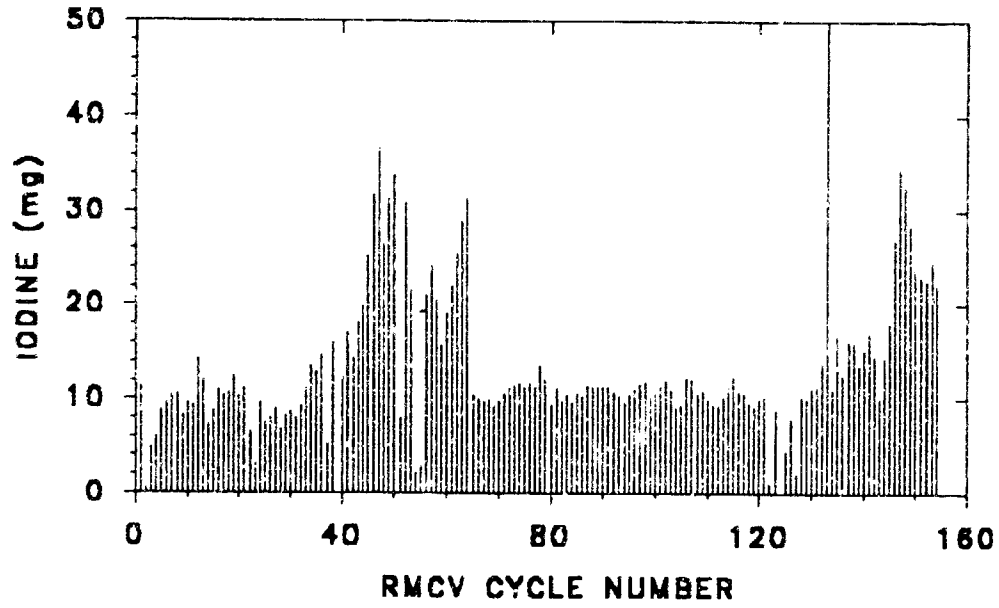

Figure 5.10 I_2 Depletion During Regeneration - Ersatz Reclaimed Potable Water.

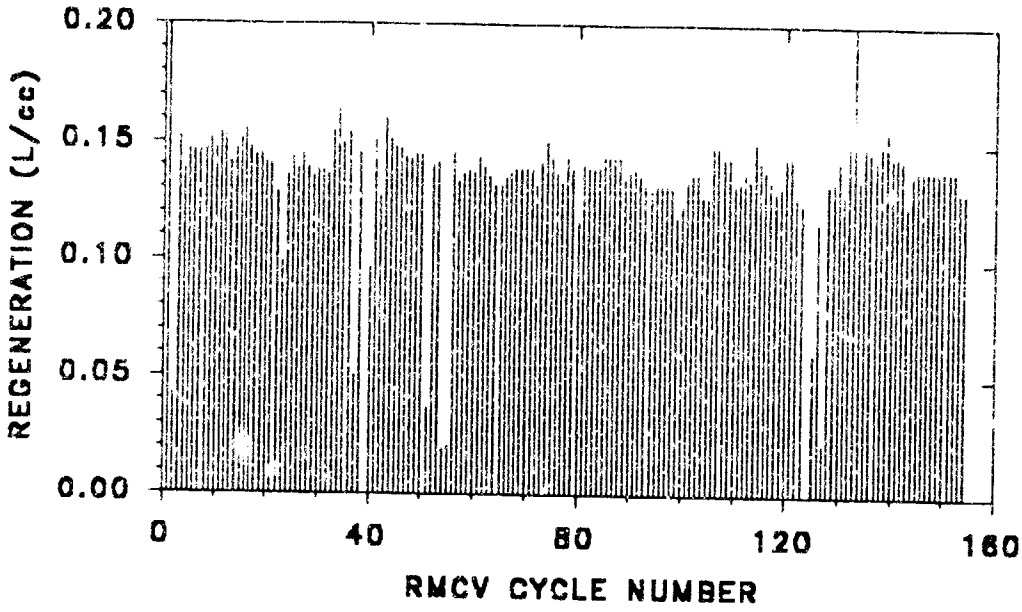

Figure 5.11 Cyclic Throughput During Regeneration - Ersatz Reclaimed Potable Water.

challenge stream at an average concentration of 6.22 mg/L. RMCV-2 experienced 312 cycles of washout and regeneration, with cyclic throughputs varying from 20 L/cm^3 per cycle to less than 1 L/cm^3 per cycle, for an overall average cyclic throughput of 7.67 L/cm^3.

The life cycle test histories for RMCV-2 are shown in Figures 5.12, 5.13, 5.14, 5.15, and 5.16, which present the first, second, third, fourth, and fifth 500 L-cm^{-3} increments of flow history respectively.

During the shakedown period, corresponding to the first 250 L/cm^3 of throughput, RMCV-2 exhibited erratic behavior. Once system hardware and software were debugged, stable operation was achieved. System upsets occured with greater frequency for this challenge stream than for any other. These were usually manifested in the form of low flow rates and correspondingly high back pressures caused by accumulated particulate matter in the glass wool at the inflow face of the MCV. This also occasionally caused the partial or

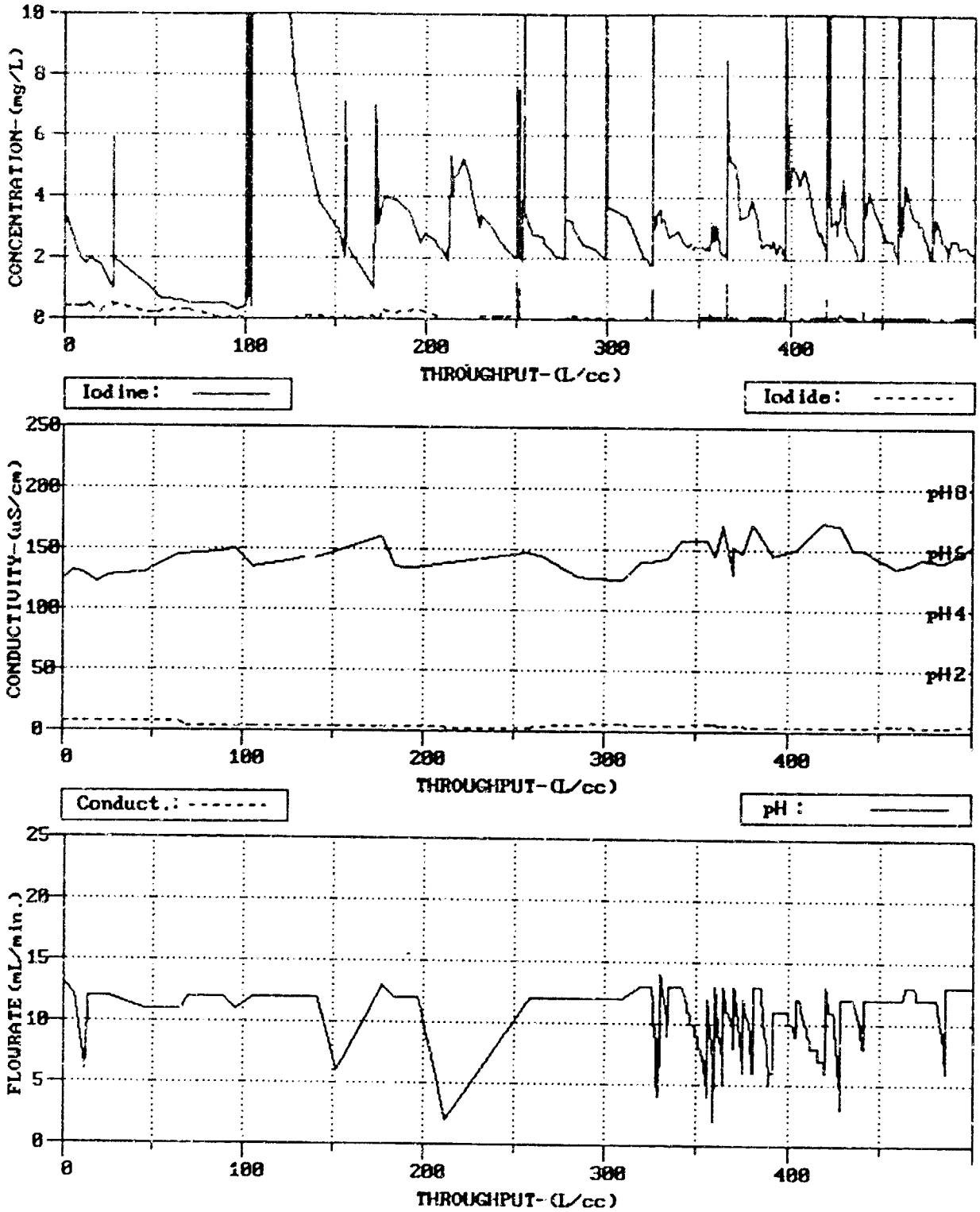

Figure 5.12 RMCV Life Cycle Test - Ersatz Reclaimed Hygiene Water: 0-500 L/cm^3.

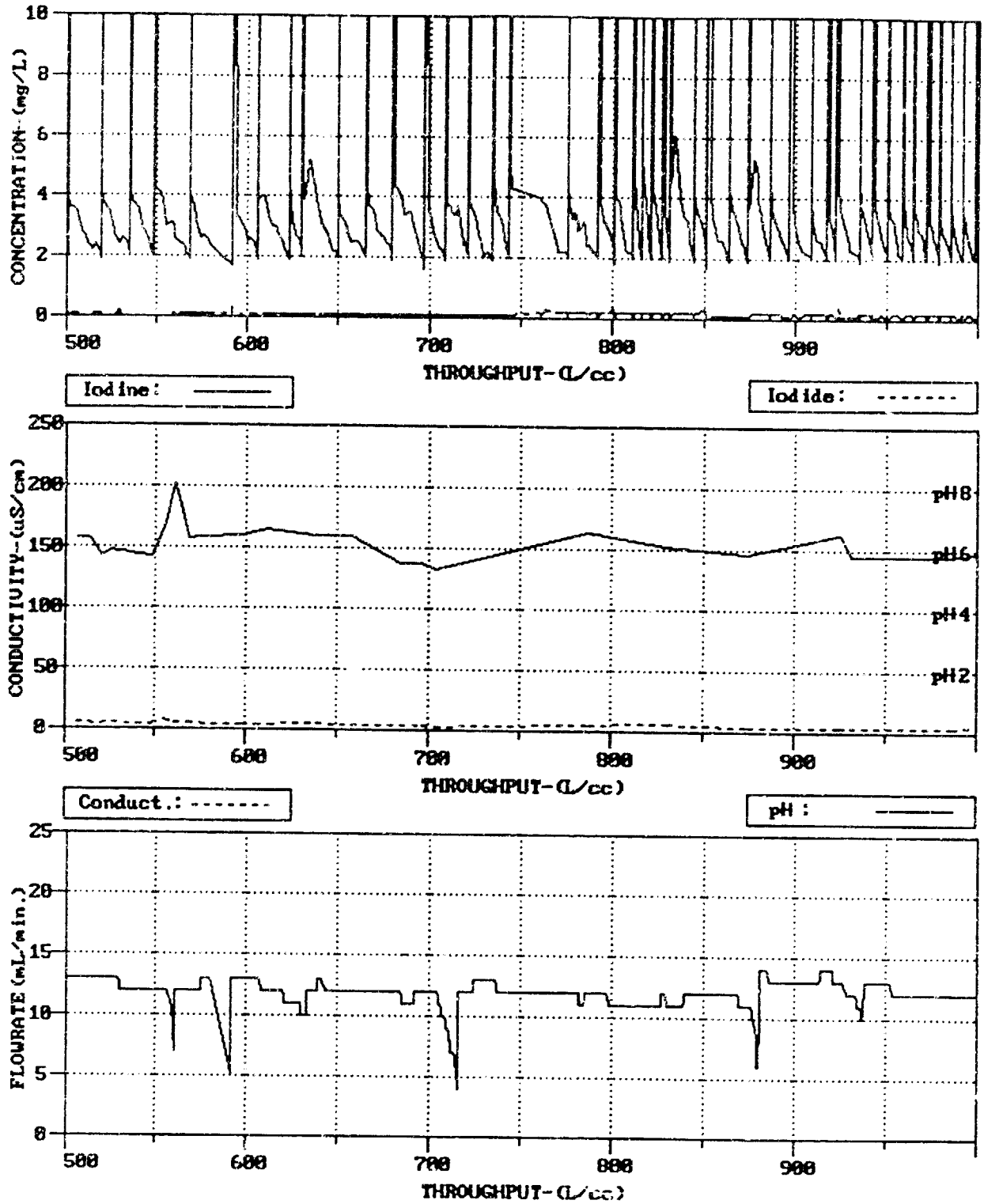

Figure 5.13 RMCV Life Cycle Test - Ersatz Reclaimed Hygiene Water 500-1000 L/cm^3.

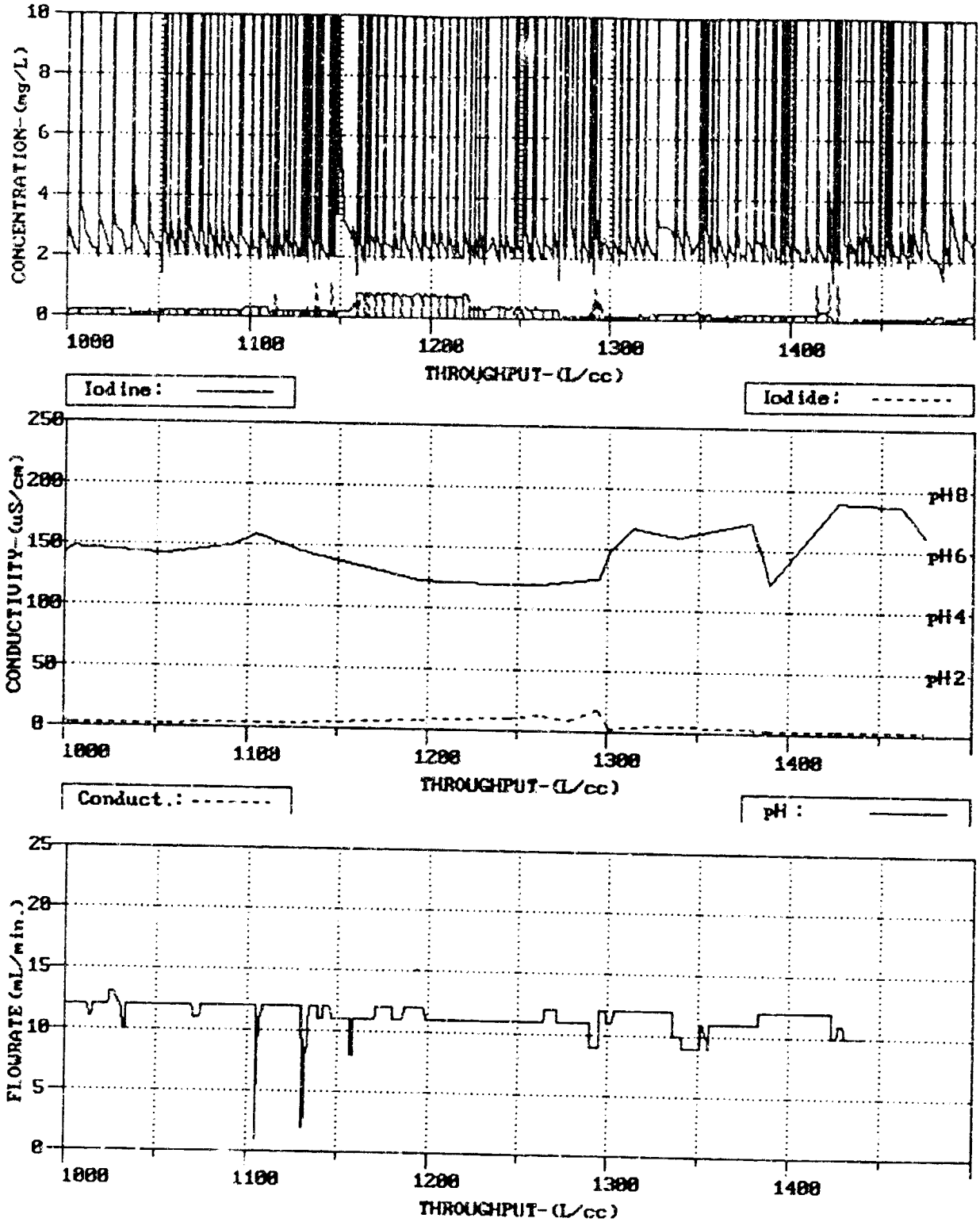

Figure 5.14 RMCV Life Cycle Test - Ersatz Reclaimed Hygiene Water 1000-1500 L/cm^3.

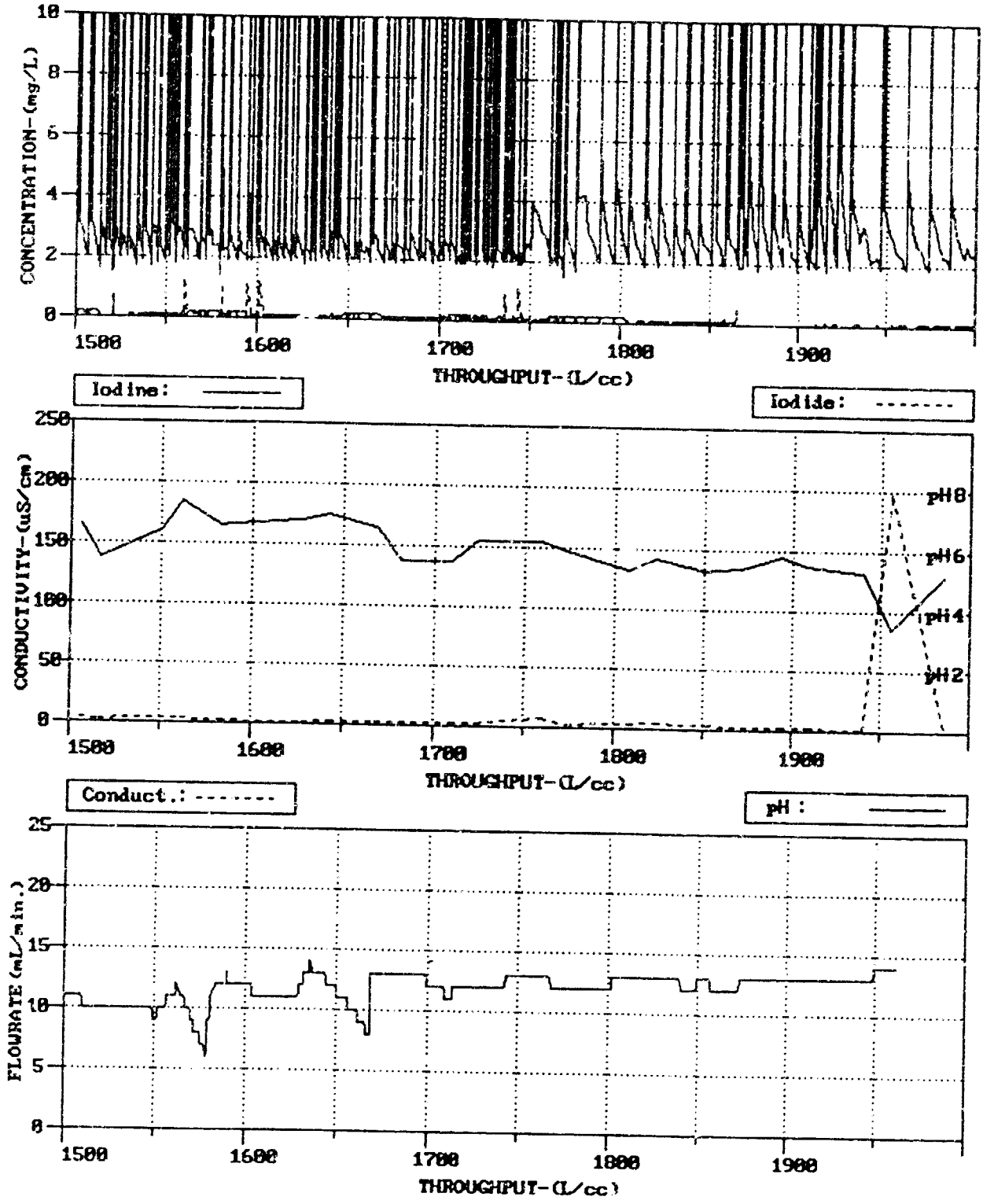

Figure 5.15 RMCV Life Cycle Test - Ersatz Reclaimed Hygiene Water: 1500-2000 L/cm^3

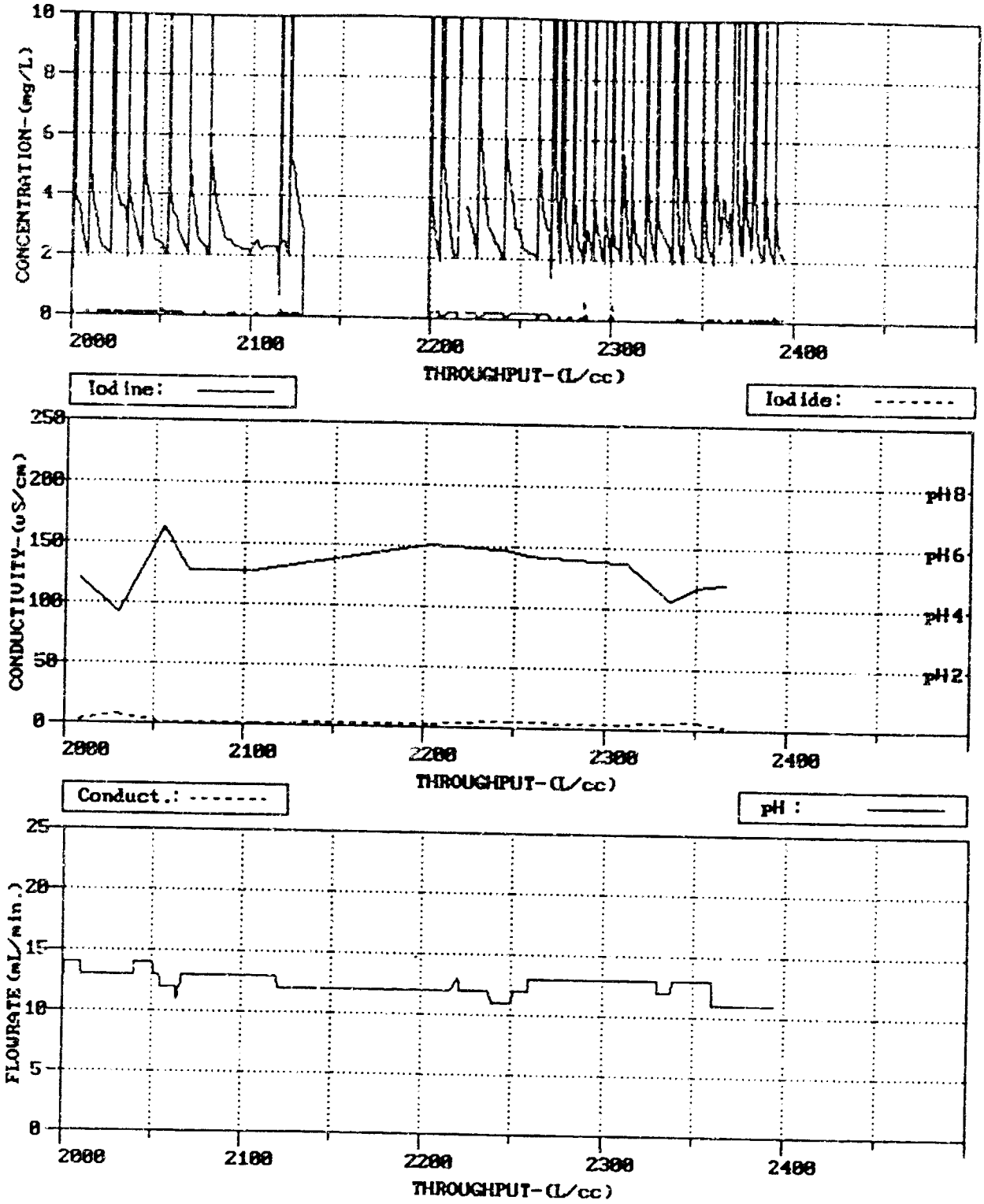

Figure 5.16 RMCV Life Cycle Test - Ersatz Reclaimed Hygiene Water: 2000-2394 L/cm^3.

complete loss of flow due to leaks.

For RMCV-2 regenerations were given a minimum duration of 50 minutes, after which regeneration was terminated by an I_2 concentration greater than 10 mg/L. At 120 minutes regenerations were programmed to terminate irrespective of the effluent I_2 concentration. This feature was never invoked in the control of RMCV-2

The shortening of cyclic throughputs and the corresponding increase in frequency of regeneration with the passage of time is more evident for the RMCV serving the ersatz reclaimed hygiene water challenge stream than for any other. By approximately 1050 L/cm^3, cyclic throughput had diminished to between 5 - 7 L/cm^3, and then further decreased to less than 1 L/cm^3 after 1720 L/cm^3 of cumulative flow. This drastic reduction in cyclic throughput corresponded to the depletion of the I_2 crystal bed which was re-packed with 10 cm^3 of crystalline I_2 at the 1770 L/cm^3 mark. Cyclic throughputs of 6 - 7 L/cm^3 resulted.

At approximately 1950 L/cm^3, an experiment was conducted on RMCV-2 testing the hypothesis that the extremely high regeneration frequency noted for this unit is attributable to loss of I^- from the MCV resin anionic sites, causing a reduction in I_2 loading capacity. A single regeneration was conducted in which the I_2 crystal bed was bypassed and a 1 g/L KI solution was allowed to flow through the MCV at a flow rate of approximately 10 cm^3/min. This attempt to replace lost I^- was then followed by a conventional regeneration. For the 300 L/cm^3 of cumulative flow following this experiment, cyclic throughputs in the range of 10 - 13 were exhibited. However, by the 2270 L/cm^3 mark the cycles had narrowed once again to the 6 - 7 L/cm^3 range. Flow to RMCV-2 was terminated at 2393.6 L/cm^3.

Cyclic I_2 depletion, cyclic I^- depletion, and cyclic throughput versus cycle number are illustrated in Figures 5.17, 5.18, and 5.19 respectively. MCV resin I_2 depletion and throughput during the regeneration phase of RMCV-2 operation versus cycle number are illustrated in Figures 5.20 and 5.21 respectively.

The high average I_2 concentration of > 6 mg/L in the MCV effluent is a direct

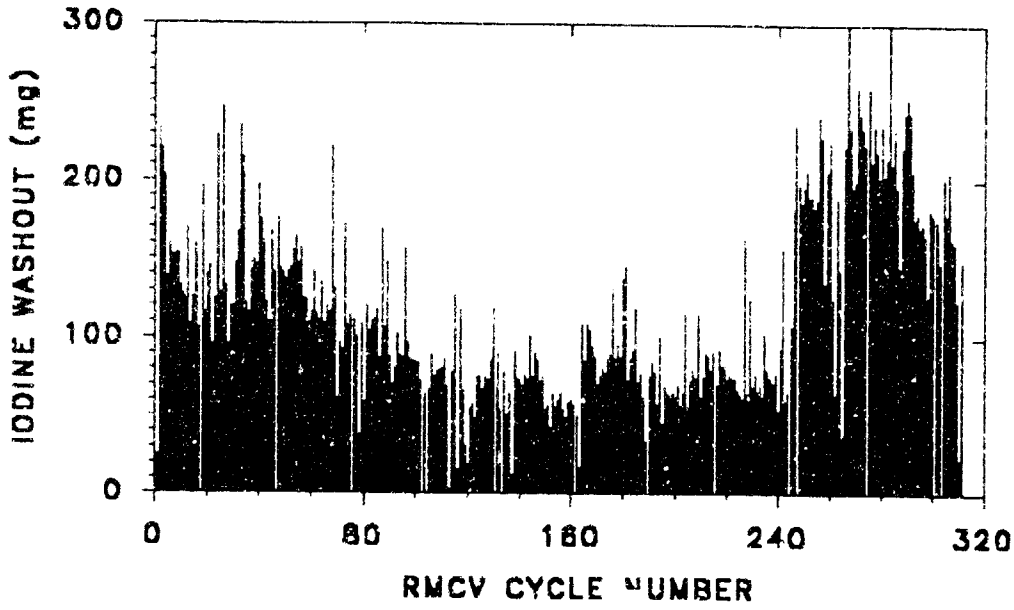

Figure 5.17 Cyclic I_2 Depletion - Ersatz Reclaimed Hygiene Water.

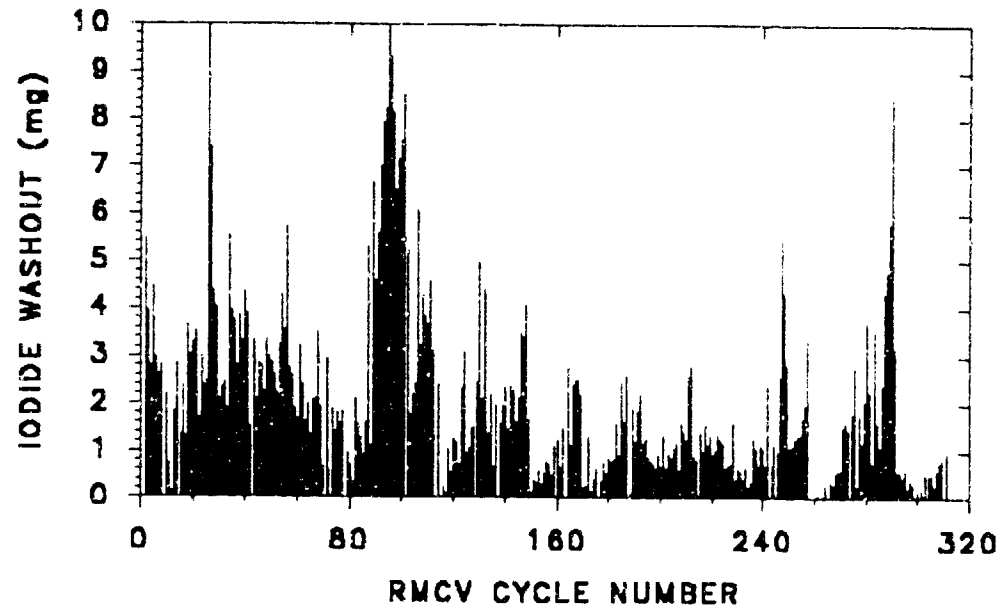

Figure 5.18 Cyclic I^- Depletion - Ersatz Reclaimed HygieneWater.

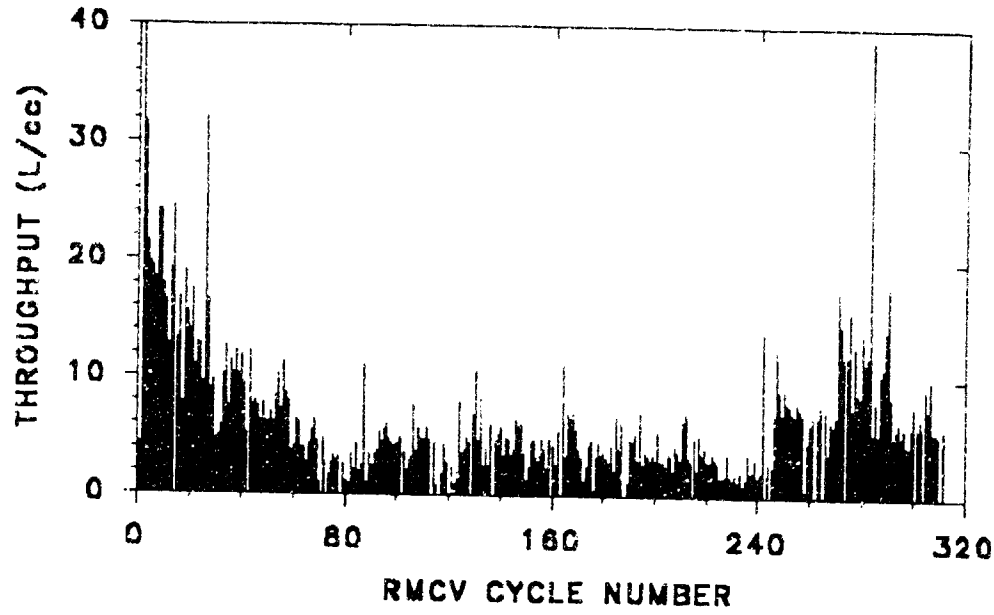

Figure 5.19 Cyclic Throughput - Ersatz Reclaimed Hygiene Water.

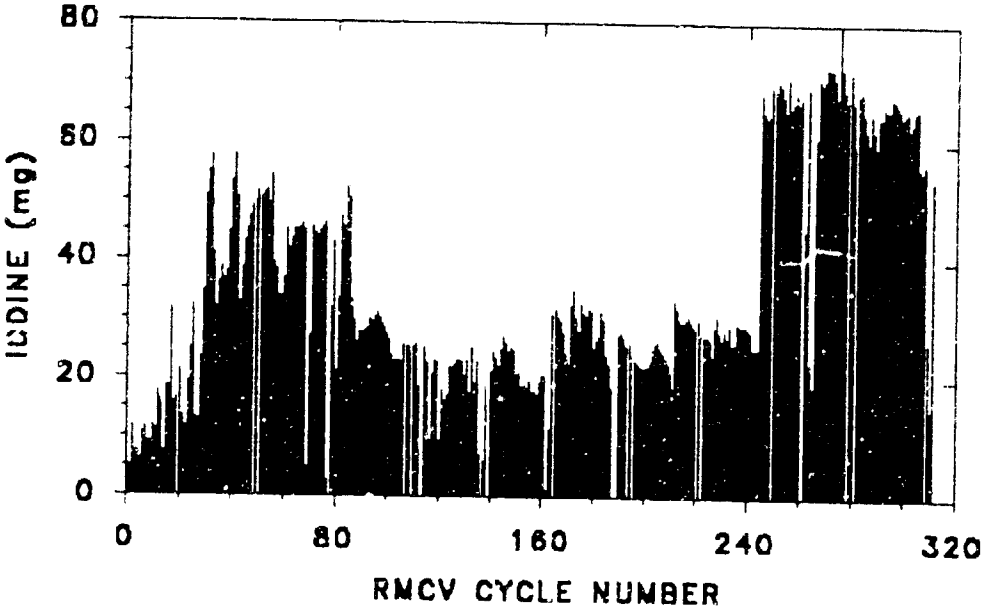

Figure 5.20 Cyclic I_2 Depletion During Regeneration- Ersatz Reclaimed Hygiene Water.

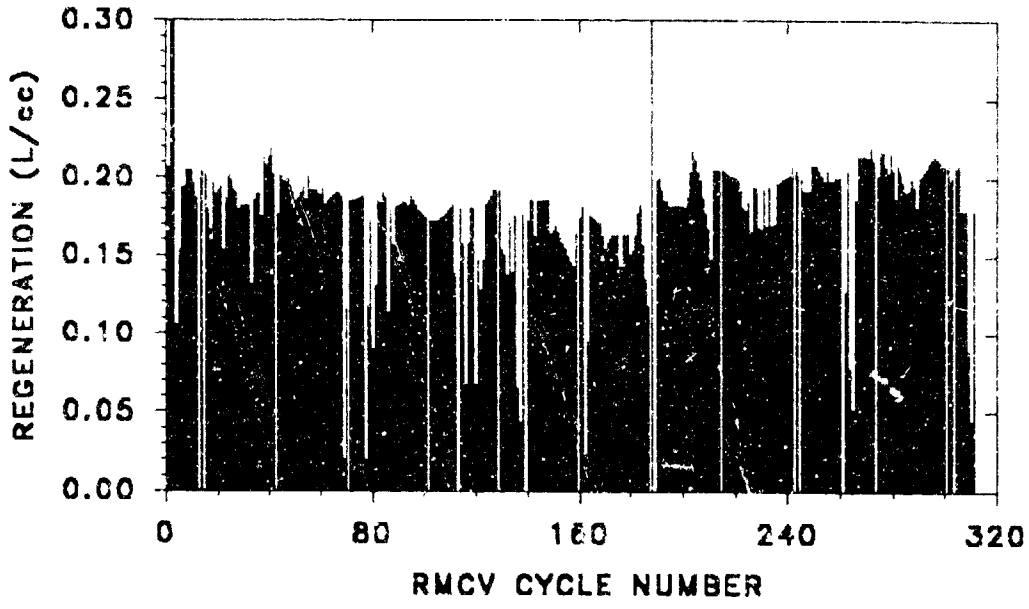

Figure 5.21 Cyclic Throughput During Regeneration - Ersatz Reclaimed Hygiene Water.

consequence of the extremely high frequency of regenerations for this unit. While control of I_2 levels to between 2.0 - 4.0 mg/L in the washout phase of the cycle was generally good, the transient spikes of higher concentration encountered during regeneration contributed proportionally more to the total cyclic I_2 depletion than for any other challenge stream. As will be discussed in greater detail in Section 6, this transient during regeneration is largely a phenomenon of the residence time of the strong I_2 regeneration liquor within the MCV resin bed. The life history data indicate clearly that a greater MCV residence time is required to achieve an acceptable level of RMCV performance using the ersatz reclaimed hygiene water as challenge solution.

5.3 RMCV-3: Ersatz Humidity Condensate.

The RMCV serving the ersatz humidity condensate challenge stream was designated

2 OF 4

N93-27122 UNCLAS

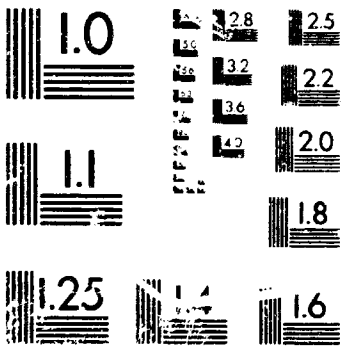

as RMCV-3. During the course of the long term life cycle testing this unit accumulated 2,533 L/cm^3 of total throughput. The average pH of the MCV effluent was 3.4. More than 19 grams of I_2 were transfered to the challenge stream at an average concentration of 3.06 mg/L. RMCV-3 went through 218 cycles of washout and regeneration, with cyclic throughputs varying from 15 L/cm^3 per cycle to 5 L/cm^3 per cycle, for an overall average cyclic throughput of 11.6 L/cm^3. Using the MCV design value of 20 L/cm^3, this constitutes a 126 fold extension of MCV life.

The life cycle test histories for RMCV-3 are shown in Figures 5.22, 5.23, 5.24, 5.25, 5.26, and 5.27, which present the first, second, third, fourth, fifth, and sixth 500 L-cm^{-3} increments of flow history respectively.

The shakedown period for RMCV-3 lasted roughly 180 L/cm^3, after which stable operation was achieved. Regenerations for this unit were given a minimum duration of 50 minutes, after which regeneration was terminated by an I_2 concentration greater than 10 mg/L. At approximately 280 L/cm^3 RMCV-3 over-regenerated due to a disruption of flow to the on-line I_2 monitor. Subsequently, a maximum regeneration time of 120 minutes was coded into the RMCV.EXE master control program for this unit.

As with the other RMCVs, the predominant trend with increasing cumulative flow was the gradual lessening of cyclic throughput. Significantly, from the outset the RMCV serving the ersatz humidity condensate exhibited a higher frequency of regeneration than those of the other challenge streams. Also the decrease in cyclic throughput was less pronounced than that of other streams, becoming most significant at the 1100 L/cm^3 mark. In conjunction with the increased frequency of regeneration noted at this time, was also the observed presence within the MCV resin bed of particulate matter which created back pressure sufficient to make the Tygon tubing bulge. At 1300 L/cm^3 of cumulative throughput, RMCV-3 was taken out of service and the particulate matter removed by rinsing with DI water. The RMCV was placed back in service with an immediate corresponding increase in cyclic throughput from 5.5

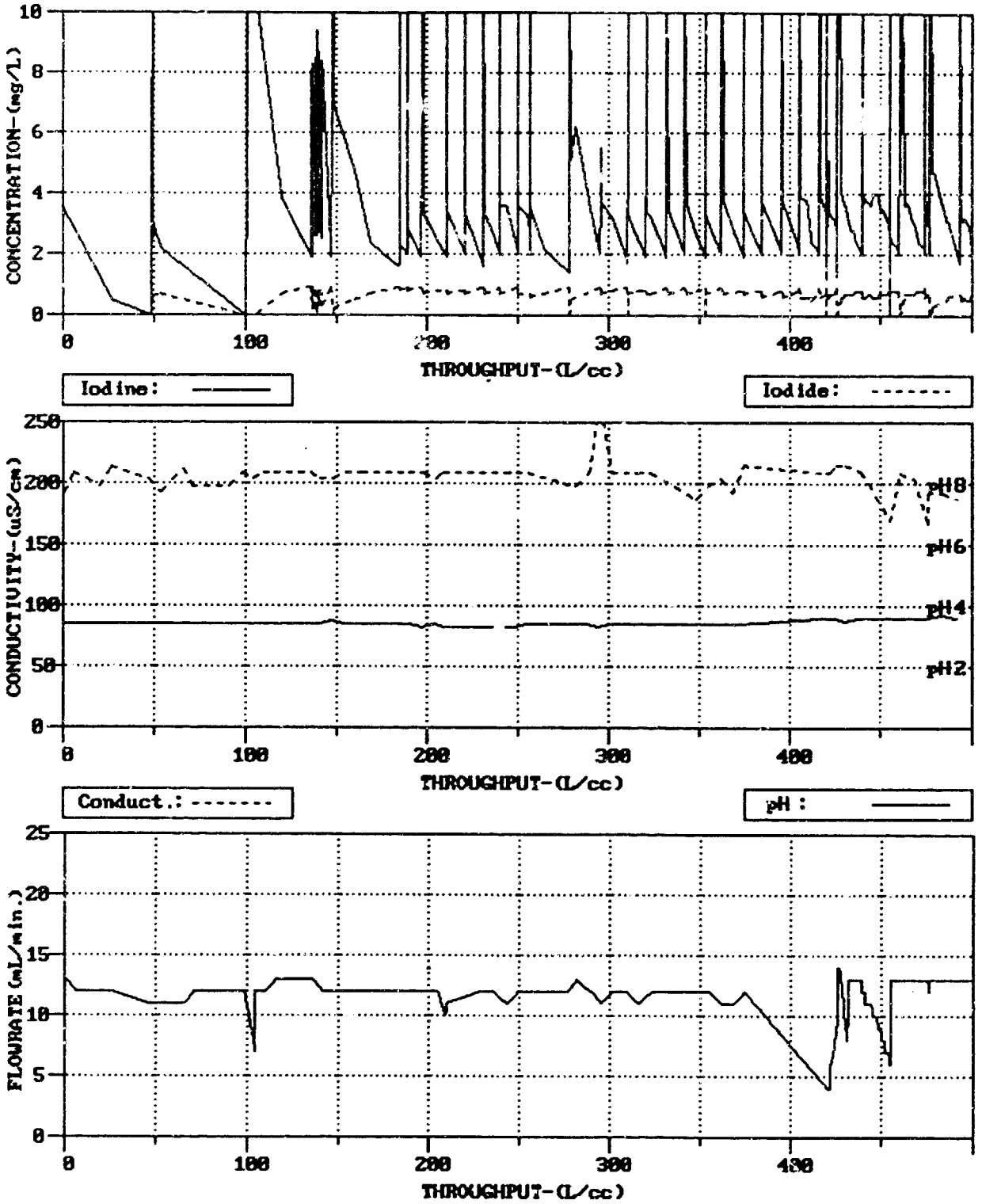

Figure 5.22 RMCV Life Cycle Test - Ersatz Humidity Condensate: 0-500 L/cm^3.

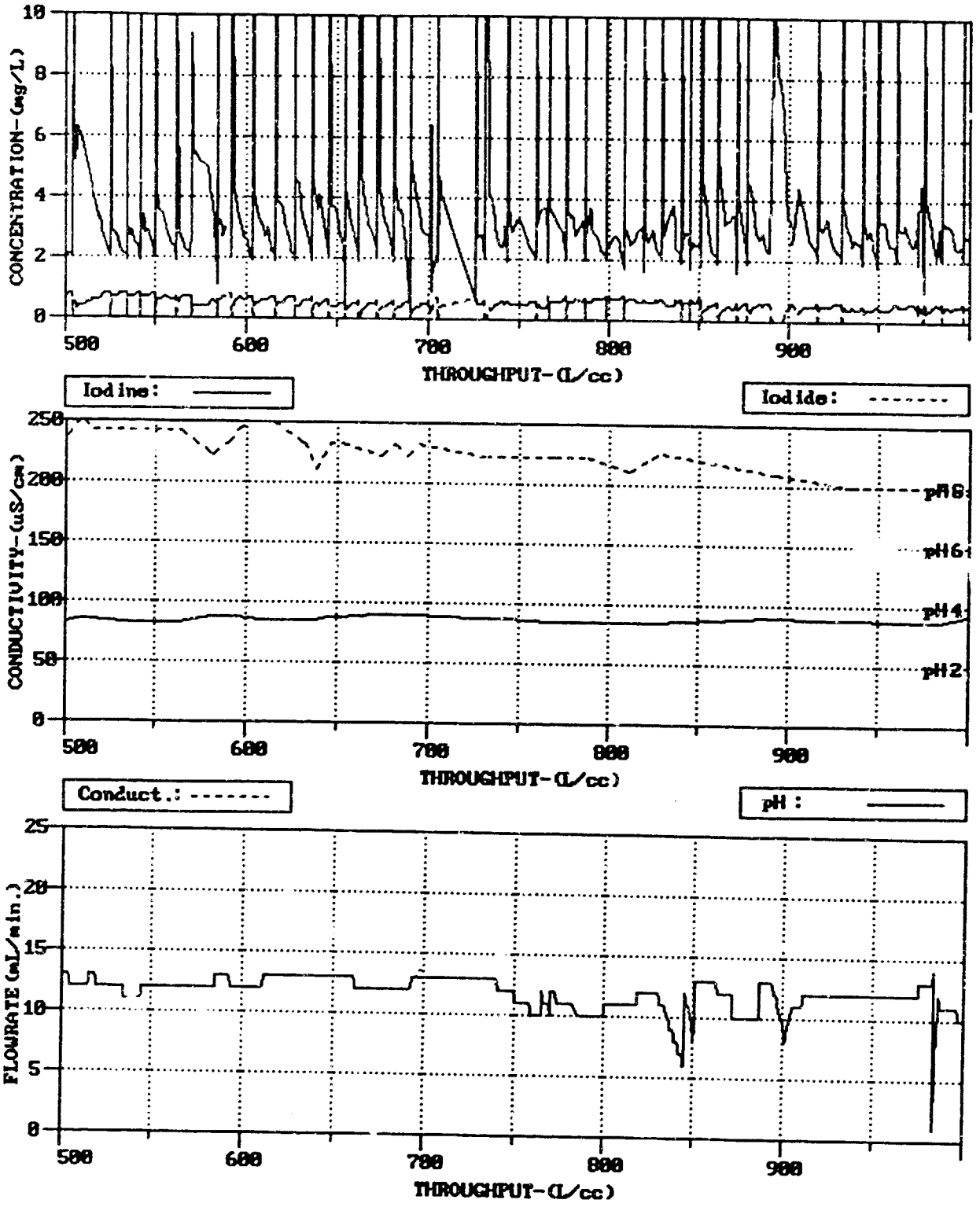

Figure 5.23 RMCV Life Cycle Test - Ersatz Humidity Condensate: 500-1000 L/cm^3.

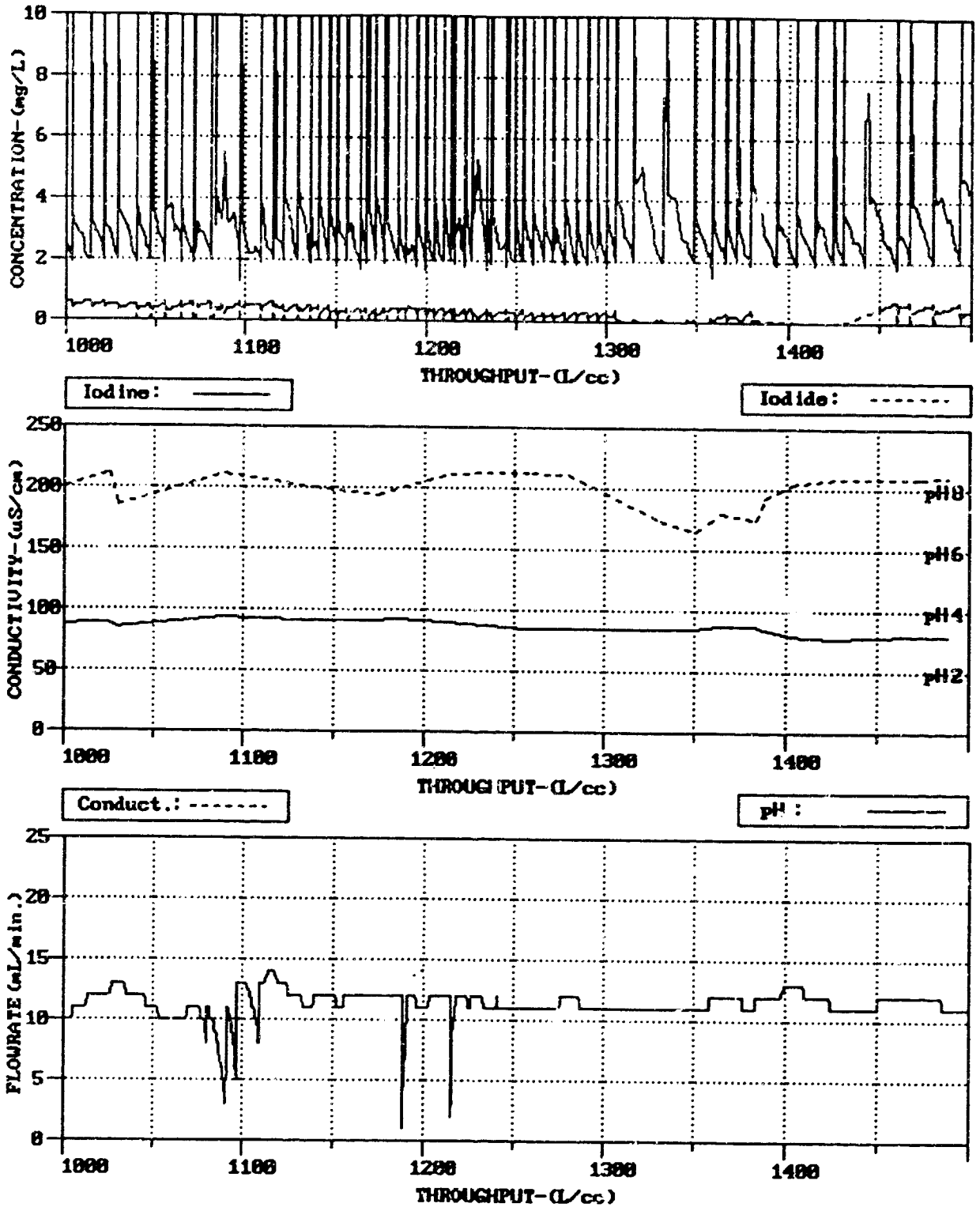

Figure 5.24 RMCV Life Cycle Test - Ersatz Humidity Condensate:1000-1500 L/cm^3.

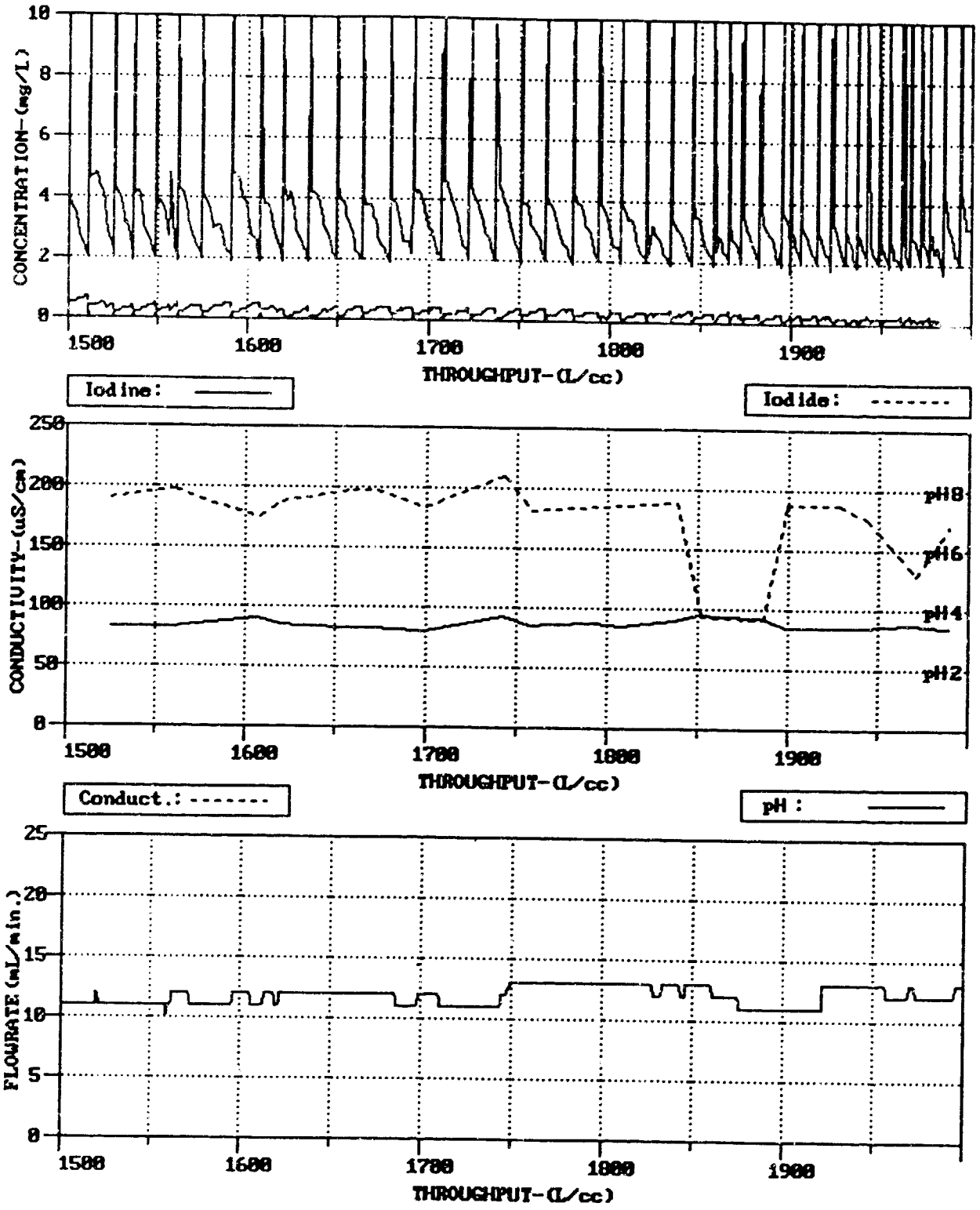

Figure 5.25 RMCV Life Cycle Test - Ersatz Humidity Condensate: 1500-2000 L/cm^3.

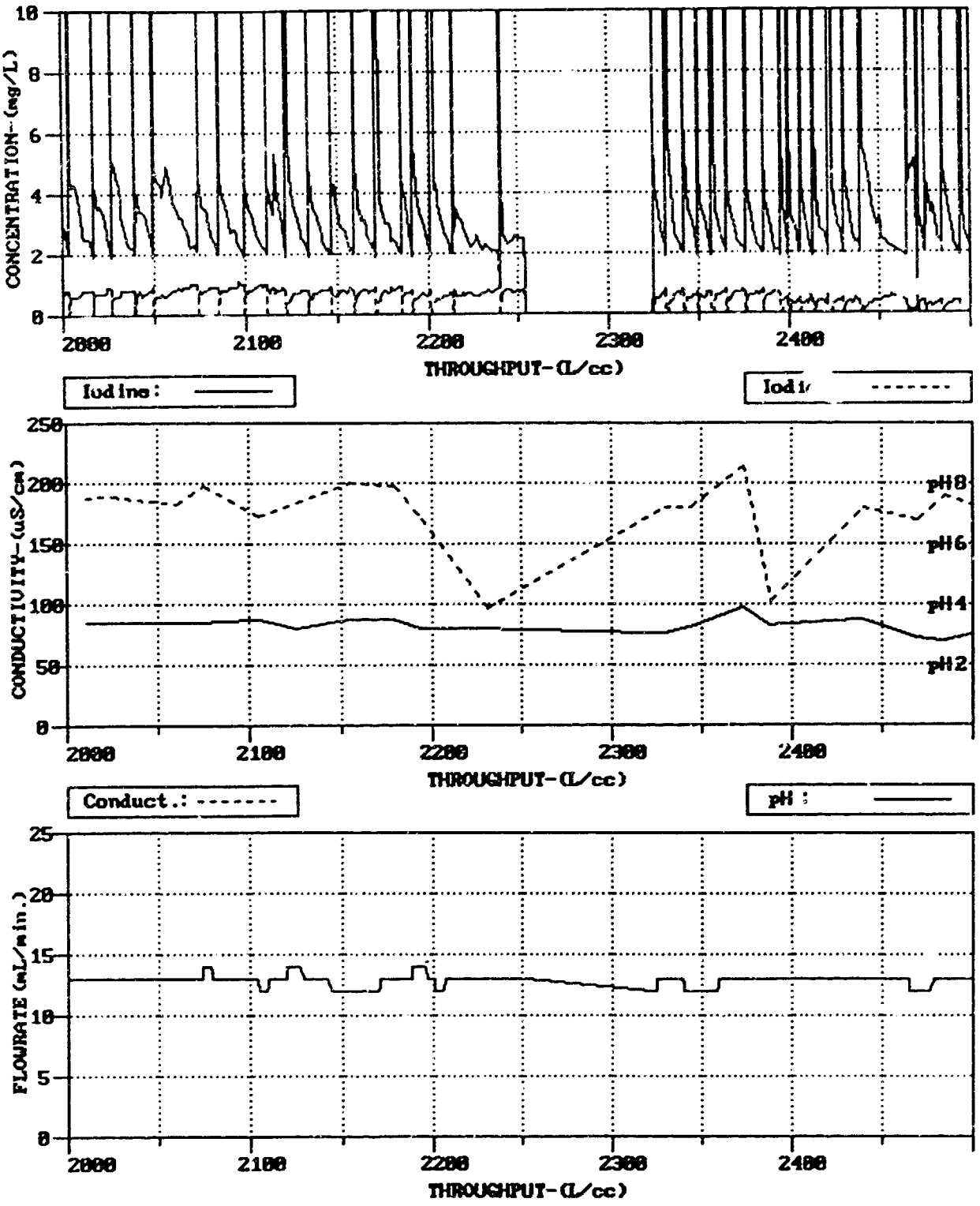

Figure 5.26 RMCV Life Cycle Test - Ersatz Humidity Condensate:2000-2500 L/cm^3.

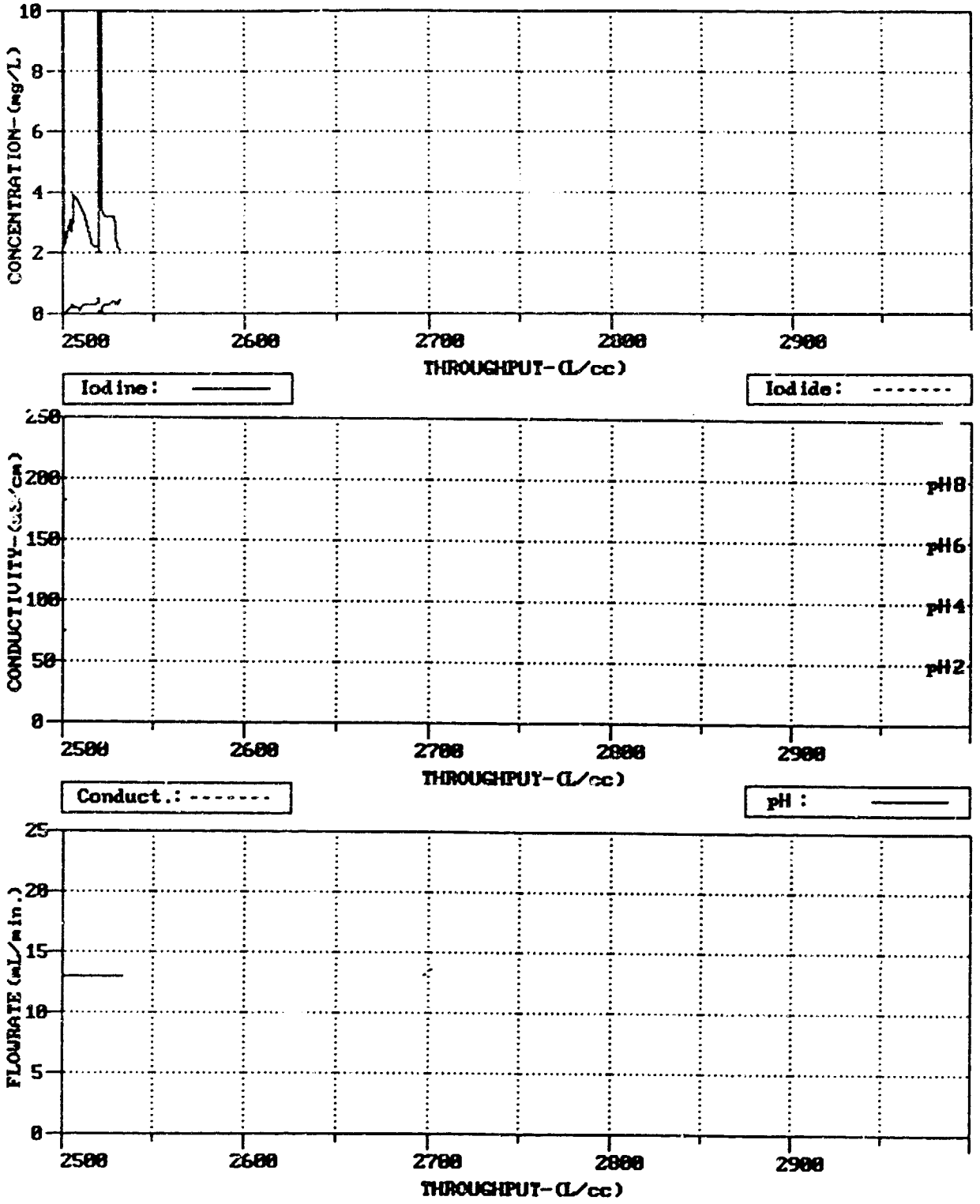

Figure 5.27 RMCV Life Cycle Test - Ersatz Humidity Condensate: 2500-2533 L/cm^3.

L/cm^3 to approximately 14 L/cm^3.

By 1900 L/cm^3 the cyclic throughput had once again narrowed to 6 - 8 L/cm^3 due to depletion of the iodine crystal bed. Replenishment of the crystal bed with 10 cm^3 of iodine resulted in an immediate lengthening of the washout period and a corresponding reduction in regeneration frequency. Iodine concentrations between 2255 - 2325 L/cm^3 were not recorded due to operator error. Flow to RMCV-3 was terminated at 2533..05 L/cm^3.

Cyclic I_2 depletion, cyclic I^- depletion, and cyclic throughput versus cycle number are illustrated in Figures 5.28, 5.29, and 5.30 respectively. MCV resin I_2 depletion and throughput during the regeneration phase of RMCV operation versus cycle number are illustrated in Figures 5.31 and 5.32 respectively. Cyclic I_2 depletion correlates well with the observed trend in cyclic throughput. Three maxima in both cyclic throughput and cyclic I_2 depletion correspond to the initial MCV state, improved performance following removal of particulates from the MCV, and improved performance following re-loading the iodine crystal bed.

Additionally, with the RMCV serving the humidity condensate challenge stream, significant washout of I^- is exhibited. A total of approximately 2.3 grams of I^- was lost from the MCV during the life cycle tests, for an average concentration of 0.37 mg/L. In large part this is due to the oxidation of formic acid by molecular iodine. This topic is treated in detail in Section 7. Inspection of Figure 5.30 reveals that cyclic I^- depletion correlates well with both cyclic throughput and cyclic I_2 depletion. The higher natural frequency of regenerations exhibited by this RMCV may be in large part due to the additional mechanism for removal of I_2 from the system by reduction to I^-.

5.4 RMCV-4: Ersatz Urine Distillate.

The RMCV serving the ersatz urine distillate challenge stream was designated as RMCV-4. This unit accumulated 2,611.7 L/cm^3 of total throughput, a value higher than

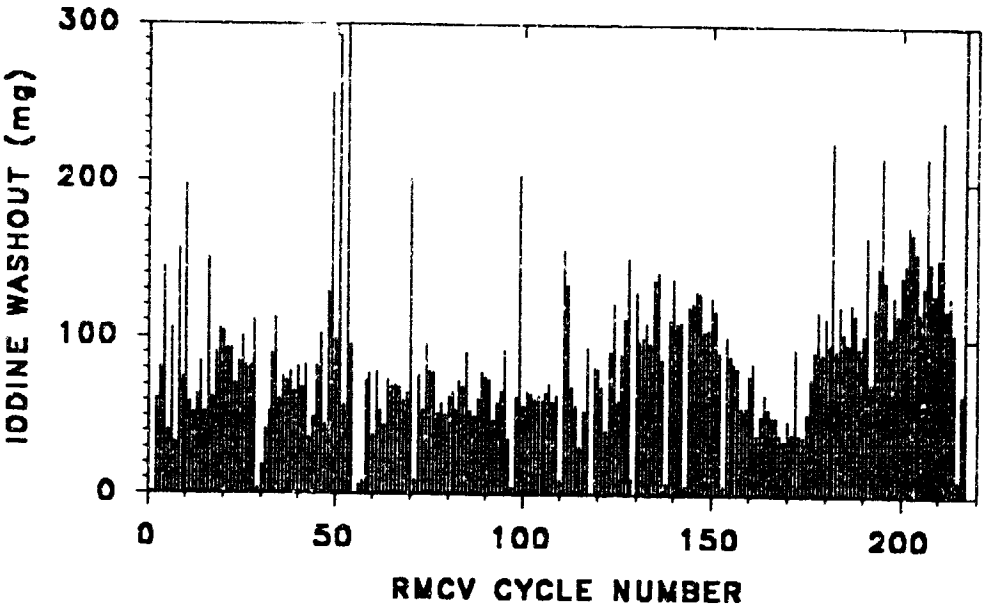

Figure 5.28 Cyclic I_2 Depletion - Ersatz Humidity Condensate.

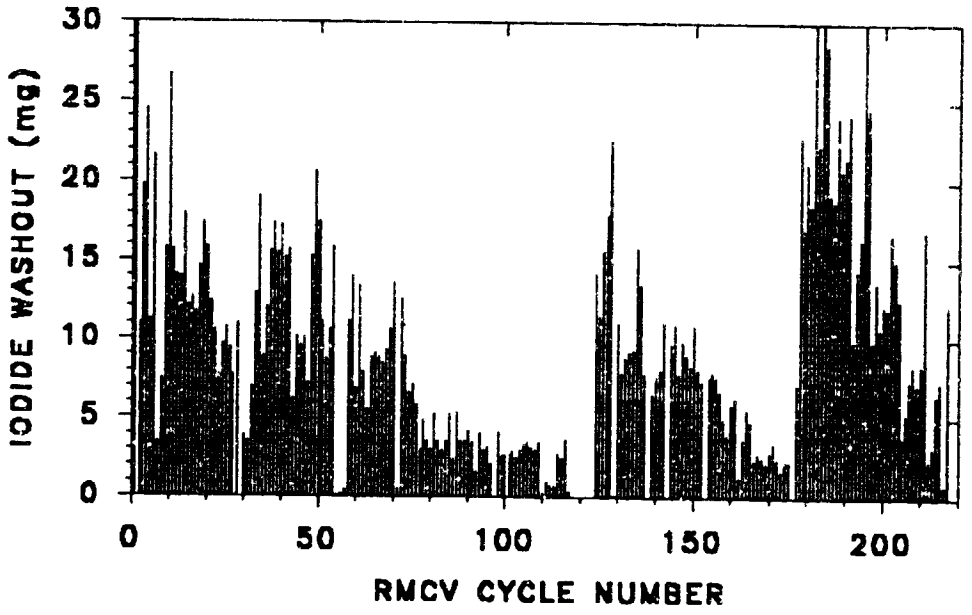

Figure 5.29 Cyclic I^- Depletion - Ersatz Humidity Condensate.

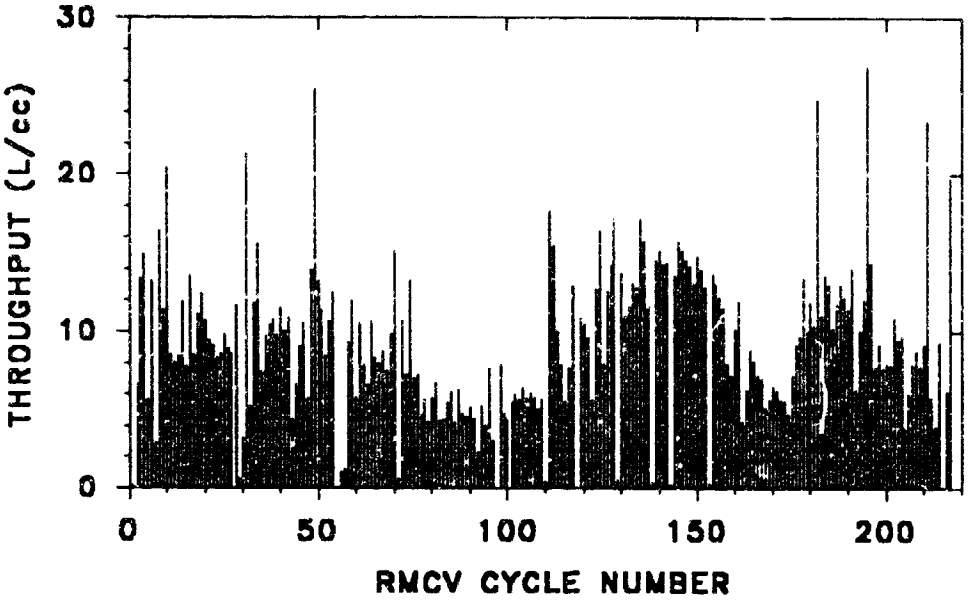

Figure 5.30 Cyclic Throughput - Ersatz Humidity Condensate.

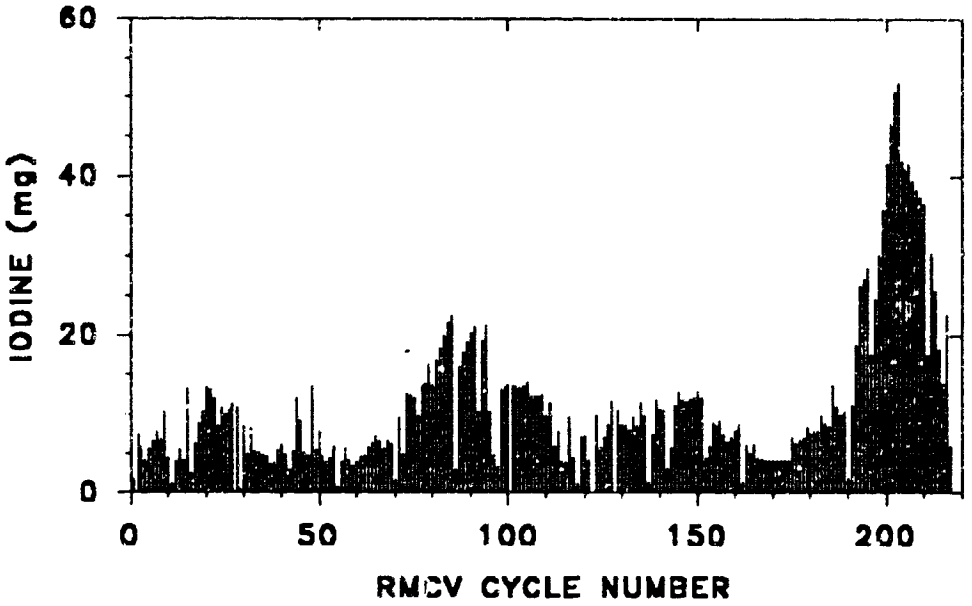

Figure 5.31 Cyclic I_2 Depletion During Regeneration - Ersatz Humidity Condensate.

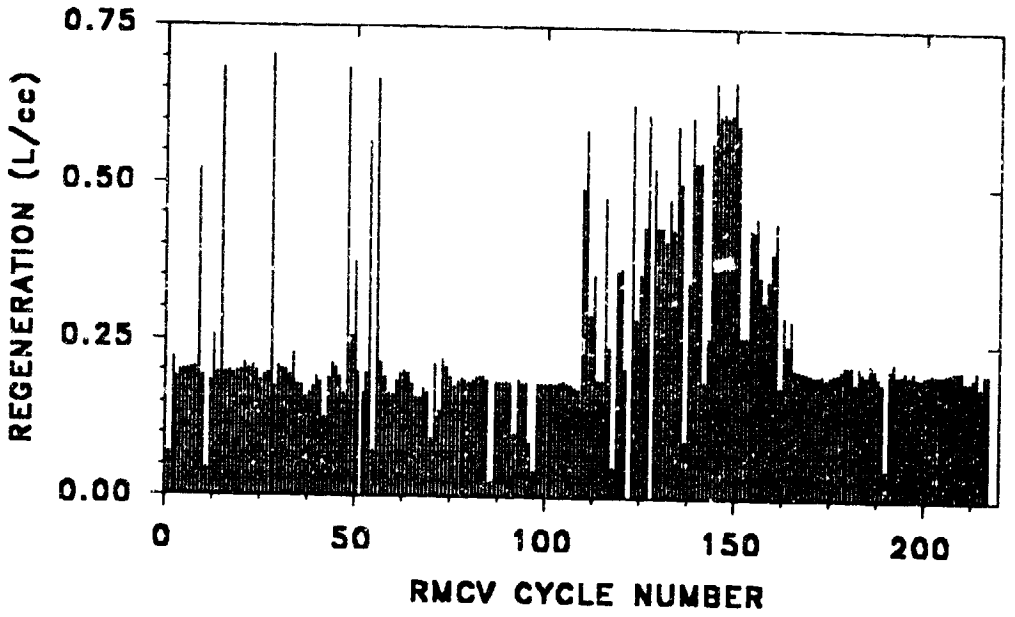

Figure 5.32 Cyclic Throughput during Regeneration - Ersatz Humidity Condensate.

that of any other RMCV. The average pH of the MCV effluent was 3.8. More than 18 grams of I_2 were imparted to the challenge stream at an average concentration of 2.79 mg/L .RMCV-4 operations totalled 176 cycles of washout and regeneration, with cyclic throughputs varying from 20 L/cm^3 per cycle to 7 L/cm^3 per cycle, for an overall average cyclic throughput of 14.8 L/cm^3. Using the MCV design value of 20 L/cm^3, this consitiues a 131 fold extension of MCV life.

RMCV-4 presented the least operational difficulty of any of the RMCVs. This is evident from examination of the life cycle test histories shown in Figures 5.33, 5.34, 5.35, 5.36, 5.37, and 5.38, which present the first, second, third, fourth, fifth, and sixth 500 L-cm^3 increments of flow history respectively.

The shakedown period for RMCV-4 lasted roughly 230 L/cm^3, after which stable

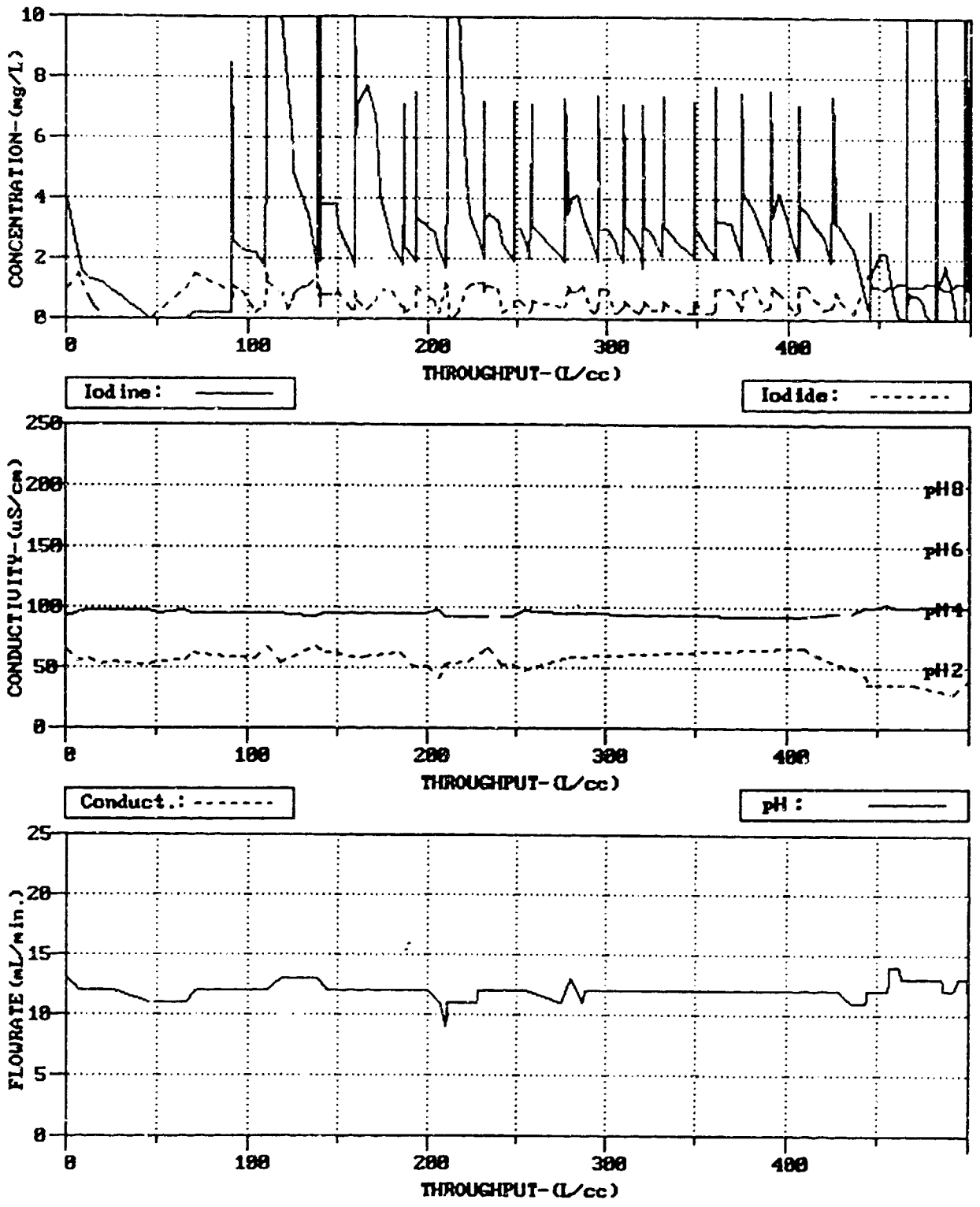

Figure 5.33 RMCV Life Cycle Test - Ersatz Urine Distillate: 0 - 500 L/cm^3.

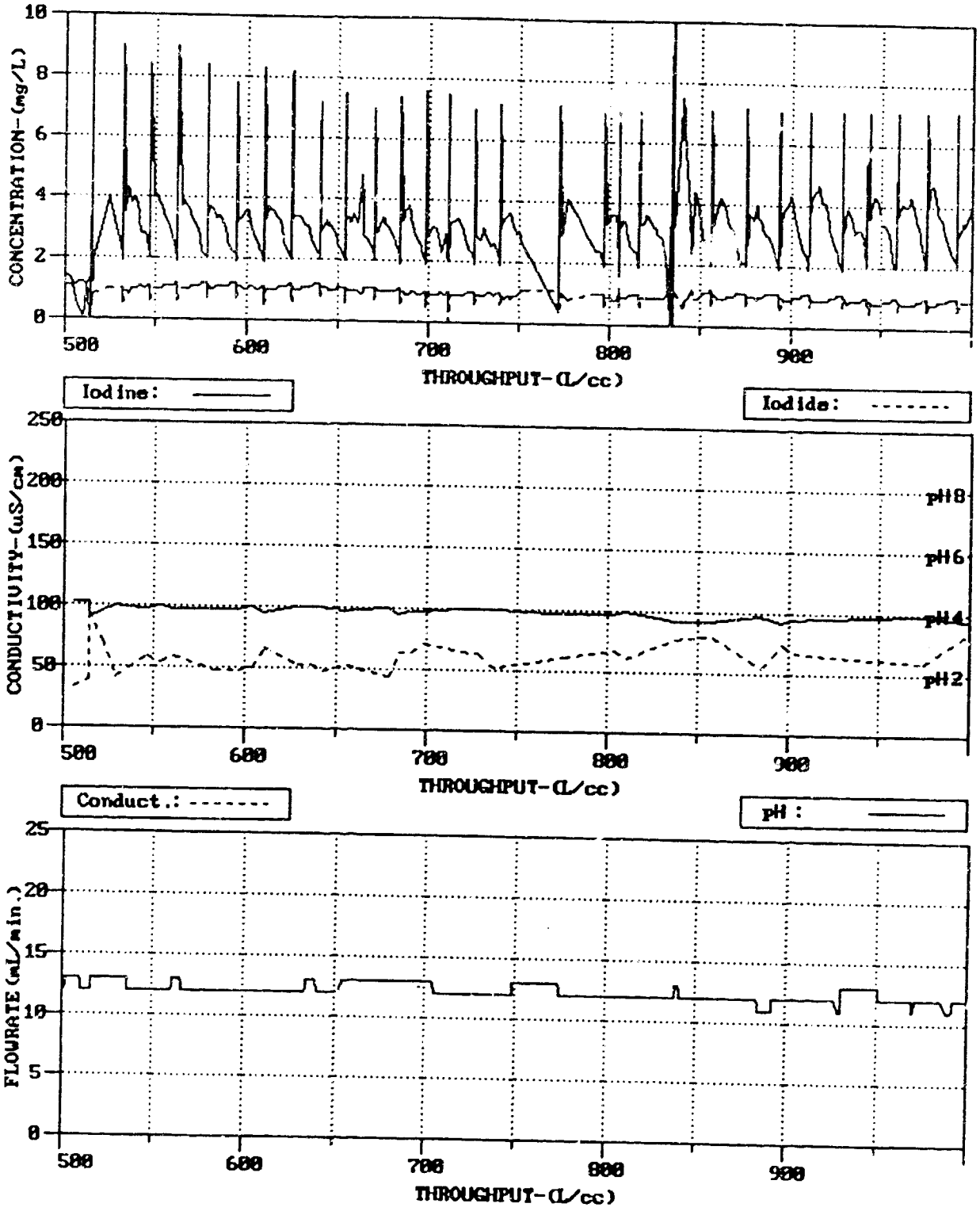

Figure 5.34 RMCV Life Cycle Test - Ersatz Urine Distillate: 500 - 1000 L/cm^3.

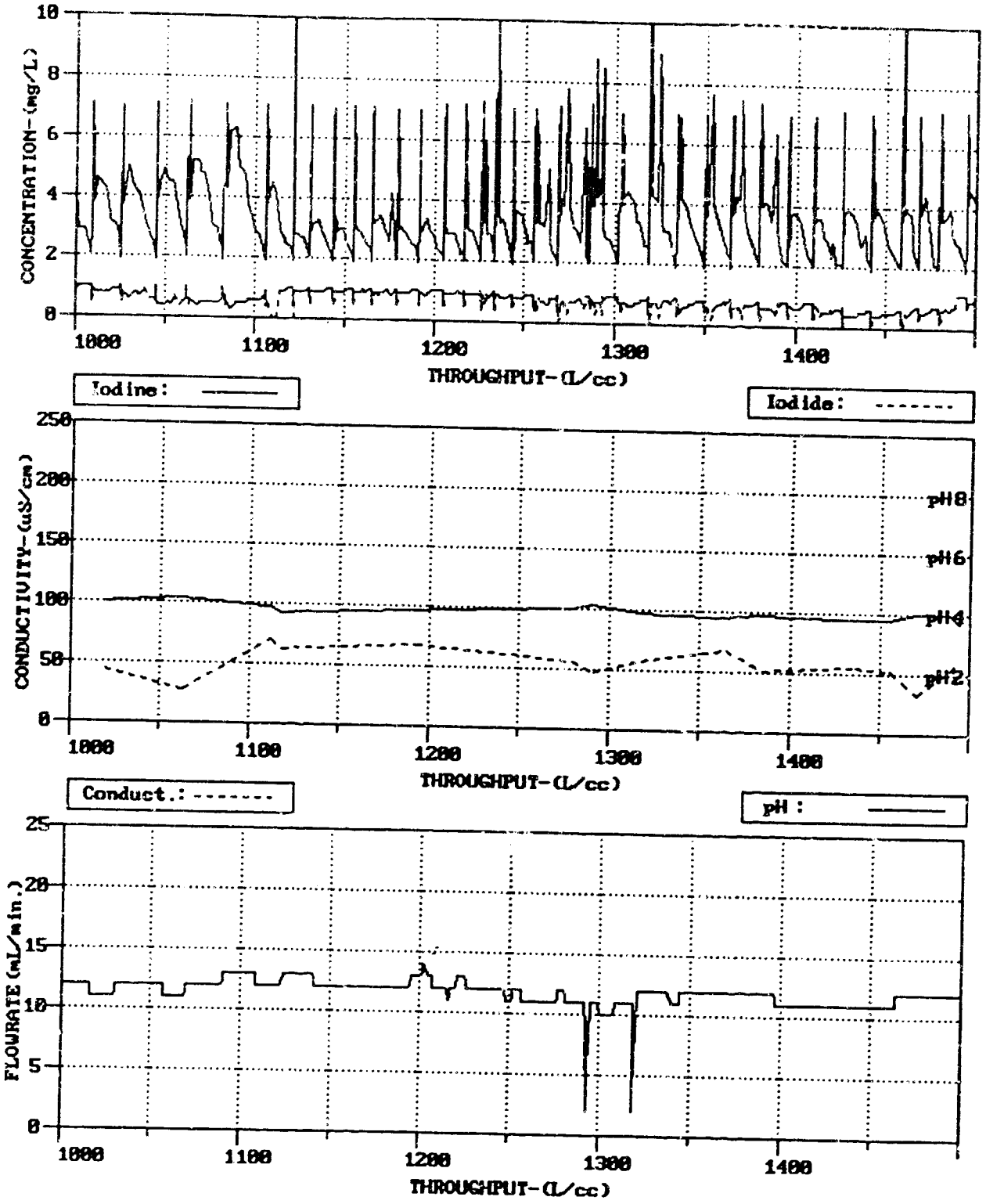

Figure 5.35 RMCV Life Cycle Test - Ersatz Urine Distillate: 1000 - 1500 L/cm^3.

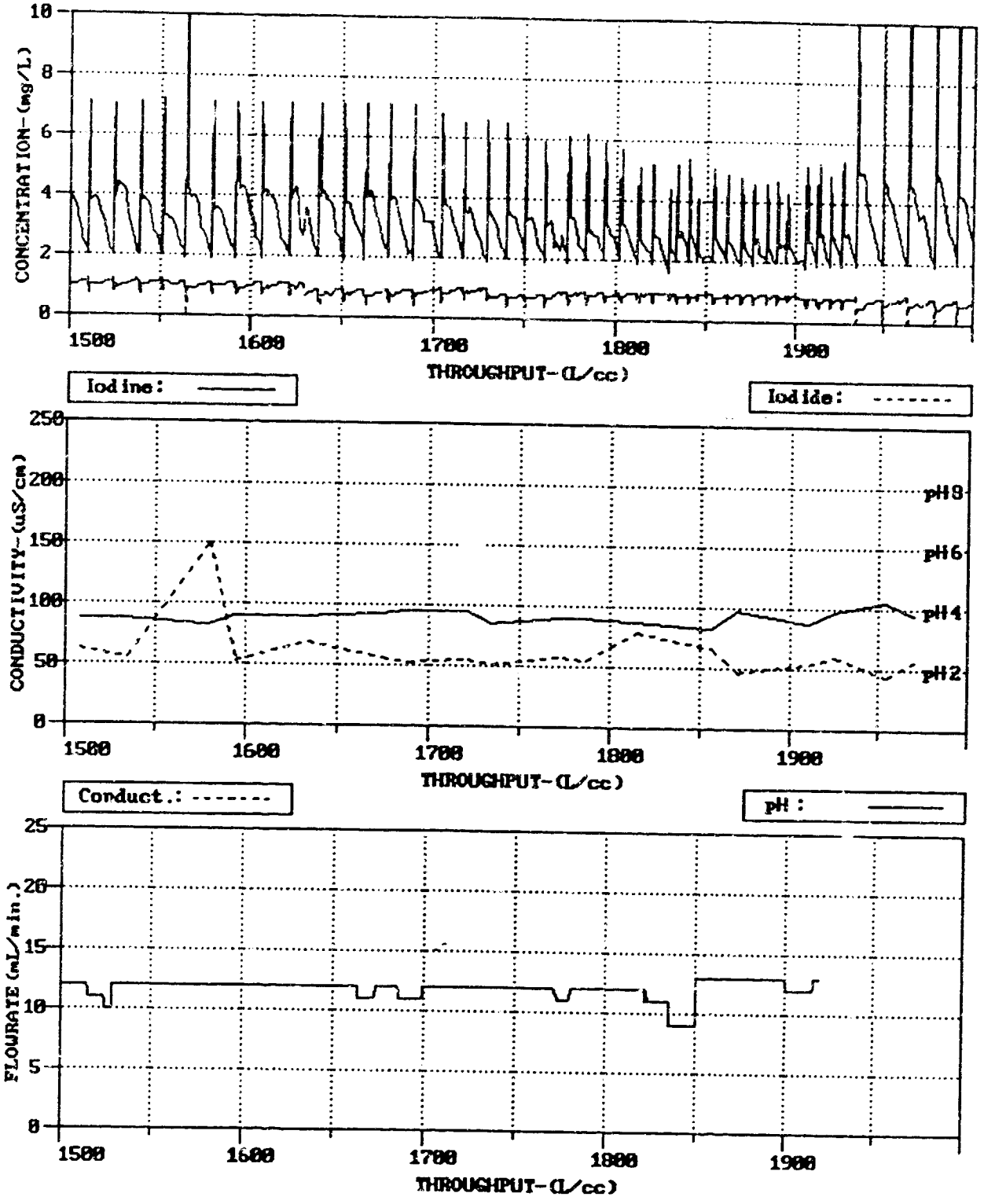

Figure 5.36 RMCV Life Cycle Test - Ersatz Urine Distillate: 1500 - 2000 L/cm^3.

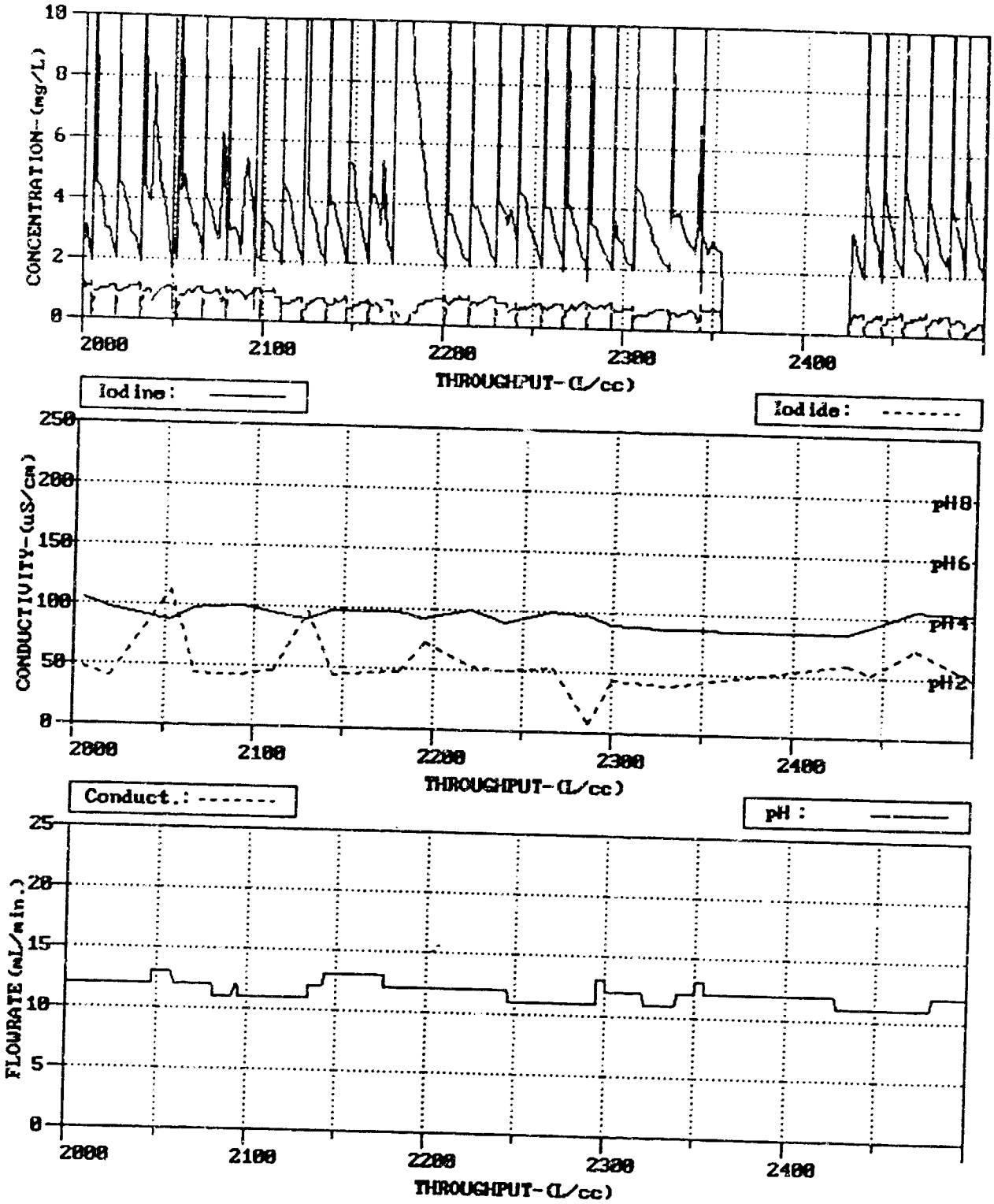

Figure 5.37 RMCV Life Cycle Test - Ersatz Urine Distillate: 2000 - 2500 L/cm^3.

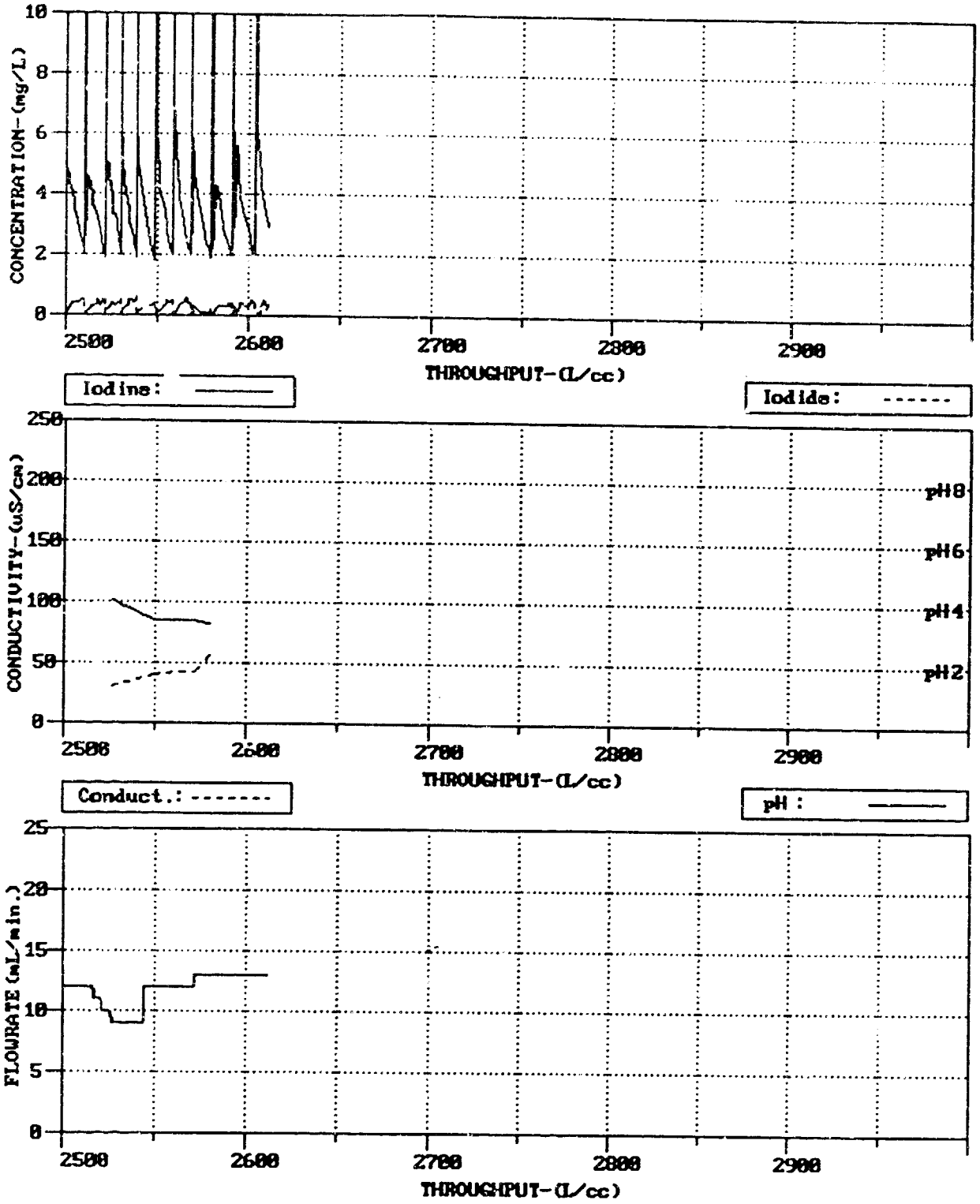

Figure 5.38 RMCV Life Cycle Test - Ersatz Urine Distillate: 2500-2612 L/cm^3.

operation was achieved. Regenerations for this unit were given a minimum duration of 60 minutes, after which regeneration was terminated by an I_2 concentration greater than 7 mg/L.

With RMCV-4, the decrease in period between regenerations with increasing cumulative flow is less significant than for any of the other RMCVs. From the outset RMCV-4 exhibited cyclic throughputs of approximately 17 L/cm^3, a value greater than for the initial ersatz humidity condensate (RMCV-3), but less than for the other two RMCVs. Cyclic throughputs diminished only slightly therafter. At the 1200 L/cm^3 mark cyclic throughputs of 10 - 11 L/cm^3 were observed. Clean-up of particulate matter as described above for RMCV-3 resulted in improved cyclic throughputs of approximately 14 L/cm^3. Reductions in cyclic throughput to 7 L/cm^3 occured near the 1800 L/cm^3 mark which corresponded to depletion of the solid state iodine crystal bed. The addition of 10 cm^3 of iodine crystals at 1940 L/cm^3 caused an immediate increase to approximately 12.5 L/cm^3. Flow to RMCV-4 was terminated at 2611.6 L/cm^3.

Cyclic I_2 depletion, cyclic I^- depletion, and cyclic throughput versus cycle number are illustrated in Figures 5.39, 5.40, and 5.41 respectively. MCV resin I_2 depletion and throughput during the regeneration phase of RMCV-4 operation versus cycle number are illustrated in Figures 5.42 and 5.43 respectively. Cyclic I_2 depletion correlates well with the observed trend in cyclic throughput.

Significant I^- levels were also detected in the RMCV-4 effluent. As with RMCV-3, this is largely due to the oxidation of formic acid by elemental iodine. This topic is treated in greter detail in Section 7. Inspection of Figure 5.40 reveals that cyclic I^- depletion correlates well with both cyclic throughput and cyclic I_2 depletion.

5.5 Conclusions.

Clearly the small column scale long term life cycle testing has demonstrated the potential for greater than a one hundred fold life extension of MCVs using the regenerative

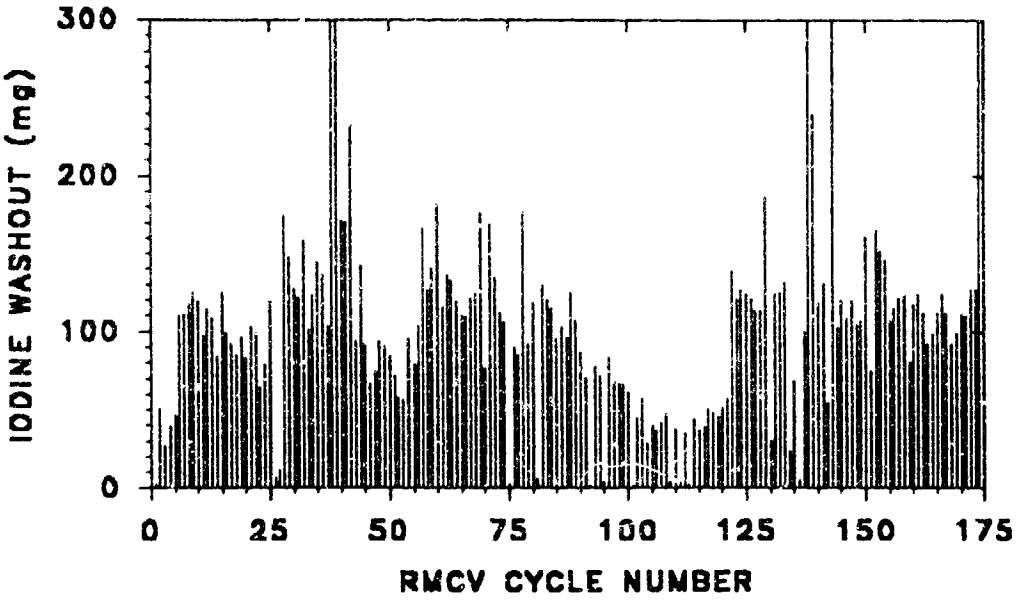

Figure 5.39 Cyclic I_2 Depletion - Ersatz Urine Distillate.

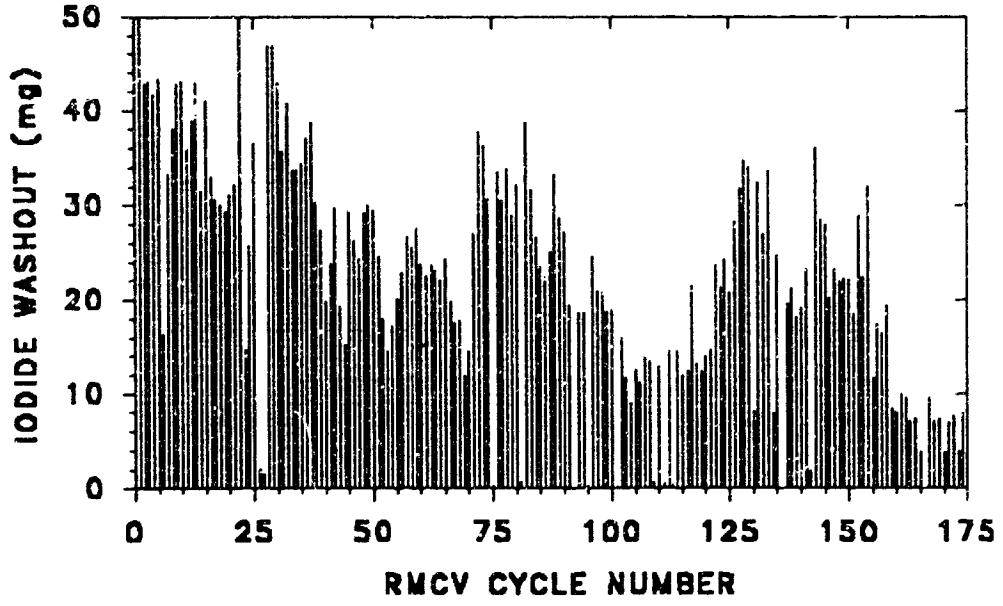

Figure 5.40 Cyclic I^- Depletion - Ersatz Urine Distillate.

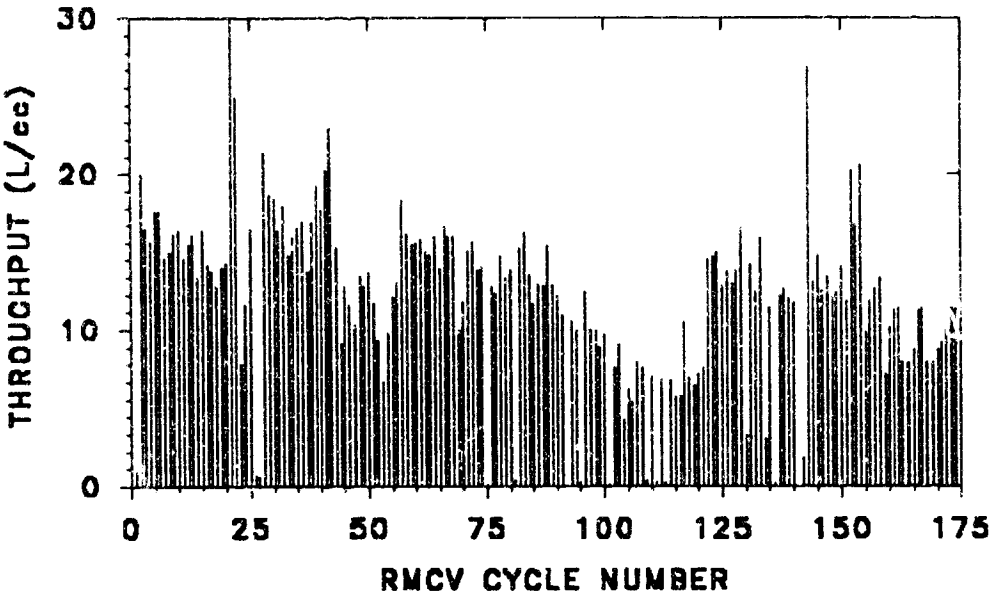

Figure 5.41 Cyclic Throughput - Ersatz Urine Distillate.

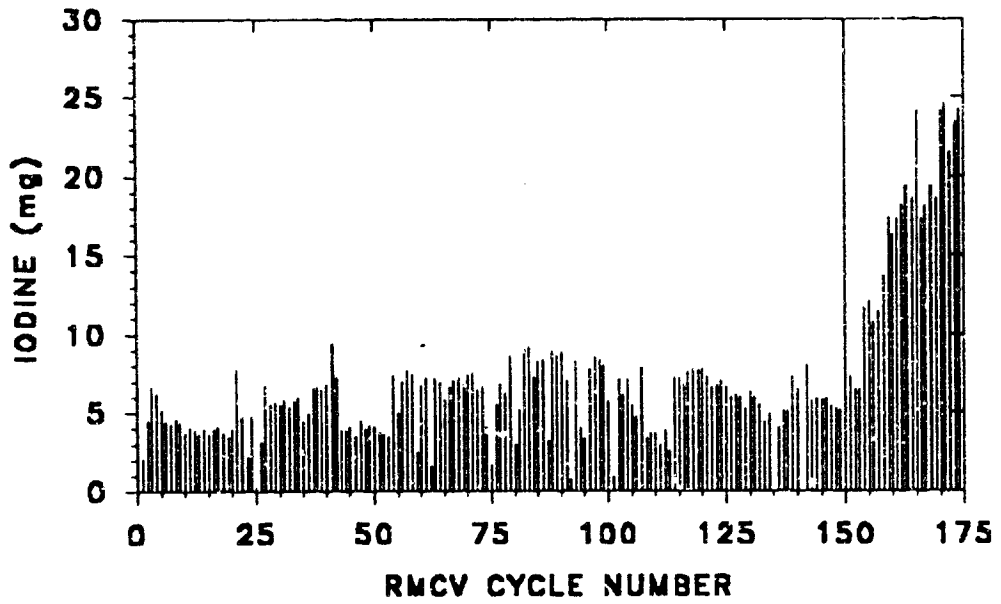

Figure 5.42 Cyclic I_2 Depletion During Regeneration - Ersatz Urine Distillate.

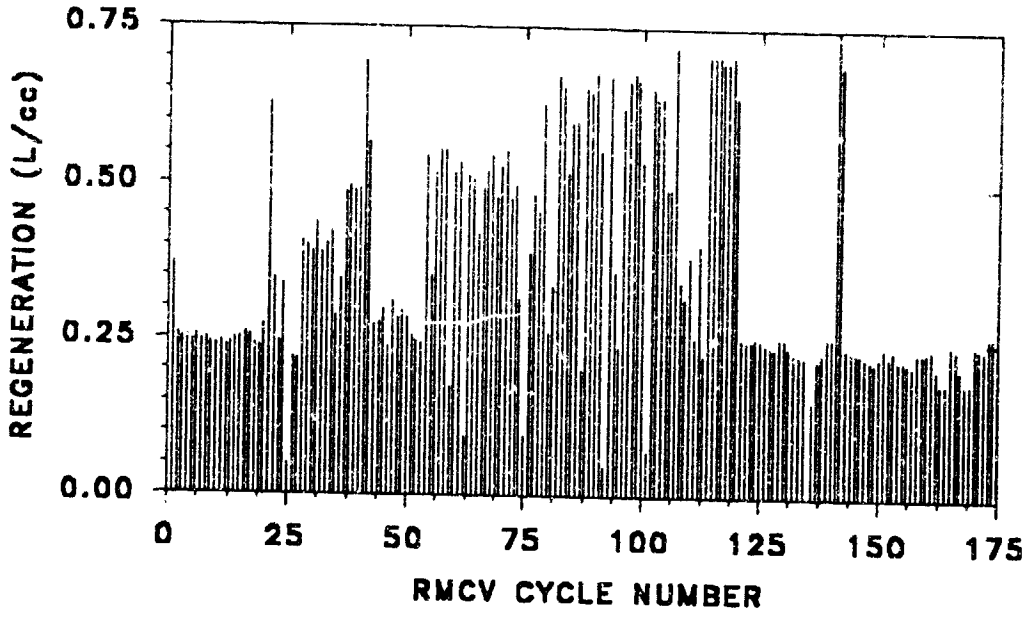

Figure 5.43 Cyclic Throughput during Regeneration - Ersatz Urine Distillate.

MCV technology. As an example, application of the 131 fold life extension exhibited by RMCV-4, to the Space Station *Freedom* MCV baselined for a 90 day life, indicates that a single RMCV could be designed to function without replacement for the entire 30 year life of the space station. This would eliminate the requirement for replacement of 120 MCVs, with the concomitant savings in astronaut manhours and resupply expendables.

While all four RMCVs continued to function for the duration of the long term life cycle tests, several potential mechanisms of performance deterioration have been identified. The accumulation of particulate matter, believed to be remnants of dead microorganisms, such as was observed with the RMCV receiving ersatz reclaimed hygiene water challenge solution, can cause problems by both occlusion of ion exchange sites on the surface of the MCV resin

and by the restriction of flow channels, resulting in a high pressure drop across the resin bed.

The indication of degraded RMCV performance is a diminution of the cyclic throughput. To a greater or lesser extent this phenomenon was indicated in all four of the RMCVs under study. At least two causitive factors seem to be in operation. One is the slow replacement of I^- at the anion exchange sites, resulting in the decrease in loading capacity of the resin for I_2. This was indicated by the experiment performed on RMCV-2 in which partial improvement in performance was obtained by flowing a strong KI solution through the resin bed. However, that the improvement in performance was limited, indicates that another mechanism of resin degradation, such as loss or blockage of ion exchange sites, is also in operation.

The life cycle test results also clearly indicate the increase in regeneration frequency attributable to the diminishing I_2 concentrations in the regeneration liquor as the solid state I_2 crystal bed nears the end of its useful life. This is a direct consequence of the decreasing residence time of the challenge solution within the crystal bed and will be discussed in greater detail in Section 6 which follows.

6

RMCV PARAMETRIC TESTING

6.0 Overview.

A program of testing has been conducted to identify the primary variable parameters which are responsible for the operational characteristics of the RMCV, and to determine the optimal values of these variables necessary to achieve maximum RMCV system performance. The second RMCV test stand, designated variously as the Accelerated Test Stand, and the Parametric Test Stand, was dedicated to these studies. The design and operational features of the test stand have been presented in Section 2. The information obtained via the parameteric test program has been applied in the design of the prototype RMCV which is discussed in detail in Section 10. A variety of tests were conducted. Since the expendable MCV is a fully developed and well understood technology, parametric testing focused specifically on the regeneration operation. The two factors of primary importance to the regeneration process are the residence times of the challenge solution within the MCV and within the bed of I_2 crystals. In accordance with the convention adopted for MCV development, residence time (t_r), or open bed contact time, is taken to mean the ratio,

$$\frac{V_b \frac{cm^3}{}}{Q \frac{cm^3}{min.}} = t_r \text{ min.} \qquad \text{(Eqn. 6.1),}$$

where V_b is packed bed volume and Q is flow rate. No attempt was made to determine bed porosities or fluid volumes within the interstitial spaces between ion exchange resin beads or I_2 crystals. Residence time experiments were conducted using room temperture ersatz reclaimed potable water and 1.7 ^oC ersatz humidity condensate, representing the two extremes of chemical complexity.

The particle size distribution of the crystalline I_2 used in the preparation of packed crystal beds was determined. Packed beds were then prepared in narrow crystal size ranges

and their dissolution behavior studied as functions of residence time and throughput. In addition to optimization of the crystal bed design for maximum regeneration efficiency, another goal of these experiments was to determine the operational requirements for production of high levels of aqueous I_2 for possible use in microbial decontamination external to the RMCV.

Some additional experimentation was performed which was less directly related to prototype RMCV development. Tests were conducted investigating the performance of the small column RMCVs with non-buffered challenge solutions of varying initial pH, ranging from pH = 2 to pH = 10. Also, MCVs prepared from Amberlite 401S ion exchange resin were evaluated for a short period using ersatz reclaimed potable water, ersatz reclaimed hygiene water, ersatz humidity condensate, and ersatz urine distillate challenge solutions.

6.1 Residence Time Experiments.

A series of tests were conducted in which the effects of varying residence times for both the I_2 crystal bed and the MCV were examined. MCV resin beds of 2.5 cm^3 and I_2 crystal beds of approximately 6.8 cm^3 were used. Residence times were varied by adjusting the flow rate. The MCVs were first washed down to an effluent I_2 value of approximately 2.0 mg/L. Regeneration was then invoked and the concentrations of I_2 in both the crystal bed effluent and the MCV effluent were recorded as functions of throughput. MCV effluent I_2 levels were determined using the diode array spectrophotometer in its normal mode of operation as the test stand on-line iodine monitor. I_2 levels in the crystal bed effluent were monitored by the LCV method, using 200 µL samples withdrawn from the in-line sample port.

The test results for the ersatz reclaimed potable water stream are given in Figures 6.1, 6.2, 6.3, and 6.4, corresponding to the MCV residence times of 0.203, 0.212, 0.294, and

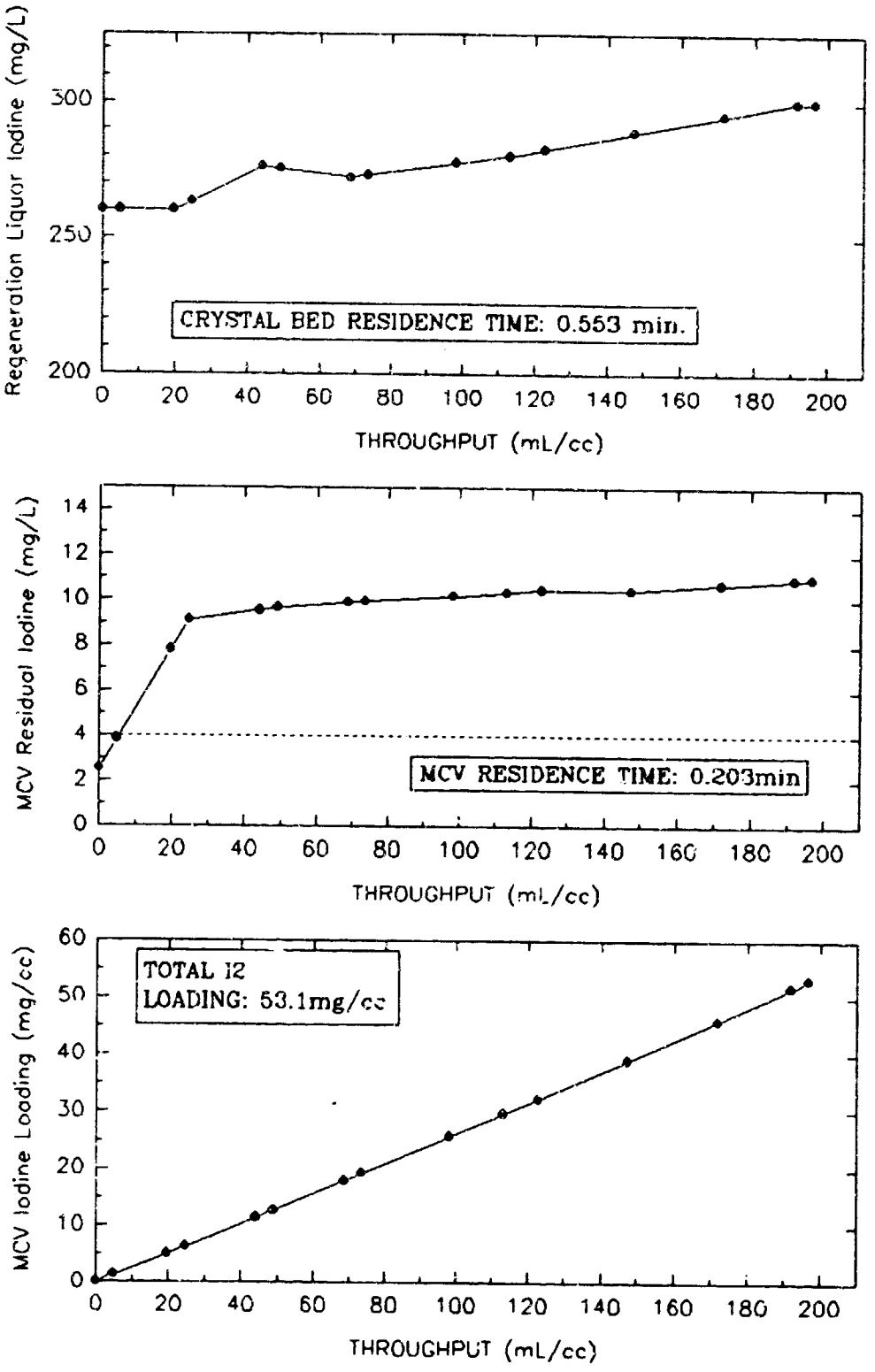

Figure 6.1 Residence Time Experiments: Ersatz Reclaimed Potable Water. MCV = 0.203 min., I_2 Bed = 0.553 min.

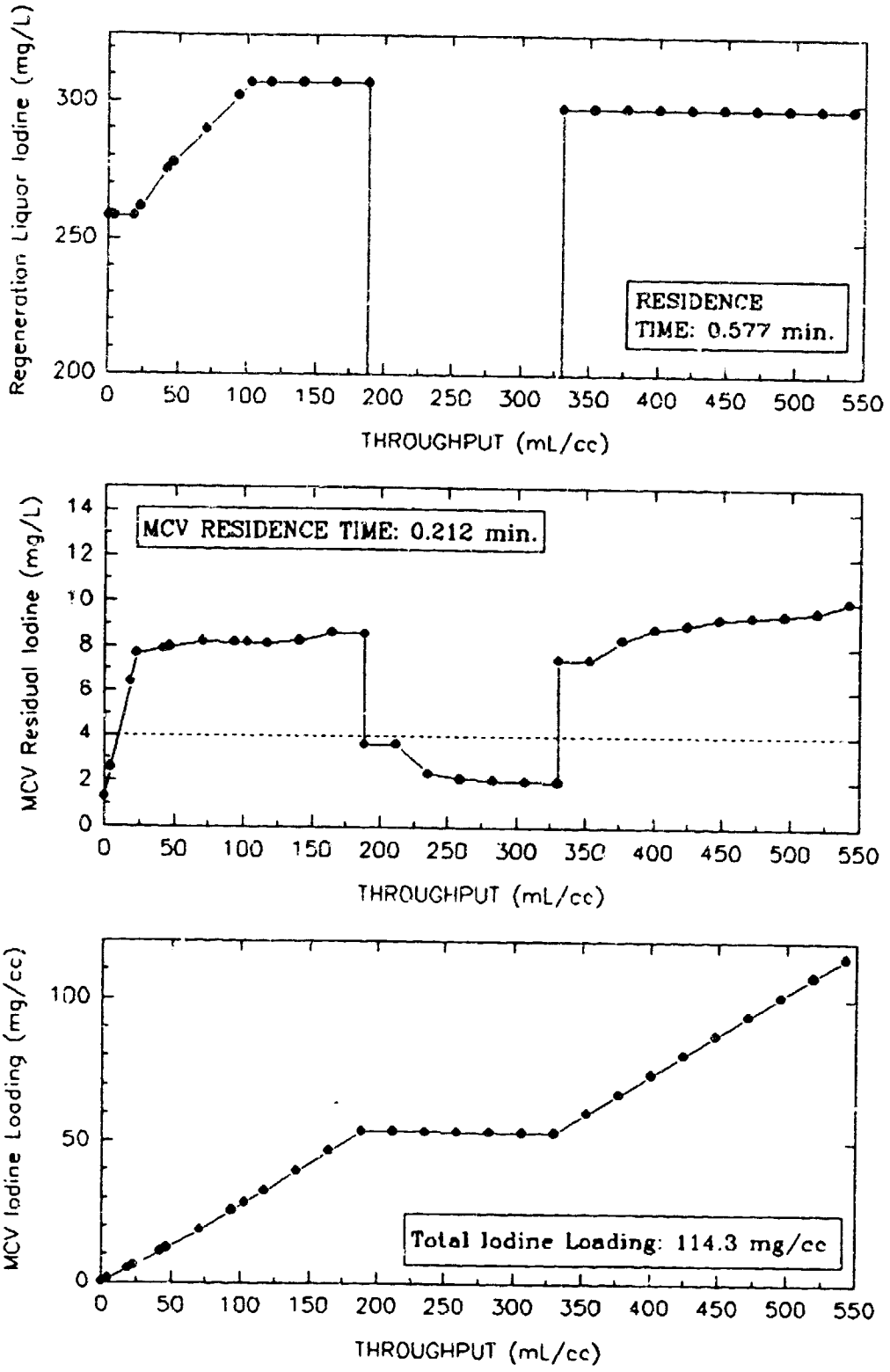

Figure 6.2 Residence Time Experiments: Ersatz Reclaimed Potable Water. MCV = 0.212 min., Crystal Bed = 0.577 min.

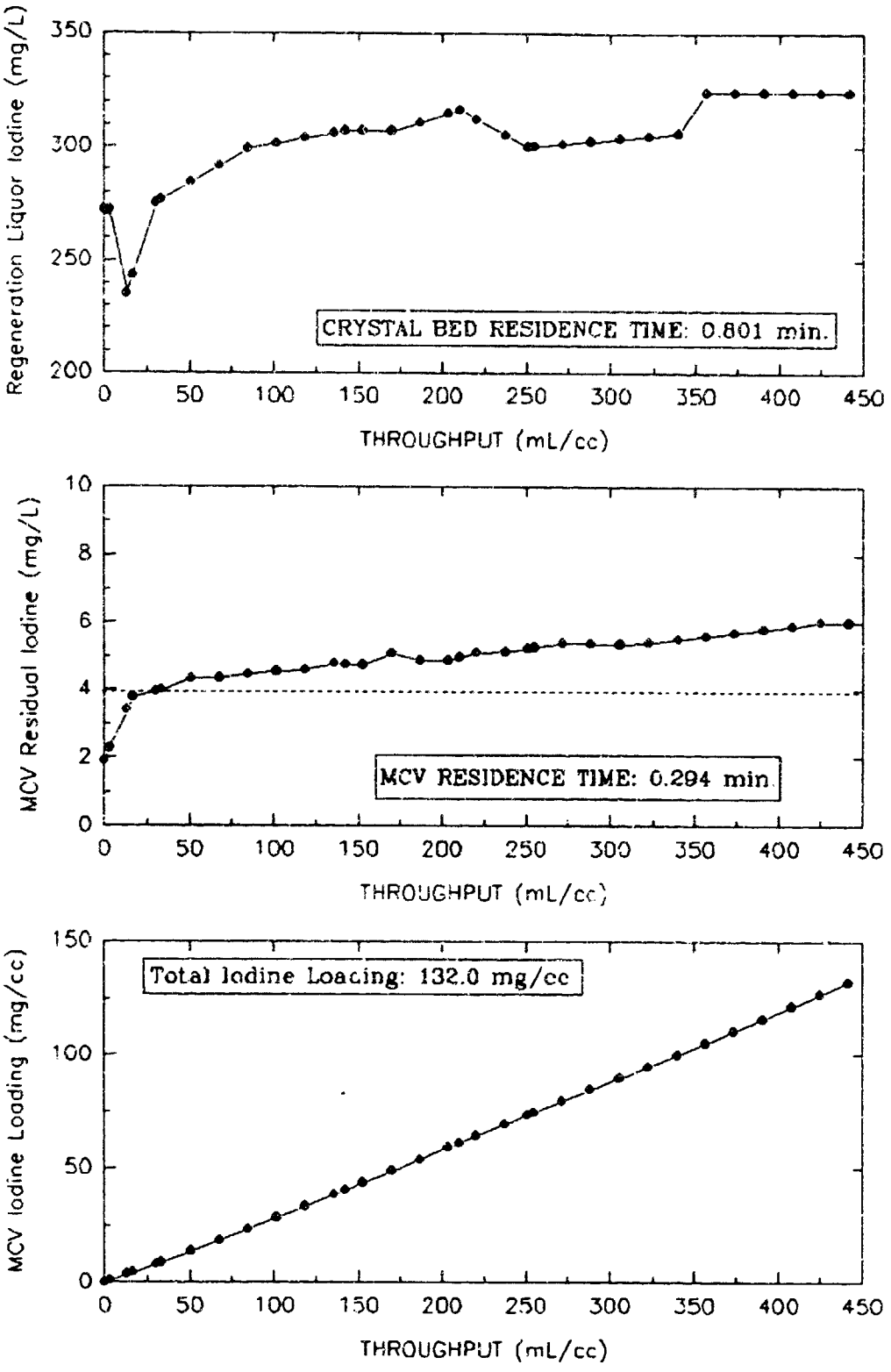

Figure 6.3 Residence Time Experiments: Ersatz Reclaimed Potable Water. MCV = 0.294 min., Crystal Bed = 0.801 min.

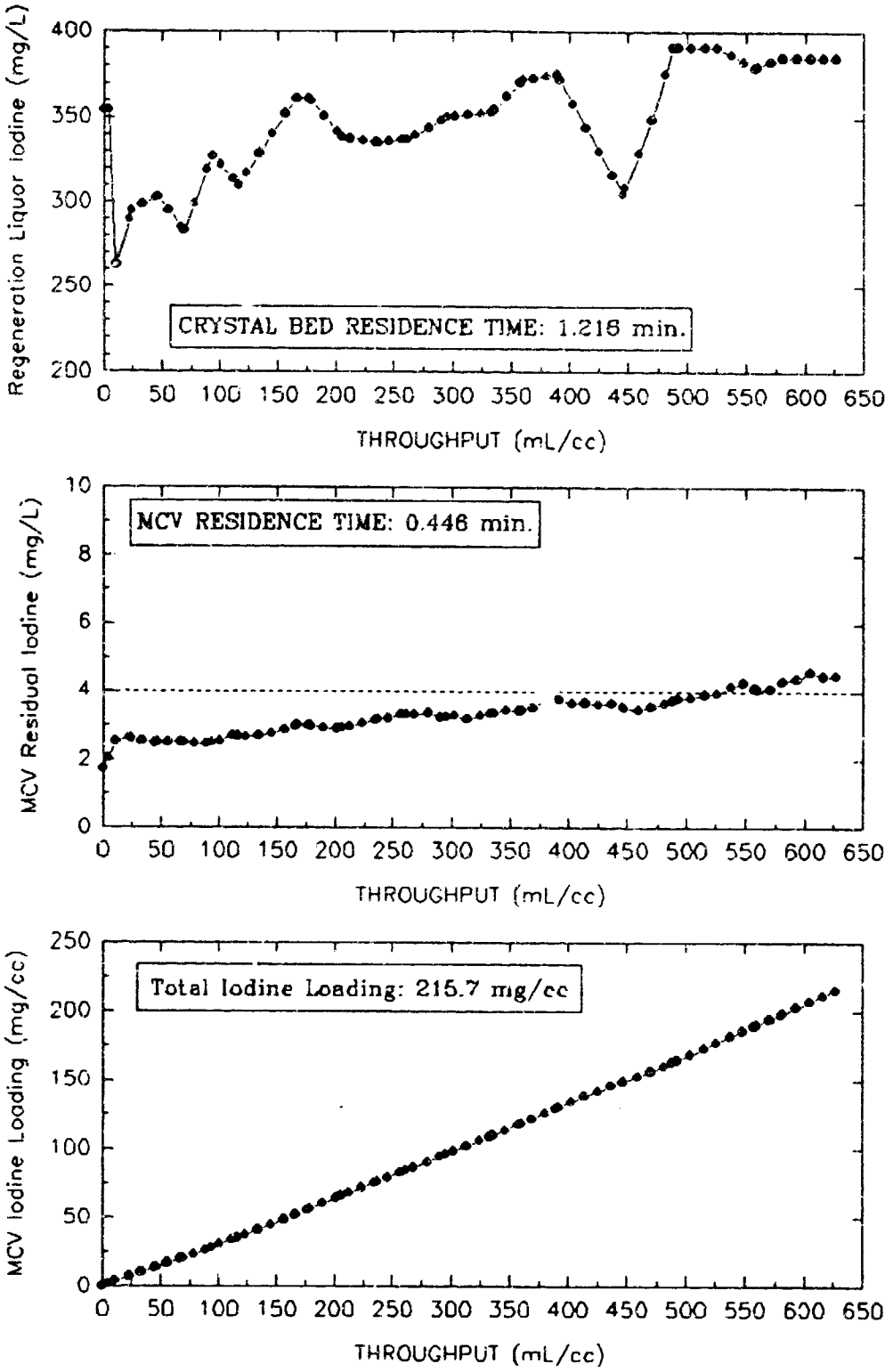

Figure 6.4 Residence Time Experiments: Ersatz Reclaimed Potable Water. MCV = 0.464 min., Crystal Bed = 1.216 min.

0.446 minutes respectively, and corresponding to I_2 crystal bed residence times of 0.533, 0.577, 0.801, and 1.216 minutes respectively. Each of these figures presents, from top to bottom, plots of crystal bed effluent I_2 versus throughput, MCV effluent I_2 versus throughput, and total MCV I_2 loading versus throughput. Figures 6.5, 6.6, and 6.7 present the test results for the ersatz humidity condensate stream with MCV residence times of 0.198, 0.202, and 0.379 minutes respectively, and I_2 crystal bed residence times of 0,640, 0.649, and 1.032 minutes respectively.

For the ersatz reclaimed potable water stream, the crystal bed effluent I_2 levels approach saturation as the residence times increase above 1.0 minute This is in marked contrast to the behavior exhibited by the RMCV serving the ersatz humidity condensate challenge stream, where lower crystal bed effluent I_2 levels are consistently observed. With the ersatz humidity condensate, the initial state of the regeneration liquor shows I_2 levels near saturation values. However upon initiation of the regeneration event, I_2 levels fall rapidly to lower values which then remain relatively constant. The trend of increasing concentration with increasing throughput, is evident, but to a lesser extent than with the ersatz reclaimed potable water. The lower I_2 levels may in part be due to the chemical composition of the ersatz humidity condensate, but are largely attributable to the lower temperature of this challenge stream. I_2 values are initially high when static challenge solution bathes the iodine crystals at room temperature, but as soon as 1.7 ^{o}C solution flows through the bed, I_2 values drop due to the lower solubility of iodine in the aqueous medium at this temperature, and due to the slower kinetics of dissolution.

The trend seen for the MCVs serving both challenge streams is similar. With MCV residence times of approximately 0.2 minutes, I_2 levels of 8 - 12 mg/L are seen early in the regeneration process. This corresponds to the behavior seen at this residence time in the long term life cycle RMCV tests. As the residence time increases, effluent I_2 concentration lessens during regeneration, until at residence times of approximately 0.4 minutes normal I_2

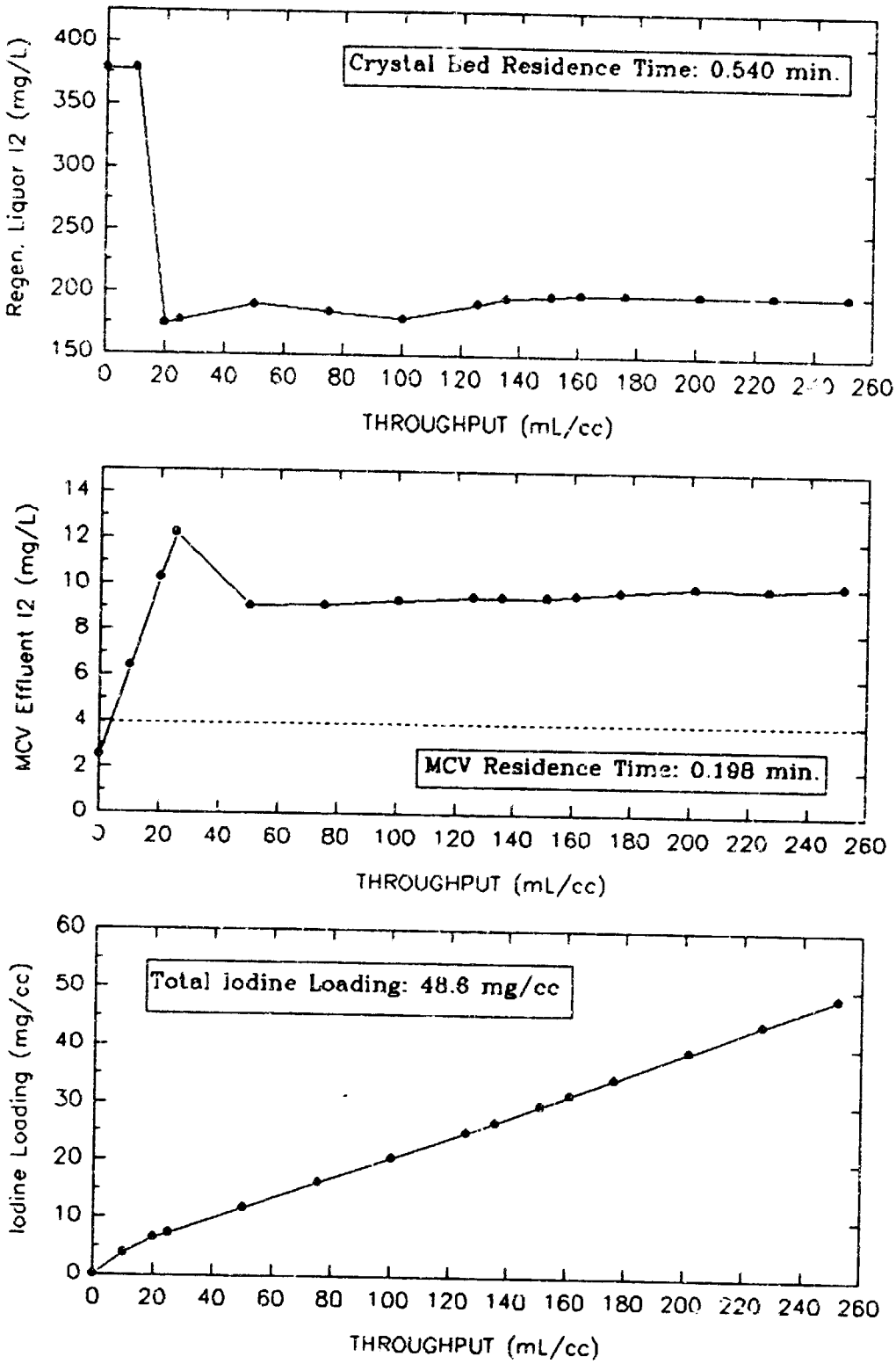

Figure 6.5 Residence Time Experiments: Ersatz Humidity Condensate. MCV = 0.198 min., I_2 Bed = 0.640

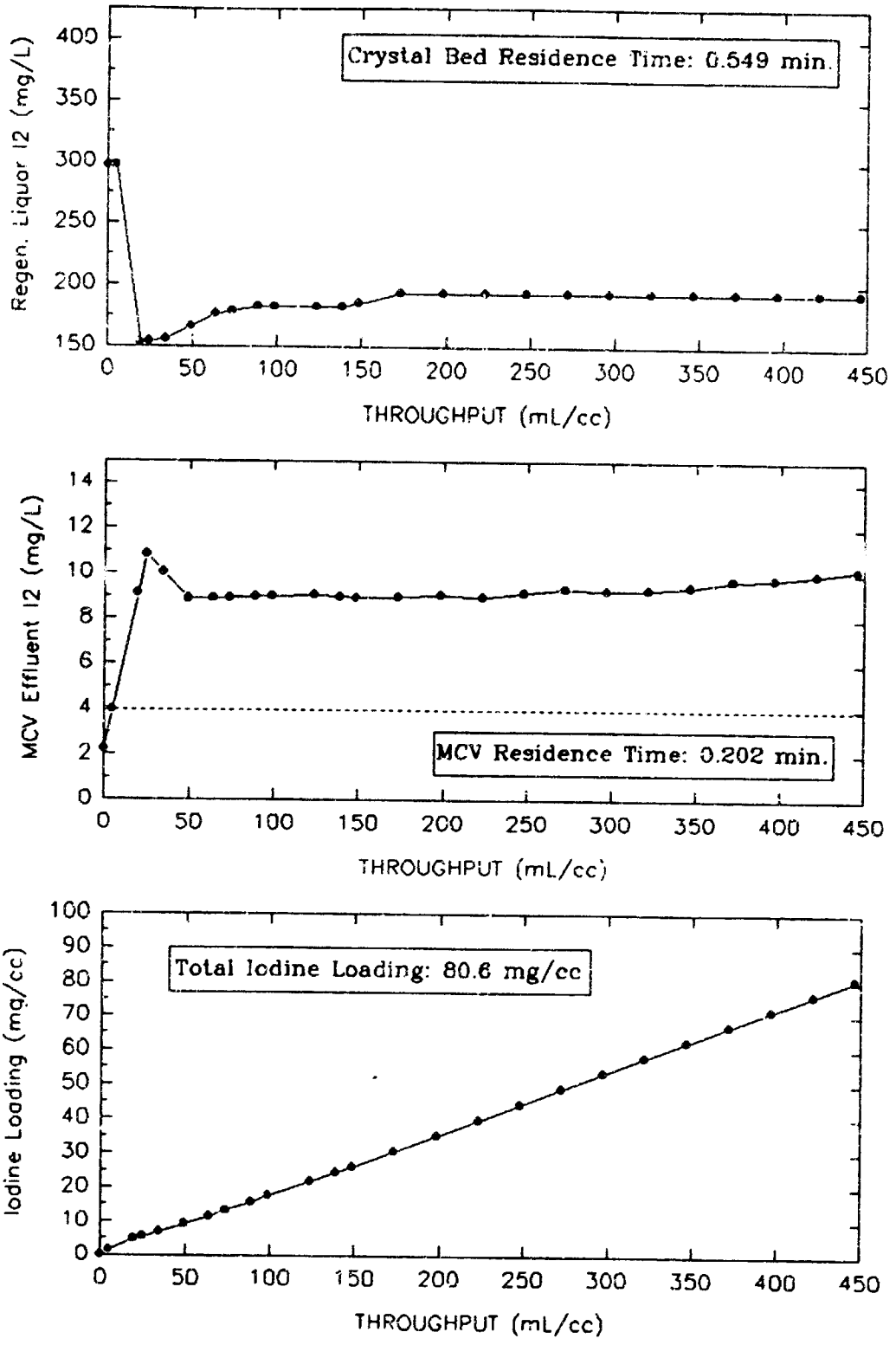

Figure 6.6 Residence Time Experiments: Ersatz Humidity Condensate. MCV = 0.202 min., I_2 Bed = 0.649

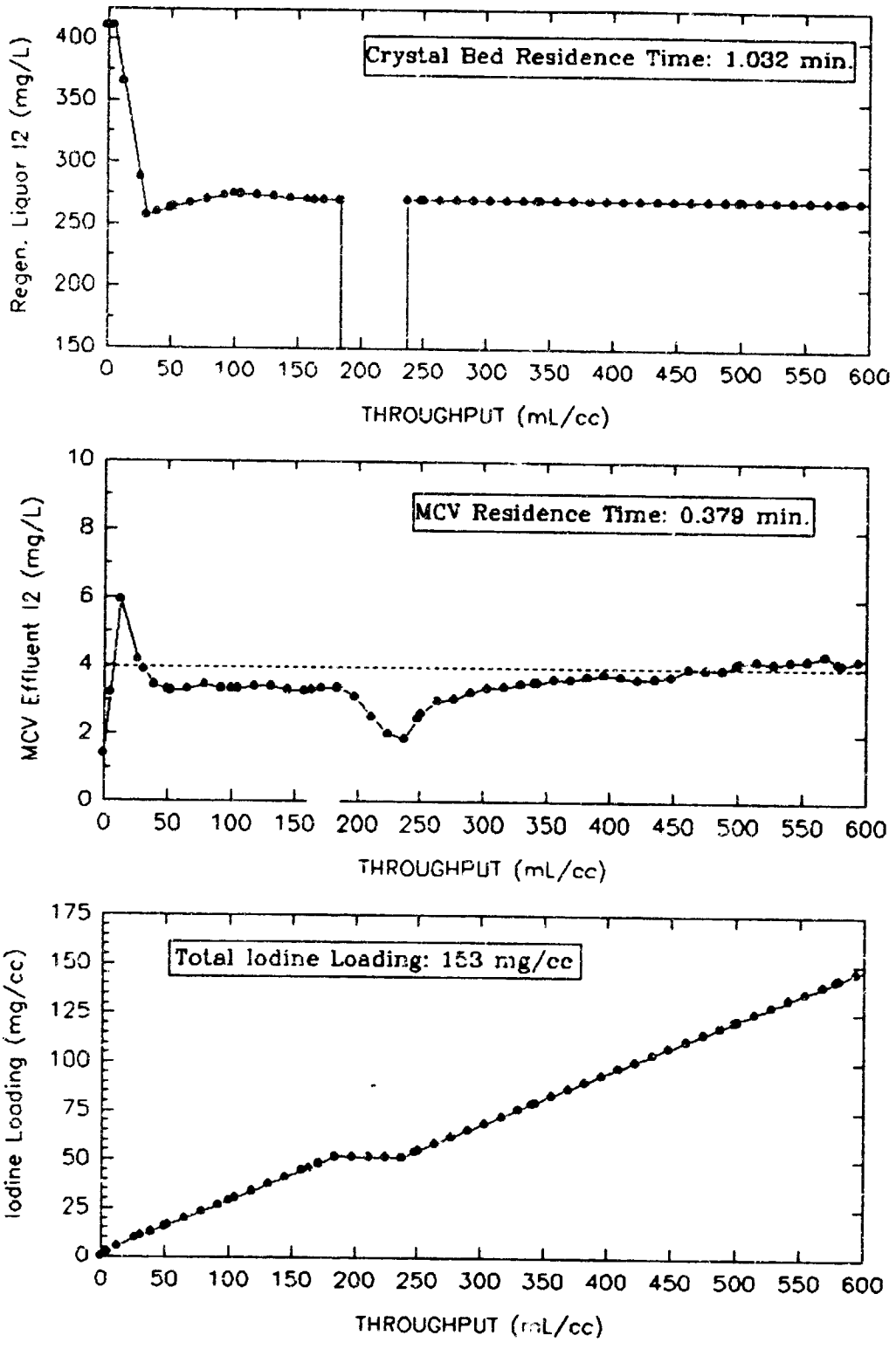

Figure 6.7 Residence Time Experiments: Ersatz Humidity Condensate. MCV = 0.379 min., I_2 Bed = 1.032 min.

values are attained. For ersatz reclaimed potable water, the relationships between I_2 concentrations in the regeneration liquor and in the MCV effluent versus residence time are illustrated in Figure 6.8 a and b respectively. The linear proportionality between MCV I_2 loading rate and MCV residence time is shown in Figure 6.9.

6.2 Iodine Crystal Size Experiments.

Experiments were conducted to determine the influence of iodine crystal size on the efficiency of the MCV regeneration process. The size distribution of the iodine crystals used in the preparation of the regeneration beds was determined by screening, using U.S. Standard Mesh sieves. The results are shown in Figure 6.10. The predominant size fraction occurs between 600 - 850 μ and consitutes approximately 25 % of the crystal mass. Next in importance are the 850 - 1180 μ, and the 1180 - 2360 μ fractions which represent approximately 20 % and 18 % of the crystal mass respectively. Only a few percent of crystals are greater than 2360 μ. Less than 8 % of crystals are smaller than 300 μ.

Crystal beds were prepared from those particle size fractions having sufficient mass. Effluent I_2 concentrations were then determined over a series of residence times using the ersatz reclaimed potable water challenge stream. Residence times were varied by flow rate adjustment. I_2 concentrations were determined in real time using the diode array spectrophotometer fitted with a 1 cm path length flow cell. Once the residence time relationships were established, constant flow at a residence time between 0.4 - 0.5 minutes was maintained until the crystal beds were depleted.

The aqueous I_2 concentrations in the crystal bed effluent versus throughput and the cumulative I_2 depletion versus throughput are shown in Figures 6.11, 6.12, 6.13, 6.14, and 6.15 for the 850 - 1180 μ, 600 - 850 μ, 425 - 600 μ, 300 - 425 μ, and < 300 μ crystal size fractions respectively. With the exception of the 300 - 425 μ size fraction, the depletion curves exhibit nearly constant effluent I_2 concentrations of approximately 225 mg/L during

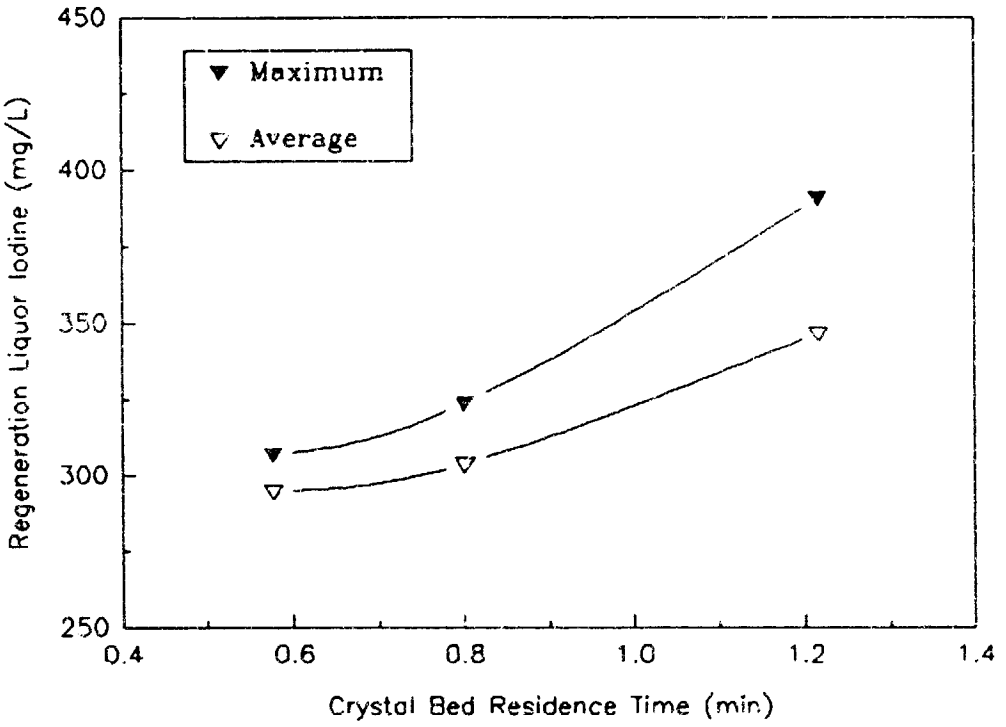

a) I_2 Crystal Bed

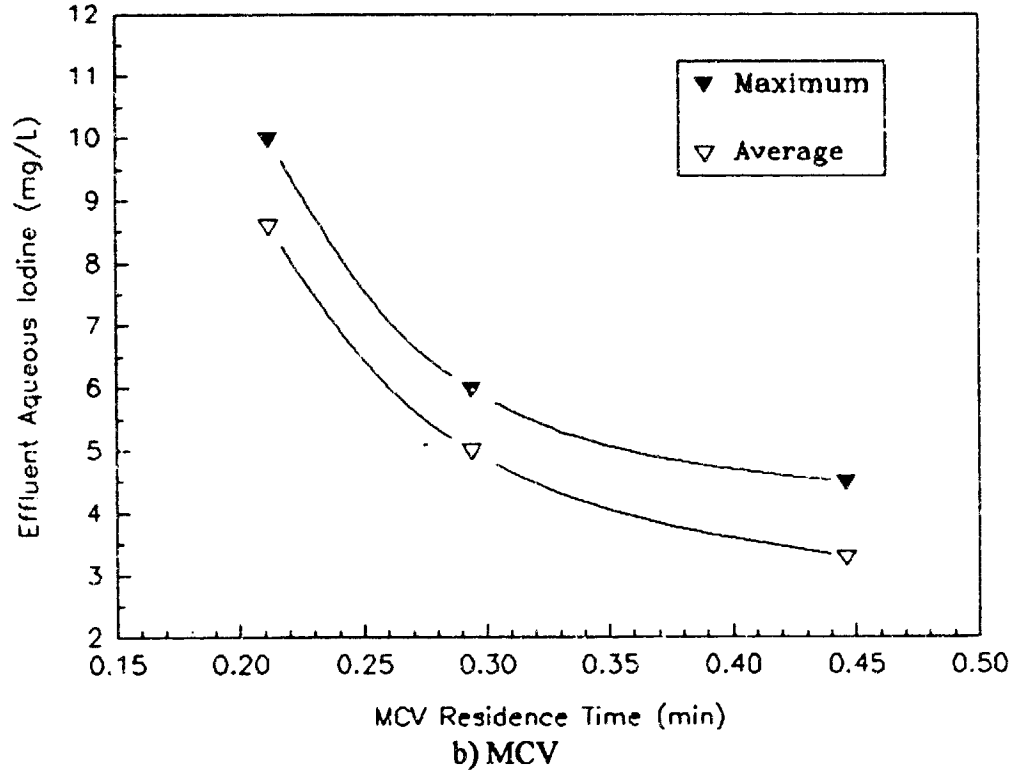

b) MCV

Figure 6.8 Effluent I_2 versus Residence Time.

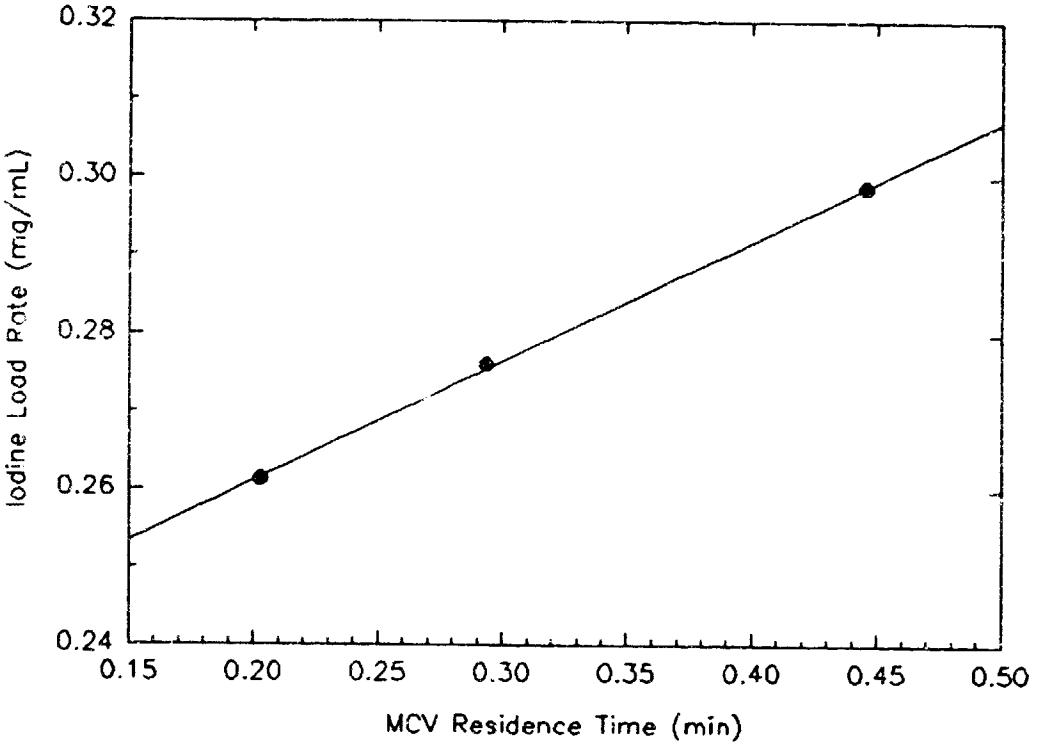

Figure 6.9 I_2 Loading Rate during Regeneration versus MCV Residence Time.

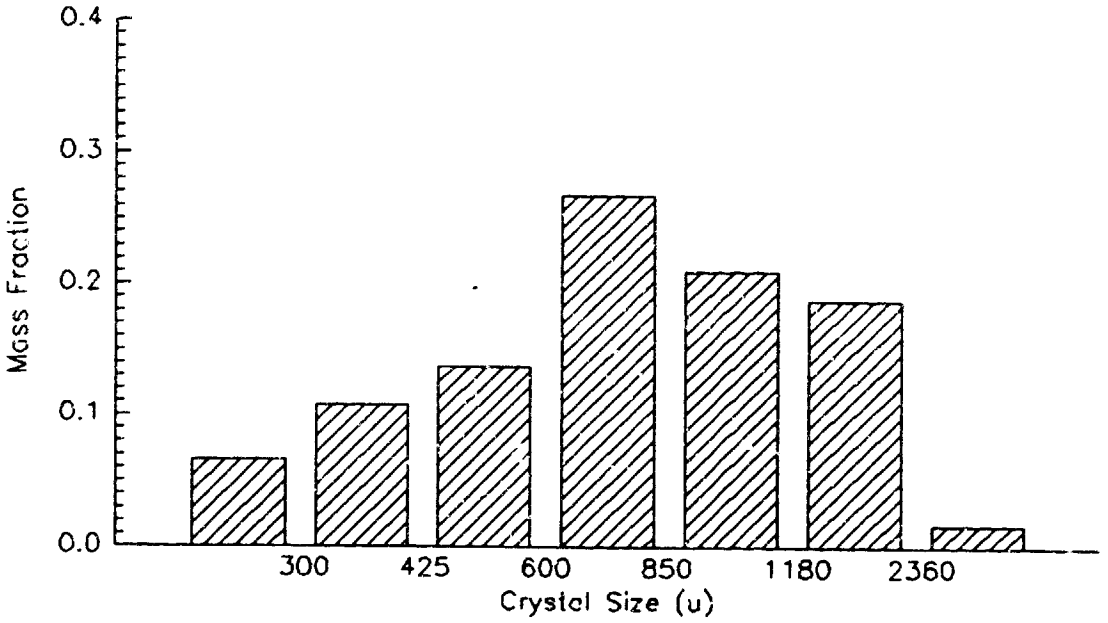

Figure 6.10 Size Distribution of I_2 Crystals.

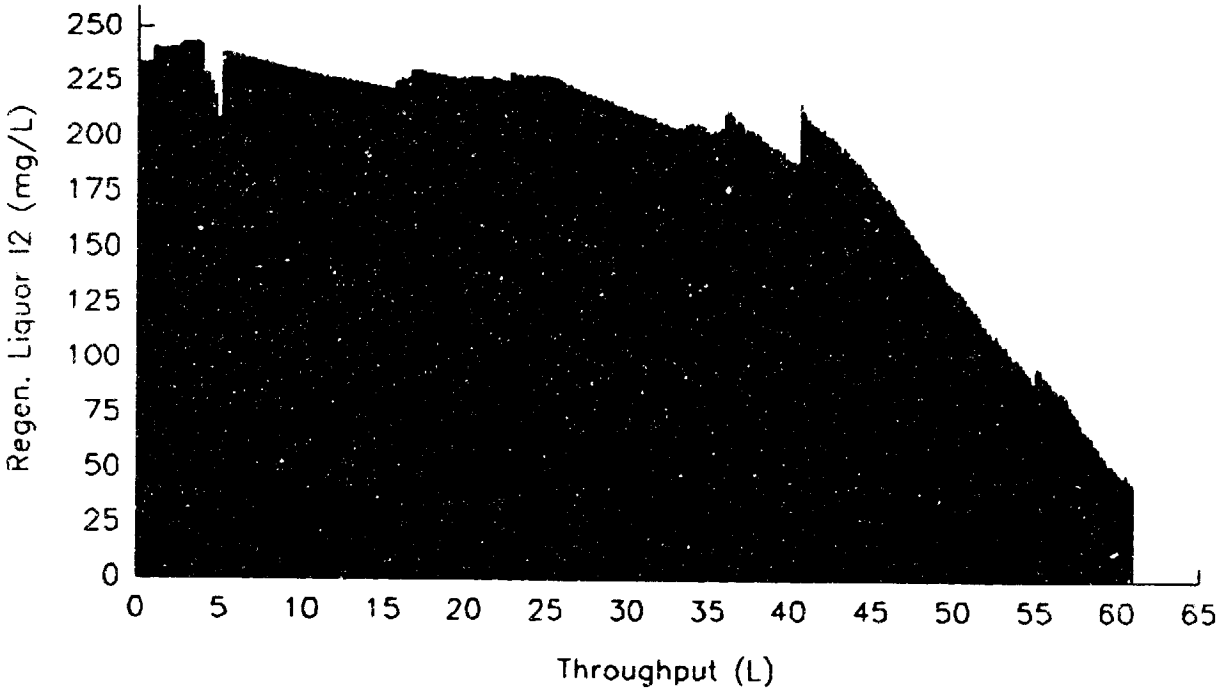

a) Effluent Iodine versus Throughput

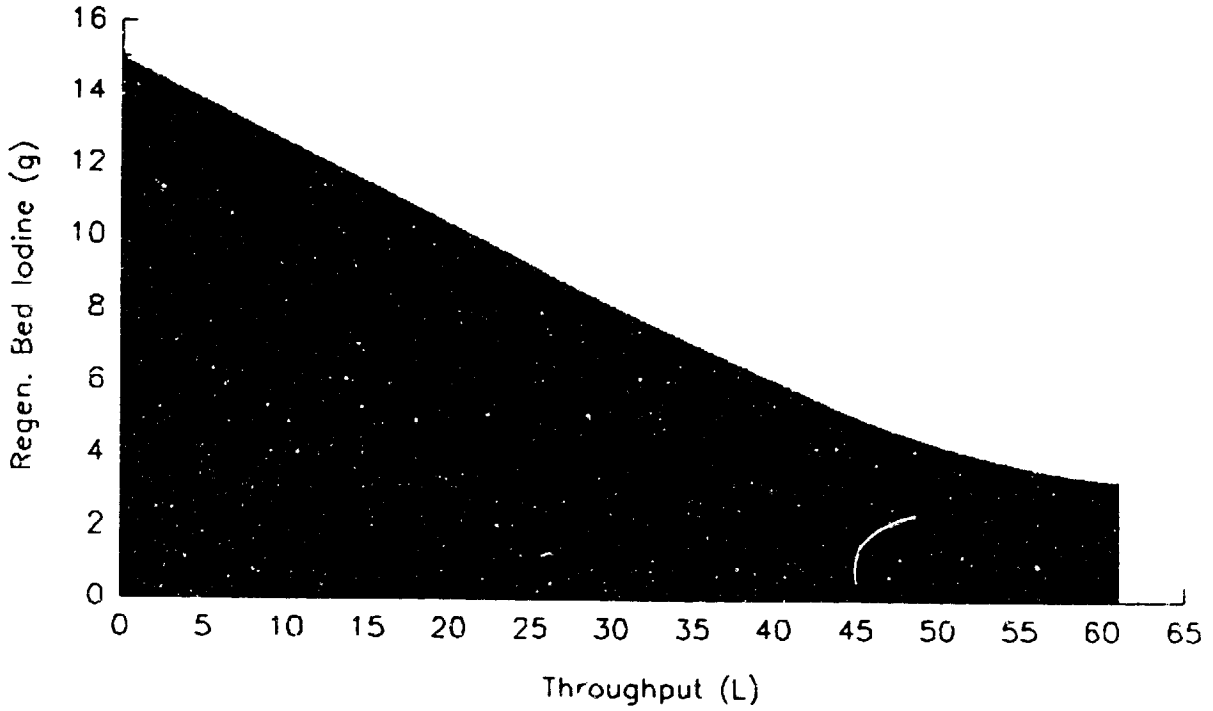

b) Iodine Depletion versus Throughput

Figure 6.11 850 - 1180 µ Crystal Bed Washout

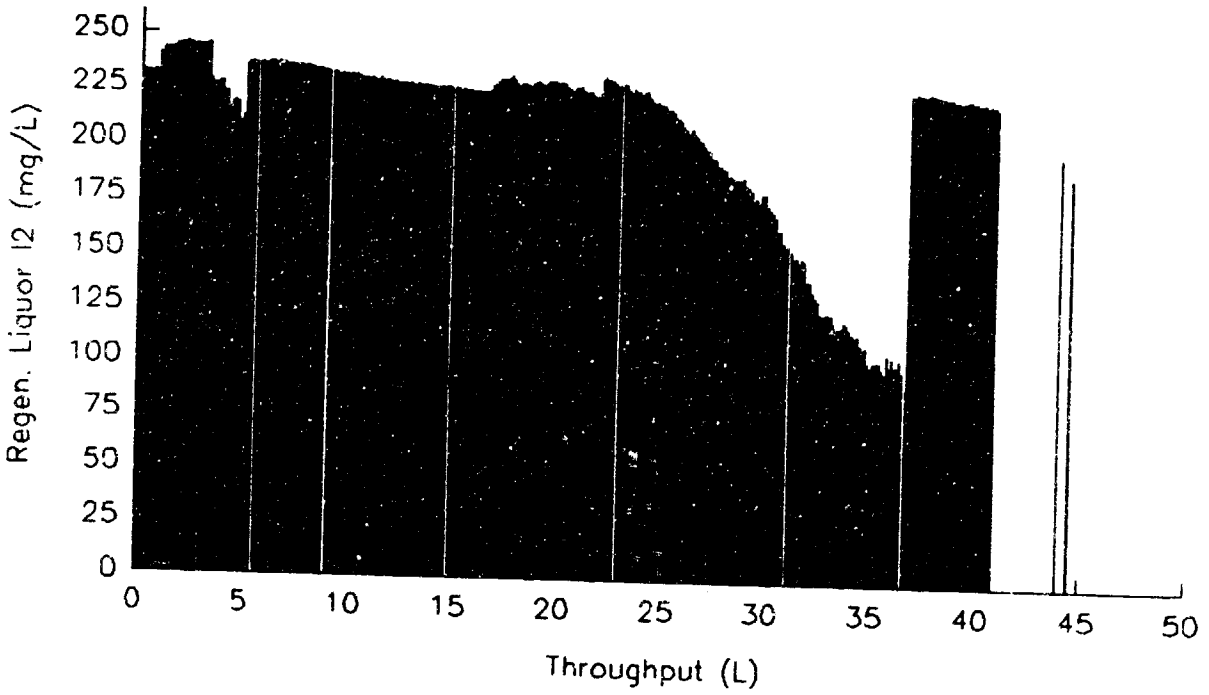

a) Effluent Iodine versus Throughput

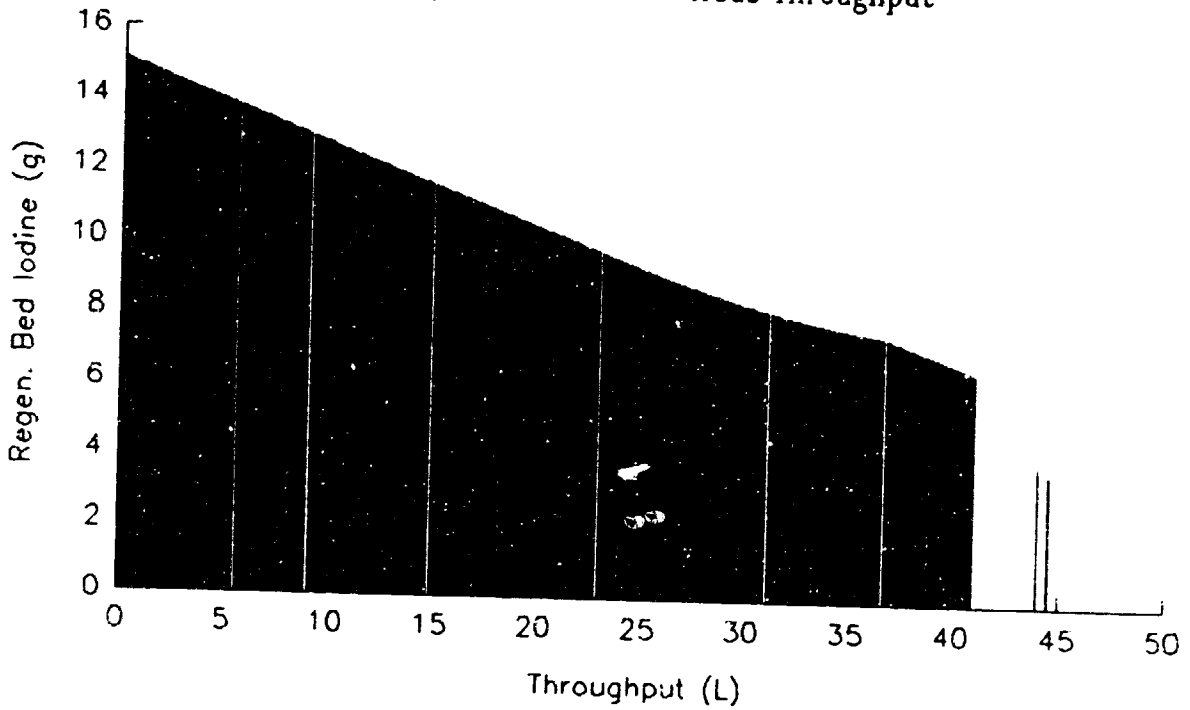

b) Iodine Depletion versus Throughput

Figure 6.12 600 - 850 µ Crystal Bed Washout.

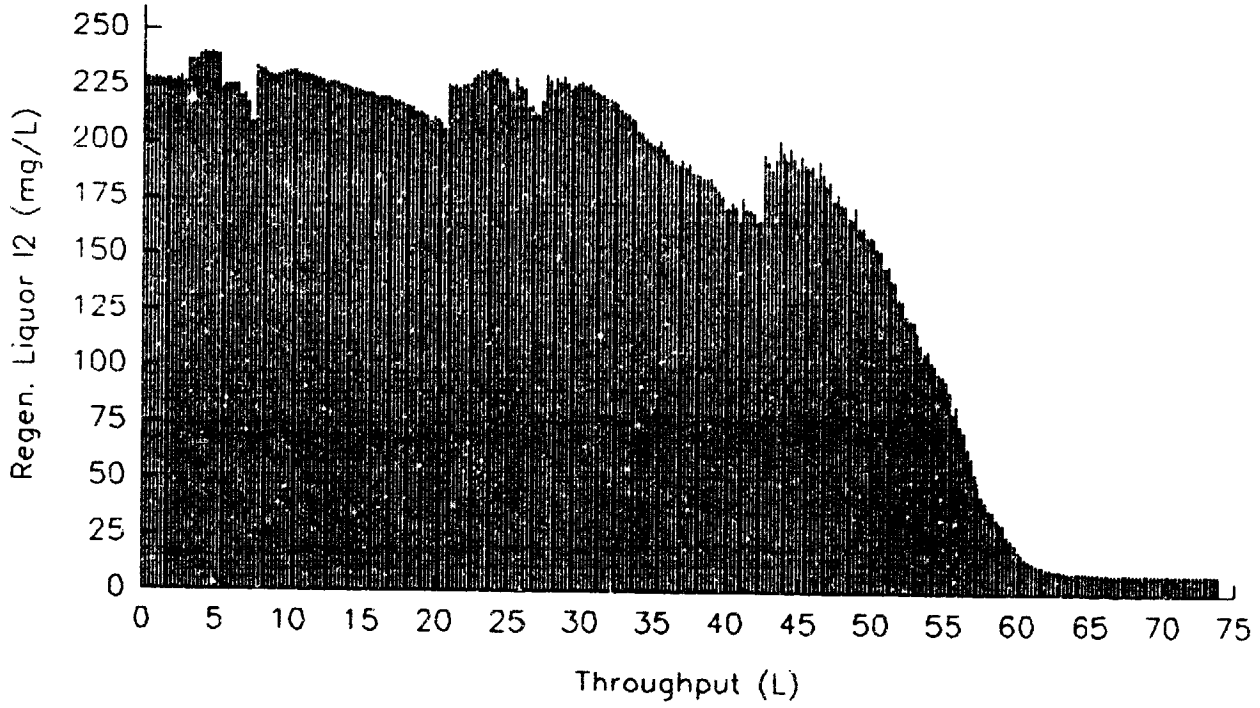

a) Effluent Iodine versus Throughput

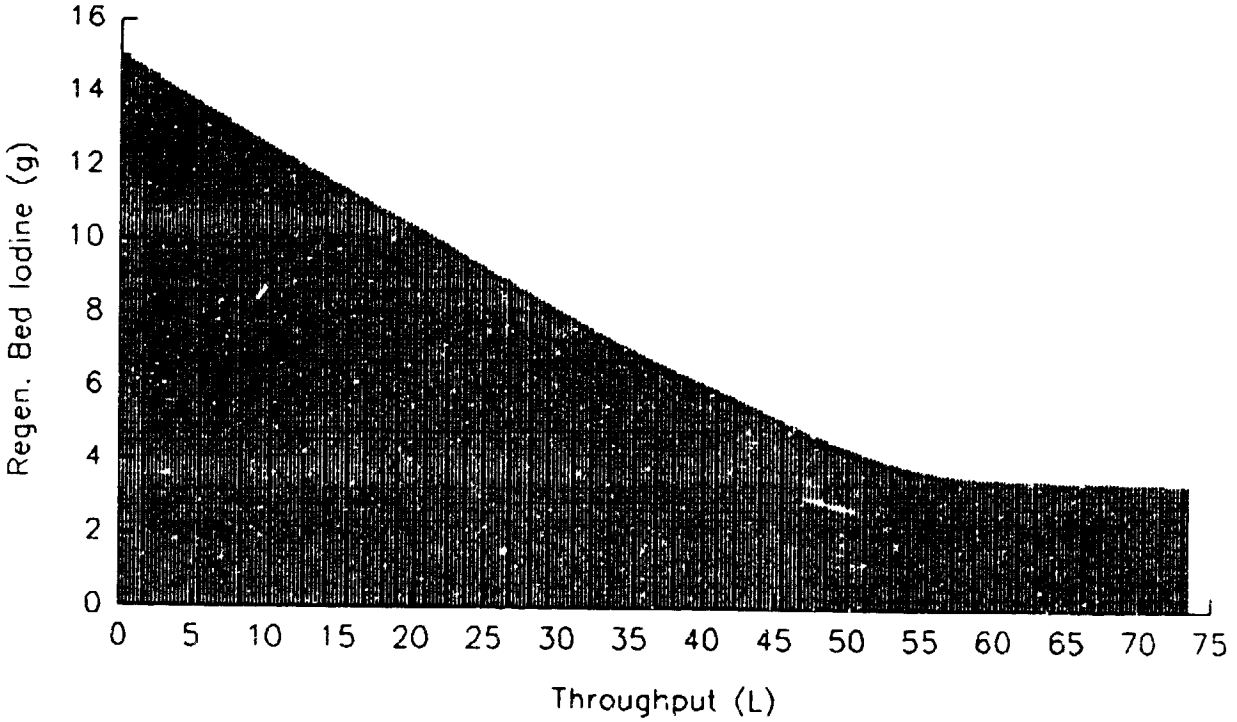

b) Iodine Depletion versus Throughput

Figure 6.13 425 - 600 μ Crystal Washout.

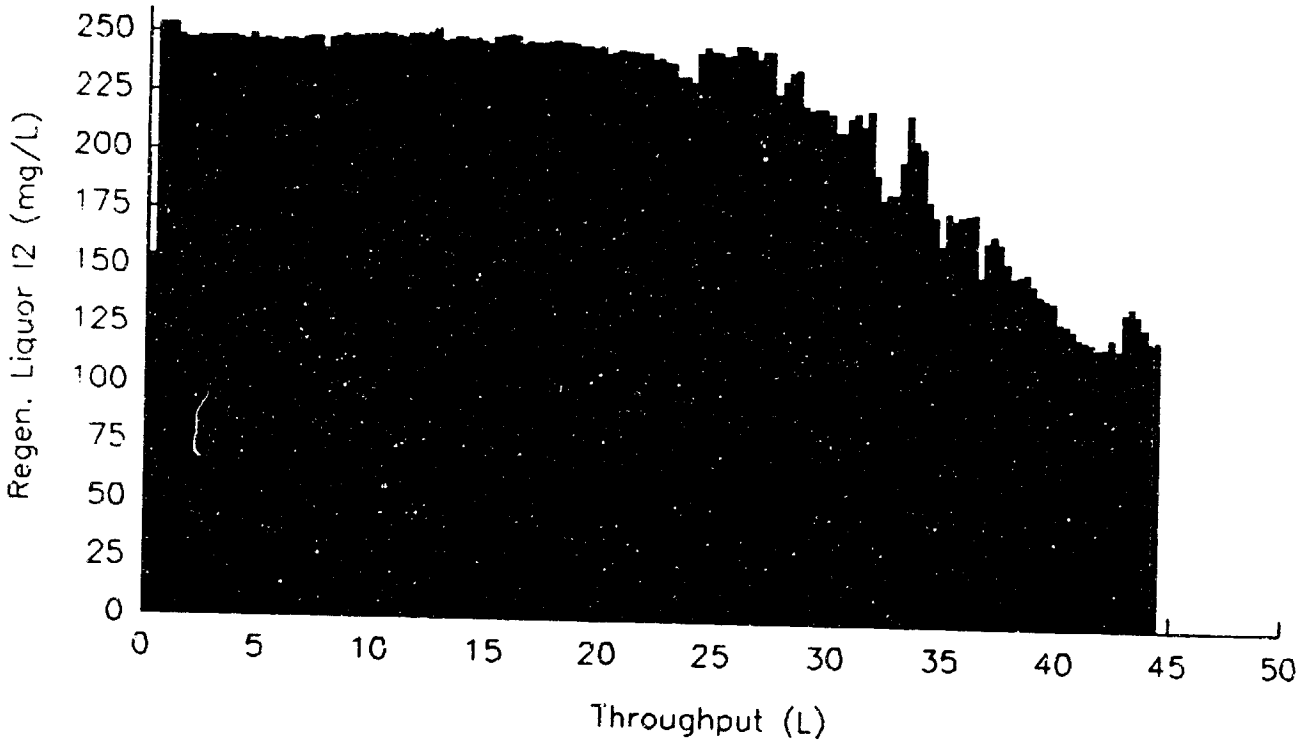

a) Effluent Iodine versus Throughput

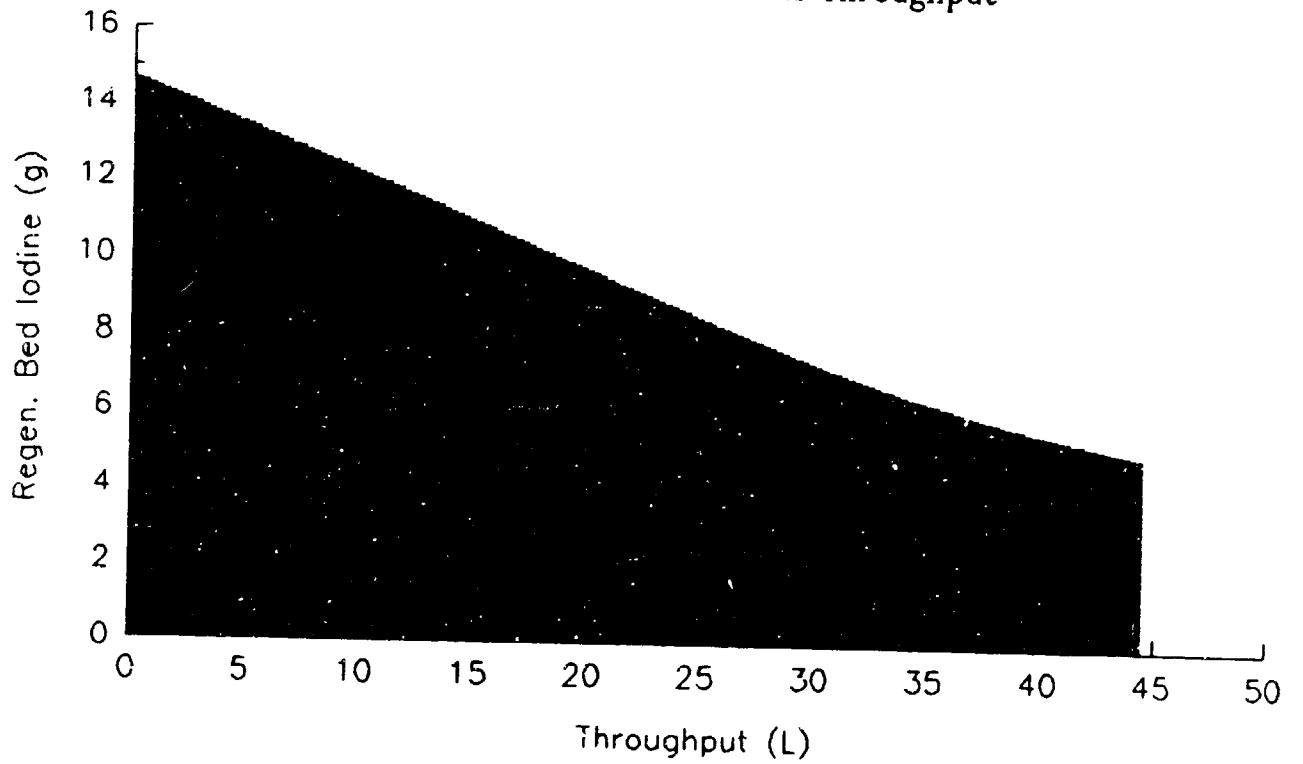

b) Iodine Depletion versus Throughput

Figure 6.14 300 - 425 µ Crystal Bed Washout.

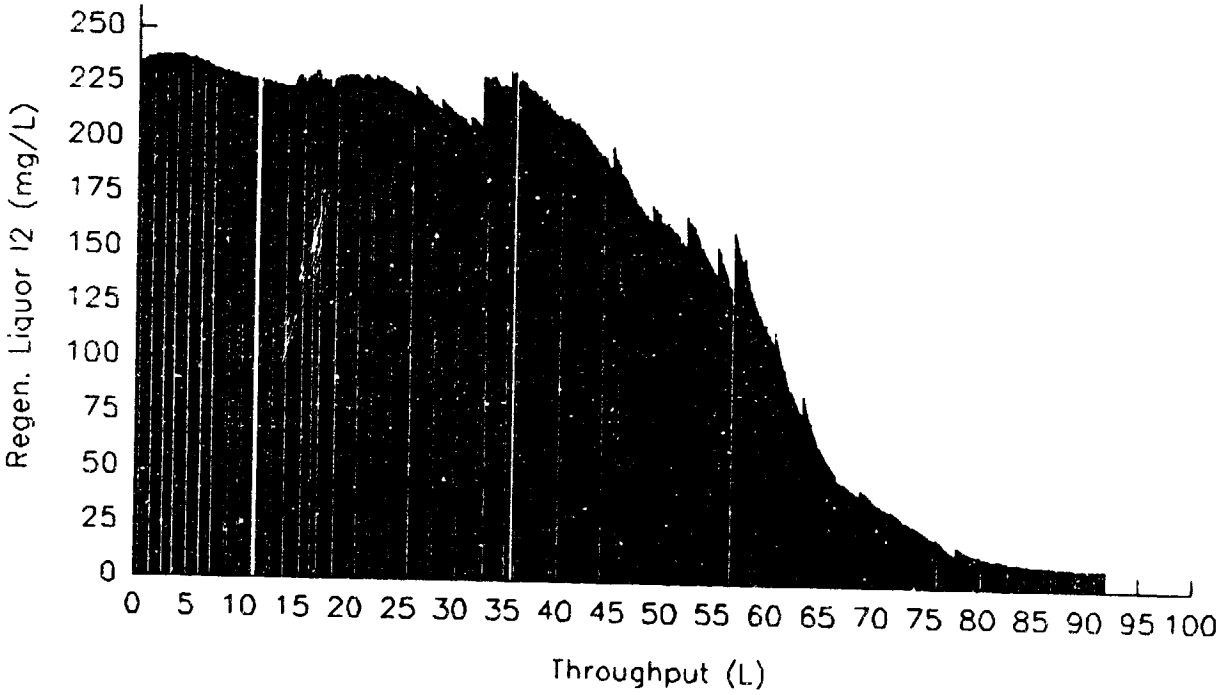

a) Effluent Iodine versus Throughput

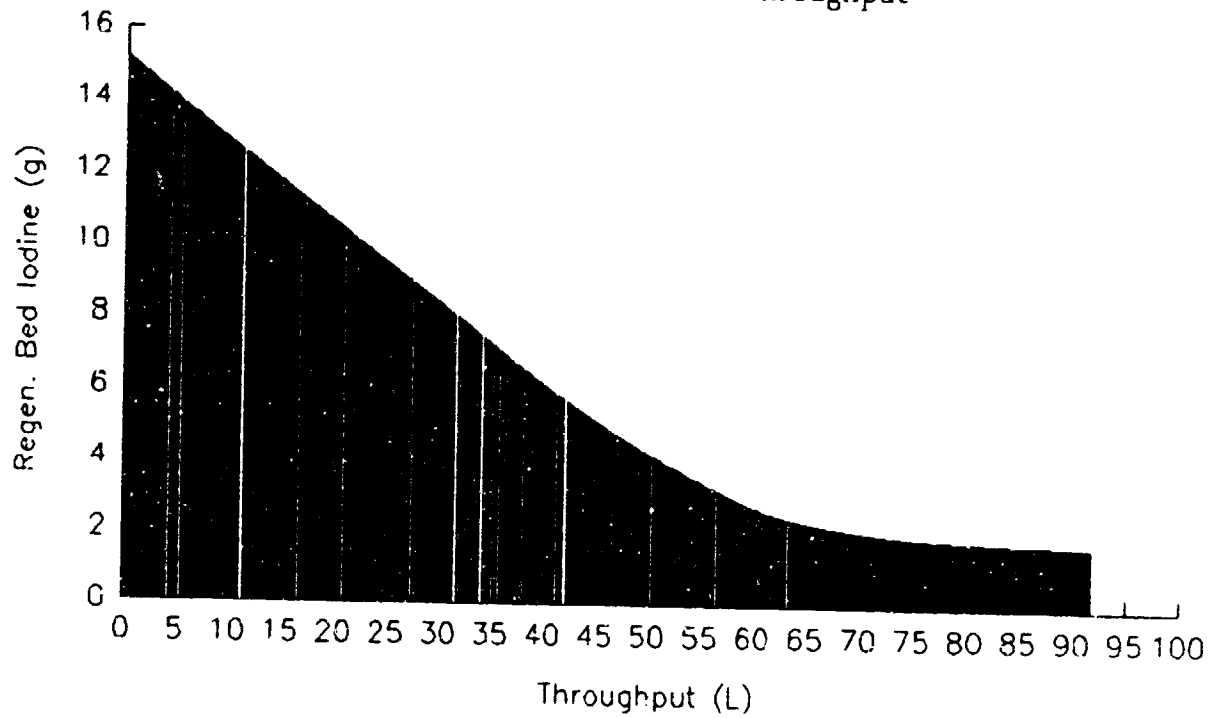

b) Iodine Depletion versus Throughput

Figure 6.15 < 300 μ Crystal Bed Washout.

the stable phase of crystal bed washout lasting between 25 and 50 liters of throughput. The 300 - 425 μ crystal size fraction produced I_2 levels of approximately 250 mg/L. For each of the fractions, as the crystal bed neared ultimate depletion, the effluent I_2 values dropped sharply.

Figure 6.12 depicts a premature decline in effluent I_2 concentration at approximately 25 liters throughput. This was the consequence of the formation of a bypass channel within the crystalline iodine bed. The bed was repacked by gentle tapping on the glass column at 38 liters throughput. This caused the I_2 concentration to immediately rise to expected levels. To a lesser extent, the effects of assymetric bed dissolution caused by the formation of prefered channels of flow can be seen in the other figures also. In all cases these problems were remedied by gentle tapping on the columns.

For constant residence time, the relationship between average aqueous I_2 concentration versus crystal size is given in Figures 6.16, 6.17, 6.18, and 6.19 for the residence times of 1.0, 0.4, 0.2, and 0.1 minutes respectively. Inspection of these data indicate that with the exception of the largest particle size fraction, 850 - 1180 μ, the I_2 values are relatively independent of crystal size. I_2 values for the largest crystal size fraction at residence times less than 1.0 minute are significantly below that of the other size fractions.

Curves depicting the dependence of effluent I_2 concentrations on residence time for the particle size fractions 300 - 425 μ, 425 - 600 μ, 600 - 850 μ, and 850 - 1180 μ are given in Figures 6.20, 6.21, 6.22, and 6.23 respectively. At very short residence times between 0 - 0.2 minutes, large changes in effluent I_2 values result from small changes in residence time. The magnitude of this effect diminishes with increasing residence times. At residence times above 1.0 minutes, effluent concentrations trend toward constant levels independent of residence times. In general, the smaller crystal sizes require less residence time to achieve equivalent concentrations of I_2.

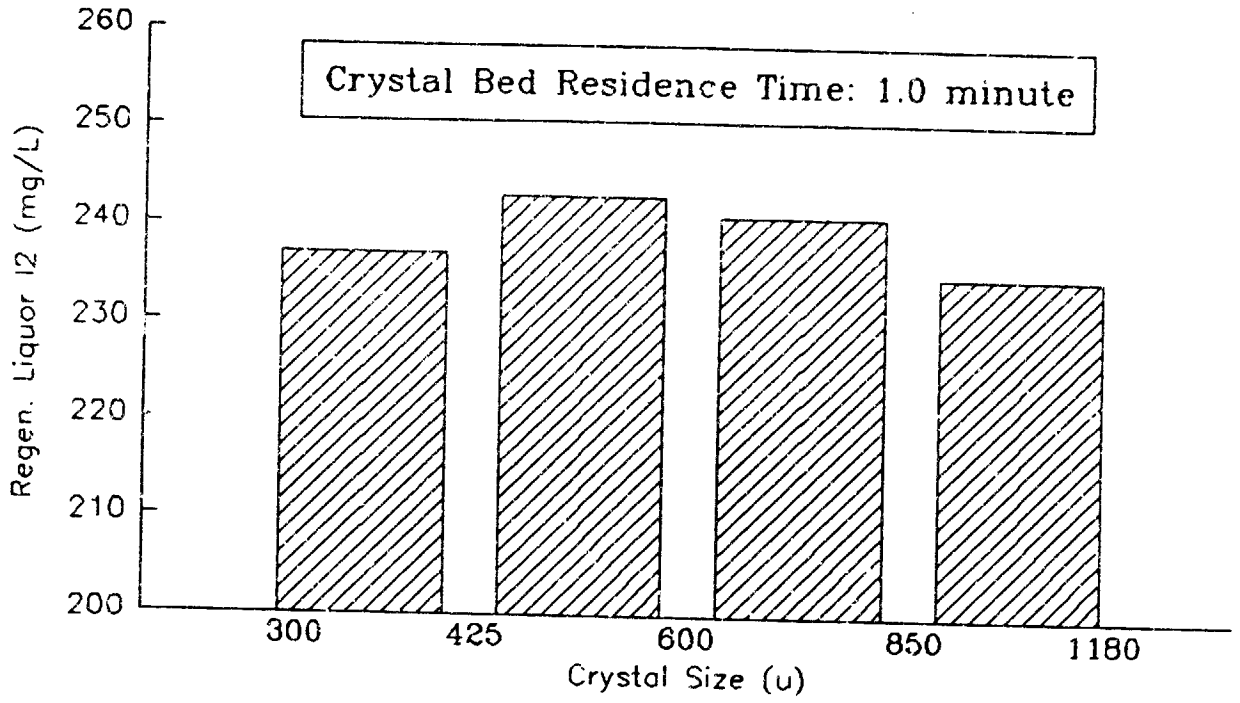

Figure 6.16 Aqueous I_2 versus Crystal Size - 1.0 Minute Residence Time.

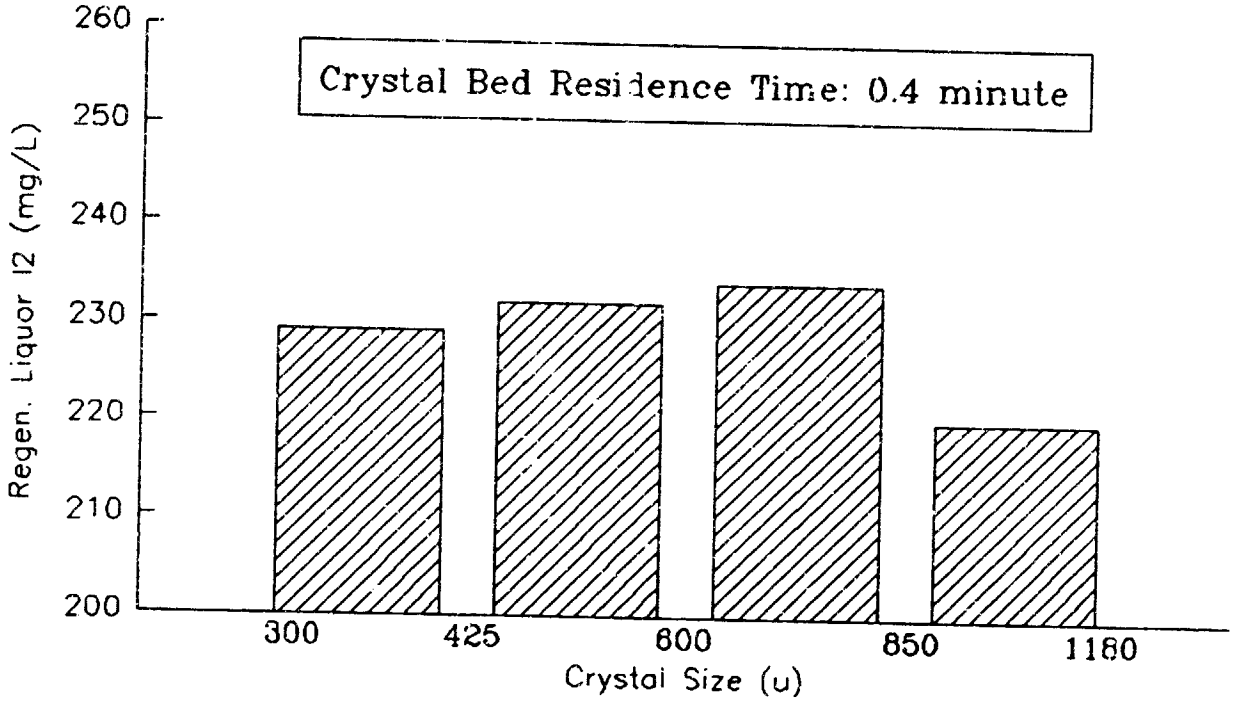

Figure 6.17 Aqueous I_2 versus Crystal Size - 0.4 Min. Residence Time.

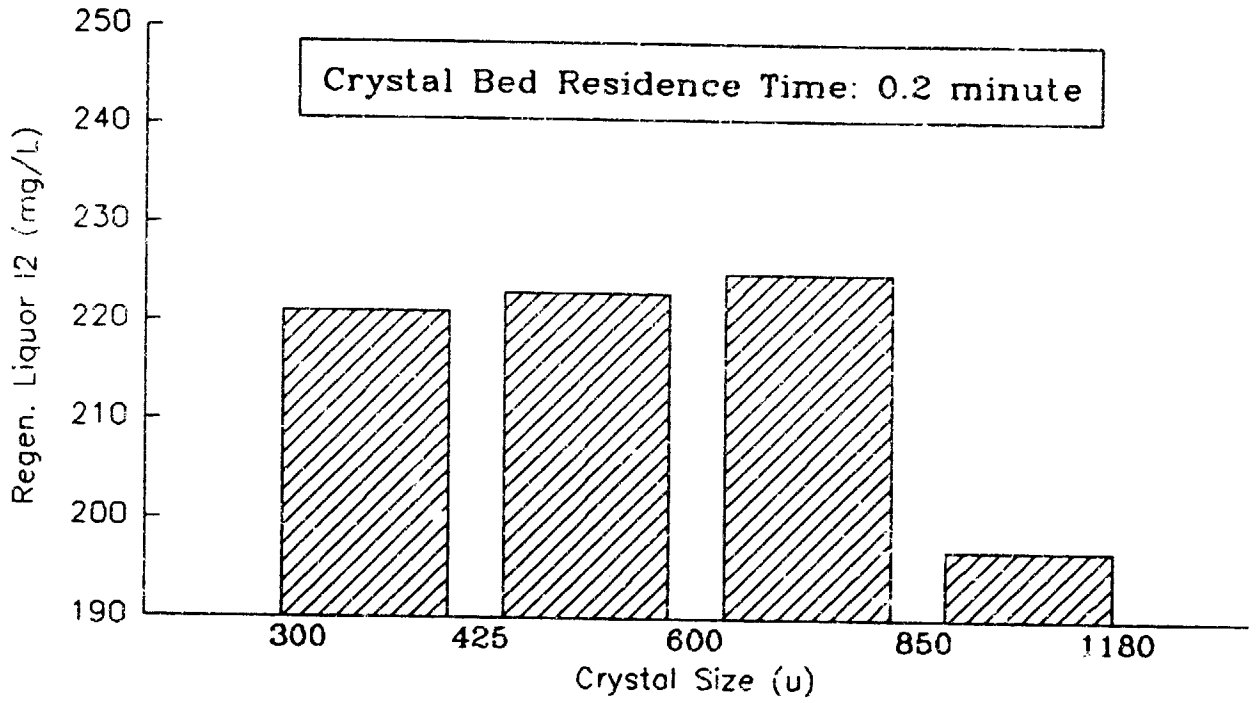

Figure 6.18 Aqueous I_2 versus Crystal Size - 0.2 Minute Residence Time.

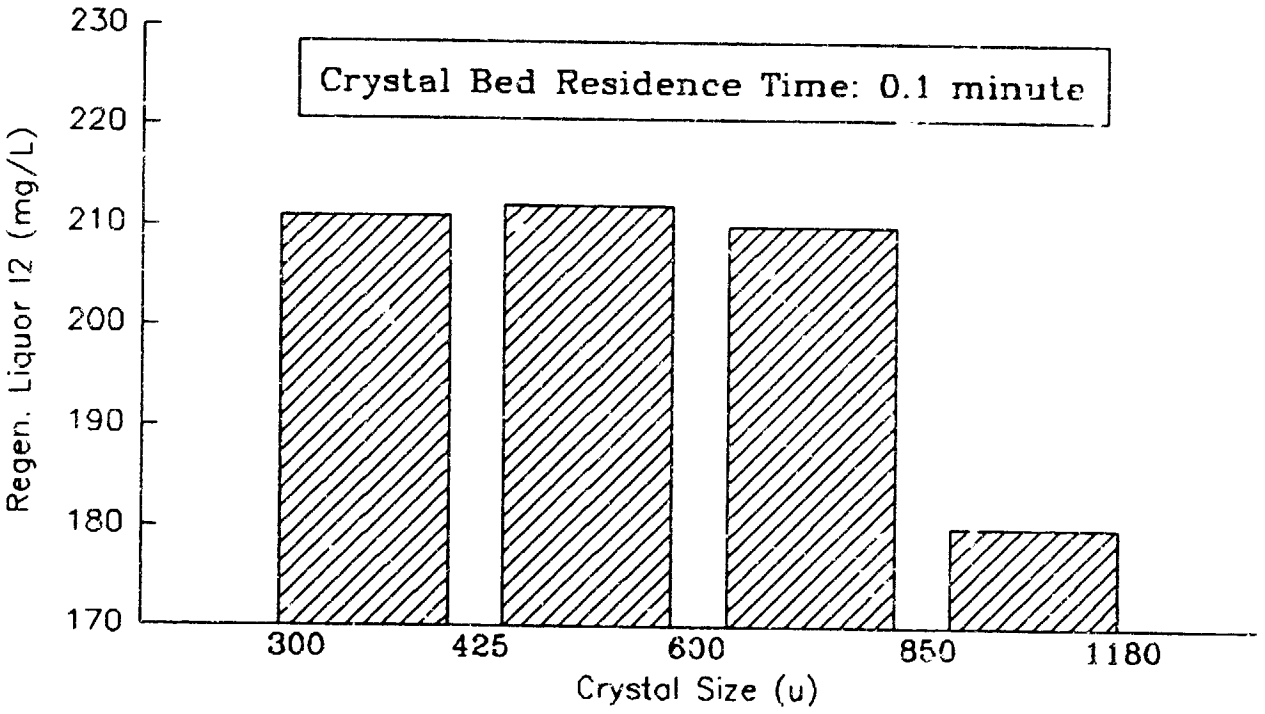

Figure 6.19 Aqueous I_2 versus Crystal Size - 0.1 Minute Residence Time.

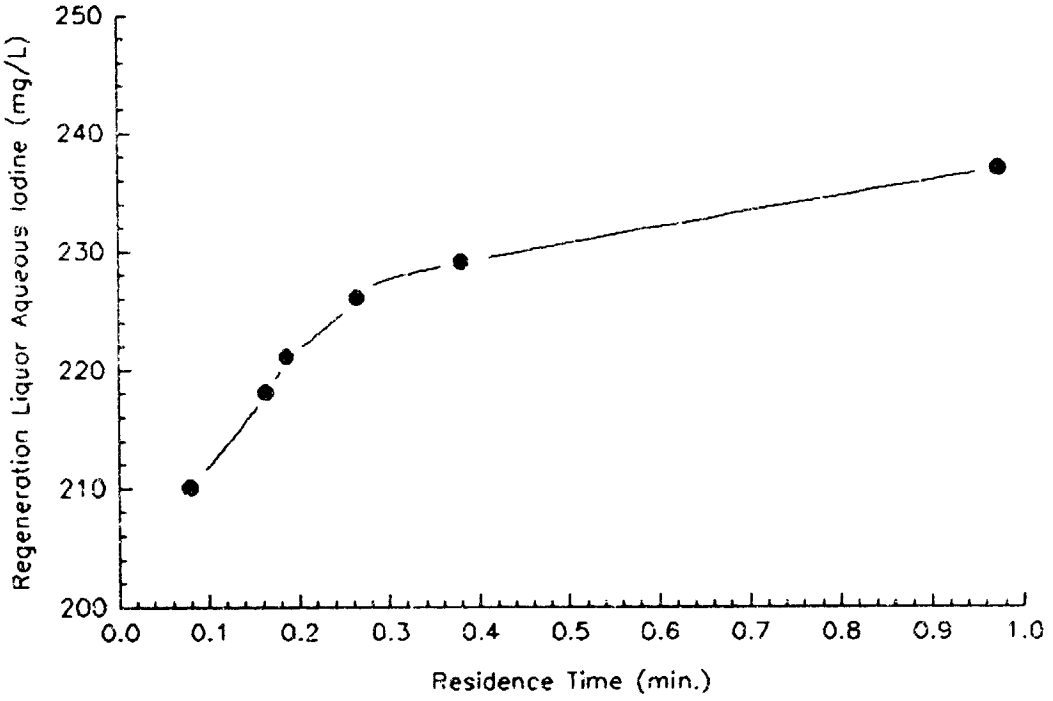

Figure 6.20 300 - 425 μ Crystal Bed Effluent versus Residence Time.

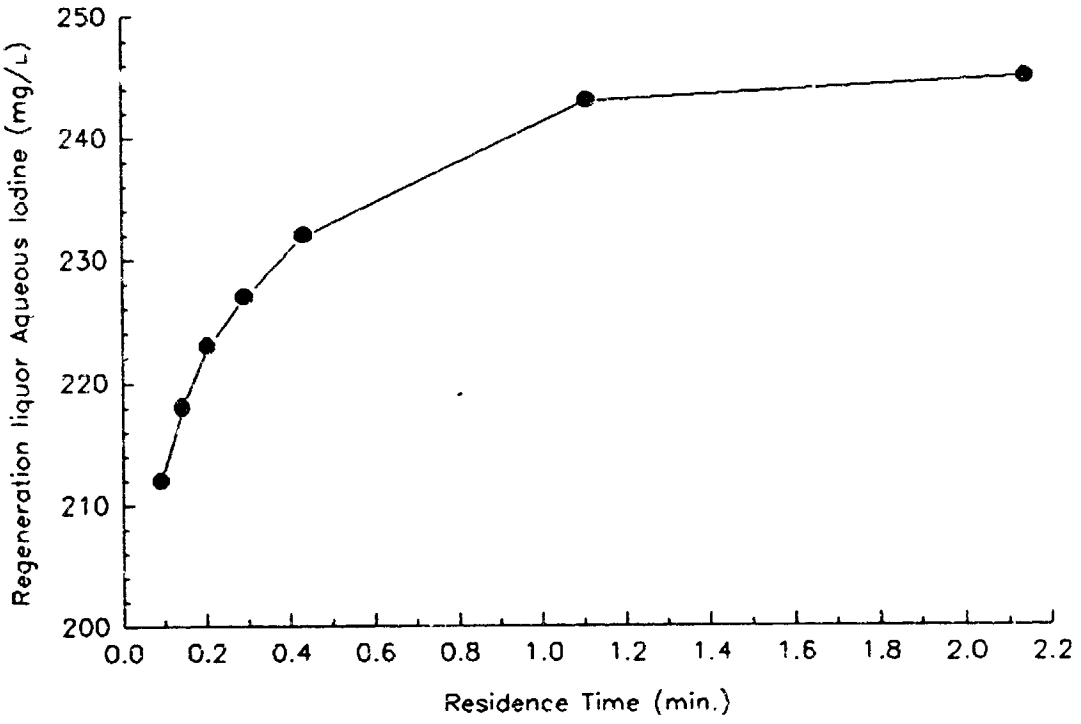

Figure 6.21 425 - 600 μ Crystal Bed Effluent versus Residence Time.

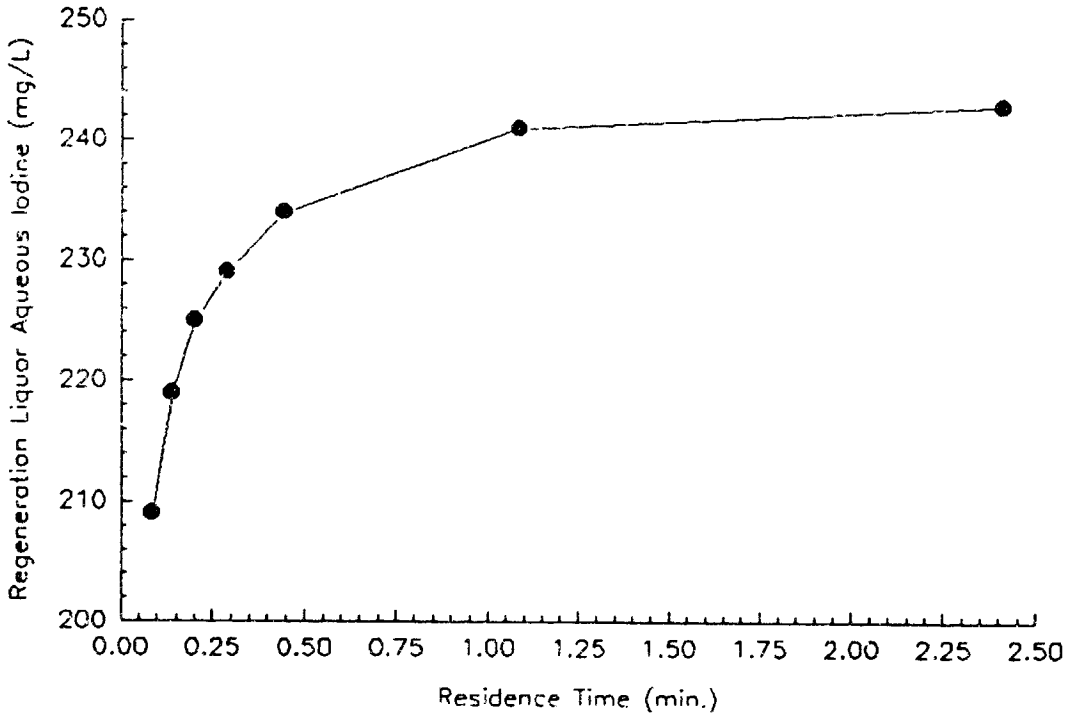

Figure 6.22 600 - 850 μ Crystal Bed Effluent versus Residence Time.

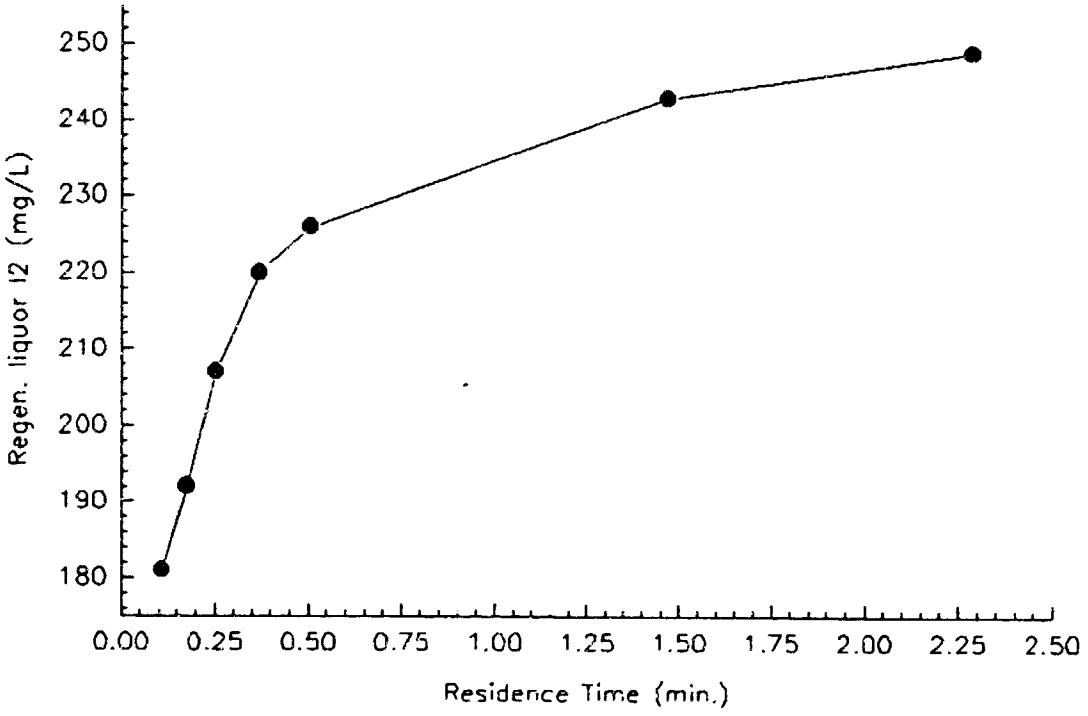

Figure 6.23 850 - 1180 μ Crystal Bed Effluent versus Residence Time.

None of the crystal bed effluent I_2 concentrations monitored during the crystal size experiments yielded the high $\geq$ 300 mg/L levels encountered during the residence time tests. Significantly, the two sets of test results were obtained by strikingly different sampling and analytical methodologies. During the residence time experiments, the test stand diode array spectrophotometer was dedicated to monitoring the low levels of I_2 in the MCV effluent. The high levels of I_2 produced by the crystal beds were of necessity determined by the LCV colorimetric method, using individually collected 200 µL samples. In the crystal size series of experiments crystal bed effluent I_2 concentrations were continuously tracked by the on-line diode array spectrophotometer, using a 1 cm path length cell.

The discrepancy between the two sets of data is most probably due to a combination of sampling and analytical method bias associated with the LCV iodine determinations. While the trends delineated by the first series of crystal bed residence time experiments are representative, the absolute magnitude of the reported I_2 values are biased high. The relationship between crystal bed residence time and I_2 concentration in the regeneration liquor developed using the crystal size experimental data reported in this sub-section is considered to be representative of RMCV operations from both a qualitative and quantitative perspective.

6.3 RMCV Operation at High and Low pH.

The contaminant models selected for use as RMCV challenge solutions represent a relatively narrow range of pH, which on average varies between pH = 3.5 to pH = 6.5. In order to investigate a broader pH range, acidic challenge solutions at pH = 2 and pH = 4 were prepared by acidification of DI water with HCl, and alkaline challenge solutions at pH = 8 and pH = 10 were prepared by addition of NaOH to DI water. These non-buffered solutions were then fed to 2.5 cm^3 small column scale MCVs. The test results are given in Figures 6.24, 6.25. 6.26, and 6.27 for pH values of 2, 4, 8, and 10 respectively.

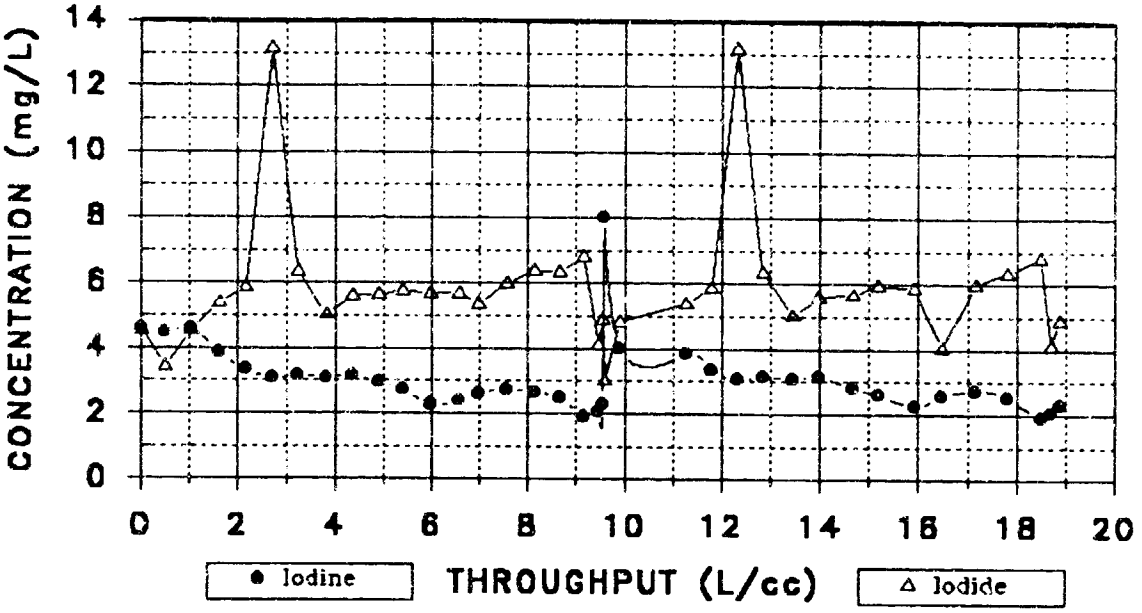

Figure 6.24 RMCV Challenged with HCl Solution at pH = 2.

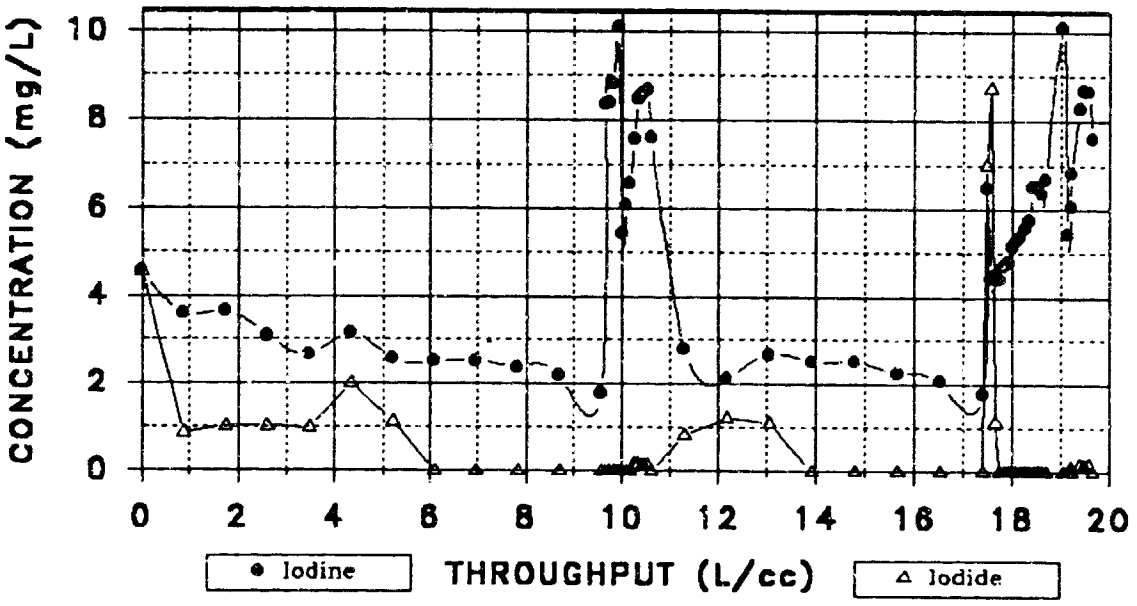

Figure 6.25 RMCV Challenged with HCl Solution at pH = 4.

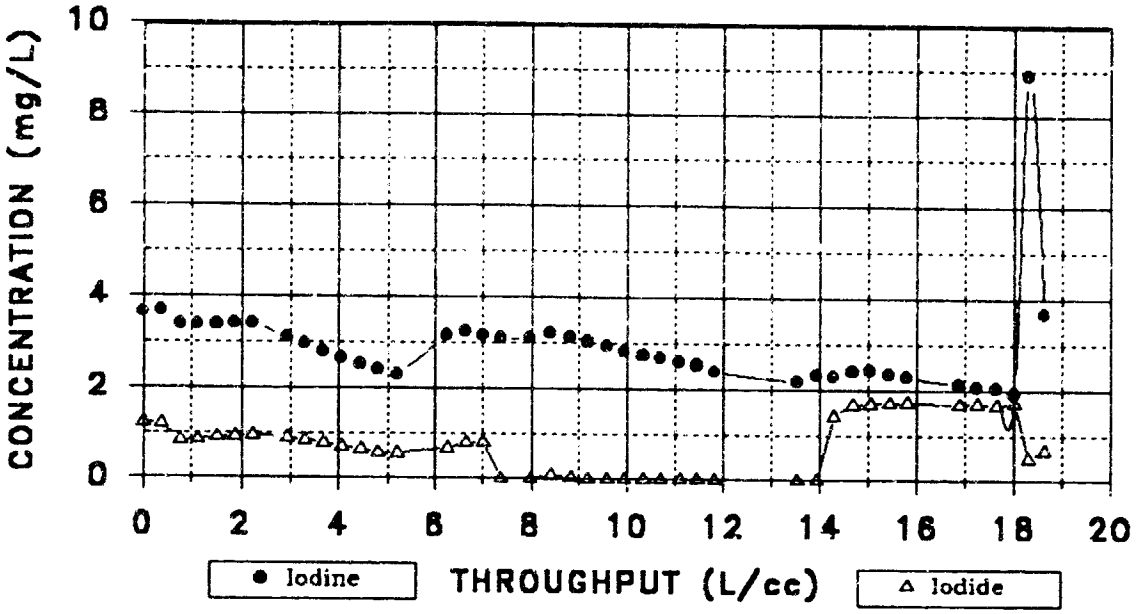

Figure 6.26 RMCV Challenged with NaOH at pH = 8.

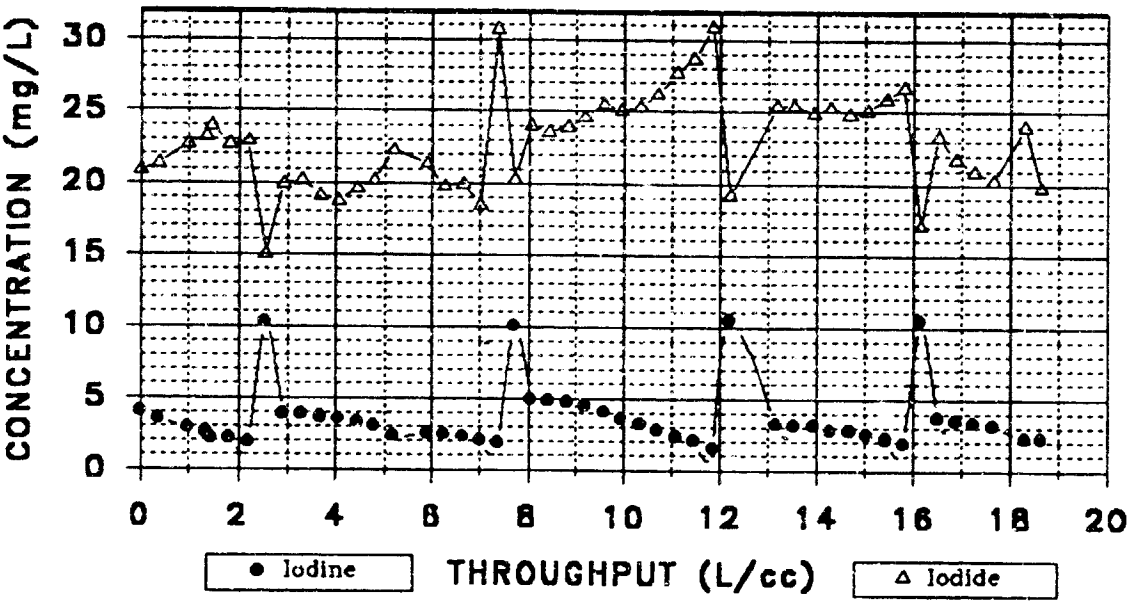

Figure 6.27 RMCV Challenged with NaOH at pH = 10.

The pH = 2 challenged RMCV cycled through two regenerations, averaging approximately 19 L/cm^3 of throughput per cycle. In comparison to the response of typical RMCV challenge streams, I^- levels were elevated to approximatley 6.0 mg/L, with reproducible spikes to 13.0 mg/L at approximately 2.5 L/cm^3 of throughput into each cycle. The high I^- levels may be due to displacement at the resin anion exchange sites by Cl^-, present at approximately 0.01 M. At pH = 4 the levels of I^- ranged between 1 - 2 mg/L. The RMCV serving this stream underwent two regenerations with average cyclic throughputs of appriximately 9.5 L/cm^3. The levels of iodide present at this pH are also possibly due to displacement by Cl^-. In summary, the unusual effects of the two experiments at acidic pHs are believed to be due to the presence of a competing anion, rather than to the effects of increased acidity.

The effluent I_2 levels from the RMCV challenged with pH = 8 solution wandered up and down before triggering a regeneration after 18 L/cm^3 of throughput. Effluent I^- levels varied between 0 - 1.7 mg/L. The source of iodide could be either displacement by OH^- or the result of hydrolytic disproportionation reactions, or both. At pH = 10 the RMCV underwent five washouts and four regenerations in approximately 19 L/cm^3 of total throughput. Extremely high levels of I^- were observed in the effluent ranging between 15 - 30 mg/L, and mirroring the symmetry of the I_2 washout curve. This behavior is probably due to hydrolytic reactions resulting in the formation of iodate, hypoiodous acid, and iodide. This subject will be treated extensively in Section 7.

6.4 Amberlite 401S Resin Tests.

The Phase I increment of RMCV development[90,222] was conducted using MCVs prepared using Amberlite 401S anion exchange resin. For comparison puposes, small column tests were run using this resin. The test results are given in Figures 6.28, 6.29, 6.30, and 6.31 for the ersatz reclaimed potable water, ersatz reclaimed hygiene water, ersatz humidity condensate, and ersatz urine distillate challenge streams respectively.

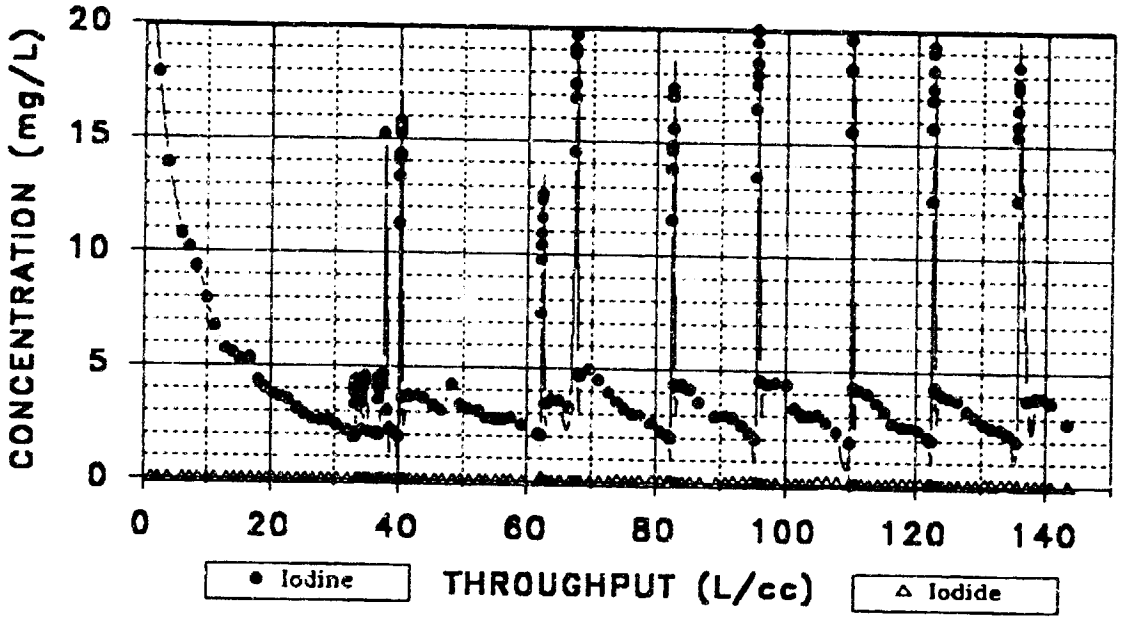

Figure 6.28 Amberlite 401S - Ersatz Reclaimed Potable Water.

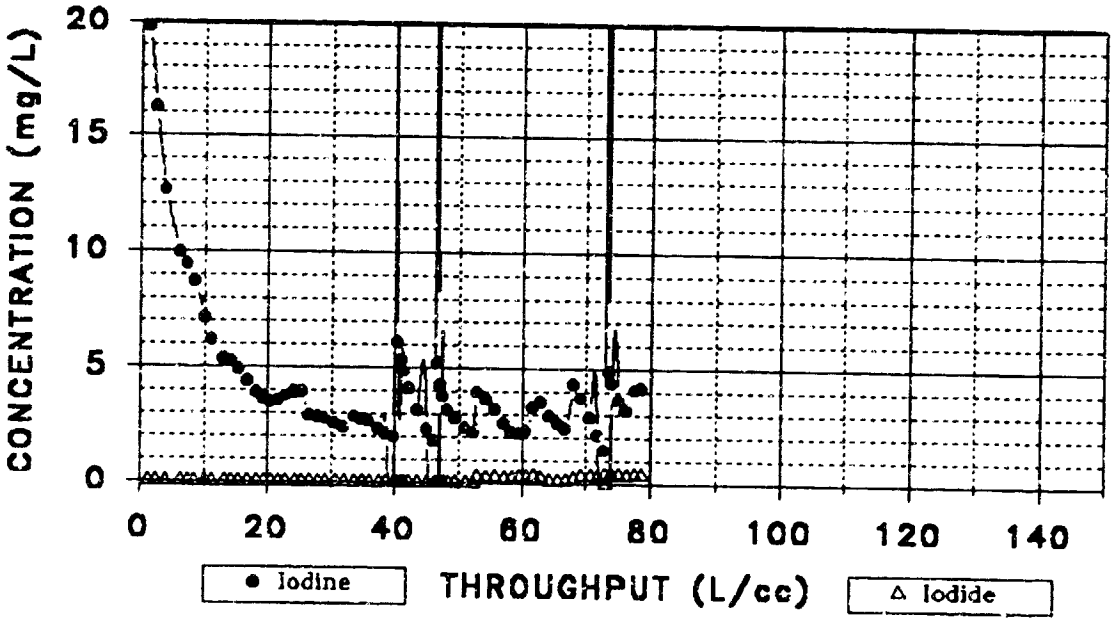

Figure 6.29 Amberlite 401S - Ersatz Reclaimed Hygiene Water.

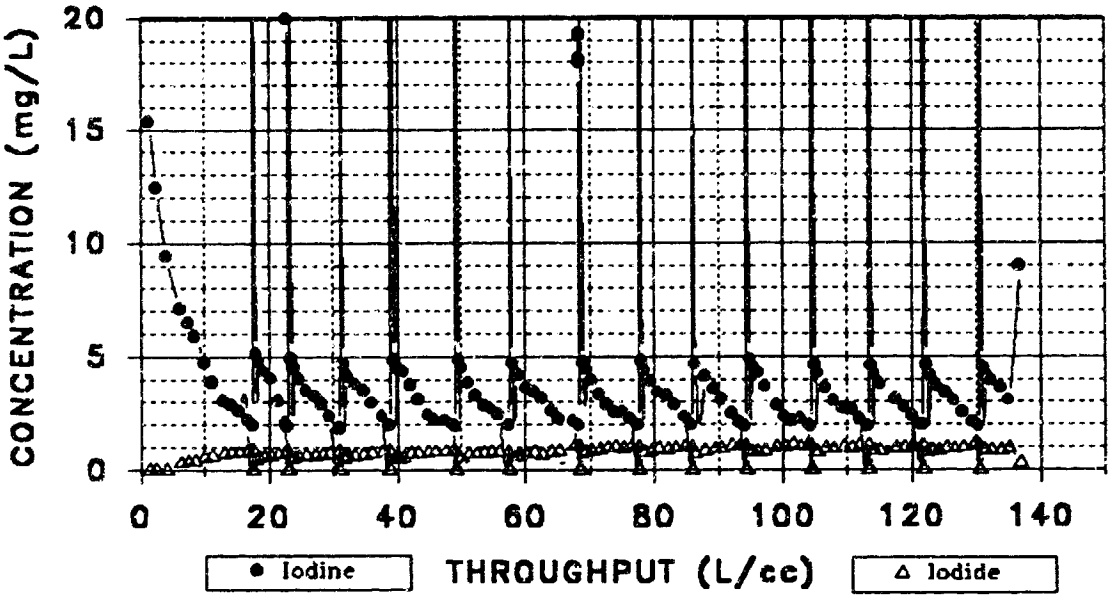

Figure 6.30 Amberlite 401S - Ersatz Humidity Condensate .

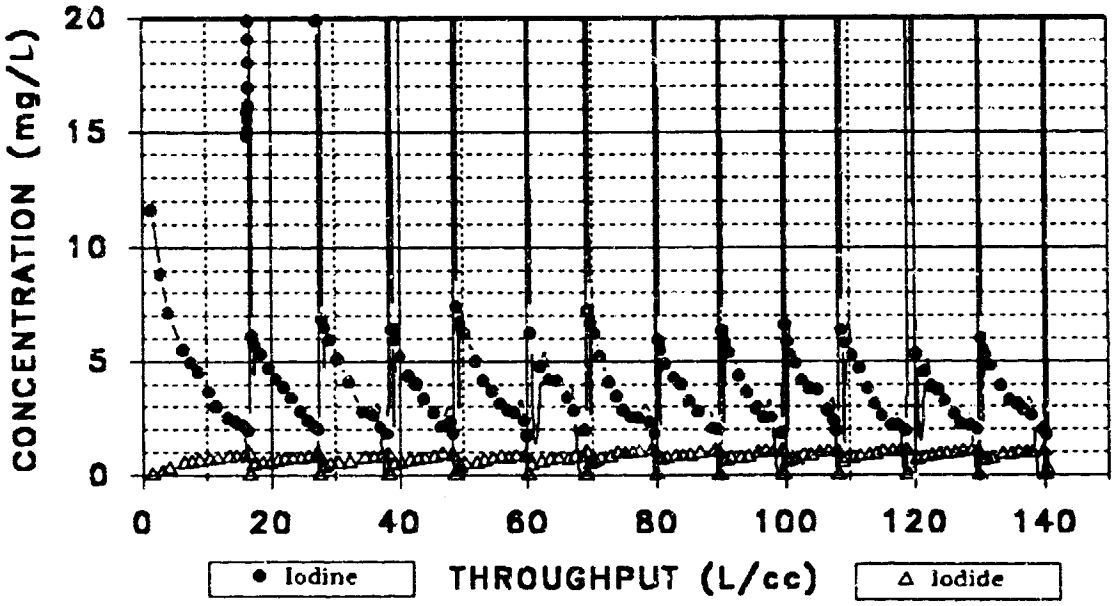

Figure 6.31 Amberlite 401S - Ersatz Urine Distillate.

The 401 S resin was prepared using the standard procedures for MCV resin. Two noteworthy properties of this resin are its low anion exchange capacity of 0.46 meq/cm^3 and its poor mechanical strength. The initial washouts for RMCVs serving all four of the challenge streams exhibited high I_2 residuls ranging between 12 - 25 mg/L. Following the protracted intial washout, the RMCV serving the ersatz reclaimed potable water stream underwent seven cycles of operation in approximately 100 L/cm^3 of throughput for an average cyclic throughput of approximately 13 L/cm^3.

The RMCV challenged with ersatz reclaimed hygiene water experienced repeated mechanical difficulties. For this reason little useful information was obtained for this challenge stream.

After an initial washout from 15 mg/L, the RMCV challenged with ersatz humidity condensate achieved stable operation, cycling through 14 regenerations in approximately 130 L/cm^3 of throughput. The RMCV challenged with ersatz urine distillate also stabilized quickly and underwent a series of 13 regenerations in 130 L/cm^3 of throughput. With this resin the natural cyclic frequency trends among the challenge solutions are the same as those noted for units prepared from standard iodinated MCV resin.

7

RMCV CHEMISTRY

7.0 Overview.

Several aspects of the chemistry of aqueous I_2 solutions are particularly relevant to the application of RMCV technology. Of foremost concern is the reactivity of molecular iodine. This is a concern from the standpoint of both the potential loss of effective biocide and the possible formation of unwanted inorganic or organic iodinated species. Aqueous I_2 reacts with water to form a number of inorganic derivatives, most notably hypoiodous acid (HOI), iodate anion (IO_3^-), and iodide. The extent to which these reactions proceed is a function of pH, temperature, and initial I_2 concentration. Both the equilibrium and kinetics of these reactions at iodine concentrations typical of RMCV operation have been examined in detail and the results are presented below.

Another aspect of aqueous I_2 chemistry which has received considerable attention during the course of the RMCV development work is the characterization of the decay of I_2 concentrations in the ersatz humidity condensate and the ersatz urine distillate challenge solutions. This work has resulted in the identification of the primary causitive reaction and in determination of the order, rate constants, frequency factor and Arrhenius activation energy describing the reaction kinetics[14]. Additionally, a survey of the literature has been conducted to ascertain possible routes of formation of iodinated organics in the RMCV challenge streams. Armed with this information, a limited number of attempts have been made to identify iodinated organics. This work has been limited by the availability of standard reference materials, the need for development of suitable analytical methodologies, and also by the time constraints of the performance period of the Phase II effort. The results of these investigations are presented in detail below.

7.1 The Chemistry of Aqueous I_2 Speciation.

7.1.1 Aqueous I_2 Equilibria at 25 °C.

Aqueous iodine can be lost from solution by phase transition to the gaseous state[274,388] as illustrated in equation 7.1 below:

$$I_{2(aq)} \leftrightarrow I_{2(v)} \qquad K_1=\frac{[I_{2(v)}]}{[I_{2(aq)}]}=0.0136 \qquad \text{(Eqn.7.1)}.$$

The linear relationship between vapor phase I_2 concentration in micro-atomospheres (μA) and aqueous I_2 concentration (mg/L) for closed systems at equilibrium is illustrated in Figure 7.1. The reaction[103,229,230,335,349] between aqueous I_2 and I^- forming I_3^- was introduced in Section 4, and is given below in equation 7.2,

$$I_2 + I^- \leftrightarrow I_3^- \qquad K_2=\frac{[I_3^-]}{[I_2][I^-]}=736 \qquad \text{(Eqn.7.2)}.$$

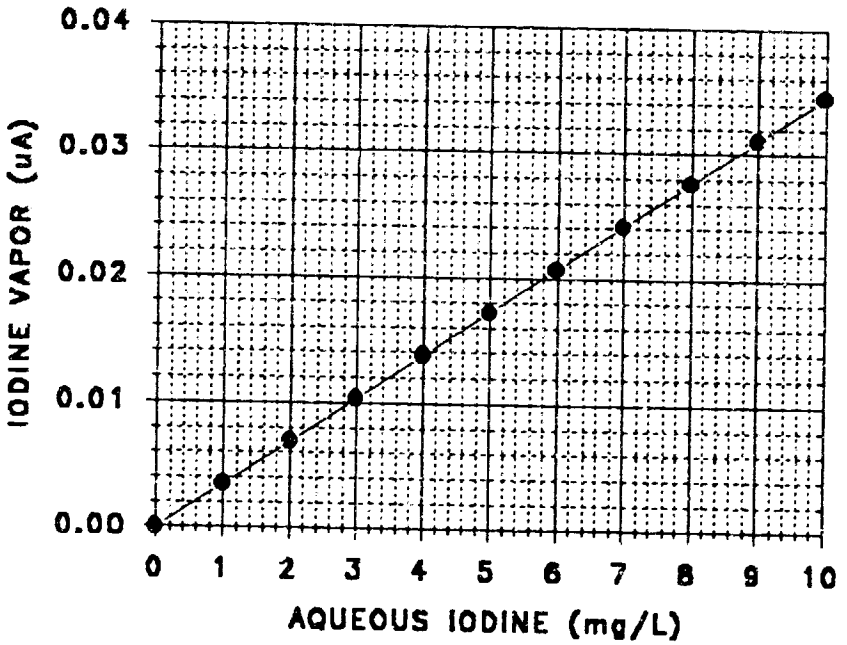

Figure 7.1 Equilibrium of I_2 Vapor as a Function of Aqueous I_2.

Aqueous I_2 undergoes a hydrolytic disproportionation[6,26,313,336,415] to form HOI and I^- as shown by equation 7.3,

$$I_2 + H_2O \leftrightarrow HOI + H^+ + I^- \qquad K_3=\frac{[HOI][H^+][I^-]}{[I_2]}=4.83\times10^{-13} \qquad \text{(Eqn.7.3)}.$$

Additional reactions associated with the products of the initial hydrolysis reaction include the dissociation of hypoiodous acid (Eqn. 7.4),

$$HOI \leftrightarrow H^+ + OI^- \qquad K_4=\frac{[H^+][OI^-]}{[HOI]}=2.30\times10^{-11} \qquad \text{(Eqn.7.4)},$$

and the formation of I_2OH^-, I_2O^{-2}, and H_2OI^+ as shown in equations 7.5, 7.6 and 7.7 respectively.

$$OI^- + I^- + H_2O \leftrightarrow I_2OH^- + OH^- \qquad K_5=\frac{[I_2OH^-][OH^-]}{[OI^-][I^-]}=0.13 \qquad \text{(Eqn.7.5)}.$$

$$OI^- + I^- \leftrightarrow I_2O^= \qquad K_6=\frac{[I_2O^=]}{[OI^-][I^-]}=0.045 \qquad \text{(Eqn.7.6)}.$$

$$H_2OI^+ \leftrightarrow HOI + H^+ \qquad K_7=\frac{[H_2OI^+]}{[HOI][H^+]}=0.03 \qquad \text{(Eqn.7.7)}.$$

A second hydrolytic disproportionation reaction results in the formation of

iodate[178,313,336,415] and iodide as shown in equation 7.8,

$$3I_2 + 3H_2O \leftrightarrow IO_3^- + 5I^- + 6H^+ \qquad K_8=\frac{[IO_3^-][I^-]^5[H^+]^6}{[I_2]^3}=1.25\times10^{-47} \quad \text{(Eqn.7.8)},$$

and in the formation of iodic acid (HIO_3)[59,350,408,445] by the reaction of equation 7.9,

$$HIO_3 \leftrightarrow H^+ + IO_3^- \qquad K_9=\frac{[H^+][IO_3^-]}{[HIO_3]}=0.164 \qquad \text{(Eqn.7.9)}.$$

Very small quantities of periodate (IO_4^-) can also be formed by disproportionation of iodate by the reaction given in equation 7.10,

$$4IO_3^- \leftrightarrow 3IO_4^- + I^- \qquad K_{10}=\frac{[IO_4^-]^3[I^-]}{[IO_3^-]^4}=1.0\times10^{-53} \qquad \text{(Eqn.7.10)}.$$

Undissociated periodic acid exits primarily in the hydrated form as H_5IO_6 (orthoperiodic acid)[67,94], and is related to the periodate anion by the series of equilibria expressed in equations 7.11 - 7.14.

$$H_5IO_6 \leftrightarrow H_4IO_6^- + H^+ \qquad K_{11}=\frac{[H_4IO_6^-][H^+]}{[H_5IO_6]}=5.01\times10^{-4} \qquad \text{(Eqn.7.11)}.$$

$$H_4IO_6^- \leftrightarrow H_3IO_6^{-2} + H^+ \qquad K_{12}=\frac{[H_3IO_6^{-2}][H^+]}{[H_4IO_6^-]}=2.00\times10^{-7} \qquad \text{(Eqn.7.12)}.$$

$$H_3IO_6^{-2} \leftrightarrow H_2IO_6^{-3} + H^+ \qquad K_{13}=\frac{[H_2IO_6^{-3}][H^+]}{[H_3IO_6^{-2}]}=1.05\times10^{-15} \quad \text{(Eqn.7.13).}$$

$$H_4IO_6^- \leftrightarrow IO_4^- + 2H_2O \qquad K14=\frac{[IO_4^-]}{[H_4IO_6^-]}=40 \quad \text{(Eqn.7.14).}$$

7.1.2 Numerical Solution of Multiple Equilibria.

For the purposes of estimating the equilibrium distributions of the various iodine containing inorganic species resulting from an initial addition of elemental iodine (I_2) to water, simultaneous solutions of these multiple equilibria were obtained under varying conditions of pH and initial I_2 concentration. A preliminary examination of the above system of interrelated equilibria revealed that the concentrations of iodinated species formed by the reactions given in equations 7.10 through 7.14 are insignificant, under the conditions of interest. For this reason, they were eliminated from further consideration. Also, since aqueous I_2 concentrations are necessarily very low ($\approx$ 1.5 mM for a saturated solution at 25 ^oC) an activity coefficient of 1 was assumed for all iodine containing species. This simplification allowed the use of concentrations directly while introducing only minimal error.

The simplified model of elemental iodine equilibrium speciation includes equations 7.2 through 7.9. The method of simultaneous solution of the system of non-linear equilibria was patterned after that of Palmer and Lietzke[334]. Initial conditions specified at the outset of each run were the equilibrium pH and the total iodine of the system introduced at t_o as I_2. The numerical solution was achieved using a Newton-Raphson type iterative algorithm[346] written in the C programming language. A source code listing for the program ISPECIES.EXE is included in Appendix I. An iodine mass balance was used as the primary convergence

criterion. The iterative solution was allowed to progress until the difference in masses between the sum of all calculated iodine species $[I_j]$ and the original I_2 addition $[I_2]_o$ was fractionally 1 part per million or less, i.e.,

$$| \{ [I_2]_o - \Sigma[I_j] \} / [I_2]_o | \leq 10^{-6} \qquad \text{(Eqn. 7.15).}$$

Secondarily, the solutions were validated by back calculation of the equilibrium constants K_2 through K_9 from the molar concentrations generated by the numerical solution for each of the iodine containing species, using the equilibrium expressions given in equations 7.2 - 7.9.

From a kinetics perspective, the time required for true equilibrium to become established is determined by the slowest or rate limiting step. In the system under consideration, the hydrolytic disproportionation reaction forming IO_3^- is rate limiting. This reaction proceeds quite slowly. By comparison, the hydrolysis reaction resulting in the formation of HOI is very fast, virtually instantaneous. Because of the drastic differences in reaction rates between the two hydrolysis reactions, a pseudo-equilibrium situation is almost instantaneously established upon additon of I_2 to an aqueous system. This pseudo-equilibrium distribution of iodine containing species is dominated by the rapid formation of HOI. Slowly with time, the psuedo-equilibrium concentration of species changes to the true equilibrium distribution which is dominated by the hydrolytic formation of IO_3^-.

Because of the lengthy periods of time required to establish true equilibrium under certain circumstances, it was realized that the nearly instantaneous psuedo-equilibrium distribution of iodine species may also be useful in the characterization of RMCV chemistry. For this reason, numerical solutions of the system of equilibria represented by equations 7.2 through 7.7 inclusively were also obtained using analogous methods over a range of initial pHs and elemental iodine concentrations. The C language source code for the program IPSEUDO.EXE is listed in Appendix I.

Representative results of the numerical solutions for both the true equilibrium situatuion and for the nearly instantaneous pseudo-equilibrium situation are presented below for a selection of I_2 concentrations of importance to RMCV operation.

7.1.3 True Equilibrium I_2 Speciation at 25 °C.

During regeneration, the RMCV solid state I_2 crystal bed produces an aqueous I_2 solution, with $I_2 \approx 300$ mg/L. The equilibrium distribution of I_2, I^-, I_3^-, HOI, IO_3^-, OI^-, HIO_3, I_2OH^-, I_2O^{-2}, and H_2OI^+, as a function of pH for this initial I_2 concentration, is presented in Figure 7.2a and 7.2b using linear and logarithmic concentration scales respectively. All concentrations are given in mg/L as I. At 300 mg/L the iodine is almost completely in the I_2 form between pH = 0 and pH = 4. Between pH = 4 and pH = 7.5 the iodine as I_2 rapidly declines to concentrations asymptotically approaching zero. In the range between pH = 4 and pH = 8 I_3^- occurs in a Gaussian distribution with peak centroid at pH ≈ 6.25, and peak level of $[I_3^-] \approx 85$ mg/L. At pH ≈ 4.5, I^- appears and rapidly increases to a constant level of approximately 250 mg/L for pH ≥ 8. IO_3^- appears at pH ≈ 5.5 and rapidly increases to $[IO_3^-] \approx 50$ mg/L.

In the small column scale long term life cycle RMCV tests, due to the short residence times of challenge solutions within the MCVs, I_2 concentrations of approximately 10 mg/L were often detected in the RMCV effluents during regeneration. Figure 7.3 presents the equilibrium iodine speciation for this concentration as a function of pH. At the high hydrogen ion concentrations between pH = 0 and pH = 1, a significant level of H_2OI^+ is formed. The peak concentration of H_2OI^+ occurs at pH = 0 and constitutes approximately 6 % of total iodine. At 10 mg/L of I, the onset of I_2 decline is shifted to lower pH by 0.4 units in comparison to the 300 mg/L values. The corresponding build up of IO_3^- and I^- also begins at somewhat lower pH.

In the washout cycle of RMCV operation, I_2 concentrations are maintained between

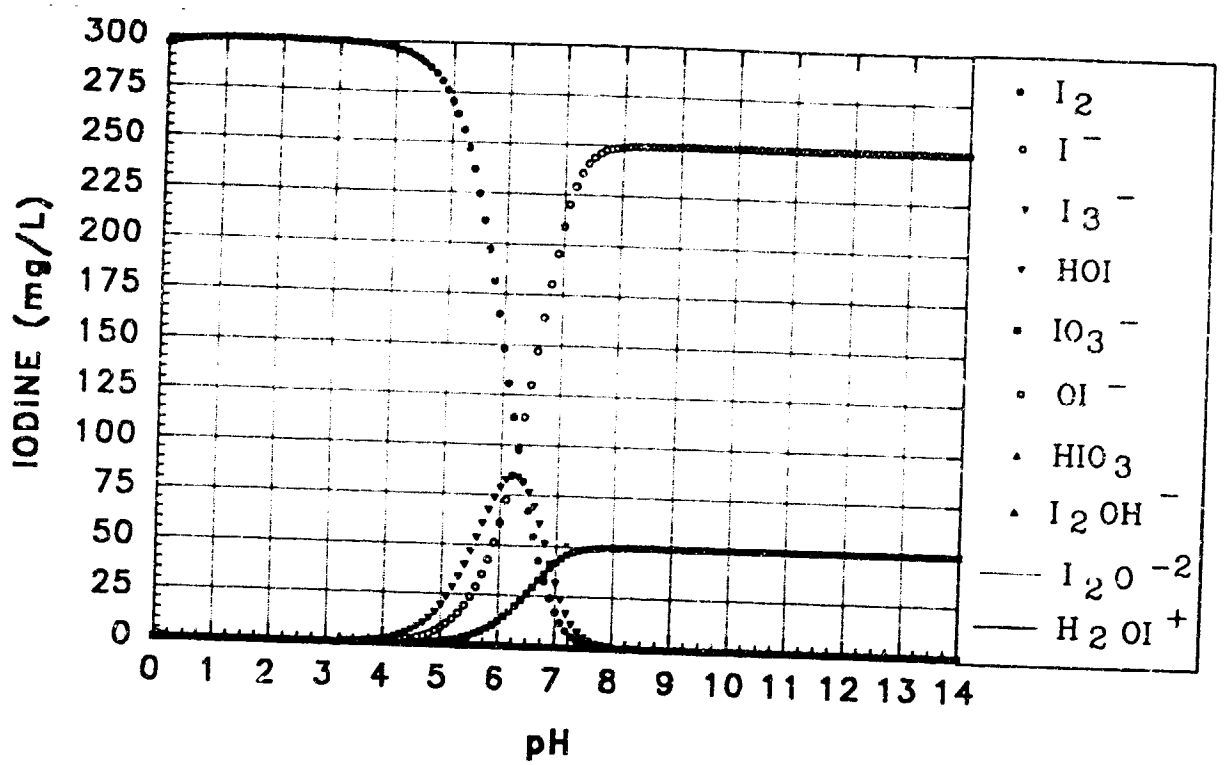

a) Linear Concentration Scale.

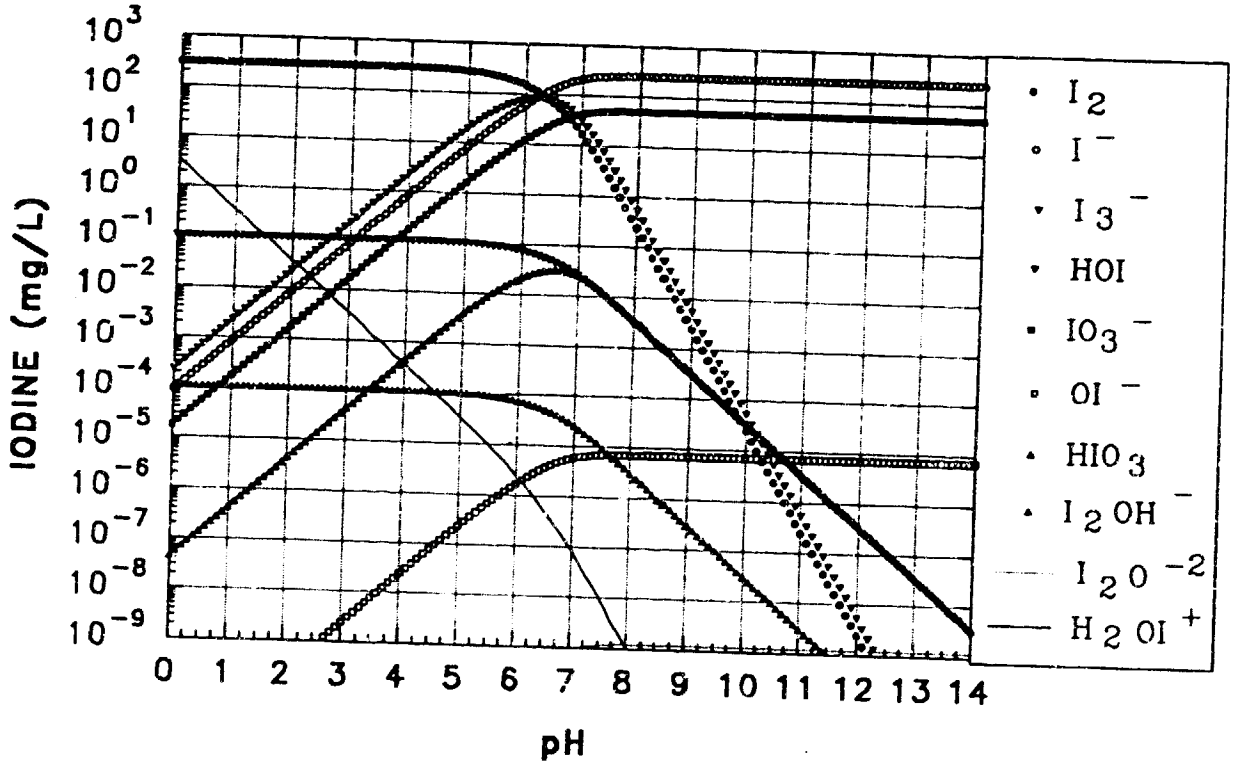

b) Logarithmic Concentration Scale.

Figure 7.2 Equilibrium Iodine Speciation - 300 mg/L I.

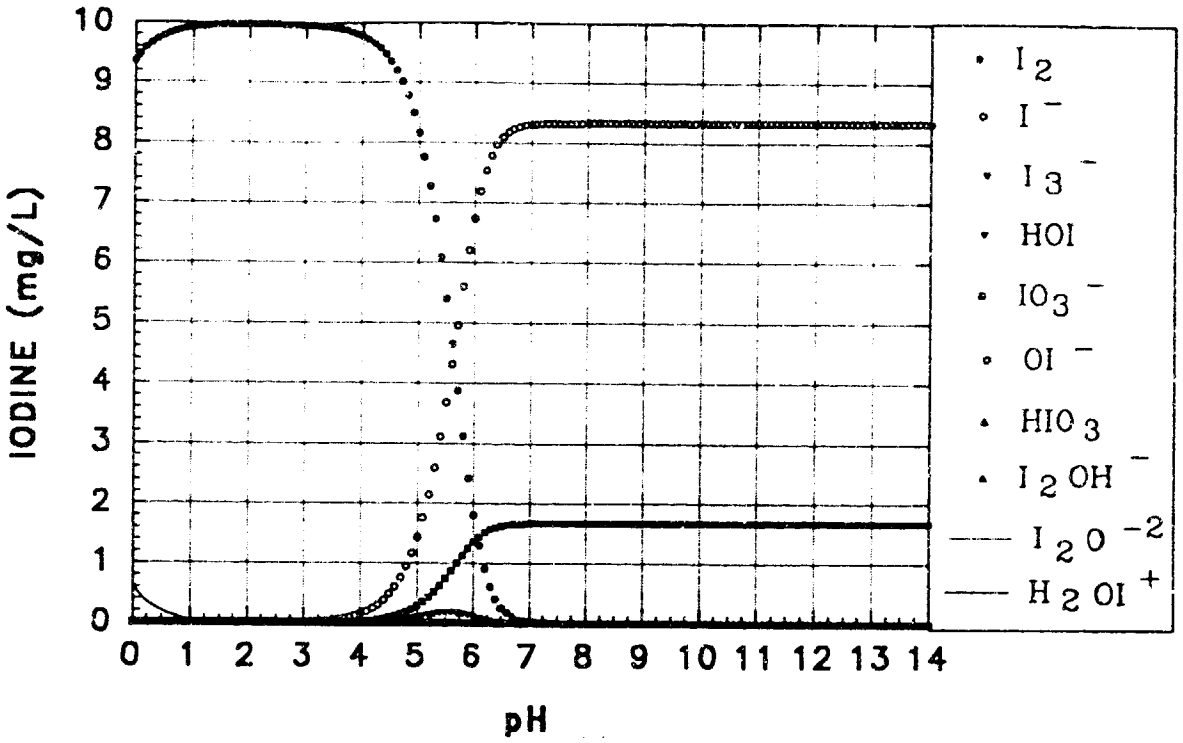

a) Linear Concentration Scale.

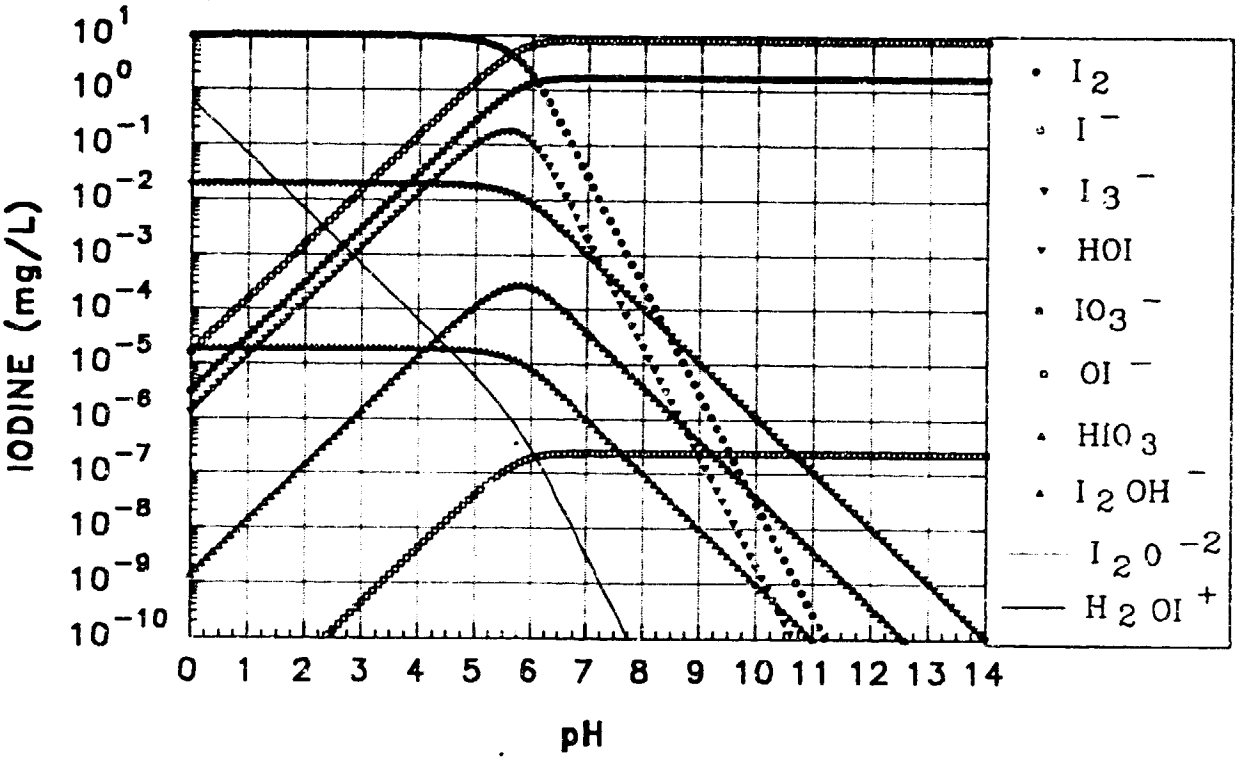

b) Logarithmic Concentration Scale.

Figure 7.3 Equilibrium Iodine Speciation - 10 mg/L I.

4.0 mg/L and 2.0 mg/L. The equilibrium iodine speciation versus pH is presented for these concentrations in Figures 7.4 and 7.5 respectively. Inspection of the variation in equilibrium distribution of iodinated species, between the concentration range of 300 mg/L to 2 mg/L reveals several trends. As the concentration of total aqueous iodine decreases, the formation of I_3^- declines markedly, while the H_2OI^+ fraction increases at low pH. Also the pHs at which I_2 decline, IO_3^- and I^- build up begin, are shifted down scale.

Based upon the above, it is clear that the true equilibrium speciation is dominated by the slow hydrolysis reaction forming 5 equivalents of iodide and 1 equivalent of iodate. This reaction is pH and concentration dependent, with the effects of pH being manifested at lower values as the total iodine concentration decreases. The major equilibrium iodinated species of concern for the concentrations and pHs encountered by RMCV operations are I_2, I^-, I_3^-, and IO_3^-. The relationships between the fractional occurence of a given species and the total iodine concentration, while pH is held constant, are presented for I_2, I^-, I_3^-, and IO_3^- as Figure 7.6, 7.7, 7.8, and 7.9 respectively. The multiple curves of each figure present fractional speciation over the range of pH between 2 and 12.

7.1.4 Pseudo-equilibrium (fast)I_2 Speciation at 25 ^{0}C.

While the true equilibrium iodine speciation is dominated by the slow hydrolytic disproportionation reaction forming IO_3^- and I^-, the pseudo-equilibrium iodine speciation reactions are dominated by the hydrolytic disproportionation reaction forming HOI and I^-. This reaction is extremely fast, virtually instantaneous. Upon addition of I_2 to an aqueous system, the distribution of iodine species corresponding to the pseudo-equilibrium state immediately prevails. The distribution of species then changes continuously and slowly until the true equiibrium distribution is achieved. Because of the length of time involved in achieving true equilibrium at the iodine concentrations and pHs encountered in RMCV operations, the pseudo-equilibrium situation may be more representative of the actual

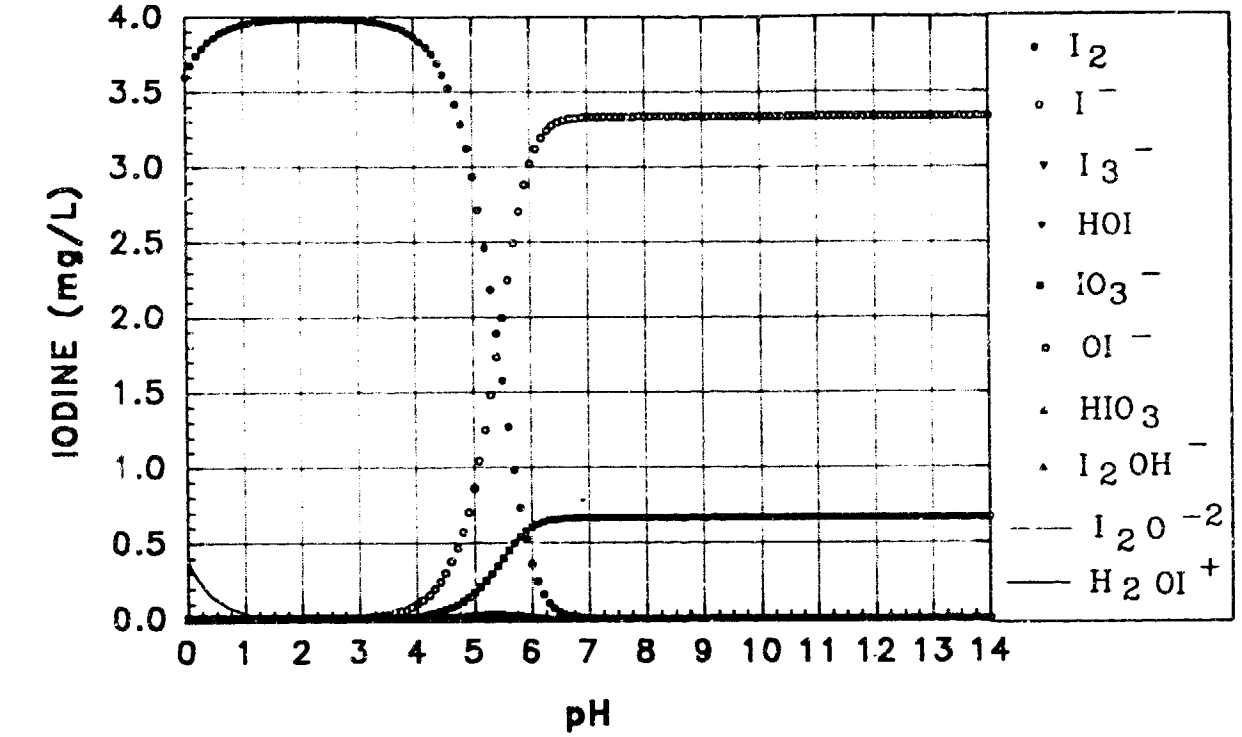

a) Linear Concentration Scale.

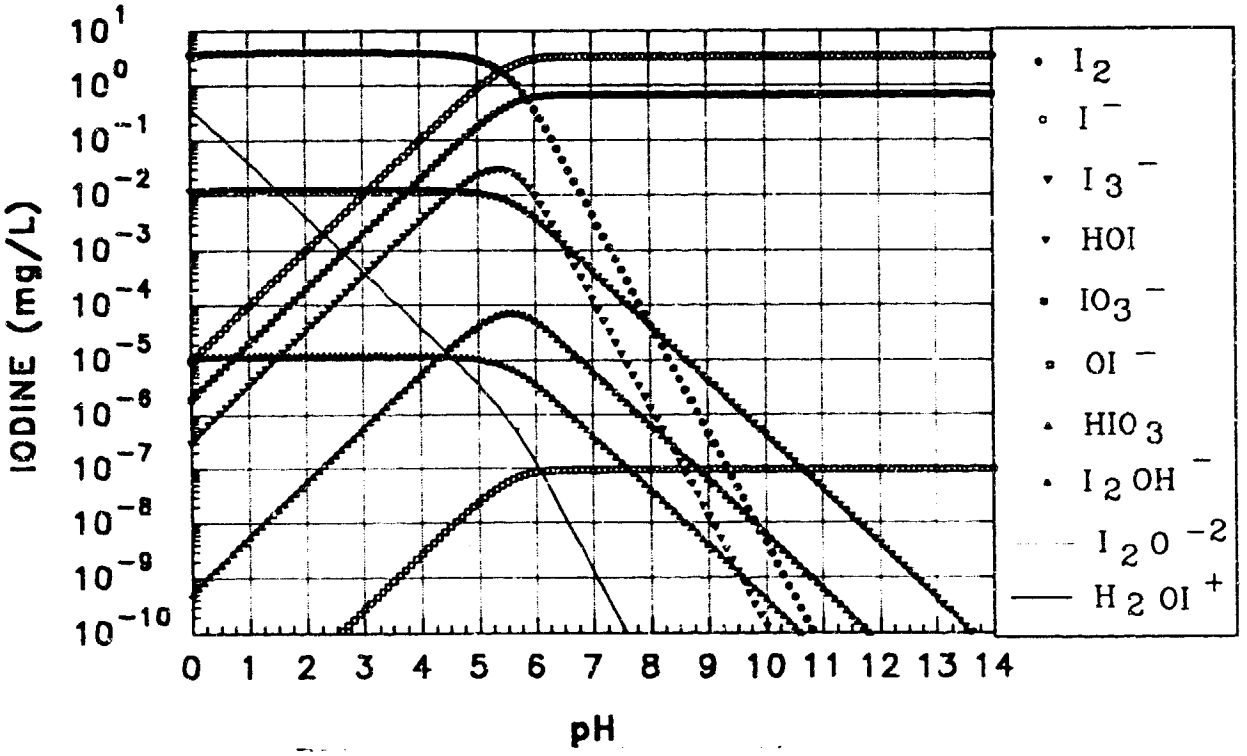

b) Logarithmic Concentration Scale.

Figure 7.4 Equilibrium Iodine Speciation - 4 mg/L I.

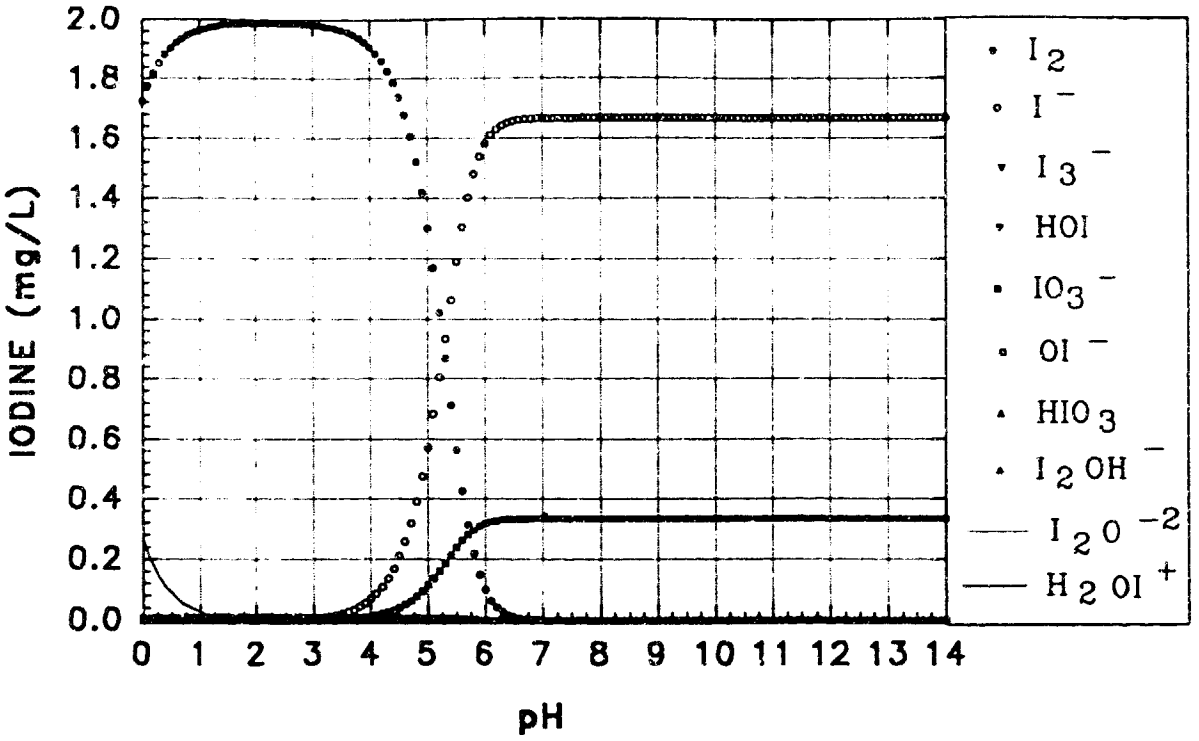

a) Linear Concentration Scale.

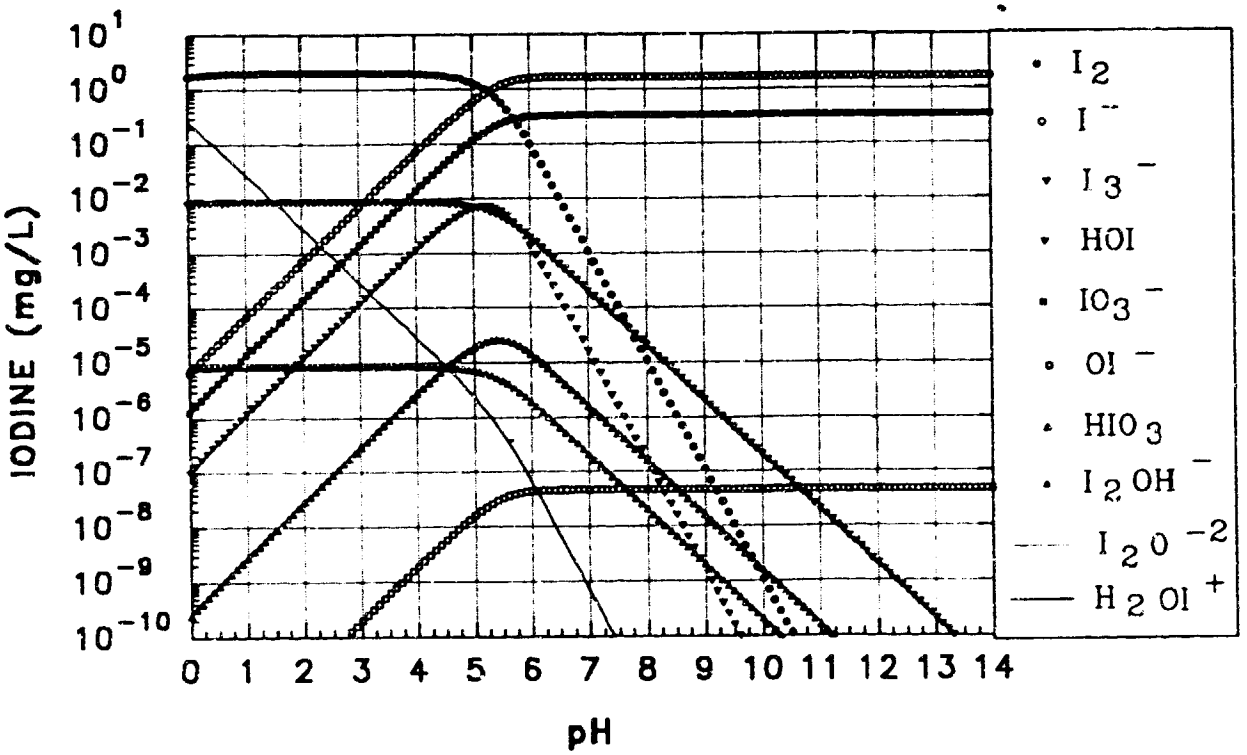

b) Logarithmic Concentration Scale.

Figure 7.5 Equilibrium Iodine Speciation - 2 mg/L I.

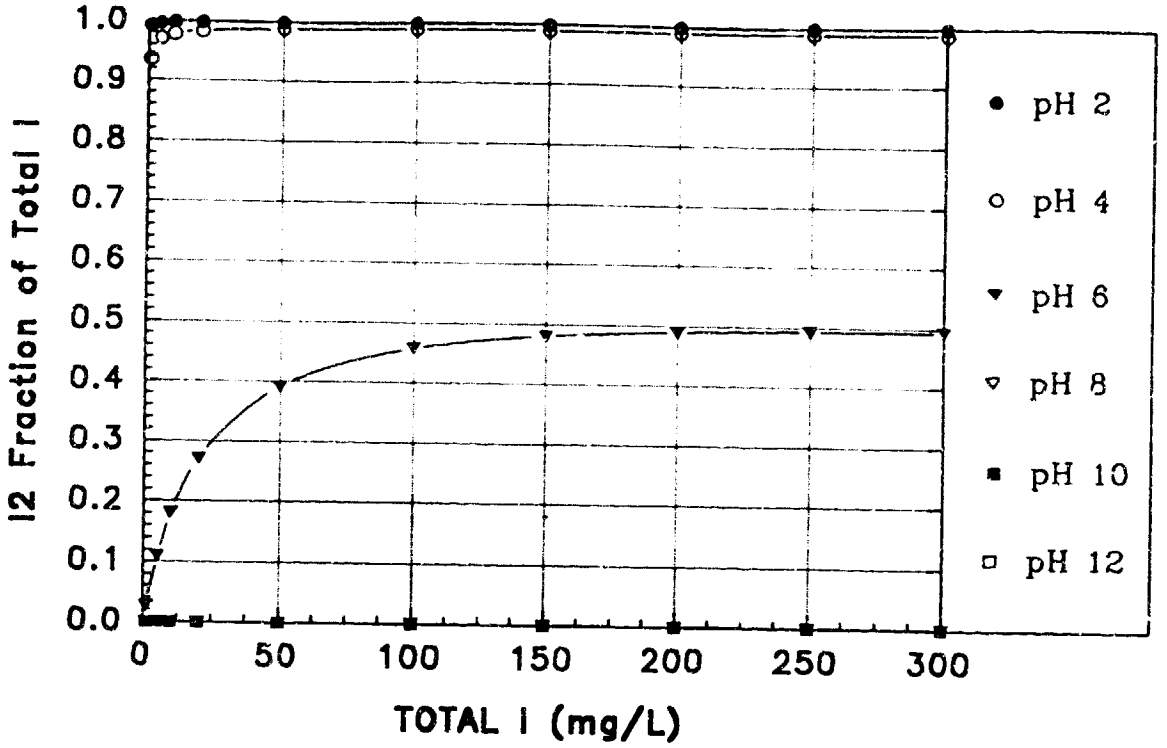

a) Linear Concentration Scale.

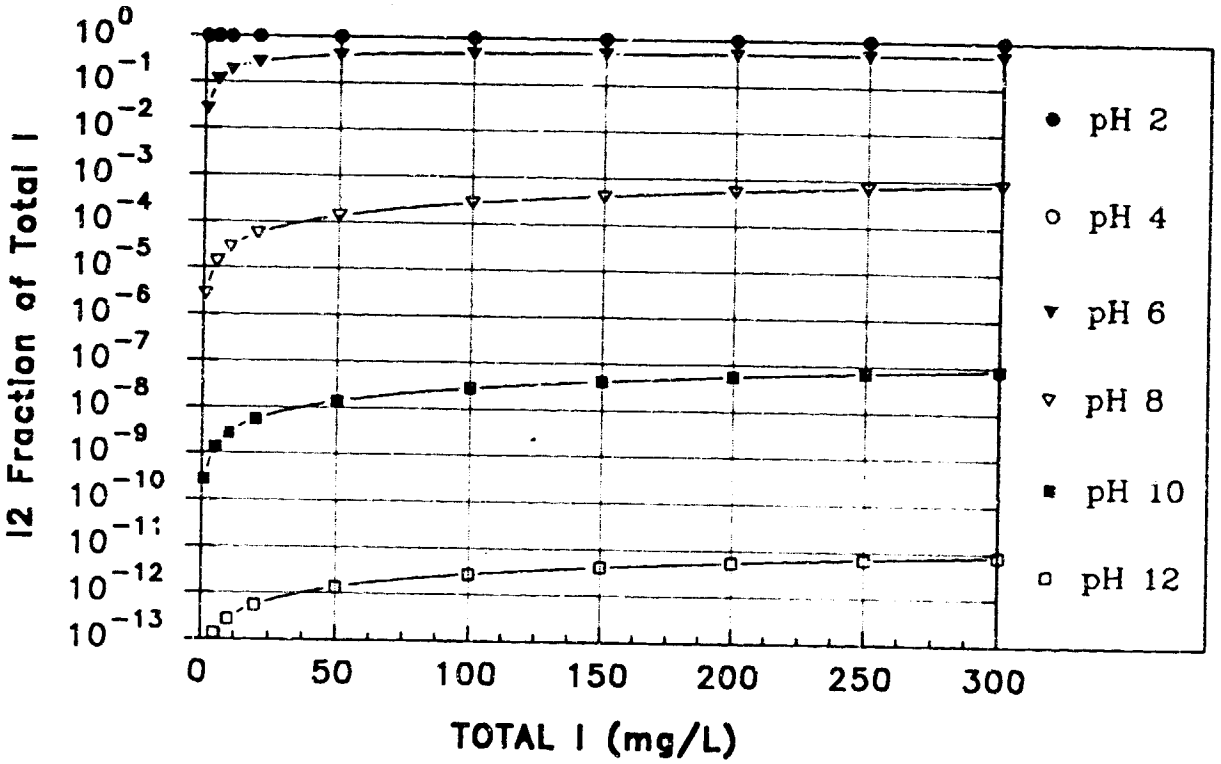

b) Logarithmic Concentration Scale.

Figure 7.6 Equilibrium Fractional Occurence of I_2 verus Total I.

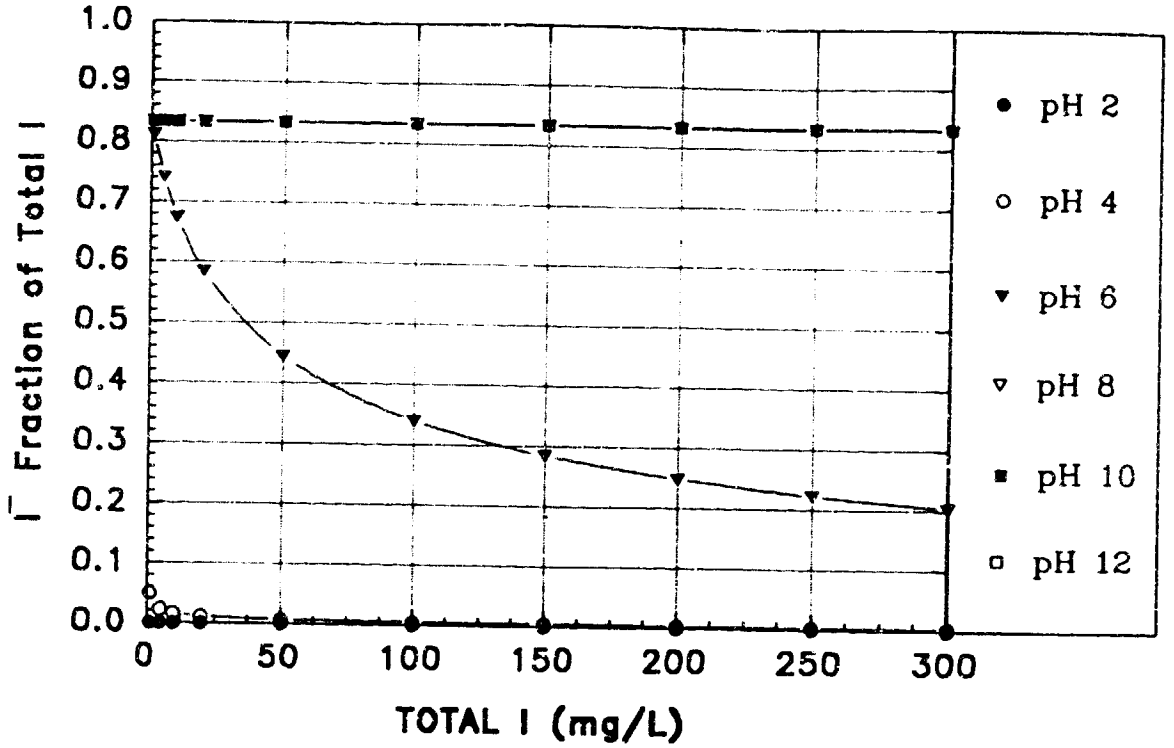

a) Linear Concentration Scale.

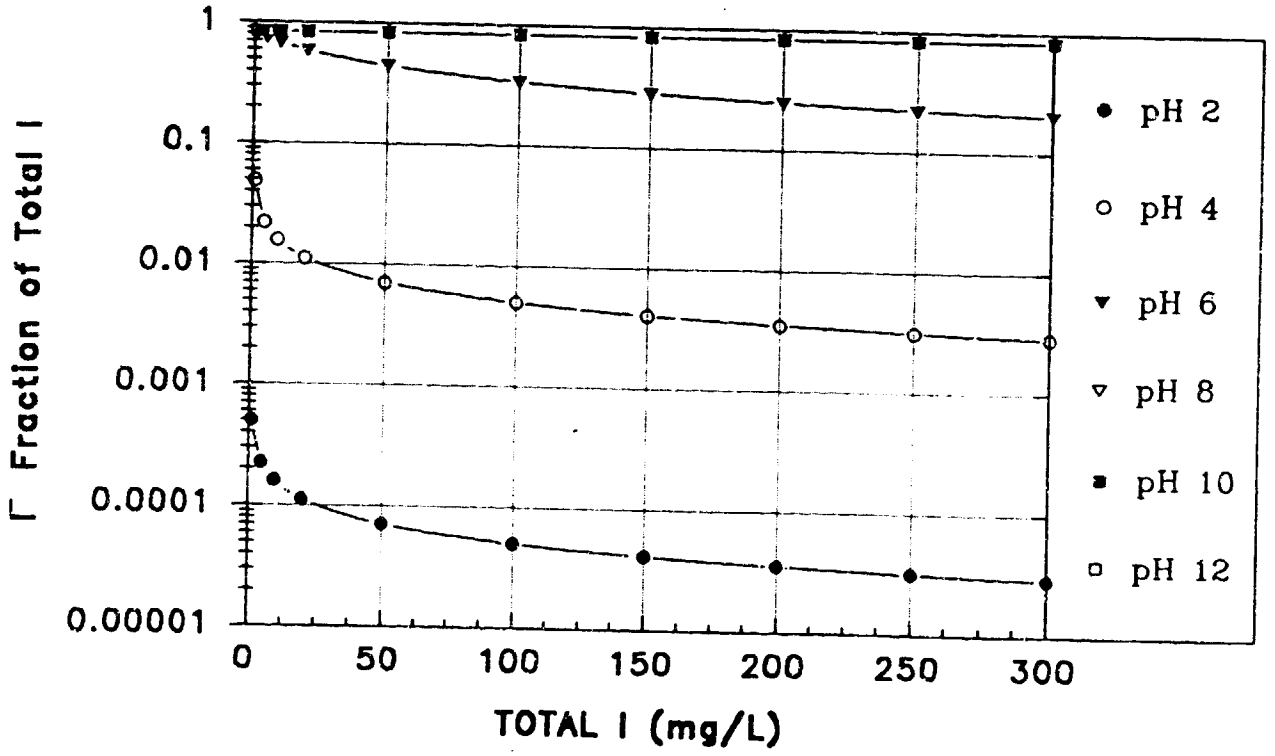

b) Logarithmic Concentration Scale.

Figure 7.7 Equilibrium Fractional Occurence of I^- versus Total I.

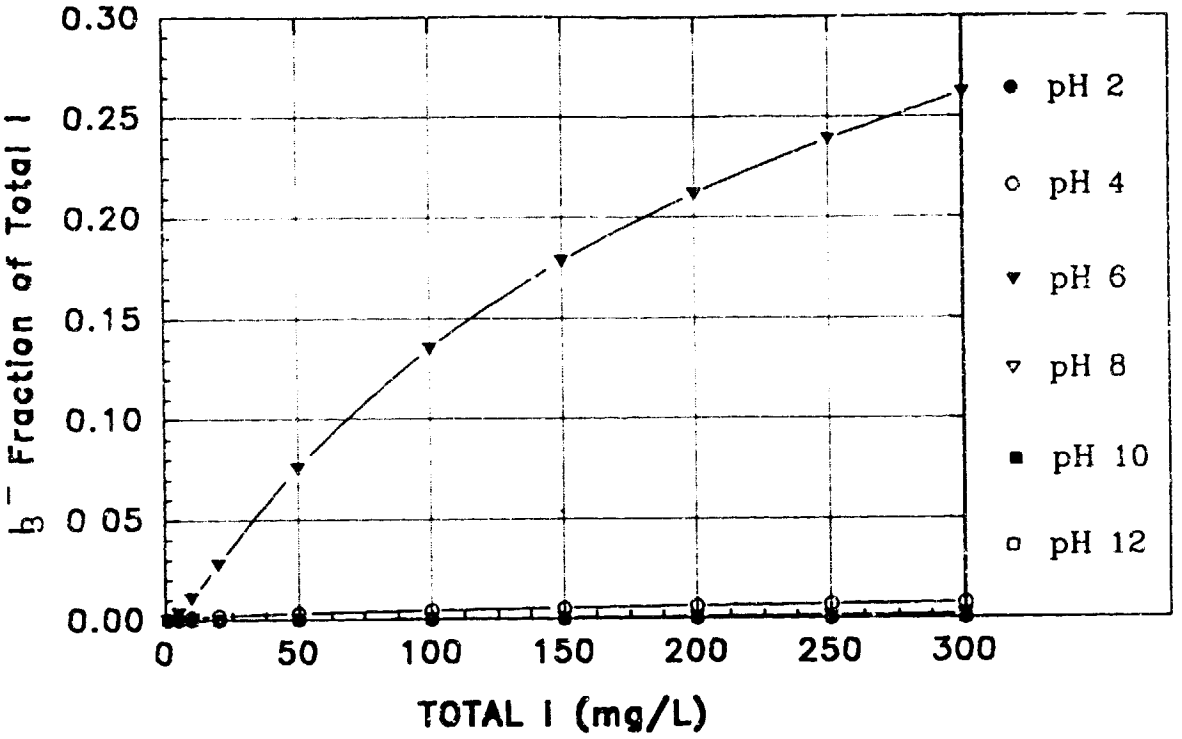

a) Linear Concentration Scale.

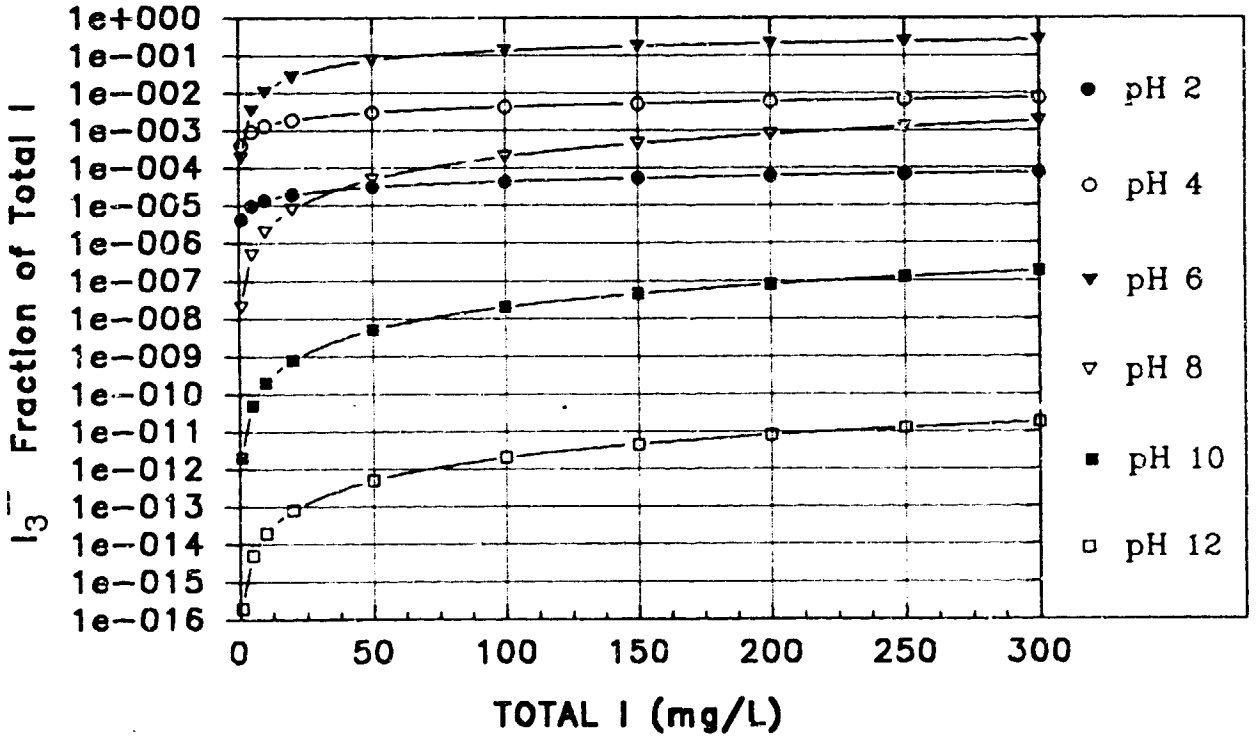

b) Logarithmic Concentration Scale.

Figure 7.8 Equilibrium Fractional Occurence of I_3^- versus Total I.

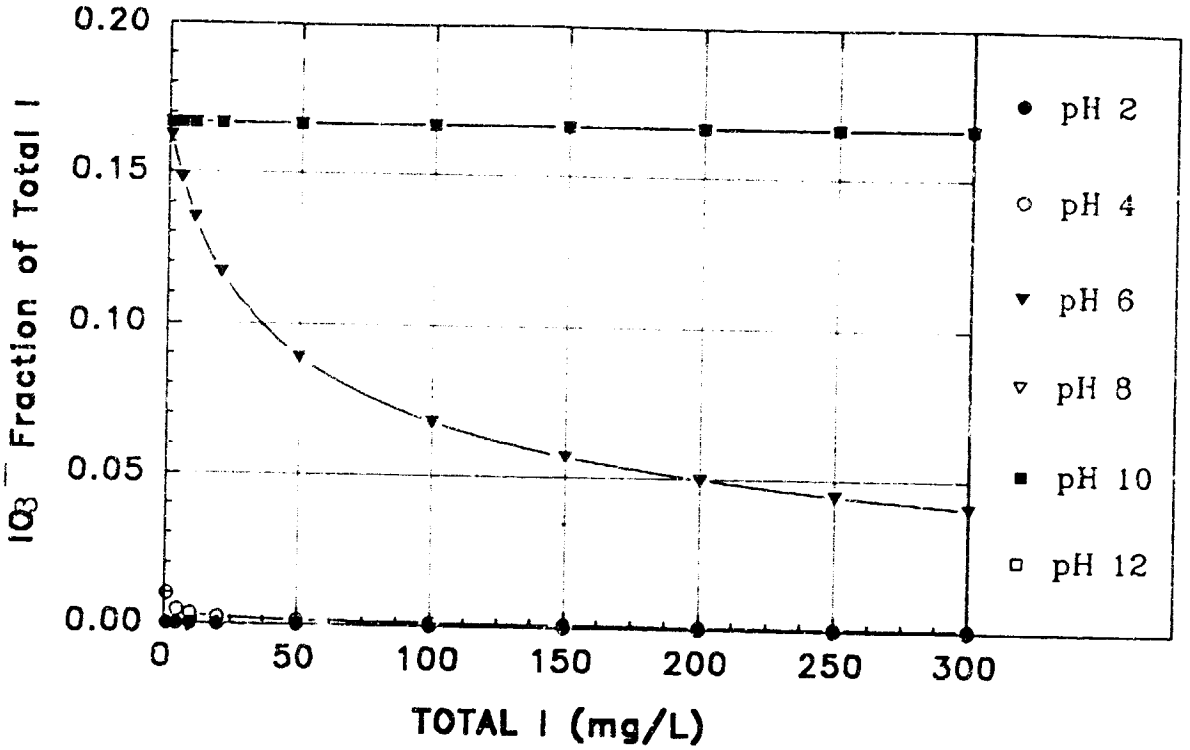

a) Linear Concentration Scale.

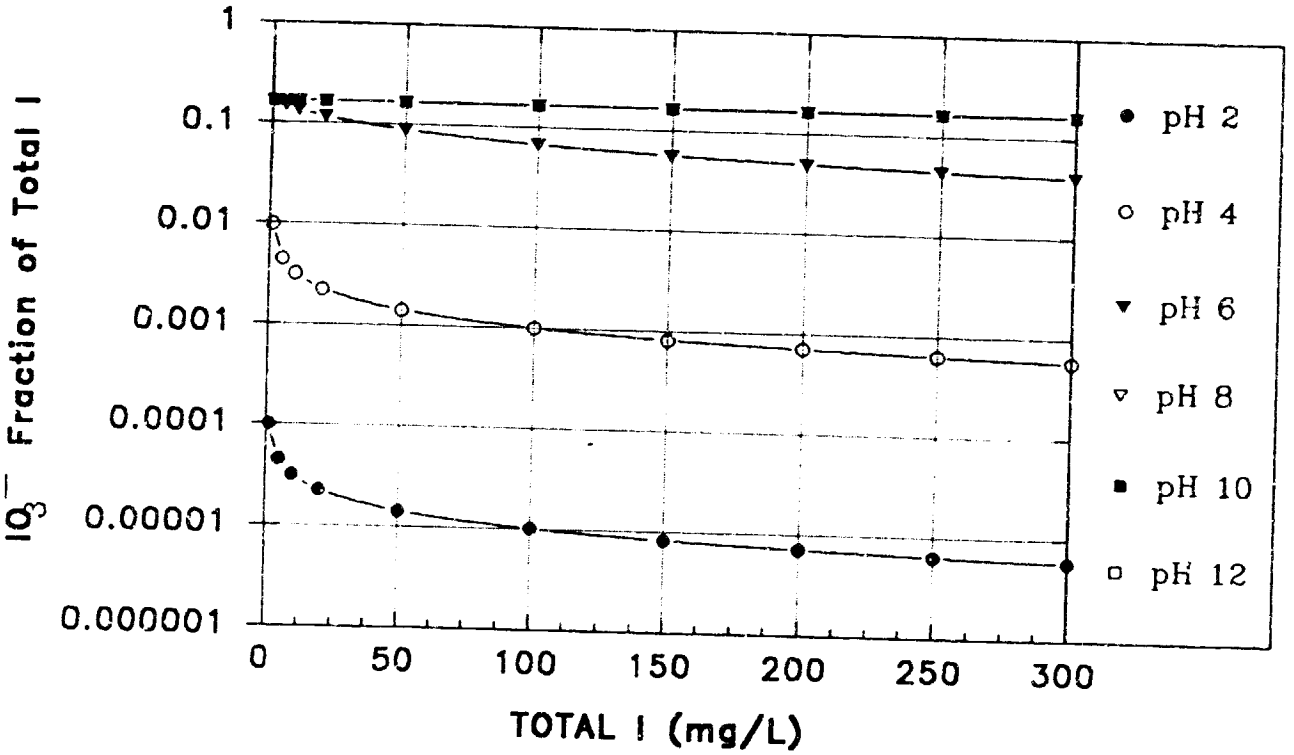

b) Logarithmic Concentration Scale.

Figure 7.9 Equilibrium Fractional Occurence of IO_3^- versus Total I.

abundances of the various species. The pseudo-equilibrium distribution of iodine species as a function of pH is presented in Figure 7.10 for an initial aqueous I_2 concentration of 300 mg/L. At this iodine concentration, I_2 levels diminish with increasing pH, beginning at pH = 4.5 and become insignificant at pH ≥ 11.5. Gaussian distributions for I_3^-, HOI, and I_2OH^- are evident, with peak centroids at pH ≈ 9, pH ≈ 10, pH ≈ 10.4, and approximate peak levels of 62 mg/L, 65 mg/L and 35 mg/L respectively. I^- levels rise from near zero at pH = 5 to 150 mg/L at pH ≥ 12. Above pH = 10, OI^- the dissociated hypoiodite anion increases to approximately 150 mg/L at ¬H = 13.5.

Similar representations of the pseudo-equilibrium distribution of iodine containing species are presented in Figures 7.11, 7.12, and 7.13 for 10 mg/L, 4 mg/L, and 2 mg/L initial I_2 concentrations. At these low levels of total iodine, only I_2, I^-, HOI and OI^- occur at significant levels. Given the pH range encountered during RMCV operation, this list can be shortened to I_2, I^-, and HOI. The observed trends for the pseudo-equilibrium case are similar to those observed with the true equilibrium case, in that the corresponding effects of speciation due to hydrolysis occur at lower pH values as the total iodine concentration of the system decreases. In comparison to the true (slow) equilibrium distribution of species, corresponding effects of hydrolysis are seen at higher pH values for the pseudo-equilibrium case.

At the 2 mg/L minimum I_2 concentration specified for routine RMCV operation, the effects of the fast hydrolysis reactions can be substantial. Under acidic conditions typical of the ersatz humidity condensate and the ersatz urine distillate, between pH = 3 and pH = 4, roughly 98% of the iodine added to the system by the MCV as I_2 will remain in this form. At the pH values of ersatz reclaimed hygiene water and ersatz reclaimed potable water, both of which vary between pH = 5 and pH = 7 and with an average pH ≈ 6, the effect of the fast hydrolysis is more pronounced. At pH = 5 iodine is approximately 93% in the I_2 form. At

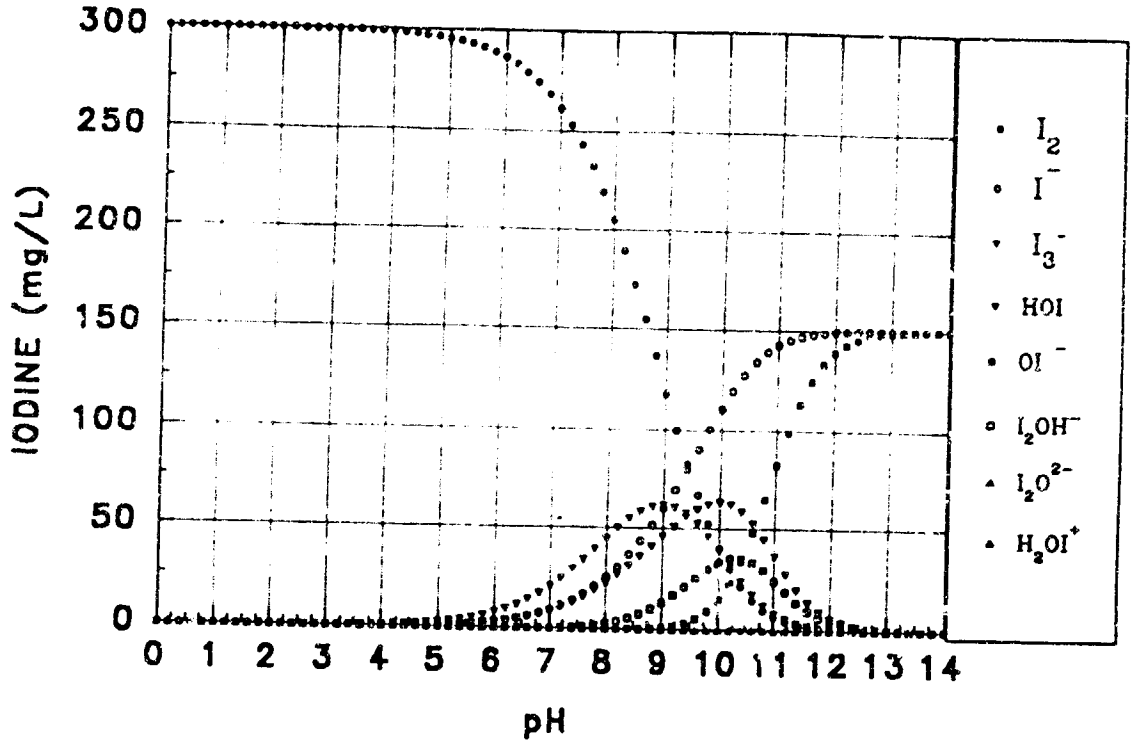

a) Linear Concentration Scale.

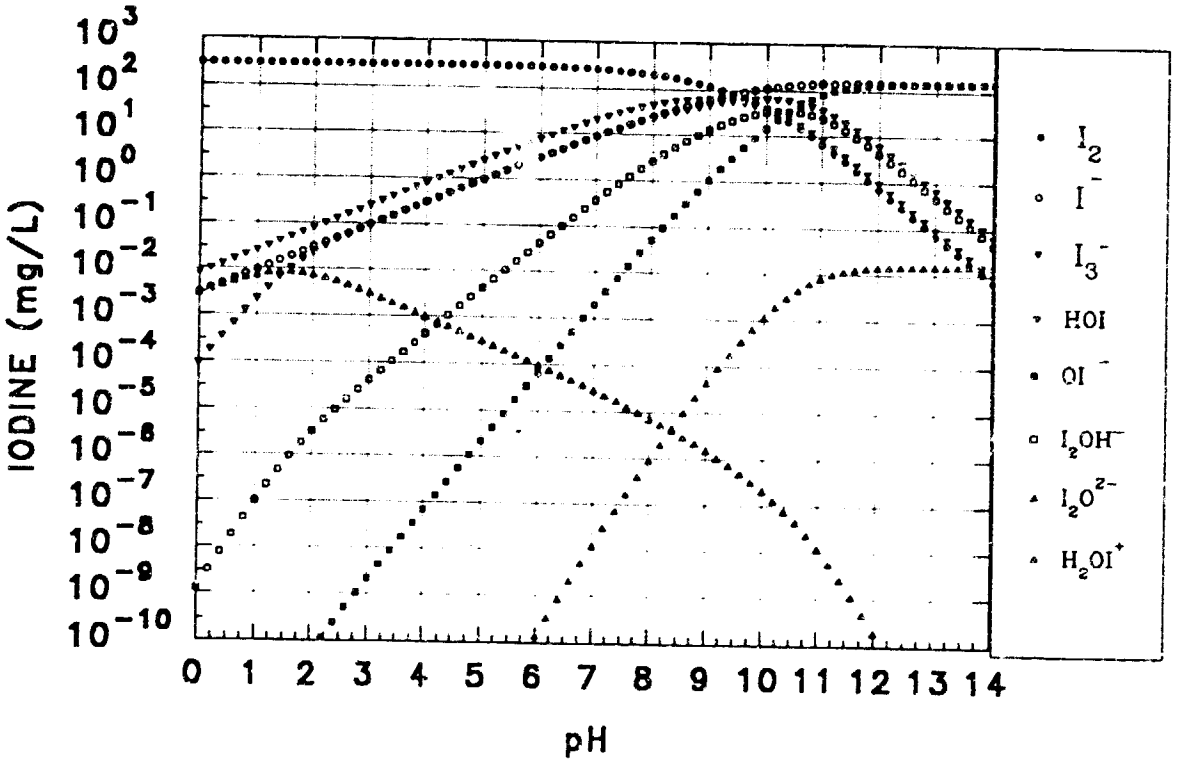

b) Logarithmic Concentration Scale.

Figure 7.10 Pseudo-equilibrium Iodine Speciation versus pH - 300 mg/L Total I.

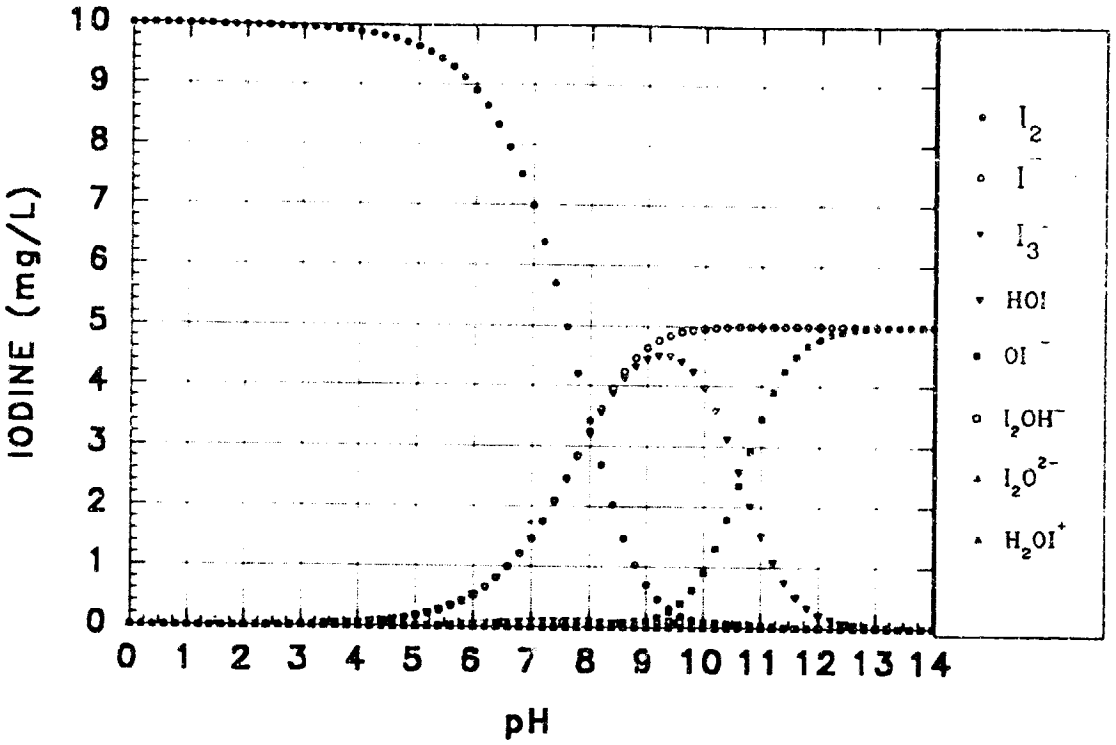

a) Linear Concentration Scale.

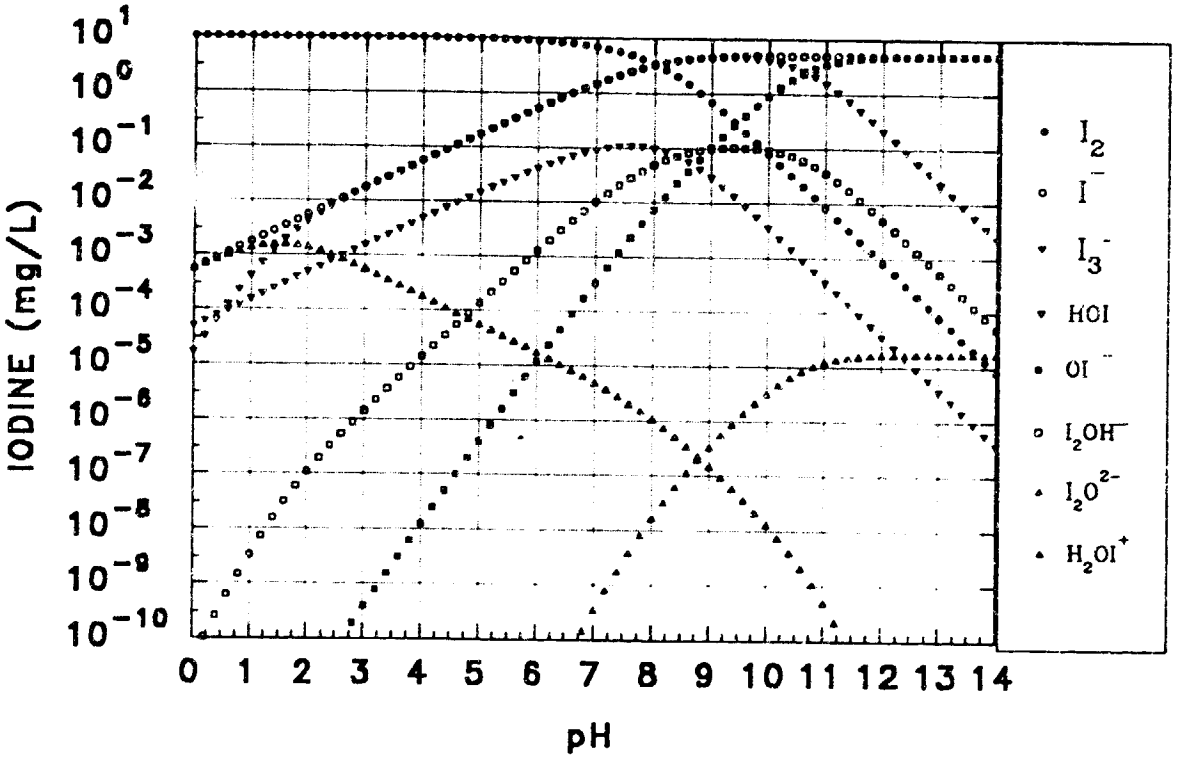

b) Logarithmic Concentration Scale.

Figure 7.11 Pseudo-equilibrium Iodine Speciation versus pH - 10 mg/L Total I.

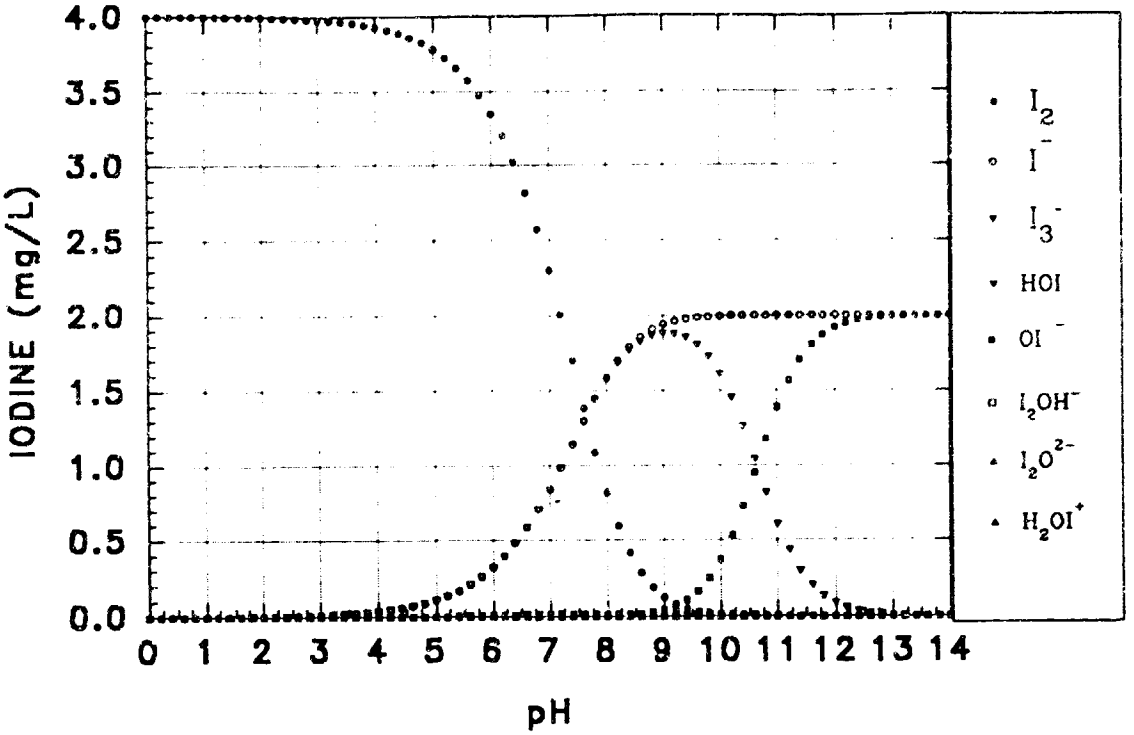

a) Linear Concentration Scale.

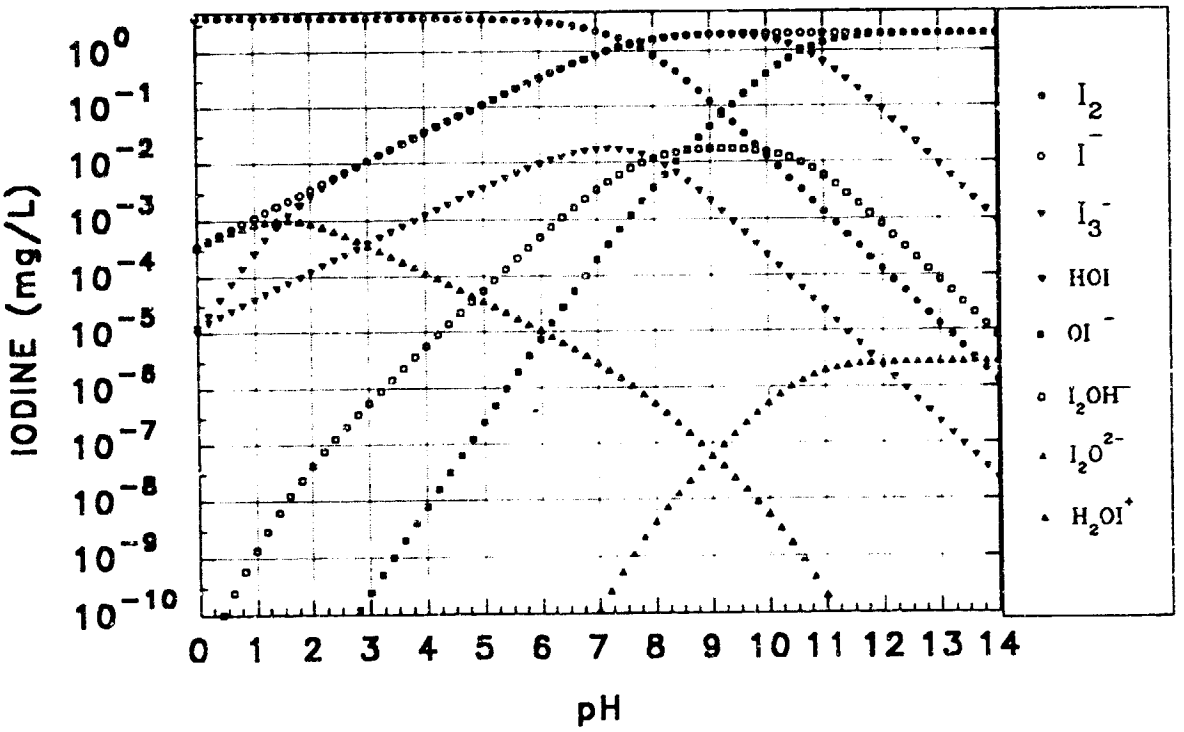

b) Logarithmic Concentration Scale.

Figure 7.12 Pseudo-equilibrium Iodine Speciation versus pH - 4 mg/L Total I.

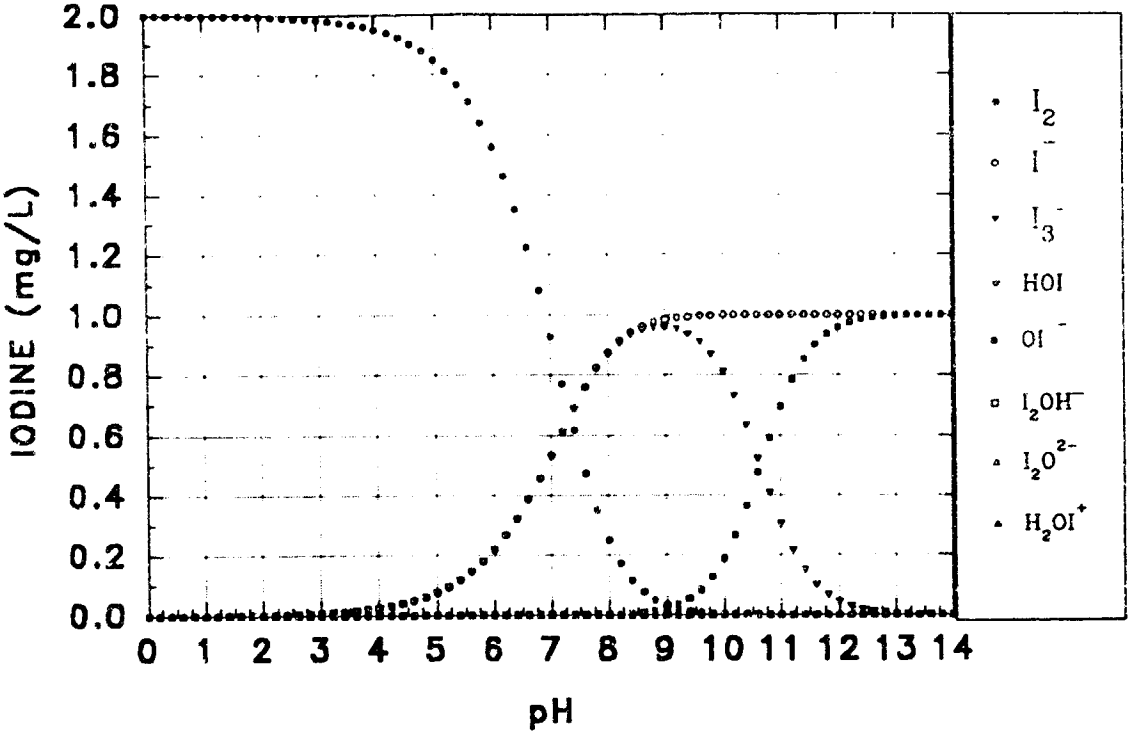

a) Linear Concentration Scale.

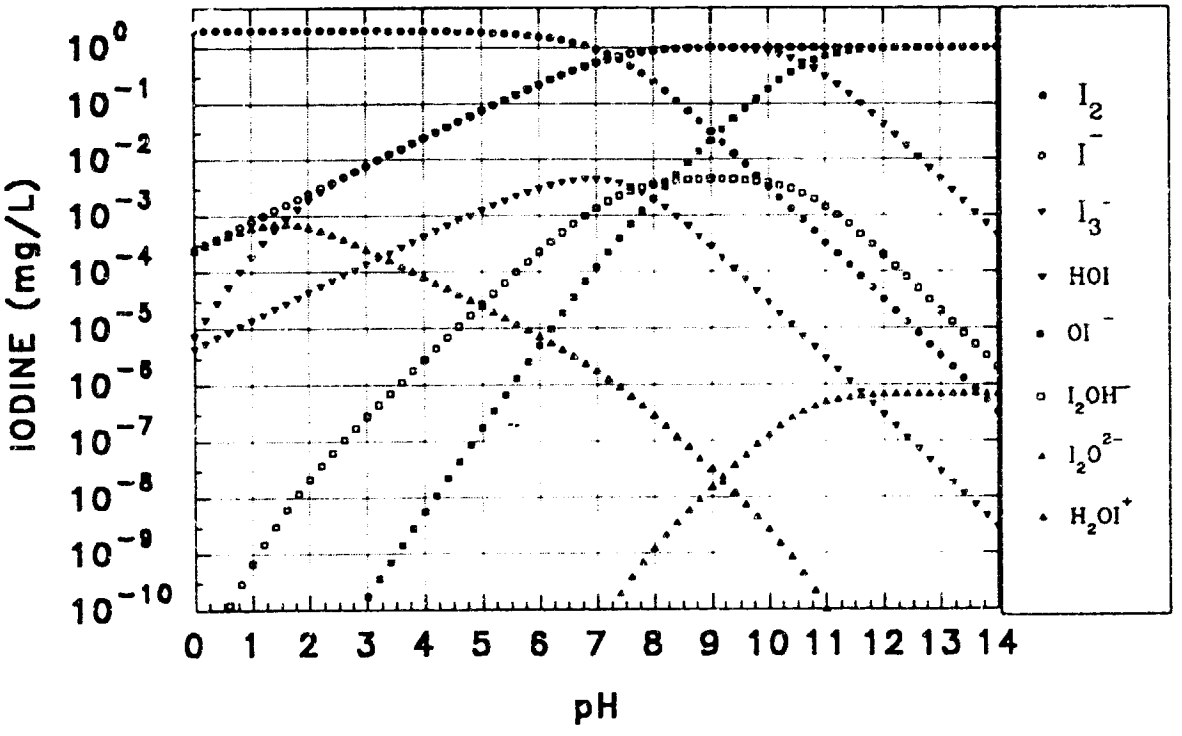

b) Logarithmic Concentration Scale.

Figure 7.13 Pseudo-equilibrium Iodine Speciation versus pH - 2 mg/L Total I.

pH = 6 this drops to 78% and to approximately 42% at pH = 7.

All of the equilibria examined thus far have been derived assuming an initial addition of only elemental iodine to the aqueous system. As we have shown in Section 5, RMCV operations also add variable quantities of I^- to the MCV effluent, the magnitude being dependent upon the chemical compositions of the respective challenge solutions. Attempts to model this situation have been partially successful. The program IIFAST.EXE, written in the C programming language, is a modification of ISPECIES.EXE. This program begins within initial conditions of both I_2 and I^- present, and adds the conservation of oxidation state as an additional convergence criterion. The program fails to converge with some regularity, but has also generated valid solutions over the pH range between pH = 0 and pH = 14, for certain initial concentrations of the two iodine species.

Addition of I^- as an initial condition results in the presence of I_3^- at all pH values for which I_2 is present. This effect is most evident at high iodine concentrations. At low iodine levels the most dramatic effect is the upscale pH shift of the onset of hydrolysis. Figure 7.14a and 7.14b present the pseudo-equilibrium iodine speciation for addition of 2.0 mg/L of I_2 and 0.2 mg/L of I^- to the aqueous system on linear and logarithmic scales respectively. Examination of the figure indicates that at pH = 4, 5, 6, and 7, I_2 levels are 1.99, 1.94, 1.7, and 1.04 mg/L respectively. In the absence of an external source of I^-, the corresponding I_2 concentrations (see Figure 7.13) are 1.95, 1.85, 1.55, and 0.92 mg/L respectively.

Similar solutions for the pseudo-equilibrium distribution of 2.0 mg/L of I_2 with 0.6 and 1.0 mg/L of I^- are given in Figures 7.15 and 7.16 respectively. Source code for the program IIFAST.EXE is listed in Appendix I.

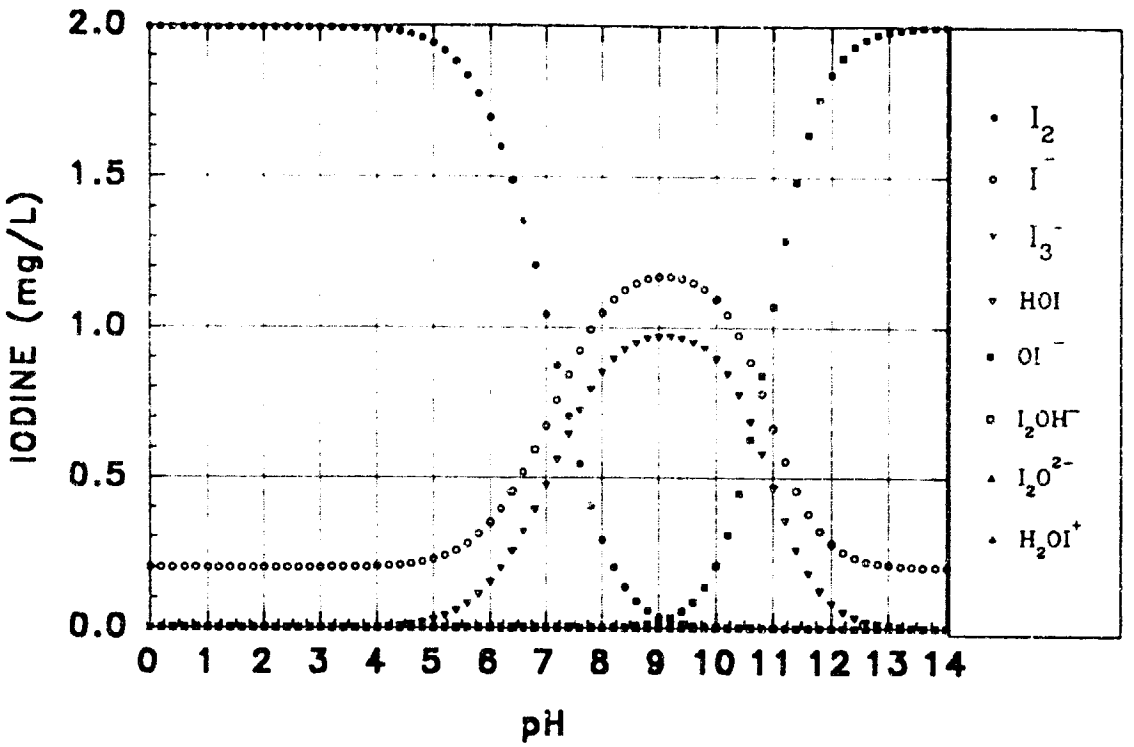

a) Linear Concentration Scale.

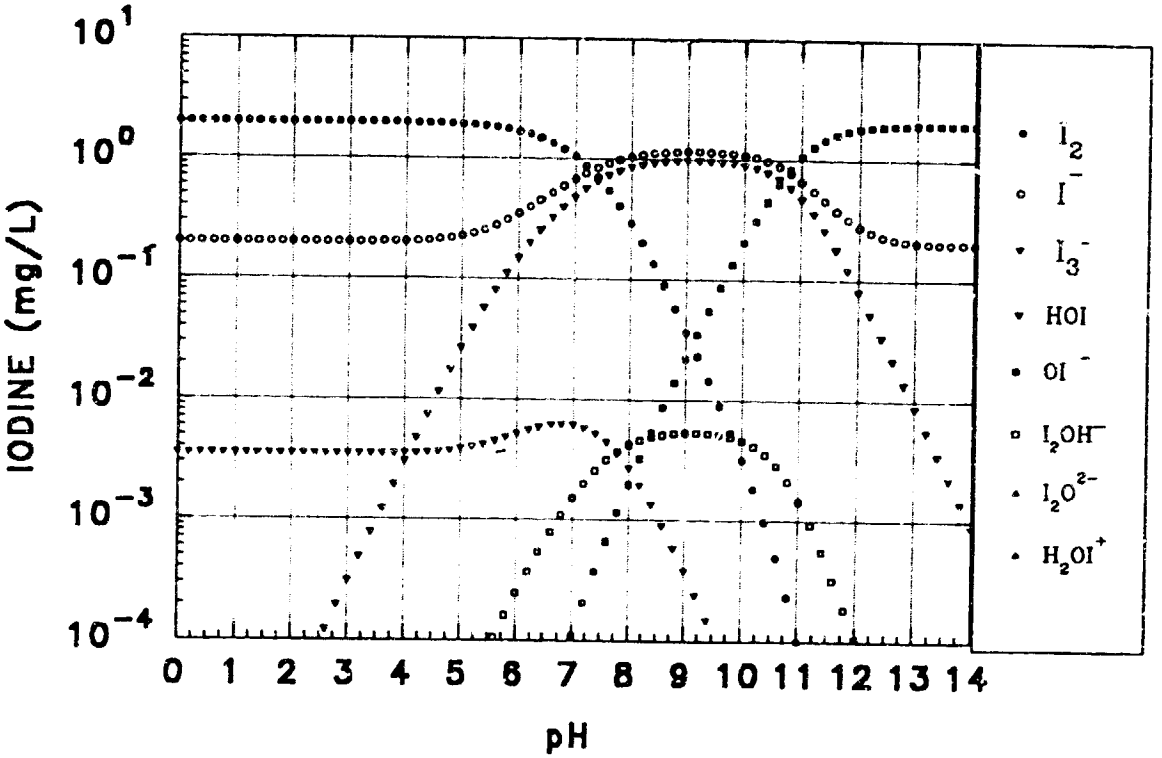

b) Logarithmic Concentration Scale.

Figure 7.14 Pseudo-equilibrium Speciation - (2 mg/L I_2 + 0.2 mg/L I^-)

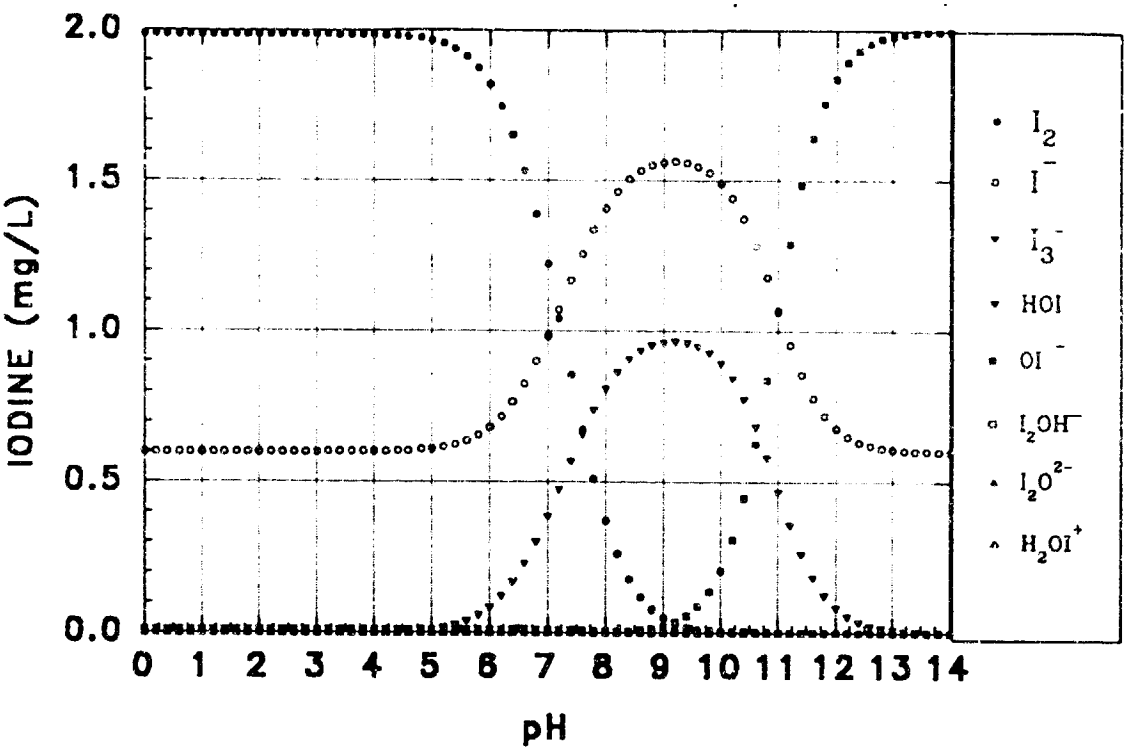

a) Linear Concentration Scale.

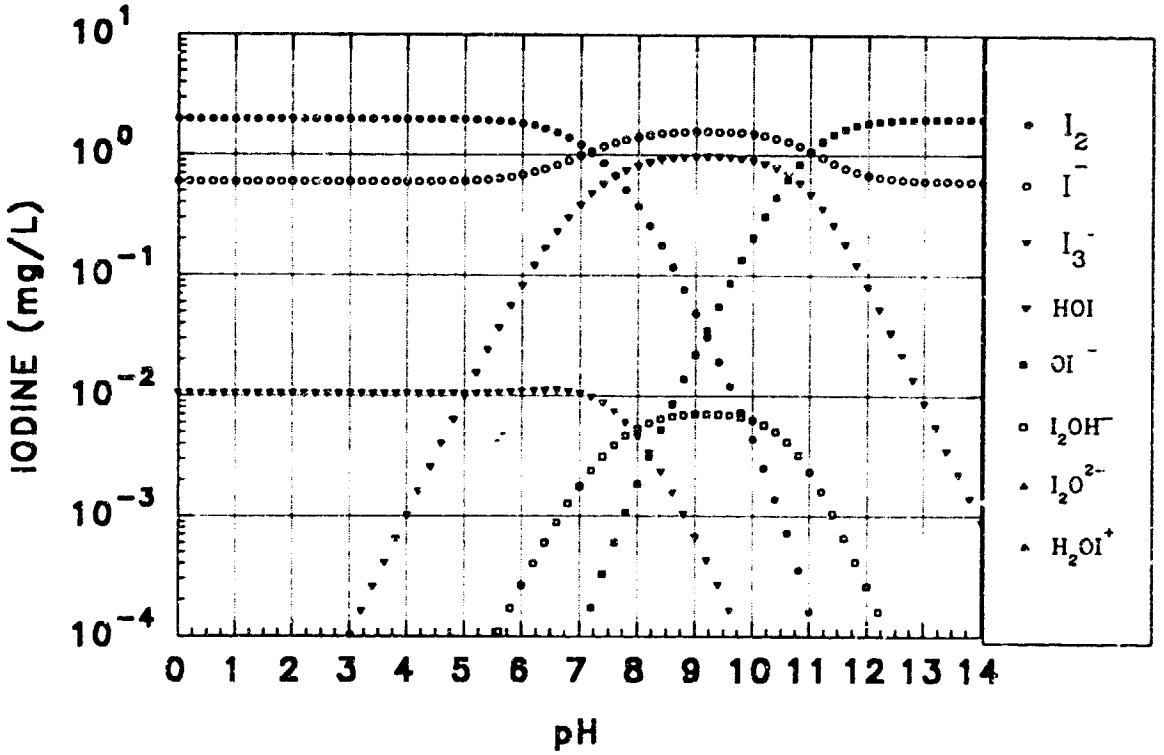

b) Logarithmic Concentration Scale.

Figure 7.15 Pseudo-equilibrium Speciation - (2 mg/L I_2 + 0.6 mg/L I^-)

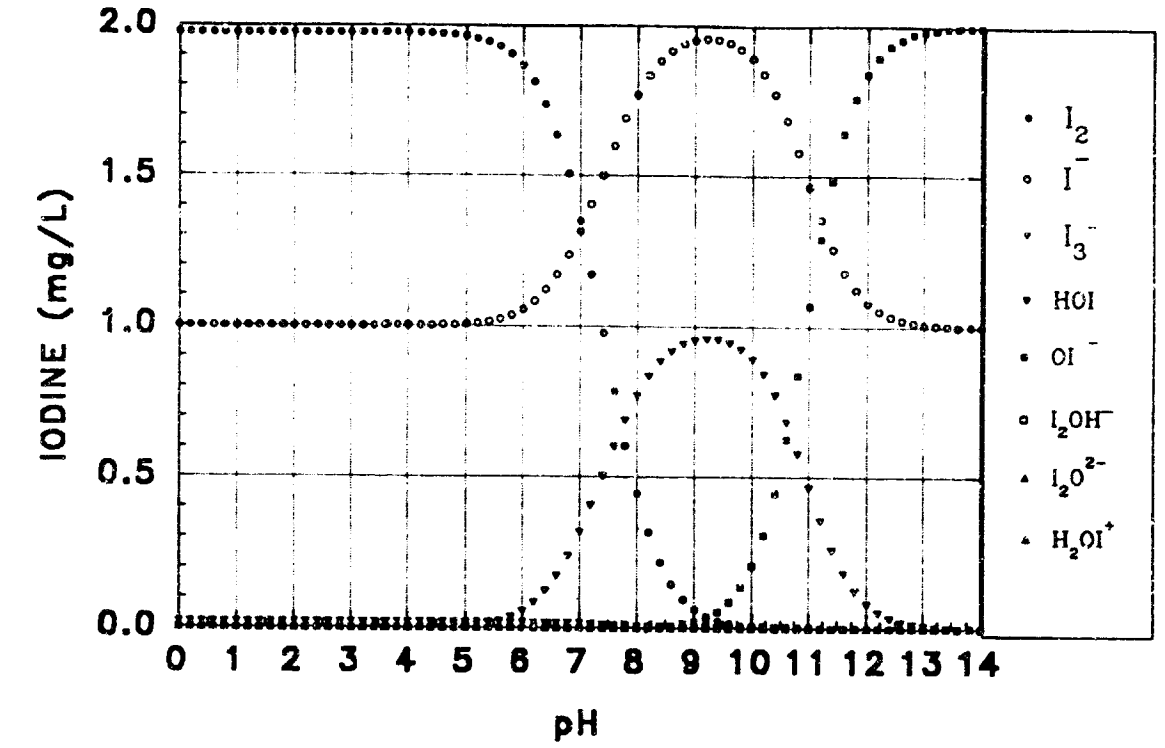

a) Linear Concentration Scale.

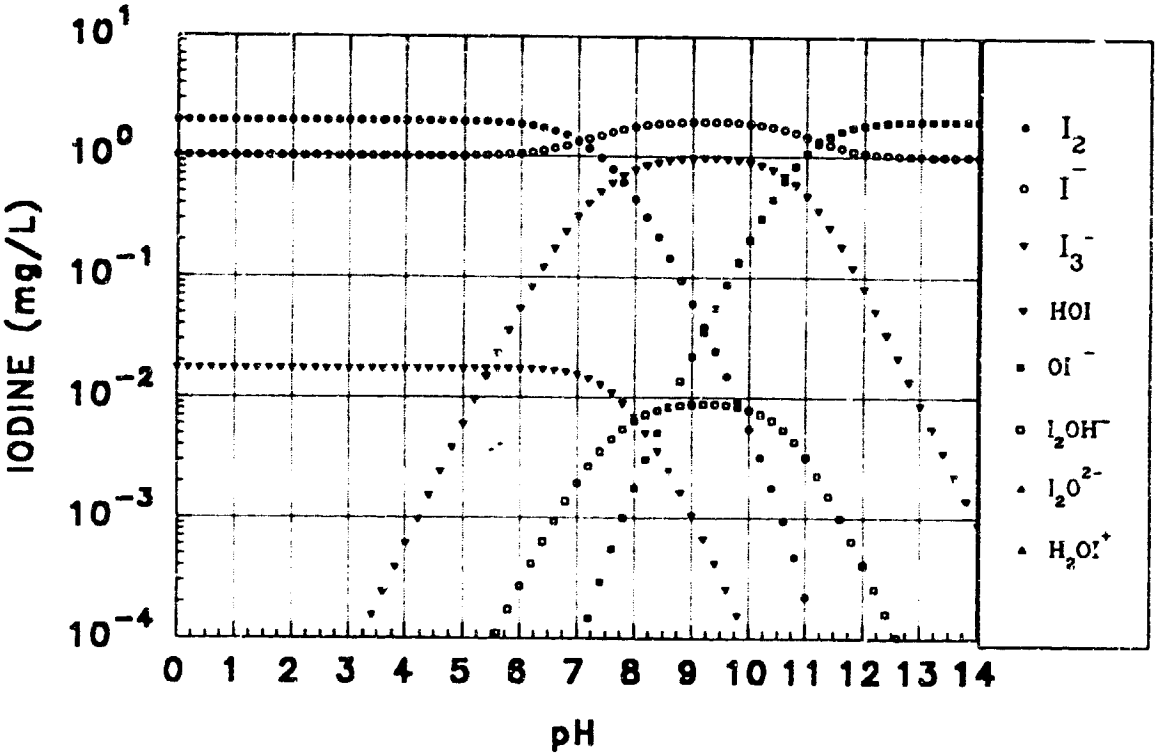

b) Logarithmic Concentration Scale.

Figure 7.16 Pseudo-equilibrium Speciation - (2 mg/L I_2 + 1.0 mg/L I^-)

7.1.5 Kinetics of Equilibrium I_2 Speciation at 25 °C.

In the pseudo-equilibrium case and the true equilibrium case we are confronted with strikingly different distributions of iodine containing inorganic species. The susceptibilty to hydrolysis as a function of pH also varies between the fast and slow reactions, with equivalent loss of iodine in the I_2 form occuring at lower pH values for the slow reaction than for the fast hydrolysis to HOI and I^-.

At the moment that elemental iodine is introduced to the aqueous stream by flow through a bed of iodinated ion exchange resin, the pseudo-equilibrium distribution of species is attained. This initial distribution of species slowly changes until the equilibrium state is reached. Without further information, it is difficult to ascertain specifically what distribution of species results for a given pH and initial iodine concentration at any given time following iodination. For this reason an examination of the kinetics of iodine speciation was undertaken to provide clarification of the relative importance of the fast and slow reactions.

For the sake of simplicity, only those species having been found to occur in significant quantities by the equilibrium speciation modeling were incorporated into the speciation kinetics model. These species were: I_2, I^-, HOI, OI^-, and IO_3^-. The numerical modelling was patterned after the method of Palmer and Leitzke[334], and used reaction rate constants obtained from the literature[125,140,261,302,313]. The kinetic model was set up as the system of linear first order ordinary differential rate equations:

$$\frac{d[I_2]}{dt} = -k_1[I_2] + k_{-1}[I^-][HOI + OI^-][H^+] \qquad \text{(Eqn. 7.16)}$$

$$\frac{d[I^-]}{dt} = k_1[I_2] - k_{-1}[I^-][HOI + OI^-][H^+] + \frac{2}{3}k_2[HOI]^2 + \frac{2}{3}k_3[HOI][OI^-] - k_{-2}[IO_3^-][I^-]^2[H^+]^2$$

(Eqn. 7.17)

$$\frac{d[HOI]}{dt} = k_1[I_2] - k_{-1}[I^-][HOI + OI^-][H^+] - k_2[HOI]^2 - k_3[HOI][OI^-] + 3k_{-2}[IO_3^-][I^-]^2[H^+]^2$$

(Eqn. 7.18)

$$\frac{d[IO_3^-]}{dt} = \frac{1}{3}k_2[HOI]^2 + \frac{1}{3}k_3[HOI][OI^-] - k_{-2}[IO_3^-][I^-]^2[H^+]^2 \qquad \text{(Eqn. 7.19)}$$

where $k_1 = 3.0\ s^{-1}$ is the first order rate constant for the hydrolysis of I_2 forming HOI, $k_{-1} = 4.4 \times 10^{12}\ M^{-2}s^{-1}$ is the third order rate constant for the reverse reaction, $k_2 = 250\ M^{-1}s^{-1}$ and $k_3 = 120\ M^{-1}s^{-1}$ are the second order rate constants of the two term rate law of Thomas et al.[415] for the formation of IO_3^- and $k_{-2} = 3.0 \times 10^8\ M^{-4}s^{-1}$ is the fifth order rate constant for the reverse reaction.

The system of differential equations was solved using Mathematica, a symbolic mathematical processor[442]. Source code for the program IKINETIC.MA, written in the Mathematica language, is listed in Appendix I. In this initial value problem, at t_o all iodine begins in the I_2 form. This simulates the introduction of elemental iodine into an aqueous stream by an MCV. To obtain a solution, only the pH of the system and the initial I_2 concentration is specified. Solutions were obtained for the time interval between 0 and 10,000 seconds (2.78 hours), where possible. At initial conditions of low iodine concentration and low pH, singularities were encountered over this time interval, which made solution impossible. In some cases, solution over a shorter time interval was possible. In all cases, solutions were obtained between 0 and 300 seconds (5 minutes). This time interval corresponds to the residence time of the RMCV effluents in the 10 cm path length flow-through spectrophotometer cell for the small column scale long term life cycle test stand. All concentrations are given as mg/L of I.

The iodine speciation kinetics for $[I_2]_o = 300$ mg/L and pH = 7 is illustrated in Figure 7.17a and 7.17b, showing the full time scale and an expanded scale representation of the first

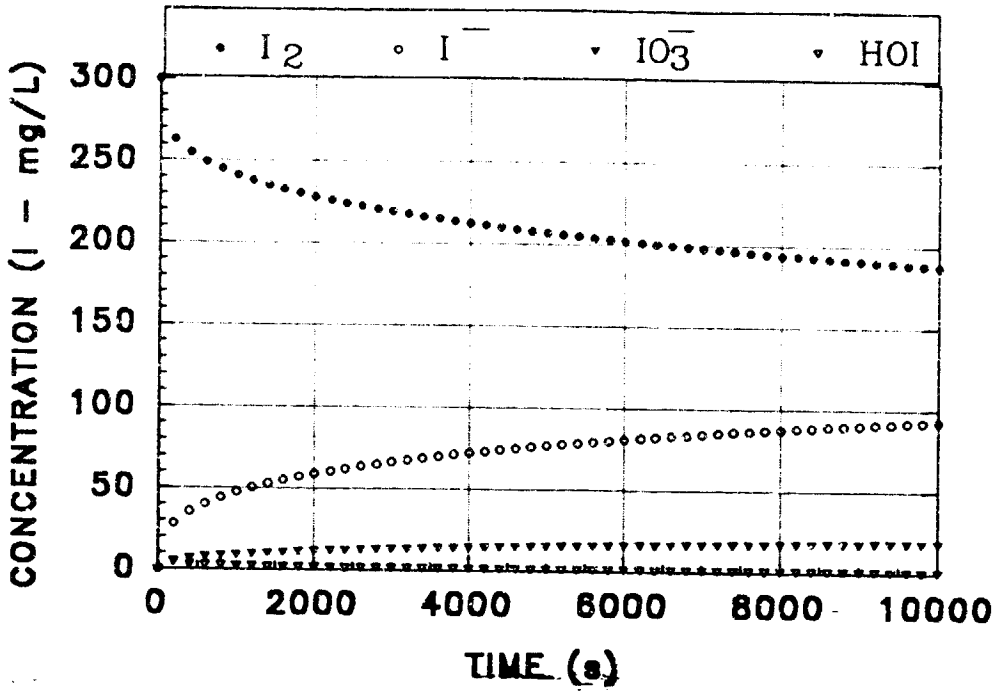

a) 0 - 10,000 s Time Scale.

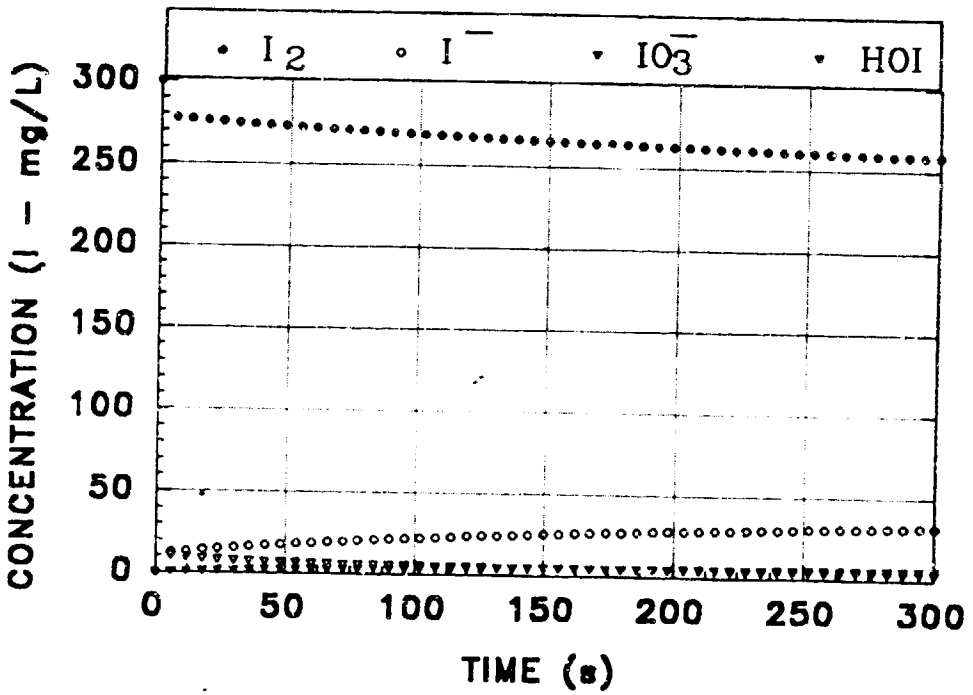

b) 0 - 300 s Time Scale.

Figure 7.17 I_2 Speciation Kinetics - 300 mg/L I at pH = 7.

300 seconds respectively. I_2 concentration is seen to immediately drop to a level of approximately 278 mg/L. At the same time, HOI and I^- appear at equivalent concentrations of approximately 11 mg/L. This is the maximum concentration that HOI will attain and results from the pseudo-equilibrium speciation dominated by the fast hydrolysis reaction. Ever afterward the concentration of HOI slowly diminishes as does the I_2 concentration, while I^- and IO_3^- slowly increase. After 10,000 seconds (2.78 hours) equilibrium has not been reached.

Figure 7.18 presents the solution of the initial value problem for pH = 7 and $[I_2]_o$ = 4.0 mg/L. The hydrolysis kinetics reinforces the observation that with all other parameters held constant, lower concentrations of elemental iodine suffer proportionally greater from the effects of hydrolysis. At 4.0 mg/L and pH = 7, I_2 levels drop within seconds to approximately 2.0 mg/L, and continue to decrease slowly thereafter, reaching approximately 0.75 mg/L after 10,000 seconds, at which time the system has yet to attain equilibrium. And as can be seen in Figure 7.19, the effects at pH = 7 for $[I_2]_o$ = 2.0 mg/L are even more pronounced.

Analogous solutions of the system of rate equations for $[I_2]_o$ values of 300 mg/L, 4.0 mg/L and 2.0 mg/L at pH = 6 are presented in Figures 7.20, 7.21, and 7.22 respectively. It can be seen that at this pH, an intial value of 300 mg/L I_2 rapidly drops to 290 mg/L, 4.0 mg/L decreases to 3.25 mg/L and 2.0 mg/L falls to 1.5 mg/L. The rates of both slow and fast hydrolysis reactions are diminished in comparison to those at pH = 7. This trend continues at pH = 5 as shown in Figures 7.23 and 7.24 illustrating hydrolysis kinetics for initial conditions of 4.0 mg/L and 2.0 mg/L I_2 respectively. The rates of I_2 hydrolysis in the 2.0 mg/L - 4.0 mg/L operational window of the RMCV become insignificant with further reduction of pH, as can be seen from inspection of Figures 7.25 and 7.26, representing pH = 4 and pH = 3 respectively.

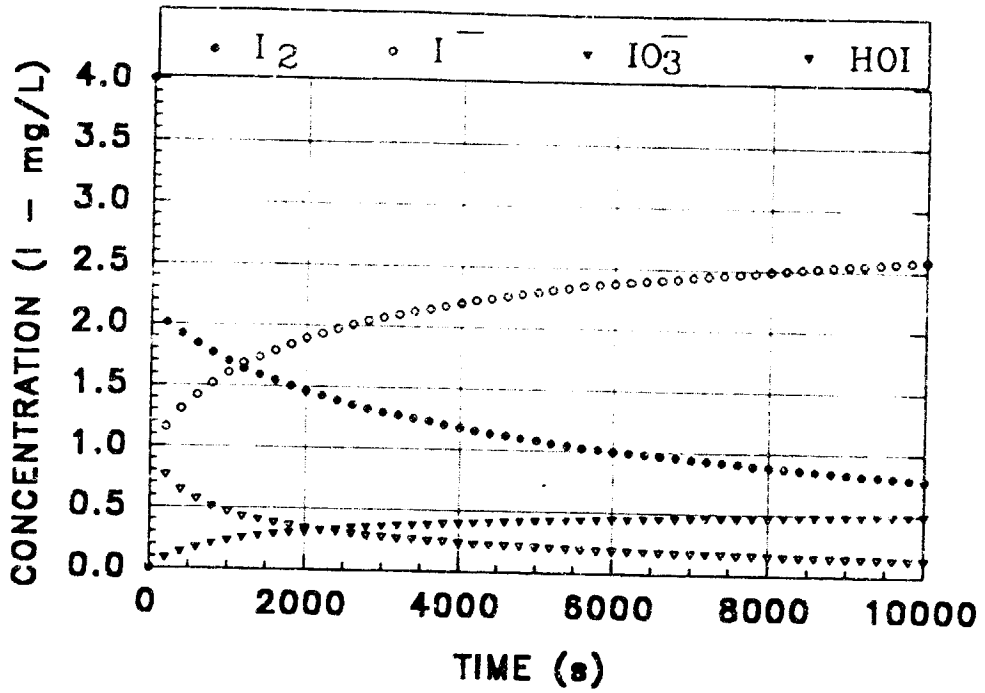

a) 0 - 10,000 Second Time Scale.

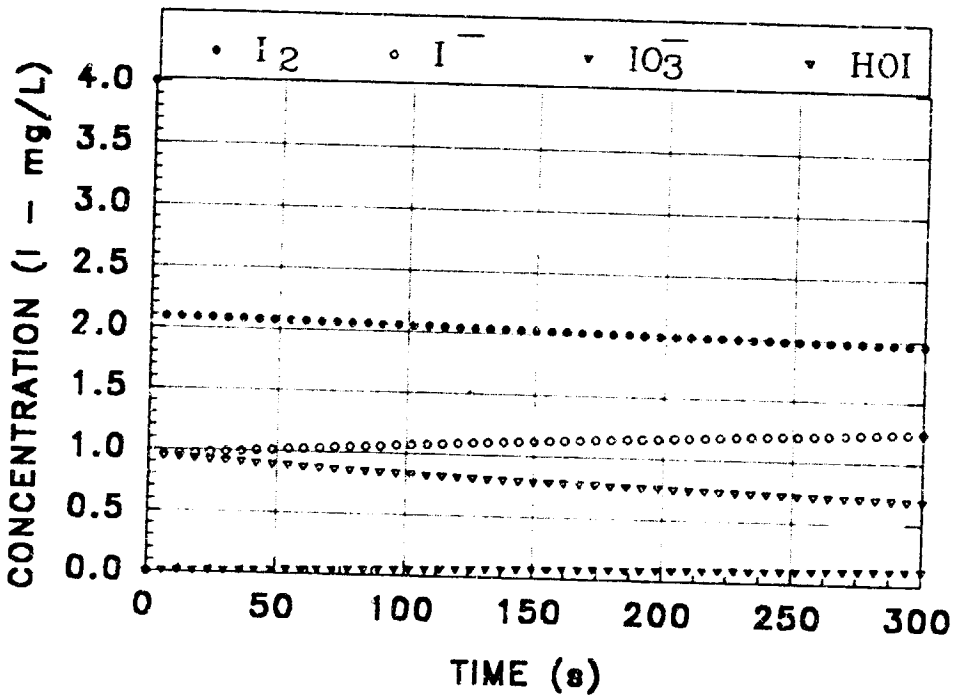

b) 0 - 300 Second Time Scale.

Figure 7.18 I_2 Speciation Kinetics - 4.0 mg/L I at pH = 7.

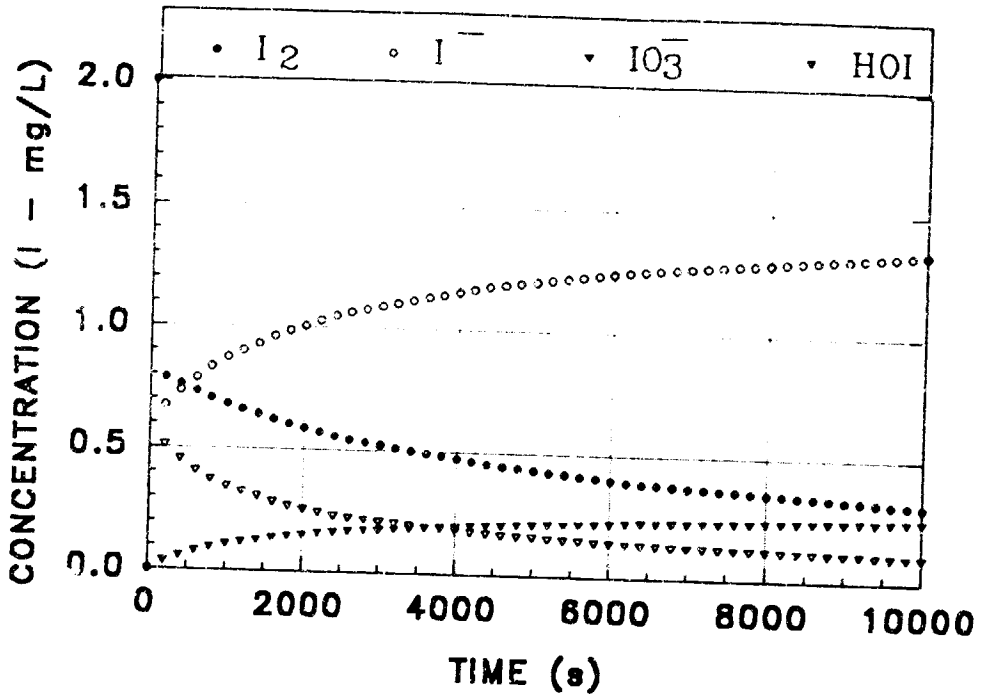

a) 0 - 10,000 Second Time Scale.

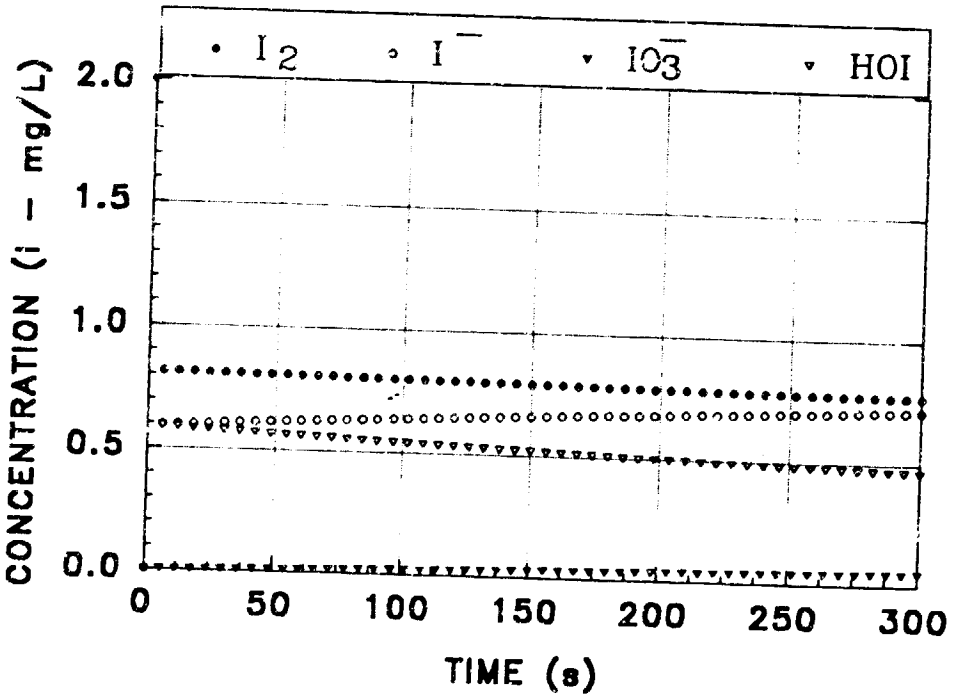

b) 0 - 300 Second Time Scale.

Figure 7.19 I_2 Speciation Kinetics - 2.0 mg/L I at pH = 7.

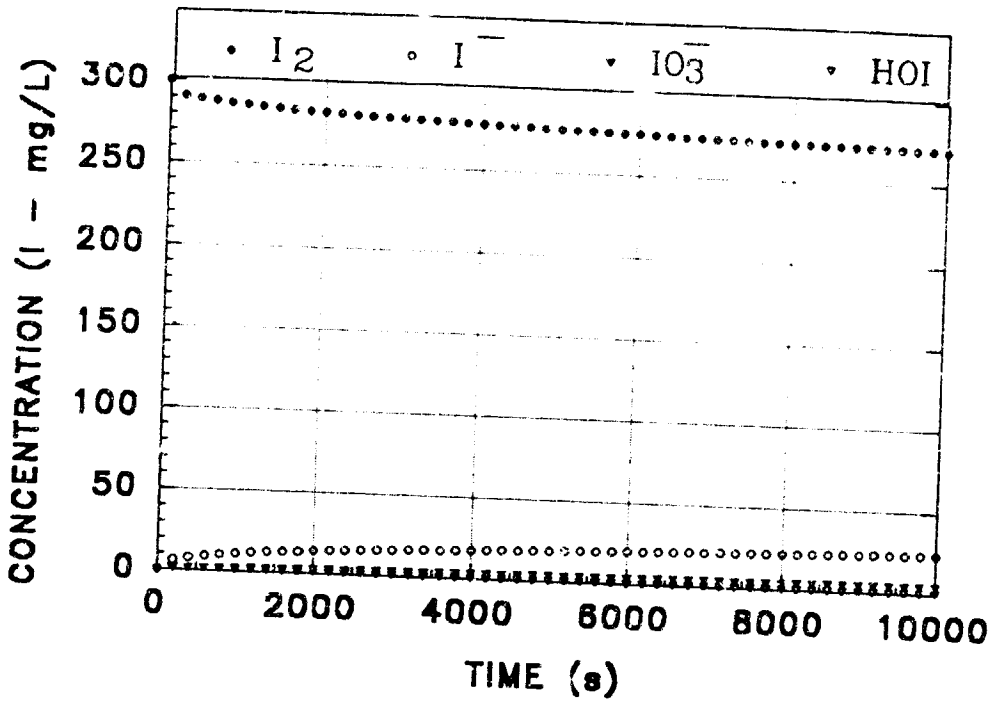

a) 0 - 10,000 Second Time Scale.

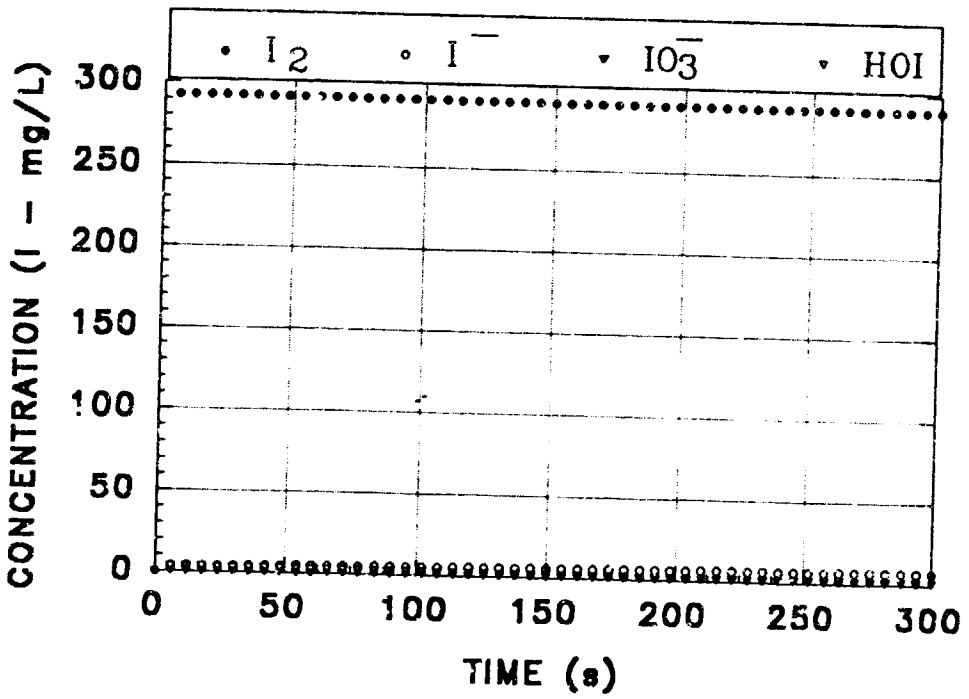

b) 0 - 300 Second Time Scale.

Figure 7.20 I_2 Speciation Kinetics - 300 mg/L I at pH = 6.

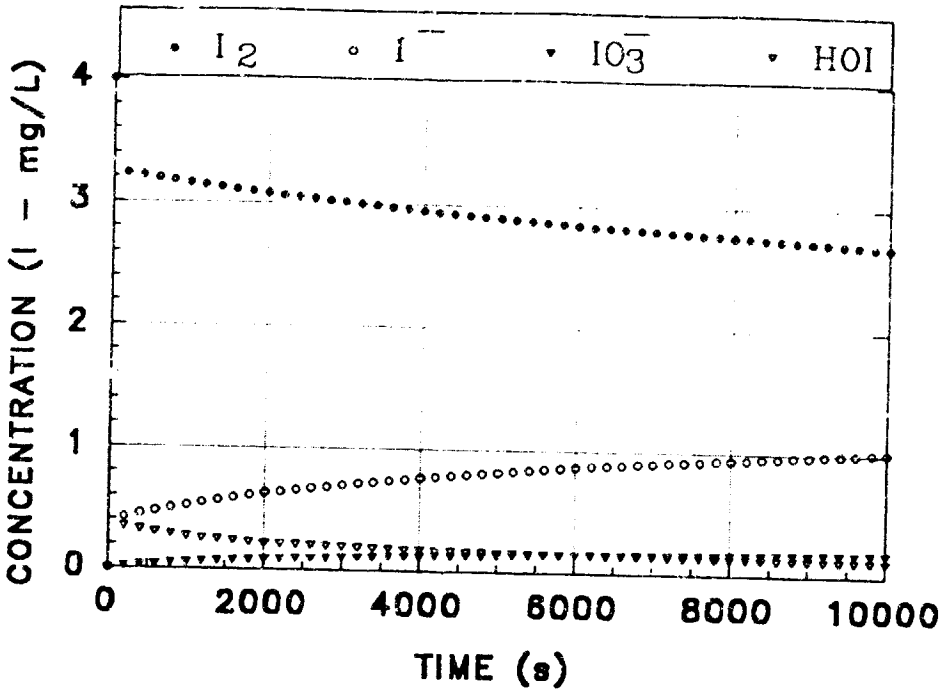

a) 0 - 10,000 Second Time Scale.

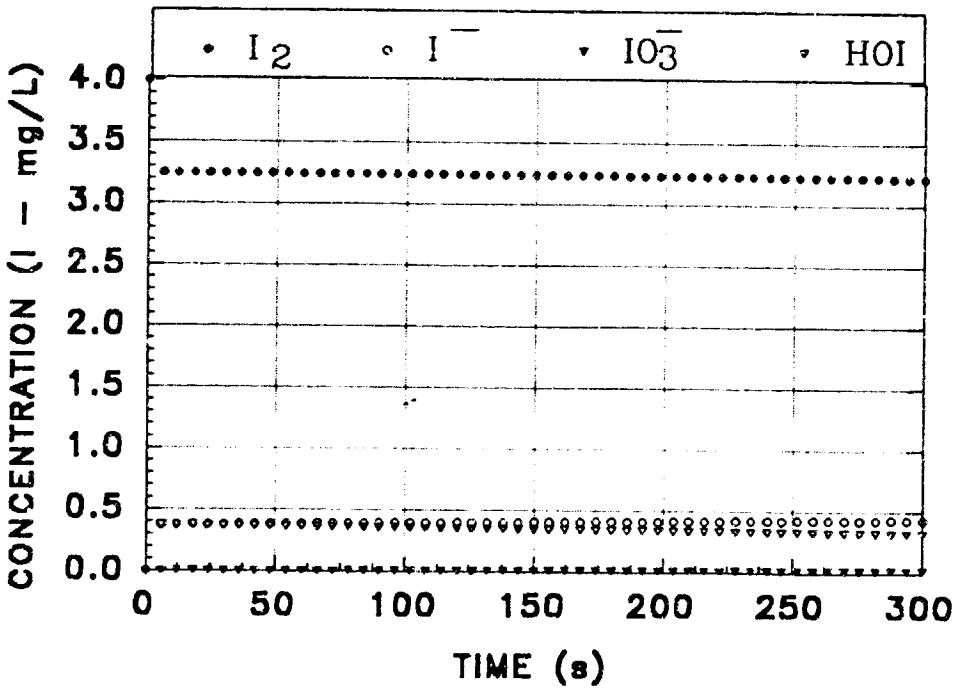

b) 0 - 300 Second Time Scale

Figure 7.21 I_2 Speciation Kinetics - 4.0 mg/L I at pH = 6.

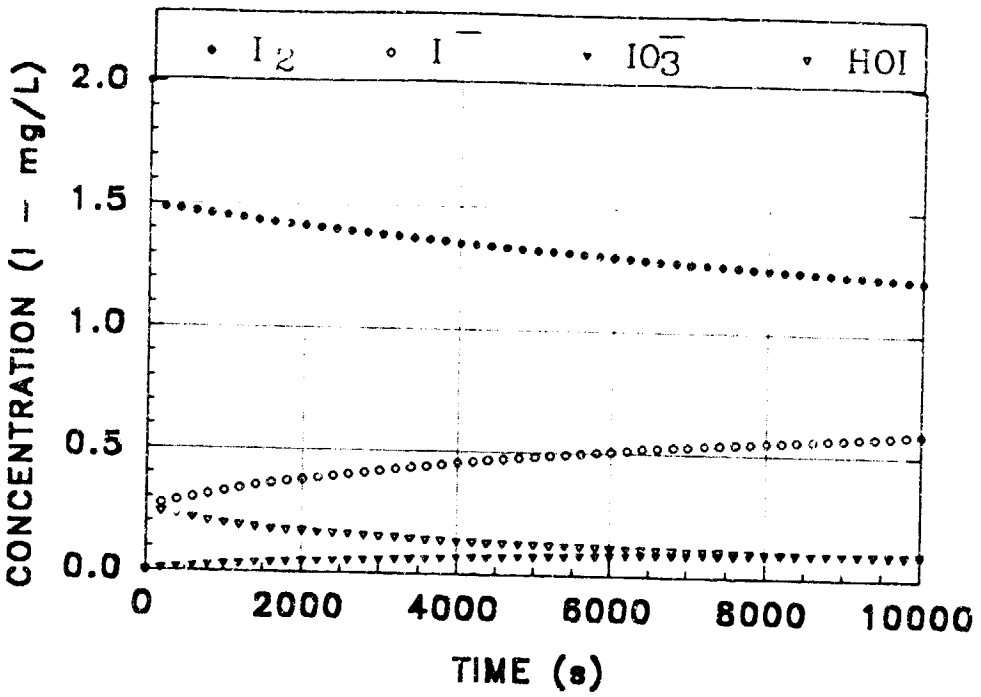

a) 0 - 10,000 Second Time Scale.

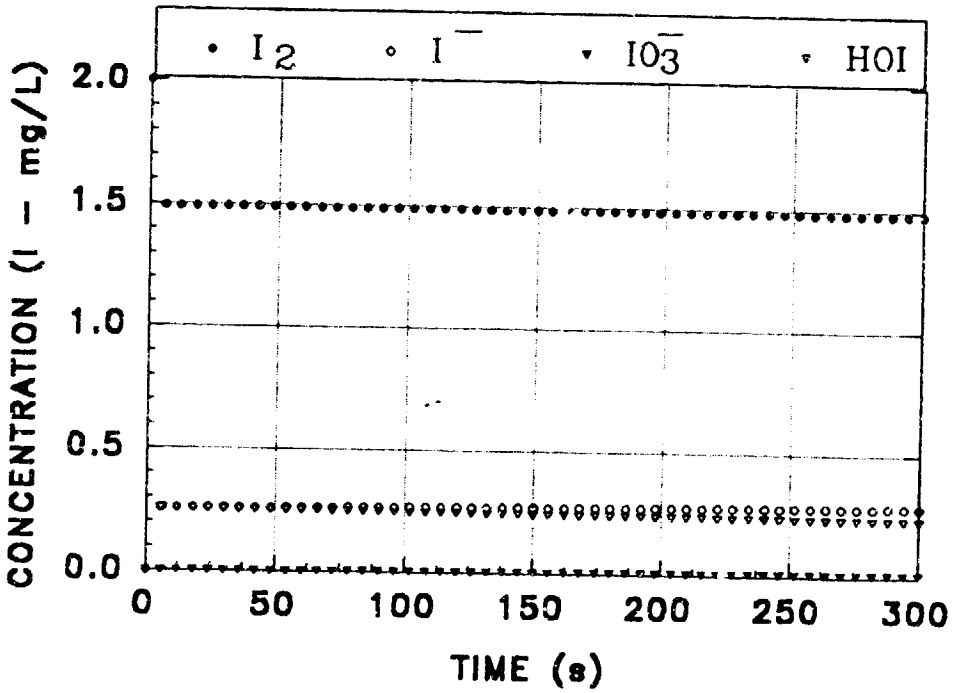

b) 0 - 300 Second Time Scale

Figure 7.22 I_2 Speciation Kinetics - 2.0 mg/L I at pH = 6.

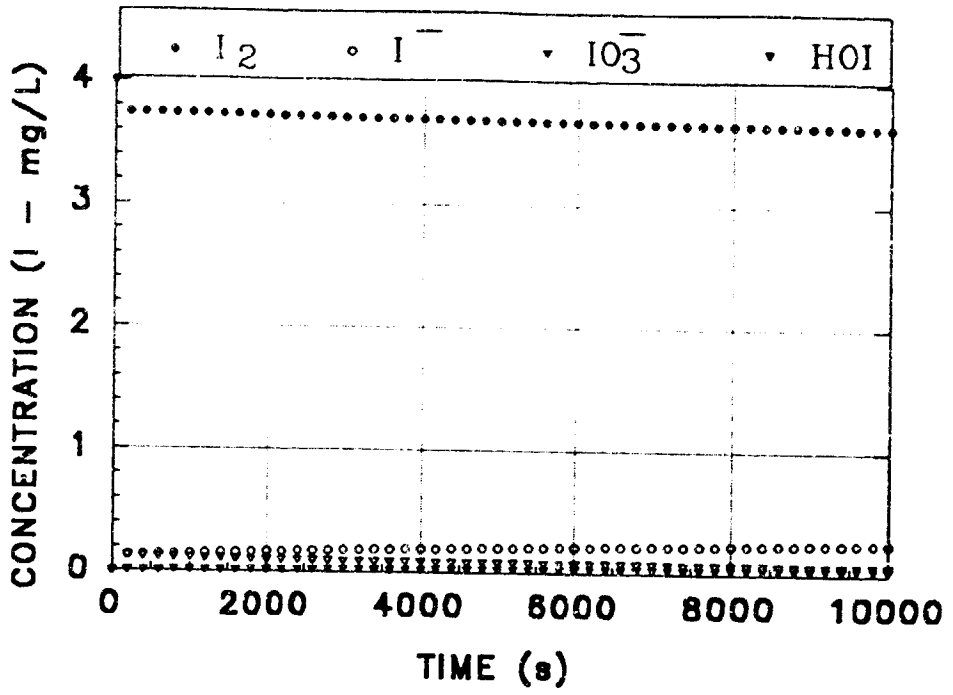

a) 0 - 10,000 Second Time Scale.

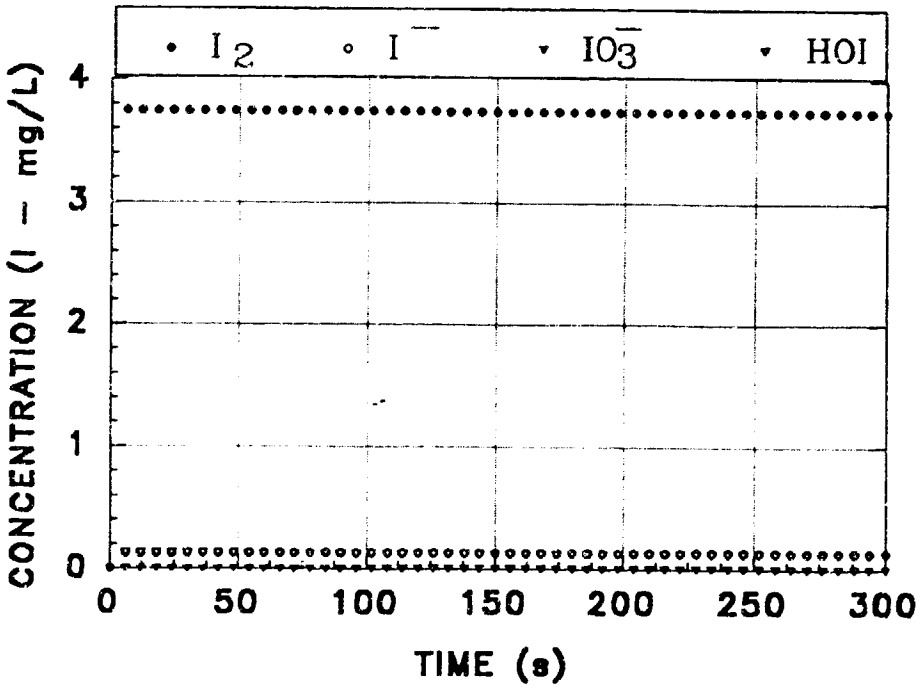

b) 0 - 300 Second Time Scale

Figure 7.23 I_2 Speciation Kinetics - 4.0 mg/L I at pH = 5.

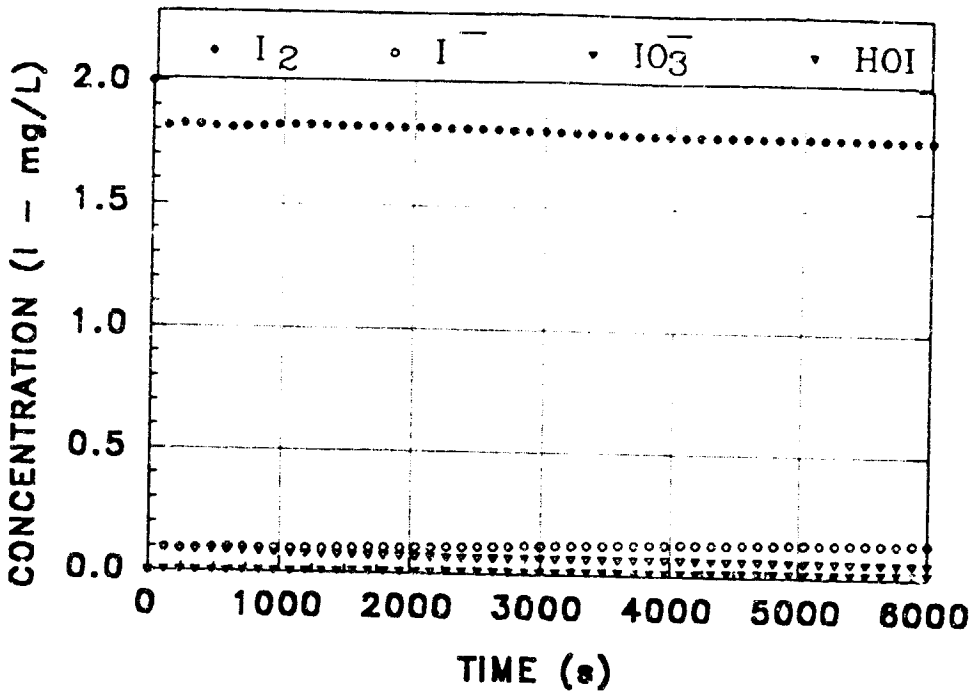

a) 0 - 6,000 Second Time Scale.

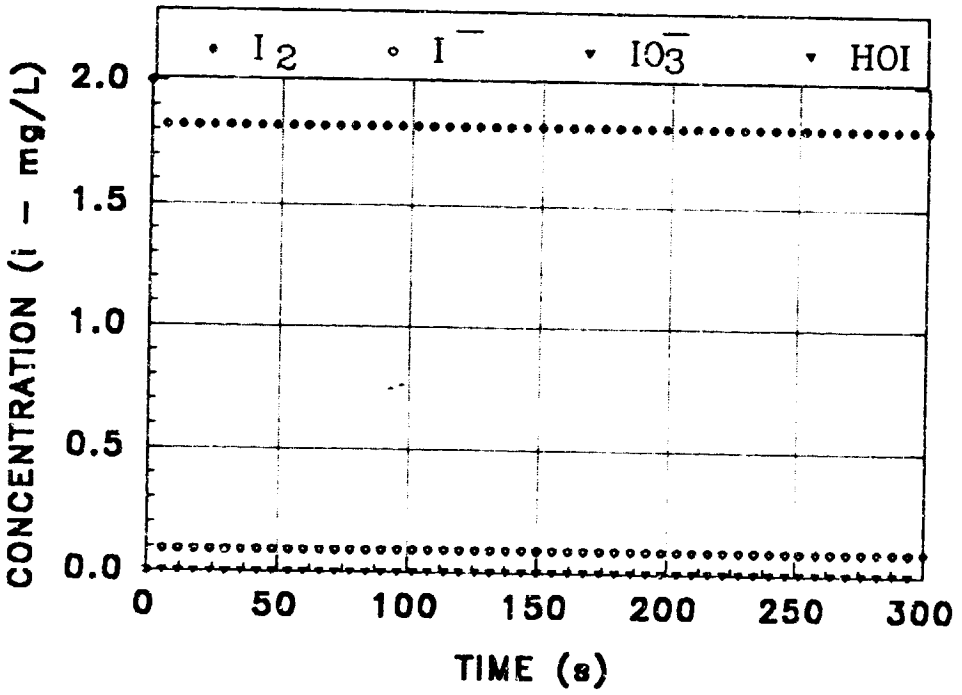

b) 0 - 300 Second Time Scale

Figure 7.24 I_2 Speciation Kinetics - 2.0 mg/L I at pH = 5.

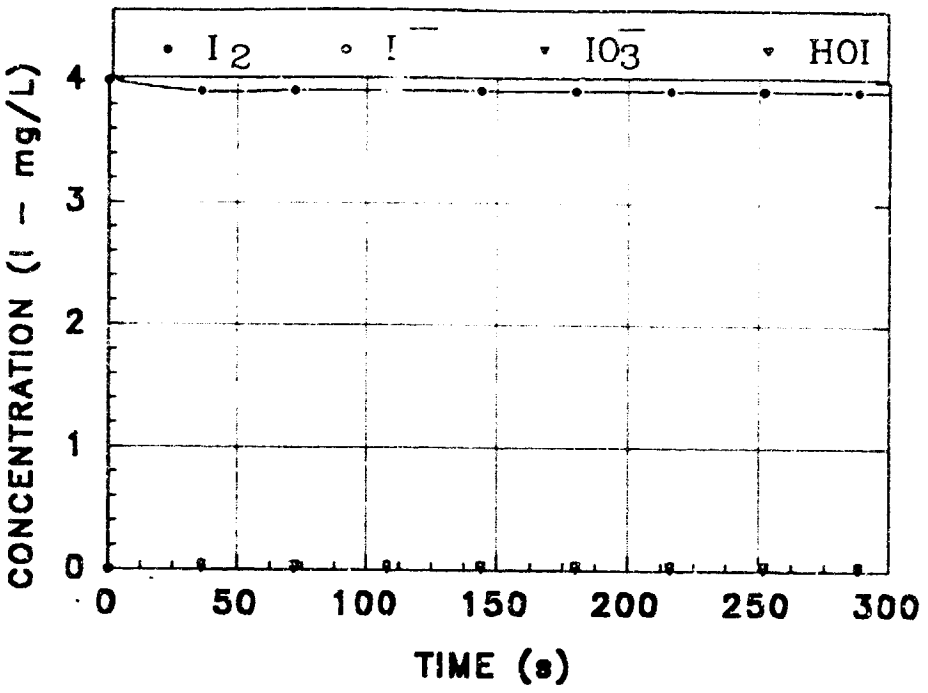

a) 4.0 mg/L I, 0 - 300 Second Time Scale.

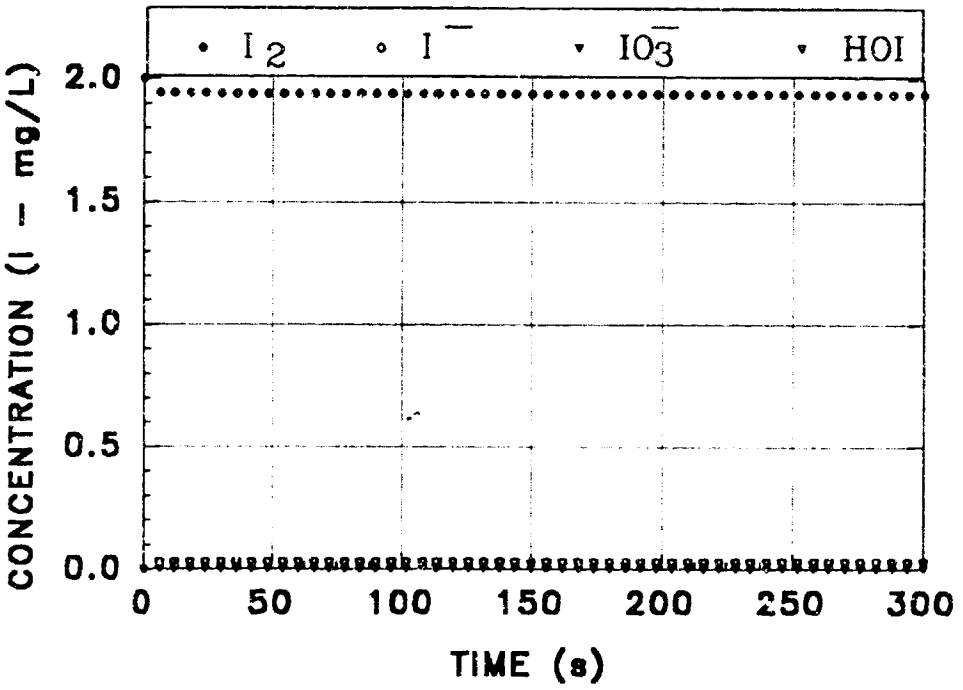

b) 2.0 mg/L I, 0 - 300 Second Time Scale

Figure 7.25 I_2 Speciation Kinetics at pH = 4.

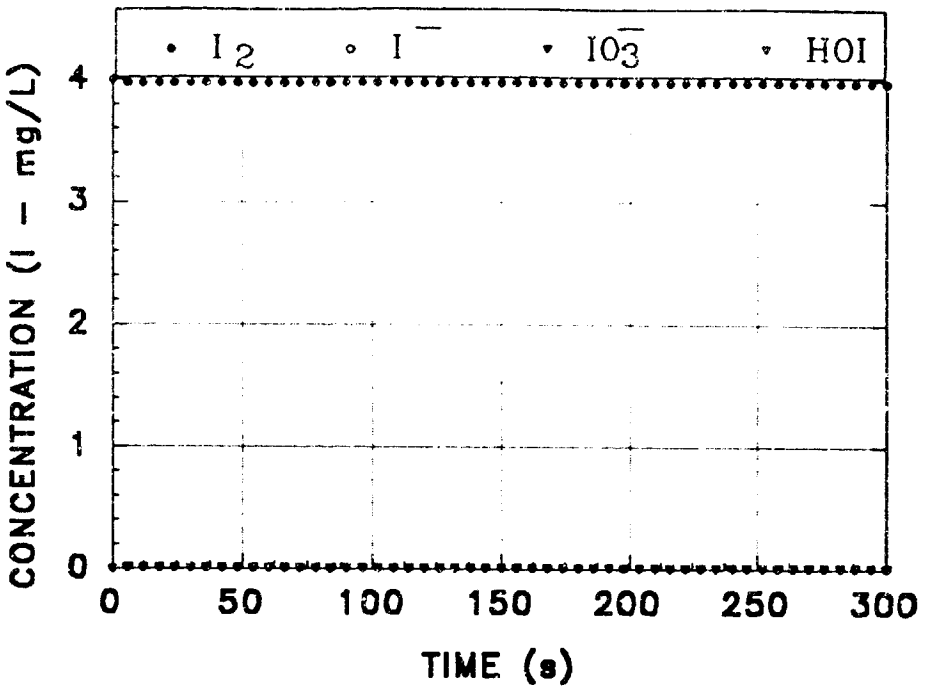

a) 4.0 mg/L I, 0 - 300 Second Time Scale.

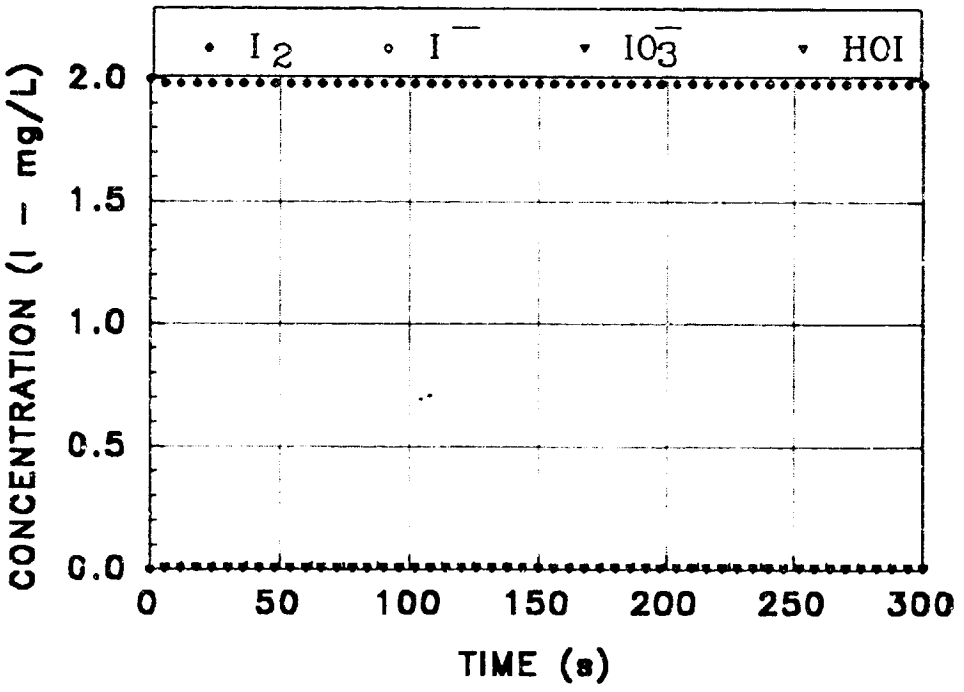

b) 2.0 mg/L I, 0 - 300 Second Time Scale

Figure 7.26 I_2 Speciation Kinetics at pH = 3.

7.2 Chemistry and Kinetics of I_2 Loss in Ersatz Humidity Condensate and Ersatz Urine Distilate.

A significant decline in I_2 concentration is associated with the iodination of heavily contaminant-laden process water streams such as the ersatz humidity condensate and ersatz urine distillate challenge streams used in the present study The acidity of these solutions, between pH = 3 and pH = 4, precludes the loss of I_2 via the hydrolysis reactions discussed above.

Instead, I_2 loss is attributable to reaction with organic constituents. This phenomenon has been investigated using time resolved UV-VIS absorption spectrophotometry of iodinated ersatz humidity condensates and iodinated ersatz urine distillates. Rates of iodine loss have also been studied using single contaminant systems at equivalent concentrations. The predominant reactive species have been identified as thiourea and formic acid[14]. Pseudo-first-order rate constants have been determined for ersatz contaminant model mixtures and for individual reactive constituents. Second order rate constants have been determined for the bimolecular reaction of iodine and formic acid. The relationship between rate constant and temperature has also been established for this reaction.

The overall strategy of the I_2 decay investigation has been to first characterize the phenomenon in the subject ersatz contaminant model, and then to dissect the model chemically, component by component, by examining aqueous binary iodine-contaminant mixtures at equivalent ersatz model concentrations, to determine which species exhibit significant reactivity toward iodine. Individual experiments were performed by iodinating the test solutions to an initial concentration of 20 mg/L I_2 and subsequently monitoring the decline in I_2 concentration as a function of time.

The ersatz humidity condensate mixture is the more chemically complex of the two RMCV chailenge streams. Though they occur in markedly different concentrations, the three predominant constituents of both contaminant models are the carboxylic acids: formic acid, acetic acid, and propionic acid. The ersatz humidity condensate mixture and the four

predominant individual organic constituents of this contaminant model, formic acid, acetic acid, propionic acid and caprolactam were selected for inital experimentation.

The reaction vessel consisted of a thermally insulated and jacketed Teflon stoppered 5 cm path length cylindrical quartz spectrophotometer cell, as described in Section 2. The cell volume was 30 cm^3. Experiments were conducted by spiking 30 cm^3 of the appropriate matrix, resident within the spectrophotometer cell, with sufficient concentrated (1,000 mg/L) ethanolic I_2 stock solution to attain an approximate 20 mg/L initial I_2 concentration. The solutions were then rapidly mixed, initial I_2 determined, and the acquisition of spectra for the determination of I_2 concentrations at periodic intervals initiated using the HP 8452A diode array spectrophotometer.. At the termination of the experiment both I_2 and I^- concentrations were determined by the LCV method.

First and second order kinetic models were derived using least squares approximation techinques[3,8,4]. Goodness of fit of the experimental data with that derived from the various kinetic models was judged using the statistical correlation coefficient (r^2)[3,8,4]. This approach assumes that all errors are random. Most experiments were performed in duplicate.

7.2.1 I_2 Decay in Ersatz Humidity Condensate.

Earlier ersatz humidity condensate models often contained thiourea, stemming from a tentative GC-MS identification of unknown peaks in Spacelab humidity condensate as thioureas . The original version of the humidity condensate model, from which the RMCV project working ersatz humidity condensate model was derived, contained thiourea. Another ersatz humidity condensate, designed as a challenge solution for a catalytic oxidation system under development at Umpqua Research Company, also contained thiourea[1].

Our attempts to characterize the reaction kinetics of thiourea with elemental iodine, both separately and as a component of an ersatz humidity condensate mixture, were frustrated by the extreme rapidity with which the reaction goes to completion. It was observed that within one or two seconds, the reaction proceeds to a point at which one or another of the reactants has been completely consumed. From the standpoint of the time resolution capability

of our experimental system the reaction is virtually instantaneous. All iodine was recovered in the form of I^-, as determined by LCV method.

The reaction responsible for the observed instantaneous I_2 loss is the oxidation of two equivalents of thiourea by a single equivalent of molecular iodine to produce the dimeric formamidine disulfide and two equivalents of hydrogen iodide[434].

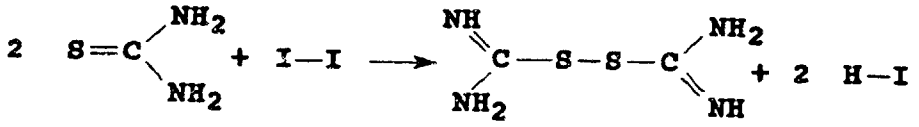

(Eqn 7.20)

Formamidine disulfide may then undergo further reaction, liberating elemental sulfur,

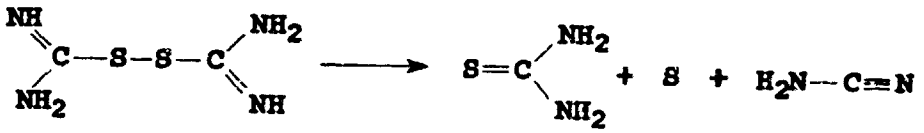

(Eqn. 7.21)

cyanamid and thiourea. Hence it is possible for one equivalent of thiourea to consume up to 1.5 equivalents of I_2 . From this we have concluded that it is impractical to maintain an I_2 residual in thiourea containing media. To do so would require addition of excess I_2 and would result in unacceptably high levels of I^- and other reaction products. Fortunately, it is unlikely that thiourea in any significant level will be encountered in real ECLSS process water streams. For these reasons, the exclusion of thiourea from the ersatz humidity condensate model used in the RMCV development program seems warranted.

The decay of an initial 20 mg/L I_2 concentration in ersatz humidity condensate matrix is illustrated in Figure 7.27. Symmetry of the curve is exponential, with a decay

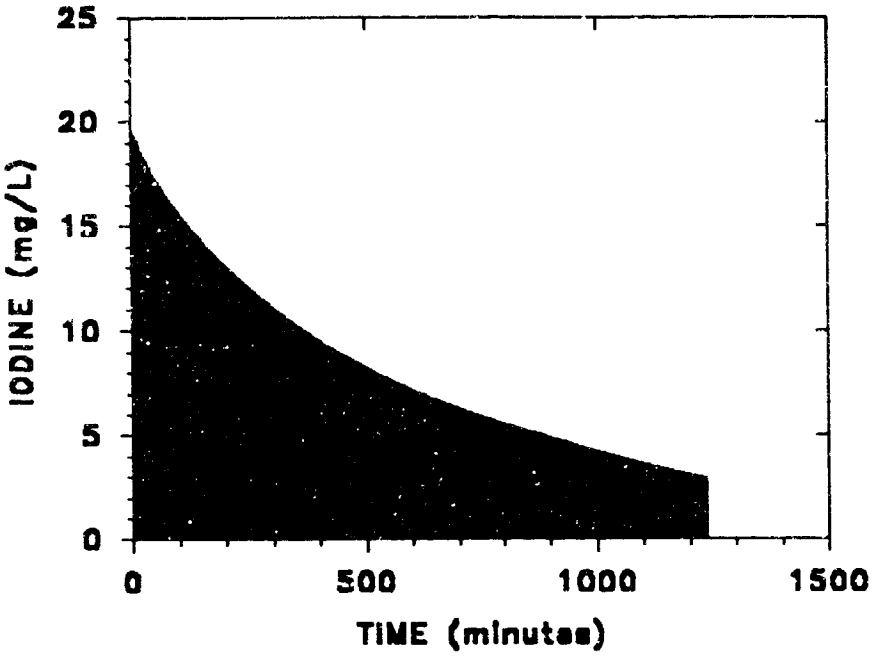

a) 1st Experiment

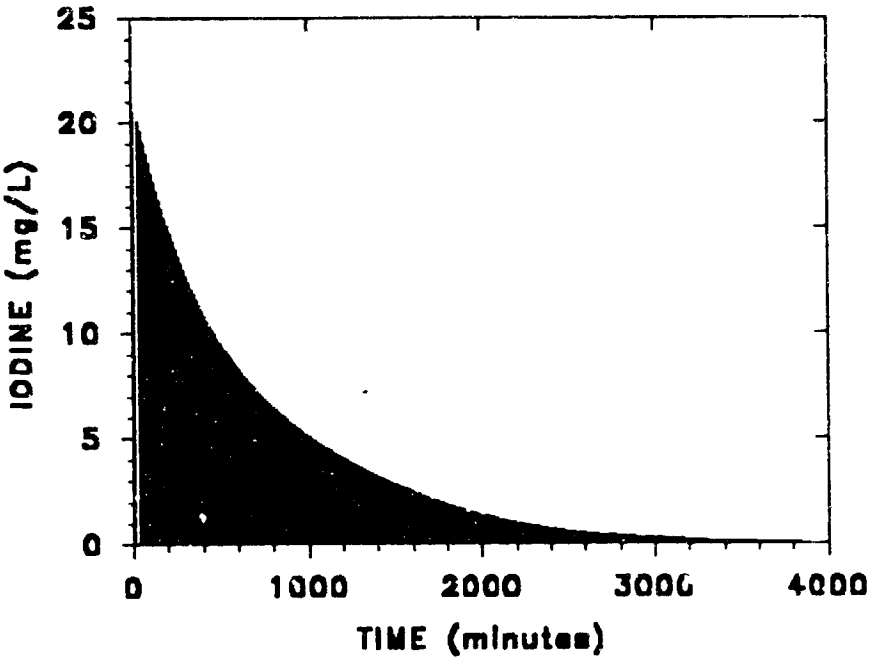

b) 2nd Experiment

Figure 7.27 I_2 Decay in Ersatz Humidity Condensate Matrix

half-life on the order of 500 - 600 minutes. First order kinetic models were derived using the relationship:

$$\frac{d[I_2]}{dt} = -k[I_2] \qquad [I_2] = [I_2]_0 \, e^{-kt} \qquad \text{(Eqn. 7.22).}$$

The least square fit of the data in Figure 7.27a and 7.27b to the integral form of the expression above yields pseudo-first order rate constants (k) of 0.00144 min^{-1} and 0.00145 min^{-1}, and correlation coefficients (r^2) of 0.9932 and 0.9977 for the first and second I_2 decay experiments in ersatz humidity condensate respectively. Figure 7.28 presents comparisons of the observed iodine decay versus that predicted by the pseudo-first order model.

Some insight into the nature of the elemental iodine decay process in ersatz humidity condensate can be gained by examination of the changing absorbance spectra. The qualitative change in absorption spectra with time, during iodine decay in ersatz humidity condensate, is presented in Figure 7.29. In this three dimensional surface representation, absorbance and wavelength are depicted on vertical and horizontal axes respectively. The time axis is represented as depth, with time increasing from front to back. The low wavelength region of non-specific absorbance has been cut and the scale expanded. Etched into the flattened top of the cut-off low wavelength region is a furrow running from front to back. To the right of this is the 270 nm line indicative of I_2 and further to the right is the 288 nm I_3^- spectral line. It is noteworthy that this furrow disappears with time, indicating that the 270 nm peak height is diminishing. The flattened region to the right of the furrow widens with time, indicating growth of the 288 nm peak relative to the 270 nm peak. Reduction of intensity of the I_2 spectral lines with time, is also seen in the height of the 460 nm peak, but is not readily apparent from the angle at which the plot is viewed. What is strikingly apparent is the

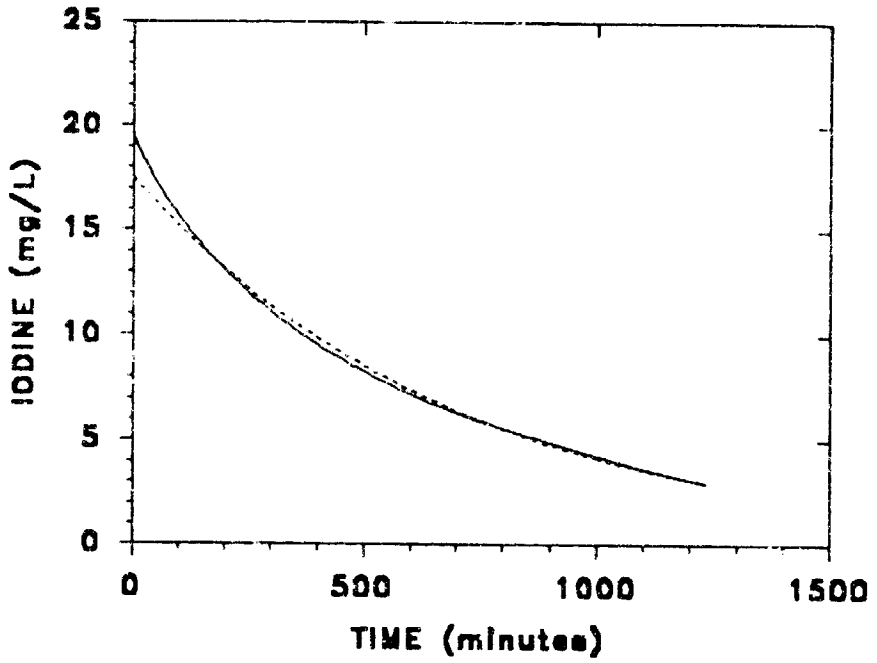

a) 1st Experiment

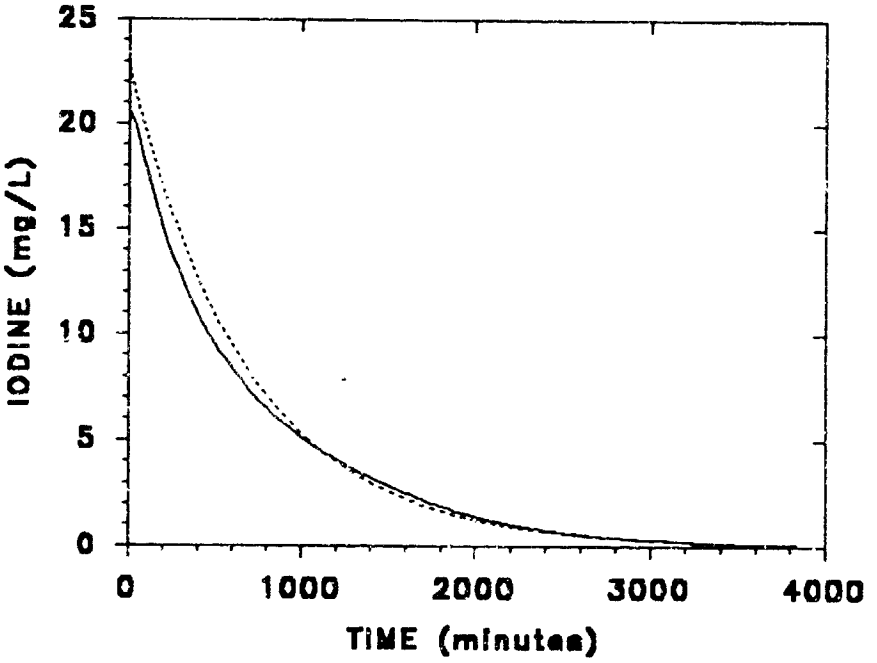

b) 2nd Experiment

Figure 7.28 Ersatz Humidity Condensate - I_2 (Data = solid, 1st Order Model = dashed)

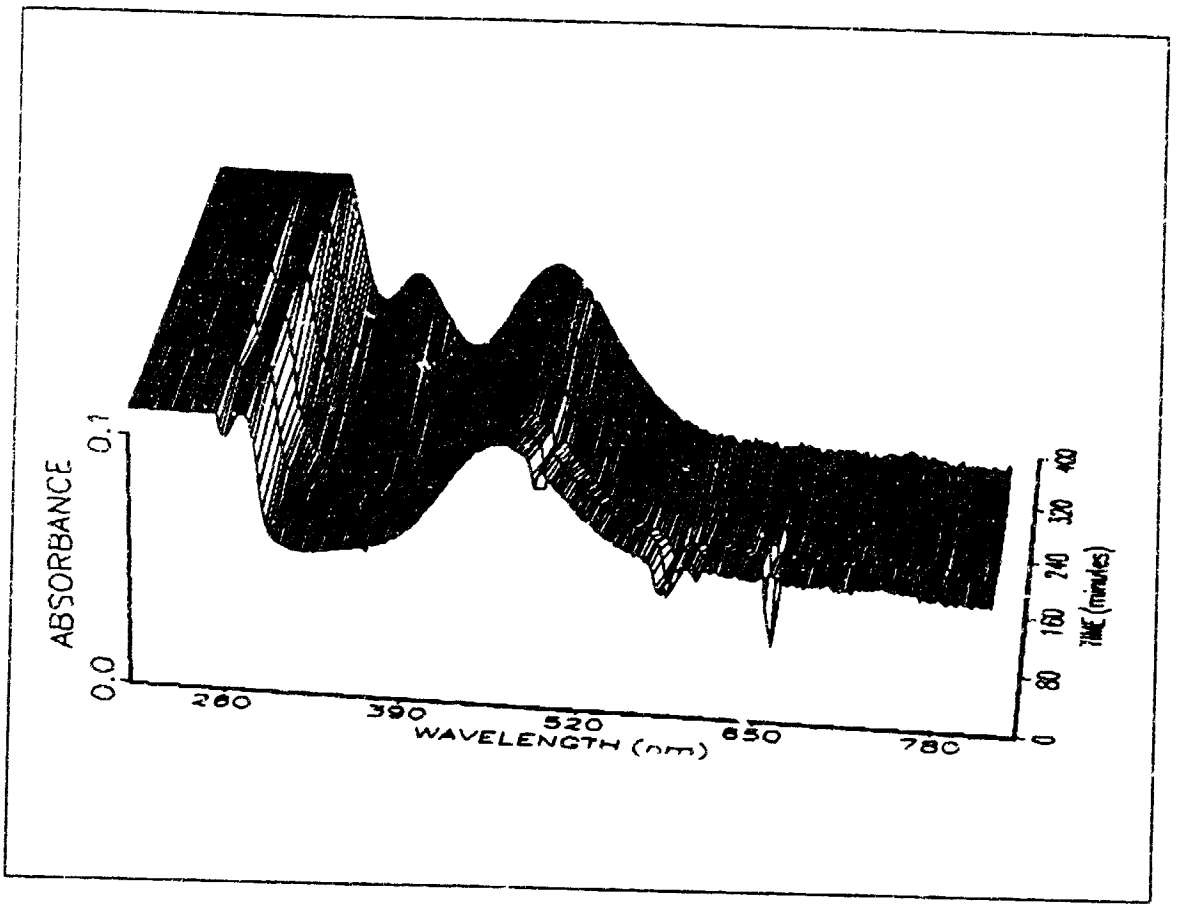

Figure 7.29 Time Series of UV-vis Spectra - I_2 in Ersatz Humidity Condensate .

appearance and increase with time of I_3^- absorbance at 350 nm. This demonstrates the production of iodide during the reaction.

Analysis of the reaction mixture upon termination of multiple experiments in ersatz humidity condensate reveals complete conversion of reacted I_2 to I^-. This is very significant. If any iodinated organics are being produced, it can only be through minor side reactions and can only result in sub-part per million levels of product.

Similar kinetic experiments were conducted individually, for each of the major constituents of the humidity condensate model: formic acid, acetic acid, propionic acid, and caprolactam at the corresponding concentrations. Additionally a deionized water blank experiment was conducted. In this way, formic acid was identified as the primary reactive

species present within the ersatz humidity condensate mixture. All other tested contaminants behaved similarly to the deionized water blank. We concluded that the principal reaction responsible for elemental iodine decay in the ersatz humidity condensate model under investigation is the oxidation of formic acid to carbon dioxide as shown in equation 7.23. In this process elemental iodine is reduced to iodide anion.

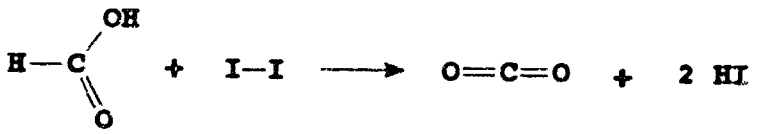

(Eqn. 7.23)

Two experimental I_2 decay curves in formic acid (pH = 3, at 2.5 mM) are presented in Figure 7.30a and 7.30b. Fitting of these data to first order kinetic models yields a rate constant (k) of 0.00104 min^{-1} and an r^2 of 0.9954 for the first experiment and a rate constant of 0.00088 min^{-1} and an r^2 of 0.9962 for the duplicate experiment. Figure 7.31 presents both experimental iodine concentrations and those predicted by the derived rate constants.

These data were also fitted to a bi-molecular second order kinetic model of the form,

$$\frac{[I_2]}{[HCO_2H]} = \frac{[I_2]_0}{[HCO_2H]_0} e^{([I_2]_0 - [HCO_2H]_0)kt} \qquad \text{(Eqn. 7.24)}$$

The resulting rate constant (k) of 0.00042 $M^{-1}min^{-1}$ and r^2 of 0.9974 for the first experiment and k of 0.00037 $M^{-1}min^{-1}$ and r^2 of 0.9985 for the second experiment show a marginal improvement over the first order model. The reaction appears to be a true second order process, but pseudo-first-order under conditions of excess formic acid. Figure 7.32 is a linearized plot which compares observed data to the predictions of the second order model. A_0 and B_0 represent the initial molarities of formic acid and I_2 respectively.

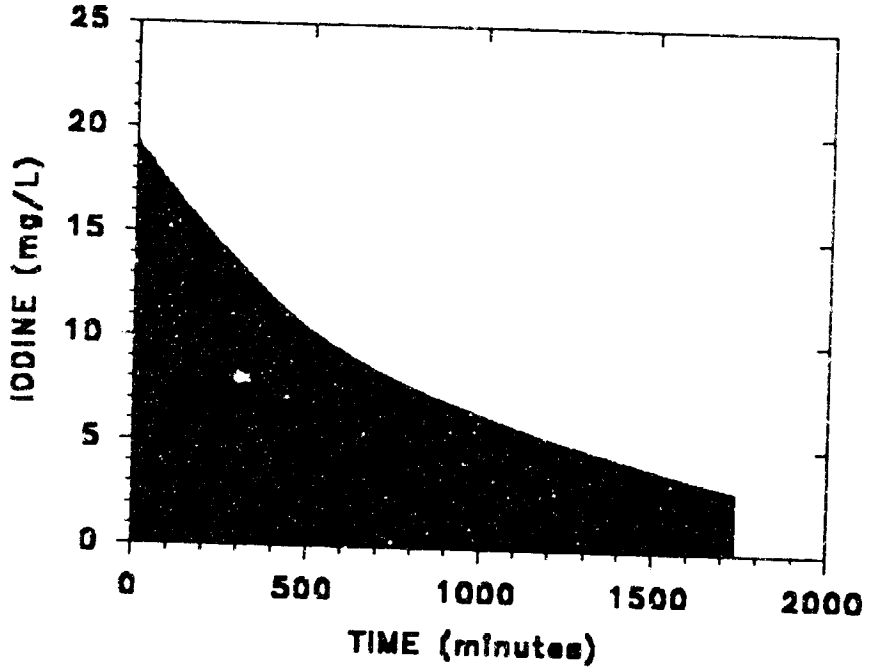

a) 1st Experiment

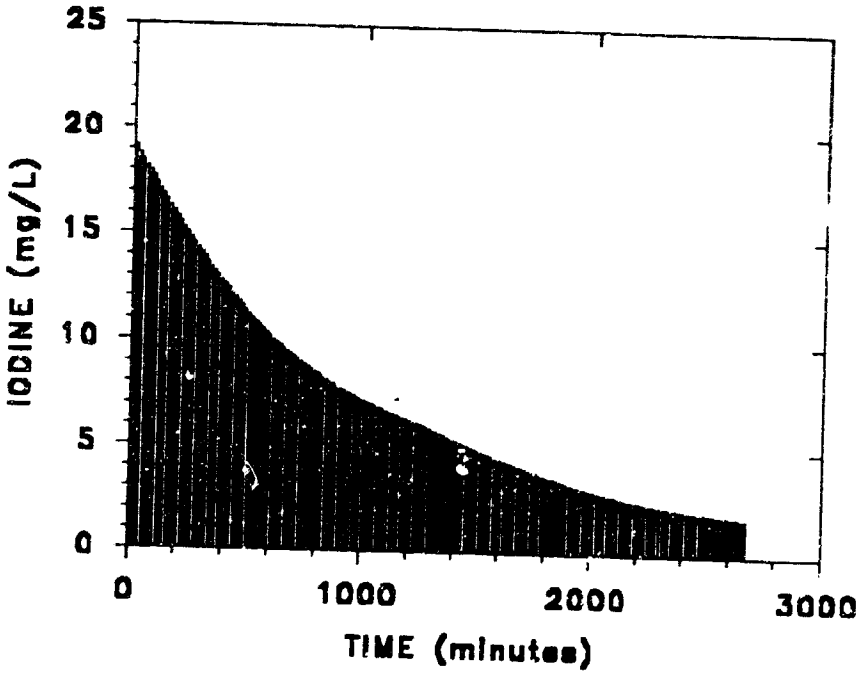

b) 2nd Experiment

Figure 7.30 Elemental Iodine Decay in 2.5 mM Formic Acid.

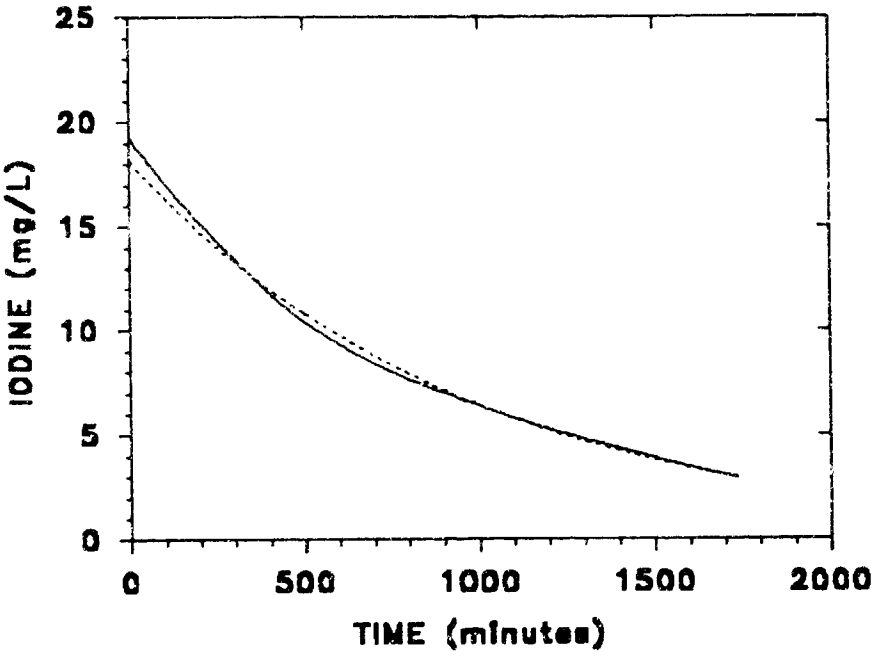

a) 1st Experiment

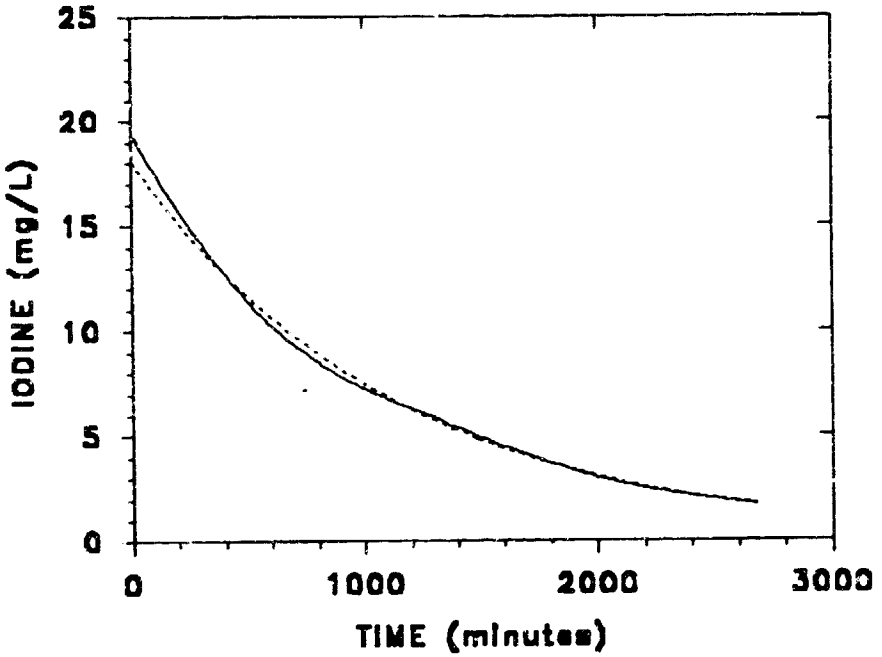

b) 2nd Experiment

Figure7.31 Iodine Reaction with Formic Acid (Observed=solid, 1st Order Model=dash).

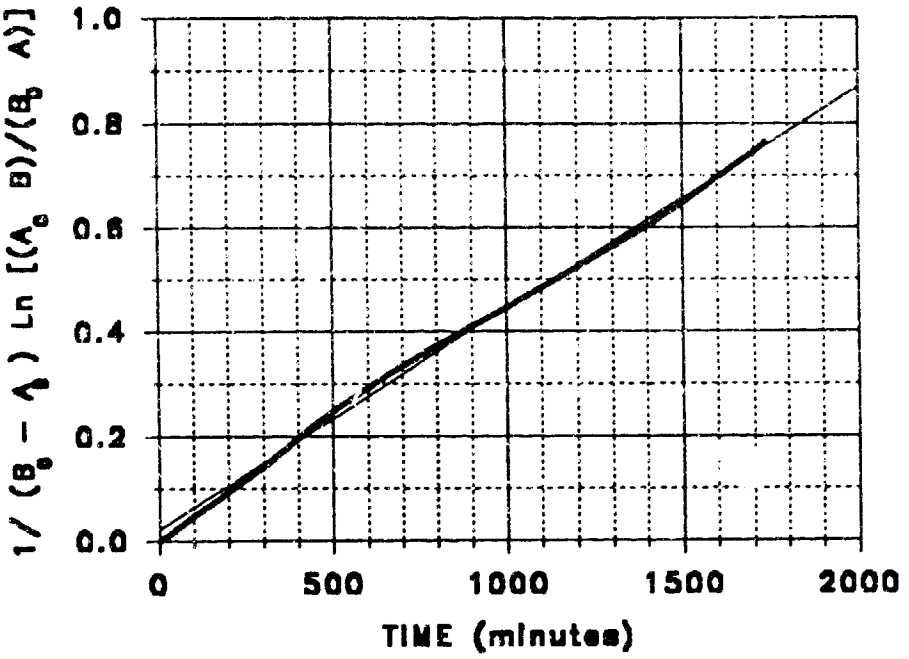

a) 1st Experiment

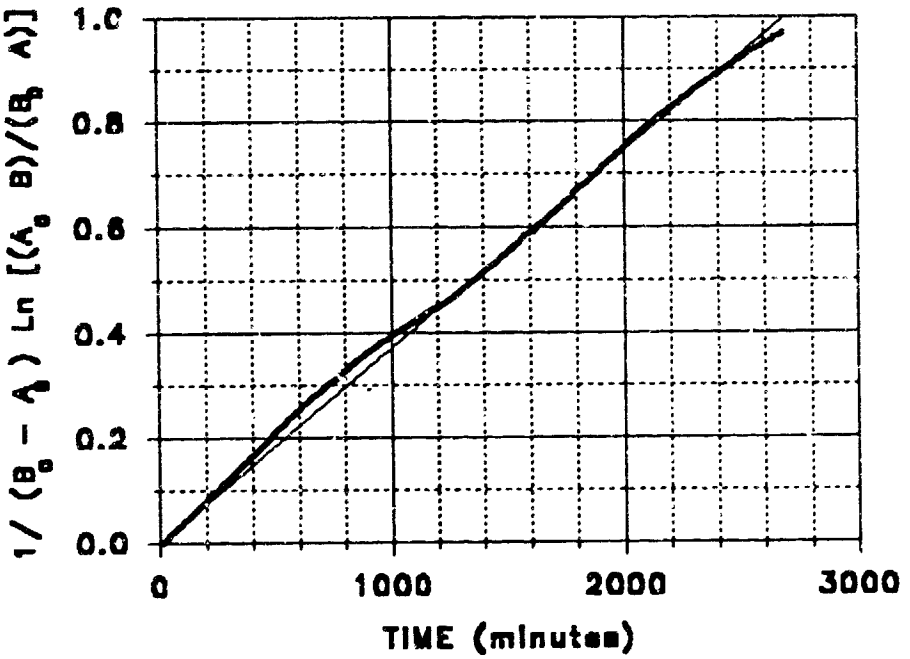

b) 2nd Experiment

Figure 7.32 Formic Acid - I_2 Second Order Rate Model- (Observed=dark,Model=light).

Reaction kinetics of the formic acid - I_2 system were characterized at two additional temperatures, 37 ^oC and 46 ^oC . These data are presented in Table 7.1. For the elevated temperature experiments, the second order rate model consistently provids a better correlation with the observed iodine decay than does the first order rate model. The Arrhenius plot of the second order data is presented in Figure 7.33. The relationship between the rate constant and temperature is expressed by,

$$k = A\ e^{-\frac{E_a}{RT}} \qquad \text{(Eqn. 7. 25),}$$

where R is the universal gas constant (8.3143 $J\text{-}^oK^{-1}\text{-}Mol^{-1}$) and T is temperature in ^oK. Strong linearity is indicated by the correlation coefficient (r^2) of 0.9993. The test results yield an Arrhenius activation energy (E_a) of 89.3 $J\text{-}mMol^{-1}$ and a frequency factor (A) of 2.46 x 10^{12} $L\text{-}mMol^{-1}\text{-}min^{-1}$.

Table 7.1 Summary of Iodine Decay Kinetics in 2.5 mM Formic Acid.

Temperature (^oC)	22	37	46
2nd Order k ($M^{-1}min^{-1}$)	0.000372 0.000423	0.00209	0.00569
Correlation Coefficient (r^2)	0.9985 0.9974	0.99974	0.99906
1st Order k (min^{-1})	0.00088 0.00104	0.00512	0.0140
Correlation Coefficient (r^2)	0.9962 0.9954	0.99909	0.99732

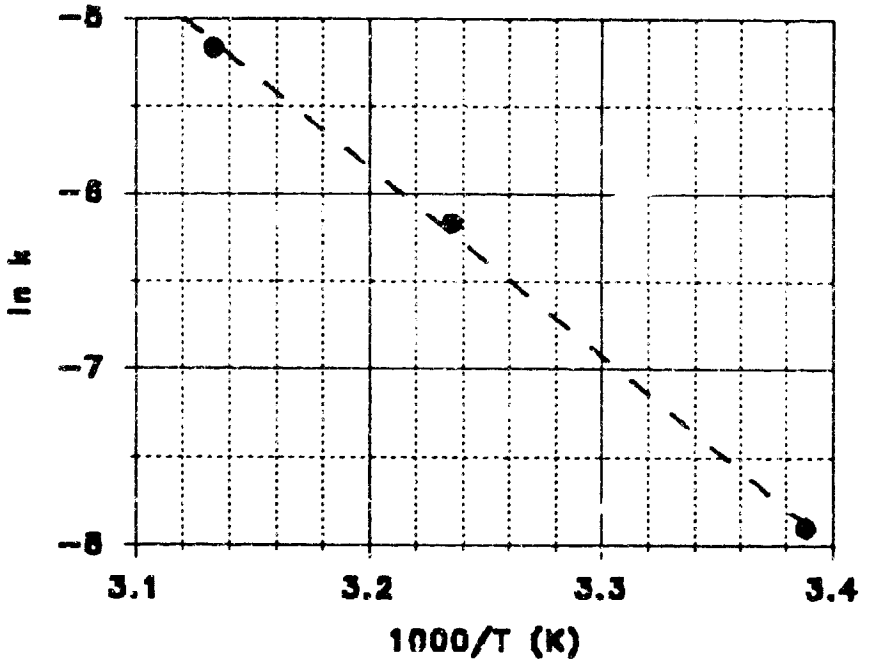

Figure 7.33 Arrhenius Plot - I_2 in Formic Acid- 2nd Order Rate Constant.

7.2.2 I_2 Decay in Ersatz Urine Distillate.

The decay of elemental iodine in ersatz urine distillate is shown in Figure 7.34. Because the three predominant constituents of the ersatz urine distillate model are components previously tested in connection with the study of ersatz humidity condensate, it can be concluded that formic acid will most probably be the predominant reactive species in this matrix as well. Examination of Figure 7.34 indicates that I_2 decay in ersatz urine distillate differs from that of humidity condensate primarily in that much longer I_2 half-lives are evident. This is to be expected for a second order process in which reaction rates are dependant upon the concentrations of both reactants. In this case the formic acid concentration is much lower, 0.22 mM as compared to 2.5 mM in the humidity condensate model. The pseudo-first order rate constant (k) of 0.000127 min^{-1} yields an r^2 value of 0.9860. This value reflects a lower order of correlation than seen for applications of the first order model to I_2 decay in ersatz humidity condensate. As can be seen from inspection of Figure 7.35, the major discrepancies

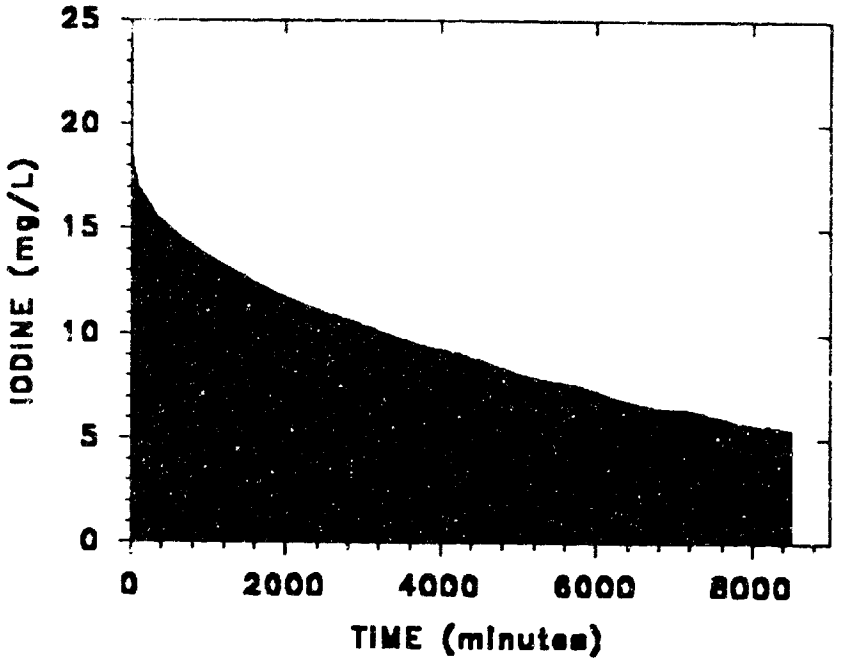

Figure 7.34 I_2 Decay in Ersatz Urine Distillate.

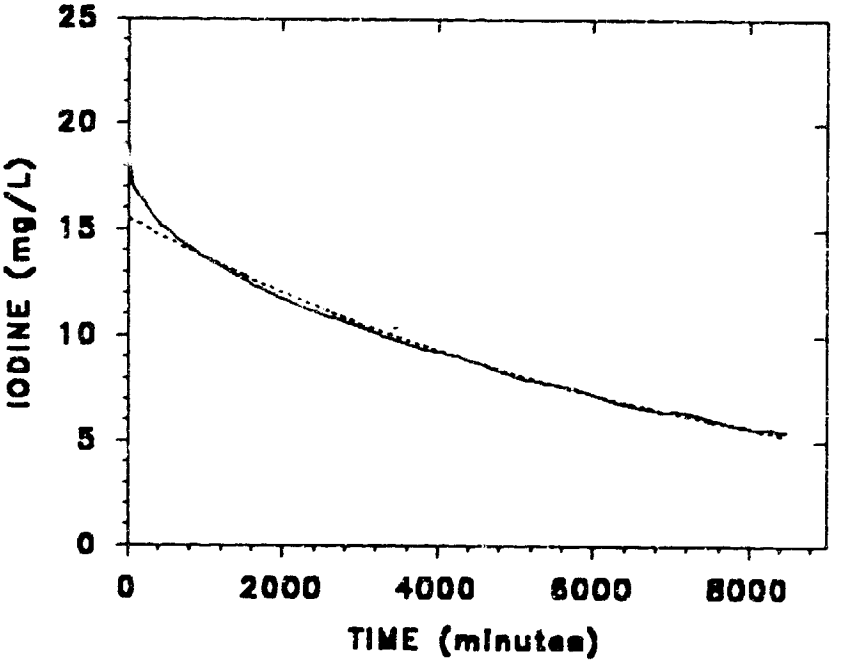

Figure 7. $_2$ in Ersatz Urine Distillate-(Observed=solid, 1st Order Model=dash).

between actual iodine values and those predicted by first order kinetics, occur in the early stages of the experiment. As illustrated in Figure 7.36, a substantially improved fit of the data is provided by the second order kinetic model, with a rate constant (k) of 0.000597 $M^{-1}min^{-1}$ and an r^2 of 0.9970. This model too shows significant deviation at the early stages of the reaction . Analysis of the reaction mixture at the termination of the experiment indicated that all iodine was quantitatively recovered as the sum of unreacted I_2 and I^-.

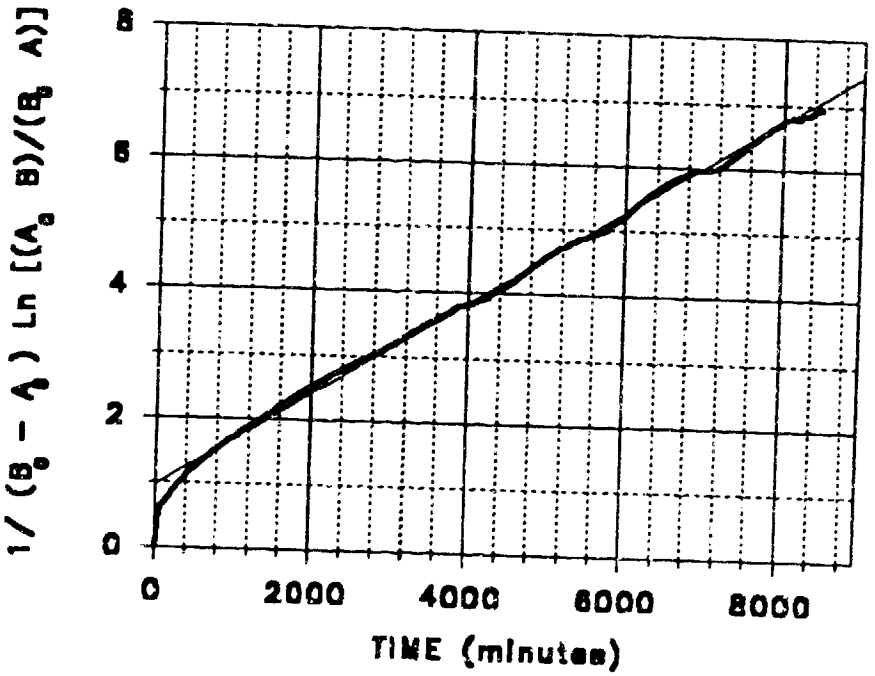

Figure 7.36 Iodine Decay in Ersatz Urine Distillate- 2nd Order Model- (Observed=dark, Model = light).

7.2.3 I_2 Decay Conclusions.

The second order bimolecular reaction of elemental iodine with formic acid, producing carbon dioxide and iodide anion, has been identified as the primary mechanism underlying the decay of residual I_2 in ersatz humidity condensate. That the reaction is second order is indicated by the consistently higher correlation coefficients of the second order model

as compared to the first order model. This trend is consistent over all temperatures and concentration ranges investigated. Using the derived Arrhenius activation energy and frequency factor, rates of elemental iodine loss in this medium can be estimated with reasonable accuracy over a range of temperatures.

Preliminary analyses[377] of humidity condensates collected during the STS-45 mission have indicated formic acid concentrations ranging between 5.0 mg/L and 10.0 mg/L. These two values have been used as input to the 2nd order rate model to project biocidal I_2 loss rates assuming an initial iodination of the humidity condensate with 4.0 mg/L I_2. The results are shown in Figure 7.37. Examination of these data indicate that, for residence times typical of closed loop regenerative life support systems, loss of I_2 does not present a serious operational difficulty.

The situation is somewhat more complicated in the ersatz urine distillate. The aforementioned reaction appears to be the primary mode of iodine decay in this matrix also. However, based upon the divergence between observed iodine concentrations versus those predicted by the kinetic models in the very early stages of the experiment, it seems that our understanding of this system is incomplete. It is entirely possible that competing reactions are at work. If so, it is a strong possibility that the unknown reaction or reactions are reversible, as the reacted elemental iodine has been recovered quantitatively as I^- at the termination of these experiments. It is also possible that a charge transfer complex is formed between I_2 and the aromatic ring portion of phenol and/or benzoic acid, and that this either impedes the reaction at early times, or interferes with the spectrophotometric quantitation of I_2.

The kinetics of the reaction of iodine with formic acid and formate salts have received some attention[23,24,45,68,84,114,182,201]. Considerable disparity exists among the rate constants determined under various conditions. Our own work suggests that reaction rates are pH dependent, with reaction rates increasing as acidity decreases. This would explain small differences observed between ersatz humidity condensate decay rates, and those

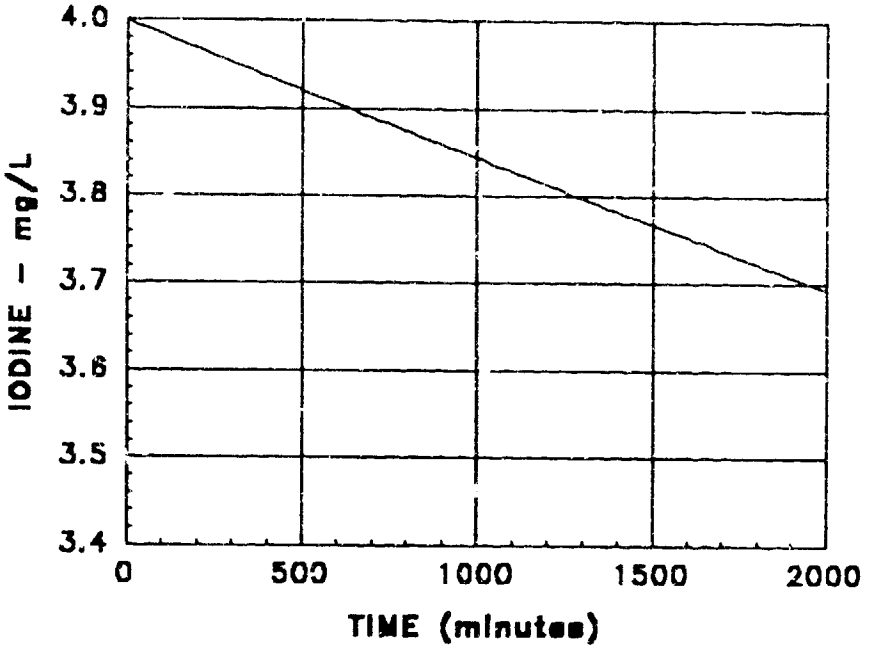

a) 5 mg/L Formic Acid

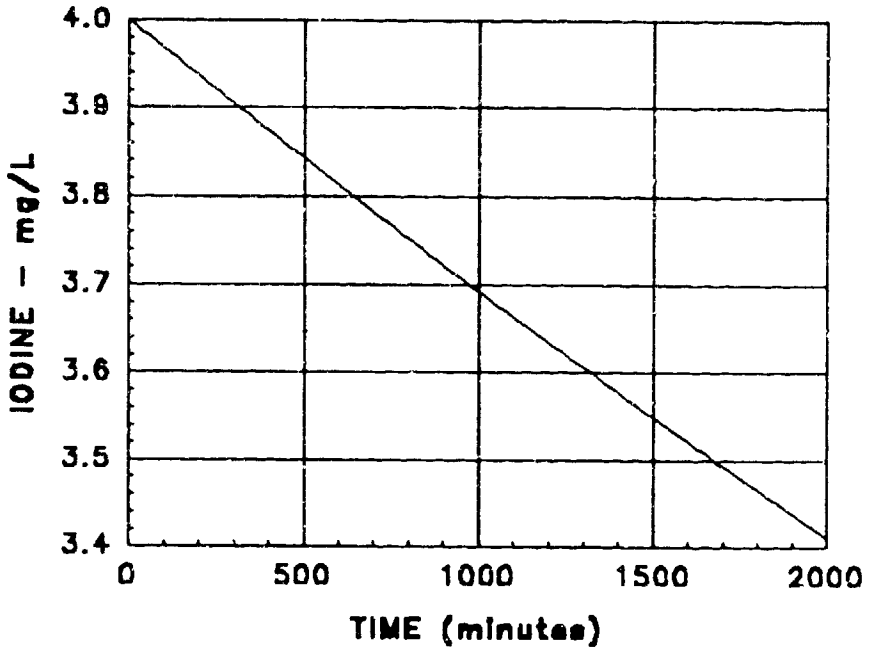

b) 10 mg/L Formic Acid

Figure 7.37 Projected Decay of 4.0 mg/L I_2 in STS-45 Humidity Condensate.

projected from pure formic acid - iodine kinetic data. It would also explain the somewhat larger disparity between predicted and observed decay of I_2 in ersatz urine distillate.

7.3 The Search for Iodinated Organics.

Prior to the identification of the reaction of iodine with formic acid, the mechanism of I_2 loss in ersatz humidity condensate and ersatz urine distillate was strongly suspected to involve the formation of iodinated organic reaction by-products. A limited investigation of the formation of iodinated organics was undertaken at the same time as the kinetics experiments described in sub-section 7.2, and consisted of a literature review, analytical methods development and analysis of iodinated RMCV challenge streams.

A survey of the literature was conducted in order to determine probable routes of formation of iodinated organics (see Section 12). Based upon the chemical composition of the RMCV challenge solutions, the following reactions were considered: the iodination of phenol[43,173,333],

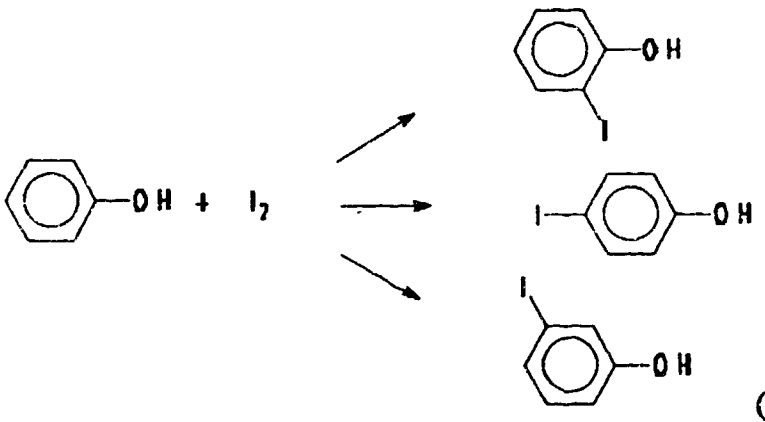

(Eqn. 7.26),

the iodination of benzoic acid[96,98,362],

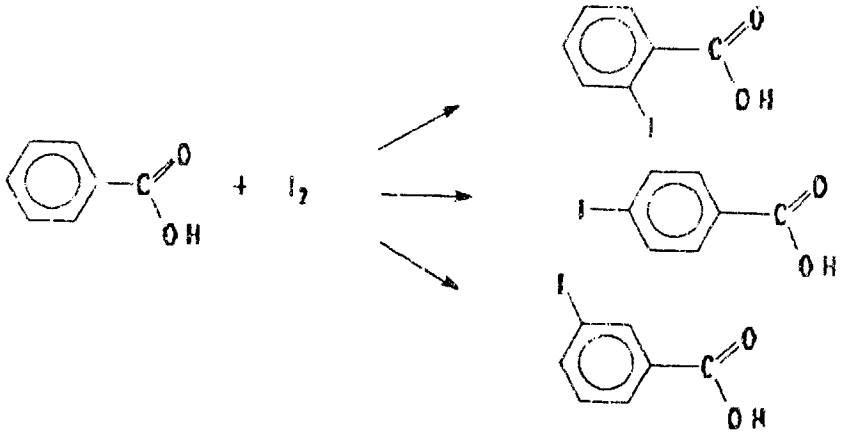

(Eqn. 7.27)

the iodoform reaction[169,383],

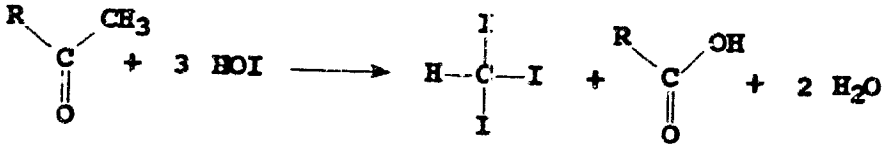

(Eqn. 7.28),

the iodination of acetone[16,27,65,66,104,174,245,353,360,443],

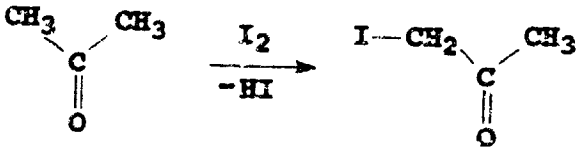

(Eqn. 7.29),

and the α-iodination of carboxylic acids[236],

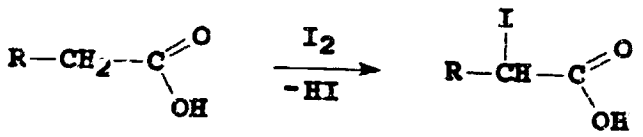

(Eqn. 7.30).

As potential products formed by the above reactions with constituents of the RMCV challenge streams, 1,000 mg/L stock solutions of the following compounds were prepared in ethyl acetate : 3-iodophenol, 4-iodophenol, 2-iodobenzoic acid, 3-iodobenzoic acid, 4-iodobenzoic acid, iodoacetic acid and iodoform. Each of these stock solutions were then diluted 1:1000 in DI water and analyzed by EPA Method 502.2, using purge and trap capillary column gas chromatography with Hall Electrolytic Conductivity and Photoionization detectors. None of the iodinated organic compounds were detected by this method.

With the exception of iodoform, the above stock solutions were then diluted 1:1000 in toluene and derivatized using diazomethane, forming O-methyl ether derivatives of the iodophenols and forming O-methyl ester derivatives of the iodinated benzoic acids and iodoacetic acid. Separation and detection of these compounds was then attempted using an adaptation of EPA Method 515.1[419], using a packed OV-17 column and electron capture detection (ECD). The three mono-iodinated benzoic acid isomers were not resolved, but were separated from the mono-iodinated phenols, which also were not resolved. Iodoacetic acid was not identified.

Iodoacetone was prepared, separated and quantified using the method of Hasty[186,187,293], which involves solvent extraction separation and concentration of iodoacetone into hexane, followed by packed column gas chromatography with ECD detection. Iodoform was separated, detected, and quantified, using similar methodology.

Representative effluents from the ersatz humidity condensate and ersatz urine distillate RMCV streams, with residual I_2 levels between 4.0 mg/L and 3.5 mg/L, were analyzed by the methods described above. No iodinated organics were found at a detection limit of approximately 1 mg/L. Lower detection limits could not be achieved because of the co-extraction of I_2 into the organic solvents and the resulting elevation of the ECD baseline. Thiosulfate was not used to reduce I_2 because of the instability of the iodophenols and iodobenzoic acids.

Ersatz humidity condensate and ersatz urine distillate matrices were iodinated with 10 mg/L I_2, representative of the spike of elevated concentration seen during regeneration in the long term life cycle testing. These samples were analyzed for Total Organo-halogen (TOX) content using method SM 5320[85], which yielded 0.49, 0.36 and 0.05 mg/L for an iodinated DI water blank, ersatz urine distillate and ersatz humidity condensate respectively. TOX is by convention reported as chlorine As iodine the TOX values become 1.75, 1.29, 0.18 mg/L respectively. Because of the lack of specificity of the method, it is not clear what proportion of the TOX numbers are attributable to iodine.

Taken together, the I_2 speciation equilibria and kinetics data reported in the previous sub-sections, the results of limited chemical analysis outlined above, and the results of the TOX assays suggest that, under conditions of normal RMCV operation, organohalogen forming reactions do not proceed at an appreciable rate in comparison to other mechanisms of I_2 loss. It is most probable that iodinated organic compounds, if they do exist, are limited to the sub-part-per-million concentration regime in the RMCV effluent streams.

8

RMCV SUPER-IODINATION
for
MICROBIAL DECONTAMINATION

8.0 Overview.

In its normal operational mode, the RMCV produces water containing biocidal I_2 concentrations confined to the narrow range between 4.0 mg/L and 2.0 mg/L. Within this range, the I_2 levels are sufficient to inhibit microbial growth within the water supply but also low enough to maintain the aesthetic quality as drinking water. The RMCV has an additional capability of operation in the super-iodination mode when output of high levels of aqueous I_2 are desired for disinfection of surfaces, prevention and control of biofilm formation, or to remedy severe microbial upsets in water reclamation process streams.

In the super-iodination mode, the MCV is bypassed. Flow of the influent stream is diverted to the solid state I_2 crystal bed, as in a normal regeneration, but the I_2 crystal bed effluent is routed directly to the point of use, rather than to the MCV. In this way, a strong aqueous I_2 solution of approximately 250 mg/L is made available for situations in which major disinfection capability is required. Experiments have been conducted which demonstrate both the long term reliable production of super-iodinated aqueous solutions from the RMCV solid state I_2 crystal bed and the efficacy of the super-iodinated solutions for the disinfection of surfaces and the control of biofilm.

8.1 Production of Super-iodinated Water.

The design requirements for the steady production of super-iodinated aqueous solutions using packed iodine crystal beds were determined as part of the parametric testing presented in Section 6. The key requirement for output of stable I_2 levels approaching saturation is a residence time of 1.0 minutes or greater. For residence times above this value, the super-iodinated aqueous concentrations of approximately 250 mg/L are attained. In operational terms, this means that a properly designed iodine crystal bed will output this concentration, independent of flow rate so long as maxima are not exceeded.

Figure 8.1 illustrates the flow history of a small column I_2 bed of approximately 10

cm^3 volume, similar in size to those used for the long term life cycle testing. In this example, DI water was fed to the crystal bed at a flow rate of approximately 8 cm^3/min. Inspection of the graph reveals that I_2 levels of approximately 250 mg/L were produced for over 2,500 cm^3 of continuous flow. In this experiment, the I_2 levels began falling only after the crystal bed was sufficiently depleted as to reduce the residence time of the aqueous stream below 1.0 minute. Expressed in terms of a scaled up crystal bed capable of processing the Space Station *Freedom* baseline flow rate of 120 cm^3/min, this would correspond to a continuous production of more than 37 liters of super-iodinated disinfectant solution.

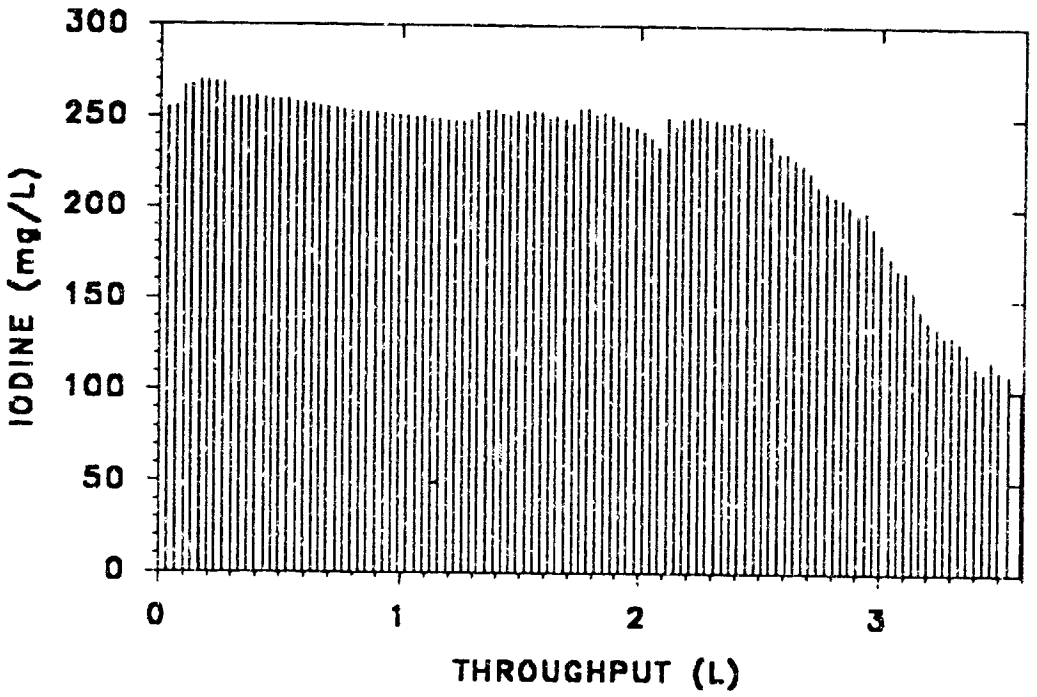

Figure 8.1 Solid State Crystal Bed Effluent I_2 Concentration versus Throughput, 10 cm^3 bed volume - 10 cm^3/min flow rate.

8.2 Disinfection of Surfaces using Super-iodinated Water.

A simple experiment was conducted to establish the efficacy of the strong aqueous I_2 solution produced by operation of the RMCV in the super-iodination mode as a surface disinfectant. Two Teflon coupons with surface areas of approximately 40 cm^2 were passively exposed to laboratory air for a period of six months. The coupons were occasionally handled with bare hands, such as for the measurement of surface areas.

Two similar coupons were contaminated by placing 15 mL of a suspension of *Pseudomonas pickettii* (5.65 x 10^6 CFU/mL) directly on the exposed surface. After one hour the bacterial supsensions were decanted and the coupons were air dried. An aqueous 300 mg/L I_2 solution was produced from a 6.8 cm^3 solid state crystal bed at a flow rate of 5.0 cm^3/min. The surface of one coupon from each pair was completely cleaned, using a calcium alginate swab saturated with the concentrated I_2 solution, followed by a rinse with sterile distilled water to remove excess I_2.

Surface bacteria were recovered using sterile type 2 Calgiswabs (calcium alginate) wetted in buffered sterile water. The swabs were placed in 100 mL sterile buffered water, and the microflora transfered to the aqueous medium by agitation. The number of bacteria were determined as CFU/cm^2 by filtration through a sterile 0.45 µm GN-6 membrane filter, and plating on R2A agar media which were then incubated at 35 °C and counted on day 2 and day 7. The test results are summarized in Table 8.1. No bacterial survivors were isolated from the surfaces of either of the coupons disinfected using the super-iodinated water.

8.3 Control of Biofilm using Super-iodinated Water.

An aqueous 300 mg/L I_2 solution was produced from a 6.8 cm^3 solid state crystal bed at a flow rate of 5.0 cm^3/min for use in the biofilm control tests. Five liters of sterile buffered distilled water, containing 6 g of tryptic soy broth (Difco) were seeded with

Table 8.1 Surface Contamination Super-iodination Test Results.

COUPON	CFU/100mL	CFU/cm^2
Air Exposure	17	0.42
Air Exposure + I_2	0	0
Pseudomonas sp.	2.0×10^5	4.9×10^3
Pseudomonas + I_2	0	0

Pseudomonas pickettii isolated from the laboratory DI water supply for use as the biofilm forming medium. Autoclave sterilized Teflon coupons, 2.54 cm x 2.54 cm x 0.3 cm, were immersed in the biofilm forming medium. Biofilm was grown on the coupons for variable time periods of 24 hr, 40 hr, 72 hr, and 88 hr. Coupons were then exposed to the super-iodinated solution for various times, after which the coupons were rinsed, excess I_2 destroyed with thiosulfate, and the number of bacteria determined as CFU/cm^2 by filtration of the rinse water through a sterile 0.45 µm GN-6 membrane filter, plating on R2A agar media which were then incubated at 35 ^{o}C and counted on day 2 and day 7.

The first series of tests were conducted using coupons with the 24 hour biofilm. Duplicate coupons were exposed to the super-iodinated solution for 30, 60, and 90 minutes. The results of this test are presented in Table 8.2. These data indicate a reduction in microbial population by six orders of magnitude for a 30 minute contact time. The 60 minute contact time produced a further lessening of survivors by one half. The effects of the 90 minute contact time are only marginally better than for the 60 minute contact time.

The results of the 40 hour, 72 hour, 72 hour multiple exposure, and 88 hour biofilm superiodination tests are presented in Tables 8.3, 8.4, 8.5, and 8.6 respectively.

Table 8.2 Test Results for Super-iodination of the 24 Hour Biofilm.

EXPOSURE min	CFU/mL	CFU/cm^2	AVERAGE CFU/cm^2
0	1.89×10^5	1.18×10^6	
0	2.36×10^5	1.48×10^6	1.33×10^6
30	0.21	1.32	
30	0.13	0.78	1.05
60	0.08	0.50	
60	0.10	0.63	0.56
90	0.08	0.50	
90	0.05	0.31	0.41

Table 8.3 Test Results for Super-iodination of the 40 Hour Biofilm.

EXPOSURE min.	CFU/mL	CFU/cm^2	AVERAGE CFU/cm^2
0	2.06×10^5	1.29×10^6	
0	3.70×10^5	2.32×10^6	1.81×10^6
30	1.41	8.84	
30	0.55	3.45	6.14
60	0.66	4.11	
60	0.09	0.55	2.33
90	0.10	0.63	
90	0.01	0.06	0.35
120	0.09	0.56	
120	0.10	0.63	0.59

Table 8.4 Super-iodination of the 72 Hour Biofilm-Single Exposure.

EXPOSURE min.	CFU/mL	CFU/cm^2	AVERAGE CFU/cm^2
0	1.64×10^5	1.03×10^6	
0	5.50×10^5	3.45×10^6	2.24×10^6
30	11.0	69.0	
30	19.8	124.1	96.6
60	0.8	5.0	
60	1.4	8.8	6.9

Table 8.5 Super-iodination of 72 Hour Biofilm-multiple exposure.

EXPOSURE min./min.	CFU/mL	CFU/cm^2	AVERAGE CFU/cm^2
30/30	0.34	2.1	
30/30	0.33	2.1	2.1
60/30	0.05	0.3	
60/30	0.03	0.2	0.2
60/60	0.03	0.2	
60/60	0.11	0.7	0.4

Table 8.6 Test Results for Super-iodination of the 88 Hour Biofilm.

EXPOSURE min.	CFU/mL	CFU/cm^2	AVERAGE CFU/cm^2
0	4.20×10^5	2.63×10^6	
0	3.90×10^5	2.45×10^6	2.54×10^6
30	41.8	262	
30	16.8	105	184
60	3.1	19.3	
60	6.8	42.6	31.0
90	0.19	1.18	
90	0.84	5.25	3.22
120	0.38	2.35	
120	0.09	0.55	1.45

Clearly, as the biofilm ages, a greater contact time is required to produce an equivalent microbial kill. The 40 hour biofilm required a super-iodinated water contact time of 60 minutes to achieve an approximate 6 order of magnitude microbial reduction. The 72 hour biofilm data are complicated by the fact that both single and repetitive iodinations were conducted. In the single exposure test, a 60 ninute contact time yielded three times as many survivors as did two repetitive 30 minute contacts, resulting in 300,000 fold and 1,000,000 fold reductions in bacterial populations respectively. Between 90 minutes and 120 minutes

were required to achieve an equivalent microbial contact kill for the 88 hour biofilm.

8.4 Conclusions.

Based upon the simple experiments outlined above, the RMCV operating in the super-iodination mode is capable of drastically reducing the levels of surface microbial contamination. It is effective against a young biofilm, but not able to reduce the biofilm forming bacterial population to zero. It is capable of disinfection of contaminated surfaces, but not capable of complete sterilization.

As an added capability of the RMCV, operation in the super-iodination mode could be quite useful in dealing with transient episodes of microbial contamination aboard spacecraft. Alternatively, stand-alone iodine crystal beds could be developed for the purpose of surface decontamination and biofilm control. The super-iodination mode of operation was incorporated into the design of the prototype RMCV and is discussed further in Section 10.

9

MATERIALS COMPATIBILITY with ELEMENTAL IODINE

9.0 Overview.

From a materials compatibility perspective, there are several problematic aspects of I_2 chemistry. Both aqueous I_2 and I_3^- are moderately strong oxidizing agents, with a standard reduction potential of +0 535 volts for the half reactions,

$I_2 + 2e^- \rightarrow 2I^-$ (Eqn. 9.1) and $I_3^- + 2e^- \rightarrow 3I^-$ (Eqn. 9.2).

As previously discussed in Section 7, I_2 oxidizes formic acid to CO_2. I_2 can also oxidize a host of other substances including metallic zinc, cadmium, copper, chromium, and iron. This presents a problem with respect to the suitability of metals and alloys for use in the construction of RMCVs. The reactivity of I_2 with unsaturated organic materials can also cause problems. I_2 forms adducts with olefins in which I is added to both sides of the double bond, as shown in equation 9.3,

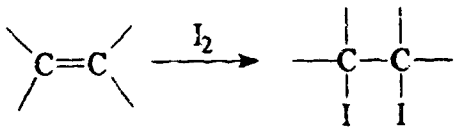

(Eqn. 9.3).

This may pose problems with plastics and related polymeric substances. I_2 also readily diffuses into and discolors a variety of organic materials used in the fabrication of O-rings, tubing, valves, fittings, connectors, etc. The volatility of aqueous I_2 and the tendency of crystalline I_2 to sublime, makes isolation of components from potential deleterious effects, difficult to achieve.

For these reasons, a materials compatibility testing program was implemented in order to identify suitable construction materials for incorporation into the prototype RMCV under development. Twelve materials were initially selected for evaluation, these included: 304 stainless steel, 316 stainless steel, 316L stainless steel, 347 stainless steel, 410 stainless steel, titanium-2, titanium-7, titanium-9, titanium-4901, Teflon, polypropylene, and Viton A. At a later date, Hasteloy G, Hasteloy C , and Teflon coated stainless steel were added to the test program.

Coupons of the various materials were contacted with I_2 in three states: dry crystals, moist crystals, and saturated aqueous solutions ($I_2 \approx$ 300 mg/L at 21 °C, $I_2 \approx$ 900 mg/L at 54.4 °C) ,and housed within bor silicate glass containers, and enclosed with Teflon lined screw-caps. Coupons contacted with each of the I_2 states were prepared in duplicate, one held at room temperture, the other held at 54.4 °C. The coupons were periodically inspected, cleaned, dried and weighed. All weights were obtained using an analytical balance sensitive to 0.0001 gram. Repetitive weighings yielded results that were reproducible to within 0.0005 gram. Weight changes less than 0.0005 gram were not considered significant. The results of these tests are discussed below.

9.1 Corrosion of Stainless Steels by I_2 .

The results of the iodine corrosion tests for the five stainless steels: 304 stainless steel, 316 stainless steel, 316L stainless steel, 347 stainless steel, and 410 stainless steel, are illustrated in Figures 9.1, 9.2, 9.3, 9.4, and 9.5. The initial and successive coupon weights are summarized in in Tables 9.1, 9.2, 9.3, 9.4, and 9.5 respectively.

9.1.1 Exposure to Saturated Iodine Solution.

Saturated aqueous I_2 at room temperature has little or no effect on 304, 316, 316L and 347 stainless steels. However, significant weight loss of the 410 stainless steel coupon is evident under these conditions, with a total weight loss from approximately 7.17 g to 6.36 g over the 300 days of exposure.

Significant corrosion rates are obtained for all stainless steel coupons held at 130 °F. Under these conditions, both 304 and 316 stainless steel coupons are virtually completely dissolved following 180 days of exposure. 316L stainless steel appears more robust, with 50 % weight loss after 180 days, but complete disappearance after 300 days. After 300 days,

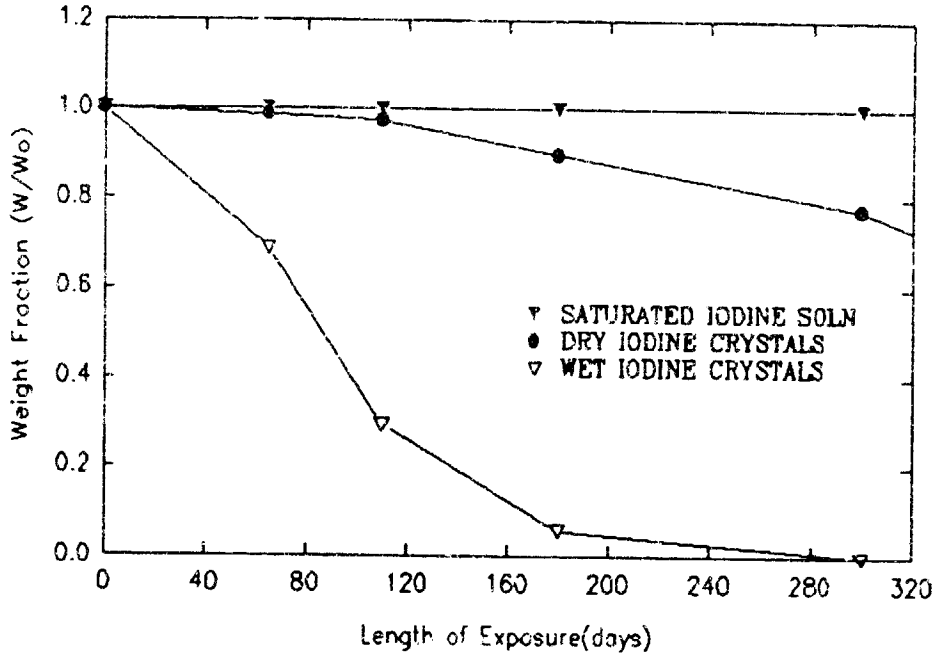

a) 21.1C

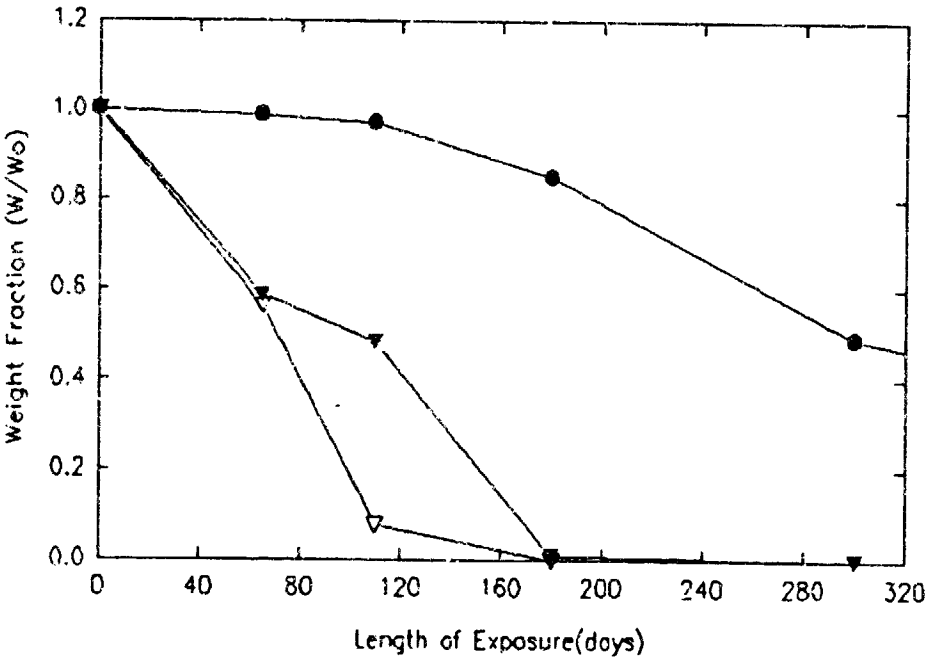

b) 54.4C

Figure 9.1 Iodine Corrosion Tests - 304 Stainless Steel.

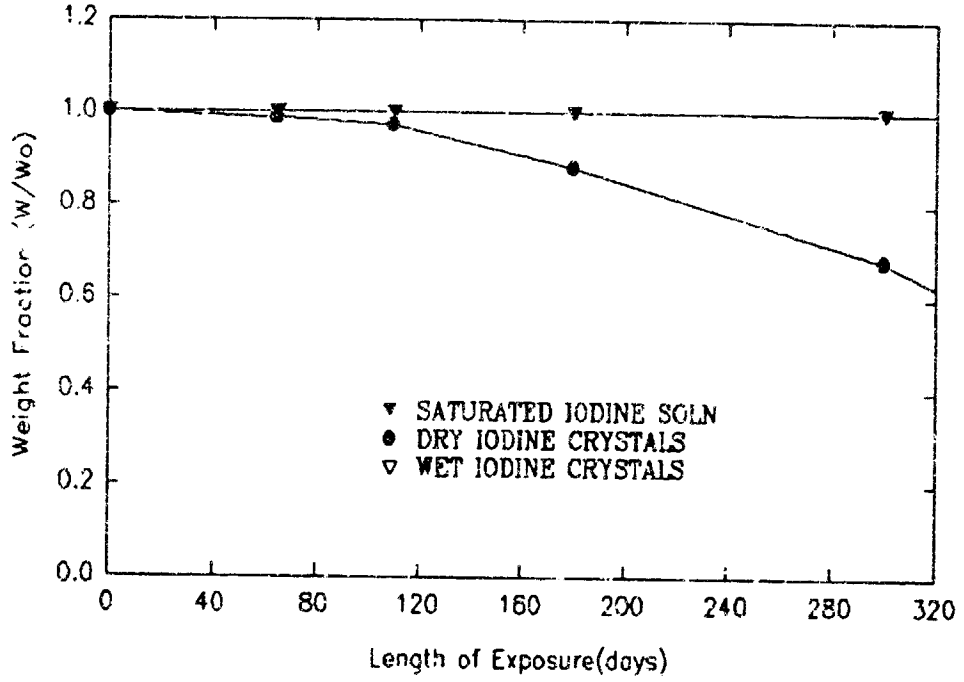

a) 21.1C

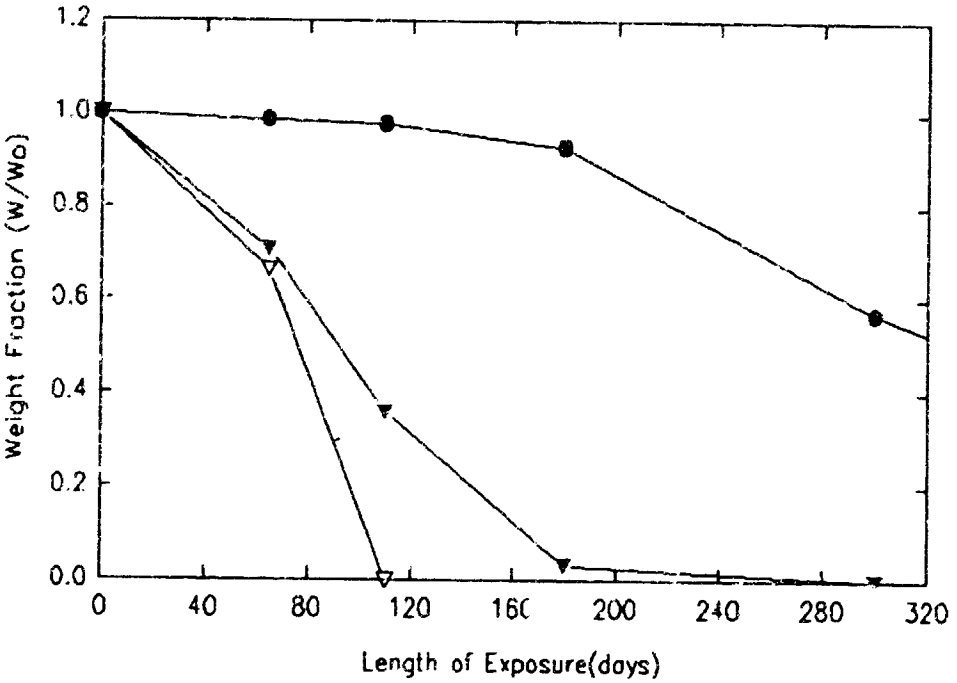

b) 54.4C

Figure 9.2 Iodine Corrosion Tests - 316 Stainless Steel.

TABLE 9.1 Corrosion Tests - 304 Stainless Steel

COUPON WEIGHT (GRAMS)

T	IODINE STATE	INITIAL 12/11/90	2/16/91	4/1/91	6/11/91	10/11/91
21.1C	Dry	7.5403	7.4420	7.3403	6.7620	5.8463
	Wet	7.3590	5.0571	2.1604	0.4190	-0-
	Sat	7.6297	7.6285	7.6281	7.6278	7.6278
54.4C	Dry	7.1146	7.0240	6.9034	6.0474	3.4846
	Wet	7.7830	4.3683	0.6019	-0-	------
	Sat	7.9529	4.0757	3.3550	0.0603	-0-

TABLE 9.2 Corrosion Tests - 316 Stainless Steel

COUPON WEIGHT (GRAMS)

T	IODINE STATE	INITIAL 12/11/90	2/16/91	4/1/91	6/11/91	10/11/91
21.1C	Dry	7.6848	7.5836	7.4640	6.7799	5.2253
	Wet	7.9629	7.9605	7.9603	7.9609	7.9600
	Sat	7.9205	7.9204	7.9195	7.9203	7.9209
54.4C	Dry	8.1601	8.0420	7.9645	7.5622	4.6341
	Wet	7.5360	4.9940	-0-	------	------
	Sat	7.4197	5.2359	2.6647	0.2296	-0-

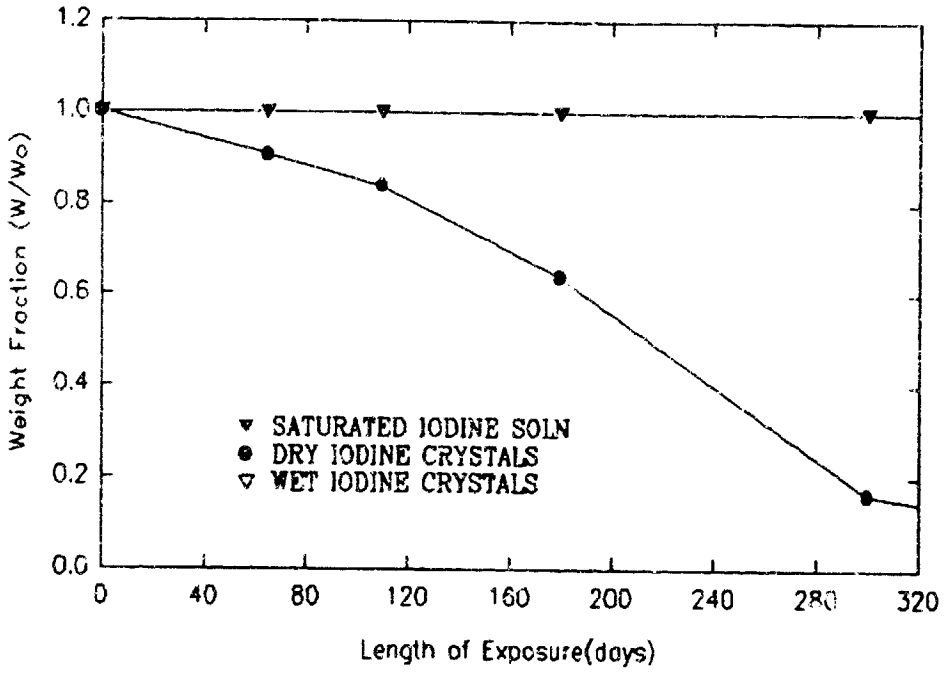

a) 21.1C

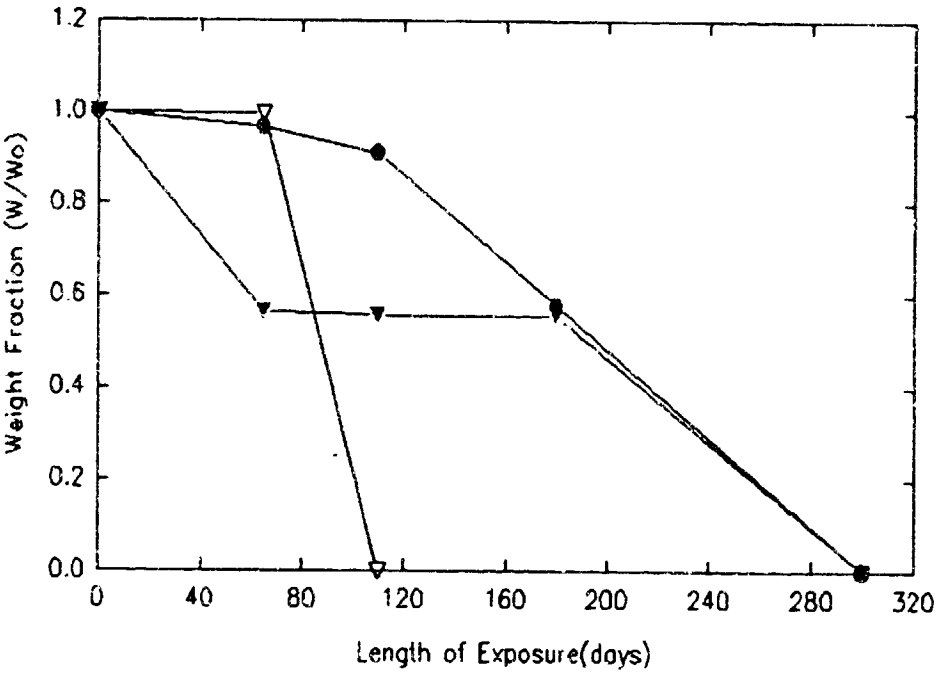

b) 54.4C

Figure 9.3 Iodine Corrosion Tests - 316L Stainless Steel.

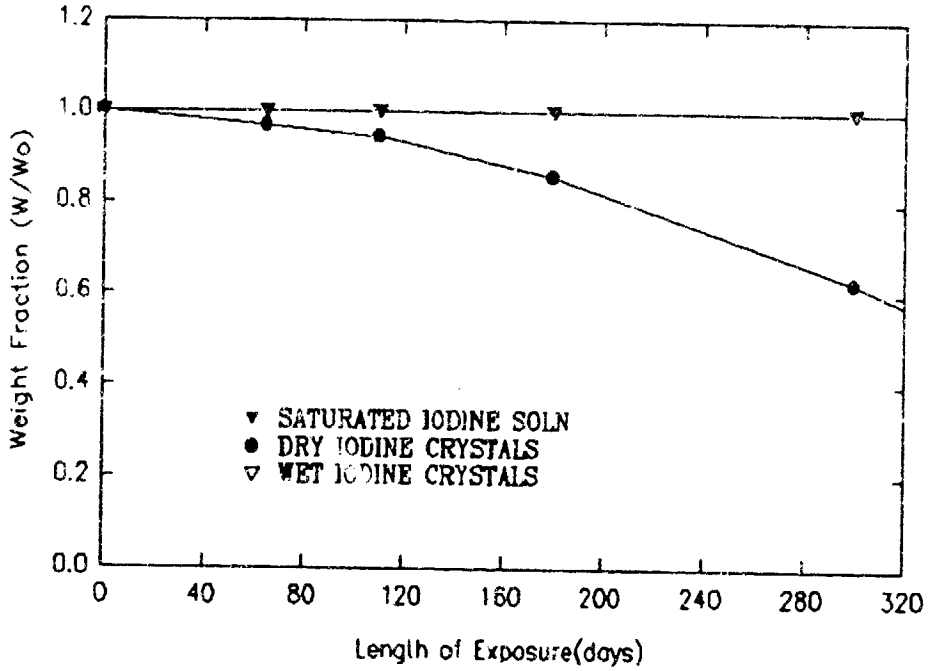

a) 21.1C

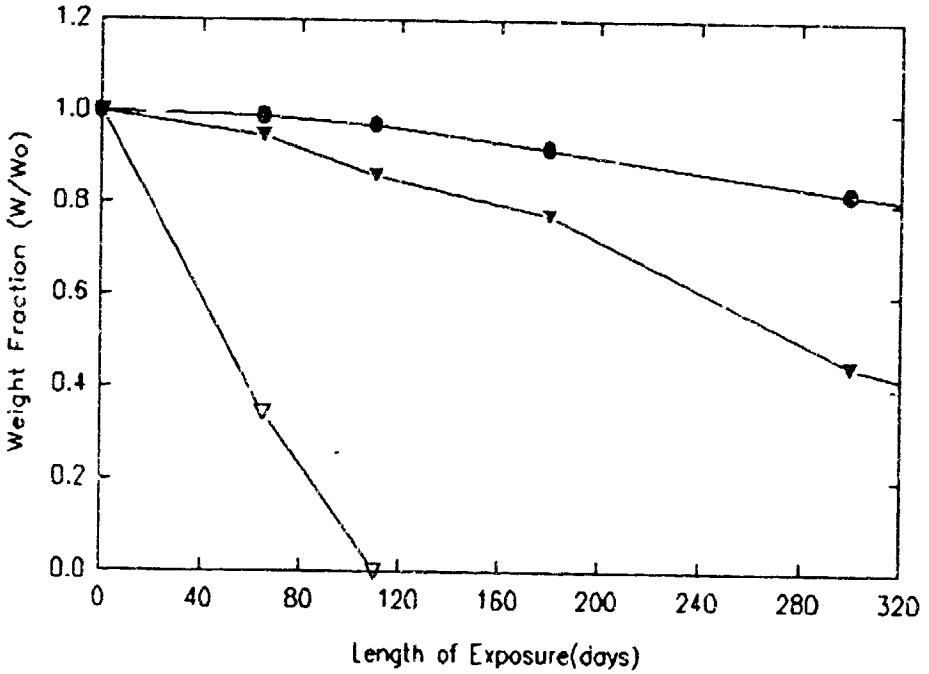

b) 54.4C

Figure 9.4 Iodine Corrosion Tests - 347 Stainless Steel.

TABLE 9.3 Corrosion Tests - 316 L Stainless Steel

T	IODINE STATE	COUPON WEIGHT (GRAMS) INITIAL 12/11/90	2/16/91	4/1/91	6/11/91	10/11/91
21.1C	Dry	2.0109	1.8206	1.6839	1.2819	0.3260
	Wet	2.2125	2.2118	2.2120	2.2123	2.2122
	Sat	2.0846	2.0804	2.0834	2.0841	2.0851
54.4C	Dry	2.0591	1.9905	1.8714	1.1910	-0-
	Wet	2.1570	2.1483	-0-	------	------
	Sat	2.0505	1.1554	1.1409	1.1404	-0-

TABLE 9.4 Corrosion Tests - 347 Stainless Steel

T	IODINE STATE	COUPON WEIGHT (GRAMS) INITIAL 12/11/90	2/16/91	4/1/91	6/11/91	10/11/91
21.1C	Dry	6.0586	5.8645	5.7212	5.1967	3.7964
	Wet	6.1758	6.1706	6.1699	6.1700	6.1701
	Sat	6.0229	6.0230	6.0218	6.0230	6.0237
54.4C	Dry	6.1173	6.0491	5.9380	5.6231	5.0279
	Wet	6.0700	2.0751	-0-	------	------
	Sat	6.2136	5.8865	5.3485	4.7909	2.7688

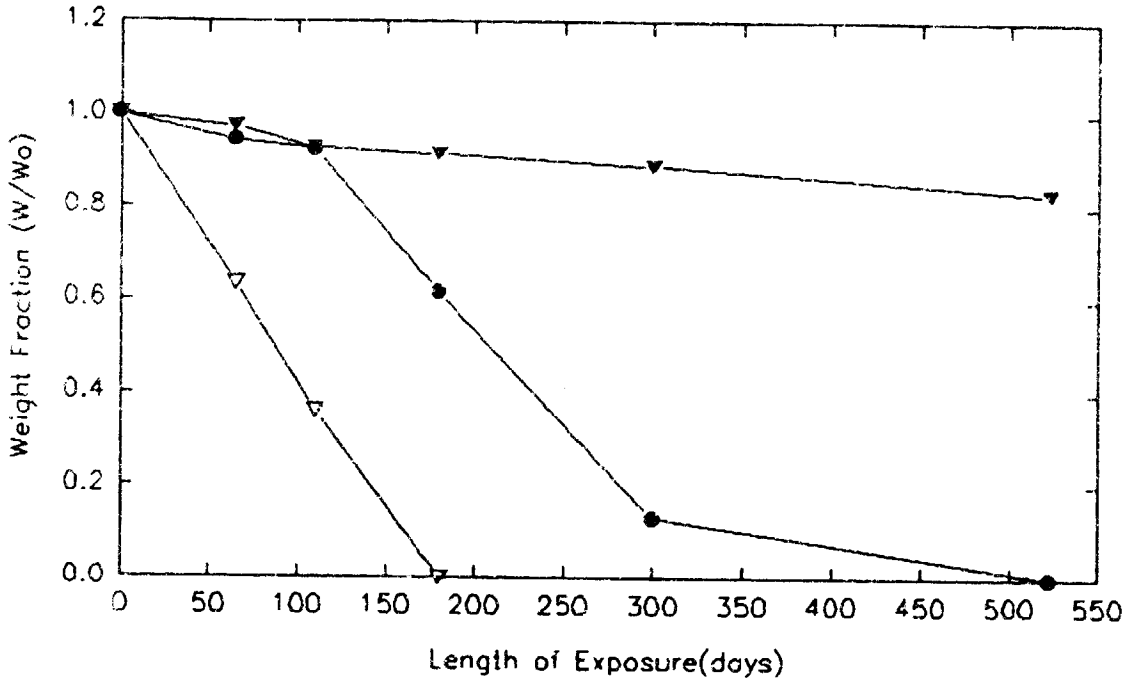

a) 21.1C

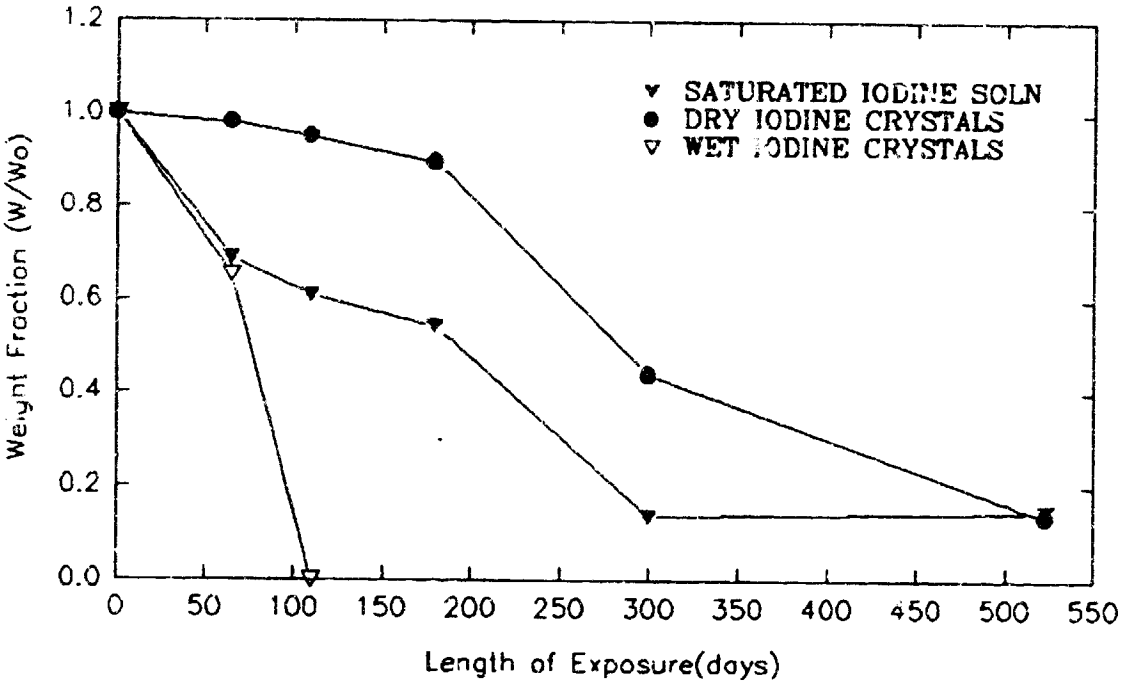

b) 54.4C

Figure 9.5 Iodine Corrosion Tests - 410 Stainless Steel.

TABLE 9.5 Corrosion Tests - 410 Stainless Steel

COUPON WEIGHT (GRAMS)

T	IODINE STATE	INITIAL 12/11/90	2/16/91	4/1/91	6/11/91	10/11/91
21.1C	Dry	7.1330	6.7261	6.5810	4.3777	0.9095
	Wet	7.1802	4.5469	2.5750	-0-	------
	Sat	7.1673	6.9649	6.6328	6.5373	6.3600
54.4C	Dry	7.5111	7.3628	7.1390	6.7195	3.2925
	Wet	7.1806	4.6795	-0-	------	------
	Sat	6.7741	4.6506	4.1200	3.6758	0.9219

TABLE 9.6 Corrosion Tests - Titanium-2

COUPON WEIGHT (GRAMS)

T	IODINE STATE	INITIAL 12/11/90	2/16/91	4/1/91	6/11/91	10/11/91
21.1C	Dry	8.4770	8.4768	8.4777	8.4773	8.4770
	Wet	7.1798	7.1809	7.1812	7.1818	7.1810
	Sat	8.6290	8.6298	8.6287	8.6305	8.6304
54.4C	Dry	7.6365	7.2936	7.2863	7.2834	7.2829
	Wet	9.5639	9.5655	9.5654	9.5647	9.5648
	Sat	7.6824	7.6835	7.6836	7.6837	7.6834

approximately 40 % of the 347 stainless steel coupon material was still intact. As expected, 410 stainless is corroded at a higher rate at elevated temperature.

9.1.2 Exposure to Moist Crystalline I_2 .

At room temperature the response to contact with moist iodine crystals varied between the stainless steels. 304 stainless steel and 410 stainless steels were vigorously attacked under these conditions, each virtually disappearing after 180 days of exposure, while 316, 316L, and 347 stainless steels were not significantly corroded after 300 days.

At 54.4 ^{o}C all stainless steel were vigorously attacked by the wet iodine crystals. After approximately 100 days of exposure, all stainless steel coupons were completely dissolved.

9.1.3 Exposure to Dry Crystalline I_2.

The effects of exposure to dry iodine crystals at room temperature ranged from moderate to severe. After 300 days of exposure approximately 80 %, 65 %, 20 %, 60 %, and 20 % of the coupon material remained for 304, 316, 316L, 347, and 410 stainless steels respectively.

The rates of corrosion of the coupons were accelerated for 304, 316, and 316L stainless steels at 54.4 ^{o}C. Surprisingly, the rates of corrosion for 347, and 410 stainless steels were lower than the rates evident at room temperature.

9.2 Corrosion of Titanium by I_2.

Experimental results for the Titanium-2, Titanium-7, Titanium-9, and Titanium-4901 coupons are illustrated in Figures 9.6, 9.7, 9.8, and 9.9 respectively. The initial and successive coupon weights are summarized in in Tables 9.6, 9.7, 9.8, and 9.9 respectively. Neither exposure to the saturated I_2 solution nor exposure to moist I_2 crystals resulted in any discernable corrosion of any of the titanium coupons under study.

Only exposure to dry crystalline iodine at 130 ^{o}F resulted in corrosive weight losses, which in comparison to the stainless steels were minimal. All of the titanium coupons so

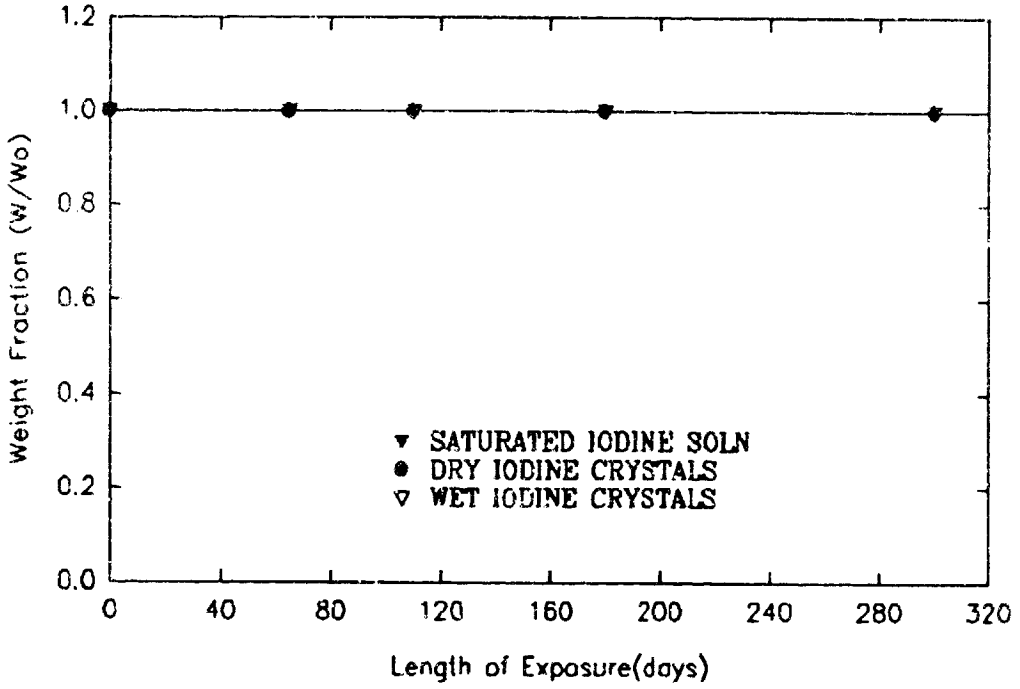

a) 21.1C

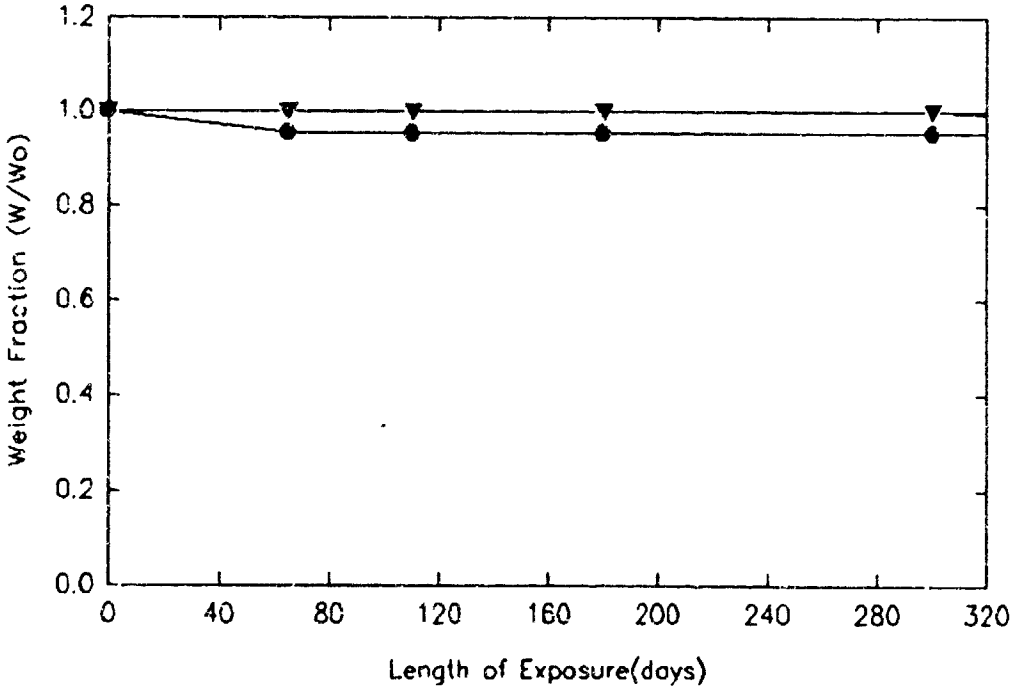

b) 54.4C

Figure 9.6 Iodine Corrosion Tests - Titanium - 2

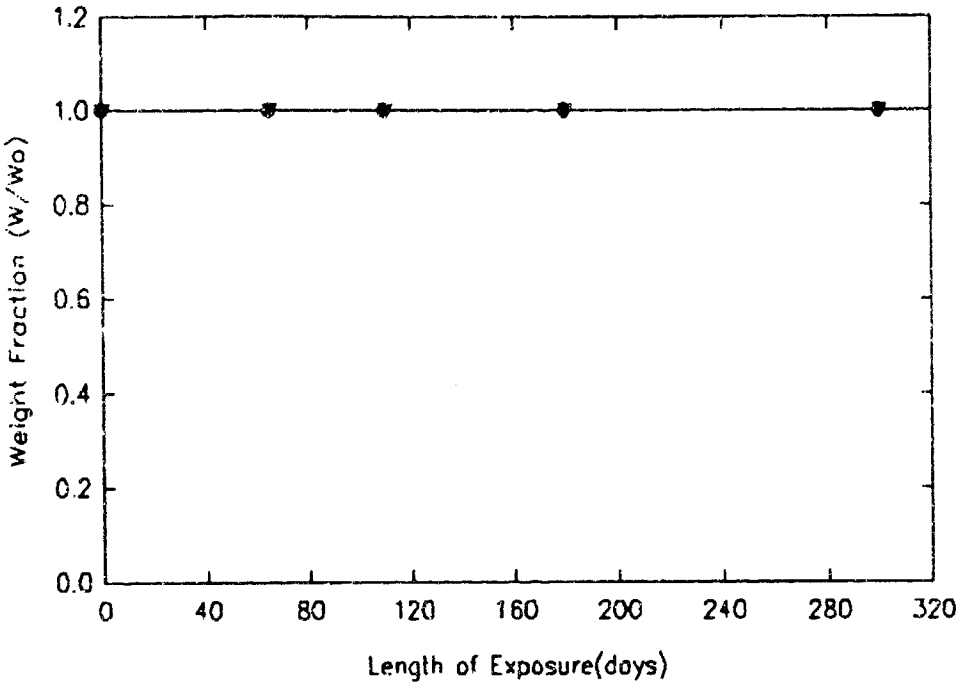

a)21.1C

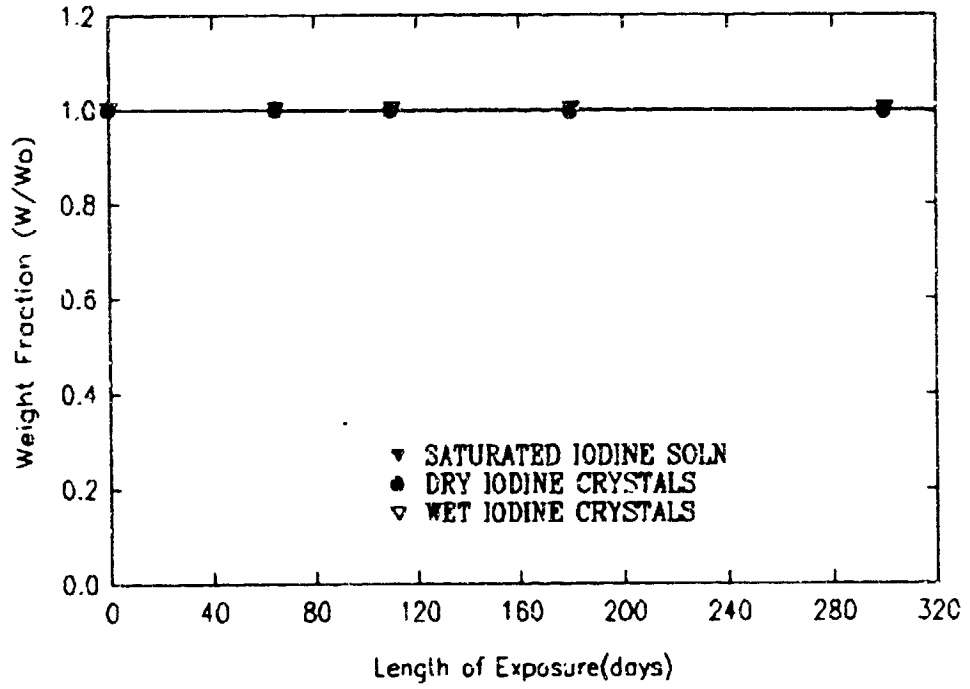

b)54.4C

Figure 9.7 Iodine Corrosion Tests - Titanium - 7

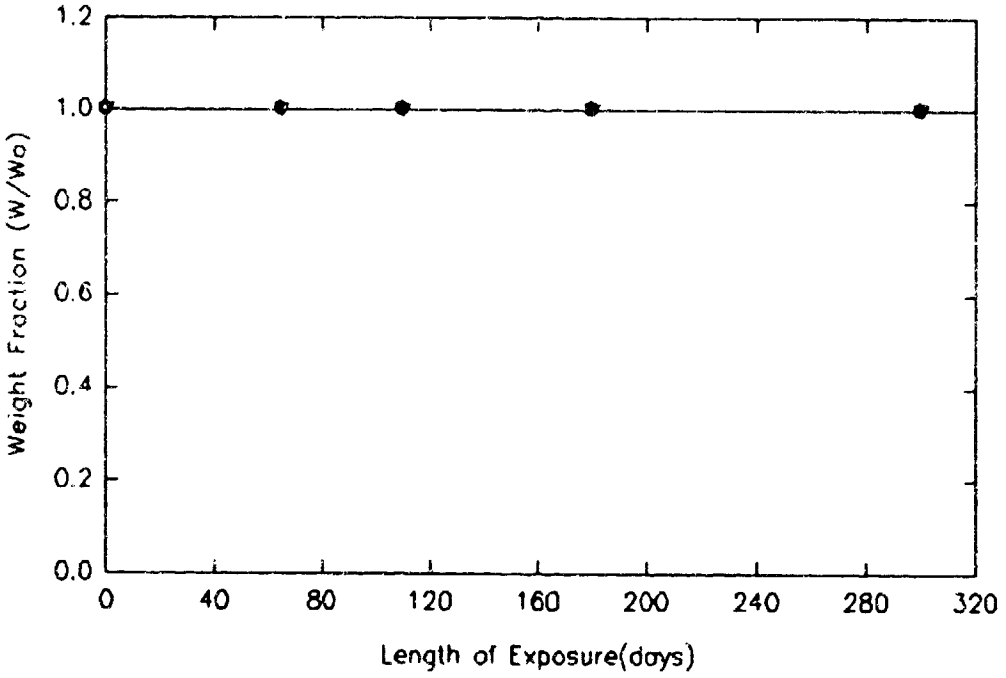

a) 21.1C

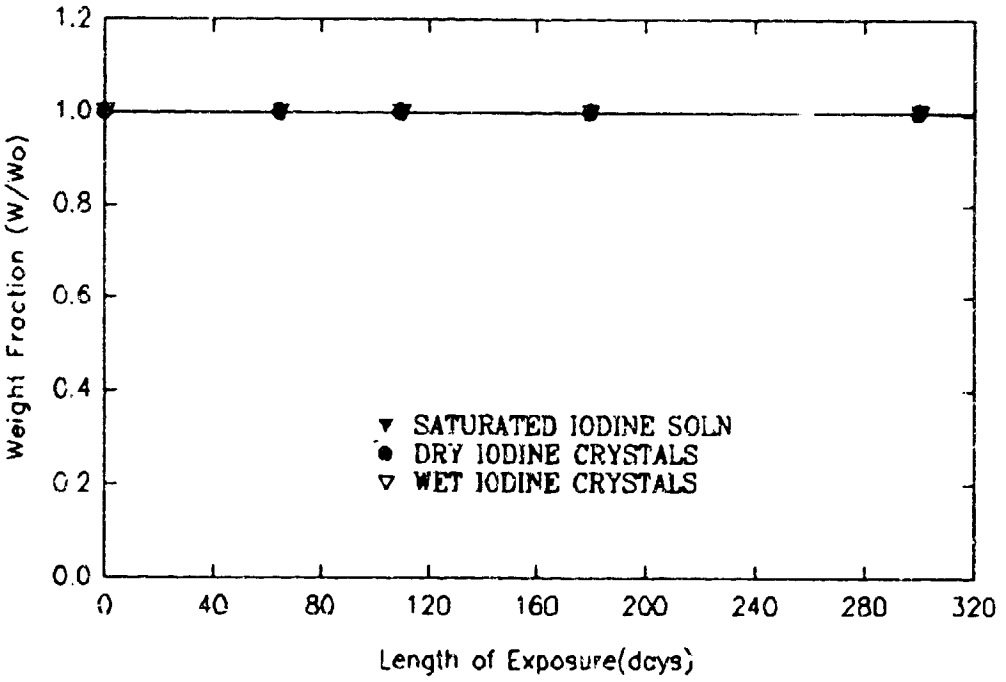

b) 54.4C

Figure 9.8 Iodine Corrosion Tests - Titanium - 9.

TABLE 9.7 Corrosion Tests - Titanium-7

COUPON WEIGHT (GRAMS)

T	IODINE STATE	INITIAL 12/11/90	2/16/91	4/1/91	6/11/91	10/11/91
21.1C	Dry	6.0791	6.0795	6.0805	6.0798	6.0797
	Wet	5.3906	5.3926	5.3918	5.3923	5.3916
	Sat	5.9115	5.9123	5.9115	5.9133	5.9137
54.4C	Dry	5.6360	5.6305	5.6228	5.6202	5.6220
	Wet	5.5917	5.5938	5.5940	5.5931	5.5937
	Sat	5.8606	5.8623	5.8624	5.8625	5.8634

TABLE 9.8 Corrosion Tests - Titanium-9

COUPON WEIGHT (GRAMS)

T	IODINE STATE	INITIAL 12/11/90	2/16/91	4/1/91	6/11/91	10/11/91
21.1C	Dry	5.6415	5.6415	5.6424	5.6417	5.6422
	Wet	7.0713	7.0730	7.0722	7.0728	7.0723
	Sat	6.0859	6.0868	6.0855	6.0874	6.0873
54.4C	Dry	6.1810	6.1738	6.1725	6.1725	6.1729
	Wet	5.5805	5.5827	5.5788	5.5778	5.5783
	Sat	6.5409	6.5438	6.5425	6.5424	6.5431

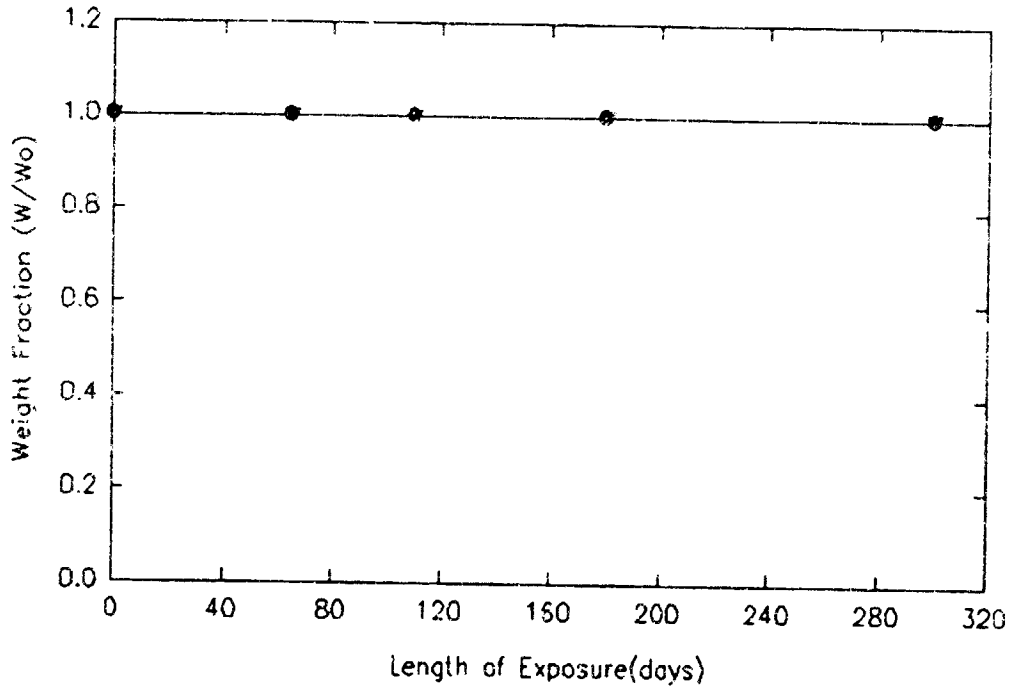

a) 21.1C

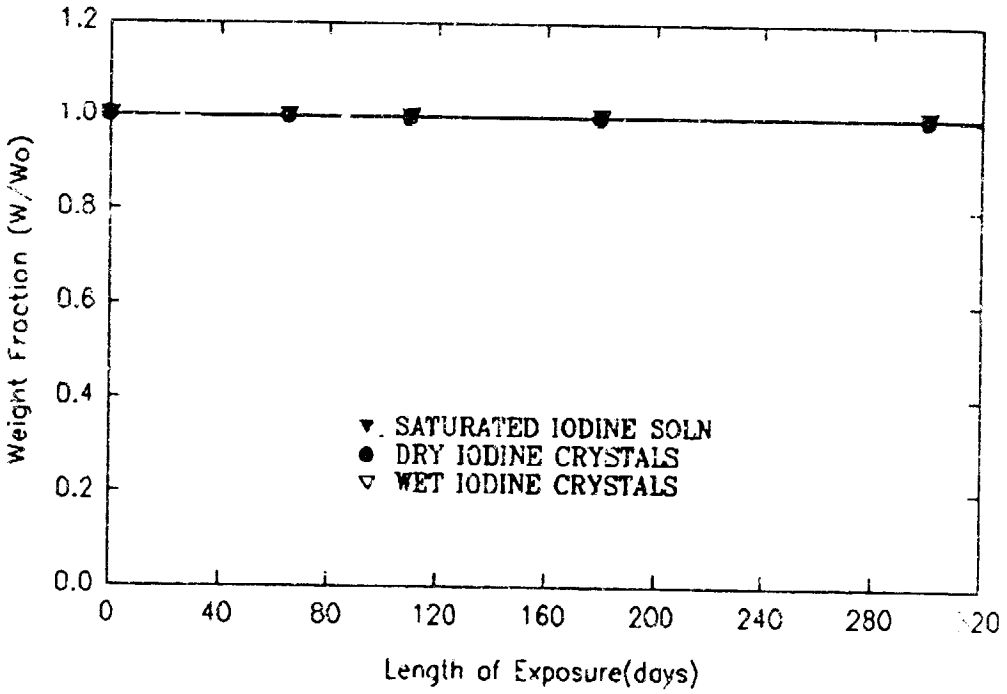

b) 54.4C

Figure 9.9 Iodine Corrosion Tests - Titanium - 4901.

TABLE 9.9 Corrosion Tests - Titanium-4901

T	IODINE STATE	COUPON WEIGHT (GRAMS) INITIAL 12/11/90	2/16/91	4/1/91	6/11/91	10/11/91
21.1C	Dry	3.9930	3.9932	3.9943	3.9948	3.9949
	Wet	4.2803	4.2820	4.2819	4.2826	4.2821
	Sat	4.1648	4.1662	4.1646	4.1670	4.1674
54.4C	Dry	4.1606	4.1479	4.1431	4.1420	4.1422
	Wet	4.0679	4.0680	4.0683	4.0665	4.0679
	Sat	4.5435	4.5458	4.5455	4.5454	4.5455

TABLE 9.10 Corrosion Tests - HASTELOY C

T	IODINE STATE	COUPON WEIGHT (GRAMS) INITIAL 05/92	9/19/92			
21.1C	Dry	23.383	23.158			
	Wet	24.336	24.336			
	Sat	24.551	24.551			
54.4C	Dry	23.571	23.571			
	Wet	21.699	21.698			
	Dry	24.775	24.774			

exposed were heavily stained. The Titanium-2 specimen was the most severely corroded, showing an approximate 350 mg weight loss from an intial weight of 7.64 g. This coupon also showed some evidence of physical damage in the form of moderate pitting.

9.3 Corrosion of Hasteloy C and Hasteloy G by I_2.

Both of these alloys were added to the materials compatibility test program after tests of the original twelve materials had begun. For this reason, the time-span of their exposures to I_2 is shorter. Experimental results for the Hasteloy C and Hasteloy G coupons are illustrated in Figures 9.10 and 9.11 respectively. The initial and successive coupon weights are summarized in Tables 9.10, and 9.11 respectively.

9.3.1 Corrosion of Hasteloy C.

Hasteloy C was the last alloy incoporated into the material compatibility study. It was subjected to approximately 120 days of I_2 exposure. In this time, none of the corrosive states at either ambient or elevated temperture resulted in any significant weight loss or visual signs of degradation.

9.3.2 Corrosion of Hasteloy G.

The test coupons were subjected to approximately one year of I_2 exposure. At room temperature, Hasteloy G was not significantly corroded by either wet I_2 crystals or the saturated aqueous I_2 solution. However, exposure to dry crystalline I_2 at room temperature resulted in an overall 10 % weight loss for the test coupon.

The experiments conducted at 54.4 ^{0}C resulted in very slight corrosion of the coupons exposed to either the saturated aqueous I_2 solution or dry I_2 crystals. The fractional weight loss for the coupon exposed to dry crystals was slightly greater than that for the coupon exposed to the saturated solution. At elevated temperature, the wet crystal exposure state resulted in complete dissolution of the coupon after approximately 250 days. These

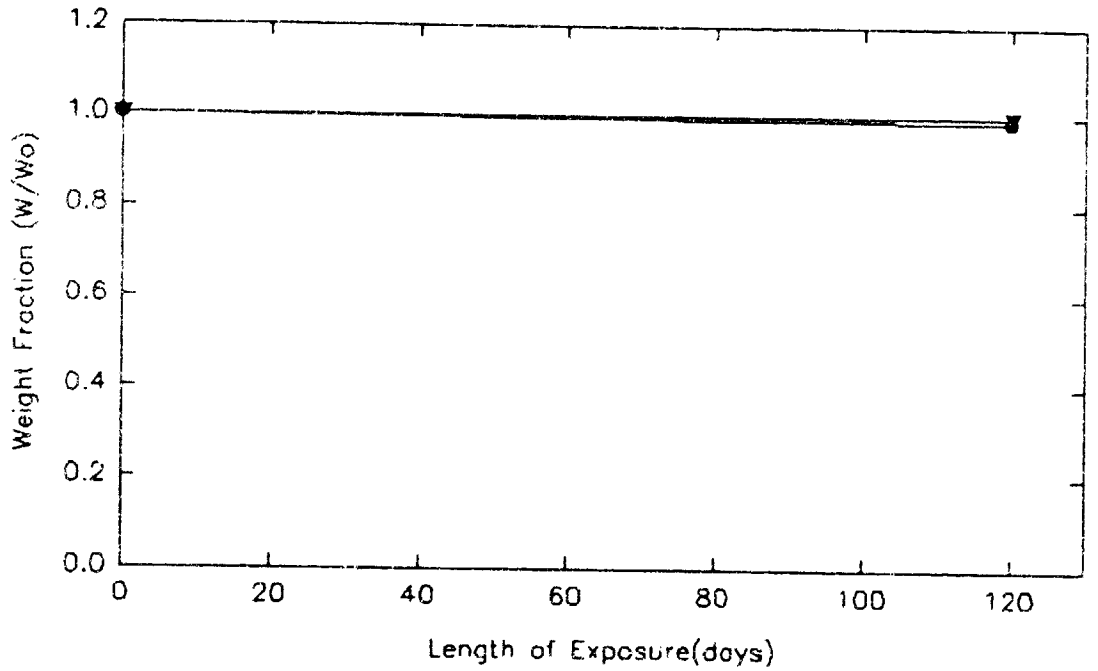

a) 21.1C

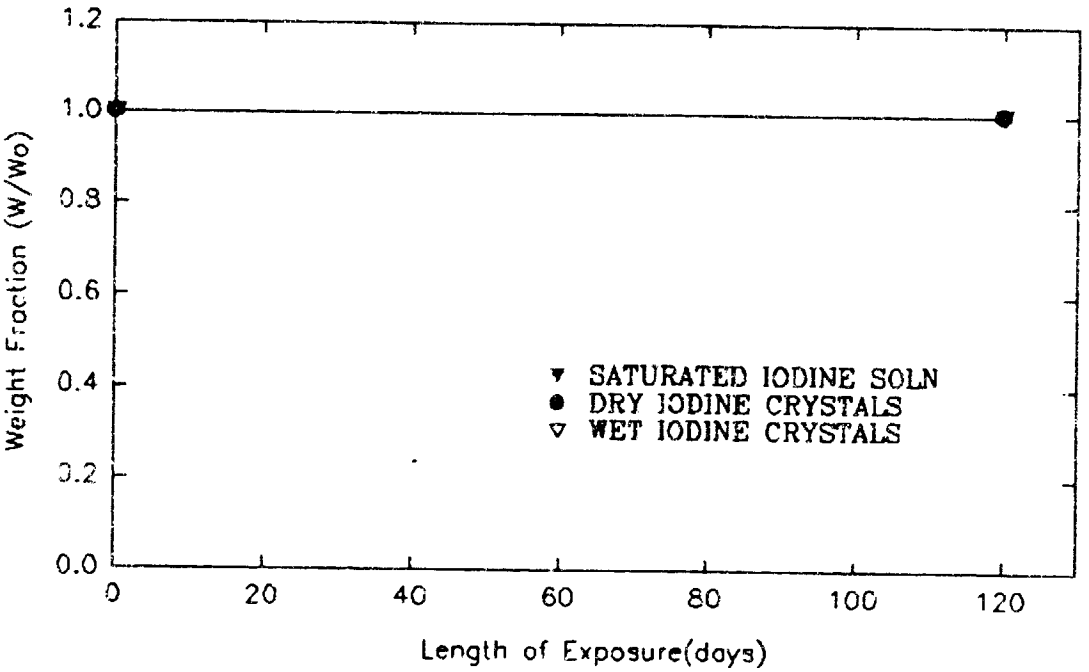

b) 54.4C

Figure 9.10 Iodine Corrosion Tests - Hasteloy C

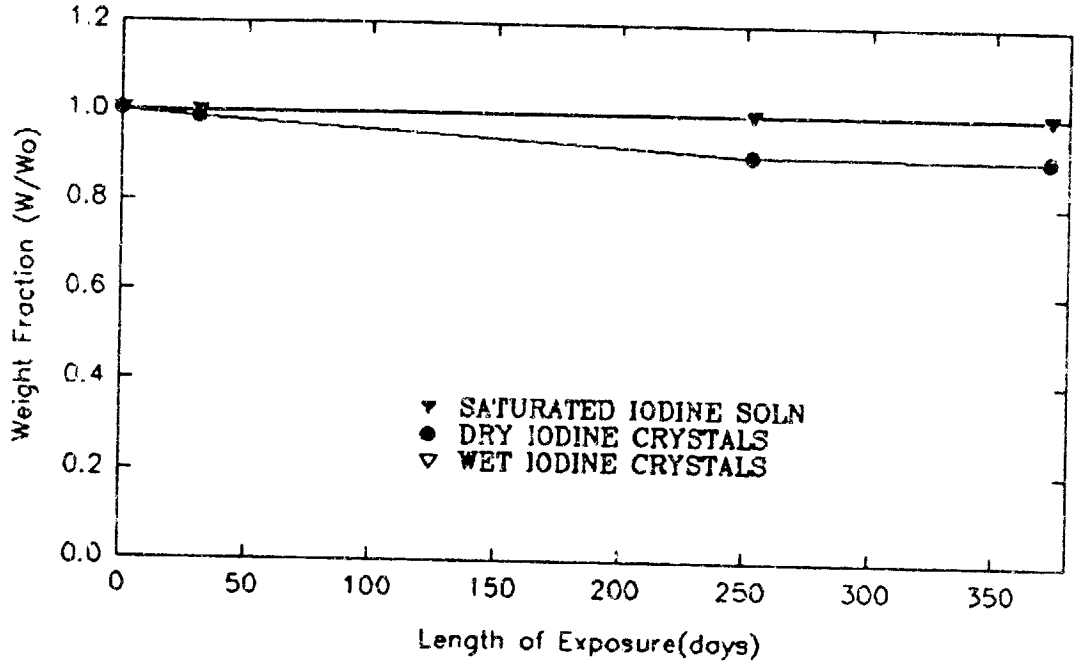

a) 21.1C

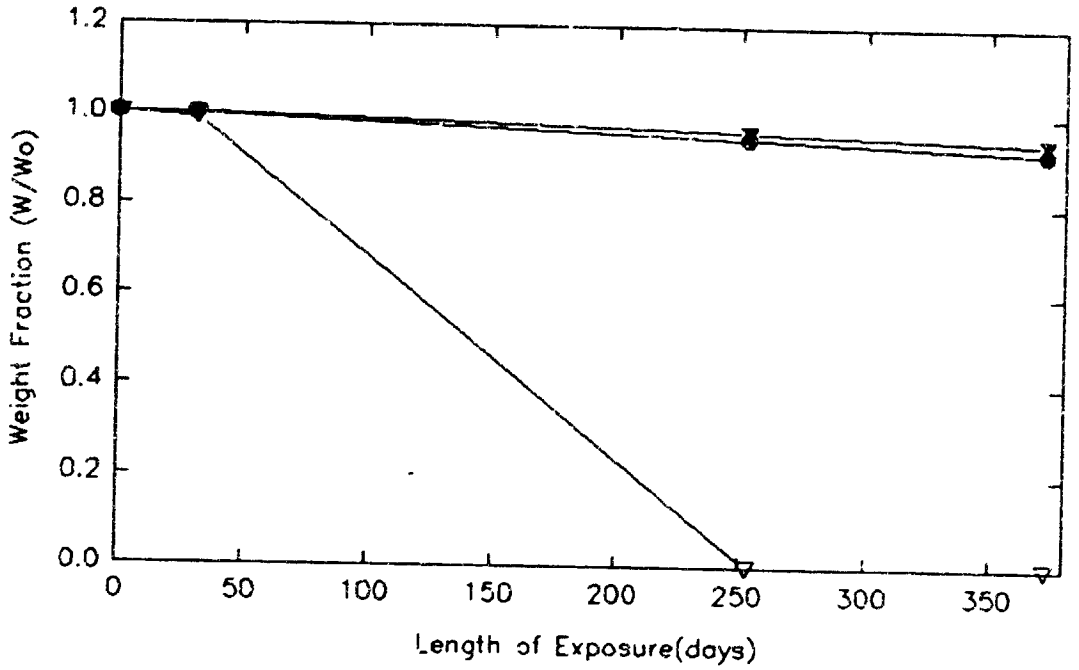

b) 54.4C

Figure 9.11 Iodine Corrosion Tests - Hasteloy G

TABLE 9.11 Corrosion Tests - HASTELOY G

COUPON WEIGHT (GRAMS)

T	IODINE STATE	INITIAL 9/10/91	10/11/91	5/23/92	9/19/92	
21.1C	Dry	3.5017	3.4451	3.1722	3.1617	
	Wet	3.1434	3.1379	3.1372	3.1379	
	Sat	3.4032	3.4015	3.4024	3.4025	
54.4 C	Dry	3.6120	3.6012	3.3405	3.3298	
	Wet	3.2260	3.2009	0	0	
	Dry	3.5503	3.5505	3.4269	3.3453	

TABLE 9.12 Corrosion Tests - TEFLON

COUPON WEIGHT (GRAMS)

T	IODINE STATE	INITIAL 12/11/90	2/16/91	4/1/91	6/11/91	10/11/91
21.1 C	Dry	3.0688	3.0689	3.0702	3.0701	3.0702
	Wet	3.0013	3.0028	3.0026	3.0030	3.0022
	Sat	3.0127	3.0137	3.0122	3.0150	3.0143
54.4 C	Dry	3.2170	3.2195	3.2185	3.2192	3.2190
	Wet	3.0523	3.0536	3.0543	3.0530	3.0531
	Sat	2.9886	2.9898	2.9906	2.9900	2.9893

experiments indicate that the extent of the corrosion resulting from exposure to dry I_2 crystals is less at elevated temperature than at room temperature. The reason for this seemingly anomalous behaviour is not known. Light staining was observed for each coupon exhibiting weight loss.

9.4 Compatibility of Organic Materials with I_2.

Experimental results for the Teflon, polypropylene, Viton A, and Teflon coated 302 stainless steel coupons are illustrated in Figures 9.12, 9.13, 9.14, and 9.15 respectively. The initial and successive coupon weights are summarized in Tables 9.12, 9.13, 9.14, and 9.15 respectively.

Of the organic materials studied, Teflon was the least affected by contact with iodine. All of the Teflon coupons registered very small weight (W) gains, with $\Delta Ws \approx 0.05$ % for 300 days of exposure. This is most probably due to the combined effects of diffusion and adsorption. Each of the Teflon coupons exhibited a light purple stain.

Polypropylene coupons exhibited significantly higher weight increases with $\Delta Ws \approx 0.8$ % at room temperature, and with ΔWs ranging between 3 % and 8 % at 54.4 ^{o}C. Marked discoloration of the polypropylene coupons was observed, the severity being greater for the elevated temperature iodine exposure states. In all cases, the originally semi-translucent polypropylene coupons became dark brown and opaque. These effects are attributable to diffusion, adsorption, and chemical reaction.

The Viton A coupons exhibited weight gains substantially greater than those of Teflon and less than those of polypropylene. An intermediate level of discoloration was also evident. Anomalously high weight gains were observed for the wet I_2 crystals and the saturated I_2 solution at 54.4 ^{o}C after approximately 100 days of exposure. This is believed due to incomplete cleaning of the coupon surface prior to drying and weighing.

The Teflon coated 302 stainless steel springs were added to the materials compatibility

program after testing of the original twelve materials had been initiated. Under all conditions of iodine exposure, Teflon coated 302 stainless steel initially exhibited strong resistance to the adverse effects of I_2. Later in the experiment however, all forms of I_2 exposure, with the exception of the saturated I_2 solution at ambient temperature, resulted in rapid degradation, until complete destruction of the springs were observed after approximately 350 days of exposure. Microscopic examination revealed small point defects in the Teflon coating, through which I_2 was able to directly attack the stainless steel. The spring exposed to saturated aqueous I_2 at room temperture exhibited no deleterious effects.

9.5 Analysis of Saturated I_2 Solutions for Dissolved Metals.

Samples of the liquid remai ing in the saturated I_2 solutions for the metallic coupons were collected after 110 days of exposure, where possible. These were analyzed by atomic absorption spectrophotometry for Fe, Ni, Cr, and Ti. Insufficient liquid volume was obtained for analysis of the saturated iodine solutions initially bathing the 316 and 410 stainless steel coupons at 54.4 ^{o}C. Due to the variable effects of evaporation, and plating of once dissolved metals on the container sufrace, the results of analysis were not considered either representative or useful. The practice was discontinued.

9.6 Conclusions.

The materials of choice for use in the fabrication of prototype RMCV components to be exposed to prolonged periods of high aqueous elemental iodine concentrations, particularly at elevated temperature, or which are to be exposed directly to dry iodine crystals, are Teflon and titanium grades 7, 9, and 4901. Grade 2 titanium is suitable for exposure to high concentrations of aqueous I_2, but not to dry crystals. For components which are only to be subjected to less corrosive states, or to transient episodes of higher corrosivity, Teflon coated stainless steel, one of the Hasteloys, or stainless steels should prove adequate.

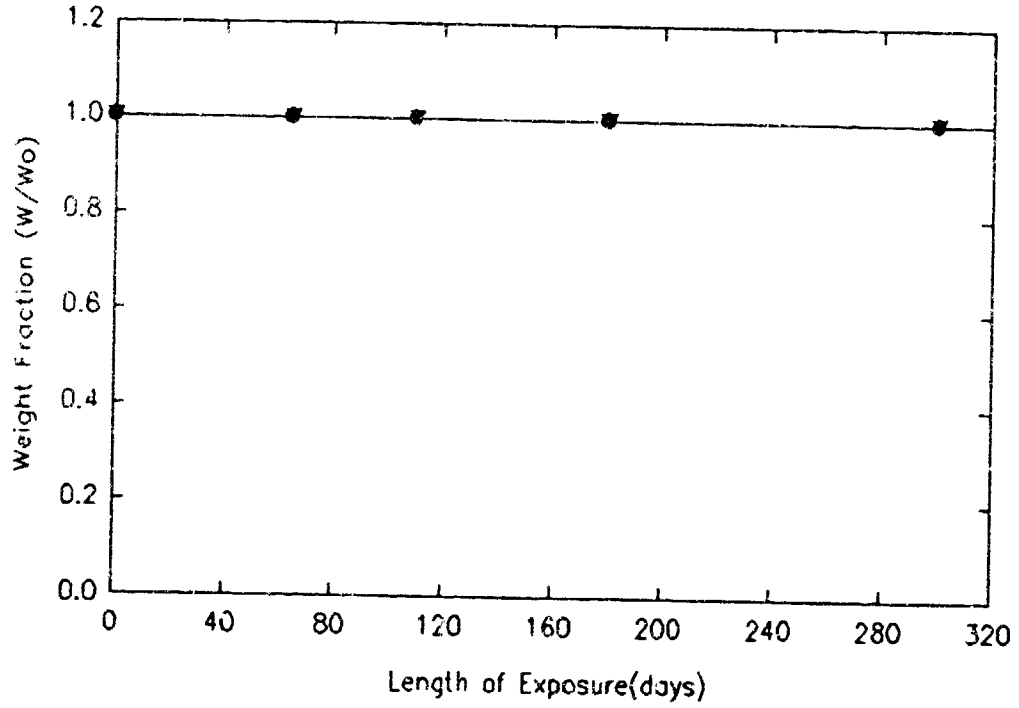

a) 21.1 C

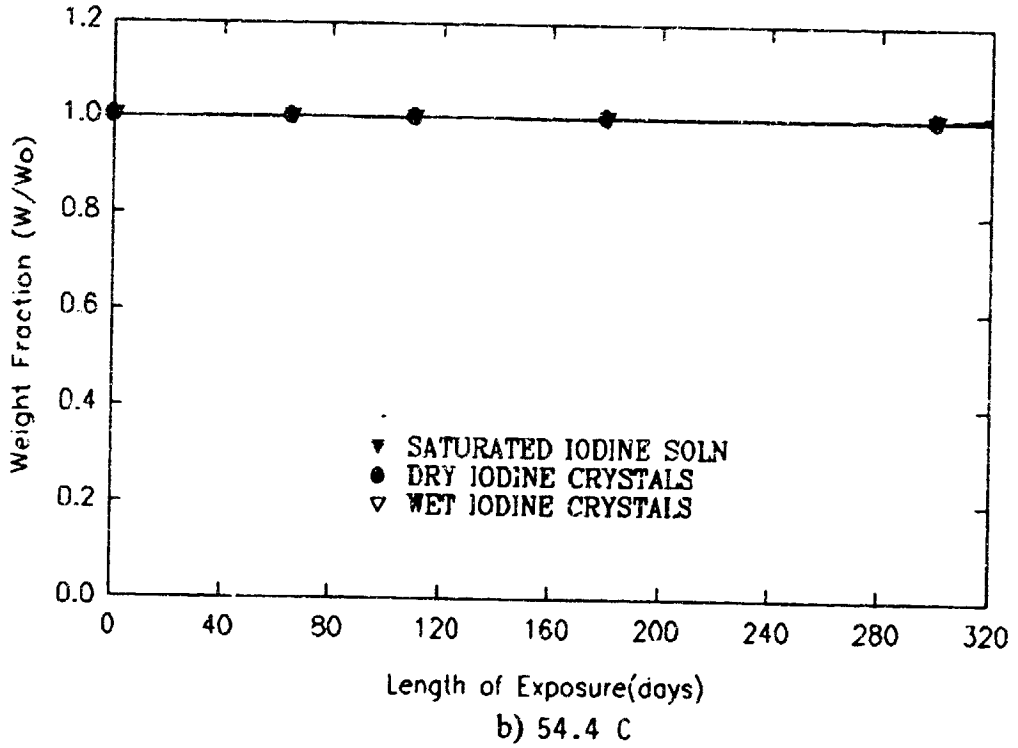

b) 54.4 C

Figure 9.12 Iodine Corrosion Tests - Teflon .

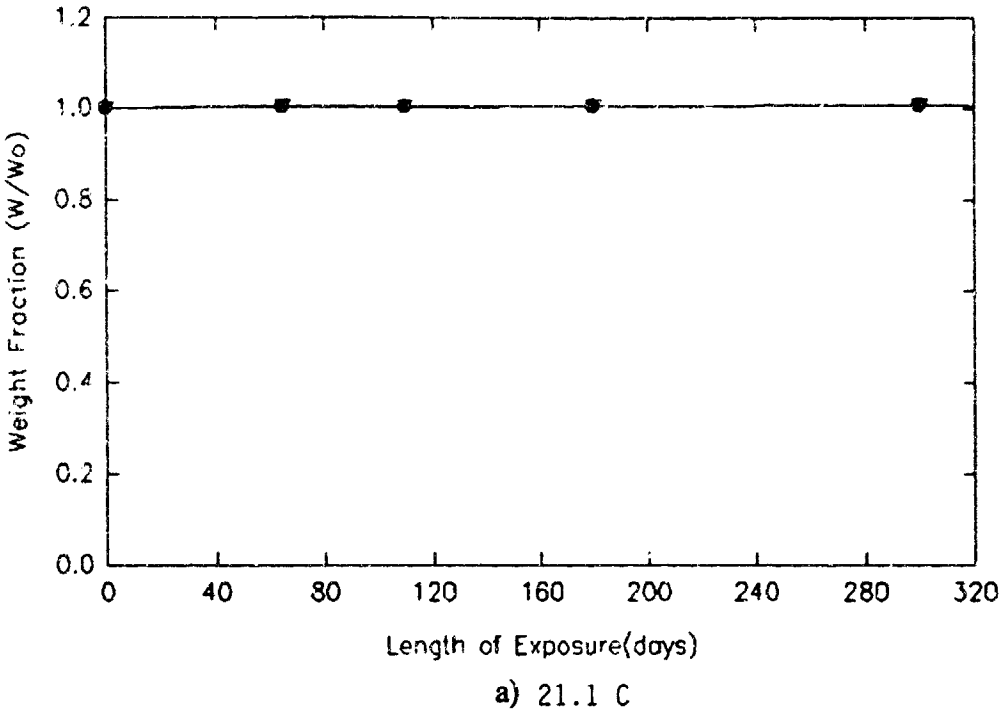

a) 21.1 C

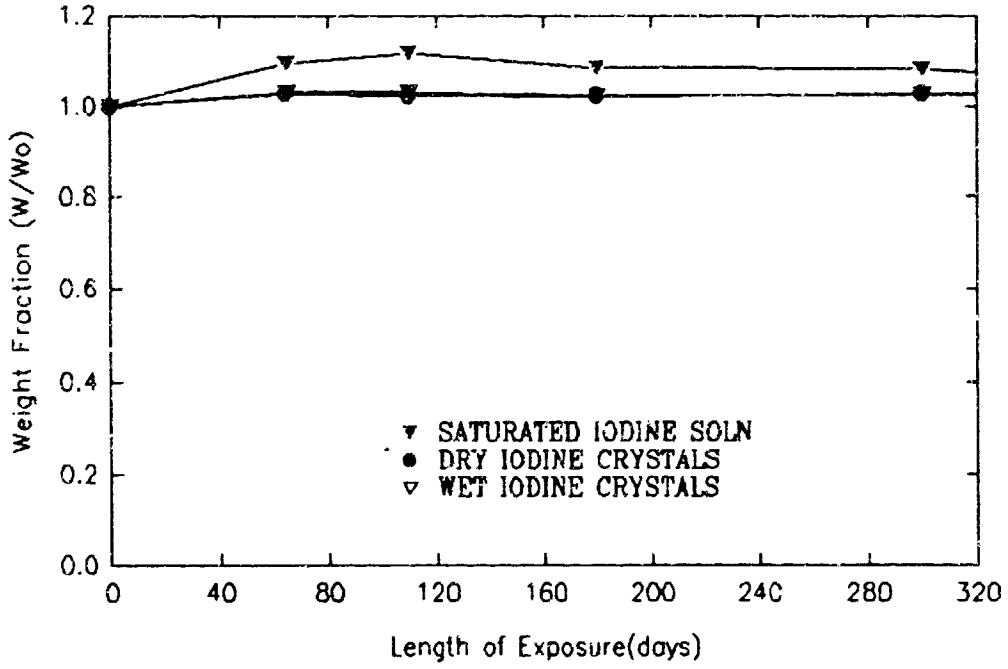

b) 54.4 C

Figure 9.13 Iodine Corrosion Tests - Polypropylene.

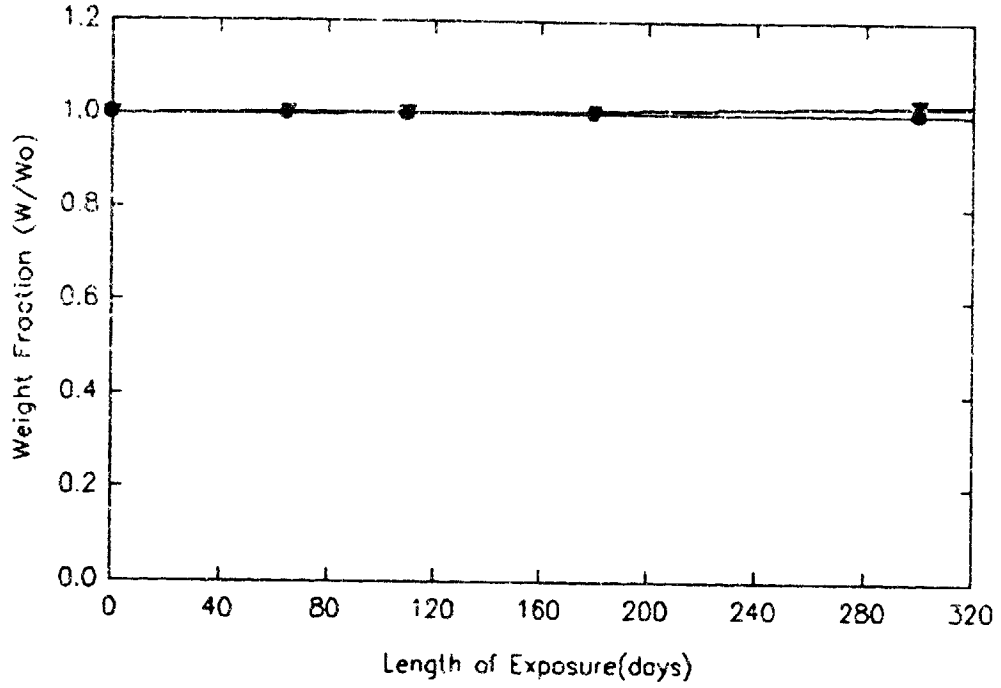

a) 21.1 C

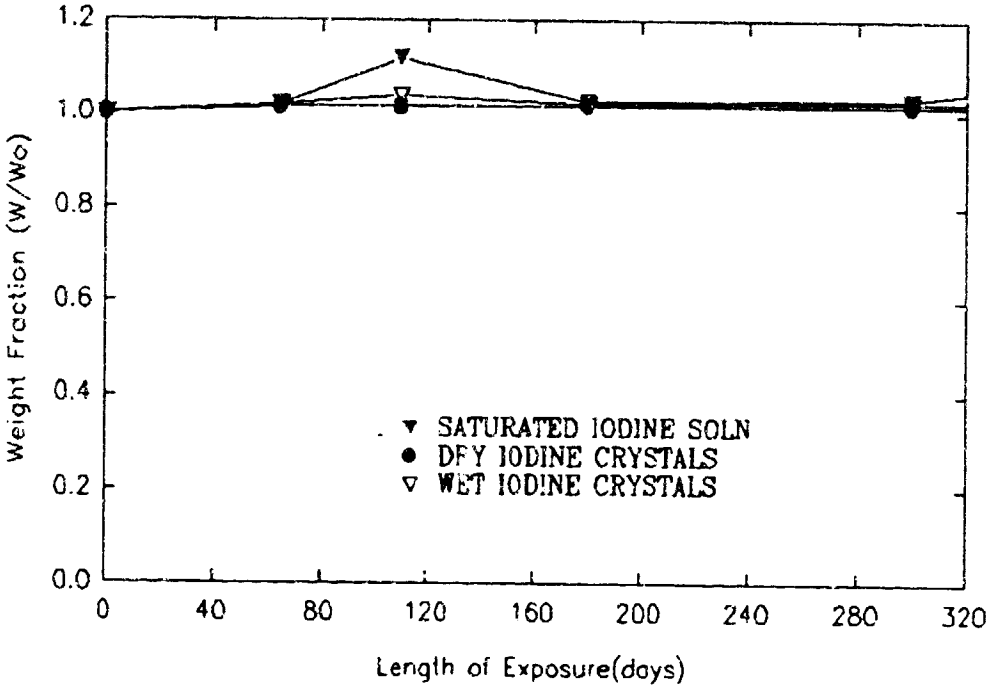

b) 54.4 C

Figure 9.14 Iodine Corrosion Tests - Viton A.

TABLE 9.13 Corrosion Tests - POLYPROPYLENE

COUPON WEIGHT (GRAMS)

T	IODINE STATE	INITIAL 12/11/90	2/16/91	4/1/91	6/11/91	10/11/91
21.1 C	Dry	1.4698	1.4731	1.4740	1.4762	1.4812
	Wet	1.5441	1.5511	1.5501	1.5537	1.5580
	Sat	1.4988	1.5025	1.5010	1.5074	1.5095
54.4 C	Dry	1.5925	1.6357	1.6293	1.6286	1.6357
	Wet	1.5814	1.6314	1.6306	1.6180	1.6212
	Sat	1.6205	1.7739	1.8115	1.7567	1.7535

TABLE 9.14 Corrosion Tests - Viton A

COUPON WEIGHT (GRAMS)

T	IODINE STATE	INITIAL 12/11/90	2/16/91	4/1/91	6/11/91	10/11/91
21.1 C	Dry	0.8465	0.8470	0.8475	0.8480	0.8490
	Wet	1.2479	1.2540	1.2531	1.2588	1.2762
	Sat	1.3428	1.3465	1.3466	1.3537	1.3690
54.4 C	Dry	0.8476	0.8600	0.8603	0.8618	0.8617
	Wet	1.3378	1.3650	1.3900	1.3663	1.3684
	Sat	0.7173	0.7313	0.8024	0.7358	0.7377

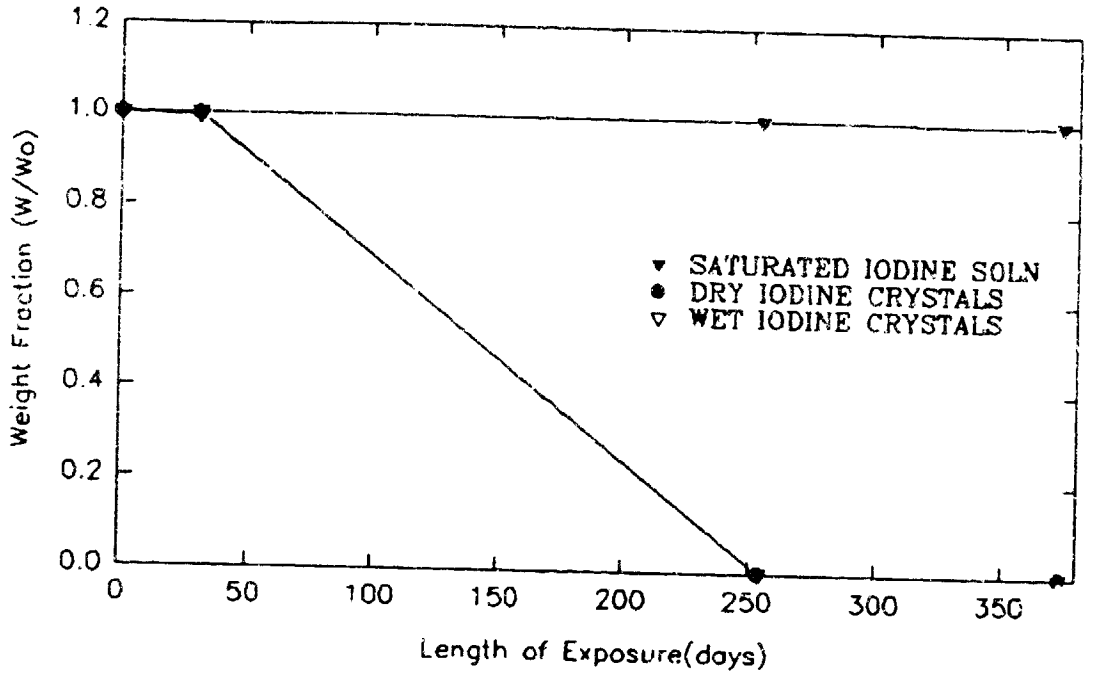

a) 21.1 C

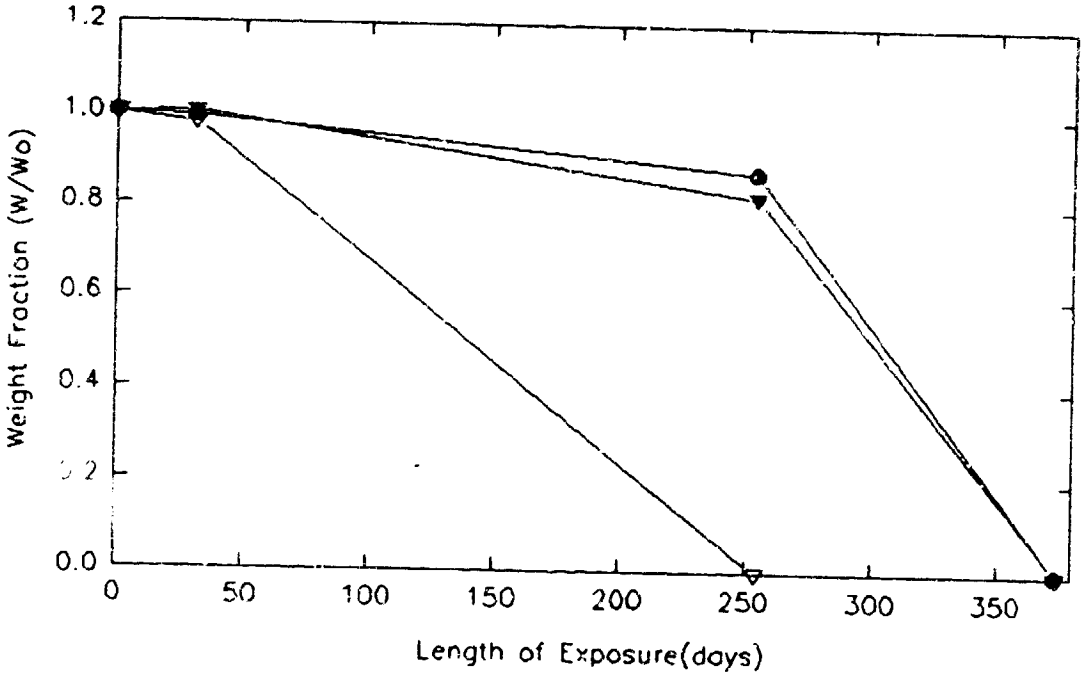

b) 54.4 C

Figure 9.15 Iodine Corrosion Tests - Teflon coated 302 SS Spring.

TABLE 9.15 Corrosion Tests - TEFLON Coated Stainless Steel Springs

COUPON WEIGHT (GRAMS)

T	IODINE STATE	INITIAL 9/10/91	10/11/91	5/22/92	9/19/92	
21.1 C	Dry	21.5739	21.5339	0	0	
	Wet	21.1225	21.0070	0	0	
	Sat	21.4191	21.4240	21.421	21.403	
54.4 C	Dry	21.6119	21.4291	18.872	0	
	Wet	21.7773	21.3144	0	0	
	Sat	23.1999	23.2405	19.033	0	

10

PROTOTYPE REGENERATIVE MICROBIAL CHECK VALVE DEVELOPMENT

10.0 Overview.

For the purpose of completely demonstrating the utility of the regenerative microbial check valve concept, a full scale autonomous prototype has been designed, fabricated, tested and delivered to NASA - Johnson Space Center. Successful development of the prototype RMCV was the culmination of the Phase II increment of the regenerative biocide delivery unit investigation.

Prototype RMCV development drew heavily upon the information gained from both the long term life cycle testing and parametric testing phases of the program. In large measure the parametric tests were specifically tailored to provide performance data to be used in scaling up the RMCV process from small column scale to the Space Station *Freedom* design flow rate of 120 cm^3/min.. DI water, representing reclaimed potable water from a closed loop regenerative water processor, was selected as the challenge stream for prototype testing. Acceptable materials of construction for the prototype RMCV were identified via the materials iodine-compatibility tests outlined in Section 9.

10.1 Prototype RMCV Design.

The envelope of operation specified for the prototype RMCV was to maintain residual biocide levels in the range of 2.0 - 4.0 mg/L I_2 for a room temperature DI water challenge stream flowing at a nearly constant flow rate of 120 cm^3/min. The prototype was required to have a minimum six month life. It was also considered desirable for the prototype to undergo a minimum of six regenerations during the six month period alioted to prototype performance evaluation. The prototype RMCV was required to operate in the super-iodination mode on a demand basis.

10.1.1 MCV and Solid I_2 Bed Sizing.

The information required for determination of the proper bed sizes for both the MCV iodinated resin bed and the solid state I_2 crystal regeneration bed were determined through

the parametric testing program presented in Section 6. The primary sizing considerations were to: minimize transient I_2 concentrations in excess of 4.0 mg/L during regeneration by selecting a suitable residence time of the challenge solution in the MCV; to maximize aqueous I_2 concentration in the regeneration crystal bed effluent by selection of a suitable residence time of the challenge solution in the I_2 crystal bed; and to maintain a length to diameter (L/D) ratio greater than 2.0 in both beds to assure uniform flow characteristics and to prevent flow channeling through the beds.

Figure 10.1 presents the relationship between effluent I_2 concentration and MCV residence time during regeneration. The minimum MCV residence time required to prevent the effluent I_2 concentration from exceeding 4.0 mg/L during regeneration is approximately 0.45 minutes. The relationship between aqueous I_2 concentration in the regeneration liquor versus crystal bed residence time is illustrated in Figure 10.2 The minimum crystal bed residence time required to provide a 240 mg/L effluent I_2 concentration at room temperature is approximately 1 minute. The linear relationships between flow rate and bed size required to achieve these two residence times are shown in Figure 10.3. The prototype design flow rate of 120 cm^3/min corresponds to minimum bed volumes of 54 cm^3 and 120 cm^3 for the MCV bed and the I_2 crystal bed respectively.

The maximum bed volumes were determined by more pragmatic limitations. The prototype MCV bed size was required to be small enough to undergo a minimum of six cycles of washout and regeneration within the six month prototype evaluation period. The solid state I_2 crystal bed volume was required to be small enough to be housed in a compact RMCV prototype frame, yet having sufficient volume to cycle through a minimum of six regenerations.

At the prototype design flow rate of 120 cm^3/min, for a selected bed diameter of 3.81 cm (1.5") I.D., the minimum bed lengths as determined by residence time requirements are 4.83 cm (1.9") and 10.4 cm (4.1") for the MCV and I_2 crystal bed respectively. In this

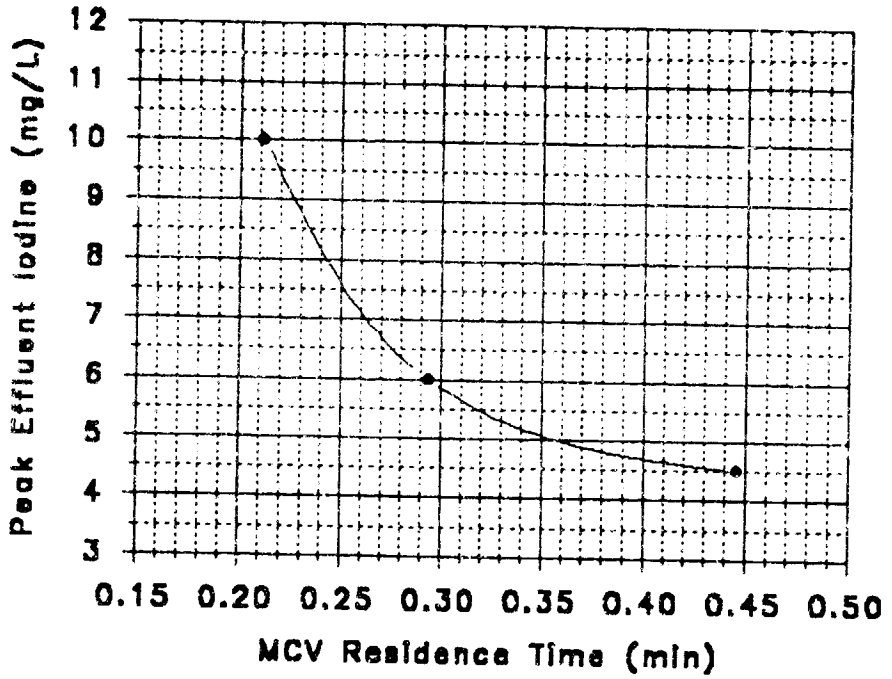

Figure 10.1 Effluent I_2 versus MCV Residence Time During Regeneration.

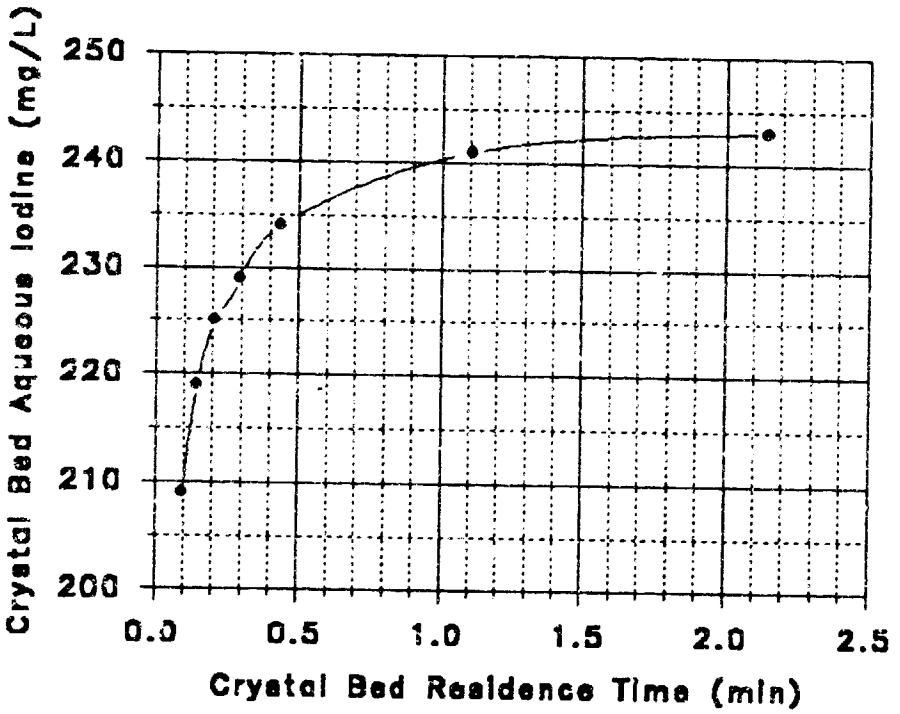

Figure 10.2 Regeneration Liquor I_2 versus Crystal Bed Residence Time.

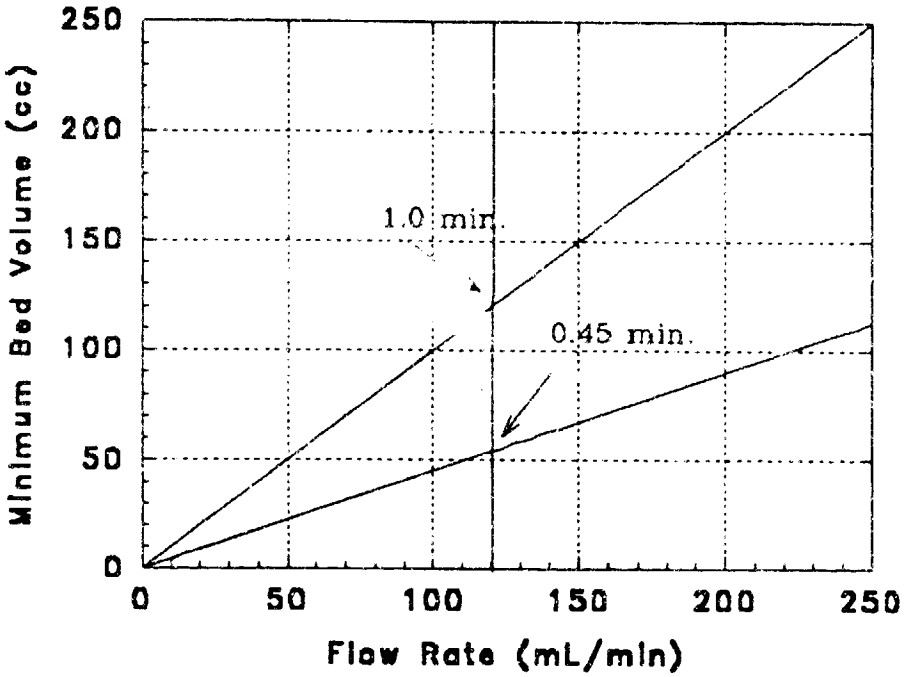

Figure 10.3 Bed Volume versus Flow Rate for Minimal Residence Times.

configuration, however, the MCV falls short of the minimum L/D ratio of 2. To meet this requirement a minimum bed length of 7.62 cm (3.0") is needed. Based upon these considerations, a 100 cm^3 MCV similar to those in use on Shuttle Orbiter missions was selected for the prototype. This MCV has a residence time of 0.833 minutes, nearly twice the minimum required, and satisfies the L/D requirement.

A typical washout capacity for freshly prepared iodinated MCV resin is 20 L/cm^3. At prototype design flow rates, this corresponds to 2,000 Liters per washout for the selected MCV, and to 15.5 RMCV cycles of washout and regeneration for the six month test period. This approximate calculation indicated that the selected MCV would undergo a sufficient number of regenerations for evaluation of the RMCV prototype and its control system.

For the I_2 crystal bed, because its contents are being depleted with time, the minimum residence time requirement dictates the length of the bed at the end of its useful life. In the

case of a 3.81 cm (1.5") I.D. bed, when the compressed crystal bed depth reaches 10.41 cm (4.1") , the residence time has decreased to the minimum. At its initial state, the bed length must be increased by an amount corresponding to the total I_2 depletion expected for the duration of its useful life.

As an estimate of the iodine mass lost to the effluent stream during a six month period, an average concentration of 3.0 mg/L in the MCV effluent over this time period was assumed. This overestimate provided a considerable margin of safety. The particle size distribution for the I_2 crystals and the known packing densities for each particle size allowed an estimate of an average packing density of 2.7 g/cm^3 for the bulk iodine crystals. Using these assumptions an estimate of the iodine volume used in a six month period was made,

$$\frac{3\ \frac{mg}{L} \quad 31{,}104\ L}{2{,}700\ \frac{mg}{cm^3}} = 34.6\ cm^3 \qquad \text{(Eqn. 10.1).}$$

The cross sectional area (A) for the crystal bed is,

$$A = \pi\,(3.81/2\ cm)^2 = 11.4\ cm^2 \qquad \text{(Eqn. 10.2),}$$

and the expected linear bed shrinkage that occurs over a six month period is,

$$\frac{34.6\ cm^3}{11.4\ cm^2} = 3.04\ cm \qquad \text{(Eqn. 10.3).}$$

Hence a total bed length of 13.45 cm (5.3") was found sufficient for maintenance of the required residence time over the six month test period.

A length of 15.24 cm (6") was chosen for the prototype I_2 crystal bed design. With the additonal 1.78 cm margin of safety, estimated bed life was increased to approximately 285 days. The 3.81 x 15.24 (1.5 " x 6.0 ") dimensions correspond to an initial bed volume of 175 cm^3 and to an initial residence time of 1.46 minutes.

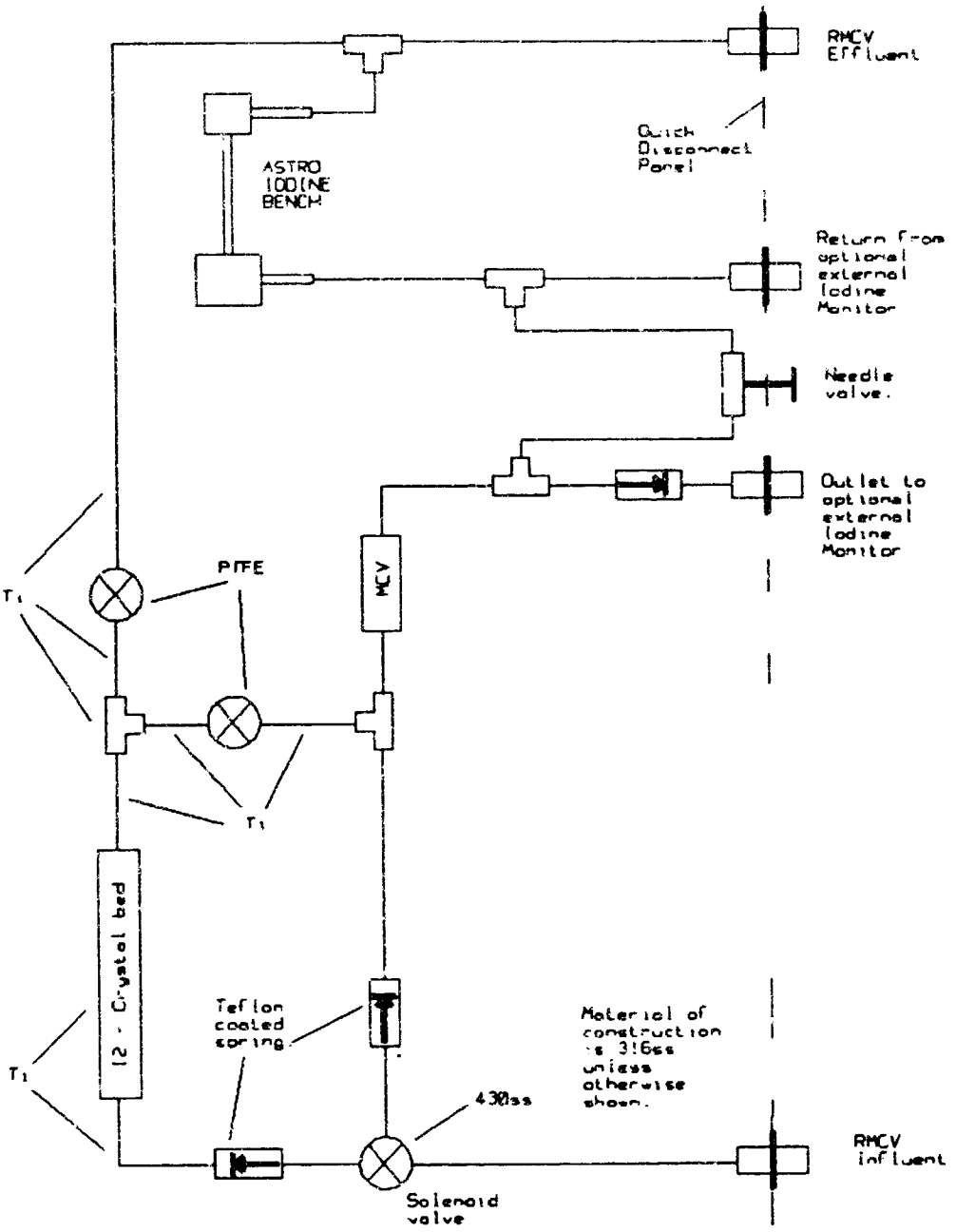

Figure 10.4 Prototype RMCV Plumbing Schematic.

10.1.2 RMCV Flow Path Hardware.

A plumbing diagram of the prototype RMCV is presented in Figure 10.4. The prototype RMCV has been constructed of materials which render it suitable for use at room temperature only. Of the twelve substances evaluated as potential materials of construction for the prototype RMCV, Teflon, Viton A, Titanium (all grades), 316 stainless steel, and 316L stainless steel were found to be suitable for use at room temperature. At elevated temperatures (54.4 ^{o}C) the stainless steels are attacked by elemental iodine as is Grade 2 Titanium. A more complete discussion of the compatibility of construction materials with elemental iodine is given in Section 9.

The MCV housing selected for the RMCV prototype is the standard 3.81 cm ID model provided to NASA for Shuttle Orbiter missions. The MCV is illustrated in Figure 10.5. The MCV cartridge is constructed of 316 stainless steel with the interior surface protected by a Teflon coating. The spring used in the MCV is composed of Teflon coated 302 stainless steel.. The 3.81 cm ID by 15.24 cm solid state iodine crystal bed shown in Figure 10.6, was fabricated from grade 2 Titanium and uses a Teflon coated 302 stainless steel spring.

An ATKOMATIC model L-01365-08 three way diverter valve, rated at 6.5 W for 115 VAC and 60 Hz, is used to invoke regeneration. Two check valves are placed so as to isolate the diverter valve, constructed of 430F stainless steel, from the high aqueous I_2 concentrations encountered during regeneration. Two FURON model MT2-122NCA1 Teflon three way valves, rated at 2W each for 115 VAC and 60 Hz, are used to select between the normal regeneration mode of operation or the super-iodination mode in which the MCV is bypassed.

All plumbing is 0.635 cm (1/4") I.D. Miscellaneous check valves, tubing, fittings, etc., that are directly contacted with concentrated aqueous I_2 during RMCV operations, are constructed of either Grade 2 Titanium, Teflon, Viton A, or 316 stainless steel.

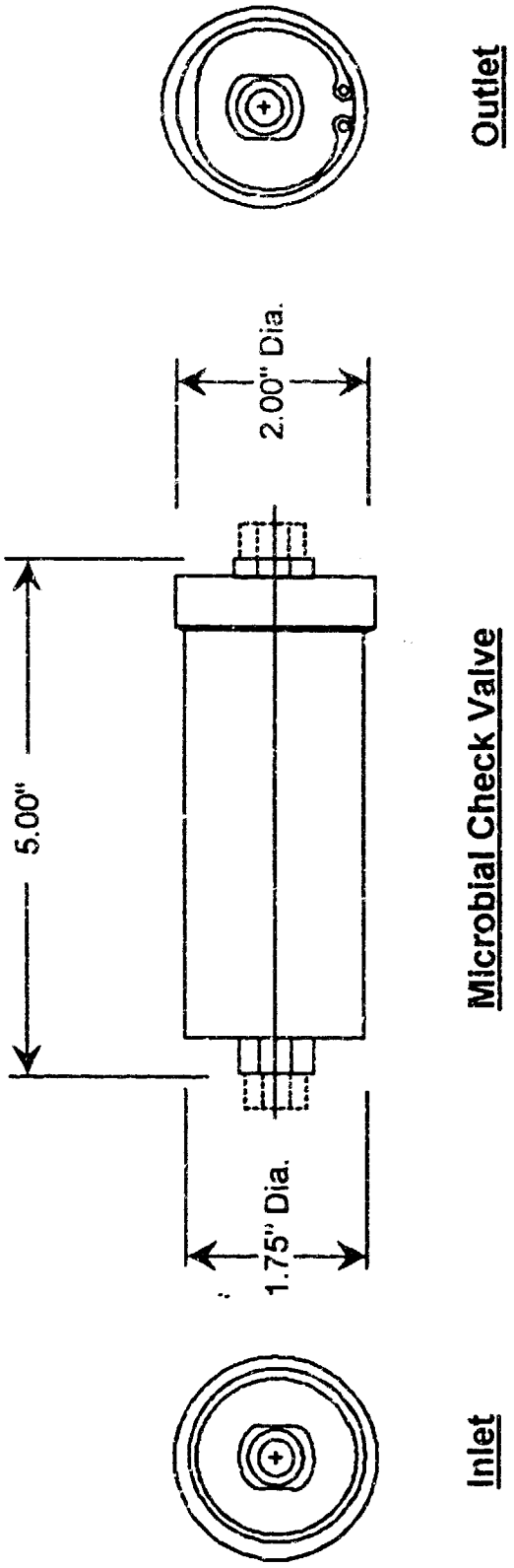

Figure 10.5 100 cm^3 Stainless Steel Microbial Check Valve.

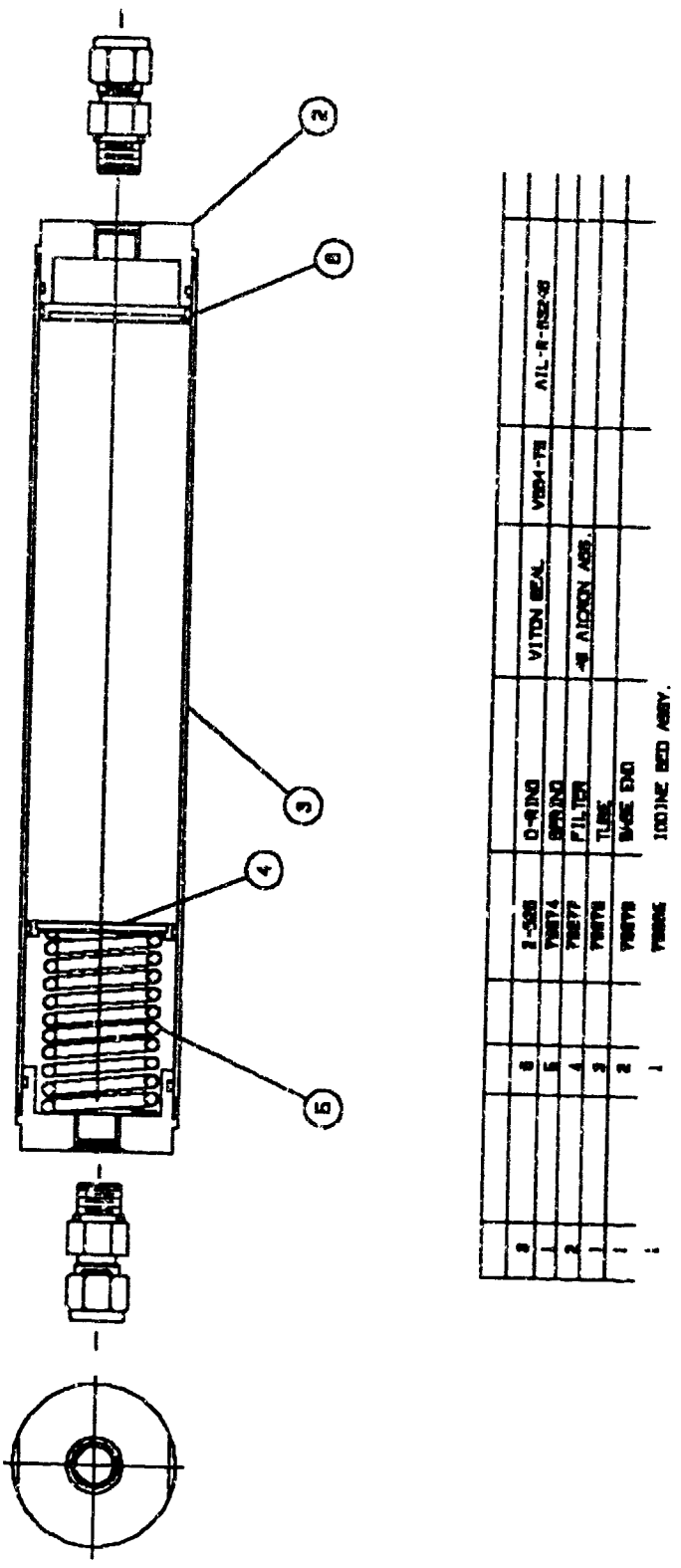

Figure 10.6 Titanium Housing for 15.24 cm I_2 Crystal Bed.

The materials compatibility study, detailed in Section 9, revealed no adverse effects on grade 2 titanium for any of the room temperture modes of I_2 exposure. However, at an elevated temperature (54.4 °C) Grade 2 Titanium in contact with dry iodine crystals did show moderate corrosion. Also, Teflon coated springs were found to be strongly attacked by all exposure conditions except that of saturated aqueous iodine at room temperature. For these reasons, the iodine crystal bed, fabricated for the Prototype RMCV, should not be stored in contact with dry iodine crystals. As a general operational precaution, it is recommended that the iodine crystal bed always be plumbed for influent to enter the *spring end* of the cartridge to preclude any possibility of an iodine crystal contacting the spring.

10.1.3 The Prototype RMCV Control System.

A block diagram of the prototype electronic control system is shown in Figure 10.7. Overall control is achieved using a Z80 microprocessor based microcontroller (Octagon Systems model 5080), housed within a card cage (Octagon Systems model 5207-RMH) and driven by an Octagon Systems model 5100 power supply with 5 V and 12 V outputs. Residual I_2 concentrations are transmitted from the system iodine monitor via an RS -232 serial data link to the microcontroller where they are stored in system RAM (128K). Decisions to initiate and terminate regenerations are made by the microcontroller based upon the I_2 concentration information. The microcontroller is capable of utilizing quantitative data originating from either the onboard system I_2 monitor provided by Astro International or from a photo diode array spectrophotometer. The regeneration diverter valves and the super-iodination valve are controlled through a digital I/O interface to the microcontroller which sinks power to an external relay for each valve.

The control code is written onto a 32 K EEPROM chip resident on the microcontroller board. This code is automatically executed on system power-up. User interaction with the microcontroller is achieved via a sixteen character keypad (Octagon Systems model KP-1) and an 80 character liquid crystal display (Octagon Systems model

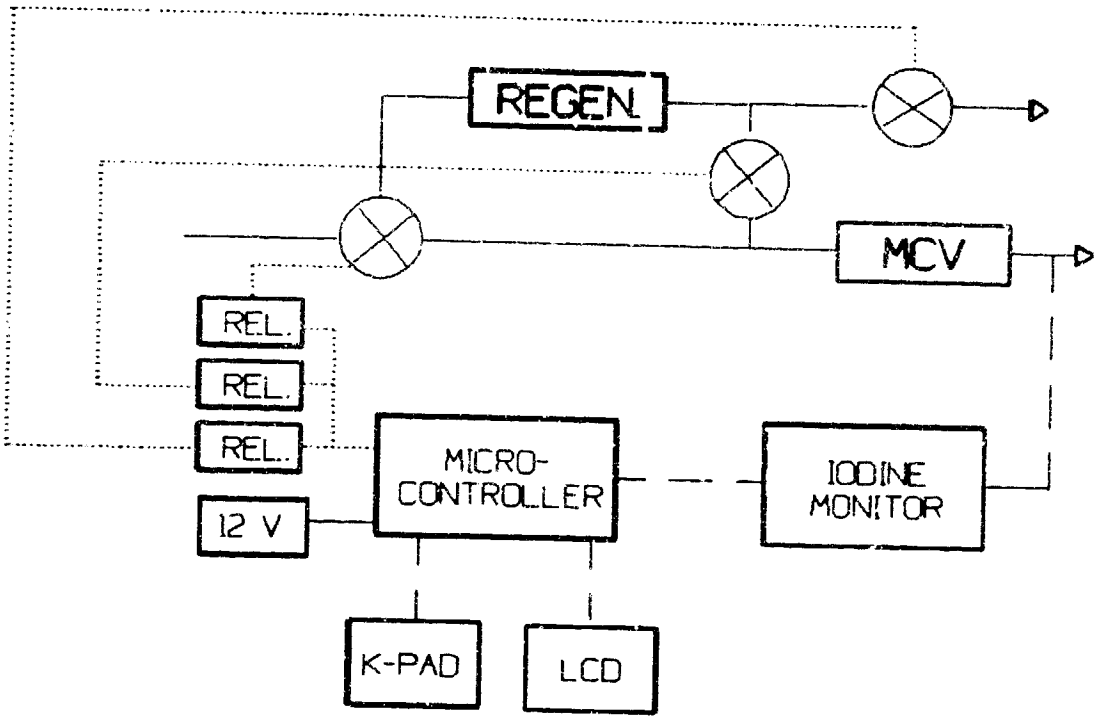

Figure 10.7 Prototype RMCV Control Schematic.

2783). A complete listing of the master control program BOOTRMCV.BAS, written in CAMBASIC is included in Appendix I. A more detailed description of operational features of the control software is presented in the RMCV Prototype Operations Manual (Appendix II).

The control algorithms were written to serve with any MCV - I_2 crystal bed combination that meet the minimum design requirements discussed in sub-section 10.1. The parameters that must be modified via keyboard entry for the algorithm to function properly, are the flow rate, the crystal bed effluent I_2 concentration, and the MCV bed volume if these differ from the 120 cm^3/min., 240 mg/L, and 100 cm^3 values currently used.

10.1.4 The On-Line Iodine Monitor.

The prototype RMCV system iodine monitor was provided by Astro International

Corporation. This unit is the latest version of the Iodine Bench under development for deployment aboard Space Station *Freedom* as a component of the Process Control Water Quality Monitor (PCWQM). The system has been described by Dougherty et al[16]. The Iodine Bench quantifies aqueous I_2 by monitoring absorbance at 467 nm using an LED light source and a 15 cm path-length flow cell designed for a flow rate of 120 cm^3/min.

Prior to acceptance of the Astro Iodine Bench as system I_2 monitor an extensive intercomparison was conducted between prototype RMCV effluent I_2 values generated by the Astro Iodine Bench, by the diode array spectrophotometer, and by the LCV colorimetric technique. The results of this intercomparison are presented in Figure 10.8. As indicated in Figure 10.8a, the I_2 values resulting from the Astro Iodine Bench tracked well with those originating from the other methods, but with a constant offset of approximately +0.5 mg/L. Figure 10.8b shows the generally good agreement between the three methods following recalibration of the Astro Iodine Bench.

Integration of the Astro Iodine Bench with the Prototype RMCV necessitated a re-design of the Iodine Bench's control system. The primary requirement was to reduce the size of the control electronics package needed to operate the Astro Iodine Bench, and to minimuze redundancies. In the configuration in which the Astro Iodine Bench was initially evaluated as a potential system I_2 monitor, control was provided by an IBM compatible PC-XT with A/D and D/A capability. The Iodine Bench control software had been written in MicrosoftC and resided on a 5 1/4 " floppy disk.

An Octagon Systems 5010 single board PC compatible computer was selected to replace the full size PC. The re-designed Astro Iodine Bench control electronics are outlined in the block diagram of Figure 10.9. The components consist of an Octagon Systems 5207-RMH rack mounted card cage, Octagon 5100 power supply, Octagon 5010 microcontroller card, Octagon 5800 floppy disk controller card, Metrabyte DACO2 digital to analog converter card, and Metrabyte DAS-O8LT analog to digital converter card. Both the Astro

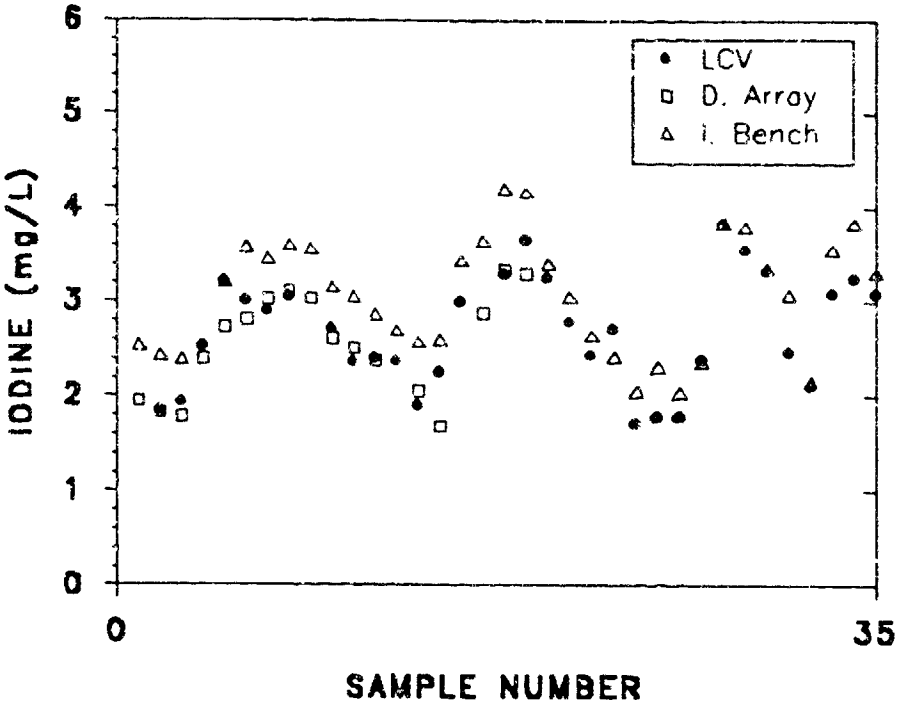

a) Prior to Recalibration of the Astro Iodine Bench.

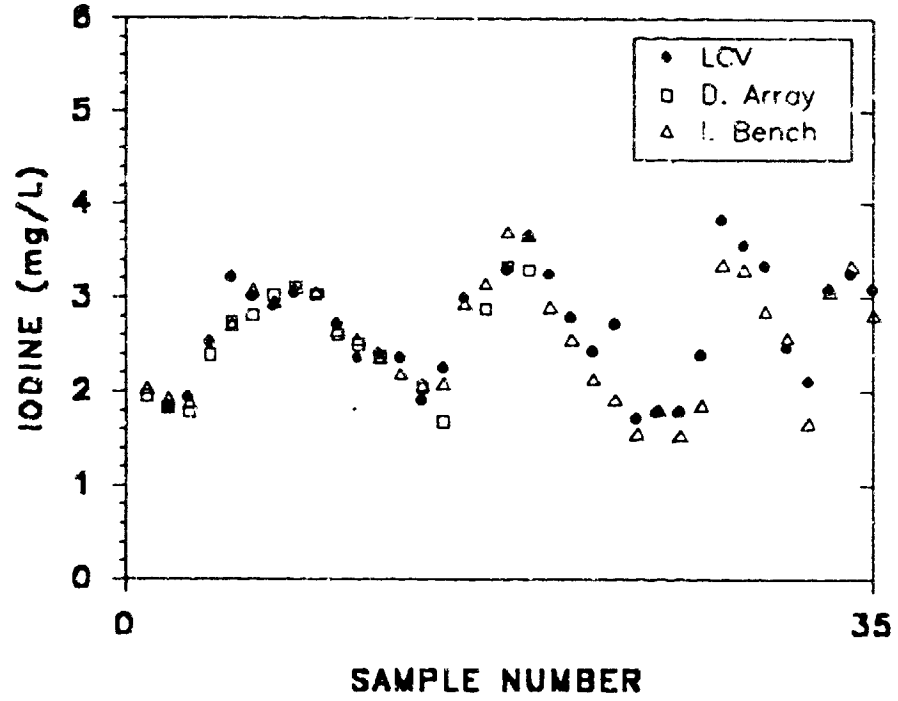

b) Following Recalibration of the Astro Iodine Bench.

Figure 10.8 Intercomparison of Prototype Effluent I_2 by Various Methods.

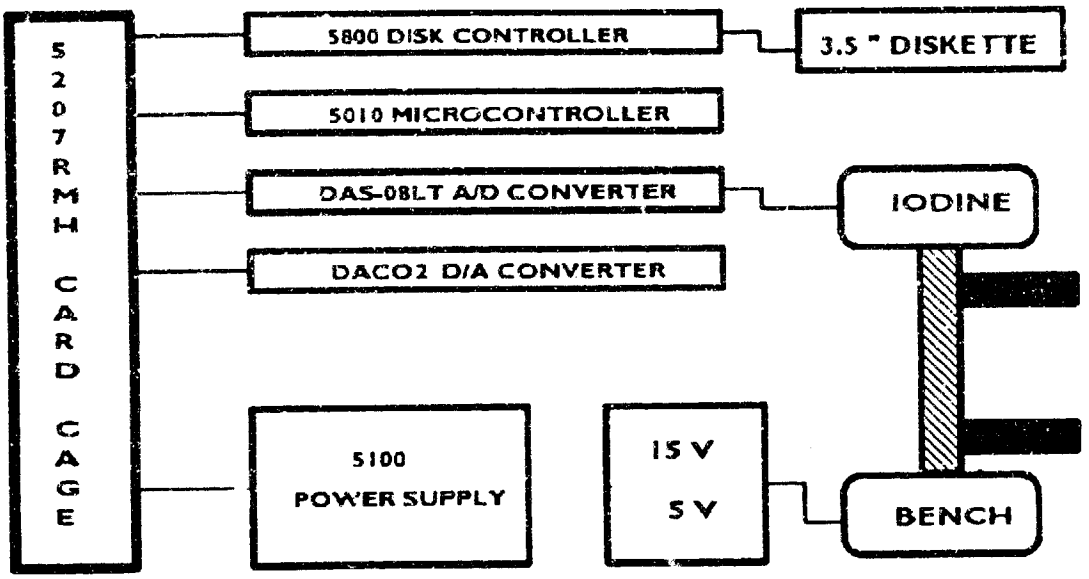

Figure 10.9 Astro Iodine Bench Control Schematic.

Iodine Bench microcontroller and the prototype system controller utilize the same card cage and power supply.

All modifications to the Astro Iodine Bench were made by Astro International Corporation personnel at their League City. Texas facility. Control algorithms for the Astro Iodine Bench were rewritten and the code loaded into EEPROM. Communication between the Iodine Bench microcontroller and the RMCV controller card occurs via a serial RS-232C data link. The Hewlett Packard 8452A diode array spectrophotometer configured with a 10 cm path-length flow-through cell can also be used either in a primary or secondary iodine monitoring role. This instrument is not able to accomodate the full prototype RMCV flow rate. For this reason an RMCV effluent bypass loop was added to the system. The diode

array spectrometer may be connected to the inlet and outlet to this loop. Flow is then established using a needle valve to adjust the flow rate through the spectrophotometer cell.

10.2 The Integrated Prototype RMCV.

A schematic illustration of the prototype RMCV enclosure and the layout of key components is shown in Figure 10.10. The unit consists of a 15 inch cubic frame containing the stainless steel MCV, Titanium I_2 crystal bed housing, Astro Iodine Bench, and associated valves, fittings, and plumbing.

Located above the RMCV frame is the electronics enclosure which houses the card cage, controllers, power supplies, breadboard mounted electromechanical relays, A/D, D/A and interface boards. Mounted on the forward face of the electronics enclosure are the liquid crystal display and 16-key keypad. Attached to the side of the electronics enclosure are two RS-232C D-subminiature 9 pin connectors for interface to an IBM PC compatible computer. These serial ports can be used to upload modified control code to the microcontroller EEPROM, to download RMCV performance data stored in RAM, or to communicate MCV effluent I_2 values between a diode array spectrophotometer and the RMCV microcontroller.

Mounted at the lower right hand side of the frame is a Quick Disconnect (QD) panel. providing QDs for the process stream inlet and outlet. Two additional QDs are provided for use with the photodiode array spectrophotometer as an optional in-line iodine monitor. A needle valve located at the QD panel allows the user to adjust the split stream flow rate to an external iodine monitor. Additional details are presented in the Prototype RMCV Operational Manual attached to this document as Appendix II.

10.3 The Prototype RMCV Operational Test.

The prototype RMCV was subjected to a six month operational test. Initial DI water flow was established at a nominal 120 cm^3/min and continued without significant

PART NUMBER P/N - 09223

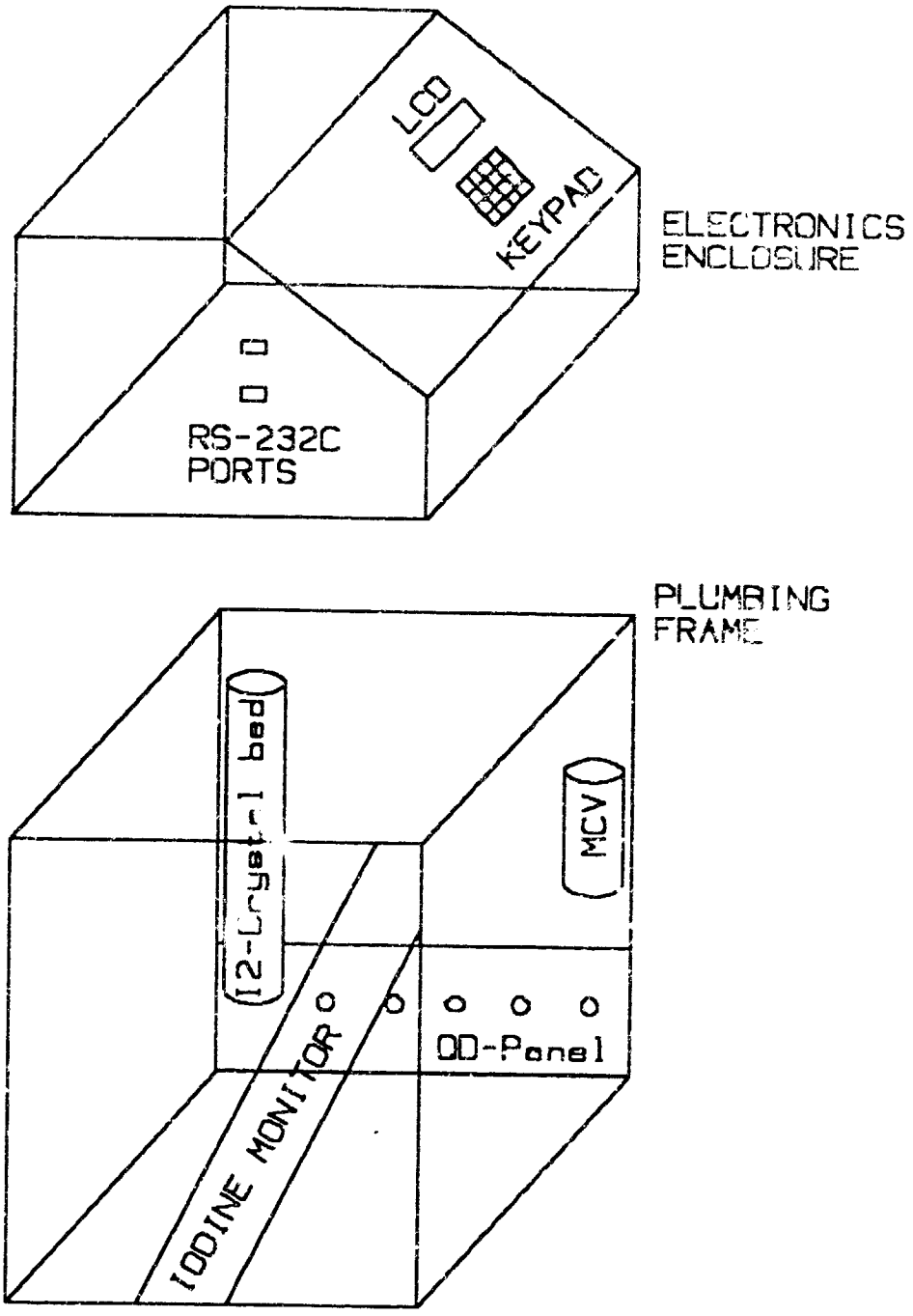

Figure 10.10 Integrated Prototype RMCV.

interruption until the test was concluded. The operational history of the prototype is illustrated in Figure 10.11. During the test period, the prototype RMCV underwent nine complete cycles of washout and regeneration. Each regeneration was autonomously initiated by the microcontroller. Debugging of the control code and evaluation of the regeneration control procedure were performed concurrently with the test period.

During the test period, I_2 levels in the MCV effluent were determined by UV-VIS spectrophotometry using a diode array spectrophotometer, by a closely related spectrophotometric technique using the Astro Iodine Bench, and by the classical LCV colorimetric procedure. Continuous I_2 data are not available for the test period as the Iodine Bench results are not recorded on storage media. These data were stored in microcontroller RAM, but displaced when either memory was filled or power was lost. For this reason, LCV derived I_2 and I^- values have been used in Figure 10.11.

With the exception of the washout following the first regeneration event, the I_2 concentration did not exceed 4.0 mg/L. This was due to the optimized residence time of the prototype MCV. The most noteworthy feature of the prototype RMCV performance during the six month test period is the extremely slow response of the full scale system to regeneration. Failure to fully anticipate this operational characteristic led to an over-regeneration at the end of the first cycle.

In contrast to the virtually immediate rise in MCV effluent I_2 concentrations experienced with small column scale RMCVs, the full scale unit shows little if any rise in effluent I_2 during the event. Instead, following regeneration, residual I_2 levels rise very slowly over the course of several days, until a maximum is reached. Once this point is attained, a typical MCV washout follows. Thus the full scale RMCV cycle consists of a wash-up phase following regeneration, followed by a normal washout once the maximum residual I_2 concentration for the cycle has been reached. The wash-up time period is typically shorter than the washout time period. This is likely due to higher concentration gradients established

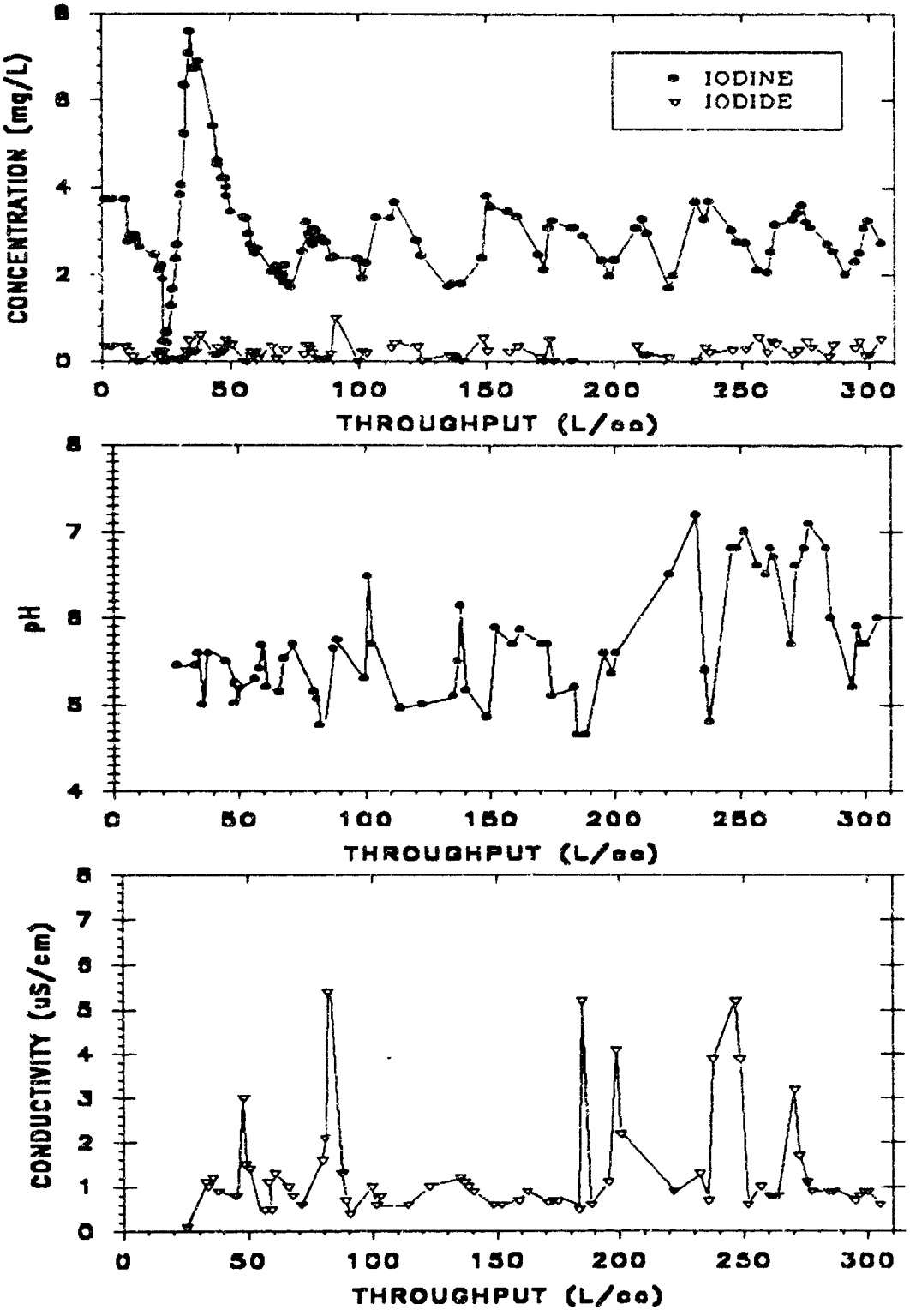

Figure 10.11 6 Month Prototype RMCV Flow History.

across the MCV resin bed following regeneration.

Freshly iodinated MCV resin is of relatively uniform composition. Once initial flow through the resin bed begins, however, an I_2 concentration gradient is established with the minimum concentration at the inflow face and the maximum concentration at the outflow face. During regeneration, the I_2 concentration gradient is strongly reversed. The wash-up period corresponds to the time interval required to re-establish the original gradient. The total cyclic time period from regeneration through washout is analogous to the retention time of a chromatographic peak.

Irrespective of the type of system iodine monitor in use at a particular time, the microcontroller performs a running integration of the area under the wash-up/washout curve to determine the total I_2 depletion for the cycle. This calculation assumes a fixed flow rate. The length of the regeneration period is then calculated as the time required to replace the I_2 lost from the system, assuming that the concentrated regeneration liquor contains 240 mg/L of I_2. The iodine crystal bed has been designed to output this concentration as a minimum at room temperature for the bulk of its useful life as long as a minimum residence time is met as discussed in sub-section 10.1. Both the flow rate and the regeneration liquor iodine concentration assumed values can be altered by the operator via keypad input. Regenerations during the six month test period typically required between four and five hours for completion. The average cyclic throughput during the test period was approximately 30 L/cm^3.

At the end of the six month test period, the operation in the super-iodination mode was tested. A split of the RMCV effluent was routed to a diode array spectrophotometer fitted with a 1 cm path length flow-through cell. Super-iodination was invoked by keypad input. The test results are illustrated in Figure 10.12. The prototype RMCV, at the end of its 6 month design life, output 60 liters of strongly iodinated water at a relatively uniform concentration of approximately 240 mg/L. Further flow produced a gradual decline in the

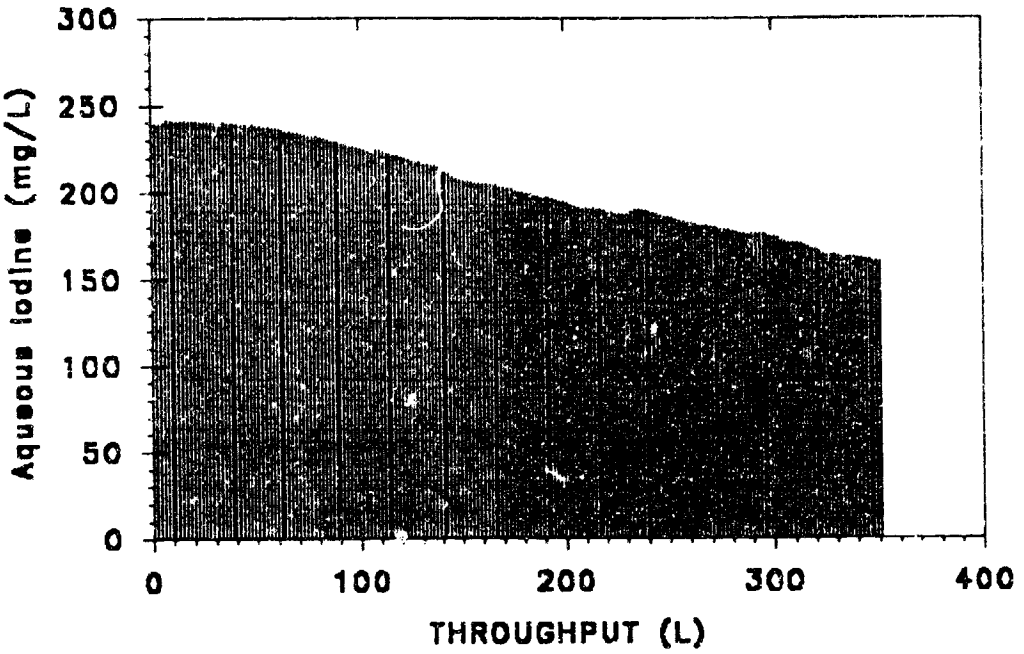

Figure 10.12 Prototype RMCV in Super-Iodination Mode.

aqueous I_2 concentration. After more than 350 liters of flow, levels of approximately 175 mg/L were observed. At this point all prototype RMCV operations were terminated.

An inspection of the Grade 2 Titanium housing revealed no evidence of corrosion. Calculation yielded an expected 9.88 cm of crystalline iodine remaining at the end of the test period, 9.22 cm of remaining iodine were found. This small discrepancy is probably due to the increased packing density of the iodine crystals resulting from the tension of the Teflon coated spring.

10.4 Conclusions.

The prototype RMCV test program was an unqualified success. The feasibility of full scale RMCV operations has been fully demonstrated. With the substantially higher MCV

residence time of the full scale unit the transient peak of high I_2 concentration, observed in small column tests during regeneration, has been totally eliminated. The system has proven capable of maintaining I_2 concentrations within the narrow range of 2.0 - 4.0 mg/L indefinitely. Additionally, operation in the super-iodination mode has confirmed that a concentrated aqueous iodine solution can be prepared on demand for use during transient episodes of microbial contamination.

11

CONCLUSIONS

The advanced RMCV development program has been very successful. Fully autonomous RMCVs have been designed, fabricated and tested, from the small column scale to the full scale prototype tested at the Space Station *Freedom* water processor design flow rate.

The small column life cycle testing demonstrated dramatic improvements in long term MCV performance via the *in situ* regenerative process, exhibiting total throughputs up to 2,611 L/cm^3. MCV life extensions of 120 - 130 fold were demonstrated, limited only by the duration of the Phase II performance period. At the conclusion of the life cycle testing the RMCVs were still fully functional. The RMCVs were shown to operate with a variety of influent streams of diverse chemical compositions including simulated: reclaimed potable water, reclaimed hygiene water, humidity condensate and urine distillate. The challenge streams of differing chemical compositions were found to exhibit characteristic cyclic frequencies, which, on average, ranged between 7.67 - 16.49 L/cm^3.

The primary symptom of deteriorating RMCV performance was observed as a gradual increase in the frequency of regeneration, with a corresponding reduction in cyclic throughput. Potential causative factors responsible for performance degradation were identified as loss of I^- from the MCV resin anion exchange sites, and the blockage of ion exchange sites by physical coating of the resin beads by particulate matter. The loss of I^- from the MCV resin is thought to be due to both displacement by other anions such as Cl^-, and to a reduction in the number of ion exchange sites due to slow mechanical degradation of the resin. Blockage of the uptake of I_2 from the regeneration liquor by materials coating the resin beads or precipitated in the interstitial spaces is felt to be largely attributable to the accumulation of materials originating from dead microorganisms. This suggests the need for adequate filtration of the RMCV influent stream. Inclusion of the capability for an MCV resin bed backwash may be a useful design feature to achieve the longest possible continuous operation

of a full scale RMCV.

The design features necessary for optimal RMCV performance have been determined through a program of parametric testing. These were incorporated into the design of a full scale autonomous prototype RMCV which operated continuously for a six month test period. In this time, the prototype RMCV underwent nine cycles of washout and regeneration and accumulated a total throughput in excess of 300 L/cm^3. No indications of deteriorating performance were observed. Operation of the prototype RMCV gave every indication that a much greater life for the full scale system is possible. This unit has been completely refurbished and delivered to NASA-JSC.

A secondary use of RMCV technology, in the delivery, on demand, of very strong aqueous I_2 solutions (225 - 300 mg/L) for use in the disinfection of microbial surface contamination and in the control of biofilm formation has been demonstrated. Both small column and full scale tests have been successfully conducted. The efficacy of the strong aqueous I_2 solution has been shown against both surface microorganisms and young biofilms. This technology can potentially be applied against episodes of transient system microbial upset, as a means of removing surface microbial contaminants, as a means of controlling biofilm formation, and as a preventative measure in systems which are particularly vulnerable to microbial contamination.

In addition, the RMCV development program has resulted in several related accomplishments of potential benefit. Methodology for the use of the diode array spectrophotometer as an on-line real time iodine monitor has been fully developed. The compatibility of a variety of materials with elemental iodine over a range of exposure situations has been determined.

The chemistry of aqueous I_2 has been explored. The oxidation of formic acid, contained within both ersatz humidity condensate and ersatz urine distillate, by I_2 has been identified, and the kinetics of the second order bimolecular reaction has been investigated. In

these experiments the reacted I_2 was quantitatively recovered as I^-, indicating that iodinated organic disinfection byproducts were not being formed in significant quantities.

The complex system of equilibria responsible for aqeuous iodine speciation has been modeled and studied under conditions of varying pH and total iodine concentration. The kinetics of aqueous iodine sepeciation have also been modeled under conditions of varying pH and total iodine concentration. The results of these studies have clearly indicated not only the pH sensitivity of both the slow and the fast hydrolytic disproportionation reactions, but also the concentration dependence which renders low I_2 levels, such as those encountered in MCV effluents, significantly more susceptible to hydrolysis. The speciation equilibria and kinetics also suggest that for a closed loop system of given volume and given water recycle rate, an optimal pH can be identified to minimize the formation of I^- as a consequence of the addition of a biocidal I_2 residual. This pH will certainly be below 7.0.

Based upon the highly successful results of the Phase II RMCV development program, a Phase III continuation of this work culminating in Flight Hardware is clearly warranted. Based upon the test results to date, it is certain that an autonomous RMCV system can be designed to function with a minimum of human intervention and minimal resupply penalty for the 30 year life of the Space Station. This technology is ideally suited for inclusion in the environmental control and life support systems required for a manned Mars mission or a Lunar Base. Also, growing interest in the use of elemental iodine as a disinfectant to control waterborne bacterial pathogens, particularly in third world countries, suggests the potential for RMCV technology to be applied commercially to public drinking water supplies.

12

REFERENCES and BIBLIOGRAPHY

1. Akse, J.R., J. Thompson, B. Scott, C. Jolly, and D.L. Carter, Catalytic Oxidation for Treatment of ECLSS & PMMS Waste Streams, SAE 921274 presented at 22nd International Conference on Environmental Systems, Seattle, July 13-16, 1992.

2. Al-Abachi, M.Q., T.S. Al-Ghabsha and M.S. Al-Hafidh, Some Observations on the Indirect Spectrophotometric Microdetermination of Iodine or Bromine in Organic Compounds Using Chloranil, Microchem. J. 41, 372 (1990).

3. Al-Wehaid, A. and A. Townshend, Flow-Injection Amplification for the Spectrophotometric Determination of Iodide, Anal. Chim. Acta 198, 45 (1987).

4. Alamgir, M. and I.R. Epstein, Complex Dynamical Behavior in a New Chemical Oscillator: The Chlorite-Thiourea Reaction in a CSTR, Int. J. Chem. Kinet. 17, 429 (1985).

5. Alfassi, Z.B. and D.M. Golden, Kinetics of the Reaction of Iodine with Acrolein. Bond Dissociation Energy of the Carbonyl C-H Bond, J. Am. Chem. Soc. 95, 319 (1973).

6. Allen, T.L. and R.M. Keefer, The Formation of Hypoiodous Acid and Hydrated Iodine Cation by the Hydrolysis of Iodine, J. Am. Chem. Soc. 77, 2956 (1955).

7. Allmand, A.J. and L. Reeve, The Photochemical Decomposition of Aqueous Formic Acid Solutions, J. Chem. Soc., 2852 (1926).

8. Andrews, L.J. and R.M. Keefer, The Interaction of Iodine with Cyclohexene and Vinyl Halides, J. Am. Chem. Soc. 74, 458 (1952).

9. Anson, F.C. and J.J. Lingane, Anodic Chronopotentiometry with latinum and Gold Electrodes. The Iodide-Iodine-Iodate System, J. Am. Chem. Soc. 79, 1015 (1957).

10. Anson, F.C., The Effect of Surface Oxidation on the Voltammetric Behavior of Platinum Electrodes. The Electroreduction of Iodate, J. Am. Chem. Soc. 81, 1554 (1959).

11. Arbon, R.E. and E.P. Grimsrud, Selective Detection of Iodinated Hydrocarbons by the Electron Capture Detector with Negative Ion Hydration and Photodetachment, Anal. Chem. 62, 1762 (1990).

12. Astro International Corp., Development of the Water Quality Monitor and UV Oxidation Analyzer for Space Station Reclaimed Waters, Final Report, Phase I, Contract No. NAS8-36656, prepared for Marshall Space Flight Center, June 1990.

13. Astro International, Engineering Selection Considerations for Design of Processor Controlled Water Quality Monitoring System Iodine Measurements, Doc. AIC-SS-1094A, July 30, 1990.

14. Atwater, J.E., R.R. Wheeler, Jr., J.T. Olivadoti, and R.L. Sauer, Chemistry and Kinetics of I_2 Loss in Urine Distillate and Humidity Condensate, SAE 921314 presented at 22nd Internation Conference on Environmental Systems, Seattle, July 13-16, 1992.

15. Atwater, J.E., R.R. Wheeler, Jr., J.T. Olivadoti, R.L. Sauer, and D.T. Flanagan, Regenerable Microbial Check Valve: Life Cycle Tests Results, SAE 921316 presented at 22nd International Conference on Environmental Systems, Seattle, July 13-16, 1992.

16. Aumont G. and J-C. Tressol, Improved Routine Method for the Determination of Total Iodine in Urine and Milk, Analyst 111, 841 (1986).

17. Aveston, J. and D.A. Everest, The Adsorption of Bromine and Iodine by Anion-Exchange Resins, Chem. Ind. (London), 1238 (1957).

18. Awtrey, A.D. and R.E. Connick, The Rate Law and Mechanism of the Reaction of Iodine with Thiosulfate Ion: The Formation of the Intermediate $S_2O_3I^-$, J. Am. Chem. Soc. 73, 1341 (1951).

19. Awtrey, A. and R.E. Connick, The Absorption Spectra of I_2, I_3^-, I^-, IO_3^-, $S_4O_6^{-2}$ and $S_2O_3^{-2}$. Heat of the Reaction $I_3^- = I_2 + I^-$, J. Am. Chem. Soc. 73, 1842 (1951).

20. Awtrey, A. and R.E. Connick, Corrections to: [The Absorption Spectra of I_2, I_3^-, I^-, IO_3^-, $S_4O_6^{-2}$ and $S_2O_3^{-2}$. Heat of the Reaction $I_3^- = I_2 + I^-$, J. Am. Chem. Soc. 73, 1842 (1951)], J. Am. Chem. Soc. 76, 6417 (1954).

21. Awtrey, A.D. and R.E. Connick, Rate Law and Mechanism of the Reaction of Iodine with Tetrathionate Ion, J. Am. Chem. Soc. 73, 4546 (1951).

22. Ayres, R.L., C.J. Michejda, and E.P. Rack, Reactions of Iodine with Olefins. I. Kinetics and Mechanism of Iodine Addition to Pentene Isomers, J. Am. Chem. Soc. 93, 1389 (1971).

23. Bafna, S.L., W.V. Bhagwat and G.L. Maheshwari, Reactions of Iodine: I-Reaction Between Iodine & Sodium Formate in Dark, J. Sci. Ind. Res. 11B, 226 (1952).

24. Bafna, S.L., W.V. Bhagwat and G.L. Maheshwari, Reactions of Iodine: II-Reaction Between Iodine & Formic Acid, J. Sci. Ind. Res. 11B, 228 (1952).

25. Bafna, S.L., W.V. Bhagwat and M.A. Tilak, Reactions of Iodine: III-Reaction Between Iodine & Sodium Malonate, J. Sci. Ind. Res. 11B, 230 (1952).

26. Bafna, S.L., K.P. Govindan and W.V. Bhagwat, Reactions of Iodine: Part IV-Reaction Between Iodine & Malonic Acid, J. Sci. Ind. Res. 11B, 376 (1952).

27. Bafna, S.L., Catalysis by Ion-Exchange Resins: Acetone-Iodine Reaction, J. Phys. Chem. 59, 1199 (1955).

28. Bali, A. and K.C. Malhotra, Behavior of Some Iodine Compounds in Disulphuric Acid, J. Inorg. Nucl. Chem. 38, 411 (1976).

29. Banks, D.F., Organic Polyvalent Iodine Compounds, Chem. Rev. 66 (1966).

30. Barkley, R., C. Hurst, A. Dunham, J. Silverstein, and G.M. Brion, Generation of Iodine Disinfection By-Products (IDP's) in a Water Recycle System, SAE 921362 presented at 22nd International Conference on Environmental Systems, Seattle, July 13-16, 1992.

31. Barnes, I., V. Bastian, K.H. Becker and R.D. Overath, Kinetic Studies of the Reactions of IO, BrO, and ClO with Dimethylsulfide, Int. J. Chem. Kinet. 23, 591 (1991).

32. Barton, A.F.M. and G.A. Wright, Kinetics of the Iodate-Iodide Reaction: Catalysis by Carboxylate and Phosphate Ions, J. Chem. Soc. (A), 2096 (1968).

33. Bathgate, R.H. and E.A. Moelwyn-Hughes, The Kinetics of Certain Ionic Exchange Reactions of the Four Methyl Halides in Aqueous Solution, J. Chem. Soc., 2642 (1959).

34. Beckman Instruments, Inc., Advanced Prototype Automated Iodine Monitor System, Final Report Contract No. NAS9-14761, prepared for NASA-Johnson Space Center, January, 1976.

35. Beilby, A.L. and A.L. Crittenden, Non-Additive Polarographic Waves in the Anodic Oxidation of Iodide, J. Phys. Chem. 64, 177 (1960).

36. Bell, R.P. and E. Gelles, The Halogen Cations in Aqueous Solution, J. Chem. Soc., 2734 (1951).

37. Bell, R.P. and E. Gelles, Equilibria in the Halogenation of Some Organic Substances in Aqueous Solution, Proc. R. Soc. (London) A 210, 310 (1952).

38. Bell, R.P. and P. Engel, Kinetics of the Reaction between Ethyl Iodomalonate and

Iodide Ions, J. Chem. Soc., 24 ' (1957).

39 Benitez, J., M. del Mar Graciani, C.D. Hubbard, and F. Sanchez-Burgos, Kinetic Salt Effects in the Reaction ofPermanganate Ions with Iodide Ions in Concentrated Electrolyte Solutions, J. Solution Chem. 19, 19 (1990).

40. Benson, S.W. and A.N. Bose, The Iodine-catalyzed, Positional Isomerization of Olefins. A New Tool for the Precise Measurement of Thermodynamic Data, J. Am. Chem. Soc. 85, 1385 (1963).

41. Benson, S.W., A.N. Bose and P. Nangia, The Kinetics of the Iodine-catalyzed Positional Isomerism of Butene-1. The Resonance Energy of the Allyl Radical, J. Am. Chem. Soc. 85, 1388 (1963).

42. Berliner, E., Kinetics of the Iodination of Aniline, J. Am. Chem. Soc. 72, 4003 (1950).

43. Berliner, E., Kinetics of the Iodination of Phenol, J. Am. Chem. Soc. 73, 4307 (1951).

44. Berne, E. and M.J. Weill, A Remeasurement of the Self-Diffusion Coefficients of Iodide Ion in Aqueous Sodium Iodide Solutions, J. Phys. Chem. 64, 272 (1960).

45. Bhagwat, W.V., The Reaction Between Aqueous Iodine and Sodium Formate, J. Ind. Chem. Soc. 17, 304 (1940).

46. Bhale, V.M., S.L. Bafna and W.V. Bhagwat, Reaction of Malonic and Monoalkyl Malonic Acids with Iodine, Z. Phys. Chem. 12, 298 (1957).

47. Bhale, V.M., K.V.N. Rao and S.L. Bafna, Reaction of Malonic & Monoalkyl Malonic Acids with Halogens: Part II - Some Further Considerations, J. Sci. Ind. Res. 20B, 128 (1961).

48. Bharadwaj, L.M., D.N. Sharma and Y.K. Gupta, Kinetics and Mechanism of Oxidations by Peroxydiphosphate Ions-V. Oxidation of Iodide in Aqueous Perchloric Acid, J. Inorg. Nucl. Chem. 39, 1621 (1977).

49. Bhat, S.N., Charge-Transfer Complex: the Blue Shifted Iodine Band by the Constant Activity Method, J. Inorg. Nucl. Chem. 37, 276 (1975).

50. Bhattacharya, A.K. and N.R. Dhar, Influence of Intensity on the Velocity of Photochemical Reactions, J. Ind. Chem. Soc. 6, 473 (1929).

51. Blagrove, R.J. and L.C. Gruen, Spectrophotometric Determination of Thiourea, Mikrochim. Acta 639 (1971).

52. Blasius, E. and U. Wachtel, Versuch des Nachweises eines Polaren Jodpyridinkomplexes mittels Ionenaustauscher, Fresenius' Z. Anal. Chem. 138, 106 (1953).

53. Boehm, A.M., A.K. Colling, Jr., M.J. Heldmann, J.W. Steele, R.G. Shaw, Space Station Water Processor: Current Flight Design, SAE 921112 presented at 22nd Internation Conference on Environmental Systems, Seattle, July 13-16, 1992.

54. Bok, L.D.C., J.G. Leipoldt and S.S. Basson, A Kinetic Study of the Reaction between Octacyanotunstate(V) and Iodide Ions, J. Inorg. Nucl. Chem. 37, 2151 (1975).

55. Bonner, O.D., Osmotic and Activity Coefficients of the Sodium Salts of Formic, Acetic and Propionic Acids, J. Solution Chem. 17, 999 (1988).

56. Bradbury, R.B., The Mechanism of the Reaction between Glycerol and Hydriodic Acid, J. Am. Chem. Soc. 74, 2709 (1952).

57. Bray, W.C., A Periodic Reaction in Homogeneous Solution and its Relation to Catalysis, J. Am. Chem. Soc. 43, 1262 (1921).

58. Bray, W.C. and H.A. Liebhafsky, Reactions Involving Hydrogen Peroxide, Iodine and Iodate Ion. I. Introduction, J. Am. Chem. Soc. 53, 38 (1931).

59. Bray, W.C. and A.L. Caulkins, Reactions Involving Hydrogen Peroxide, Iodine and Iodate Ion. II. The Preparation of Iodic Acid. Preliminary Rate Measurements, J. Am. Chem. Soc. 53, 44 (1931).

60. Bray, W.C. and J.B. Ramsey, The Simultaneous Reduction of Vanadic Acid and Oxygen by Iodide. Induced Catalysis of Oxygen Reactions, J. Am. Chem. Soc. 55, 2279 (1933).

61. Briggs, T.S. and W.C. Rauscher, An Oscillating Iodine Clock, J. Chem. Ed. 50, 496 (1973).

62. Brion, G.M., and J. Silverstein, Inactivation of a Model Coliphage Virus in Water by Iodine, SAE 921361 presented at 22nd International Conference on Environmental Systems, Seattle, July 13-16, 1992.

63. Brusa, M.A. and A.J. Colussi, A Kinetic Study of the Reaction between Formic Acid and HOBr, Int. J. Chem. Kinet. 14, 479 (1982).

64. Brydon, D.L. and J.I.G. Cadogan, Radical Abstraction of Iodine from Aromatic Iodides: Benzyne Formation from o-Iodo-N-nitrosoacetanilide, Chem. Comm., 744 (1966).

65. Buchberger, W. and K. Winsauer, Determination of Traces of Iodide in Serum and Urine by Ion Chromatography, Mikrochim. Acta III, 347 (1985).

66. Buchberger, W. and U. Huebauer, Selective Determination of Bromide and Iodide in Serum and Urine by Gas Chromatography, Mikrochim. Acta III, 137 (1989).

67. Buist, G.J., W.C.P. Hipperson and J.D. Lewis, Equilibria in Alkaline Solutions of Periodates, J. Chem. Soc. (A), 306 (1969).

68. Buist, G.J., The Oxidation of Organic Compounds by Non-metallic Anions, in Comprehensive Chemical Kinetics, vol.6, C.H. Bamford, and C.F.H. Tipper, Eds., Elsevier, New York, 1972.

69. Bujake, J.E. Jr. and R.M. Noyes, Mechanisms of Exchange Reactions of t-Butyl Iodide with Elementary Iodine, J. Am. Chem. Soc. 83, 1555 (1961).

70. Bujake, J.E. Jr., M.W.T. Pratt and R.M. Noyes, Mechanisms of Exchange Reactions of Primary and Secondary Alkyl Iodides with Elementary Iodine, J. Am. Chem. Soc. 83, 1547 (1961).

71. Bull, R.J., K.D. Thrall and T.T. Sherer, Thyroid Effects of Iodine and Iodide in Potable Water, SAE Paper No. 911401, presented at 21st International Conference on Environmental Systems, San Francisco, July 15-18, 1991.

72. Bunnett, J.F. and D.J. McClennan, Iodine Scrambling Accompanying Base-Catalyzed Isomerization of 1,2,4-Triiodobenzene, J. Am. Chem. Soc. 90, 2190 (1968).

73. Bunker, D.L. and N. Davidson, A Further Study of the Flash Photolysis of Iodine, J. Am. Chem. Soc. 80, 5085 (1958).

74. Burger, J.D. and H.A. Liebhafsky, Thermodynamic Data for Aqueous Iodine Solutions at Various Temperatures, An Exercise in Analytical Chemistry, Anal. Chem. 45, 600 (1973).

75. Burns, G. and W.H. Wong, Study of Atomic Recombination Over a Wide Pressure Range, J. Am. Chem. Soc. 97, 710 (1975).

76. Cain, W.P. and R.M. Noyes, Detailed Mechanisms of Exchange Reactions between Iodine and Allyl Iodide, J. Am. Chem. Soc. 1, 2031 (1959).

77. Carter, D.L., H.Cole, M. Habercom, and G. Griffith, Determination of Organic Carbon and Ionic Accountability of Various Waste and Product Waters Derived from ECLSS Water Recovery Tests and Spacelab Humidity Condensate, SAE 921313

presented at 22nd International Conference on Environmental Systems, Seattle, July 13-16, 1992.

78. Carter, J.S., The Salting-out Effect. The Influence of Electrolytes on the Solubility of Iodine in Water, J. Chem. Soc., 2861 (1925).

79. Castleman, A.W., Jr., I.N. Tang and H.R. Munkelwitz, The Chemical States of Fission-Product Iodine Emanating into a High Temperature Aqueous Environment, J. Inorg. Nucl. Chem. 30, 5 (1968).

80. Chambers, J.F., The Conductance of Concentrated Aqueous Solutions of Potassium Iodide at 25° and of Potassium and Sodium Chlorides at 50°, J. Phys. Chem. 62, 1136 (1958).

81. Chan, R.J.-H., C. Ueda and T. Kuwana, A 200% Efficient Electrolysis Cell, J. Am. Chem. Soc. 105, 3713 (1983).

82. Chang, S.L., The Use of Active Iodine as a Water Disinfectant, J. Am. Pharm. Assn. 47, 417 (1958).

83. Chia, Y.-T. and R.E. Connick, The Rate of Oxidation of I^- to Hypoiodite Ion by Hypochlorite Ion, J. Phys. Chem. 63, 1518 (1959).

84. Chow, B.F., Studies on the Relationship between the Rates of Reactions and Oxidation-Reduction Potentials. I. Oxidation of Formate Ion by Halogens in the Dark, J. Am. Chem. Soc. 57, 1437 (1935).

85. Ciesceri, L.S., A.E. Greenberg, R.R. Trussel, Eds., Standard Methods for the Examination of Water and Wastewater, 17th Edition, APHA, Washington (1989).

86. Cohen, E.D. and C.N. Trumbore, The Exchange Reaction of Ethyl Iodide and Iodine, J. Am. Chem. Soc. 87, 964 (1965).

87. Colombo, G.V. and D.P Putnam, Microbial Check Valve for Shuttle, ASME Paper 78-ENAs-27, presented at 8th Intersociety Conference on Environmental Systems, San Diego, July 10-13, 1978.

88. Colombo, G.V., D.R. Greenley, D.F. Putnam, Water System Microbial Check Valve Development, Final Report, Contract NAS9-15079, Umpqua Research Company, July 1978.

89. Colombo, G.V. and D.R. Greenley, Advanced Microbial Check Valve Development, Final Report, Contract NAS9-15854, Umpqua Research Company, June 1980.

90. Colombo, G.V., C.D. Jolly and R.L. Sauer, Regenerable Biocide Delivery Unit, SAE Paper No. 911406, presented 21st International Conference on Environmental Systems, San Francisco, July 15-18, 1991.

91. Cooke, D.O., A Double-Barreled Chemical Oscillator, Int. J. Chem. Kinet. 14, 1047 (1982).

92. Corain, B. and A.J. Poe, Iodoplatinate(II) Species in Aqueous Solution, J. Chem. Soc. (A), 1318 (1967).

93. Creeth, A.M. and M. Spiro, A Re-formulation of the Wagner and Traud Additivity Principle: Catalytic and Electrochemical Experiments with Iodide Modified Surfaces, J. Electroanal. Chem. 312, 165 (1991).

94. Crouthamel, C.E., A.M. Hayes and D.S. Martin, Ionization and Hydration Equilibria of Periodic Acid, J. Am. Chem. Soc. 73, 82 (1951).

95. Czapski, G., J. Jortner and G. Stein, The Oxidation of Iodide Ions in Aqueous Solution by Atomic Hydrogen, J. Phys. Chem. 63, 1769 (1959).

96. Danen, W.C. and D.G. Saunders, Halogen Abstraction Reactions. I. Free-Radical Abstraction of Iodine from Substituted Iodobenzenes, J. Am. Chem. Soc. 91, 5924 (1969).

97. Danen, W.C. and R.L. Winter, Halogen Abstraction Studies. II. Free-Radical Abstraction of Iodine from Aliphatic Iodides. Evidence to Support Anchimeric Assistance by Neighboring Halogen in Homolytic Reactions, J. Am. Chem. Soc. 93, 716 (1971).

98. Danen, W.C., D.G. Saunders and K.A. Rose, Halogen Abstraction Studies. IV. Abstraction of Iodine by Phenyl Radicals from 2-Substituted Iodobenzenes and Iodoferrocene, J. Am. Chem. Soc. 95, 1612 (1973).

99. D'Aprano, A., J. Komiyama and R.M. Fuoss, Conductance of Potassium Iodide in Mixed Solvents, J. Solution Chem. 5, 279 (1976).

100. Darbee, L.R. and G.M. Harris, Thermal Isotopic Exchange between Ethyl Iodide and Molecular Iodine in the Liquid Phase, J. Phys. Chem. 61, 111 (1957).

101. Darrall, K.G. and G. Oldham, The Diffusion Coefficients of the Tri-iodide Ion in Aqueous Solutions, J. Chem. Soc. (A), 2584 (1968).

102. Dateo, C.E., M. Orban, P. De Kepper and I.R. Epstein, Bistability and Oscillations in the Autocatalytic Chlorite-Iodide Reaction in a Stirred-Flow Reactor, J. Am. Chem.

Soc. 104, 504 (1982).

103. Davies, M. and E. Gwynne, The Iodine-Iodide Interaction, J. Am. Chem. Soc. 74, 2748 (1952).

104. Dawson, H.M. and F. Powis, The Conditions of Isodynamic Change in the Aliphatic Ketones. Part I. The Autocatalytic Reaction between Acetone and Iodine, J. Chem. Soc. 101, 1503 (1912).

105. Dawson, H.M. and J.S. Carter, Acid and Salt Effects in Catalyzed Reactions, Part I., J. Chem. Soc., 2282 (1926).

106. Dawson, H.M. and N.C. Dean, Acid and Salt Effects in Catalyzed Reactions, Part II. The Minimum Reaction Velocities for Acid-Salt Mixtures, J. Chem. Soc., 2872 (1926).

107. Degn, H., Evidence of a Branched Chain Reaction in the Oscillating Reaction of Hydrogen Peroxide, Iodine and Iodate, Acta Chem. Scand. 21, 1057 (1967).

108. De Keeper, P., I.R. Epstein and K. Kustin, Bistability in the Oxidation of Arsenite by Iodate in a Stirred Flow Reactor, J. Am. Chem. Soc. 103, 6121 (1981).

109. De Keeper, P. and I.R. Epstein, A Mechanistic Study of Oscillations and Bistability in the Briggs-Rauscher Reaction, J. Am. Chem. Soc. 104, 49 (1982).

110. Dess, H.M. and R.W. Parry, The Oxidation of Arsenic(III) Fluoride with Bromine and Iodine, J. Am. Chem. Soc. 78, 5735 (1956).

111. Dhar, N., Catalysis. Part IV. Temperature Coefficients of Catalysed Reactions, J. Chem. Soc. 111, 707 (1917).

112. Dickenson, R.G. and H. Lotzkar, The Kinetics of the Thermal Isomerization of Cinnamic Acid Catalyzed by Iodine, J. Am. Chem. Soc. 59, 472 (1937).

113. Dolan, S.P., S.A. Sinex and S.G. Capar, On-Line Preconcentration and Volatilization for Inductively Coupled Plasma Atomic Emission Spectrometry, Anal. Chem., 63, 2539 (1991).

114. Dosaj, S.S. and W.V. Bhagwat, Dark Reaction between Sodium Formate and Iodine, J. Ind. Chem. Soc. 11, 330 (1934).

115. Dozsa, L., D.A. Durham and M.T. Beck, Catalysis of the Iodine-Azide Reaction by Inert Thiocyanato Complexes, J. Inorg. Nucl. Chem. 31, 3659 (1969).

116. Dougherty, D.R., J.R. Novotny, E.L. Jeffers, T. Poorman, Continuous Monitoring of Effluent Iodine Levels of Space Station Water Using Solid State Technology, SAE 921265 presented at 22nd International Conference on Environmental Systems, Seattle, July 13-16, 1992.

117. Dubler, E. and L. Linowsky, Proof of the Existence of Linear,Centrosymmetric Polyiodide Ion I_4^{2-} The Crystal Structure of $Cu(NH_3)_4I_4$, Helv. Chim. Acta 58, 2604 (1975).

118. Duchin, K.L., Y.S. Lee and J.W. Mills, Quenching of I_2 Vapor Fluorescence Excited with He-Ne Laser Light, A Kinetics -Spectroscopy Experiment, J. Chem. Ed. 50, 858 (1973).

119. Dushman, S., The Rate of Reaction between Iodic and Hydriodic Acids, J. Phys. Chem. 8, 453 (1904).

120. Egger, K.W., D.M. Golden and S.W. Benson, Iodine Catalyzed Isomerization of Olefins. II. The Resonance Energy of the Allyl Radical and the Kinetics of the Positional Isomerization of 1-Butene, J. Am. Chem. Soc. 86, 5420 (1964).

121. Egger, K.W. and S.W. Benson, Iodine and Nitric Oxide Catalyzed Isomerization of Olefins. V. Kinetics of the Geometrical Isomerization of 1,3-Pentadiene, a Check on the Rate of Rotation about Single Bonds, and the Allylic Resonance Energy, J.Am. Chem. Soc. 87, 3314 (1965).

122. Egger, K.W. and S.W. Benson, Nitric Oxide and Iodine Catalyzed Isomerization of Olefins. VI. Thermodynamic Data from Equilibrium Studies of the Geometrical and Positional Isomerization of n-Pentenes, J. Am. Chem. Soc. 88, 236 (1966).

123. Egger, K.W. and S.W. Benson, Nitric Oxide and Iodine Catalyzed Isomerization of Olefins. VII. The Stabilization Energy in the Pentadienyl Radical and the Kinetics of the Positional Isomerization of 1,4-Pentadiene, J. Am. Chem. Soc. 88, 241 (1966).

124. Egger, K.W., Iodine-Catalyzed Isomerization of n-Heptenes. Thermodynamic Data for Positional and Geometrical Isomerization and the cis Effect in the Entropy Difference of Geometrical Isomer Pairs, J. Am. Chem. Soc. 89, 504 (1966).

125. Eigen, M. and Kustin, K., The Kinetics of Halogen Hydrolysis, J. Am. Chem. Soc., 84, 1355 (1962).

126. Eiland, H.M. and M. Kahn, Some Observations on the Oxidation of Iodine at Low Concentrations, J. Phys. Chem. 65, 1317 (1961).

127. Ellis, K.V. and H.B.R. van Vree, Iodine Used as a Water Disinfectant in Turbid

Waters, Wat. Res. 23, 671 (1989).

128. Elving, P.J. and C.L. Hilton, Polarographic Behavior of Organic Compounds. XII. Relative Ease of Carbon-Halogen Bond Fission in the Iodobenzoic Acids, Phthalic Anhydrides and Phthalates, J. Am. Chem. Soc. 74, 3368 (1952).

129. Espenson, J.H., Kinetics and Mechanism of the Aquation of Iodopentaaquochromium(III) Ion and of Oxidation of Coordinated Iodide Ion in Acidic Solution, Inorg. Chem. 3, 968 (1964).

130. Espenson, J.H., Mechanisms of the Reaction of Vanadium(IV) and Chromium(VI) and of the Induced Oxidation of Iodide Ion, J. Am. Chem. Soc. 86, 5101 (1964).

131. Esteso, M.A., F.F. Hernandez-Luis, L.F. Fernandez-Merida and O.M. Bonzalez-Diaz, Activity Coefficients in Mixed-Electrolyte Solutions at 25°C: Na-Formate + NaCl System, J. Solution Chem. 18, 265 (1989).

132. Eyal, E. and A. Treinin, A Spectrophotometric Study of the System $I_2 + Br^-$, J. Am. Chem. Soc. 86 (1964).

133. Faull, R.F. and G.K. Rollefson, The Effect of Iodine on the Rate of Decomposition of Ethylene Oxide, J. Am. Chem. Soc. 59, 1361 (1937).

134. Field L. and C.M. Lukehart, The Sulfur-Iodine Bond, in Sulfur in Organic and Inorganic Chemistry, Vol.4, A. Senning, Ed., Marcel Dekker, New York (1982).

135. Ferranti, F., A Kinetic Study of the Reaction between Octacyanomolybdate(V) and Iodide Ions, J. Chem. Soc. (A), 134 (1970).

136. Fina, L.R., N Hassouna, G.L. Horacek, J.P. Lambert and J.L. Lambert, Viricidal Capability of Resin-Triiodide Demand-Type Disinfectant, Appl. Environ. Microbiol. 44, 1370 (1982).

137. Fishman, M.J. and M.W. Skougstad, Indirect Spectrophotometric Determination of Traces of Bromide in Water, Anal. Chem. 35, 146 (1963).

138. Forbes, G.S. and A.F. Nielson, Photoiodination of the Butenes, Propylene and Ethylene at Low Temperatures. Preparation and Photolysis of 1,2-Diiodobutane, J. Am. Chem. Soc. 59, 693 (1937).

139. Forster, D. and D.M.L. Goodgame, Iodine Adducts of Co-ordinated Isothiocyanate Groups, J. Chem. Soc. (A), 170 (1966).

140. Forster, E.L.C., The Rate of Formation of Iodates in Alkaline Solutions of Iodine, J.

Phys. Chem. 7, 640 (1903).

141. Freiberg, L.A., On the Mechanism of Oxidation of Enolizable Nonmethyl Ketones by Base and Iodine. The Role of Atmospheric Oxygen, J. Am. Chem. Soc. 89, 5297 (1967).

142. Friedman, H.B. and B.E. Anderson, Neutral Salt Action. I. The Effect of Neutral Salts on the Velocity of the Reaction $2Fe(CN)_6^{-3} + 3I^- \rightarrow 2Fe(CN)_6^{-4} + I_3^-$, J. Am. Chem. Soc. 61, 116 (1939).

143. Freund, T. and N. Nuenke, The Kinetics of the Reduction of Iodate Ion by Borohydride Ion in Basic Aqueous Solutions, J. Am. Chem. Soc. 84, 2678 (1962).

144. Fujii, T., T. Uehiro and Y. Nojiri, Real-Time Monitoring of Iodine in Process Off-Gas by Inductively Coupled Plasma-Atomic Emission Spectroscopy, Anal. Chem. 62, 414 (1990).

145. Fujiwara, T., N. Tanimoto, J-J. Huang and T. Kumamaru, Generation of Chemiluminescence upon Reaction of Iodine with Luminol in Reversed Micelles and Its Analytical Applicability, Anal. Chem. 61, 2800 (1989).

146. Fukutomi, H. and G. Gordon, Kinetic Study of the Reaction between Chlorine Dioxide and Potassium Iodide in Aqueous Solution, J. Am. Chem. Soc. 89, 1362 (1967).

147. Funai, I.A. and M.A. Blesa, Kinetics and Mechanism of the Reaction of Iodine with Isonicotinoylhydrazide, Can. J. Chem. 62, 2923 (1984).

148. Furrow, S.D., Kinetics and Mechanism for the Iodination of Methylmalonic Acid, Int. J. Chem. Kinet. 11, 131 (1979).

149. Furrow, S.D. and R.M. Noyes, The Oscillatory Briggs-Rauscher Reaction. 1. Examination of Subsystems, J. Am. Chem. Soc. 104, 38 (1982).

150. Furrow, S.D. and R.M. Noyes, The Oscillatory Briggs-Rauscher Reaction. 2. Effects of Substitutions and Additions, J. Am. Chem. Soc. 104, 42 (1982).

151. Furrow, S.D. and R.M. Noyes, The Oscillatory Briggs-Rauscher Reaction. 3. A Skeleton Mechanism for Oscillations, J. Am. Chem. Soc. 104, 45 (1982).

152. Furuichi, R., I. Matsuzaki and H.A. Liebhafsky, Rate of the Dushman Reaction at Low Iodide Concentrations.Experimental Method and Temperature Coefficient, Inorg. Chem. 11, 952 (1972).

153. Furuyama, S., D.M. Golden and S.W. Benson, Kinetics Studies of the Reactions

CH_2I_2+ HI --> CH_3I + I_2 and 2 CH_3I --> CH_4+ CH_2I_2, The Heat of Formation of the Iodomethyl Radical, Int. J. Chem. Kinet. 1, 283 (1969).

154. Furuyama, S., D.M. Golden and S.W. Benson, Kinetic Study of the Reaction CHI_3 + HI --> CH_2I_2 + I_2 . A Summary of Thermochemical Properties of Halomethanes and Halomethyl Radicals, J. Am. Chem. Soc. 91, 7564 (1969).

155. Gardener, I.J. and R.M. Noyes, Effects of Substituents on the Radical Exchange Reaction between Benzyl Iodide and Iodine, J. Am. Chem. Soc. 83, 2409 (1961).

156. Gaswick, D.C. and J.H. Krueger, Kinetics and Mechanism of the Chromium (VI)-Iodide Reaction, J. Am. Chem. Soc. 91, 2240 (1969).

157. Geiger, A. and H.G. Hertz, Proton Magnetic Relaxation Study of Water Orientation Around I^- and Li^+, J. Solution Chem. 5, 365 (1976).

158. Gensch, K.-H., I.H. Pitman and T. Higuchi, Oxidation of Thioethers to Sulfoxides by Iodine. II. Catalytic Role of Some Carboxylic Acid Anions, J. Am. Chem. Soc. 90, 2096 (1968).

159. Gerin, M. and J. Fresco, Potentiometric Properties of Trialkylammonium ion-exchangers, Can. J. Chem. 58, 1412 (1980).

160. German, E.D. and R.R. Dogonadze, The Kinetics of Nucleophilic Substitution Processes in the Alkyl Halides. Part B-Analysis of Experimental Data, Int. J. Chem. Kinet. 6, 467 (1974).

161. Gibson, H.W., The Chemistry of Formic Acid and its Simple Derivatives, Chem. Rev. 69, 673 (1969).

162. Gillespie, R.J. and J.B. Senior, Cations and Oxy Cations of Iodine. II. Solutions of Iodosyl Sulfate, Iodine Dioxide, and Iodic Acid-Iodine Mixtures in Sulfuric Acid and Dilute Oleum, Inorg. Chem. 3, 972 (1964).

163. Gillespie, R.J. and J.B. Milne, The Iodine Cation I_2+, Chem. Comm., 158 (1966).

164. Ginn, S.G.W. and J.L. Wood, The Structure of the Tri-iodide Ion, Chem. Comm., 262 (1965).

165. Golden, D.M., K.W. Egger and S.W. Benson, Iodine-Catalyzed Isomerization of Olefins. I. Thermodynamic Data from Equilibrium Studies of Positional and Geometrical Isomerization of 1-Butene and 2-Butene, J. Am. Chem. Soc. 86, 5416 (1964).

166. Golden, D.M., A.S. Rodgers and S.W. Benson, The Kinetics and Mechanism of the Reaction $I_2 + C_3H_6 = C_3H_5I + I$ and the Heat of Formation of the Allyl Radical, J. Am. Chem. Soc. 88, 3196 (1966).

167. Goldman, S., R.G. Bates and R.A. Robinson, Osmotic Coefficients and Activity Coefficients of Iodic Acid at High Concentrations, J. Solution Chem. 3, 593 (1974).

168. Goodenough, R.D., J.F. Mills and J. Place, Anion Exchange Resin (Polybromide Form) as a Source of Active Bromine for Water Disinfection, Env. Sci. Technol. 3, 854 (1969).

169. Gould, J.P., M. Giabbai and J-S. Kim, Formation of Iodinated Trihalomethanes, in Water Chlorination: Chemistry, Environmental Impact and Health Effects, Vol. 5, R.L. Jolley, R.J. Bull, W.P. Davis, S. Katz, M.H. Roberts, Jr., and V.A. Jacobs, Eds., Lewis, Chelsea, MI (1985).

170. Gowda, B.T. and J.I. Bhat, Mechanistic Studies with Positive Iodine. Kinetics of Oxidation of Thiocyanate Ion by Iodine Monochloride and Aqueous Iodine in Perchloric Acid Medium, Int. J. Chem. Kinet. 21, 621 (1989).

171. Gregory, J. and M.J. Semmens, Sorption of Carboxylate Ions by Strongly Basic Anion Exchangers, J. Chem. Soc. Faraday Trans. 68, 1045 (1972).

172. Griffiths, T.R. and R.H. Wijayanayake, Combined Effects of Temperature and Pressure upon the Charge Transfer to Solvent Spectrum of Iodide in Water and Non-aqueous Solvents, J.Chem. Soc. Faraday Trans. 69, 1899 (1973).

173. Grovenstein, E., Jr., N.S. Aprahamian, C.J. Bryan, N.S. Gnanapragasam, D.C. Kilby, J.M. McKelvey, Jr., and R.J. Sullivan, Aromatic Halogenation. IV. Kinetics and Mechanism of Iodination of Phenol and 2,6-Dibromophenol, J. Am. Chem. Soc. 95, 4261 (1973).

174. Grys, St., The Gas-Liquid Chromatographic Determination of Inorganic Iodine, Iodide and Tightly Bound Iodine in Milk, J. Chromatog. 100, 43 (1974).

175. Guthrie, J.P., J. Cossar and A. Klym, The pK_a of Acetone: A Kinetic Method for Determining the pK_as of Ketones in Aqueous Solution, J. Am. Chem. Soc. 104, 895 (1982).

176. Haim, A. and H. Taube, The Reactions of Iodopentamminecobalt(III) with Various "One-electron" Oxidation-Reduction Reagents, J. Am. Chem. Soc. 85, 495 (1963).

177. Haim, A. and H. Taube, The Reactions of Iodopentaamminecobalt(III) with Various "Two- Electron" Oxidizing Agents, J. Am. Chem. Soc. 85, 3108 (1963).

178. Haimovich, O. and A. Treinin, The Disproportionation of Hypoiodite, J. Phys. Chem. 71, 1941 (1967).

179. Hamilton, D.W. and R.M. Noyes, Effects of Substituents on the Exchange of Iodine with Benzoyl Iodides in Nonpolar Solvents, J. Am. Chem. Soc. 91, 1740 (1969).

180. Hammes, G.G. and B. Widom, On the Mechanism of the Hydrogen-Iodine Reaction, J. Am. Chem. Soc. 96, 7621 (1974).

181. Hammick, D.L., W.K. Hutchison and F.R. Snell, The Rate of Reaction of Bromine with Aqueous Formic Acid, J. Chem. Soc., 2715 (1925).

182. Hammick, D.L. and M. Zvegintzov, The Rate of Reaction Between Formic Acid and Iodine in Aqueous Solution, J. Chem. Soc., 1105 (1926).

183. Hand, E.S. and W.P. Jencks, Nonlinearity in Buffer-Rate Relationships. The Significance of Carboxylate-Acid Complexes, J. Am. Chem. Soc. 97, 6221 (1975).

184. Hanna, A., A. Saul and K. Showalter, Detailed Studies of Propagating Fronts in the Iodate Oxidation of Arsenous Acid, J. Am. Chem. Soc. 104, 3838 (1982).

185. Hashmall, J.A., B.E. Mills, D A. Sl ..ey and A. Streitwieser, Jr., A Comparison of Valence Shell and Core Ionization Potentials of Alkyl Iodides, J. Am. Chem. Soc. 94, 4445 (1972).

186. Hasty, R.A., A Gas Chromatographic Method for the Microdetermination of Iodine, Mikrochim. Acta 348 (1971).

187. Hasty, R.A., Gas Chromatographic Microdetermination of Iodine by Derivatization with Ketones, Mikrochim. Acta 621 (1973).

188 Hasty, R.A., Reduction of Iodate by Hydrazine: Application of the Iodide Ion Selective Electrode to the Uncatalyzed Reaction, Mikrochim. Acta 925 (1973).

189. Hatch, G.L., An Iodinated Anion Exchange Resin for the Production of Disinfecting Levels of Iodine and Hypiodous Acid, paper presented at American Chemical Society, Division of Environmental Chemistry Meeting, Anaheim, California, March 12-17, 1977.

190. Hatch, G.L., J.L. Lambert and L.R. Fina, Some Properties of the Quaternary Ammonium Anion-Exchange Resin-Triiodide Disinfectant for Water, Ind. Eng. Chem. Prod. Res. Dev. 19, 259 (1980).

4 OF 4

N93-27122 UNCLAS

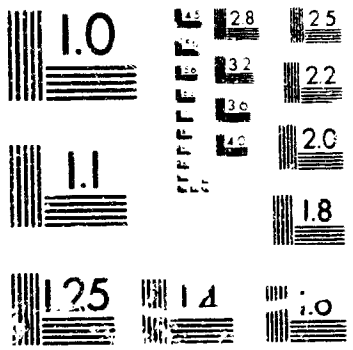

191 Hatch, G.L., Preparation of Iodinated Anion-Exchange Resins for the Controlled Release of Disinfecting Levels of Iodine and Hypoiodous Acid, Ind. Eng. Chem. Prod. Res. Dev. 20, 382 (1981).

192. Hatch, G.L., Effect of Temperature on the Starch-Iodine Spectrophotometric Calibration Line, Anal. Chem. 54, 2002 (1982).

193. Hatch, G.L., Hypoiodous Acid, Iodine, and Iodide Determination with Leuco Crystal Violet and N-Chlorosuccinimide-Succinimide Reagents, Anal. Chem. 56, 2238 (1984).

194. Heurtebise, M. and W.J. Ross, Application of an Iodide-Specific Resin to the Determination of Iodine in Biological Fluids by Activation Analysis, Anal. Chem. 43, 1438 (1971).

195. Heurtebise and W.J. Ross, Radiochemical Separations with Halogenated Resins, Anal. Chem. 44, 596 (1972).

196. Higuchi, T. and K.-H. Gensch, Oxidation of Thioethers by Iodine to Sulfoxides. Catalytic Role of Certain Inorganic Nucleophiles, J. Am. Chem. Soc. 88, 5486 (1966).

197. Higuchi, T., I.H. Pitman and K.-H. Gensch, Asymmetric Oxidation of Thioethers to Sulfoxides. Configurational Specificity Induced by Optically Active Organic Catalysts, J. Am. Chem. Soc. 88, 5676 (1966).

198. Hildebrand, J.H., H.A. Benesi and L.M. Mower, Solubility of Iodine in Ethyl Alcohol, Ethyl Ether, Mesitylene, p-Xylene, 2,2-Dimethylbutane, Cyclohexane and Perfluoro-n-heptane, J. Am. Chem. Soc. 72, 1017 (1950).

199. Hildebrand, J.H. and D.N. Glew, The Entropy of Solution of Iodine, J. Phys. Chem. 60, 618 (1956).

200. Hildebrand, J.H., The Entropy of Solution of Iodine at Constant Volume, J. Phys. Chem. 64, 370 (1960).

201. Hiller, F.W. and J.H. Krueger, The Rate and Mechanism of the Iodine-Formate Reaction in Dimethyl Sulfoxide-Water Solvents, Inorg. Chem. 6, 528 (1967).

202. Hine, J., N.W. Burske, M. Hine and P.B. Langford, The Relative Rates of Formation of Carbanions by Haloforms, J. Am. Chem. Soc. 79, 1406 (1957).

203. Hogge, E.A. and M.B. Kraichman, The Limiting Current on a Rotating Disc Electrode in Potassium Iodide-Potassium Triiodide Solutions, J. Am. Chem. Soc. 76, 1431 (1954).

204. Holder, D.W.,Jr., and R.M. Bagdigian, Phase III Integrated Water Recovery Testing at MSFC: Closed Hygiene and Potable Loop Test Results and Lesson Learned, SAE 921117 presented at 22nd International Conference on Environmental Systems, Seattle, July 13-16, 1992.

205. Howlett, K.E. and S. Sarsfield, Kinetics and Mechanisms of Redox Reactions in Aqueous Solutions. Part II. The Reactions between Chromium(VI) and Iodide, J. Chem. Soc (A), 683 (1968).

206. Hsia, K.-L. and R.M. Fuoss, Conductance of the Alkali Halides. XI. Cesium Bromide and Iodide in Water at 25°, J. Am. Chem. Soc. 90, 3055 (1968).

207. Hunter, W.H. and L.M. Seyfried, A Catalytic Decomposition of Certain Phenol Silver Salts. V. The Action of Iodine on the Sodium Salt of Trichlorophenol, J. Am. Chem. Soc. 43, 151 (1921).

208. Huq, R., Kinetics of the Reaction between Methyl Iodide and Silver Nitrate in Aqueous Solution, J. Chem. Soc. Faraday Trans. 68, 1824 (1972)

209. Hwang, R.J. and S.W. Benson, Kinetics of Iodination of Hydrogen Sulfide by Iodine and the Heat of Formation of the SH Radical, Int. J. Chem. Kinet. 11, 579 (1979).

210. Hwang, R.J. and S.W. Benson, Thermochemistry of the Reaction of Hydrogen Sulfide withIodine and the Heat of Formation of HSI-a New Sulfur Compound, J. Am. Chem. Soc. 101, 2615 (1979).

211. Indelli, A. and E.S. Amis, Activation Energy Measurements in the Reaction between Iodide and Persulfate Ions in the Presence of Different Salts, J. Am. Chem. Soc. 82, 332 (1960).

212. Indelli, A., G. Nolan, Jr. and E.S. Amis, Salt Effects in the Reaction between Bromate and Iodide Ions, J. Am. Chem. Soc. 82, 3233 (1960).

213. Indelli, A., Salt Effects in the Reactions between Iodate and Iodide, J. Phys. Chem. 65, 240 (1961).

214. Jaffe, R.L., J.M. Henry and J.B. Anderson, Molecular Dynamics of the Hydrogen Iodide and Hydrogen-Iodide Exchange Reactions, J. Am. Chem. Soc. 98, 1140 (1976).

215. Jeffers, E.L. and C.D. Jolly, Development of the Process Control Water Quality Monitor for Space Station Freedom, SAE Paper No. 911432, presented at 21st International Conference on Environmental Systems, San Francisco, July 15-18, 1991.

216. Jeffers, E.L., and J. Novotny, Process Control Water Quality Monitor for Space Station Freedom - Development Update, SAE 921264 presented at 22nd International Conference on Environmental Systems, Seattle, July 13-16, 1992.

217. Jenkins, F.E. and G M. Harris, Some Isotopic Exchange Reactions of Iodine Cyanide, J. Phys. Chem. 61, 249 (1957).

218. Johnson, C.E., Jr. and S. Winstein, Oxidation-Reduction. I. The Kinetics of the Reduction of Iodine by Titanous Ion, J. Am. Chem. Soc. 73, 2601 (1951).

219. Johnson, C.E., Jr. and S. Winstein, Oxidation-Reduction. II. Catalysis of the Titanous Chloride-Iodine Reaction by Quinones and Phenazines, J. Am. Chem. Soc. 74, 755 (1952).

220. Johnson, C.E., Jr. and S. Winstein, Oxidation-Reduction. III. The Kinetics of the Reduction of Sodium Anthraquinone beta-Sulfonate by Titanous Ion and Oxidation by Iodine, J. Am. Chem. Soc. 74, 3105 (1952).

221. Johnson D.C. and S. Bruckenstein, A Study of the Kinetics of the Oxidation of Arsenic(III) by Electrogenerated Iodine in Alkaline Media, J. Am. Chem. Soc. 90, 6592 (1968).

222. Jolly, C.D., Regenerable Biocide Delivery Unit, Final Report, Contract NAS9-18113, Umpqua Research Company, August 1989.

223. Jordan, J. and R.A. Javick, Rate and Mechanism of the Electrooxidation of Iodide, J. Am. Chem. Soc. 80, 1264 (1958).

224. Jortner, J., R. Levine, M. Ottoleinghi and G. Stein, The Photochemistry of the Iodide Ion in Aqueous Solution, J. Phys. Chem. 65, 1232 (1961).

225. Kagawa, K., F. Tokuyama and M. Ishihane, Emmision from I_3^- on the Surface of Potassium Iodide, J. Luminescence 50, 197 (1991).

226. Kamson, O.F., Flow-Injection Determination of Some Sulphur Anions Via the Catalyzed Iodine-Azide Reaction, Anal. Chim. Acta 211, 299 (1988).

227. Kaner, R.J. and I.R. Epstein, Induction and Inhibition of Chemical Oscillations by Iodide Ion in the Belousov-Zhabotinskii Reaction, J. Am. Chem. Soc. 100, 4073 (1978).

228. Kasai, P.H. and D. McLeod, Jr., Electron Spin Resonance Study of Pyrolysis and Photolysis of 2-Iodoacetic Acid and 2-Iodoacetamide, J. Am. Chem. Soc. 94, 7975 (1972).

229. Katzin, L.I. and E. Gebert, Solvent Effects in the Iodide-Iodine-Triiodide Complex Equilibrium, J. Am. Chem. Soc. 76, 2049 (1954).

230. Katzin, L.I. and E. Gebert, The Iodide-Iodine-Triiodide Equilibrium and Ion Activity Coefficient Ratios, J. Am. Chem. Soc. 77, 5814, (1955).

231. Kaur, S. and T.S. Lobana, Spectrophotometric Determination and Thermodynamic Parameters of Species Formed on Reactions of Some Mono- and Di-Tertiary-Phosphine Sulphides with Molecular Iodine in Different Solvents, J. Inorg. Nucl. Chem. 43, 2439 (1981).

232. Ke, P.J., R.J. Thibert, R.J. Walton and D.K. Soules, Catalytic Determination of Iodine in Serum at Nanogram Levels Using the As(III)/Ce(IV) Reaction, Mikrochim. Acta 569 (1973).

233. Kern, D.M. and C.-H. Kim, Iodine Catalysis in the Chlorite-Iodide Reaction, J. Am. Chem. Soc.87, 5309 (1965).

234. Kertesz, M. and F. Vonderiszt, Electronic Structure of Long Polyiodide Chains, J. Am. Chem. Soc. 104, 5889 (1982).

235. Kimball, J.W., R.L. Kramer and E.E. Reid, The Iodometric Estimation of Mercaptans, J. Am. Chem. Soc. 43, 1199 (1921).

236. Kimpe, N.D. and R. Verhe, The Chemistry of alpha-Haloketones, alpha-Haloaldehydes and alpha-Haloimines, John Wiley & Sons, New York (1988).

237. Kleemann, E. and G. Herrmann, Uber die Adsorption von Tellur(IV), Jodid und Jodat an Anionenaustauschern, J. Chromatog. 3, 275 (1960).

238. Kleinberg, J. and J. Sattizahn, Exchange between Radioactive Iodine and Derivatives of Monopyridine Iodine(I) in Pyridine, J. Am. Chem. Soc. 73, 1865 (1951).

239. Kolthoff, I.M. and J. Jordan, Voltammetry of Iodine and Iodide at Rotated Platinum Wire Electrodes, J. Am. Chem. Soc. 75, 1571 (1953).

240. Kokkinidis, G., E. Hatzigrigoriou, D Sazou and A. Varvagolis, Electrochemical Reduction of Some Hypervalent Iodine Compounds, Electrochim. Acta 36, 1391 (1991).

241. Kolthoff, I.M. and S.E. Khalafalla, Effect of Iodide and Bromide on the One-Electron Polarographic Reduction of Hexammine Cobalt(III) Chloride, J. Am. Chem. Soc. 85, 664 (1963).

242. Korosov, F., Reaction of Tantalum, Colombium and Vanadium with Iodine, J. Am. Chem. Soc. 61, 838 (1939).

243. Krestov, G A., A.M. Kolker and V.P. Korolev, Peculiar Properties of Sodium Iodide in Alcohols, Acetone, and Alcohol-Water Mixtures at Lower Temperatures, J. Solution Chem. 11, 593 (1982)

244. King, K.D., D.M. Golden, G.N. Spokes and S.W. Benson, Very Low Pressure Pyrolysis IV. The Decomposition of i-Propyl Iodide and n-Propyl Iodide, Int. J. Chem. Kinet. 3, 411 (1971).

245. King, L.C. and R.J. Hlavecek, The Reaction of Ketones with Iodine and Thiourea, J. Am. Chem. Soc. 72, 3722 (1950).

246. Krzewska, S. and H. Podsiadky, Studies on the Reaction of Copper(II) with Thiourea-I. Silver-Silver Thiourea Electrode for Determination of Free Thiourea Concentration in $HClO_4$ Medium, J. Inorg. Nucl. Chem. 42, 83 (1980).

247. Krzewska, S., L. Pajdowski and H. Podsiadky, Studies on the Reaction of Copper(II) with Thiourea-II. The Modification of Bjerrum's Method. The Determination of Equilibrium in Simultaneous Redox and Complexation Reactions, J. Inorg. Nucl. Chem. 42, 87 (1980).

248. Krzewska, S., H. Podsiadky and L. Pajdowski, Studies on the Reaction of Copper(II) with Thiourea-III. Equilibrium and Stability Constants in Cu(II)-Thiourea-$HClO_4$ Redox System, J.Inorg. Nucl. Chem. 42, 89 (1980).

249. Lambert, J.L., G.L. Hatch and B. Mosier, Iodide and Iodine Determination in the Parts-per-Billion Range with Leuco Crystal Violet and N-Chlorosuccinimide-Succimide Reagents, Anal. Chem. 47, 915 (1975).

250. Lambert, J.L., G.T. Fina and L.R. Fina, Preparation and Properties of Triiodide-, Pentaiodide-, and Heptaiodide-Quaternary Ammonium Strong Base Anion-Exchange Resin Disinfectants, Ind. Eng. Chem. Prod. Res. Dev. 19, 256 (1980).

251. Lang, R.P., Molecular Complexes and their Spectra. XIV. Iodine Complexes with Thiourea and Thioacetamide, J. Am. Chem. Soc. 84, 1185 (1962).

252. Larsen, A.A., C. Moore, J. Spraque, B. Cloke, J. Moss and J.O. Hoppe, Iodinated 3,5-Diaminobenzoic Acid Derivatives, J. Am. Chem. Soc. 78, 3210 (1956).

253. Lasselle, P.A. and J.G. Aston, The Conductivity of Sodium Iodide Solutions at 25° and the Limiting Conductance of the Iodide Ion, J. Am. Chem. Soc. 55, 3067 (1933).

254. Lawler, R.G., H.R. Ward, R.B. Allen and P.E. Ellenbogen, Chemical Exchange Broadening and Chemically Induced Dynamic Nuclear Polarization during a Free Radical Initiated Chain Iodine Transfer Reaction, J. Am. Chem. Soc. 93, 787 (1971).

255. Leaist, D.G., Ternary Diffusion with Charged-Complex Formation in Aqueous I_2 + NaI and I_2 + KI Solutions, J. Solution Chem. 17,359 (1988).

256. Leary, J.A. and M. Kahn, Isotopic Exchange between Potassium Iodide and Benzyl Iodides. Solvent Effects, J. Am. Chem. Soc. 81, 4173 (1959).

257 Leffler, J.E., D.C. Ward and A. Burdurogiu, Substituent Effects on the Rate and Mechanism of the Decomposition of Phenyliodine Dicarboxylates, J. Am. Chem. Soc. 94, 5339 (1972).

258. Leopold, K.R. and A. Haim, Equilibrium, Kinetics, and Mechanism of the Malonic Acid-Iodine Reaction, Int. J. Chem. Kinet. 9, 83 (1977).

259. Levine, S. and R.M. Noyes, Mechanisms of Exchange Reactions between Elementary Iodine and Aromatic Iodides, J. Am. Chem. Soc. 80, 2401 (1958).

260. Lewis, C. and D.A. Skoog, Spectrophotometric Study of a Thiocyanate Complex of Iodine, J. Am. Chem. Soc. 84, 1101 (1962).

261. Li, C.H. and C.F. White, Kinetics of Hypoiodite Decomposition, J. Am. Chem. Soc. 65, 335 (1943).

262. Liebhafsky, H. A., Reactions Involving Hydrogen Peroxide, Iodine and Iodate Ion. III. The Reduction of Iodate by Hydrogen Peroxide, J. Am. Chem. Soc. 53, 896 (1931).

263. Liebhafsky, H. A., Reactions Involving Hydrogen Peroxide, Iodine and Iodate Ion. IV. The Oxidation of Iodine to Iodate Ion by Hydrogen Peroxide, J. Am. Chem. Soc. 53, 2074 (1931).

264. Liebhafsky, H.A., The Catalytic Decomposition of Hydrogen Peroxide by the Iodine-Iodide Couple at 25°, J. Am. Chem. Soc. 54, 1792 (1932).

265. Liebhafsky, H.A., The Catalytic Decomposition of Hydrogen Peroxide by the Iodine-Iodide Couple. II. The Rate of Oxidation, in Neutral Solution, of Hydrogen Peroxide by Iodine, J. Am. Chem. Soc. 54, 3499 (1932).

266. Liebhafsky, H.A., The Catalytic Decomposition of Hydrogen Peroxide by the Iodine-Iodide Couple. III. The Rate of Oxidation, in Acid Solution, of Hydrogen Peroxide by Iodine, J. Am. Chem. Soc. 54, 3504 (1932).

267. Liebhafsky, H.A. and A. Mohammad, Kinetics of the Reduction, in Acid Solution, of Hydrogen Peroxide by Iodide Ion, J. Am. Chem. Soc. 55, 3977 (1933).

268. Liebhafsky, H.A., The Hydrolysis of Bromine. The Hydration of the Halogens. The Mechanism of Certain Halogen Reactions, J. Am. Chem. Soc. 61, 3513 (1939).

269. Liebhafsky, H.A. and L.S. Wu, Reactions Involving Hydrogen Peroxide, Iodine, and Iodate Ion. V. Introduction to the Oscillatory Decomposition of Hydrogen Peroxide, J. Am. Chem. Soc. 96, 7180 (1974).

270. Liebhafsky, H.A., W.C. McGavock, R.J. Reyes, G.M. Roe and L.S. Wu, Reactions Involving Hydrogen Peroxide, Iodine, and Iodate Ion. 6. Oxidation of Iodine by Hydrogen Peroxide at 50 °C, J. Am. Chem. Soc. 100, 87 (1978).

271. Liebhafsky, H.A. and G.M. Roe, The Detailed Mechanism of the Dushman Reaction Explored by Computer, Int. J. Chem. Kinet. 11, 693 (1979).

272. Liebhafsky, H.A., R. Furuichi and G.M. Roe, Reactions Involving Hydrogen Peroxide, Iodine, and Iodate Ion. 7. The Smooth Catalytic Decomposition of Hydrogen Peroxide, Mainly at 50 °C, J. Am. Chem. Soc. 103, 51 (1981).

273. Lii, R.-R. and S.I. Miller, Kinetics, Mechanism, and Isotope Rate Effect of the Base-Catalyzed Formation of 1-Haloalkynes from Acetylenes and Sodium Hypohalites, J. Am. Chem. Soc. 95, 1602 (1973).

274. Lin, C.-C., Volatility of Iodine in Dilute Aqueous Solutions, J. Inorg. Nucl. Chem. 43, 3229 (1981).

275. Lin, S., Y. Chen and Z. Wu, Determination of Iodide Ion in Environmental Water by Chemiluminescent Measurement, Fenxi Huaxue 16, 269 (1988). Chem. Abst. 10H81, October 1988.

276. Linke, W.F., Solubilities of Inorganic and Metal-organic Compounds, vol.1, 4th Ed., Van Nostrand, New York, 1958.

277. Luther, G.W., C.B. Swartz and W.J. Ullman, Direct Determination of Iodide in Seawater by Cathodic Stripping Square Wave Voltammetry, Anal. Chem. 60, 1721 (1988).

278. Luty, T. and J.C. Raich, Molecular to Atomic Transformation in Solid Iodine under High Pressure, Can. J. Chem. 66, 812 (1988).

279. Lynn, K.R. and P.E. Yankwich, Kinetics of the Reactions of Sodium Cyanide with

Some Alkyl Iodides, J. Phys. Chem. 64, 1719 (1960).

280. MacInnes, D.A. and M.O. Dayhoff, The Partial Molal Volumes of Potassium Chloride, Potassium and Sodium Iodides and of Iodine in Aqueous Solution at 25°, J. Am. Chem. Soc. 74, 1017 (1952).

281. MacInnes, D.A., C.-C. Yang and A.R. Pray, A Redetermination of the Value of the Faraday with the Iodine Coulometer, J. Phys. Chem. 61, 662 (1957).

282. MacNevin, W.M. and W.N. Carson, Jr., Catalysis of the Reaction of Carbon Monoxide with Iodine in Acid Solution, J. Am. Chem. Soc. 72, 42 (1950).

283. Mahootian, F., D.J. Hauri and J.E. Earley, New Region of Oscillations in the Chlorite-Bromate-Iodide System of Internally Coupled Chemical Oscillators, J. Phys. Chem. 96, 1014 (1992).

284. Maguin, F., A. Mellouki, G. Laverdet, G. Poulet, and G. LeBras, Kinetics of the Reactions of the IO Radical with Dimethyl Sulfide, Methanethiol, Ethylene and Propylene, Int. J. Chem. Kinet. 23, 237 (1991).

285. Mailen, J.C. and T.O. Tiffany, The Reaction of Iodine with Concentrated Nitric Acid, J. Inorg. Nucl. Chem. 37, 127 (1975).

286. Mailen, J.C., Equilibrium in the Oxidation of Iodine by Hyperazeotropic Nitric Acid, J. Inorg. Nucl. Chem. 37, 1019 (1975).

287. Majid, Y. A. and K.E. Howlett, Kinetics and Mechanisms of Redox Reactions in Aqueous Solutions. Part I. The Reaction between Cyanoferrate(III) and Iodide, J. Chem. Soc. (A), 679 (1968).

288. Manno, P.J. and W.H. Johnston, Extremely Slow Reactions. I. The Isotopic Exchange Reaction between Iodobenzene and Potassium Iodide, J. Am. Chem. Soc. 79, 807 (1957).

289. Marchetti, A. and D.R. Kearns, Spectroscopic and Photochemical Investigation of the Triplet States of p-Diiodobenzene and Other Iodoaromatics, J. Am. Chem. Soc. 89, 5335 (1967).

290. Marchin, G.L., L.R. Fina, J.L. Lambert and G.T. Fina, Effect of Resin Disinfectants-I_3 and -I_5 on Giardia muris and Giardia lamblia, Appl. Environ. Microbiol. 46, 965 (1983).

291. Marchin, G.L. and L.R. Fina, Contact and Demand-Release Disinfectants, CRC Crit. Rev. Environ. Cont. 19, 277 (1989).

292. Marchin, G.L., Application of the Pentaiodide Strong Base Resin Disinfectant to the U.S. Space Program, SAE Paper 901380, presented at 20th Intersociety Conference on Environmental Systems, Williamsburg, July 9-12, 1990.

293. Maros, L., M. Kaldy and S. Igaz, Simultaneous Determination of Bromide and Iodide as Acetone Derivatives by Gas Chromatography and Electron Capture Detection in Natural Waters and Biological Fluids, Anal. Chem. 61, 733 (1989).

294. Marshall, B.W. and E.A. Moelwyn-Hughes, The Kinetics of the Reaction between Methyl Iodide and Potassium Cyanide in Aqueous Solution, J. Chem. Soc., 2640 (1959).

295. Martin, D., J.L. Jourdain, G. Laverdet and G. LeBras, Kinetic Study of the Reaction of IO with CH_3SCH_3, Int. J. Chem. Kinet. 19, 503 (1987).

296. Mason, C.F.V., J.D. Farr and M.G. Bowman, The Reaction of the Alkaline Earth Metal Oxides with Iodine in the Presence of Water as Part of a Thermochemical Hydrogen Cycle, J. Inorg. Nucl. Chem. 42, 799 (1980).

297. Mauger, E. and E. Berliner, The Kinetics of Iodination of Propiolic Acid, J. Am. Chem. Soc. 94, 194 (1972).

298. McAlpine, R.K., The Reaction of Dilute Iodine and Ammonia Solutions, J. Am. Chem. Soc. 74, 725 (1952).

299. McFeters, G.A. and B.H. Pyle, Consequences of Bacterial Resistance to Disinfection by Iodine in Potable Water, SAE Paper No. 871489, presented at 17th Intersociety Conference on Environmental Systems, Seattle, July 13-15, 1987.

300. Mehra, H.C. and W.T. Frankenberger, Jr., Simultaneous Determination of Cyanide, Chloride, Bromide, and Iodide in Environmental Samples Using Ion Chromatography with Amperometric Detection, Microchem. J. 41, 93 (1990).

301. Mellouki, A., G. Laverdet, J.L. Jourdain and G. Poulet, Kinetics of the Reactions Br + NO_2 + M and I + NO_2 + M, Int. J. Chem. Kinet. 21, 1161 (1989).

302. Meyers, O.E. and J.W. Kennedy, The Kinetics of Iodine-Iodate Isotopic Exchange Reaction, J. Am. Chem. Soc. 72, 897 (1950).

303. Middaugh, R.L., R.S. Drago and R.J. Niedzielski, The Donor Properties of Some Carbonyl Compounds, J. Am. Chem. Soc. 86, 388 (1964).

304. Miller, L.L. and Hoffmann, The Electrochemical Formation of Carbonium and

Iodonium Ions from Alkyl and Aryl Iodides, J. Am. Chem. Soc. 89, 593 (1967).

305. Miller, L.L., E.P. Kujawa and C.B. Campbell, Iodination with Electrolytically Generated Iodine(I), J. Am. Chem. Soc. 92, 2821 (1970).

306. Miller, L.L. and B.F. Watkins, Scope and Mechanism of Aromatic Iodination with Electrochemically Generated Iodine(I), J. Am. Chem. Soc. 98, 1515 (1976).

307. Miller, M.L. and M. Doran, Concentrated Salt Solutions. II. Viscosity and Density of Sodium Thiocyanate, Sodium Perchlorate and Sodium Iodide, J. Phys. Chem. 60, 186 (1956).

308. Miller, M.L., Concentrated Salt Solutions. III. Electrical Conductance of Solutions of Sodium Thiocyanate, Sodium Iodide and Sodium Perchlorate, J. Phys. Chem. 60, 189

309. Miller, S.I. and R.M. Noyes, Iodide-ion Catalysis of the Elimination of Iodine from trans-Diiodoethylene and of the Addition of Iodine to Acetylene, J. Am. Chem. Soc. 74, 3403 (1952).

310. Moelwyn-Hughes, E.A. and A.R. Legard, The Kinetics of the Addition of Iodine to beta-Phenylpropiolic Acid, J. Chem. Soc., 424 (1933).

311. Muckle, S., Treatment of Spacecraft Humidity Condensate to Produce Potable Water, Masters Thesis, University of Houston, May 1990.

312. Mullineaux, R.D. and J.H. Raley, High Temperature Reactions of Iodine with Hydrocarbons. II. Aromatization, J. Am. Chem. Soc. 85, 3178 (1963).

313. Murray, H.D., The Hydrolysis of Iodine as Measured by the Iodine Electrode, J. Chem. Soc., 882 (1925).

314. Muthakia, G.K. and S.B. Jonnalagadda, Kinetics and Mechanism of Indigo Carmine-Acidic Iodate Reaction. An Indicator Reaction for Catalytic Determination of Ru(III), Int. J. Chem. Kinet. 21, 519 (1989).

315. Nakahara, T. and T. Wasa, Indirect Determination of Iodine in Seawater and Brine by Atmospheric Pressure Helium Microwave Induced Plasma Atomic Emission Spectrometry Using Continuous-Flow Cold-Vapor Generation of Mercury, Microchem. J. 41, 148 (1990).

316. Nakahara, T., S. Yamada and T. Wasa, Continuous-Flow Determination of Trace Iodine by Atmospheric-Pressure Helium Microwave-Induced Plasma Atomic Emission Spectrometry Using Generation of Volatile Iodine from Iodide, Appl. Spectrosc. 44,

1673 (1990).

317. Nakashima, M. and R.M. Noyes, Exchange and Decomposition Reactions of Isobutyl Iodide with Iodine, Int. J. Chem. Kinet. 1, 391 (1969).

318. Nakashima, M., C.Y. Mok and R.M. Noyes, Kinetics of Exchange of Iodine Atoms with Aromatic Iodides, J. Am. Chem. Soc. 91, 7635 (1969).

319. Nangia, P.S. and S.W. Benson, The Thermodynamics of the Dehydrogenation of Propane by Iodine Vapor, J. Am. Chem. Soc. 86, 2770 (1964).

320. Neptune, J.A. and E.L. King, The Rate Law for the Reaction of Selenious Acid and Iodide Ion, J. Am. Chem. Soc. 75, 3069 (1953).

321. Ng, K.C., A.H. Ali and J.D. Winefordner, Atomic Emission Detection of Non-Metals in Vapors Injected into Helium Hollow Cathode Discharge, Spectrochim. Acta 46, 309 (1991).

322. Niedzielski, R.J., R.S. Drago and R.L. Middaugh, Donor Properties of Some Sulfur Compounds, J. Am. Chem. Soc. 86, 1694 (1964).

323. Nikolov, G. St. and D. Mihailova, Kinetics of the Reaction of Iodide Ion Oxidation with Vanadium(V) in Sulphuric Acid Medium, J. Inorg. Nucl. Chem. 31, 2499 (1969).

324. Nolan, M.F., J.N. Pendlebury and R.H. Smith, Kinetics of the Reactions Br_2 + HCN, BrCN + I^-, $S(CN)_2$ + I^- in Aqueous Acid Solution, Int. J. Chem. Kinet. 7, 205 (1975).

325. Nomura, T. and T. Mimatsu, Electrolytic Determination of Traces of Iodide in Solution with a Piezoelectric Quartz Crystal, Anal. Chim. Acta 143, 237 (1982).

326. Noszticzius, Z., E. Noszticzius and Z.A. Schelly, On the Use of Ion-Selective Electrodes for Monitoring Oscillating Reactions. 1 Potential Response of the Silver Halide Membrane Electrodes to Hypohalous Acids, J. Am. Chem. Soc. 104, 6194 (1982).

327. Noyes, R.M. and D.J. Sibbett, Mechanisms of Exchange Reactionsbetween Elementary Iodine and Organic Iodides, J. Am. Chem. Soc. 75, 767 (1953).

328. Noyes, R.M., Hydrogen Iodide Revisited. Continued Significance of the Sullivan Experiments, J. Am. Chem. Soc. 96, 7623 (1974).

329. Nyman, C.J. and R.A. Plane, Polymerization in Cobalt Periodate Solutions, J. Am. Chem. Soc. 83, 2617 (1961).

330. Ogata, Y. and K. Aoki, Iodination of Aromatic Compounds with a Mixture of Iodine and Peracetic Acid. III. Autocatalysis and Relative Rates, J. Am. Chem. Soc. 90, 6187 (1968).

331. Olmsted, John, III, and G. Karal, Iodine-Sensitized Photoformation of Singlet Oxygen, J. Am. Chem. Soc. 94, 3305 (1972).

332. Orban, M. and I.R. Epstein, Oscillations and Bistability in Hydrogen-Platinum-Oxyhalogen Systems, J. Am. Chem. Soc. 103, 3723 (1981).

333. Painter, B.S. and F.G. Soper, Acid Catalysis in the Iodination of Phenol. Iodination by Acyl Hypoiodites, J. Chem. Soc., 342 (1947).

334. Palmer, D.A. and M.H. Lietzke, The Equilibria and Kinetics of Iodine Hydrolysis, Radiochim. Acta 31, 37 (1982).

335. Palmer, D.A., R.W. Ramette and R.E. Mesmer, Triiodide Ion Formation Equilibrium and Activity Coefficients in Aqueous Solution, J. Solution Chem. 13, 673 (1984).

336. Palmer, D.A., R.W. Ramette and R.E. Mesmer, Potentiometric Studies of the Thermodynamics of Iodine Disproportionation from 4 to 209 °C, J. Solution Chem. 13, 685 (1984).

337. Pantel, S., Catalytic-Kinetic Determination of Thioureas by a Biamperostataic Method with Iodine-Azide as the Indicator Reaction, Anal. Chim. Acta 152, 215 (1983).

338. Paquette, J. and B.L. Ford, Iodine Chemistry in the + 1 Oxidation State. I. The Electronic Spectra of OI^-, HOI, and H_2OI^+, Can. J. Chem. 63, 2444 (1985).

339. Peach, M.E., Sulfur-Iodine Compounds, Int. J. Sulfur. Chem. 8, 151 (1973).

340. Pendlebury, J.N. and R.H. Smith, Kinetics of the Reversible Reaction Between Arsenious Acid and Aqueous Iodine, Int. J. Chem. Kinet. 6, 663 (1974).

341. Perrin, D.D., Dissociation Constants of Inorganic Acids and Bases in Aqueous Solution, Pure Appl. Chem. 20, 133 (1969).

342. Piekarski, H., A. Piekarska and S. Taniewska-Osinska, Dissolution Enthalpy of NaI in Water- Alcohol Mixtures at 288.15 and 308.15 K. Enthalpy of Interaction in Electrolyte-Alcohol-Water Systems, Can. J. Chem. 62, 856 (1984).

343. Pilipenko, A.T., A.V. Terletskaya and O.V. Zui, Determination of Iodide and Bromide by Chemiluminescence Methods Coupled with Dynamic Gas Extraction, Fresenius' Z. Anal. Chem. 335, 45 (1989).

344. Popov, A.I., R.H. Rygg and N.E. Skelly, Studies on the Chemistry of Halogens and of Polyhalides. IX. Electrical Conductance Study of Higher Polyiodide Complex Ions in Acetonitrile, J. Am. Chem. Soc. 78, 5740 (1956).

345. Popov, A.I., R.E. Humphrey and W.B. Person, Studies on the Chemistry of Halogens and of Polyhalides. XIX. Formation Constants of Halogen Complexes from Infrared Measurements, J. Am. Chem. Soc. 82, 1850 (1960).

346. Press, W.H., B.P. Flannery, S.A. Teukolsky, W.T. Vetterling, Numerical Recipes: The Art of Scientific Computing, Cambridge University Press, New York (1985).

347. Porter, R.N., D.L. Thompson, L.B. Sims and L.M. Raff, The Crucial Role of Dynamic Effects in the Hydrogen-Iodine Reaction, J. Am. Chem. Soc. 92, 3208 (1970).

348. Raley, J H., R.D. Mullineaux and C.W. Bittner, High Temperature Reactions of Iodine with Hydrocarbons. I. Dehydrogenation, J. Am. Chem. Soc. 85, 3174 (1963).

349. Ramette, R.W. and R.W. Sanford, Jr., Thermodynamics of Iodine Solubility and Triiodide Ion Formation in Water and in Deuterium Oxide, J. Am. Chem. Soc. 87, 5001 (1965).

350. Ramette, R.W. and D.A. Palmer, Thallium(I) Iodate Solubility Product and Iodic Acid Dissociation Constant from 2 to 75 °C, J. Solution Chem. 13, 637 (1984).

351. Ramos, G.R., M.C.G. Alvarez-Coque and R.M.V. Carneras, Analytical Applications of the Catalysed Iodine - Azide Reaction, A Review, Analyst 111, 1001 (1986).

352. Rao, T.S., M.M. Murhe, R.B. Dabke and T. Harikrishna, Study of Rapid Reactions by the Steady State Principle: Kinetics of the Reaction between Vitamin C and Iodine in Aqueous Solution, Current Sci. 59, 370 (1990).

353. Rappe, C., Halogenation of Ketones. VII. Base-Catalyzed Halogenation of Butanone-2. Evidence for two Different Reactions, Acta Chem. Scand. 21, 857 (1967)

354. Rappe, C., Halogenation of Ketones. VII. Studies on the Mechanisms of the two Base-Catalyzed Halogenations of 2-Butanone. Indications of Non-Enolic Mechanisms, Acta Chem. Scand. 21, 1823 (1967).

355. Rastogi, R.P. and B.L. Dubey, Solid-State Reaction between Iodine and Mercurous Halides, J. Am. Chem. Soc. 89, 200 (1967).

356. Rastogi, R.P., B.L. Dubey and N.K. Pandey, Solid-State Reaction between Thallous Carbonate and Iodine, J. Inorg. Nucl. Chem. 34, 2127 (1972).

357. Ray, B.R., D.M. Beeson and H.F. Crandall, Centrifugal Electromotive Force: The Transference Numbers of Lithium, Rubidium and Cesium Iodides. The Iodide-Iodine Complex, J. Am. Chem. Soc. 80, 1029 (1958).

358. Rehr, A. and M. Jansen, $(I_3O_6)^+$, a Novel Polyoxo Cation of Iodine, Angew. Chem. Int. Ed. Engl. 30, 329 (1991).

359. Reynolds, W.L., The Reaction between Potassium Ferrocyanide and Iodine in Aqueous Solutions, J. Am. Chem. Soc. 80, 1830 (1958).

360. Roe, A. and E.L. Albenesius, The Isotope Effect. III. The Reaction of Acetone-1-C^{14} with Alkaline Hypoiodite, J. Am. Chem. Soc. 74, 2402 (1952).

361. Rogers, A.S., D.M. Golden and S.W. Benson, The Thermochemistry of the Gas Phase Equilibrium $I_2 + C_3H_6 = C_3H_5I + HI$, J. Am. Chem. Soc. 88, 3194 (1966).

362. Rogers, A.S., D.M. Golden and S.W. Benson, Kinetics of the Reaction of Iodobenzene and Hydrogen Iodide. The Heat of Formation of the Phenyl Radical and Its Implications on the Reactivity of Benzene, J. Am. Chem. Soc. 89, 4578 (1967).

363. Roliefson, G.K. and R.F. Faull, The Effect of Iodine on the Rates of Decomposition of Formaldehyde, Acetaldehyde and Propionaldehyde, J. Am. Chem. Soc. 59, 625 (1937).

364. Roy, J.C., W.H. Hamill and R.R. Williams, Jr., Diffusion Kinetics of the Photochemical and Thermal Dissociation-Recombination of Trihalide Ions, J. Am. Chem. Soc., 77, 2953 (1955).

365. Rudra, S., H. Talukdar and K.K. Kundu, Ion-Ion-Solvent Interactions in Aqueous Ionic Cosolvent Systems. III. Thermodynamics of Hydrogen Bromide and Hydrogen Iodide from Water to Aqueous Solutions of Sodium Nitrate from EMF Measurements at Different Temperatures and the Structuredness of the Solvents, Can. J. Chem. 65, 2843 (1987).

366. Rutz, J.A., S.V. Muckle, R.L. Sauer, Iodine Addition Using Triiodide Solutions, SAE 921315 presented at 22nd International Conference on Environmental Systems, Seattle, July 13-16, 1992.

367. Saluja, P.P.S., K.S. Pitzer and R.C. Phutela, High-Temperature Thermodynamic Properties of Several 1:1 Electrolytes, Can. J. Chem. 64, 1328 (1986).

368. Sanden, G.N., B.S. Fields, J.M. Barbaree, W.E. Morrill and J.C. Feeley, Bactericidal Activities of Tri- and Penta-Iodinated Resins against Legionella pneumophila, Wat.

Res. 26, 365 (1992).

369. Sansoni, B., Spezifische Molekuladsorption von Jod an Anionenaustauschern, Angew Chem. 73, 493 (1961).

370. Santana, H. de and M.L. A. Temperini, Spectrochemical Study of Iodide, Iodate and Periodate on a Silver Electrode in Alkaline Aqueous Solution, J. Electroanal. Chem. 316, 93 (1991).

371. Sauer, R.L. and D.S. Janik, Medical Effects of Iodine Disinfection Products in Spacecraft Water, SAE Paper No. 871487 presented at 17th Intersociety Conference on Environmental Systems, Seattle, July 13-15, 1987.

372. Schlegel, J.H. and J. Perrine, The Oxidation of Iodide by Bromate in Fused Alkali Metal Nitrates, J. Inorg. Nucl. Chem. 34, 2087 (1972).

373. Schmulbach, C.D. and R.S. Drago, Molecular Addition Compounds of Iodine. III. An Infrared Investigation of the Interaction Between Dimethylacetamide and Iodine, J. Am. Chem. Soc. 82, 4484 (1960).

374. Schultz, J.R. et al., Biofilm Formation and Control in a Simulated Spacecraft Water System: Interim Results, SAE Paper No 891543, presented at 19th Intersociety Conference on Environmental Systems, San Diego, 1989.

375. Schultz, J.R., R.D. Taylor, T. Flannagan, S.E. Carr, R.J. Bruce, J.V. Svoboda, M.H. Huls, R.L. Sauer, and D.L. Pierson, Biofilm Formation and Control in a Simulated Spacecraft Water System: Two-Year Results, SAE Paper No. 911403, presented at 21st International Conference on Environmental Systems, San Francisco, July 15-18, 1991.

376. Schultz, J.R., D.T. Flannagan, R.J Bruce, P.D. Mudgett, S.E. Carr, J.A. Rutz, M.H. Huls, R.L. Sauer, and D.L. Pierson, Biofilm Formation and Control in a Simulated Spacecraft Water System: Three Year Results, SAE 921310 presented at 22nd International Conference on Environmental Systems, Seattle, July 13-16, 1992.

377. Schultz, J.R., personal communication, August 1992.

378. Schweitzer, P. and R.M. Noyes, Kinetics of Iodine Bromide Formation in Concentrated Sulfuric Acid. A Concerted Termolecular Process, J. Am. Chem. Soc. 93, 3561 (1971).

379. Scudi, J.V., The Iodination of p-Aminobenzenesulfonamide and Some Symmetrical Azobenzenesulfonamides, J. Am. Chem. Soc. 59, 1480 (1937).

380. Secco, F., A. Indelli and P.L. Bonora, A Kinetic Study of the Reaction of Arsenic Acid with Iodide Ions, Inorg. Chem. 9, 337 (1970).

381. Secco, F. and S. Celsi, A Kinetic Study of the Reaction between Peroxydisulphate Ion and Iodine, J. Chem. Soc. (A), 1092 (1971).

382. Seelye, R.N. and T.A. Turney, The Iodoform Reaction, J. Chem. Ed. 36, 572 (1959).

383. Seitz, R.W. and D.M. Hercules, A Quantitative Study of Chemiluminescence from the Iodine-Luminol Reaction, J. Am. Chem. Soc. 96, 4094 (1974).

384. Selby, S.M., Ed., Standard Mathematical Tables, 22nd Edition, CRC Press, Cleveland (1974).

385. Sharma, K.R. and R.M. Noyes, Oscillations in Chemical Systems. VII. Effects of Light and of Oxygen on the Bray-Liebhafsky Reaction, J. Am. Chem. Soc. 97, 202 (1975).

386. Sharma, K.R. and R.M. Noyes, Oscillations in Chemical Systems. 13. A Detailed Molecular Mechanism for the Bray-Liebhafsky Reaction of Iodate and Hydrogen Peroxide, J. Am. Chem. Soc. 98, 4345 (1976).

387. Shine, H.J. and D.M. Hoffman, The Decomposition of Acetyl Peroxide: The Effect of Iodine, J. Am. Chem. Soc. 83, 2782 (1961).

388. Shirley, D.A. and W.F. Giauque, The Entropy of Iodine. Heat Capacity from 13 to 327 K. Heat of Sublimation, J. Am. Chem. Soc. 81, 4778 (1959).

389. Shreeve, W.W., F. Leaver and I. Siegel, A Method for the Specific Conversion of Iodoform to Carbon Dioxide, J. Am. Chem. Soc. 74 (1952).

390. Shu, Z.X. and S. Bruckenstein, Iodine Adsorption Studies at Platinum, J. Electroanal. Chem. 317, 263 (1991).

391. Shum, L.G.S. and S.W. Benson, The Oxidation of HI at Low Temperatures and Heat of Formation of HO_2, Int. J. Chem. Kinet. 15, 323 (1983).

392. Shum, L.G.S. and S.W. Benson, Thermochemistry and Kinetics of the Reaction of Methyl Mercaptan with Iodine, Int. J. Chem. Kinet. 15, 433 (1983).

393. Shum, L.G.S. and S.W. Benson, Iodine Catalyzed Pyrolysis of Dimethyl Sulfide. Heats of Formation of CH_3SCH_2I, the CH_3SCH_2 Radical and the Pibond Energy in CH_2S, Int. J. Chem. Kinet. 17, 277 (1985).

394. Simoyi, R.H., J. Masere, C. Muzimbaranda, M. Manyonda and S. Dube, Travelling

Wave in the Chlorite-Thiourea Reaction, Int. J. Chem. Kinet. 23, 419 (1991).

395. Skell, P.S. and R.R. Paul, Stereospecific trans Photoaddition of Elementary Iodine to Aliphatic Olefins. Bridged Iodoalkyl Radicals, J. Am. Chem. Soc. 86, 2956 (1964).

396. Slaugh, L.H., R.D. Mullineaux and J.H. Raley, High Temperature Reactions of Iodine with Hydrocarbons. III. Rearrangement of Aliphatic Free Radicals, J. Am. Chem. Soc. 85, 3180 (1963).

397. Smith, R.H., Kinetics of the Reversible Reaction Between Iodine and Cyanide in Aqueous Acid Solution, Aust. J. Chem. 23, 431 (1970).

398. Smith, R.H. and J. Kilford, Kinetics of the Molybdate Catalyzed Oxidation of Iodide by Hydrogen Peroxide, Int. J. Chem. Kinet. 8, 1 (1976).

399. Solly, R.K. and S.W. Benson, Carbon-Hydrogen Bond Strengths in Methyl Formate and the Kinetics of the Reaction with Iodine, Int. J. Chem. Kinet. 1, 427 (1969).

400. Solly, R.K., D.M. Golden and S.W. Benson, Thermochemical Properties of Iodoacetone. Intramolecular Electrostatic Interactions in Polar Molecules, J. Am. Chem. Soc. 92, 4653 (1970).

401. Solly, R.K. and S.W. Benson, Kinetics of the Gas-Phase Reaction of Benzaldehyde with Iodine. The Heat of Formation and Stabilization Energy of the Benzoyl Radical, J. Am. Chem. Soc. 93, 1592 (1971)

402. Solly, R.K. and S.W. Benson, Kinetics of the Gas-Phase Unimolecular Decomposition of the Benzoyl Radical, J. Am. Chem. Soc. 93, 2127 (1971).

403. Souchay, P., Polarographie des Periodates Applications Analytiques, Anal. Chim. Acta 2, 17 (1948).

404. Spencer, J.G., Jr., and L.G. Hepler, Heats of Solution of Ammonium, Potassium and Sodium Iodates and of Sodium Bromate; Heat of Reaction of Iodine Pentoxide with Aqueous Hydroxide, J. Phys. Chem. 64, 499 (1960).

405. Stegemann, H., A. Rohde, A. Reiche, A. Schnitke and H. Fullbier, Room Temperature Molten Polyiodides, Electrochim. Acta 37, 379 (1992).

406. Stern, J.H. and N.W. Gregory, The Condensation Coefficient of Iodine, J. Phys. Chem. 61, 1226 (1957).

407. Straaten, H.V.D. and A.H.W. Aten, Jr., The Exchange between Organic Iodides and Inorganic Iodine in Aqueous Solution, J. Am. Chem. Soc. 76, 3798 (1954).

408. Strong, L.E. and A.D. Pethybridge, Aqueous Iodic Acid: Conductance and Thermodynamics, J Solution Chem. 16, 841 (1987).

409. Stroup, T.L., S.H. Schwartzkopf and G.L. Marchin, Iodine Microbial Control of Hydroponic Nutrient Solution, SAE Paper No. 911490, presented at 21st International Conference on Environmental Systems, San Francisco, July 15-18, 1991.

410. Subbarao, P.V., P.S.N. Murty and R.V.S. Murty, Kinetics of Oxidation of Iodide by Vanadium(V)-Oxalic Acid Catalysis, J. Inorg. Nucl. Chem. 40, 295 (1978).

411. Subramonian S. and D. Clifford, Aqueous-Phase Ion Solvation and the Selectivity of Anion Exchange Resins for Monovalent Ions, J. Solution Chem. 18, 529 (1989).

412. Symons, M.C.R., The Formation of Iodine Cations. Part I. Magnetic Evidence, J. Chem. Soc., 387 (1957).

413. Tamelen, E.E. van and M. Shamma, Assignment of the Olefinic Position in Unsaturated Acids by Means of the Iodolactonization Reaction, J. Am. Chem. Soc. 76, 2315 (1954).

414. Taylor, S.L., L.R. Fina and J.L. Lambert, New Water Disinfectant : an Insoluble Quaternary Ammonium Resin-Triiodide Combination that Releases Bactericide on Demand, Appl. Microbiol. 20, 720 (1970).

415. Thomas, T.R., D.T. Pence and R.A. Hasty, The Disproportionation of Hypoiodous Acid, J. Inorg. Nucl. Chem. 42, 183 (1980).

416. Thoma, J.A. and D. French, The Starch-Iodine-Iodide Interaction. Part I. Spectrophotometric Investigations, J. Am. Chem. Soc. 82, 4144 (1960).

417. Triolo, R. and M.H. Lietzke, Adsorption on Mixtures of Ion Exchangers, J. Inorg. Nucl. Chem. 42, 913 (1980).

418. Tschuikow-Roux, E. and K.R. Maltman, Application of the Modified Semi-Ion Pair Model for the Evaluation of Activation Energies for HX(X=F, Cl, Br, I, OH) Addition to Olefins, Int. J. Chem. Kinet. 7, 363 (1975).

419. U.S. Environmental Protection Agency, Methods for the Determination of Organic Compounds in Drinking Water, EPA/600/4-88/039, December (1988).

420. Uchiyama, S., M. Ono and S. Suzuki, Coulometric Cell Using Porous Carbon Felt, Anal. Chem. 60, 1835 (1988).

421. Upton, S.J., M.E. Tilley, G.L. Marchin, and L.R. Fina, Efficacy of a Pentaiodide Resin Disinfectant on Cryptoslporidium parvum (Apicomplexa: Cryptosporidiidae) Oocysts In Vitro, J. Parisit. 74, 719 (1988).

422. Vandegrift, G.F and J. Rocek, Catalysis in Oxidation Reactions. II. The Oxalic Acid Catalyzed Oxidation of Iodide, J. Am. Chem. Soc. 98, 1371 (1976).

423. Vandegrift, G.F. and J. Rocek, Chromic Acid Oxidation of Iodide, J. Am. Chem. Soc. 99, 143 (1977).

424. Vincent, H., Y. Monteil and M.P. Berthet, The Thiotrithiazyl Iodated Polyhalides, J. Inorg. Nucl. Chem. 42, 5 (1980).

425. Wakita, H., G. Johansson, M. Sandstrom, P.L. Goggin, and H. Ohtaki, Structure Determination of Zinc Iodide Complexes Formed in Aqueous Solution, J. Solution Chem. 20, 643 (1991).

426. Walkley, J. and J.H. Hildebrand, Partial Vapor Pressure and Entropy of Solution of Iodine, J. Phys. Chem. 63, 1174 (1959).

427. Walsh, J.M., C.C. Brawner, and R.L. Sauer, Development of an Automated Potable Water Bactericide Monitoring Unit, ASME 75-ENAs-36, presented at 5th Intersociety Conference on Environmental Systems, San Francisco, July 21-24, 1975.

428. Walsh, R. and S.W. Benson, Kinetics and Mechanism of the Gas Phase Reaction between Iodine and Isopropyl Alcohol and the Tertiary Carbon-Hydrogen Bond Strength in Isopropyl Alcohol, J. Am. Chem. Soc. 88, 3480 (1966).

429. Walsh, R and S.W. Benson, Kinetics and Mechanism of the Gas Phase Reaction between Iodine and Formaldehyde and the Carbon-Hydrogen Bond Strength in Formaldehyde, J. Am. Chem. Soc. 88, 4570 (1966).

430. Walsh, R. and S.W. Benson, Corrections to : [Kinetics and Mechanism of the Gas Phase Reaction between Iodine and Formaldehyde and the Carbon-Hydrogen Bond Strength in Formaldehyde, J. Am. Chem. Soc. 88, 4570 (1966).], J. Am. Chem. Soc. 89, 727 (1967).

431. Wang, R.T., G. Rabai and K. Kustin, Kinetics and Mechanism of the Iodine Oxidation of Hydroxylamine, Int. J. Chem. Kinet. 24, 11 (1992).

432. Warrick, P., Jr., E.M. Wewerka and M.M. Kreevoy, The Reactions of Iodine in Solution with Elementary Mercury, J. Am. Chem. Soc. 85, 1909 (1963).

433. Wells, C.F. and D. Whatley, Kinetics of the Oxidation of Formic Acid by Aquomanganese(III) Ions in Aqueous Perchlorate Media, J. Chem. Soc. Faraday Trans. 68, 434 (1972).

434. Werner, E.A., The Interaction of Iodine and Thiocarbamide. The Properties of Formamidine Disulphide and its Salts, J. Chem. Soc. 101, 2166 (1912).

435. Westermark, T., Sorption of Organic Vapors in Organic Ion Exchanging Substances, Acta Chem. Scand. 14, 1857 (1960).

436. Wilcomb, B.E., T.M. Mayer, R.B. Bernstein and R.W. Bickes, Jr., Crossed Molecular Beam Measurement of the Intrinsic Activation Barrier for the Endoergic Reaction Hg + I_2 --> HgI + I, J. Am. Chem. Soc. 98, 4676 (1976).

437. Williams, R.J., E. Rohrman and B.E. Christensen, Organic Oxidation Equivalent Analysis. II. By the Use of Iodate. (Micro and "Sub-micro" Methods), J. Am. Chem. Soc. 59, 291 (1937).

438. Willis, C.E. and J.R. Schultz, Spacecraft Water System Disinfection Technology: Past, Present and Future Needs, SAE Paper No. 871487, presented at 17th Intersociety Conference on Environmental Systems, Seattle, July 13-15, 1987.

439. Wilson, J.N. and R.G. Dickinson, Measurement of a Reaction Rate at Equilibrium by Means of a Radioactive Indicator. The Reaction between Arsenic Acid and Iodine, J. Am. Chem. Soc. 59, 1358 (1937).

440. Wilson, M.H. and E. Berliner, The Kinetics of Iodination of Sodium Phenylpropiolate, J. Am. Chem. Soc. 93, 208 (1971).

441. Woittiez, J.R.W., H.A. van der Sloot, G.D. Wals, B.J.T. Nieuwendijk and J. Zonderhuis, The Determination of Iodide, Iodate, Total Inorganic Iodine and Charcoal-Adsorbable Iodine in Seawater, Mar. Chem. 34, 247 (1991).

442. Wolfram, S., Mathematica: A System for Doing Mathematics by Computer, 2nd Edition, Addison Wesley, New York (1991).

443. Wong, S.-W. and R.M. Noyes, Mechanism of Exchange between Iodoacetone and Elementary Iodine, J. Am. Chem. Soc. 86, 3787 (1964).

444. Woodson, J.H. and H.A. Liebhafsky, Iodide-Selective Electrodes in Reacting and in Equilibrium Systems, Anal. Chem. 41, 1895 (1969).

445. Woolley, E. M., J. O. Hill, W.K. Hannan and L.G. Helper, Thermodynamics of Ionization of Aqueous Iodic Acid, an "Almost-Strong" Electrolyte, J. Solution Chem.

7, 385 (1978).

446. Wren, J.C., J. Paquette, S. Sunder and B.L. Ford, Iodine Chemistry in the + 1 Oxidation State. II. A Raman and UV-Visible Spectroscopic Study of the Disproportionation of Hypoiodite in Basic Solutions, Can. J. Chem. 64, 2284 (1986).

447. Wyatt, W.A., F.V. Bright and G.M. Hieftje, Characterization and Comparison of Three Fiber-Optic Sensors for Iodide Determination Based on Dynamic Fluorescence Quenching of Rhodamine 6G, Anal. Chem. 59, 2273 (1987).

448. Yao, S-Z., Z-H. Mo and L-H. Nie, Determination of Ultratrace Iodide in Aqueous Solution with a Piezoelectric Detector, Anal. Chim. Acta 215, 79 (1988).

449. Yao, S-Z., Nie, L.H. and Z.H. Mo, Determination of Picomolar Concentrations of Bromide with a Piezoelectric Detector by Catalysis of the Permanganate/Iodide Reaction, Anal. Chim. Acta 217, 327 (1989).

450. Yost, D.M. and W.E. Stone, The Complex Ions Formed by Iodine Cyanide with Cyanide and Iodide Ions. The Vapor Pressure, Free Energy and Dissociation of Iodine Cyanide, J. Am. Chem. Soc. 55, 1889 (1933).

451. Young, P.R. and L.-S. Hsieh, General Base Catalysis and Evidence for a Sulfurane Intermediate in the Iodine Oxidation of Methionine, J. Am. Chem. Soc. 100, 7121 (1978).

452. Young, P.R. and L.-S. Hsieh, Mechanism of Buffer Catalysis in the Iodine Oxidation of N-Acetylmethionine Methyl Ester, J. Am. Chem. Soc. 104, 1612 (1982).

453. Ziegler, M., Sorption von Brom und Jod durch Anionen-Austauscher, Angew. Chem. 71, 283 (1959).

454. Zimmermann, H.W. and W.M. Latimer, The Heat of Reaction of Thiosulfate with Triiodide, J. Am. Chem. Soc. 61, 1554 (1939).

455. Zingaro, R.A., C.A. VanderWerf and J. Kleinberg, Evidence for the Existence of Unipositive Iodine Ion in Solutions of Iodine in Pyridine, J. Am. Chem. Soc. 73, 88 (1951).

456. Zucker, L. and L.P. Hammett, The Effect of Nuclear and Side Chain Substitution on the Oxonium Ion Catalyzed Iodination of Acetophenone Derivatives, J. Am. Chem. Soc. 61, 2779 (1939).

457. Zucker, L. and L.P. Hammett, Kinetics of the Iodination of Acetophenone in Sulfuric and Perchloric Acid Solutions, J. Am. Chem. Soc. 61, 2791 (1939).

END

DATE

FILMED

JUL 2 1993

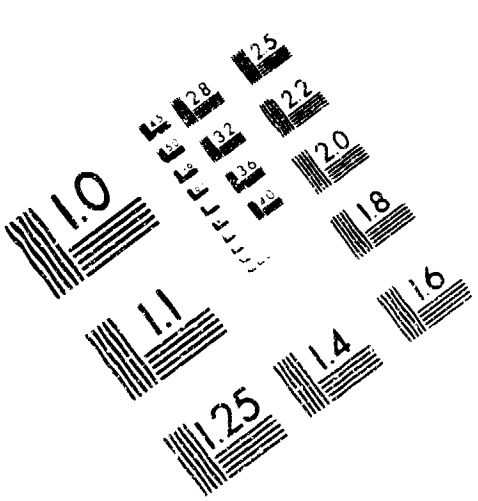

Association for Information and Image Management
1100 Wayne Avenue Suite 1100
Silver Spring Maryland 20910
301 587-8202

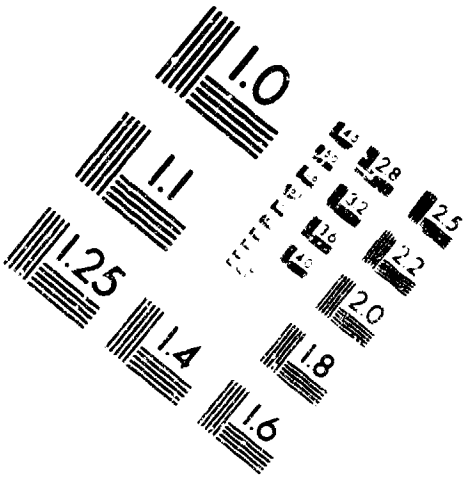

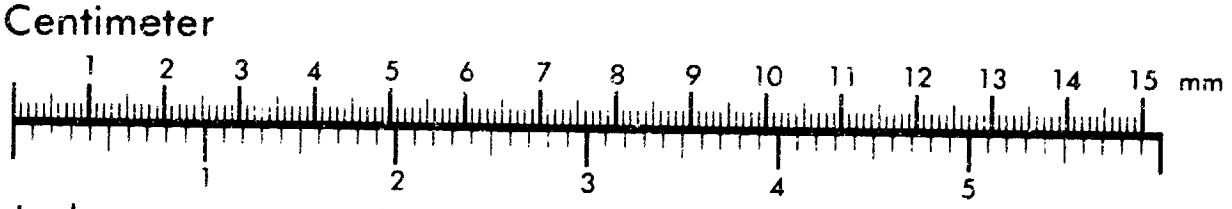

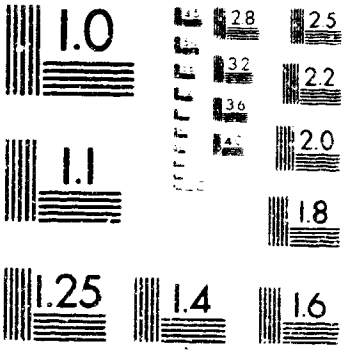

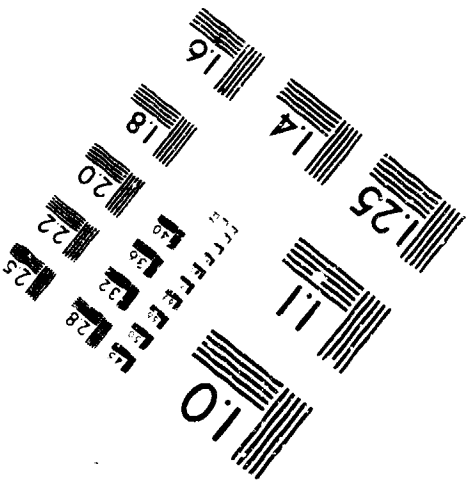

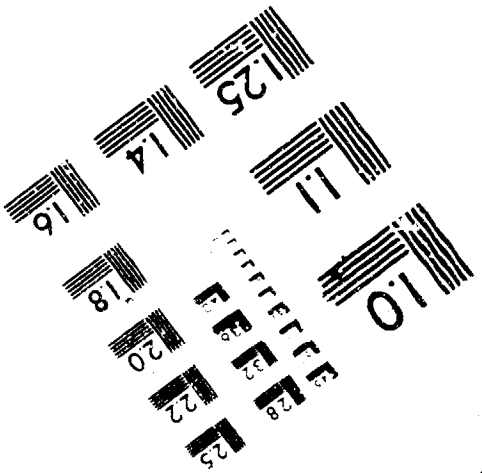

MANUFACTURED TO AIIM STANDARDS
BY APPLIED IMAGE, INC.